Investigation of the regulatory role of heme oxygenase-1 and its products during VEGF-induced angiogenesis, using *in vitro* and *in vivo* models

A thesis submitted for the degree Doctor of Philosophy and the Diploma of Imperial College

by

Andrea Bauer

National Heart and Lung Institute

Hammersmith Campus

Imperial College London

November 2012

ABSTRACT

Angiogenesis is fundamental to many physiological processes, and associated with various pathologies, including atherosclerosis and malignant disease.

Increasing evidence suggests a role for the cytoprotective enzyme heme oxygenase-1 (HO-1) and its products in angiogenesis. However, the mechanisms through which HO-1 exerts its effects remain elusive. This study aims to identify signalling pathways and novel HO-1 downstream targets regulating angiogenesis.

I show that inhibition of HO-1 with synthetic antagonist (ZnPP) or specific siRNA alters the angiogenic process at various levels. HO-1 inhibition significantly reduced vascular endothelial growth factor A (VEGF)-mediated human endothelial cell (EC) proliferation and inhibited capillary-like formation on 2D-Matrigel. Further, I demonstrate that VEGF-induced EC cell cycle progression is inhibited by HO-1 siRNA; an observation associated with decreased expression of cell cycle regulators cyclin A1 and cyclin E1. In contrast, HO-1-deficient cells were still protected from apoptosis by VEGF, most likely through induction of anti-apoptotic genes Bcl-2 and A1. Interestingly, HO-1 depletion negatively affected directional migration of EC towards a VEGF gradient; a phenotype reversed by HO-1 over-expression using an adenoviral vector. Moreover, migrating HO-1-deficient cells showed decreased cyclin A1 protein accompanied by decreased cyclin-dependent kinase 2 activity. Importantly, a combined proteomics and microarray approach has identified downstream targets of HO-1 and their potential roles in HO-1-driven angiogenesis have been investigated. For instance, HO-1 depletion results in impaired assembly of the intermediate filament vimentin. HO-1-deficient cells show reduced activity of the calcium-dependent protease calpain in response to VEGF; this observation was accompanied by a decrease in vimentin cleavage. The differences in vimentin cleavage and filament assembly may in turn account for the impaired angiogenic phenotype of HO-1-deficient cells.

Identification of HO-1 downstream target genes may reveal potential therapeutic approaches for enhancing angiogenesis at sites of ischaemia or wound healing, or alternatively inhibiting angiogenesis associated with atherosclerosis or tumourogenesis.

ACKNOWLEDGEMENTS

This study was carried out at the National Heart and Lung Institute, Vascular Sciences Section, Imperial College London. It was supported by the National Heart and Lung Foundation (Charity No. 1048073). I thank Prof Dorian Haskard for providing the research facilities in the department.

I would like to take this opportunity to express my sincere gratitude and deep appreciation to my supervisor Prof Justin Mason. I am sincerely grateful for his continuous support during my PhD, for his patience, motivation, enthusiasm and sharing his immense knowledge with me. Justin, you have greatly improved my way of thinking, producing and presenting science. Thank you.

I thank my secondary supervisors Anna Randi and Robin Wait. Your way of providing ideas, constructive criticisms, and support for my work has been of crucial importance.

I especially thank Hayley Mylroie and Clare Thornton. Ladies, you are wonderful and I thank you deeply for the great time we had together in the lab and the 'real' world. It has been a great pleasure to get to know you as colleagues but most importantly as my friends. You made my work and life in London very enjoyable and unforgettable!

I warmly thank Odile Dumont who teached me the necessary skills to conduct this work, shared her vast technical knowledge with me and become a valuable and true friend to me. I also like to thank Damien Calay and Fahad Alrashed. I very much enjoyed working with you and am deeply grateful for all your help, advice and the ideas you have contributed to my project.

I am grateful to Graeme Birdsey and Richard Starke for their constant help and advice throughout my time in the department. Thanks for sharing your wisdom with me. I have learned a lot from you guys! I thank Joseph Boyle for his extremely useful suggestions and ideas relating to this study.

It is a great pleasure to thank Danuta Mahiouz, the heart of our department. Thank you for all your help, advice and support and keeping the lab running even during the move.

Narges, Bao, Ramzi, Nicky A and Nicky D, Simon, Andrea, Amalia, Emon, Aarti, Samia, Silvia and Lourdes thank you for all your support, encouragement and help over the past few years. You all became good friends and made the time in the department unforgettable to me.

On a more personal note, I thank my dear friend Sebastian Krumscheid who brought home much closer to me during my time in London. I also like to thank Judith Wermert who I met when I was two years old and who has been my best friend ever since.

Jonas Lexow, I thank you wholeheartedly. My life in London would have not been possible without you. You stood by my side during the most difficult times, picked me up when I was down and supported me unconditionally. I thank you so much for all the beautiful memories I have of our time in London. I will never forget them and you will be a part of me forever.

I especially thank my sister Silvia and my brother Oliver, his wife Martina and their children Marlene and Lars. Thank you for believing in me and I know for sure that I can always count on you. I thank my grandparents Ruth and Heinz Bauer, and Elisabeth and August Ramschik. I will keep you in my heart forever.

Finally, I would like to dedicate this thesis to my parents Maria and Hans Bauer. There are just no words to express my gratitude for all you have done for me. Your unconditional love, endless support and the trust you have in me made me strong and this work possible. Thank you!

DECLARATION

All the work described in this thesis was performed by the author except were specifically indicated below or in the text. Figure 1.2., Fig. 1.3., Fig. 1.5., Fig. 1.6., Fig. 1.9., Fig. 1.12., Fig. 2.7. and Fig. 8.1. were obtained from the respective publications (Aird, 2007; Ley *et al.*, 2007; Widlansky *et al.*, 2003; Obaya and Sedivy, 2002; Mattila and Lappalainen, 2008; Shibuya, 2009; Dennery, 2005; Linnenbaum *et al.*, 2012; Wako Chemicals GmbH; Ivaska *et al.*, 2007). Fig. 1.4. was printed with permission from Prof Justin C Mason. The BioAnalyzer run shown in Fig. 6.12. was performed with assistance of Nathalie Lambie. Difference in-gel electrophoresis and mass spectroscopy experiments were planned in collaboration with Prof Manual Mayr and conducted by Xiaoke Yin.

CONTENTS

LIST OF FIGURES

LIST OF TABLES

ABBREVIATIONS

1D	one-dimensional
2D	two-dimensional
λ PP	lambda protein phosphatase
α-SMC	alpha smooth muscle actin
ADP	adenosine diphosphate
AGE	advanced glycation end products
AMPK	AMP-activated protein kinase
Ang	angiopoietin
Ang II	angiotensin II
ANOVA	analysis of variance
AP-2	activator protein 2
APC/C	anaphase-promoting complex
ApoE	apolipoprotein E
ARE	anti-oxidant response element
Arp2/3	actin-related protein complex-2/3
ATP	adenosine triphosphate
BAEC	bovine aortic EC
Bcl	B-cell lymphoma
bFGF	basic fibroblast growth factor
BH_4	tetrahydrobiopterin
BPB	bromphenol blue
BrdU	5-bromo-2'-deoxyuridine
BSA	bovine serum albumin
Ca^{2+}	calcium
CCNA1	cyclin A1
Cdk	cyclin-dependent kinase
cDNA	complementary DANN
cGMP	guanosine monophosphate
CIT	citron
CKI	cyclin-dependent kinase inhibitor
CMFDA	5-chloromethylfluorescein diacetate
CO	carbon monoxide
CO_2	carbon dioxide
CoPP	cobalt protophorphyrin
CORM	CO-releasing molecule
COX	cyclo-oxygenase(s)
CRP	C-reactive protein
Cu/ZnSOD	cupper/zinc superoxide dismutase
CVD	cardiovascular disease(s)
DAF	decay-accelerating factor
DDR	discoidin domain receptor(s)

DIGE	Difference in-gel electrophoresis
DFO	deferoxamine mesylate
Dll	delta-like ligand
DLR™ assay	Dual-Luciferase® Reporter Assay
DMEM	Dulbecco's Modified Eagle Medium
DMSO	dimethyl sulfoxide
DANN	deoxyribonucleic acid
DTT	DL-Dithiothreitol
EBM	endothelial basal medium
EC	endothelial cell(s)
ECGS	EC growth supplement
ECL	enhanced chemiluminescence
ECM	extracellular matrix
E. coli	*Escherichia coli*
EDTA	ethylenediaminetetraacetic acid
EGF	epidermal growth factor
EGM	endothelial growth medium
eNOS	endothelial nitric oxide synthase
EPC	endothelial progenitor cell(s)
ER	endoplasmic reticulum
ERK	extracellular signal-regulated kinase
ESAM	endothelial cell-selective adhesion molecule
ESL-1	E-selectin ligand 1
ET_A	endothelin receptor type A
ET-1	endothelin-1
ET-CORM	enzyme-triggered CORM
F-actin	filamentous actin
FAK	focal adhesion kinase
FBS	fetal bovine serum
FCS	fetal calf serum
Fe^{2+}	ferrous iron
Fe^{3+}	ferric iron
FGF	fibroblast growth factor
FHC	ferritin heavy chain
Fig	figure
FITC	fluorescein isothiocyanate
FS	forward scatter
FSCN2	fascin homolog 2
FSP1	fibroblast specific protein 1
GA	gentamycin and amphotericin-B
G-actin	globular actin
GAPDH	glyceraldehyde 3-phosphate dehydrogenase

GC	guanylate cyclase
GO	gene ontology
GP	glycoprotein
G-phase	gap-phase
Grb2	growth factor receptor-bound protein 2
h	hour(s)
HAEC	human aortic endothelial cell(s)
HAoSMC	human aortic endothelial smooth muscle cell(s)
HBSS	Hank's balanced salt solution
HCl	hydrochloric acid
HDGF	hepatic-derived growth factor
hEGF	human endothelial growth factor
HEK	human embryonic kidney
HCl	hydrochloric acid
h-FGF-β	human fibroblast growth factor beta
HKa	high molecular weight kininogen
HMEC-1	human dermal microvascular endothelial cell(s)
HO	heme oxygenase
HO-1	heme oxygenase-1
HO-2	heme oxygenase-2
H_2O	hydrogen oxide (water)
H_2O_2	hydrogen peroxide
HRP	horseradish peroxidise
HSP32	heat shock protein 32
HSV-TK	herpes simplex virus thymidine kinase
HUVEC	human umbilical vein endothelial cell(s)
HSP	heat shock protein
HUVEC	human umbilical vein endothelial cell(s)
ICAM	intracellular adhesion molecule
IF	intermediate filament
ifu	infectious unit
Ig	immunoglobin
IκB	inhibitor of kappa B
IL	interleukin
INF-γ	interferon gamma
iNOS	inducible nitric oxide synthase
IRM	Interference Reflection microscopy
JAK-STAT	Janus kinase/signal transducer and activators of transcription
JAM	junctional adhesion molecule(s)
JNK	c-jun-NH_2-terminal kinase
$K_3[Fe(CN)_6]$	potassium hexacyano-ferrate (III)
$K_3[Fe(CN)_6]*3H_2O$	potassium hexacyano-ferrate (II) trihydrate

KLF-2	Krüppel-like factor 2
LAP	latency-associated peptide
LAR II	Luciferase Assay Reagent II
LDL	low density lipoprotein
LFA-1	lymphocyte function-associated antigen 1
L-NAME	N^{ω}-nitro-L-arginine methyl ester(s)
LPS	lipopolysaccharide
LTPB	latent TGF-β binding protein
mAb	monoclonal antibody
MAC-1	macrophage antigen 1
MADCAM-1	mucosal vascular addressin cell-adhesin molecule 1
MAEC	murine aortic EC
MAPK	mitogen-activated protein kinase
MARE	Maf response element
MbCO	carbonmonoxy myoglobin
M-CSF	macrophage colony-stimulating factor
MCP-1	monocyte chemotactic protein-1
MFI	mean fluorescent intensity
Mg^{2+}	magnesium
$Mg(CH_3COO)_2$	magnesium acetate
$MgCl_2$	magnesium chloride
min	minute(s)
MMP	matrix-metalloproteinases
$MnCL_2$	manganese chloride
MnSOD	managanese superoxide dismutase
MOI	multiplicity of infection
M-phase	mitosis phase
mRNA	messenger ribonucleic acid
MTS	3-(4,5-dimethylthiazol-2-yl)-5-(3-carboxymethoxyphenyl)-2-(4-sulfophenyl)-2H-tetrazolium
MW	molecular weight
NAC	N-acetyl cysteine
NADPH	nicotinamide adenine dinucleotide phosphate-oxidase
NFκB	nuclear factor kappa B
$(NH_4)_2S_2O_8$	diammonium peroxydisulfate
NICD	notch intracellular domain
nNOS	neuronal nitric oxide synthase
NO	nitric oxide
Nrf-2	nuclear factor erythroid 2-related factor-2
O_2	oxygen
PAF	platelet-activating factor
PAI-1	plasminogen activator inhibitor-1
PAR	platelet protease-activated receptor(s)

PBS	phosphate-buffered saline
PCNA	proliferating cell nuclear antigen
PCR	polymerase chain reaction
PDGF	placenta-derived growth factor
PDTC	pyrrolidine dithiocarbamate
PECAM	platelet endothelial cell adhesion molecule
PE-Texas Red	R-phycoerythrin Texas Red
PGI_2	prostacyclin
PI	propidium iodide
PlGF	placental growth factor
PI3K	phosphoinositide 3-kinase
PKA	protein kinase A
PKC	protein kinase C
PKG	protein kinase G
PLB	passive lysis buffer
PLC-γ	phospholipase C-γ
POD	peroxidase
PPP1R12A	protein phosphatase 1, regulatory (inhibitor) subunit 12A
pRB	retinoblastoma protein
PSGL-1	P-selectin glycoprotein ligand 1
PVDF	polyvinylidene fluoride
qRT-PCR	quantitative real-time PCR
RA	rheumatoid arthritis
RAGE	receptor for AGE
Rb	retinoblastoma protein
R^3-IGF-1	insulin-like Growth Factor analogue
RFU	relative fluorescence units
ROS	reactive oxygen species
RT	room temperature
RTK	receptor tyrosine kinase
SA-β-gal	senescence-associated beta-galactosidase
SCID	severe combined immune deficient
SDF	stromal cell-derived factor
SDS	sodium dodecyl sulphate
SDS-PAGE	sodium dodecyl sulphate-polyacrylamide gel electrophoresis
SEM	standard error of the mean
ser	serine
seq	sequence
siRNA	small interfering ribonucleic acid
SLE	systemic lupus erythematosus
SMC	smooth muscle cell(s)
SnPP	tin protoporphyrin

SOS	son of sevenless
S-phase	synthesising-phase
SS	side scatter
SSRE	shear stress-response element
StRE	stress-responsive element
sVEGF-R1	soluble vascular endothelial growth factor receptor 1
Tab	Table
TBS-T	Tris buffered saline and Tween 20
TEMED	N,N,N',N'-Tetramethylethylenediamine
TF	tissue factor
TGF-β	transforming growth factor-beta
TGF-βRI	transforming growth factor-beta type I receptor
TGF-βRII	transforming growth factor-beta type II receptor
Thr	threonine
TNF-α	tumour necrosis factor-alpha
tPA	tissue plasminogen activator
Tris	Trizma^{c} base
uPA	urokinase-type plasminogen activator
VAM	vimentin associated matrix adhesion
VASP	vasodilator-stimulated phosphoprotein
VCAM	vascular cell adhesion molecule
VE-cadherin	vascular endothelia-cadherin
VEGF	vascular endothelial growth factor
VEGFR	vascular endothelial growth factor receptor
VLA4	very late antigen 4
VMSC	vascular smooth muscle cell(s)
VPF	vascular permeability factor
VVO	vesico-vacuola organelles
vWF	von Willebrand factor
WASP	Wiscott-Aldrich Syndrome protein
X-gal	5-bromo-4-chloro-3-indolyl β-D-galactosidase
ZnPP	zinc (II) protoporphyrin IX chloride
ZO	zonula-occludens

CHAPTER 1 - INTRODUCTION

1.1. THE VASCULAR ENDOTHELIUM IN HEALTH AND DISEASE

The vascular endothelium is a continuous cellular monolayer lining the interior surface of all vessels of the vascular tree, starting from the origin at the exit of the heart to its final branches, the capillaries. The endothelium is a highly dynamic and heterogeneous organ that acts in an autocrine and paracrine manner and principally serves as a physiological and physical barrier between the vascular and extra-vascular compartments. It actively regulates the passage of solutes, macromolecules and blood cells across the vascular wall, generates and integrates biological signals and plays an essential role in haemostasis, leukocyte traffic and vascular tone, maintaining an anti-thrombotic, fibrinolytic and anti-inflammatory surface (Cines *et al.*, 1998).

1.1.1. Development of the vascular endothelium

The cardiovascular system is the first organ system to form in the gastrulating embryo. Vascular development requires two organised processes to occur: vasculogenesis and angiogenesis. Vasculogenesis is the *de novo* organisation of endothelial cells (EC) into vessels in the absence of any pre-existing vascular system, and angiogenesis is the continued expansion of the vascular tree as a result of EC sprouting from existing vessels (Risau and Flamme, 1995; Risau 1997). EC derive from the embryonic mesoderm via the differentiation of mesodermal cells into hemangioblasts leading to the formation of the primitive blood islands in the yolk sac. Hemangioblasts are common progenitors of EC and hematopoietic cells. Hemangioblasts from the centre of the islands give rise to hematopoietic stem cells from which the first embryonic blood cells develop and hemangioblasts of the periphery of the islands differentiate into angioblasts, the precursors of mature EC (Risau and Flamme, 1995; Cines *et al.*, 1998; Robb and Elefanty, 1998; Carmeliet, 2000). Following activation by chemotactic and haptotactic chemoattractants such as soluble growth factors and immobilized extracellular matrix (ECM) proteins respectively, migration of angioblasts is initiated which in turn allows the fusion of the blood islands and their rearrangement into luminised, tubular structures known as the first primitive vascular plexus (Risau and Flamme, 1995; Rossant and Howard, 2002). Remodelling of the vascular plexus into larger vessels also occurs via the process of angiogenesis (Risau and Flamme, 1995). Tissues

that are vascularised by this process are generally of endodermal origin and include the lung, pancreas, and spleen as well as the heart tube and dorsal aorta, whereas tissues of ectodermal and mesodermal derivation such as kidney and brain are vascularised primarily by angiogenesis (Pardanaud *et al.*, 1989). Common to both vasculogenesis and angiogenesis is the process of vascular remodelling, involving changes in lumen diameter and vessel wall thickness to suit the functional and metabolic requirements of the local tissue (Beck and D'Amore, 1997).

Vascular development is driven by specific polypeptide growth factors and interaction with their transmembrane receptor tyrosine kinases (RTK), extracellular matrix proteins, tissue remodelling by proteinases/enzymes and specific cell-matrix and cell-cell interactions. Among the most important growth factors are basic fibroblast growth factor (bFGF) and vascular endothelial growth factor (VEGF), both playing a pivotal role in the early development of the vascular endothelium (Beck and D'Amore, 1997). This is demonstrated by the fact that mutations affecting the VEGF gene cause abnormal vascular development and ultimately embryonic lethality (Carmeliet *et al.*, 1996; Ferrara *et al.*, 1996). Interaction of bFGF and VEGF with their respective receptors results in autophosphorylation of the receptors, triggering downstream signalling cascades leading to EC proliferation and migration, and subsequent assembly into vessels (Cines *et al.*, 1998).

Once the primary capillary plexus is formed, mesenchyme and smooth muscle cells (SMC) surrounding the developing vessel synthesise and secrete angiopoietin (Ang) glycoproteins (Davis *et al.*, 1996; Maisonpierre *et al.*, 1997). Four angiopoietins, Ang-1 to -4, have been identified to date, with Ang-1 and Ang-2 promoting vascular development (Tallquist *et al.*, 1999). Ang-1 and Ang-2 drive the expansion of the vascular tree, endocardial and ventricular development, and formation of the vascular wall via binding to Tie receptor family members (Davies *et al.*, 1996; Maisonpierre *et al.*, 1997; Valenzuela *et al.*, 1999). The two Tie receptors, Tie-1 and Tie-2/TEK comprise a separate class of endothelial-specific receptor tyrosine kinases. Their intracellular structure is similar to that of VEGF receptors, while the extracellular domain is unique having epidermal growth factor (EGF)-like, immunoglobin (Ig)-like, and fibronectin type three motifs (Partanen *et al.*, 1992; Ziegler *et al.*, 1993). Both receptors Tie-1 and Tie-2 are expressed throughout the vasculature from early stages and remain predominantly endothelial-specific throughout development, while in adult life Tie-2 may also be found on monocytes

(Dumont *et al.*, 1995). All four angiopoietins (Ang-1 to-4) exclusively bind Tie-2, while ligands for Tie-1 remain unknown (Davies *et al.*, 1996; Maisonpierre *et al.*, 1997; Valenzuela *et al.*, 1999). Ang-1 is an activating ligand, promoting tyrosine phosphorylation of the receptor while Ang-2 is an inhibitory ligand, antagonising the action of Ang-1 (Maisonpierre *et al.*, 1997). Recruitment of supporting cells, i.e. pericytes and SMC, which stabilise the maturing vessels, is critical to the integrity of the developing vasculature. Ang-1 in particular recruits accessory cells and creates stable vessels (Rossant and Howard, 2002; Suburo and D'Amore, 2006).

Extracellular matrix components such as collagen type IV, fibronectin, vitronectin, and proteoglycans interact with EC via cell-matrix adhesion receptors and regulate capillary tube formation. The predominant receptors that mediate cell-matrix interactions are members of the integrin family, although other ECM receptors are also known, including dystroglycan and discoidin domain receptors (DDR; Hynes, 2007). Integrin-ligand binding anchors the cell to the ECM in turn triggering intracellular signals that regulate cytoskeletal organisation at specific sites on the surface membrane to facilitate cell movement or maintain tissue stability, and to regulate proliferation and cell survival (Hynes, 2007). Among the integrins, many have been implicated in the development of the vascular system, including collagen receptors ($\alpha_1\beta_1$, $\alpha_2\beta_1$), laminin receptors ($\alpha_3\beta_1$, $\alpha_6\beta_1$, $\alpha_6\beta_4$), fibronectin receptors ($\alpha_4\beta_1$, $\alpha_5\beta_1$), and the α_v receptors, $\alpha_v\beta_3$ and $\alpha_v\beta_5$ (Hynes *et al.*, 1999; Serini *et al.*, 2006; Hynes, 2007). EC express more than one integrin and the combination is constantly changing, suggesting that specific combinations are required as development proceeds (Cines *et al.*, 1998).

Vessel sprouting and lengthening requires angioblasts and EC to be in contact with like cells. Such cell-cell contacts are mediated by a distinct series of cell surface receptors that include platelet EC adhesion molecule (PECAM-1/CD31), a member of the Ig superfamily, and vascular endothelial (VE)-cadherin, also known as cadherin-5 (Risau and Flamme, 1995; Albelda *et al.*, 1991; Cines *et al.*, 1998). These rather weak adhesion complexes are thought to assist cell-cell recognition and facilitate the assembly of more classic junctional complexes in maturing vessels, such as tight junctions and gap junctions, depending on the underlying vascular bed (Cines *et al.*, 1998). Vascular extension and remodelling requires co-ordinated synthesis and degradation of various tissues, such as the basement membrane and ECM, by specific enzymes including matrix

metalloproteinases (MMP) and plasminogen activators, allowing EC movement and subsequent expansion of the vascular tree (Bretscher, 1996; Carmeliet and Collen, 1995).

Vascular development is a complex multi-step process, involving multiple cell types interacting with one another, surrounding cells and the ECM. Many of these molecular processes required for vasculogenesis and angiogenesis are also involved in maintaining vascular homeostasis within the adult, and are recapitulated after injury or as part of inflammatory responses (Cines *et al.*, 1998).

1.1.2. Functions of the vascular endothelium

The vascular endothelium is composed of a single layer of cells that lines the inner lumen of all blood vessels. In adults, it is estimated to comprise around 10^{13} cells, representing a weight of 1.5 kg and covering 4,000-7,000 m^2 (Wolinsky *et al.*, 1980; Augustin *et al.*, 1994; Ait-Oufella *et al.*, 2010). Endothelial cells (EC) lie at the interface of the circulating blood and the vessel wall. They are flattened cells, 50-100 µm long, 10-15 µm wide, and about 0.5 µm in thickness. Their elongated shapes are juxtaposed in a mosaic such that their long axis is orientated in the direction of blood flow. Individual EC are interconnected by cell-to-cell adherent junctions formed by junctional adhesion molecules including PECAM-1/CD31 and VE-cadherin. They are anchored to an underlying basal membrane rich in collagen and glycoproteins, forming a complex interface between the circulation and the platelet-activating, pro-coagulant vascular matrix (Dejana *et al.*, 1995; Dejana *et al.*, 2009; Ait-Oufella *et al.*, 2010).

Nowadays, the endothelium is no longer viewed as an inert tissue. EC structure and functional integrity are important in the maintenance of the vessel wall and circulatory function. Cells respond to physical and chemical signals by production and secretion of a large variety of mediators that regulate vascular homeostasis and blood flow, vascular tone, cellular adhesion and permeability, thrombosis and thrombolysis, endothelial proliferation and angiogenesis, and vessel wall inflammation (Fig. 1.1.; Galley and Webster).

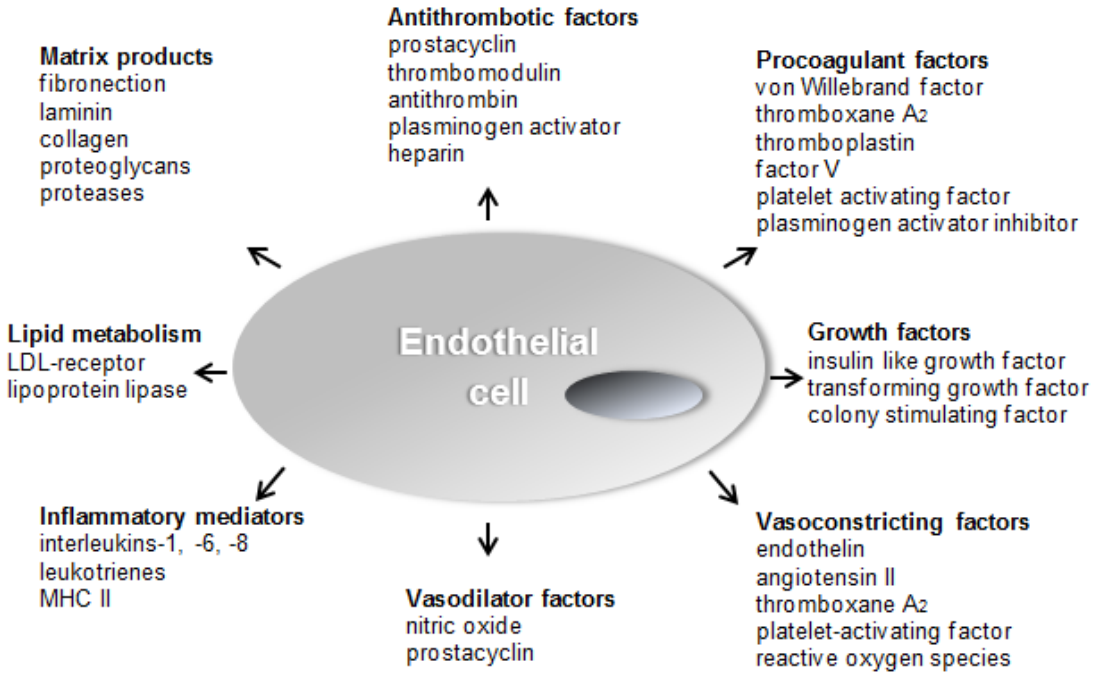

Figure 1. 1.: Metabolic and synthetic functions of the endothelium. Endothelial cells (EC) influence cellular functioning of the body through the secretion of a wide range of mediators. LDL – low density lipoprotein, MHC II – major histocompatibility complex class II (modified after Galley and Webster, 2004).

Endothelium transport and barrier functions

The endothelium functions as an important barrier to the free passage of plasma, molecules and cells from the blood to the underlying tissues and cells. Specific transport mechanisms, including trans- and paracellular permeability, and extracellular barriers such as focal adhesions, allow the transport of essential circulating blood macromolecules across EC to the subendothelial space to meet the metabolic demands of the surrounding tissue (Mann *et al.*, 2003). The endothelial barrier is maintained by two main types of intracellular junctions; tight junctions and adherens junctions. The latter are ubiquitous throughout the vasculature and provide barrier functions in most vascular beds principally via the intracellular junction protein VE-cadherin (Mehta and Malik, 2006; Rudini and Dejana, 2008; Komarova and Malik, 2010). Tight junctions are found in most vascular beds but contribute to microvascular barrier function only in a few specialised tissues, including the brain, retina and testes. The intracellular junction proteins mainly responsible for tight junction barrier function are occludin and claudin-5 (Hawkins and Davies, 2005; Mehta and

Malik, 2006; Abbott *et al.*, 2010). Small molecules and fluids tend to pass through the endothelial barrier using paracellular pathways via cell junctions, whereas larger molecules, such as albumin and low density lipoproteins (LDL), use an active transcellular route employing receptor-dependent and independent mechanisms, caveolae, vesico-vacuolar organelles (VVO) and transcellular channels (Feng *et al.*, 2002; Aird, 2007; Frank *et al.*, 2009). Endothelial transcellular permeability is mainly mediated by caveolae involving vesicle-mediated endocytosis of macromolecules at the luminal membrane, followed by transcytosis across the cell, and exocytosis at the basolateral membrane (Fig. 1.2.) (Predescu *et al.*, 2007)

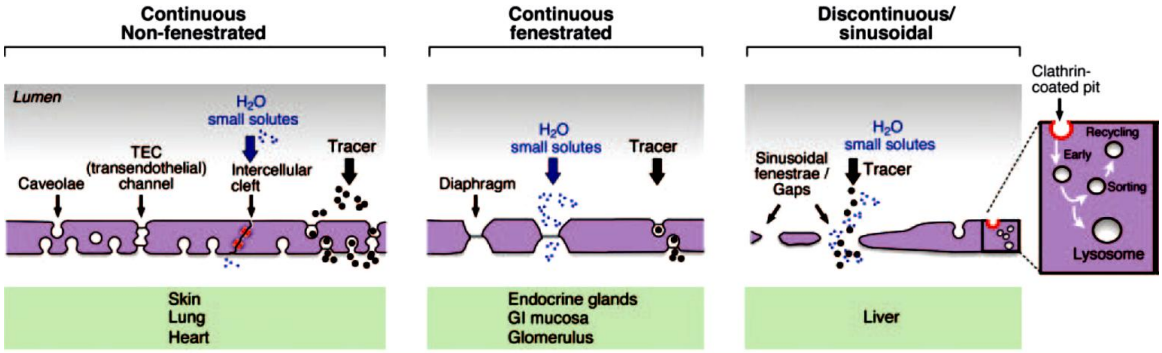

Figure 1. 2.: Vascular permeability in different vascular beds. In continuous non-fenestrated endothelium as present in skin, lung or heart, smaller molecules such as water (H_2O) and small solutes pass freely between EC, whereas larger molecules (tracer) pass through EC either via transendothelial channels (TEC) or transcytosis meditated by caveolae. Diaphragms of the fenestrae present in the continuous fenestrated endothelium as found in endorine glands, the gastrointestinal tract (GI) and the glomerulus, act as molecular filters, allowing greater permeability for H_2O and small molecules but refecting the passage of larger macromolecules. A discountinious endothelium as found in the liver is characterised by a sinusoidal fenestrae lacking diaphragms, and a poorly organised basement membrane allowing the free passage of fluids, small solutes and larger macromolecules. Clathrin-coated pits assist in receptor-mediated endocytosis (modified after Aird, 2007).

Caveolae are ‘cave-like’ invaginations in the plasma membrane containing caveolin-1, a scaffolding protein that is recruited to the membrane and regulates caveolar internalisation (Minshall *et al.*, 2003). By forming vesicles, caveolae are capable of moving considerable amounts of fluid and solutes across the cell. Focal adhesions are attachments between the endothelial basolateral membrane and surrounding ECM of the microvascular wall, principally

composed of the transmembrane receptor family of integrins. Integrins are heterodimeric glycoproteins containing an α and β subunit (Petit and Thiery, 2000; Hodivala-Dilke *et al.*, 2003; Wu, 2005). Their intracellular domains interact with the cytoskeleton either directly, or indirectly via the linker proteins paxillin, talin, vinculin, or α-actinin, and their large extracellular domains bind respective proteins present in the ECM, such as fibronectin, vitronectin, collagen, fibrinogen, and laminin (Petit and Thiery, 2000; Hodivala-Dilke *et al.*, 2003). The precise mechanisms by which focal adhesions contribute to endothelial barrier function are not completely understood, but integrin-matrix binding is essential for the establishment and stabilisation of endothelial barriers (Wu, 2005). Alterations in integrin-binding properties decrease focal adhesion strength, cause cell detachment from the ECM and EC apoptosis, or affect transendothelial flux of fluids and large solutes (Dejana and Lauri, 1990; Cheng *et al.*, 1991; Trache *et al.*, 2005; del Zoppo and Milner, 2006).

Vascular tone

The endothelium produces a variety of vasodilator and vasoconstrictor substances which regulate vasomotor tone, blood flow and pressure, and vascular haemodynamics (Fig. 1.1.). Among the most important vasodilatory substances produced by the endothelium are nitric oxide (NO) and prostacyclin (PGI_2), which are co-released from every vessel, thereby forming a particular partnership in the regulation of vascular function (Moncada *et al.*, 1976; Palmer *et al.*, 1987; de Nucci *et al.*, 1988). Important vasoconstrictors include endothelin-1 (ET-1), platelet-activating factor (PAF), thromboxane A_2, angiotensin II (Ang II), and reactive oxygen species (ROS) (Yanagisawa *et al.*, 1988; Schiffrin, 2001; Anderson *et al.*, 2000). The production of NO by the endothelium is constitutive and modulated by different stimuli, whereas the synthesis of other meditators, PGI_2, ET-1, and PAF, is inducible. The delicate balance between these mediators provides minute-by-minute control of tone and blood pressure.

NO is a highly soluble, gaseous molecule which is synthesised during oxidation of the semi-essential amino acid L-arginine and oxygen to L-citrulline by the enzyme nitric oxide synthase (NOS). NOS shares homology with the cytochrome p450 family of enzymes and requires tetrahydrobiopterin (BH_4), nicotinamide adenine dinucleotide phosphate-oxidase (NADPH) and

calcium/calmodulin for NO production (Knowles and Moncada, 1994; Scott-Burden, 1995). There are three recognised NOS isoforms which differ in their regulation and tissue expression; neuronal NOS (nNOS or NOS I), inducible NOS (iNOS or NOS II) mainly expressed in inflammatory cells and sites of inflammation, and endothelial NOS (eNOS or NOS III) the predominant isoform present in EC (Palmer *et al.*, 1988; Pollack *et al.*, 1991; Ghosh and Salerno, 2003). eNOS is constitutively expressed in the vascular endothelium and activated by increased intracellular calcium and phosphorylation in response to changes in shear forces or via receptor-mediated processes, thereby constantly generating NO (Stamler *et al.*, 1992). Laminar shear stress is the main stimulus for NO production, enhancing enzyme activity and synthesis (Féletou and Vanhoutte, 2009). Other receptor agonists stimulating eNOS include acetylcholine, bradykinin, histamine, serotonin, adenosine triphosphate (ATP) and adenosine diphosphate (ADP) (Moncada and Higgs, 2006). Released NO rapidly diffuses into neighbouring vascular smooth muscle cells (VSMC) where it binds and activates soluble guanylate cyclase (GC), leading to the generation of cyclic guanosine monophosphate (cGMP) and activation of protein kinase G (PKG) (Moncada *et al.*, 1991). PKG activation causes reduced calcium influx into VSMC, and decreased calcium/calmodulin stimulation of myosin light chain kinase. This in turn decreases the phosphorylation of myosin light chains, decreasing smooth muscle contraction and causing vasodilation (Moncada *et al.*, 1991; Moncada and Higgs, 2006; Vanhoutte *et al.*, 2009). The liberation of NO into the circulation also inhibits platelet aggregation and activation contributing to an anti-thrombotic vasculature (Riddell and Owen, 1999; Broos *et al.*, 2011).

In contrast to NO, endothelin is a potent vasoconstrictor also produced by endothelial cells, with marked effects on vascular tone. Three endothelin isoforms have been characterised, but only endothelin-1 (ET-1) is uniquely synthesised and released by the endothelium in response to stimuli including hypoxia, ischaemia and shear stress (Inoue *et al.*, 1989; Levin, 1995). Liberated ET-1 diffuses to neighbouring VSMC and binds to the abundant G-protein coupled receptor endothelin receptor type A (ET_A) present on the cell surface. Receptor binding promotes the release of intracellular calcium from the endoplasmic reticulum (ER) triggering VSMC proliferation and inducing vasoconstriction (Inoue *et al.*, 1989; Levin, 1995; Abraham and Dashwood, 2008).

Prostacyclin (PGI_2) and platelet-activating factor (PAF) are both intercellular signalling molecules synthesized by stimulated EC and derived from the metabolism of arachidonic acid. PGI_2 is an eicosanoid produced by the vascular enzymes cyclo-oxygenase (COX)-1 and COX-2, stimulating vasodilation and inhibiting platelet aggregation via paracrine signalling cascades that involve G-protein coupled receptors on nearby EC and platelets (Mitchell and Warner, 1999; Simmons *et al.*, 2004). In contrast, PAF, a phospholipid signalling via juxtacrine mechanisms, causes vasoconstriction and stimulates the adhesion of leukocytes to the endothelium (Imaizumi *et al.*, 1995; Lorant *et al.*, 1995).

Regulation of leukocyte traffic

The endothelium is of vital importance in the functioning of the immune system and regulation of immune responses. Both innate and adaptive immunity depend on the exit of leukocytes from the bloodstream and their migration across the endothelium to underlying target tissues, a process referred to as extravasation (Johnson-Léger *et al.*, 2000). Leukocyte extravasation occurs both as part of a constitutive physiological process, e.g. during lymphocyte re-circulation, and at sites of inflammation. In lymphoid organs, specialised vascular sites within postcapillary venules known as high endothelial venules (HEV) represent the major constitutive extravasation route *in vivo* (Anderson and Anderson, 1976; Anderson *et al.*, 1976; Lasky, 1992). In response to vascular injury or inflammatory stimuli the endothelium adopts an activated phenotype and rapidly upregulates its expression of cell surface leukocyte-adhesion molecules: E-selectin, P-selectin, vascular cell adhesion molecule 1 (VCAM-1) and intercellular adhesion molecule 1 (ICAM-1). This enhances the recruitment of neutrophils and stimulates secretion of soluble mediators such as cytokines (interleukin [IL]-1, IL-6) and chemoattractants (RANTES, monocyte chemotactic protein-1 [MCP-1]), which perpetuate inflammation and leukocyte recruitment (Bratt and Palmblad, 1997). Consequently, leukocytes are captured by EC initiating the leukocyte-adhesion cascade, a multistep process of successive interactions of adhesion receptors between leukocytes and EC.

Over the past decade, new insights into mechanisms underlying the adhesion process led to the expansion of the classical cascade consisting of selectin-mediated leukocyte rolling, chemokine-triggered activation, and integrin-dependent arrest, to a more detailed version now including slow

rolling, adhesion strengthening and spreading, intraluminal crawling, paracellular and transcellular migration, and migration through the basement membrane (Fig. 1.3.; Butcher, 1991; Springer, 1995; Muller, 2003; Imhof and Aurrand-Lions, 2004; Ley *et al.*, 2007). E- and P-selectin interact with their corresponding ligands P-selectin glycoprotein ligand 1 (PSGL-1) and E-selectin ligand 1 (ESL-1) on leukocytes, slowing down their velocity in the bloodstream and leading to a rolling movement on the vascular wall. Leukocyte activation enhances integrin affinity and avidity to ICAM-1 and VCAM-1 expressed on EC, resulting in the firm cell adhesion to the apical endothelial plasma membrane. Finally, leukocytes transmigrate to sites of injury via a gradient of chemotactic molecules which include MCP-1, complement components (C3a and C5a), cytokines and prostaglandins through paracellular pathways using interactions with junctional adhesion molecules (JAM), CD99 and PECAM-1, or alternatively through the transcellular route via ICAM-1 and PECAM-1 (Fabbri *et al.*, 1999; Muller, 2003; Vestweber, 2003).

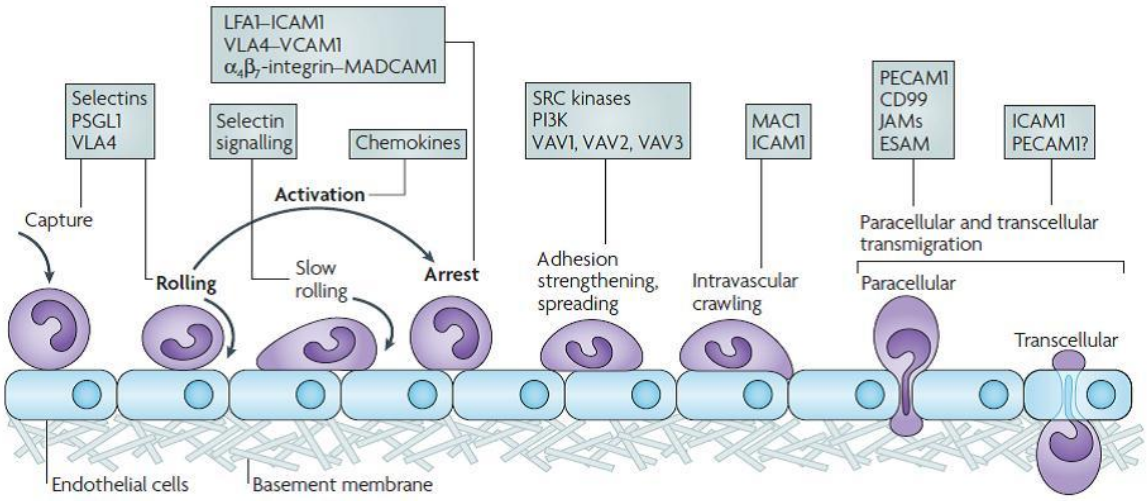

Figure 1. 3.: The leukocyte adhesion cascade. The originally described steps selectin-mediated leukocyte rolling, chemokine-triggered activation and integrin-dependent arrest are shown in bold. Additionally identified steps include capture, adhesion strengthening and spreading, intravascular crawling, and paracellular and transcellular transmigration. ESAM – endothelial cell-selective adhesion molecule, ICAM-1 – intercellular adhesion molecule 1, JAM – junctional adhesion molecule, LFA-1 – lymphocyte function-associated antigen 1, MAC-1 – macrophage antigen 1, MADCAM-1 – mucosal vascular addressin cell-adhesin molecule 1, PSGL-1 – P-selectin glycoprotein ligand 1, PECAM-1 - platelet endothelial cell adhesion molecule 1, PI3K – phosphoinositide 3-kinase, VCAM-1 – vascular cell adhesion molecule, VLA4 – very late antigen 4 (adapted from Ley *et al.*, 2007).

Regulation of haemostasis and coagulation

A crucial physiological function of the endothelium is to facilitate blood flow by providing an anti-thrombotic surface that inhibits platelet adhesion and clotting. However, when the continuity of the vascular endothelium is disrupted, EC undergo biochemical changes that culminate in their transformation to a pro-thrombotic surface promoting platelet aggregation and activation, coagulation and fibrinolysis (Cines *et al.*, 1998). Haemostasis is a defence mechanism to regulate bleeding in response to vascular wall injury and comprises a series of events classified as primary haemostasis (platelet aggregation), secondary haemostasis (blood coagulation), and tertiary haemostasis (fibrinolysis) (Arnout *et al.*, 2006). Haemostatic processes are tightly controlled by the delicate balance between anti-thrombotic and pro-thrombotic factors secreted or expressed by the endothelium and surrounding tissues (Tab. 1.1.; Ait-Oufella *et al.*, 2010). When a vascular lesion occurs, the immediate response of the endothelium is vascular constriction to reduce blood flow locally followed by platelet recruitment initiating repair mechanisms (Roth, 1992). The pivotal ligand in the initiating event in haemostatic plug formation is von Willebrand factor (vWF). vWF is a high-molecular weight multimeric glycoprotein present in the subendothelium and in plasma, where it is conformationally activated by shear forces linking platelets through the glycoprotein (GP) Ib component of the GPIb/IX/V receptor to the subendothelium (Savage *et al.*, 1996; Siedlecki *et al.*, 1996; Ruggeri, 1999). Adhering activated platelets express P-selectin and integrins on their surface to facilitate the further recruitment of circulating platelets, which are in turn activated and form a platelet aggregate (Ait-Oufella *et al.*, 2010). Aggregation requires fibrinogen, energy and calcium (Troy, 1988). By secreting the granular contents ADP and serotonin, and producing prostaglandins, platelets provide a catalytic surface for the assembly of coagulation complexes necessary for α-thrombin production and subsequent conversion of soluble fibrinogen into insoluble fibrin (Ait-Oufella *et al.*, 2010).

Thrombin is produced from factor Xa via the extrinsic coagulation pathway and is among the most potent stimulators of platelets through proteolytic cleavage and activation of platelet protease-activated receptors (PAR), especially PAR1 and PAR4 (Coughlin, 1999). Receptor activation leads to formation of fibrin and expression of pro-thrombotic factors including tissue factor (TF), plasminogen activator inhibitor-1 (PAI-1), PAF and ET-1 thereby amplifying the coagulation

cascade (Woolkalis *et al.*, 1995). Excessive thrombin generation is prevented by antithrombin and activation of the protein C pathway (Esmon, 1992; Arnout *et al.*, 2006). Activation of the fibrinolytic system results from conversion of the pro-enzyme plasminogen into the active serine proteinase plasmin, controlled by proteases secreted by EC including tissue plasminogen activator (tPA) and urokinase-type plasminogen activator (uPA). Plasmin digests fibrin components of a blood clot and releases degradation products into the circulation. Two inhibitors control the fibrinolytic system; the plasmin inhibitor α2 antiplasmin and plasminogen activator inhibitor (PAI) (Stassen *et al.*, 2004; Aid-Oufella *et al.*, 2010). Together, these physiological processes act to maintain normal functioning blood vessels and a non-thrombotic state.

Table 1. 1.: Regulation of haemostasis through secretion and expression of molecules with anti- and pro-thrombotic properties. (adapted from Ait-Oufella *et al.*, 2010).

Haemostasis		
Primary haemostasis	Activation	von Willebrand Factor (vWF)
	Inhibition	nitric oxide (NO)
Secondary haemostasis	Activation	tissue factor (TF)
	Inhibition	tissue factor pathway inhibitor
		endothelial protein C receptor
		thrombomodulin
		heparan/dermatan sulphate
Tertiary haemostasis	Activation	tissue plasminogen activator (tPA)
		urinary plasminogen activator (uPA)
	Inhibition	plasminogen activator inhibitor (PAI)

1.1.3. Intrinsic cytoprotective mechanisms of the endothelium

The endothelium is constantly exposed to a variety of factors capable of inducing an inflammatory response, including endotoxins, cytokines, complement components, activated leukocytes and oxidatively-modified lipoproteins. Thus, the endothelium has evolved various intrinsic

cytoprotective mechanisms to minimize inflammatory reactions and protect itself against injury (Bach *et al.*, 1997; Tedgui and Mallat, 2001). These mechanisms include the synthesis of anti-inflammatory cytokines, such as interleukin (IL)-10, IL-13, and IL-1RA, extracellular signalling molecules such as transforming growth factor-beta (TGFβ), and vascular endothelial growth factor (VEGF). Furthermore, activation of constitutive and inducible cytoprotective genes including endothelial eNOS, NO, PGI2, and the anti-oxidant enzyme heme oxygenase-1 (HO-1), complement regulatory proteins, as well as anti-inflammatory and anti-apoptotic genes including A1, A20, and Bcl-2. In addition, more recent studies suggest that endothelial cells at sites in the vasculature, exposed to pulsatile, unidirectional blood flow are more protected from inflammatory insults than those areas where a bidirectional, oscillatory blood flow occurs, at least in part through induction of the cytoprotective genes mentioned above (Chatzizisis *et al.*, 2007).

Interleukin-10

Interleukin (IL)-10 is an immunomodulatory cytokine produced by endothelial cells, smooth muscle cells, Th_2 lymphocytes, B-lymphocytes and monocytes/macrophages. The cytokine inhibits antigen driven proliferation and attenuates Th_1 cellular responses (Tedgui and Mallat, 2006).

IL-10 exerts its biological effects on cells via interaction with a specific cell-surface receptor belonging to the class II cytokine receptor family (Liu *et al.*, 1994). The functionally active receptor is composed of two distinct subunits; the IL-10 receptor α-chain mediates high-affinity ligand binding and signal transduction, while the β-chain serves as an accessory chain and is essential for the active receptor complex (Liu *et al.*, 1994; Spencer *et al.*, 1998). Anti-inflammatory actions of IL-10 are predominantly mediated through initiation of the Janus kinase/signal transducer and activators of transcription (JAK-STAT) pathway eventually affecting nuclear factor kappa B (NFκB) activation (Riley *et al.*, 1999). Other intracellular signalling pathways regulated by IL-10 include the mitogen-activated protein (MAP) kinases extracellular signal-regulated kinase (ERK) 1 and ERK2 (Suttles *et al.*, 1999).

Protective and anti-inflammatory properties of IL-10 are demonstrated by *in vitro* studies showing that IL-10 down-regulates ICAM-1 and VCAM-1 expression on IL-1-activated human umbilical vein endothelial cells (HUVEC), inhibits tumour necrosis factor (TNF)-induced or fibroblast growth factor (FGF)-2-induced human aortic SMC proliferation, and attenuates low density lipoprotein (LDL)-induced monocyte binding (Van der Meeren *et al.*, 1999; Selzman *et al.*, 1998; Pinderski Oslund *et al.*, 1999). The cytoprotective importance of IL-10 is further supported by *in vivo* studies; mice fed a high-fat diet demonstrate a significant reduction in NFκB activation and ICAM-1 and VCAM-1 expression in response to IL-10 overexpression, while IL-10 deficient mice show a marked increase in lipopolysaccharide (LPS)-mediated expression of ICAM-1 and VCAM-1 (Potteaux *et al.*, 2006, Morise *et al.*, 1999). These animals also demonstrate increased leukocyte infiltration into the vascular wall when fed an atherogenic diet (Mallat *et al.*, 1999). Additional mechanisms of vascular protection attributable to IL-10 include reduced superoxide anion production in blood vessels in response to LPS, protection against myocardial ischaemia-reperfusion injury, and attenuation of neo-initimal hyperplasmia in mice subjected to balloon angioplasty (Gunnett *et al.*, 2000; Hayward *et al.*, 1997; Feldman *et al.*, 2000).

Transforming growth factor-beta

Transforming growth factor-beta (TGF-β) is a potent anti-inflammatory and pro-fibrotic cytokine, playing important regulatory functions within the cardiovascular system, including proliferation, cellular differentiation and immunity. To date, three mammalian isoforms have been identified, i.e. TGF-β1, TGF-β2, and TGF-β3, which are ubiquitously found in vascular cells, including EC, arterial and venous SMC, macrophages, neutrophils and platelets (Lefer, 1991).

TGF-β superfamily members are secreted in an inactive complex with latent TGF-β binding protein (LTPB) and latency-associated peptide (LAP), proteins derived from the N-terminal region of the TGF-β gene. Extracellular activation of latent TGF-β is regulated by the plasminogen/plasmin system and is an essential step in the regulation of TGF-β function *in vivo* (Grainger *et al.*, 1994). Active TGF-β elicits its biological functions through the distinct cell-surface receptors TGF-β type 1 (TGF-βRI) and type II (TGF-βRII) receptor, upregulating the kinase activity of these receptors and their downstream effectors, the transcription factors Smad proteins

(Derynck and Zhang, 2003; Shi and Massagué, 2003). Smad-mediated signalling activates CREB, in turn blocking the association of CPB with p65/NFkB and inhibiting NFkB activity (Dabek *et al.*, 2006).

Numerous *in vitro* studies demonstrate the potent anti-inflammatory effects of TGF-β on vascular cells. TGF-β attenuates cytokine-induced expression of E-selectin on EC as well as VCAM-1 on EC and SMC, reduces MCP-1 expression in TNF-α or IL-1β-stimulated HUVEC, and inhibits IL-8-dependent transmigration of neutrophils through the TNF-α-activated endothelium (DiChiara *et al.*, 2000; Park *et al.*, 2000; Gamble *et al.*, 1995; Honda *et al.*, 1999; Smith *et al.*, 1996). In addition, TGF-β restores TNF-α-mediated endothelial vasodilation (Lefer *et al.*, 1990). The vasoprotective properties of TGF-β1 are confirmed by TGF-β1 deficient mice, which die *in utero* due to widespread uncontrolled inflammation most severely affecting the heart and lungs (Shull *et al.*, 1992). Moreover, TGF-β1 heterozygous mice (TGF-$\beta1^{+/-}$), when fed a cholate-enriched atherogenic diet, demonstrate increased endothelial activation with elevated levels of ICAM-1 and VCAM-1, and enhanced macrophage infiltration into the vascular wall compared to wild-type controls, further supporting the cytoprotective role of endogenous TGF-β1 in the vascular system (Grainger *et al.*, 2000).

Angiogenic mediators and growth factors

Vascular endothelial growth factor (VEGF), initially known as vascular permeability factor (VPF), was first discovered as a tumour-secreted factor that increases vascular permeability (Senger *et al.*, 1983). Subsequently, VEGF has been identified as an important regulator of angiogenesis and EC homeostasis, which stimulates receptor tyrosine kinases and acts as a potent mitogen for vascular endothelial cells (Greenaway *et al.*, 2004; Siemeister *et al.*, 1998). VEGF is a high affinity ligand for the tyrosine kinase receptors VEGF-R1/Flt-1 and VEGF-R2/KDR/Flk, and exerts its cellular effects through interactions with these receptors (De Vries *et al.*, 1992). Along with the proliferative effects on endothelial cells, VEGF has been recognised as a cytoprotective modulator, by protecting EC from apoptosis by increased induction of the anti-apoptotic genes A1 and Bcl-2 (Gerber *et al.*, 1998), enhanced induction of decay-accelerating factor (DAF), thereby protecting EC against complement-mediated injury (Mason *et al.*, 2001), upregulation of

endothelial NOS (Bussolati *et al.*, 2001), and stimulating synthesis of NO and PGI_2 (Kroll and Waltenberger, 1999; Laitinen *et al.*, 1997; Murohara *et al.*, 1998; He *et al.*, 1999), and induction of the cytoprotective enzyme heme oxygenase-1 (HO-1) (Bussolati *et al.*, 2004; Siner *et al.*, 2007).

Recent studies have shown that the angiogenic mediator angiopoietin-1 (Ang-1) also exhibit potent protective effects in the adult vasculature including promotion of vessel survival, inhibition of vascular leakage, and suppression of inflammatory gene expression (Brindle *et al.*, 2006). In fact, Ang-1 treated EC demonstrate increased PECAM-1 localisation to EC junctions thereby inhibiting TNF-α-induced leukocyte transmigration (Gamble *et al.*, 2000). In addition, Ang-1 abrogates leukocyte adhesion by suppressing VEGF-induced expression of adhesive and inflammatory molecules, including E-selectin, ICAM-1 and VCAM-1, and blocks TNF-α- and VEGF-mediated tissue factor (TF) expression on cultured EC (Kim *et al.*, 2001a; Gamble *et al.*, 2000; Kim *et al.*, 2002). Moreover, Ang-1 has been shown to protect against endothelial apoptosis in response to a variety of stimuli, including serum-deprivation, oxidised LDL, and TNF-α (Kwak *et al.*, 1999; Papapetropoulos *et al.*, 1999; Kim *et al.*, 2001b). Anti-inflammatory and anti-apoptotic properties of Ang-1 are mediated through binding to its endothelium specific tyrosine kinase receptor Tie-2 and activation of the PI3K/Akt signalling pathway (Kim *et al.*, 2000; Papapetropoulos *et al.*, 2000; Gamble *et al.*, 2000).

Nitric oxide

Besides its well-described role as a vasodilatory molecule, endothelial-derived nitric oxide (NO) has been recognised to exhibit potent anti-inflammatory properties, which are mainly mediated via inhibition of NFκB activation through enhanced induction and nuclear translocation of inhibitor of kappa B alpha (IκBα) (De Caterina *et al.*, 1995; Spiecker *et al.*, 1997). For instance, endogenous NO synthesis attenuates cytokine-induced endothelial activation, decreases the expression of the adhesion molecules ICAM-1 and VCAM-1, and inhibits leukocyte trafficking (Kubes *et al.*, 1991; De Caterina *et al.*, 1995). In contrast, inhibition of NO results in increased expression of MCP-1 in cultured human EC (Zeiher *et al.*, 1995). The vascular protective effects of NO are confirmed by *in vivo* studies utilising the NO synthesis inhibitor N^{ω}-nitro-L-arginine methyl ester (L-NAME) and eNOS-deficient mice. Chronic *in vivo* blockade of NO synthesis results in increased leukocyte

infiltration with increased expression of ICAM-1 and VCAM-1, enhanced expression of the pro-inflammatory mediators MCP-1, IL-6, macrophage colony-stimulating factor (M-CSF), and NFκB activation (Luvara *et al.*, 1998; Kitamoto *et al.*, 2000; Koyanagi *et al.*, 2000; Gonzalez *et al.*, 2000). In line with these findings, eNOS-deficient mice display enhanced leukocyte adhesion and increased atherosclerotic lesion size (Knowles *et al.*, 2000; Kuhlencordt *et al.*, 2001). Moreover, NO synthesis inhibition is associated with increased oxidative stress and ROS production, an effect abrogated by the anti-oxidant N-acetyl cysteine (NAC) and blockage of angiotensin II type 1 receptor (Luvara *et al.*, 1998; Gonzalez *et al.*, 2000; Usui *et al.*, 2000).

Anti-apoptotic proteins

In addition to protecting EC from apoptosis, several anti-apoptotic proteins including members of the Bcl-2 gene family (Bcl-2, Bcl-XL, and A1), A20 and heme oxygenases (HO) have been shown to possess potent anti-inflammatory properties. A1 and A20 are induced in response to inflammatory stimuli and protect EC from uncontrolled activation and cell death through an NFkB-dependent mechanism (Cooper *et al.*, 1996). Overexpression of Bcl-2, Bcl-XL, A1, or A20 inhibits VCAM-1, E-selectin, and IL-8 expression in EC by inhibiting NFκB activation (Ferran *et al.*, 1998; Stroka *et al.*, 1999). *In vivo* experiments underscore the importance of these protective genes; A20-deficient mice fail to regulate TNF-α-dependent NFκB activation and inflammation, develop severe inflammation and cachexia, are hypersensitive to LPS and TNF, and die prematurely (Lee *et al.*, 2000). Double-mutated mice, deficient in apolipoprotein E (ApoE) and haplo-insufficient for A20, demonstrate an increase in atherosclerotic aortic root lesion area correlating with increased expression of the NFκB target genes ICAM-1, VCAM-1, and M-CSF, while overexpression of A20 results in reduced lesion area (Wolfrum *et al.*, 2007). Furthermore, specific human A20 polymorphisms resulting in decreased A20 expression confer increased cardiovascular risk in diabetic patients through modulation of NFκB activation (Boonyasrisawat *et al.*, 2007).

Vasoprotective effects of laminar shear stress

The endothelium has not only evolved intrinsic cytoprotective mechanisms capable of responding to hormonal stimuli in the circulation, but may also respond to biochemical forces created by blood flow and the cardiac cycle (Davies, 1995). As a result of their unique anatomical location, EC are constantly exposed to a variety of mechanical forces. These local haemodynamic forces include pressure, created by the hydrostatic forces of blood within the blood vessel; blood pressure-derived tensile stress, created as a result of defined intracellular connections between EC that exert longitudinal forces on the cell during vasomotion; and flow-generated shear stress, which is the frictional force of the flowing blood on the endothelial surface (Davies, 1995). Shear-induced mechanotransduction transforms mechanical forces to biochemical responses, inducing endothelial structural changes, and activating signal transduction and endothelium-dependent gene and protein expression that determines endothelial cell phenotype (Davies, 1995; Pan, 2009). For instance, numerous mechanoreceptors expressed on the luminal surface of EC, including ion channels, G-proteins, VEGF-R2, VE-cadherin, PECAM-1, proteoglycans, caveolae, tyrosine kinase receptors and NADPH oxidase, have been shown to play important roles in the shear stress sensing mechanisms (Traub and Berk, 1998; Li *et al.*, 2005; Lehoux *et al.*, 2006; Chatzizsis *et al.*, 2007; Ando and Yamamoto, 2011). Receptor engagement in turn leads to the simultaneous activation of several intracellular signalling pathways, including mitogen-activated protein kinases (MAPK), protein kinase C (PKC), Rho family small GTPases, the PI3K/Akt cascade (Traub and Berk, 1998; Li *et al.*, 2005; Lehoux *et al.*, 2006; Chatzizsis *et al.*, 2007; Ando and Yamamoto, 2011), and downstream transcription factors such as Krüppel-like factor 2 (KLF-2) and nuclear factor erythroid 2-related factor-2 (Nrf-2; Dekker *et al.*, 2002; Wang *et al.*, 2006; Chen *et al.*, 2003). These transcription factors recognise specific shear stress response elements (SSRE) within the promoter of mechanosensitve genes thereby regulating their expression (Chatzizisis *et al.*, 2007).

In the arterial circulation, localised haemodynamic shear stress determines site-specific susceptibility to atherosclerosis and its progression (Fig. 1.4.; Caro *et al.*, 1969; Pan, 2009). Regions within the vasculature that are exposed to disturbed, bidirectional flow with low and oscillatory shear forces (0 to 10 dynes/cm^2) such as those in the vicinity of branch points, the

outer wall of bifurcations, and the inner wall of curvatures, are associated with an enhanced risk of endothelial dysfunction and cardiovascular diseases such as atherosclerosis and subsequent occlusive thrombosis triggering acute myocardial infarction or stroke (Cheng *et al.*, 2005; Cheng *et al.*, 2006; Suo *et al.*, 2008; VanderLaan *et al.*, 2004; Chatzizisis *et al.*, 2007; Malek *et al.*, 1999a). In contrast, at straight parts of the arterial tree, where streamlined unidirectional blood flow occurs with high laminar shear stress (10 to 70 dynes/cm^2), the endothelium adopts an anti-inflammatory and anti-coagulant surface with reduced EC turnover characterised by both decreased proliferation and apoptosis (Davies *et al.*, 1986; Kaiser *et al.*, 1997; Davies, 2000). In addition, atherosclerotic lesion size is reduced in these areas (Cheng *et al.*, 2006). Molecular mechanisms underpinning the anti-inflammatory actions of shear stress include protection against oxidative stress and inhibition of NFκB and jun-N-terminal kinase (JNK)-AP-1 pathways and their downstream targets. *In vitro* experiments demonstrate that the prolonged exposure of EC to laminar flow diminishes ICAM-1 and VCAM-1 surface expression in the unstimulated but also activated endothelium (Sampath *et al.*, 1995; Chappell *et al.*, 1998), whereas prolonged low and oscillatory shear stress enhances E-selectin, VCAM-1 expression and monocyte adhesion (Mohan *et al.*, 1999; Chappell *et al.*, 1998). The cytoprotective effects of shear stress are further demonstrated by increased secretion of the vasodilators PGI_2 and eNOS and subsequent increased bioavailability of NO (Hanada *et al.*, 2000; Topper *et al.*, 1996; Malek *et al.*, 1999b; Mashour and Boock, 1999). In addition, expression of vasoconstrictors including ET-1 (Malek and Izumo, 1992), are supressed, thereby contributing to a quiescent atheroprotective phenotype. Gene expression profiling further revealed that cultured vascular EC respond to fluid mechanical forces by modulating the messenger ribonucleic acid (mRNA) level of a large number of genes. Sustained exposure of EC to high shear laminar flow up-regulates the expression of atheroprotective, anti-oxidant transcription factors including KLF-2 and Nrf-2 and their downstream target genes such as the cytoprotective enzyme HO-1 (De Keulenaer *et al.*, 1998), manganese superoxide dismutase (MnSOD; Topper *et al.*, 1996), and cupper/zinc superoxide dismutase (Cu/ZnSOD; Inoue *et al.*, 1996), thereby reducing the production of reactive oxygen species (ROS). In contrast, disturbed flow, with associated reciprocating low shear stress, generally induces genes that promote atherogenesis (Mohan *et al.*, 1999; De Keulenaer *et al.*, 1998). The protective effects of high shear stress are further supported by *in vivo* studies

demonstrating constitutive NFκB activation and VCAM-1 expression in EC located in regions highly susceptible to atherosclerotic lesion formation, where low or oscillatory shear forces occur (Hajra *et al.*, 2000; Potteaux *et al.*, 2006).

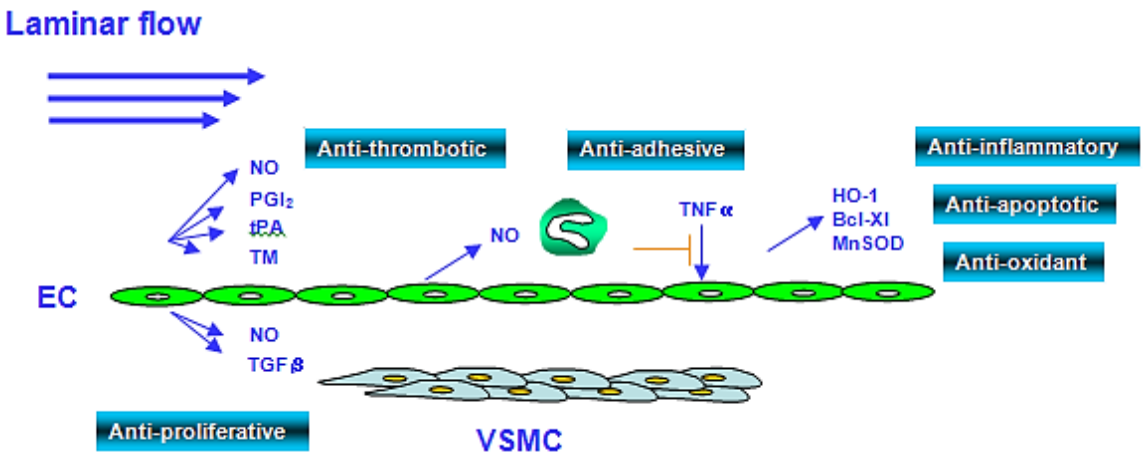

Figure 1. 4.: Cytoprotective mechanisms of laminar shear stress in the vasculature. Laminar shear stress promotes an anti-thrombotic and anti-inflammatory endothelial phenotype. It inhibits leukocyte migration and smooth muscle proliferation, while simultaneously promoting endothelial survival (printed with permission from Prof Justin C. Mason).

1.1.4. Vascular injury and its role in disease

The normal healthy endothelium serves as an autocrine and paracrine organ that controls vessel wall integrity and function by maintaining an anti-thrombotic, anti-inflammatory, and vasoregulatory phenotype. Moreover, the endothelium acts as an important regulator of vessel wall inflammation, thrombosis, and normal host defence mechanisms by adopting an 'activated' phenotype, expressing pro-inflammatory chemokines, cytokines, and surface adhesion molecules that leukocytes to the site of inflammation, to clear microorganisms and initiate wound healing and repair. However, an imbalance in these highly regulated processes may lead to a dysfunctional endothelium and subsequent perpetuation of inflammatory diseases (Cines *et al.*, 1998).

Its anatomical location constantly exposes the endothelium to potentially harmful stimuli including oxidised lipoproteins, C-reactive protein, pro-inflammatory cytokines, bacterial endotoxins such as LPS, anti-phospholipid antibodies, complement activation products, proteolytic enzymes, and haemodynamic forces. These factors may injure and activate the endothelium, promoting a shift from the constitutive, anti-inflammatory, anti-coagulant, and anti-proliferative phenotype to an

'activated' phenotype, which facilitates inflammation, thrombosis and mitogenesis (Tesfamariam and DeFelice, 2007). If persistent, the pro-inflammatory and pro-coagulant state of the activated endothelium may eventually lead to endothelial dysfunction. Endothelial dysfunction is a systemic pathological condition characterised by a shift of the endothelium towards impaired vasodilation, and a pro-inflammatory and pro-thrombotic milieu (Fig. 1.5.). Endothelial dysfunction is primarily the consequence of a reduction in NO bioavailability caused by impaired NO production by the endothelium and/or increased inactivation of NO by ROS (Kaneto *et al.*, 2010; Witting *et al.*, 2007). Endothelial dysfunction is one of the earliest events in the initiation and progression of atherosclerosis (Vanhoutte, 1997) and has been detected in patients suffering from hypercholesterolemia, hypertension, coronary and peripheral artery disease, chronic heart failure, as well as autoimmune diseases such as systemic lupus erythematosus (SLE), rheumatoid arthritis (RA), and diabetes mellitus (Ross, 1999; Schachinger *et al.*, 2000; Heitzer *et al.*, 2001; Bijl, 2003; Endemann and Schiffrin 2004; Higashi *et al.*, 2009).

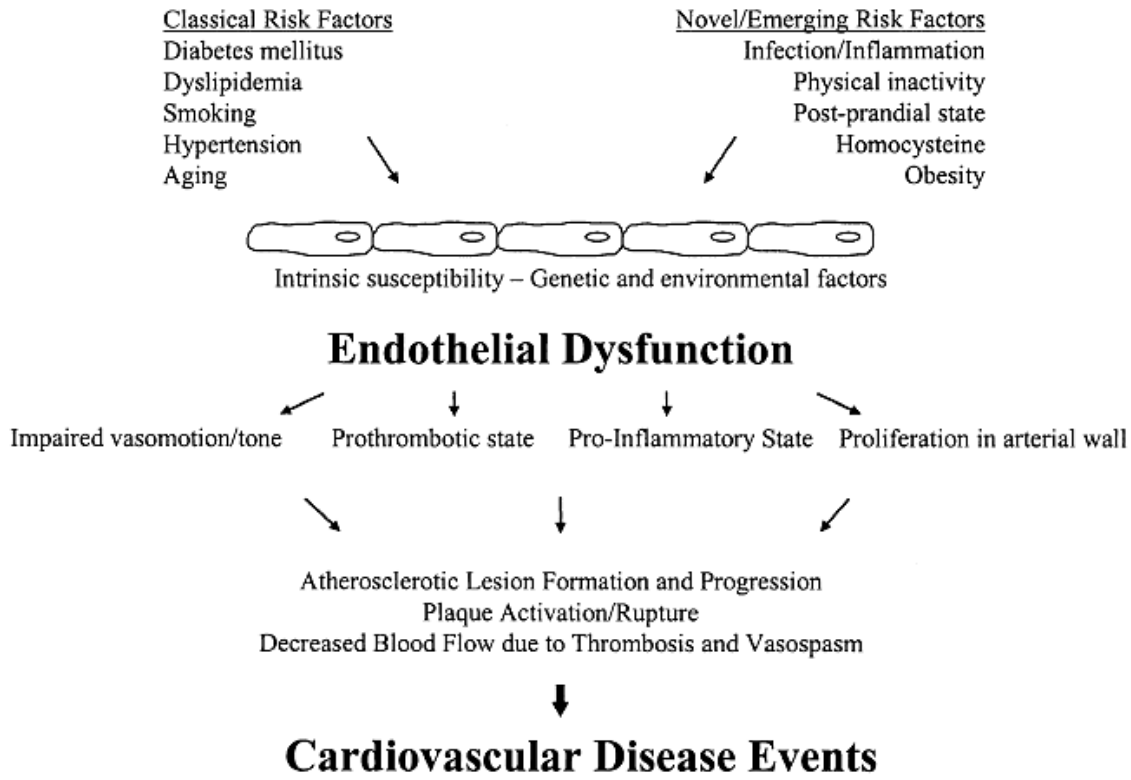

Figure 1. 5.: Endothelial dysfunction in the pathogenesis of cardiovascular diseases. The endothelium is constantly exposed to numerous cardiovascular risk factors that facilitate endothelial activation and may lead to endothelial dysfunction, the earliest step in the pathogenesis of atherosclerosis and other cardiovascular diseases (adapted from Widlansky *et al.*, 2003).

Atherosclerosis is the most prevalent disease in developed countries (Cines *et al.*, 1998). It is a multifactorial, progressive disease of large and medium-sized muscular arteries characterised by endothelial dysfunction, vascular inflammation and the accumulation of lipids, fibrous materials, calcium and cellular debris within in intima of the vessel wall. Atherosclerosis results from excessive inflammatory and fibroproliferative responses to vascular insults such as dyslipidaemia, free radicals resulting from cigarette smoke, hypertension, and diabetes mellitus, and/or genetic predisposition which culminates in the formation of oxidatively-modified LDL contributing to EC injury and activation (Ross, 1999). EC activation subsequently up-regulates the expression of leukocyte adhesion molecules such as VCAM-1 and platelet receptors, as well as pro-inflammatory chemokines (e.g. MCP-1) and cytokines such as IL-1 which facilitate the infiltration of platelets, monocytes/macrophages and T-lymphocytes into the subendothelial intima. Uptake of oxidised LDL by activated initimal macrophages, through scavenger receptors, then results in the formation of foam cells and fatty streaks and secondary secretion of free radicals, proteases and pro-inflammatory cytokines, including TNF-α and IL-1, that further contribute to vascular injury. Next, progressive lipid accumulation, extracellular matrix deposition, and SMC proliferation and migration contribute to the formation of a fibrous cap, resulting in vascular remodelling, luminal narrowing, alterations in blood flow patterns, and diminished oxygen supply to target organs.

Pathological neovascularisation has been described in the evolving plaque. Vessels of the neovascular vasa vasorum are leaky and associated with intraplaque haemorrhage and the subsequent rupture of the protective fibrous cap. In addition, elaboration of interferon gamma (INF-γ) by Th_1 cells, the predominant lymphocytes within the evolving plaque, and synthesis and release of matrix metalloproteinases (MMP) by activated macrophages result in inhibition of SMC proliferation and collagen degradation contributing to thinning and rupture of the vulnerable plaque. Plaque rapture exposes thrombogenic contents, e.g. lipid-laden foam cells, extracellular lipid and necrotic cell debris, to the circulating blood further facilitating progression of the atherosclerotic lesion (Kolodgie *et al.*, 2003; Milei *et al.*, 1998) and predisposes to thrombus formation, partial or complete obstruction of the blood vessel, and myocardial infarction (Ross, 1999; Cines *et al.*, 1998; Galley and Webster, 2004; Hansson, 2005; Rocha and Libby, 2009).

Diabetes mellitus is a major accelerator of cardiovascular disease and is associated with an increased risk of atherosclerosis. Fundamental pathogenic mechanisms in diabetes-associated vascular disease include endothelial dysfunction, vascular inflammation, and increased oxidative stress (Onat *et al.*, 2011). Hyperglycaemia alters endothelial function and contributes to vascular injury through the extensive formation of advanced glycation end products (AGEs) (Barlovic *et al.*, 2011). AGEs represent a heterogeneous group of proteins, lipids and nucleic acids, irreversibly cross-linked with reducing sugars (Barlovic *et al.*, 2011). AGEs are implicated in the pathogenesis of atherosclerosis, either directly or via receptor-mediated mechanisms. Ligand-dependent activation of receptor for AGE (RAGE) leads to increased ROS formation, and triggers activation of NFκB and other pro-inflammatory signalling pathways leading to increased synthesis of growth factors and pro-inflammatory cytokines, thereby promoting vascular dysfunction (Barlovic *et al.*, 2011).

Autoimmune diseases, including rheumatoid arthritis (RA) and systemic lupus erythematosus (SLE), have also been associated with accelerated atherosclerosis, which is preceded by endothelial dysfunction (López-Pedrera *et al.*, 2012). RA is a chronic systemic inflammatory disease predominately affecting the synovial joints and eventually leading to physical disability and linked to higher morbidity and mortality rates. Mortality risk factors include amyloidosis, infections, and underlying cardiovascular diseases (CVD), with coronary atherosclerosis representing the main cause of cardiovascular-related deaths in RA patients (Maradit-Kremers *et al.*, 2005; Szekanecz *et al.*, 2007). Among the traditional CVD risks factors, such as smoking, hypercholesterolemia, and dyslipidaemia, inflammatory and atherogenic mediators have been identified as distinct CV risks factors in RA and include acute phase proteins, autoantibodies, autoreactive lymphocytes and pro-atherogenic cytokines (Szekanecz *et al.*, 2007; López-Pedrera *et al.*, 2012). Cardiovascular events and underlying endothelial dysfunction are a leading cause of death in SLE patients. The increased frequency of atherosclerosis and thromboembolic events in patients with SLE is likely due to a combination of traditional CVD risk factors, and disease-related factors including vasculititis and steroid therapy, as well as systemic inflammatory responses that contribute to accelerated atherosclerosis in SLE including complement activation, antibodies against heat-shock proteins (HSP) and an abnormal lipid profile (Agarwal *et al.*, 2009; Sherer *et al.*, 2010).

1.2. ANGIOGENESIS IN HEALTH AND DISEASE

The vascular system ensures the efficient and simultaneous transport of gases, liquids, nutrients, signalling molecules and circulating cells between organs and tissues, a requirement for the functioning of the complex body of vertebrates. Blood vessels are responsible for systemic circulation, proceeding from the heart through the aorta, arteries, into smaller arterioles and finally into capillary beds. Capillaries form extensive networks that facilitate the exchange of gases and metabolic products before blood is returned through venules and veins to the heart and then into the lungs to be replenished by oxygen (Adams and Alitalo, 2007).

In the healthy organism the vascular system is essential for homeostasis and hence vascular malformations or dysfunction contribute to the pathogenesis of numerous diseases (Carmeliet, 2005; Adams and Alitalo, 2007). Insufficient blood supply causes tissue ischaemia, whereas in cancer stimulation of angiogenesis allows tumours access to nutrients and oxygen, stimulating their growth and metastasis. Therefore the ability to control the growth of blood vessels has considerable therapeutic potential.

1.2.1. The angiogenic process

Angiogenesis is a highly complex, multistep process, requiring the tight coordination of cell proliferation, differentiation, migration, matrix adhesion and cell-cell signalling. The destabilisation phase entails the enzymatic breakdown of the basement membrane and the loosening of junctional connections with surrounding cells. During the proliferation and migration phase, activated EC migrate towards an angiogenic stimulus, invading and proliferating into the underlying extracellular matrix. Eventually during the maturation phase, EC align to form a luminal vessel, a new basement membrane is secreted, intracellular adhesions and EC-basement membrane connections mature and pericytes are recruited to the new vessel wall (Patan, 2000; Bouïs *et al.*, 2006; Sun and Schiller, 2007). The formation of new blood vessels is strictly regulated and depends on the concerted activities of various growth factors and their receptors expressed on the surface of endothelial and accessory cells, including macrophages, mast cells, and stromal components. The delicate balance between the release of pro- and anti-angiogenic factors from these cells is essential for the regulation of angiogenesis (Tab. 1.2.).

Table 1. 2.: Endogenous pro- and anti-angiogenic factors. (adapted from Sun and Schiller, 2007).

Pro-angiogenic factors	Anti-angiogenic factors
VEGF	angiostatin
epidermal growth factor (EGF)	endostatin
platelet-derived growth factor (PDGF)	canstatin
fibroblast growth factor (FGF)	tumstatin
stromal cell-derived growth factor 1 alpha (SDF-1α)	interferon α and β
transforming growth factor beta(TGF-β)	tissue inhibitors of metalloproteinases
tumour necrosis factor alpha (TNF-α)	thrombospondin
hepatocyte growth factor (HFG)	pigment epithelium-derived factor
granulocyte colony-stimulating factor	vascular endothelial growth inhibitor
interleukin-1, -6, -8 (IL-1, IL-6, IL-8)	vasoinhibin
matrix metalloproteinases	
angiogenin	
proliferin	
pleiotropin	
ephrin	

Selection of sprouting EC

The recent recognition that specialised EC contribute to the formation of vessel branches has been an exciting breakthrough (Tab. 1.3.). During angiogenic growth, some EC within the capillary vessel wall are selected for sprouting. These cells which are known as tip cells lead the growing sprout. Tip cells extend long and motile filopodia, thin (0.1-0.3 µm), finger-like structures filled with tight parallel bundles of filamentous (F)-actin, towards the source of pro-angiogenic growth factors to enable directional and prevent disorganised vessel growth (Gerhardt *et al.*, 2003; Matilla and Lappalainen, 2008). “Stalk” cells trail behind, elongating the stalk of the sprout and forming a lumenised tube. So called “phalanx” cells, which resemble the “phalanx formation”

of ancient Greek soldiers, are the most quiescent EC, and line vessels once the new vessel branches have been consolidated (Carmeliet *et at.*, 2009; De Smet *et al.*, 2009).

Table 1. 3.: Molecular signature and properties of specialised EC involved in angiogenesis. (modified after Carmeliet *et al.*, 2009; De Smet *et al.*, 2009)

Cell type	Molecular signature	Function
Tip cell	- VEGF-R2 - VEGF-R3-1 - PDGF-BB - Unc5B - Neuropilin-1 (NRP1) ↑ Delta-like ligand-4 (Dll4) ↓ Notch	• located at the forefront of vessel branches • highly polarised nature • numerous filopodia probing the environment while migrating toward an angiogenic stimulus • do not form a lumen • proliferate minimally • detect gradients of navigator cues and integrate combinatorial molecular codes into directional migration
Stalk cell	↑ Notch ↑ Jagged1 ↓ Dll4 ↓ VEGF-R2 ↓ VEGF-R3 ↓ NRP1 ↓ CXC-R4 - Notch-related ankyrin-repeat protein (Nrarp)	• trail behind the tip cell • elongate the stalk of the sprout • do not extend filopodia • they proliferate • form junctions • lay down extracellular matrix • form a lumen
Phalanx cell		• most quiescent EC • line vessels once the vessel branches have been consolidated • form a smooth cobblestone monolayer • are covered by pericytes • stick to each other via adherens junctions • are embedded in a thick basement membrane

The fate and differentiation of EC into specialised cells involved in angiogenesis is strongly controlled by the Notch pathway. The family of Notch receptors comprises four members, Notch-1, -2, -3, and -4, which are recognised and their activation controlled by their transmembrane

ligands Delta-like ligand 1 (Dll1), Dll3, and Dll4 and Jagged1 and Jagged2 (Rocha and Adams, 2007; Carmeliet *et al.*, 2009). Activation of Notch results in a proteolytic generation of the Notch intracellular domain (NICD), which induces transcription of target genes (Roca and Adams, 2007; Carmeliet *et al.*, 2009).

Tip cells contain relatively high levels of Dll4, whereas stalk cells preferentially express a different Notch ligand, Jagged1. In quiescent EC, Dll4 and Notch signalling are thought to be balanced but upon exposure to pro-angiogenic stimuli, such as VEGF, Dll4 expression is upregulated in tip cells inducing the expression of Notch in adjacent stalk cells (Hofmann and Iruela-Arispe, 2007; Hellström *et al.*, 2007). VEGF-R2 signalling in the tip cell allows cells to extend filopodia and move ahead, while Dll4/Notch signalling leads to downregulation of VEGF-R2 and VEGF-R3 in stalk cells, thereby dampening the VEGF-induced migratory response in these cells (Tammela *et al.*, 2008; Hellström *et al.*, 2007; Suchting *et al.*, 2007). The ligand Jagged1 is a pro-angiogenic regulator that antagonises Dll4/Notch signalling suppressing the motile, invasive and sprouting phenotype of tip cells and thereby positively controls the number of sprouts and tips (Benedito *et al.*, 2009).

Endothelial proliferation and cell cycle regulation

The endothelial sprout extends via proliferation of endothelial stalk cells. The rate of proliferation depends on three different aspects. Firstly, the rate of cell division representing the time it takes to complete a cell division cycle, secondly the fraction of cells within the population undergoing cell division, and thirdly the rate of cell loss from the population due to terminal differentiation or cell death. The mammalian cell cycle can be divided into two functional phases, the DNA synthesising (S)-phase and the mitosis (M)-phase, and two preparatory gap (G)-phases, G_1 and G_2. Non-dividing cells persist in a resting state, called the G_0-phase (Lukas *et al.*, 2004; Satyanarayana and Kaldis, 2009).

The proliferative state of mammalian cells is determined by the availability of growth factors and mitogens such as VEGF in their immediate environment. The presence of extrinsic growth factors triggers numerous cytoplasmic signalling cascades, including the ERK 1/2 MAPK pathway (see section 1.2.3.), which eventually result in the sequential activation of distinct cyclin-dependent

kinase (Cdk) activities. Cdks are serine/threonine kinases that drive the ordered transition through the phases of the cell cycle. Kinase activity of all Cdks requires the binding of a positive regulatory subunit known as a cyclin (Morgan, 1997; Solomon *et al.*, 1990). Each of the phases of the cell cycle is characterised by the expression of a distinct type of cyclin (Fig 1.6.), and binding of cyclins to Cdks results in the partial activation of the Cdk enzyme. Full activation of the cyclin/Cdk complex requires further phosphorylation of the Cdk by a separate kinase, the Cdk activation kinase. Active cyclin/Cdk complexes then initiate phosphorylation of downstream targets, thereby inducing specific cell cycle events (Obaya and Sedivy, 2002; Satyanarayana and Kaldis, 2009).

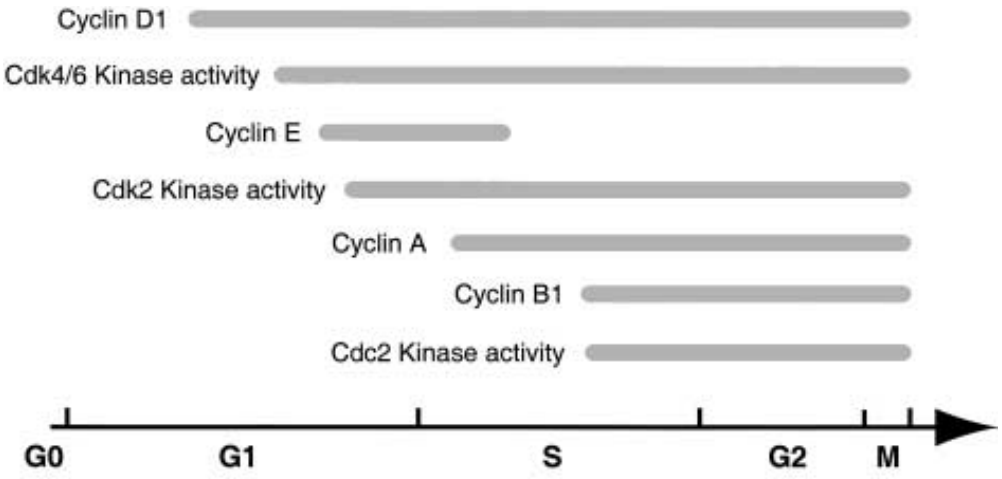

Figure 1. 6.: Cell cycle phase-specific expression patters of cyclins and Cdk activities. (adapted from Obaya and Sedivy, 2002).

In mammalian cells approximately 20 Cdk-related proteins have been identified and can be grouped in specialised G_1, G_1/S, S and G_2/M phase specific Cdks and cyclins (Obaya and Sedivy, 2002). Among the most studied cyclins are type D-cyclins that assemble with Cdk4 and Cdk6 driving progression through the G_1-phase (Inaba *et al.*, 1992). In early G_1-phase, active cyclin D/Cdk4/6 complexes initiate phosphorylation of retinoblastoma protein (pRb), which in turn leads to the release of the cell cycle transcription factor E2F. Release of E2F from pRb results in its activation and the transcription of target genes required for cell cycle progression (Weinberg, 1995; Dyson, 1998; Sherr and Roberts, 1999). Early E2F responsive genes include E- and A-type cyclins (Lundberg and Weinberg, 1998; Sherr and Roberts, 1999). Cyclin E forms a complex with Cdk2 in late G_1-phase. This leads to Cdk2 activation and further phosphorylation of pRb by the

active cyclin E/Cdk2 complex. Hyperphosphorylation of pRb in turn results in further E2F-mediated transcription and passage through the restriction point at the boundary of the G_1/S-phase, and to S-phase initiation (Fig.1.7.) (Dulic *et al.*, 1992; Koff *et al.*, 1992). In S-phase, Cdk2 is bound and activated by A-type cyclins and. cyclin A/Cdk2 activity is required for S-phase transition and control of DNA replication (Elledge *et al.*, 1992; Cardoso *et al.*, 1993). Later in G_2-phase, cyclin A also binds to and activates Cdk1 (Cdc2) and regulating G_2/M-phase transition and initation of prophase (Furuno *et al.*, 1999). Finally, cyclin B is expressed in late S-phase and G_2-phase and assembles with Cdk1 participating in the entry and completion of mitosis (Pines and Hunter, 1989; Nurse, 1990; Maller, 1991).

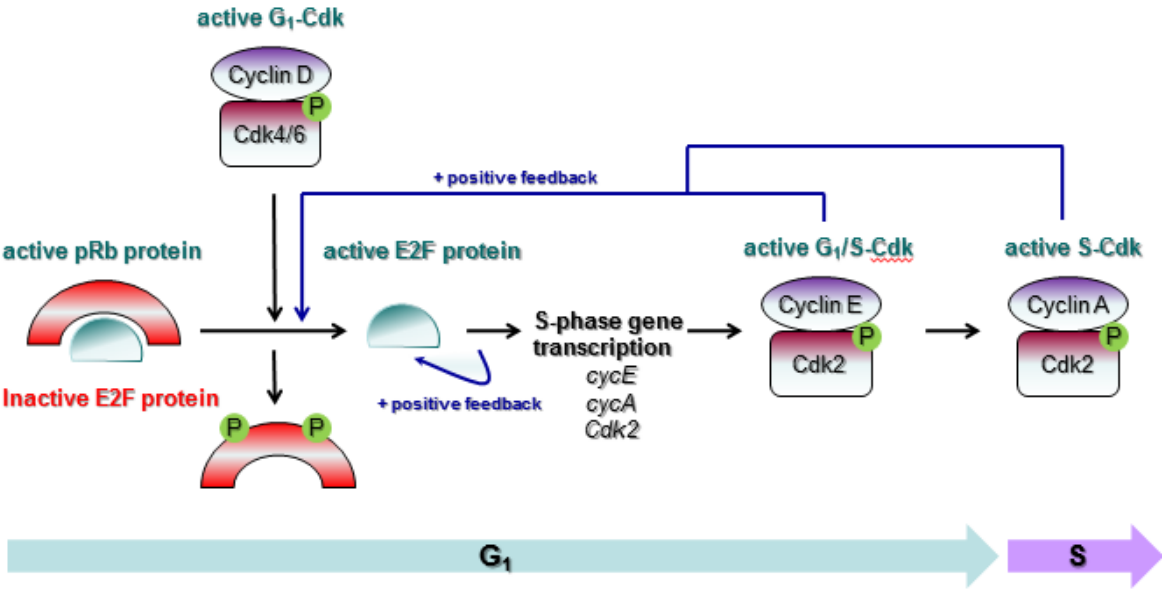

Figure 1. 7.: S-phase initiation. In its active form, retinoblastoma protein (pRb) persists in a hypophosphorylated state in G_1-phase and binds the cell cycle transcription factor E2F, thereby rendering it inactive. Upon phosphorylation of pRb by active cyclin D/Cdk4/6 complexes, E2F is released and activated, which in turn results in transcription of cell cycle regulatory genes including cyclin E (cycE) and cyclin A (cycA). Cyclin E complex with and activates Cdk2 resulting in further phosphorylation of pRb, E2F-mediated transcription, and progression to the S-phase. Active cyclin A/Cdk2 complexes mediate the transition through the S-phase.

The cell cycle is negatively regulated by cyclin-dependent kinase inhibitor (CKI) proteins. Seven CKIs have been described in mammalian cells and can be divided into two families. Family members of the inhibitor of Cdk4 (INK4) family include $p16^{INK4a}$, $p15^{INK4b}$, $p18^{INK4c}$, and $p19^{INK4d}$, and bind exclusively to and inhibit the D-type cyclin-dependent kinases Cdk4 and Cdk6. The three

members of the CIP/KIP CKI family $p21^{CIP1/WAF1}$, $p27^{KIP1}$ and $p57^{KIP2}$ are able to inhibit kinase activity of all Cdks. Binding of CKIs to active cyclin/Cdk complexes causes a conformational change in the active site of Cdks thereby decreasing their activity (Sherr and Roberts, 1995; Roussel, 1999; Obaya and Sedivy, 2002).

Endothelial cell migration

Endothelial migration is essential to angiogenesis. To migrate, cells must have an asymmetric morphology with defined leading and trailing edges. Cell motility is a multistep process and requires the activation of polarised intracellular signalling pathways that initiate cytoskeletal remodelling and protrusion formation at the leading edge, regulate integrin-mediated adhesion to the underlying substrate, as well as contraction and detachment at distinct regions of the cell (Fig. 1.8.) (Lauffenburger and Horitz, 1996; Ridley *et al.*, 2003).

Actin is a major cytoskeletal component of endothelial cells and cell migration is dependent on different actin filament structures. Monomeric globular actin subunits (G-actin) polymerise into elongated helical filaments (F-actin) at the barbed/positive end (oriented towards the plasma membrane) of the actin string, a process mediated by the actin regulatory proteins profilin, Ena/VASP and formin family members (Pollard and Borisy, 2003; Matilla and Lappalainen, 2008). Elongation of actin filaments is required for the formation of cell protrusions and pushes the leading edge forward and thus promotes cell migration (Pollard and Borisy, 2003; Chhabra and Higgs, 2007). The protrusive structures at the leading edge of a cell are called lamellipodia and filopodia. Lamellipodia are thin, sheet-like cytoplasmic protrusions composed of branched actin-networks, Lamellipodia formation is regulated by the small GTPase Rac1, as well as the actin-related protein complex-2/3 (Arp2/3) and members of the Wiscott-Aldrich Syndrome protein (WASP) family, which regulate F-actin filament branching (Ridley, 2001; Lamalice *et al.*, 2007; Matilla and Lappalainen, 2008). Filopodia are thin, finger-like membrane projections filled with tight bundles of F-actin. Formation of these structures is mainly regulated by the small GTPase Cdc42 that associates with WASP members (Ridley, 2001; Lamalice *et al.*, 2007; Matilla and Lappalainen, 2008). Filopodia act as sensors of pro-migratory stimuli, they contain integrins and cadherins in their tips or along their shafts, probing the matrix for migratory cues and promoting

cell adhesion and migration (Galbraith *et al.*, 2007). Stress fibres are contractile structures, which are also present in non-muscle cells and are composed of actin and myosin filaments grouped into bundles by myosin II. Stress fibres provide contractile forces for cell migration (Hotulainen and Lappalainen, 2006; Pellegrin and Mellor, 2007; Matilla and Lappalainen, 2008). Retraction of the cell at the trailing end is mediated by cofilin. Cofilin depolymerises and shortens the actin string at the pointed/negative end (pointing towards the inside of the cell), resulting in the release of the rear of the cell from the substrate and the promotion of forward movement (Pollard and Borisy, 2003; Huber *et al.*, 2003).

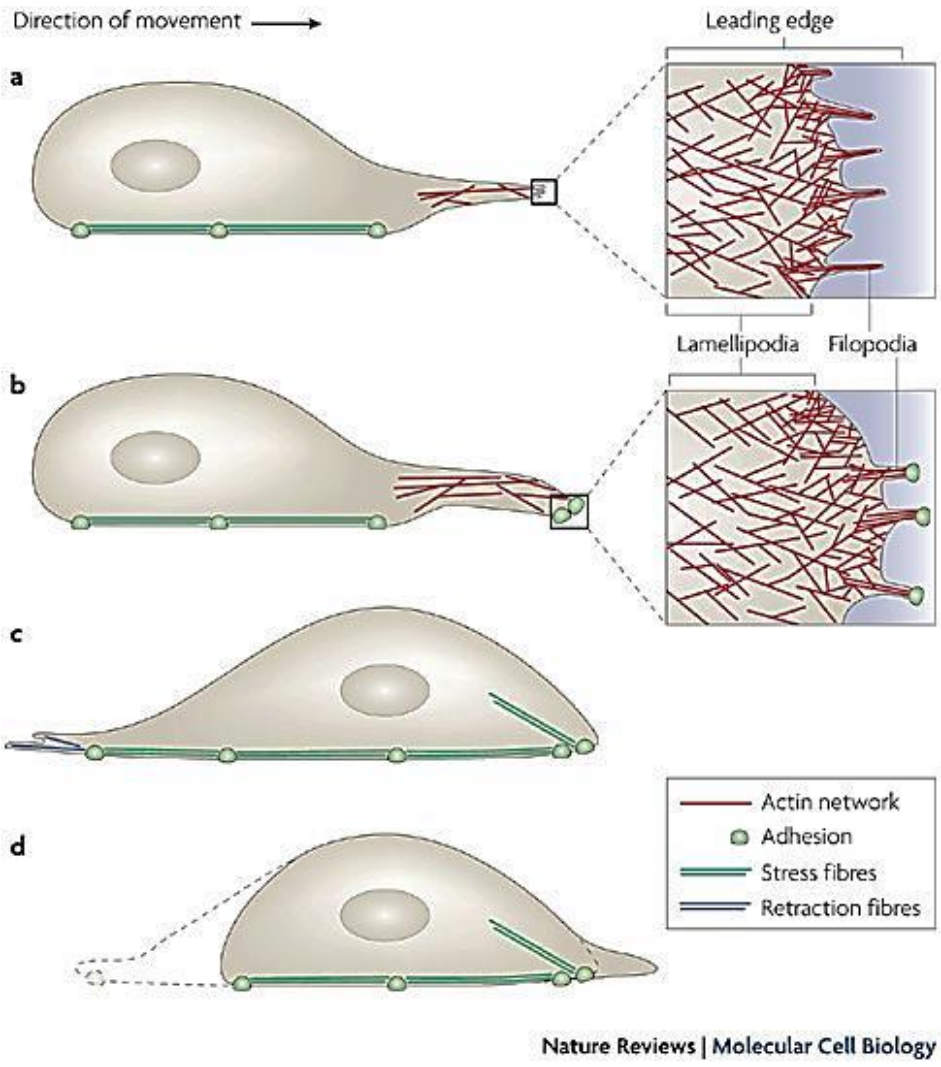

Figure 1. 8.: Sequential events during endothelial cell migration. (A) Cell motility is initiated by Cdc42-dependent sensing of migratory cues by filopodia and Rac1-dependent formation of lamellipodia. Both cell protrusions contain actin-filaments, with elongating barbed ends oriented towards the plasma membrane. (B) Protrusions attach to the substratum at the leading front via focal adhesions and integrins. (C) Stress fibre-mediated contraction forces translocate the nucleus and cell body, allowing forward movement. (D) Retraction fibres pull the rear of the cell forward, adhesions at the rear disassemble and the trailing end retracts. (adapted from Mattila and Lappalainen, 2008).

Endothelial migration involves 3 major mechanisms that determine the velocity and directionality of the growing sprout in the tissue environment, namely chemotaxis, haptotaxis and mechanotaxis (Lamalice *et al.*, 2007). The coordinated interplay of all three mechanisms is required for the angiogenic response of EC and further involves the activation of intracellular signalling cascades that converge on cytoskeletal remodelling, including activation of small GTPases, PI3K and eNOS, MAPK p38 and phosphorylation of focal adhesion kinase (FAK).

Chemotaxis is the directional migration of cells towards a gradient of soluble chemoattractants. Among the numerous cytokines, VEGF, bFGF and angipoietins are three major growth factors contributing to this type of actin-based motility. VEGF-R2-mediated activation of small GTPases of the Rho family is centrally involved in the regulation of chemotaxis. In particular, Cdc42 induces the formation of dynamic filopodia to sense guidance cues and migrate coordinately, and is also involved in the formation of stress fibres via activation of the MAPK p38 pathway (Kater *et al.*, 1995; Lamalice *et al.*, 2004). Moreover, VEGF-induced activation of Rac1 leads to the formation of lamellipodia assuring the crawling movement of cells (Lamalice *et al.*, 2004). The small GTPase RhoA is also an important regulator of EC migration and mediates VEGF-R2 phosphorylation and downstream activation of phosphatidylinositol 3-kinase (PI3K), thereby regulating the function of actin-regulatory proteins such as profiling, cofilin and FAK (van Nieuw Amerongen *et al.*, 2003; Gingras *et al.*, 2000; Rousseau *et al.*, 2000; Qi and Claesson-Welsh, 2001).

Haptotaxis is defined as the directional movement of cells towards a gradient of immobilised extracellular matrix ligands (Davis and Senger, 2005). Under physiological conditions the ECM contributes to maintain EC in a quiescent state. However, during early angiogenesis the ECM is broken down by metalloproteinases resulting in the release of mitogenic signals either generated by the proteolytic fragments or the release of embedded angiogenic stimuli such as VEGF, in turn promoting EC migration (Wang *et al.*, 2005; Lamalice *et al.*, 2007). The adhesive interaction that triggers haptotaxis of EC are mainly directed by ECM components such as collagen and fibronection and integrins expressed on EC (Davis and Senger, 2005). Focal adhesions are sites of tight adhesion where integrins connect the ECM with the cellular cytoskeleton and recruit a complex network of signalling and scaffolding proteins (Geiger *et al.*, 2001). In migrating cells,

focal adhesions and stress fibres are aligned in the direction of migration and focal adhesions are characterised by a rapid turnover, thereby allowing the forward movement of the cell. Activation of integrins initiates and regulates angiogenic signalling. Activation of integrins at focal adhesion initiates and regulates several angiogenic signalling pathways that converge on actin polymerisation, cellular contractility and cell migration (Guo and Giancotti, 2004). Active integrins trigger the activation of the small GTPases Rac and Cdc42, inducing actin polymerisation and filament assembly, presumably through activation of the Arp2/3 complex and WASP. Moreover, Rac and Cdc42 activation may result in further recruitment of integrins to the tips of filopodia thereby forming a positive feedback loop to amplify the haptotatic signal (Hsu *et al.*, 2005, Lamalice *et al.*, 2007). Concomitantly, the activation of integrins at focal adhesion sites leads to the activation of RhoA and ERK pathways, resulting in increased contractility (Guo and Giancotti, 2004; Klemke *et al.*, 1997). Together, integrin-mediated actin polymer elongation and contractility trigger haptotatic EC migration.

Mechanotaxis is the directional migration generated by mechanical forces (Li *et al.*, 2005). Due to their anatomical location, EC are constantly exposed to fluid shear stress. Shear stress is sensed by the luminal membrane of EC and its associated receptors and transmitted throughout the cell activating intracellular signalling pathways that regulate EC migration. In particular, shear stress may induces the small GTPases Rac1 and RhoA to promote lamellipodia formation in the direction of flow and to increase the contractility of stress fibres at the trailing end of the cell, respectively (Sander *et al.*, 1999; Li *et al.*, 2005).

Sprout fusion and lumen formation

To form new vascular connections, tip cells need to suppress their motile, explorative behaviour. Strong adhesive interactions that occur when tip cells encounter each other regulate fusion of adjacent sprouts and vessels. VE-cadherin, a junctional transmembrane protein that mediates adhesive interactions between adjacent EC, is a critical regulator of vascular integrity and permeability and inhibits angiogenic growth (Dejana *et al.*, 2009; Vestweber *et al.*, 2008; Lampugnani *et al.*, 2006; Abraham *et al.*, 2009). VE-cadherin has been found to be expressed in filopodia and thus VE-cadherin interactions between adjacent tip cells may stabilise the contact

and simultaneously downregulate pro-angiogenic signalling and tip cell behaviour (Almagro *et al.*, 2010; Eilken and Adams, 2010). Fantin and colleagues show that specialised macrophages polarised to the M2 type, which promote angiogenesis by releasing pro-angiogenic factors such as VEGF (Sica *et al.*, 2008; Tammela *et al.*, 2008), are located in the vicinity of vessel branches and that these tissue-resident macrophages can act as bridges between adjacent tip cells (Fantin *et al.*, 2010).

The establishment of blood flow requires the formation of a vascular lumen, which may occur in vascular endothelial sprouts before or after they have joined with other vessels, and involves cell shrinking, and vacuole formation. Intracellular and intercellular vacuoles fuse to establish a lumen in EC, which further requires integrin-matrix adhesions and activation of the small GTPases Cdc42 and Rac1 (Bayless and Davis, 2002; Davis and Bayless, 2003).

Perfusion and maturation of blood vessels

The generation of a lumen triggers the onset of blood flow. This in turn improves oxygen delivery to the growing vessel sprout and reduces local hypoxia-induced expression of pro-angiogenic factors such as VEGF (Adams and Alitalo, 2007). Perfusion also promotes maturation processes. Maturation describes the stepwise transition from an actively growing vascular bed to a quiescent, fully formed and functional network, and involves the inhibition of cell proliferation and sprouting, stabilisation of vessels and establishment of tight intracellular junctions, deposition of ECM proteins into the subendothelial basement membrane and the recruitment and incorporation of mural cells such as pericytes and vascular SMC (Jain *et al.*, 2003; Cleaver and Melton, 2003). Pericytes establish direct cell-cell contacts with EC and cover capillaries and immature vessels, whereas vascular SMC cover mature arteries and veins, and are separated from the endothelium by a basement membrane layer (Adams and Alitalo, 2007).

1.2.2. The role of vascular endothelial growth factor in angiogenesis

The most important molecule controlling blood vessel morphogenesis is vascular endothelial growth factor A (VEGF-A), which is part of a large family of potent angiogenic regulators including

placental growth factor (PlGF), VEGF-B, VEGF-C, VEGF-D, and the Orf-virus encoded VEGF-E (Ferrara *et al.*, 2003; Shibuya, 2006). Its biological importance is evidenced by the fact that the lack of only one VEGF allele results in embryonic lethality (Carmeliet *et al.*, 1996; Ferrara *et al.*, 1996).

In normal tissues, the highest levels of VEGF-A are found in the lung, kidney, heart, and adrenal gland and lower levels in liver, spleen and the gastrointestinal tract. Human VEGF-A is a 32 to 42 kDa, homodimeric, disulphide-bound glycoprotein, whose gene is organised as eight exons separated by seven introns (Houck *et al.*, 1991; Tischer *et al.*, 1991). In humans, alternative splicing results in at least seven VEGF-A isoforms, having respectively 121, 145, 148, 165, 183, 189, or 206 amino acids after cleavage (Houck *et al.*, 1991; Tischer *et al.*, 1991). VEGF-A_{121} is a freely diffusible polypetide with no heparin-binding properties, whereas VEGF-A_{189} and VEGF-A_{206} bind to heparin with high affinity and are tightly bound to ECM proteoglycans (Houck *et al.*, 1992). VEGF-A_{165} (here referred to as VEGF) is the most predominant isoform and has intermediary properties. VEGF contains only one of two possible heparin-binding domains and exists in part as a secreted, moderately diffusible protein, but a significant fraction remains bound to the cell surface and ECM (Park *et al.*, 1993). The latter may be released in a diffusible form by plasmin cleavage (Houck *et al.*, 1992).

VEGF is a high affinity ligand for the tyrosine kinase receptors (RTK) VEGF-R1/Flt1 and VEGF-R2/KDR/Flk (Terman *et al.*, 1994). Both receptors consist of seven immunoglobulin-like domains in the extracellular domain, a single transmembrane region and a consensus tyrosine kinase sequence that is interrupted by a kinase-insert domain (Shibuya *et al.*, 1990; Terman *et al.*, 1991). VEGF-R1 is also recognised by PlGF and VEGF-B, and VEGF-E as well as VEGF-C and VEGF-D bind and activate VEGF-R2 (Gale and Yancopoulous, 1999). In addition, VEGF-C and VEGF-D have high binding affinities for VEGF-R3/Flt4 (Joukov *et al.*, 1996; Achen *et al.*, 1998). Soluble VEGF-R1 (sVEGF-R1), which is physiologically released and acts as a VEGF antagonist, may be overproduced in some pathologies. sVEGF-R1 is bound and activated by PlGF and VEGF-B (Hornig and Weich, 1999). VEGF family members also interact with a family of co-receptors, namely the neuropilins NRP1 and NRP2 (Fig. 1.9.) (Soker *et al.*, 1998).

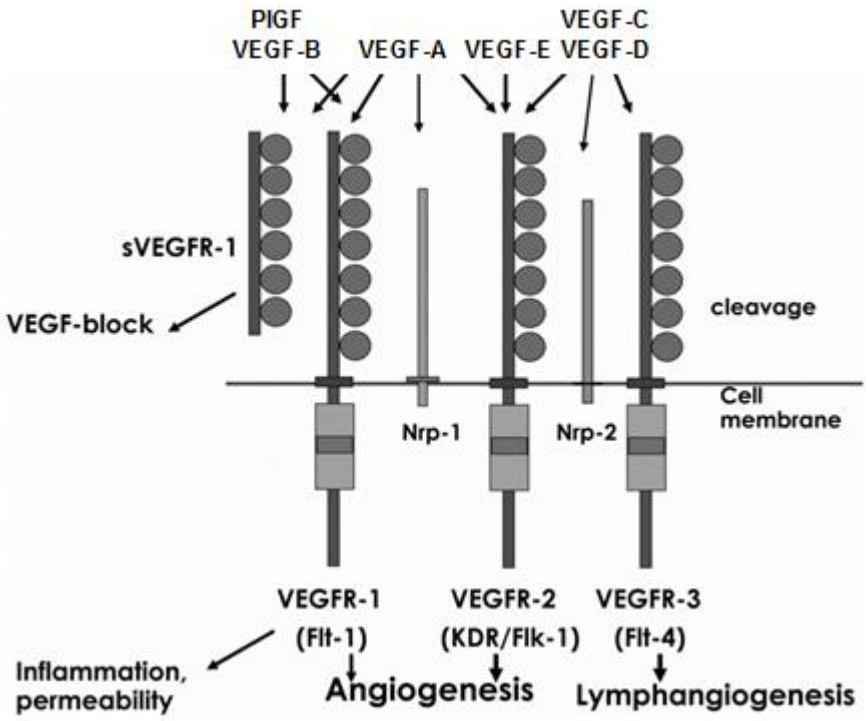

Figure 1. 9.: The VEGF family and its receptors. The VEGF family consists of the four VEGF genes VEGF-A, VEGF-B, VEGF-C, VEGF-D, the Orf-virus encoded VEGF-E, and the related growth factor PlGF. VEGF-A binds and activates the tyrosine kinase receptors (RTKs) VEGF-R1 and VEGF-R2. VEGF-R1 is also activated by PlGF and VEGF-B. VEGF-C and VEGF-B bind to and activate VEGF-R2 and VEGF-R3, whereas VEGF-E has only high binding affinity for VEGF-R2. In addition to RTKs, VEGF family members interact with neutropilin co-receptors (NRP1, NRP2) (adapted from Shibuya, 2009).

In endothelial cells, VEGF stimulates differentiation, survival, migration, proliferation, tubulogenesis and vascular permeability. This multifunctionality of VEGF results from its ability to activate diverse, complex and integrated signalling pathways (Carmeliet, 2000; Ferrara, 2000; Zachary and Gliki, 2001). VEGF-R2 is the major mediator of the mitogenic, angiogenic and permeability-enhancing effects of VEGF and its key role in angiogenesis is revealed by the lack of vascuologenesis and failure to develop blood islands and organised blood vessels in VEGF-R2 knockout mice, resulting in embryonic lethality between gestation days 8.5 and 9.5 (Shalaby *et al.*, 1995). VEGF-R2 signalling is initiated through ligand-induced receptor dimerization and autophosphorylation of tyrosine residues in the cytoplasmic domain (Fig. 1.10.).

VEGF-mediated survival is mainly regulated via PI3K signalling. PI3K-dependent activation of the anti-apoptotic kinase Akt/protein B in turn results in the phosphorylation and inactivation of the pro-apoptotic mediators Bad and caspase-9. Moreover, VEGF induces anti-apoptotic proteins, including Bcl-2 and A1, inhibitors of apoptosis proteins (IAPs), survivin and X-chromosome-linked IAP (XIAP) (Gerber *et al.*, 1998; Tran *et al.*, 1999). Akt survival signalling further mediates VEGF-induced NO production via eNOS phosphorylation (Dimmeler *et al.*, 1999; Fulton *et al.*, 1999). Moreover, VEGF-induced PI3K/Akt signalling is dependent on VE-cadherin, as indicated by reduced Akt signalling and Bcl-2 expression in response to VE-cadherin deficiency (Carmeliet *et al.*, 1999).

The proliferative effects of VEGF during the angiogenic process are mainly regulated by the MAPKs ERK1 and ERK2. VEGF-R2-dependent activation of ERK1/ERK2 is initiated by phosphorylation of growth factor receptor-bound protein 2 (Grb2) and subsequent stimulation of the guanine nucleotide exchange factor SOS (son of sevenless) and Ras activation, leading to activation of the Raf-1/MEK/ERK cascade (Ilan *et al.*, 1998). Mitogenic signalling of VEGF can be also regulated via a Ras-independent pathway involving phospholipase C-γ (PLC-γ) (Takahashi *et al.*, 1999; Gliki *et al.*, 2001). VEGF induces PLC-γ phosphorylation leading to the activation of PKC. PKC mediates activation of ERK1/2 via Raf-1 and MEK. PKC inhibition blocks VEGF signalling and subsequent angiogenic capacities of EC (Xia *et al.*, 1996; Wellner *et al.*, 1999; Higaki *et al.*, 1999; Gliki *et al.*, 2002). Studies also point towards a cross-talk between the ERK and JNK MAPK pathways in the regulation of EC proliferation. VEGF activates JNK and expression of a dominant-negative JNK-1 mutant inhibited VEGF-induced thymidine incorporation, while a dominant-negative ERK2 mutant blocked JNK activation (Pedram *et al.*, 1998).

VEGF-mediated EC migration involves activation of p38 MAPK downstream of the small GTPase Cdc42, resulting in actin remodelling and EC migration, effects inhibited by a p38 inhibitor (Rousseau *et al.*, 2000). VEGF-R2 signalling has also been shown to activate other small GTPases including RhoA and Rac1, in turn promoting cell migration (Zeng *et al.*, 2002). The vasodilator NO may also regulate VEGF-induced migration dependent on eNOS phosphorylation (Dimmeler *et al.*, 2000). Another key signalling pathway in VEGF-mediated EC migration involves

phosphorylation of FAK and focal adhesion-associated protein paxillin to recruit FAK to focal adhesion in EC (Abedi and Zachary, 1997; Abu-Ghazaleh, 2001).

Although signalling pathways regulating VEGF-induced cell permeability still remain poorly understood, they may involve PI3K/Akt-dependent phosphorylation of eNOS and subsequent NO production (Zachary, 2003). Moreover, VEGF-induced phosphorylation of components of adherens and tight junctions may be a mechanism through which endothelial cell-cell adhesions are disrupted, leading to increased permeability (Esser *et al.*, 1998; Zachary and Gliki, 2001). Indeed, VEGF stimulation promotes rapid endocytosis of VE-cadherin, thereby disrupting the endothelial barrier function. This process is initiated by VEGF-R2-dependent activation of Rac, in turn promoting p21-activated kinase (PAK)-mediated phosphorylation of VE-cadherin (Gavard and Gutkind, 2008).

VEGF-R2-dependent VEGF signalling further determines the fate of individual cells by enabling one EC to take the lead and become a tip cell, while instructing adjacent cells to become stalk cells. Such lateral inhibition relies on tip-to-stalk communication by Dll4/Notch signalling (Hellström *et al.*, 2007; Eilken and Adams, 2010). (please see section 1.1.1. Selection of sprouting EC).

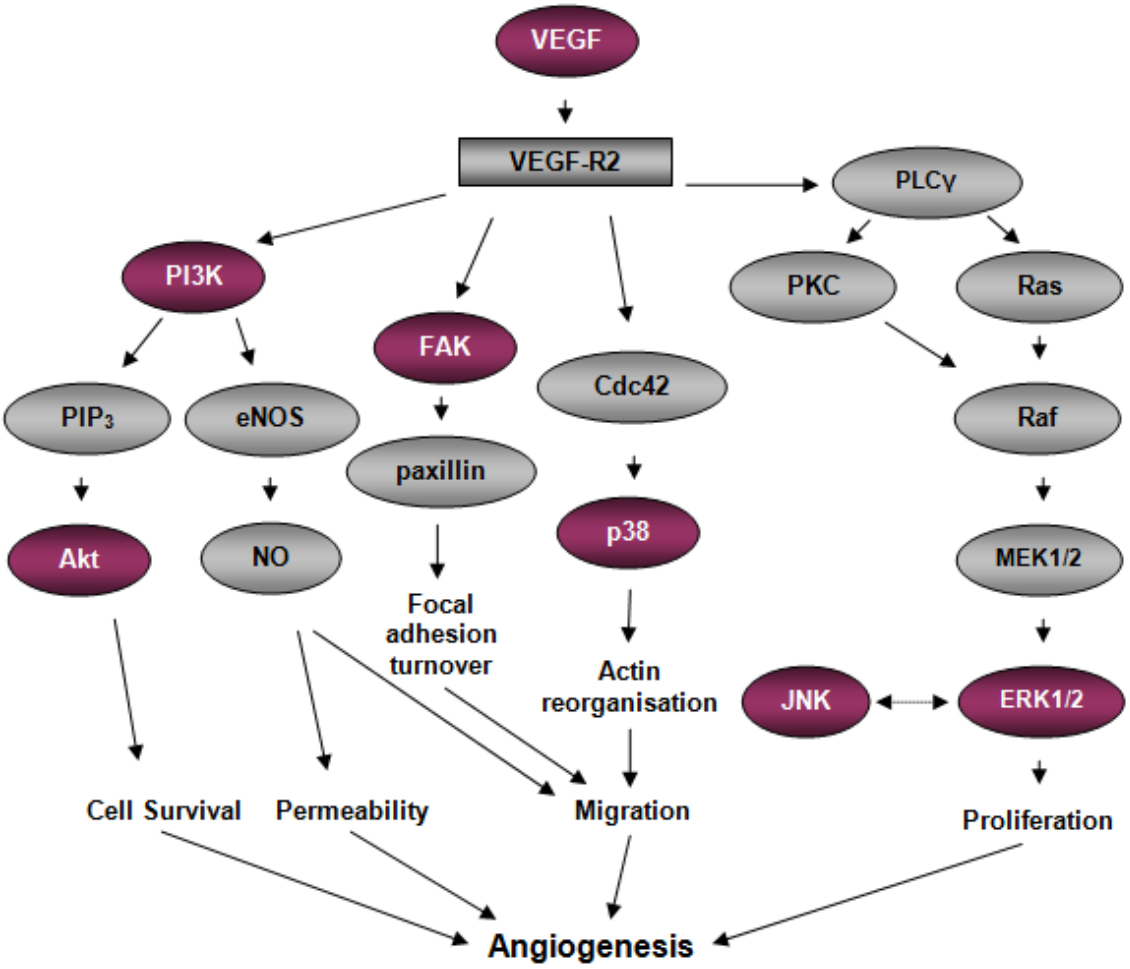

Figure 1. 10.: VEGF signalling pathways in the regulation of angiogenesis. VEGF is a high affinity ligand for the tyrosine kinase receptor VEGF-R2, which is the main signal transducing VEGF receptor for angiogenesis and mitogenesis of EC. Ligand binding results in receptor dimerization and autophosphorylation, which in turn activates PI3K/Akt, MAPK p38, ERK1/2, and JNK MAPK signalling pathways. VEGF plays important roles during angiogenic remodelling, regulating EC survival, proliferation and migration, as well as cell organisation.

1.2.3. Angiogenesis in disease

Angiogenesis occurs primarily during embryogenesis and development and only to a limited extent in postnatal life contributing to organ growth. Physiological angiogenesis in adults is mainly downregulated, with blood vessels exhibiting a quiescent phenotype, but is reactivated during the female reproductive cycle, is necessary for maturation of oocytes, and plays a profound role during pregnancy, establishing a link between the maternal and foetal circulation in the placenta. Besides those internally regulated processes, angiogenesis is an inherent feature of wound healing and repair. Moreover, dysregulated angiogenesis is involved in numerous diseases ranging from cancer to chronic inflammatory syndromes such as atherosclerosis, rheumatoid arthritis, diabetes mellitus, and ischaemic heart disease (Carmeliet, 2005; Bouïs *et al.*, 2006; Sun and Schiller, 2007).

Angiogenesis in atherosclerosis

Human arteries possess a microvasculature in their advential layers called the vaso vasorum. Normal vaso vasorum originate from coronary artery branch points at regular intervals and run longitudinally along the vessel wall. These vessels then separate to form circumferential arches around the main coronary lumen. Because diffusion of blood nutrients from the lumen is limited to a distance of ~100 µm, a primary function of these vessels is thought to be the transport of nutrients to the vessel wall (Heistadt and Marcus, 1979; Khurana *et al.*, 2005).

Angiogenesis is a recognised feature of the atherogenic process in both coronary and carotid disease. Numerous studies further confirm the presence of an increased microvessel density in vulnerable and ruptured plaques compared with stable lesions, arising from repeated activation and proliferation of the dense network of vessels in the adventitia adjacent to a plaque (Fleiner *et al.*, 2004, Jerziorska and Wooley, 1999, and Morena *et al.*, 2004). In developing lesions, new vaso vasorum invade the intima at specific sites of medial disruption, whilst the intima and media of complicated plaques in coronary atherosclerotic vessels are infiltrated with a tumour-like mass of microvessels which are prone to leak, and are associated with a high degree of macrophage infiltration and thin-cap lesions (Herrmann *et al.*, 2006; Moreno *et al.*, 2004). These angiogenic blood vessels have been identified in complex regions of human aortic lesions following CD105

(endoglin) and TGFβ-1 immunostaining (Piao and Tokunaga, 2006), and are thought to be important regulators of plaque growth and lesion instability. In addition to an association between microvessels and vulnerable plaques, the expression of several pro-angiogenic cytokines in human lesions, including VEGF and its receptors, bFGF, PDGF, HGF, and TGFβ-1, further supports a role for angiogenesis in atherosclerosis (Hughes *et al.*, 1993; Lappalainen *et al.*, 2004; Ignatescu *et al.*, 1999; Lupia *et al.*, 2003; Barrett and Benditt, 1988; Ma *et al.*, 2002). The strongest experimental evidence that angiogenesis plays a causative role in the atherogenic process has come from studies in the hypercholesterolemic ApoE$^{-/-}$ mouse model, demonstrating that the endothelium-specific anti-angiogenic agents endostatin, TNP-40 and angiostatin significantly reduce plaque formation when compared to control mice (Moulton *et al.*, 1999; Moulton *et al.*, 2003). Moreover, intraperitoneal administration of human VEGF protein into ApoE/ApoB100 double knockout mice promotes atherosclerotic plaque formation in these animals as indicated by increased EPC and macrophage/monocytes counts, plaque EC density, and macrophage infiltration (Celletti *et al.*, 2001).

Angiogenesis in rheumatoid arthritis

Rheumatoid arthritis (RA) is chronic systemic inflammatory and destructive disease predominately affecting the peripheral synovial joints (Paleolog, 2002). Disease progression involves an inflammatory response in the synovium, which significantly increases in mass due to hyperplasia of synovial cells and an increase in the volume of synovial fluid, resulting in joint swelling and pain. Blood-derived cells, including T cells, B cells, macrophages and plasma cells infiltrate the sublining of the synovium, resulting in the development of a fibrous tissue, the ‘pannus’, at the synovial interface with cartilage and bone. The pathology of the disease leads to the destruction of articular cartilage, subchondral bone, and periarticular soft tissues, producing deformities of the affected joints (Paleolog, 2002).

Angiogenesis plays a central role in the initiation and progression of RA. Indeed, the synovium of RA patients is characterised by a dense vascular network, and an increase in the number of synovial blood vessels is essential for the expansion of synovial tissue. Moreover, the number of synovial blood vessels has been found to correlate with hyperplasia of synovial cells, infiltration of

mononuclear cells, and joint stiffness (Rooney *et al.*, 1988). Further support for a role for angiogenesis in RA is the finding that EC lining the synovial blood vessel express high levels of PCNA and Ki67, both markers for active EC proliferation (Ceponis *et al.*, 1998; Walsh *et al.*, 1998). A consequence of synovial hyperplasia is the demand for oxygen and nutrients by the growing tissue resulting in local hypoxia, which in turn is a potent signal for angiogenic growth. The augmented proliferation of synovial EC further promotes hypoxia and angiogenesis, and hence synovial infiltration of inflammatory cytokines and growth factors and eventually hyperplasia (Paleolog, 2002). In fact, VEGF levels are significantly increased in serum and synovial fluid from RA patients when compared to normal controls and serum VEGF concentration correlates with C-reactive protein expression, a marker for inflammation and disease activity (Koch *et al.*, 1994; Paleolog *et al.*, 1998; Lee *et al.*, 2001). Moreover, EC lining small blood vessels in the pannus stain positive for VEGF (Koch *et al.*, 1994, Fava *et al.*, 1994; Pufe *et al.*, 2001). Other angiogenic growth factors have been reported to be expressed in synovial fluid and tissue from RA patients and may contribute to disease initiation and progress, including acidic and basic FGF, PDGF and HGF (Koch, 2000; Paleolog, 2002).

Diabetes mellitus

Diabetes mellitus is a chronic metabolic disease characterised by hyperglycaemia due to lack of (type I) or resitance to insulin (type 2) (Kolluru *et al.*, 2012). Diabetic patients are frequently afflicted with cardiovascular complications such as accelerated atherosclerosis, endothelial dysfunction, impaired neovascularisation and wound healing, demonstrate vascular abnormalities of the retina, the kidneys, and have an increased risk of organ transplant rejection (Martin *et al.*, 2003; Kolluru *et al.*, 2012). In each of these complications, abnormal angiogenesis can be implicated in the pathogenesis. Indeed, diabetic retinopathy arises from excessive angiogenesis. Hyperglycemia-induced intramural pericyte apoptosis leads to an impaired blood-retina-barrier and chronic hypoxia, followed by aberrant neovascularisation. The resulting vessels are malformed and show increased permeability and are prone to haemorrhage (Lip *et al.*, 2000; Geraldes *et al.*, 2009). In contrast, impaired diabetic wound healing is the consequence of a deficiency in angiogenesis (Martin *et al.*, 2003). Wound healing is a multistep process involving

haemostasis, inflammation and debridement, proliferation, epithelialisation, and remodelling (Loots *et al.*, 1999). The non-healing nature of diabetic wounds has been attributed to disturbances in both the inflammation/debridement phase and the proliferation phase, which prevent the wound from progressing to a later step of the healing process (Loots *et al*., 1999).

Aberrant angiogenesis is also intimately associated with solid tumour growth. The study of tumour angiogenesis is a rapidly developing field and is beyond the scope of this thesis. Angiogenesis promotes tumour growth and persistence of primary solid tumours and their metastases. An increase in vascular density allows easier access of tumour cells in the circulation and correlates with the invasive properties of tumours and thus the malignant tumour phenotype (Cavallaro and Christofori, 2000). A variety of anti-angiogenic drugs are being studied in clinical trials in various malignant diseases. For example the anti-VEGF drug avastin has been approved in the treatment of colonic carcinoma.

1.3. THE HEME OXYGENASE SYSTEM

Heme oxygenases (HO) are the rate-limiting enzymes in the degradation of heme into equimolar amounts of carbon monoxide, biliverdin/bilirubin, and free iron. In humans, two distinct isoforms have been identified, namely the inducible HO-1 and the constitutive HO-2. HO enzymes and their products play a critical role in the vasculature by exhibiting important physiological actions that are ultimately linked to endothelial cell protection, including anti-inflammatory, anti-oxidant, and anti-apoptotic effects. Induction of HO-1 is an important cellular adaptive response, minimising tissue injury and facilitating repair. In addition, a role for HO-1 in the regulation of angiogenesis has been proposed (Kim *et al.*, 2011).

1.3.1. Heme oxygenases: An introduction

Heme oxygenases catalyse the rate-limiting step in heme metabolism. Both HO isoforms oxidise heme (ferriprotoporphyrin IX) to the bile pigment biliverdin-IXα. Biliverdin-IXα is further metabolised to bilirubin-IXα by NAD(P)H:biliverdin reductase (BVR). HO-catalysed heme cleavage releases iron in its ferrous form Fe II (Fe^{2+}) and eliminates the α-methene-bridge carbon of heme as carbon monoxide (CO) (Tenhunen *et al.*, 1969). The enzymatic activity of HO requires three moles of molecular oxygen (O_2) per heme molecule oxidised and reducing equivalents from NAPDH:cytochrome *P*450 (cytochrome C) reductase (Fig. 1.11.). The generation and release of intracellular Fe^{2+} during heme metabolism induces expression of the iron-binding protein ferritin heavy chain (FHC). FHC associates with ferritin light chain to form a multimeric complex (Harrison and Arosio, 1996) and catalyses the oxidation of iron from the ferrous (Fe^{2+}) to the ferric form (Fe^{3+}) (Balla *et al.*,1992; Berberat *et al.*, 2003). HO-mediated cleavage of the α-methene-bridge carbon is inhibited by various metalloporphyrins, including the synthetic HO antagonists zinc protoporphyrin (ZnPP) and tin protoporphyrin (SnPP) (Ryter *et al.*, 2006).

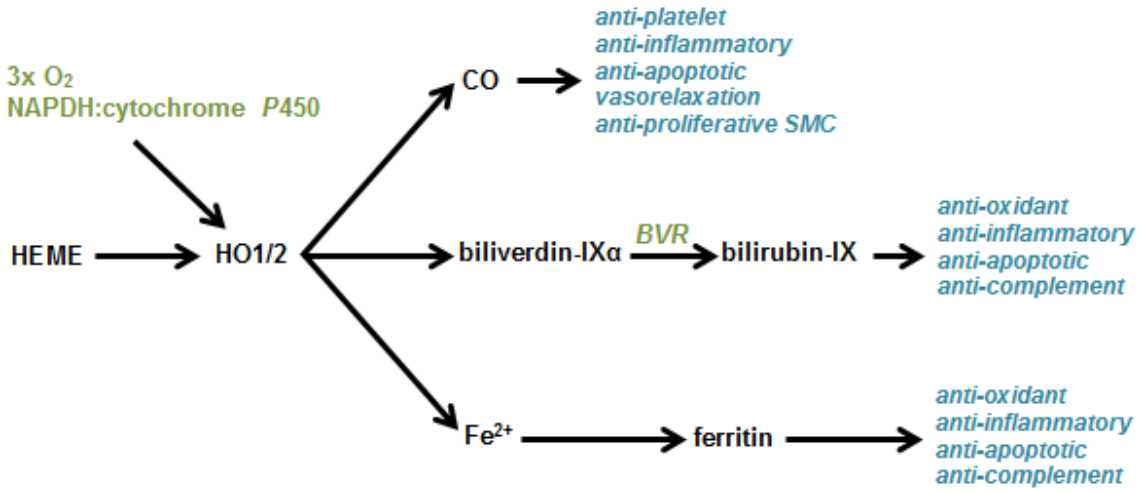

Figure 1. 11.: Oxidative degradation of heme by HO enzymes. HO isoforms (HO-1, HO-2) catalyse the degradation of heme into its products carbon monoxide (CO), ferrous iron (Fe^{2+}), thereby inducing the expression of ferritin, and biliverdin-IXα, which is converted into bilirubin-IX by the NAPDH-dependent biliverdin reductase (BVR). Enzymatic activity of HO requires 3 moles of molecular oxygen (O_2) and NAPDH:cytochrome P450 as an electron source. Each product activates several cytoprotective pathways in the vascular endothelium.

Two genetically distinct HO isoforms have been identified in mammals, the inducible isoform HO-1 and the constitutively expressed HO-2. Both proteins are products of distinct genes, but share 43% amino acid sequence homology (Fig. 1.12). HO-1 is the product of only one transcript, but HO-2 is encoded by two transcripts from one gene arising from differences in polyadenylation (McCoubry and Maines, 1994). The two HO isoforms share a heme catalytic site that allows them to have similar functions in heme degradation, but vary in terms of tissue distribution, regulation and kinetics (Maines *et al.*, 1986). Analysis of the crystal structure of mammalian HO-1 reveals that it is composed of 7 α-helicals with heme fitting into the heme pocket between the proximal and distal helix (Dennery, 2005). The crytal structure of HO-2 has not been identified yet, but differences in the structure of the two isoforms may account for their different kinetic properties. Indeed, comparison the amino acid sequence of the two isoforms, show that HO-1 and HO-2 differ at their amino and carboxy terminus. The amino terminus of HO-2 has additional residues which help to account for the differences in size of the isoforms (McCoubrey and Maines, 1993; Dennery, 2005). In addition, numerous serine phosphorylation sites have been identified for HO-

2. Although the precise mechanisms remain elusive, phosphorylation of serine residues has been shown to alter HO-2 activity (Dore *et al.*, 1996). It is therefore plausible to suggest that HO activity could be modified by posttranslational events such as phosphorylation or mutations of the amino acid sequence, which may alter the heme catalytic site. The heme pocket of HO enzymes is flexible and can open and close which allows for increased distance between heme and the catalytic site in turn affecting HO activity. Furthermore, the multi-step process of HO reaction has differing reaction rates. The biliverdin formation step is rate limiting whereas the oxygen binding followed by a second electron transfer to give biliverdin products is more rapid (Trakshel and Maines, 1989; Colas and Ortiz de Montellan, 2003). These variations in rates of synthesis of biliverdin suggest that there could be many conditions where the rate of heme degradation is altered thereby affecting the HO activity level.

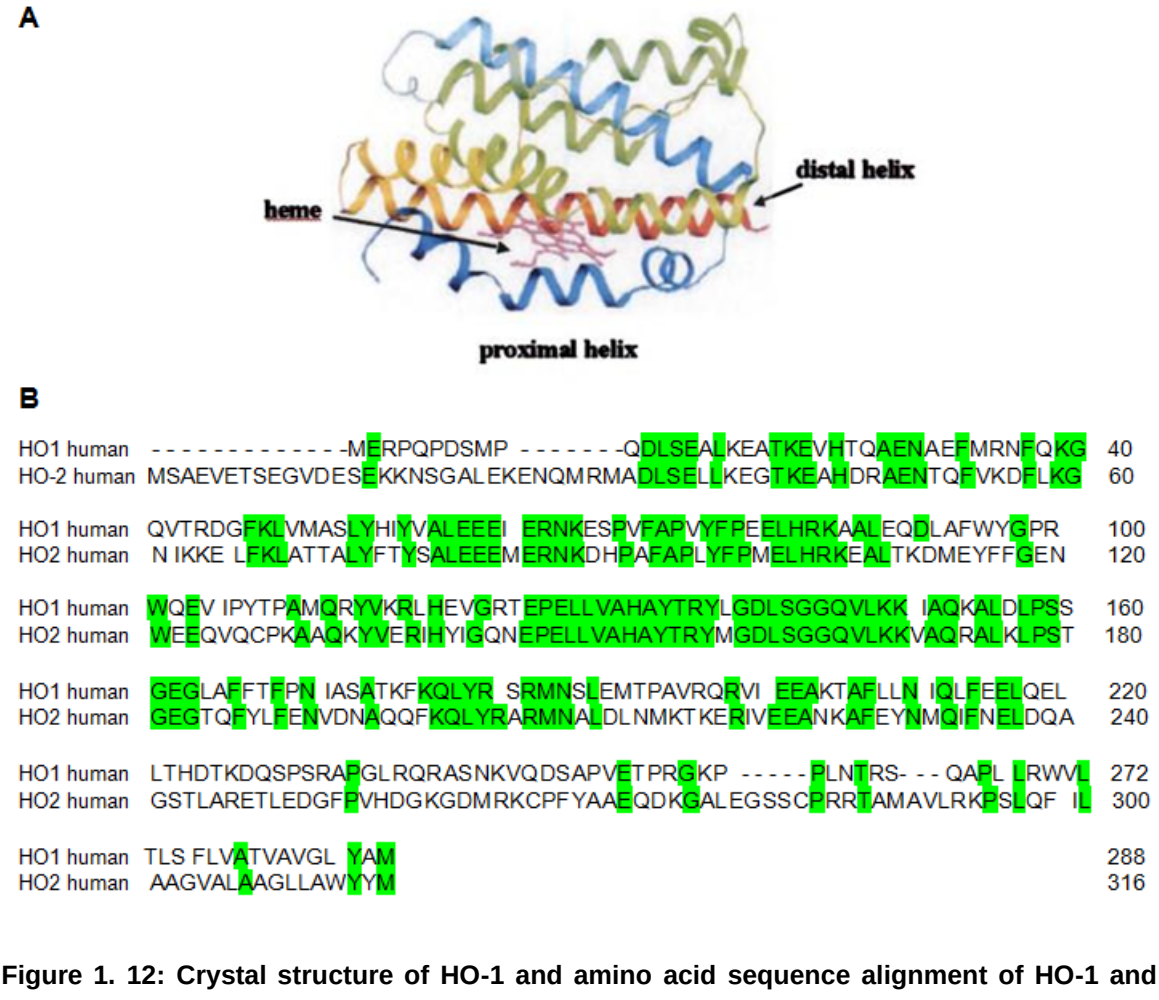

Figure 1. 12: Crystal structure of HO-1 and amino acid sequence alignment of HO-1 and HO-2. (A) Crystal structure of HO-1 (adapted from Dennery, 2005). (B) HO-1 and HO-2 share 43% amino acid homology. Conserved amino acids are marked in green (modified after Linnenbaum *et al.*, 2012).

HO-1 is a 32 kDa protein, also denoted as heat shock protein 32 (HSP32) (Keyse and Tyrrell, 1989). Apart from high expression levels in the spleen and specialised reticuloendothelial cells, HO-1 is typically expressed at low to undetectable levels under basal conditions, but rapidly responds to transcriptional activation by numerous physiological and pathological stimuli, including heme, hypoxia, heavy metals, NO and reactive oxygen species (ROS), as well as pro-inflammatory cytokines and haemodynamic forces exerted by the flowing blood (Wagner *et al.*, 1997; Ryter and Choi, 2002; Ali *et al.*, 2009). Thus, HO-1 is a stress-induced protein which aims to maintain cellular integrity (Ryter *et al.*, 2006). In regard of compartmentalisation, HO-1 is predominantly localised to the endoplasmic reticulum (ER), but can be found in other subcellular domains, including the plasma membrane and the nucleus (Ishikawa *et al.*, 1991; Shibahara *et al.*, 1985; Kim *et al.*, 2004; Ryter *et al.*, 2006).

HO-2, a 36 kDa protein, is constitutively expressed and present at high levels in the brain and testes, and is also abundantly and ubiquitously expressed in the endothelium, liver, kidney and gut (Maines, 1997; Maines *et al.*, 1986; Trakshel *et al.*, 1986; Zachary *et al.*, 1996). Unlike HO-1, HO-2 does not respond to transcriptional activation by environmental stress but may be transcriptionally modulated by corticosteroids and its activity may be dynamically regulated by post-translational modifications, as indicated by the three cysteine phosphorylation sites present in the HO-2 protein (Maines *et al.*, 1997; Raju *et al.*, 1997; Boehning *et al.*, 2003). Moreover, the function of HO-2 is poorly understood but may include a regulatory role in heme homeostasis, by sequestering heme to maintain the intracellular heme level. HO-2 may also function as an oxygen sensor and HO-2 deletion causes EC activation marked by oxidative stress, inflammation and angiogenesis, underscoring important functions of this enzyme in endothelial homeostasis (Kemp, 2005; Bellner *et al.*, 2009). In addition, HO-2 deficiency is associated with impaired reparative and inflammatory responses after injury, implicating a role for HO-2 in the regulation of these responses (Seta *et al.*, 2006). Moreover, it has been postulated that HO-2 is critical for HO-1 expression, which may explain why HO-2 null mice cannot compensate for the loss of HO-2 by increasing HO-1 expression (Sodhi *et al.*, 2009).

1.3.2. Regulation of HO-1 expression

The human HO-1 gene (*HMOX1*) is organised into five exons and four introns and is located on chromosome position 22q12 and its expression is mainly regulated at the transcriptional level (Shibahara *et al.*, 1989; Gozzelino *et al.*, 2010). *HMOX1* transcription can be induced by a variety of signal transduction pathways in an inducer-, cell-type- and species-specific manner. A significant role in the activation of HO-1 has been implicated for mitogen-activated protein kinases (MAPK). MAPKs belong to the signal transduction superfamily of serine/threonine kinases that regulate cellular growth, apoptosis, motility, differentiation, and responses to environmental stimuli. The MAPK superfamily is comprised of the extracellular signal regulated kinases (ERK1/2), the c-Jun NH_2-terminal kinase (JNK), and the p38 MAPK signalling cascade. Each kinase sequentially phosphorylates and activates its downstream target kinases, that ultimately converge on multiple target proteins, including transcription factors (Kyriakis and Avruch, 2001; Cowan and Storey, 2003).

p38 MAPK signalling has been described as the major MAPK pathway responsible for HO-1 gene activation (Kacimi *et al.*, 2000), whereas a number of *in vitro* and *in vivo* models now suggest that simultaneous activation of more than one MAPK pathway is required for optimal gene induction (Chen and Maines, 2000; Zhang *et al.*, 2002; Ryter *et al.*, 2006). Phosphorylation-dependent activation of these signalling cascades ultimately activates transcription factors that regulate *HMOX1* transcription including KLF-2, Nrf-2, CREB, NFκB, AP-1, and ETS factors that recognise specific response element-rich regions within the proximal (-0.3 kb) and distal (-4 kb and -10 kb) *HMOX1* promoter (Fig. 1.13.) (Ryter *et al.*, 2006; H. Mylroie, unpublished data). The distal -10 kb *HMOX1* promoter region has been implicated in the upregulation of HO-1 in response to organic hydroperoxides (Hill-Kapturczak *et al.*, 2003a), and the -4 kb region mediates in part the induction response to heme and cadmium (Hill-Kaptuczek *et al.*, 2003b; Takeda *et al.*, 1994), as well as shear stress, NO donor compounds, cigarette smoke, and oxidised phospholipids (Chen *et al.*, 2003; Hara *et al.*, 1999; Favatier and Polla, 2001; Kronke *et al.*, 2003). An additional response-rich region, the -0.3 kb region, has been identified in the proximal promoter adjacent to the transcriptional start site, containing binding sites for ETS transcription factors, NFκB, and activator protein 2 (AP-2) (Deramaudt *et al.*, 1999; Lavrovsky *et al.*, 1994). The dominant sequence

element in these transcription enhancer regions is the stress-responsive element (StRE), a 10 bp motif with the consensus sequence of (T/C)GCTGAGTCA. The StrRE, which is structurally and functionally similar to the Maf response element (MARE) and the anti-oxidant response element (ARE), mediates transcription to almost all HO-1 inducers via c-Jun, CREB, ATF, Maf and Nrf-2 transcription factors (Ryter *et al.*, 2006). A distinct StRE-binding factor, Bach 1, is critical for the negative regulation of *HMOX1* transcription. Bach-1 dimerises with Maf proteins and competes against Nrf-2/Maf dimers for binding at the StRE. Unlike Nrf-2, Bach 1 lacks a transactivation domain and therefore functions as a transcriptional repressor (Sun *et al.*, 2002). Although there are multiple positive regulatory elements, only two negative regulatory regions located at -981 bp and -412 bp have been identified (Takahashi *et al.*, 1999). In addition, another potential negative regulatory element specific to the human *HMOX1* promoter corresponds to a variable GT-rich region ($(GT)_n$). Both inducible and basal expression of HO-1 is variable in the human population, reflecting the presence of highly polymorphic fragments in the human *HMOX1* locus, including a $(GT)_n$ microsatellite polymorphism, ranging from 11 to 42 repeats, in the proximal *HMOX1* promoter region (Exner *et at.*, 2004). In recent years, research has shown that these $(GT)_n$ repeats affect transcription, modulate basal and induced HO-1 expression and are of clinical relevance.

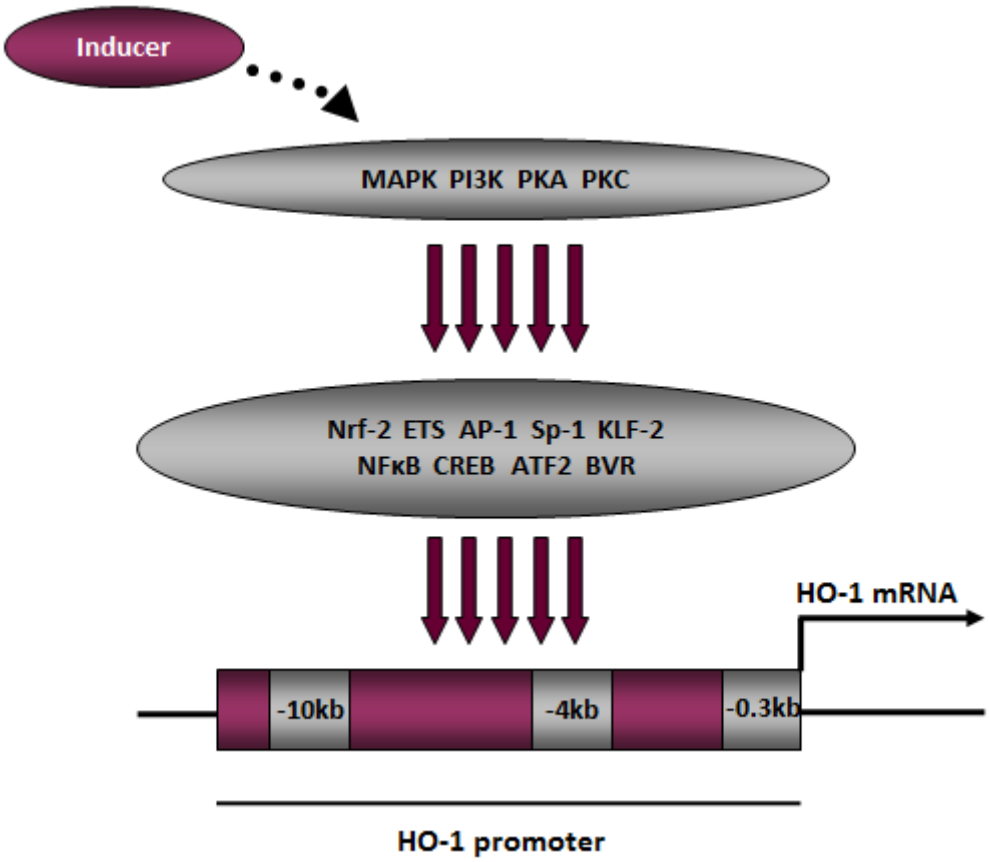

Figure 1. 13.: Signalling and transcriptional mechanisms leading to *HMOX1* activation. Numerous inducers of HO-1 activate protein phosphorylation-dependent signalling cascades that ultimately converge on the transcription factors that regulate the *HMOX1* gene by binding to specific response elements in the proximal (-0.3 kb) and/or distal (-4 kb and -10 kb) regions of the *HMOX1* promoter. AP-1 – activator protein 1, ATF-2 – activating transcription factor 2, BVR – biliverdin reductase, CREB – cAMP response element-binding protein, KLF-2 – Krüppel-like factor 2, MAPK – mitogen-activated protein kinase, NFκB – nuclear factor kappa B, Nrf-2 – NF-E2 related factor 2; PI3K- phosphoinositide 3-kinase; PKA – protein kinase A, PKC – protein kinase C, Sp-1 – specificity protein 1 (modified after Ryter *et al.*, 2006; Kim *et al.*, 2011).

1.3.3. Cytoprotective mechanisms of HO-1 and its products

Heme consists of a tetrapyrrole ring with a central iron ion and is the most abundant source of redox active iron in the human body. Heme exhibits contradictory biological functions. On the one hand heme is responsible for oxygen and mitochondrial electron support as an essential prosthetic group of haemoglobin, myoglobin and cytochromes (Wijayanti *et al.*, 2004; Mense and Zhang, 2006). On the other hand, non-protein bound free heme is inherently dangerous and greatly amplifies cellular damage arising from activated oxygen, with the vasculature being at particular risk (Balla *et al.*, 2007). Heme degradation and removal of the highly reactive heme moiety from cells and tissues by HO-1 was the initial explanation for the protective effects afforded by HO-1 (Maines *et al.*, 1993; Otterbein *et al.*, 2003; Kirkby and Adin, 2006).

The importance of HO-1 in heme and iron metabolism was first demonstrated by Tonegawa and Poss who characterised the HO-1-deficient mouse (HO-$1^{-/-}$). HO-$1^{-/-}$ mice demonstrate a state of iron overload, excess tissue iron deposition, splenomegaly, hepatitis with hepatic fibrosis and premature mortality. In addition, they suffer from chronic inflammation and exaggerated sensitivity to stress, and have been shown to develop more extensive and complex atherosclerotic lesions when bred on an Apo$E^{-/-}$ background (Poss and Tonegawa, 1997; Yet *et al.*, 2003). In man, HO-1 deficiency is a rare phenomenon and the first reported case was of a child that died at the age of six and suffered a chronic inflammatory illness characterised by intravascular haemolysis and heme-induced endothelial cell damage. The inability to handle free iron results in iron accumulation within, and enhanced oxidative modification of LDL, leading to endothelial damage, fatty streak and fibrous plaque formation within the vascular wall (Yachie *et al.*, 1999; Kawashima *et al.*, 2002). Furthermore, endothelial cells obtained from this patient were more susceptible to oxidative stress *in vitro* (Jeney *et al.*, 2002). These observations suggested that HO-1 is a critical vascular anti-oxidant and anti-inflammatory system in man.

Atherosclerosis, a multifactorial, progressive disease of large and medium-sized arteries characterised by EC dysfunction, vascular inflammation and the accumulation of lipids, fibrous materials, calcium and cellular debris within the vessel wall, is the most prevalent disease in developed countries (Cines *et al.*, 1998; Ross *et al.*, 1999). Numerous studies suggest that HO-1 is a readily inducible cytoprotective protein during atherogenesis exhibiting anti-inflammatory,

anti-oxidant and vasodilatory actions, as well as inhibitory effects on SMC proliferation. Atherosclerotic risk factors such as raised oxidised LDL, cigarette smoke and hypertension induce HO-1 (Ishizaka *et al.*, 1997; Ishikawa *et al.*, 1997; Favatier and Polla, 2001). Indeed, HO-1 expression is greatly upregulated in atherosclerotic plaques in all cell types and the degree of expression correlates with the severity of the lesion (Wang *et al.*, 1998; Morsi *et al.*, 2006). The multiple anti-inflammatory, anti-oxidant and cytoprotective properties of HO-1 are evident in several cell types involved in atherosclerosis. In endothelial cells, HO-1 overexpression inhibits ROS-mediated cell growth and apoptosis and attenuates macrophage-derived superoxide formation by inhibiting NADPH oxidase assembly and activity (Abraham *et al.*, 2003; Taille *et al.*, 2004). In addition, HO-1 inhibits TNF-α-mediated E-selectin and VCAM-1 upregulation thereby preventing leukocyte adhesion to the vascular endothelium, and attenuates oxidised LDL-induced transmigration of monocytes into the vascular wall (Kawamura *et al.*, 2005; Hayashi *et al.*, 1999; Soares *et al.*, 2004). HO-1 has an inhibitory effect on vascular SMC proliferation and migration, an important step in the process of atheroma formation, by decreasing the expression of endothelin-1 (ET-1) and placenta-derived growth factor (PDGF) (Morita and Kourembanas, 1995). Of note, these actions of HO-1 may be reproduced by its products biliverdin/bilirubin and CO.

The vascular protective effects of HO-1 have been demonstrated in several disease models involving HO-1 modulation and HO-1-deficient mice. Adenoviral-mediated induction of HO-1 attenuates vascular remodelling and neointima formation following balloon injury in rat carotid arteries, while concomitant administration of the HO-1 inhibitor SnPP abolishes this effect (Tulis *et al.*, 2001a; Tulis *et al.*, 2001b). Moreover, the HO-1 inducer probucol inhibits vascular SMC proliferation and decreases the intima-media ratio in balloon-injured rat aortas (Lau *et al.*, 2003; Deng *et al.*, 2004). LDL-deficient mice fed a high-cholesterol diet abundantly express HO-1 in atherosclerotic lesions (Alam, 1994). Moreover, HO-1 overexpression reduces atherosclerotic plaque formation in this disease model, whilst inhibition of HO activity increases plasma and tissue lipid peroxide levels and plaque formation (Ishikawa *et al.*, 2001). Yet and colleagues reported that mice deficient in both HO-1 and ApoE develop larger and more advanced atherosclerotic plaques, and more aggressive vein graft stenosis when compared to animals deficient in ApoE alone (Yet *et al.*, 2003). In contrast, selective overexpression of HO-1 using adenovirus-mediated gene transfer inhibits the development of atherosclerosis in $ApoE^{-/-}$ mice

(Juan *et al.*, 2001). Furthermore, adenoviral-mediated expression of HO-1 in the porcine vascular wall improves vascular function and inhibits SMC proliferation by activating a guanylate cyclase and cGMP-dependent pathway (Duckers *et al.*, 2001).

More recent studies have shown that the products of heme degradation carbon monoxide, biliverdin/bilirubin and an increase in intracellular ferritin are more likely to be responsible for the biological activity of HO-1 and its cytoprotective and anti-inflammatory functions (Brouard *et al.*, 2000; Soares *et al.*, 2004).

Carbon monoxide

Carbon monoxide (CO), although initially thought of as a toxic molecule, has profound influence on intracellular signalling processes, culminating in anti-inflammatory, anti-oxidant, and anti-apoptotic effects (Tenhunen *et al.*, 1969; Gozzelino *et al.*, 2010). CO is the best studied HO product and is most likely to be primarily responsible for many of the cytoprotective actions.

CO is a gaseous transcellular messenger mediating cytoprotection through activation of several signalling pathways. Like NO, CO interacts with soluble guanylate cyclase (sGC) resulting in elevation of cGMP levels that induce protective vascular relaxation (Pae *et al.*, 2008). In fact, endogenous HO-1-derived CO has been reported to elevate cGMP in vascular SMC, whilst inhibition of sGC completely abolishes vasodilation induced by CO in rabbit aortic rings (Morita *et al.*, 1995; Hussain *et al.*, 1997). Consistent with this, HO-1 inhibition attenuates hemin-induced vasodilation, suggesting a role for endogenous CO from vascular tissues in vasodilation (Wang *et al.*, 1997). Moreover, CO has been shown to inhibit platelet activation and aggregation via a guanylate cyclase/cGMP-dependent pathway (Brune and Ullrich, 1987). CO also suppresses the induction of plasminogen-activator inhibitor-1 (PAI-1) in macrophages, an important mediator of pulmonary microvascular thrombosis (Fujita *et al.*, 2001).

CO additionally exerts numerous anti-inflammatory, anti-apoptotic and anti-proliferative effects through MAPK-dependent signalling, but these may be dependent on cell type and stimuli (Morse and Sethi, 2002; Ryter *et al.*, 2006). CO suppresses the expression of pro-inflammatory cytokines such as TNF-α and IL-1β through modulation of p38 MAPK or JNK signalling pathways, and the

transcription factor AP-1, whilst enhancing the expression of anti-inflammatory mediators, including IL-10 (Otterbein *et al.*, 2000; Morse *et al.*, 2003; Ryter *et al.*, 2006).

The anti-proliferative effects of HO-1 on SMC and T-cells may also be attributed to CO. CO inhibits IL-2-dependent T-cell proliferation which may involve ERK and caspase-dependent pathways (Pae *et al.*, 2004; Song *et al.*, 2004). Similarly CO is shown to inhibit SMC proliferation and migration involving a guanylate cyclase and cGMP-dependent pathway, and this effect is associated with downregulation of endothelial-derived mitogens ET-1 and PDGF (Morita *et al.*, 1995; Morita and Kourembanas, 1995). CO also activates p38 MAPK signalling in SMC in turn inducing the expression of cell cycle inhibitor p21 and subsequent cell cycle arrest. Consistent with this, the anti-proliferative effect of CO is abolished in SMC from p21-deficient mice (Otterbein *et al.*, 2003).

Anti-apoptotic actions of CO were first demonstrated by *in vitro* studies showing enhanced protection against TNF-α-induced apoptosis in fibroblast and endothelial cultures exposed to exogenous CO (Petrache *et al.*, 2000; Brouard *et al.*, 2000). These effects mimic the anti-apoptotic effects observed with HO-1 overexpression and are exerted via the p38 MAPK signalling pathway in human EC (Brouard *et al.*, 2000). Furthermore, CO and HO-1 may inhibit TNF-α-mediated EC apoptosis through induction of anti-inflammatory genes Bcl-2, Bcl-XL, A1 and A20 via an NFκB-dependent pathway (Brouard *et al.*, 2002). Other signalling molecules which may regulate the cytoprotective effects of CO include STAT3 and HIF-1α (Otterbein *et al.*, 2003; Zhang *et al.*, 2006; Chin *et al.*, 2007). Moreover, CO exposure induces the expression of heat shock protein 70 in EC, which plays a critical role in protection against cytokine-induced apoptosis (Kim *et al.*, 2005). The anti-apoptotic effects of CO are reinforced by several animal models of disease. CO protects against liver ischaemia-reperfusion injury via activation of p38 MAPK (Amersi *et al.*, 2002), and improved survival rates of HO-1-deficient mice in an ischaemic lung injury model (Fujita *et al.*, 2001). Thus, CO mediates many of the cytoprotective effects of HO-1, which contribute to the maintenance of vascular homeostasis during inflammation and vascular injury.

Biliverdin and bilirubin

There is increasing evidence that the bile pigments biliverdin and bilirubin mediate some of the vascular protective functions of HO-1, in turn preserving EC integrity and survival, enhancing EC reactivity, and inhibiting restenosis (Ryter *et al.*, 2006).

The protective effects of biliverdin/bilirubin have been demonstrated in multiple *in vitro* and *in vivo* studies. In fact, hyperbilirubinemic rats displayed reduced expression of oxidative stress markers in response to hyperoxia, and protection against ischaemic/reperfusion injury when compared to wild type animals (Dennery *et al.*, 1995; Kitamura *et al.*, 2003). In addition, the protective effects of biliverdin/bilirubin have been demonstrated in other models of vascular inflammation including cardiac allograft rejection and post-angioplasty restenosis (Yamashita *et al.*, 2004; Ollinger *et al.*, 2005; Ollinger *et al.*, 2007), and bilirubin plasma and serum concentration levels have been shown to inversely correlate with the risk of coronary artery disease and severity of atherosclerosis in man (Schwertner *et al.*,1994; Novotny and Vitek, 2003; Schwertner and Vitek, 2008). The bile pigments biliverdin and bilirubin have been demonstrated to exhibit potent anti-oxidant properties which may account for their anti-atherogenic effects. In fact, biliverdin and bilirubin can directly scavenge ROS, inhibit the oxidation of LDL and other lipids, interact with the free radical NO and the oxidant peroxinitrite and counteract oxidative stress overall (Neuzil and Stocker, 1994; Stocker *et al.*, 1987; Schwertner *et al.*, 1998; Mancuso *et al.*, 2006). Bilirubin also exerts anti-inflammatory and anti-proliferative actions, including inhibition of the inflammatory adhesion proteins VCAM-1, P- and E-selectin and abrogation of leukocyte trafficking (Hayashi *et al.*, 1999; Keshavan *et al.*, 2005). HO-1-derived bilirubin also attenuates EC activation and dysfunction (Kawamura *et al.*, 2005). Moreover, biliverdin treatment inhibits NFκB activation in response to TNF-α and LPS (Gibbs and Maines, 2007; Wegiel *et al.*, 2009).

The anti-proliferative effects of biliverdin/bilirubin were demonstrated in vascular SMC. Administration of exogenous biliverdin/bilirubin resulted in G_1-phase cell cycle arrest, an effect associated with diminished expression of positive cell cycle regulators, including A-, D-, and E-type cyclins as well as Cdk2, resulting in hypophosphorylation and activation of pRb (Ollinger *et al.*, 2005). In addition, recent work from our laboratory demonstrated that HO-1-derived bilirubin protects EC from complement-dependent injury through induction of decay-accelerating factor

(DAF) (Kinderlerer *et al.*, 2009). The notion that oxidation of bilirubin by ROS results in the formation of biliverdin, which in turn is reduced to bilirubin by BVR, led to the postulation that this increase in bilirubin augments the protective properties of biliverdin/bilirubin, forming a cytoprotective amplification loop (Baranano *et al.*, 2002). This might relate to the ability of biliverdin reductase to exhibit serine/threonine and tyrosine activity. Indeed, BVR has been identified as a signalling molecule in various cytoprotective pathways (Salim *et al.*, 2001; Lerner-Marmarosh *et al.*, 2005). Thus, phosphorylation of cell surface-associated BVR leads to phosphorylation and activation of Akt/PKB via PI3K signalling, thereby enhancing the production of IL-10 in various cell types including macrophages and EC (Wegiel *et al.*, 2009). Furthermore, BVR also activates signalling pathways involving MAPKs and protein kinase C by direct interaction and phosphorylation (Amit and Boneh, 1993; Hansen *et al.*, 1996). Thus, the bile pigments biliverdin and bilirubin as well as biliverdin reductase represent a distinct pathway with various anti-oxidant and anti-inflammatory effects which ultimately confer vascular protection.

Ferrous iron and ferritin

Ferrous iron (Fe^{2+}), is an extremely pro-oxidative molecule and is released during the breakdown of free heme by HO-1, but is rapidly removed by ferritin. Ferritin is a ubiquitously existing intracellular multimeric protein complex consisting of a heavy chain and a light chain subunit (Harrison and Arosio, 1996). Ferritin is able to effectively sequester intracellular iron and, hence, limits the pro-oxidant capacity of Fe^{2+} by catalysing the oxidation to the ferric form Fe^{3+} (Balla *et al.*, 1992; Berberat *et al.*, 2003). It is likely that increased ferritin expression in conjunction with HO-1 expression may contribute to additional protection afforded by HO-1 (Balla *et al.*, 1992; Ryter *et al.*, 2006). Indeed, ferritin co-localises with HO-1 in atherosclerotic lesions and its expression is significantly upregulated in various cell types present in atherosclerotic plaques including macrophages, fibroblasts and EC, and this may confer protection against oxidised LDL (Juckett *et al.*, 1995). Ferritin also demonstrates EC anti-apoptotic effects, inhibits complement activation by enhancing endothelial DAF expression and may inhibit cytokine-induced leukocyte adhesion molecule upregulation (Pham *et al.*, 2004; Soares *et al.*, 2004; Kinderlerer *et al.*, 2009). *In vivo*, the salutary effects of ferritin appear to be dependent on the disease model and cell type.

In a rat model of endotoxic shock, ferritin and iron dosing was insufficient to offer protection (Otterbein *et al.*, 1997). However, overexpression of FHC attenuated ischaemia-reperfusion-induced liver injury and protected EC and hepatocytes from apoptosis (Berberat *et al.*, 2003).

The recognition of the highly inducible properties of HO-1 in conjunction with its multiple anti-inflammatory, anti-oxidant, and anti-apoptotic properties have aroused interest in HO-1 and its products as a therapeutic target for several varied inflammatory diseases including atherosclerosis, transplant rejection and ischaemia-reperfusion injury.

1.3.4. HO-1 and angiogenesis

Reparative and pathological angiogenesis is driven by various inflammatory mediators that influence the synthesis of growth factors. Indeed, reactive oxygen species and nitric oxide have been shown to regulate the synthesis and activity of VEGF, the most important molecule controlling blood vessel morphogenesis (Chua *et al.*, 1998; Murohara and Asahara, 2002; Ushio-Fukai, 2006). Moreover, expression of the cytoprotective enzyme HO-1, which is also induced by ROS and NO in the vascular endothelium, has been shown to be upregulated in response to VEGF, indicating a potential role for HO-1 in the regulation of VEGF-mediated angiogenesis. Data to date suggest that HO-1 may influence angiogenesis at various levels, affecting the proliferative and migratory capacities of endothelial cells as well as their subsequent formation into lumenised vessels.

The first evidence came from Deramaudt and colleagues in 1998, demonstrating that gene transfer of human HO-1 into coronary EC enhances their proliferation and formation of capillary-like structures (Deramaudt *et al.*, 1998). HO-1 overexpression promotes cell cycle progression of EC, but has contrary effects on that of vascular SMC (Li Volti *et al.*, 2002). Moreover, in vascular SMC, HO-1-derived CO has been shown to activate p38 MAPK signalling and upregulate caveolin-1, which in turn inhibits cell proliferation (Kim *et al.*, 2005). Supportive of the proliferative effects of HO-1 in the endothelium, studies from our laboratory show that overexpression of HO-1 utilising a recombinant adenovirus expressing the human HO-1 gene increases proliferation of EC isolated from human umbilical veins (Bussolati and Mason, 2006). In contrast, inhibition of HO-1 decreases EC proliferation, capillary formation, and cell cycle progression (Bussolati *et al.*, 2004; Li Volti *et al.*, 2005). Moreover, this effect is associated with an increased expression of the cell cycle inhibitors p21 and p27, and is restored by CO but not bilirubin (Li Volti *et al.*, 2005). The proliferative effects of HO-1 are reinforced by studies utilising aortic EC isolated from HO-1-deficient mice. When compared to HO-$1^{+/+}$ littermate controls, HO-$1^{-/-}$ MAEC demonstrate reduced proliferation (Chen *et al.*, 2004).

HO-1 may indirectly affect angiogenesis through its ability to increase VEGF synthesis. In fact, augmentation of HO-1 by inducers such as heme, cobalt protoporphyrin (CoPP), prostaglandin J_2 (PGJ_2), hydrogen peroxide (H_2O_2), or hypoxia leads to stimulation of VEGF synthesis in a HO-1-

dependent manner (Dulak *et al.*, 2002; Jozkowicz *et al.*, 2002; Marinissen *et al.*, 2006; Dulak *et al.*, 2008). Consistent with these findings, overexpression of HO-1 in vascular SMC and EC increases the production of VEGF, whilst the pharmacological antagonists SnPP and ZnPP inhibit hypoxia- and PGJ_2-induced VEGF biosynthesis (Dulak *et al.*, 2002; Jozkowicz *et al.*, 2002; Jozkowicz *et al.*, 2003). Furthermore, MAEC deficient in HO-$1^{-/-}$ show decreased VEGF synthesis in response to H_2O_2 (Ciscowski *et al.*, 2005). In a rat model of hindlimb ischaemia, overexpression of HO-1 enhances VEGF synthesis and augments the formation of vascular capillaries, and in turn improves blood flow in ischaemic tissues, an effect abolished by a pharmacologic antagonist of HO-1, ZnPP (Suzuki *et al.*, 2003). HO-1 overexpression promotes VEGF synthesis and modulates foetal growth in the rat (Kreiser *et al.*, 2002). Besides acting as an inducer of VEGF, HO-1 appears to be involved downstream of the VEGF-mediated activation of EC, further supporting the role for HO-1 in angiogenesis. Indeed, the pro-angiogenic factor VEGF and more recently stromal cell-derived factor-1 alpha (SDF-1α) have been shown to activate HO-1 expression and activity in the vascular endothelium (Bussolati *et al.*, 2004; Deshane *et al.*, 2007).

Studies from our laboratory demonstrated increased HO-1 expression in response to VEGF in primary human EC and EC of the dermal microvasculature, in turn modulating their angiogenic capacities. Induction of HO-1 with CoPP alone results in EC proliferation comparable to that seen with VEGF, whilst inhibition of HO-1 using the synthetic antagonist SnPP or ZnPP attenuates VEGF-induced EC proliferation *in vitro* (Bussolati *et al.*, 2004). Moreover, HO-1 inhibition prevents development of VEGF-induced neovessels *in vitro* and also *in vivo* and *ex vivo* (Bussolati *et al.*, 2004). In concordance with these findings, VEGF increases HO-1 protein expression in the chick embryo chorioallantoic membrane, an effect inhibited by staurosporine, indicating a potential role for protein kinase C (PKC) (Fernandez and Bonkovsky, 2003). Furthermore, the chemokine SDF-1α, an important regulator of endothelial progenitor cell migration and recruitment to sites of ischaemic injury, has been linked to HO-1-driven angiogenesis. Deshane and colleagues demonstrated that exposure to SDF-1α results in a marked upregulation of HO-1 mRNA and protein in human aortic EC (HAEC). Moreover, pharmacological and genetic inhibition of HO-1 impaired SDF-1α mediated endothelial tube formation, an effect reversed by a CO donor, CO-releasing molecule (CORM-2), but not bilirubin. This study further confirms the functional significance of HO-1 in angiogenesis by using the Matrigel plug and wound healing models in the

HO-1$^{-/-}$ mouse, demonstrating a close association of HO-1 deficiency with impaired neovascularisation and wound healing in injured tissue (Deshane *et al.*, 2007).

A role for HO-1 in endothelial migration is emerging but so far poorly understood. Exposure to the HO-1 antagonist SnPP inhibits VEGF-induced migration of primary human EC as assessed using a modified Boyden chamber (Jozkowicz *et al.*, 2003). Genetic inhibition of HO-1 in HAEC abrogates their migratory capacity in response to SDF-1α, an effect also seen in aortic EC and EPC isolated from HO-1 knockout mice (Deshane *et al.*, 2007). Moreover, the migratory properties of HO-1 overexpressing coronary microvascular EC are enhanced, as demonstrated by increased propensity to form vascular tubes in Matrigel (Deramaudt *et al.*, 1998).

The importance of HO-1 in angiogenesis is confirmed *in vivo*. Even though, HO-1-deficient mice show no obvious phenotype suggestive of defective vascular morphogenesis, the infertility of female HO-1 null mice and the high mortality rate of embryos lacking the functional HO-1 gene suggests an effect of HO-1 on developmental angiogenesis (Bainbridge and Smith, 2005; Zenclussen *et al.*, 2007; Gozzelino *et al.*, 2010). HO-1 overexpression enhances VEGF levels in the rat placenta and this is associated with increased pup size (Kreiser *et al.*, 2002). In addition, VEGF treatment increases angiogenesis simultaneously with HO-1 expression during chick embryo development, an effect attenuated by HO-1 inhibition (Fernandez and Bonkovsky, 2003). Consistent with this, HO-1 deficiency has been associated with pregnancy-related disorders such as recurrent miscarriages, intrauterine growth restriction and preeclampsia (Yachie *et al.*, 1999; Bainbridge and Smith, 2005; Lyall and Myatt, 2002). Preeclampsia is a medical condition occurring during pregnancy and the postpartum period and is characterised by hypertension and proteinuria. Moreover, preeclampsia is associated with endothelial dysfunction and elevated plasma levels of anti-angiogenic mediators soluble Flt1 (sFlt1) and soluble endoglin (sEng). Interestingly, when compared with matched wild-type controls, plasma of HO-1$^{-/-}$ mice contains higher levels of sFlt1 and sEng (Cudmore *et al.*, 2007). Accordingly, HO-1 inhibition potentiates VEGF-mediated sFLt1 release and IFNγ and TNF-α-induced sEng release from placental villous explants and EC, while adenoviral-mediated HO-1 overexpression inhibits this effect (Cudmore *et al.*, 2007). Supportive of a role for HO-1 in postnatal *in vivo* angiogenesis are the observations that pharmacological or genetic inhibition of HO-1 diminishes neovascularisation in wounded

tissues and impairs cutaneous wound healing in mice (Grochot-Przeczek *et al.*, 2009). Moreover, human HO-1 deficiency revealed both prominent intravascular haemolysis and EC dysfunction (Yachie *et al.*, 1999; Kawashima *et al.*, 2002).

Beside its role in vascular remodelling and reparative angiogenesis a link between HO-1 and pathological angiogenesis has been proposed. Indeed, several human tumours express high levels of HO-1, including renal and prostate cancer (Goodman *et al.*, 1997; Maines and Abrahamsson, 1996; Was *et al*., 2006; Fang *et al.*, 2003). Numerous *in vitro* and *in vivo* studies support the influence of HO-1 on carcinogenesis and tumour growth. However, a pro- or anti-proliferative effect of HO-1 on cancer cells appears to be highly tissue-specific (Was *et al.*, 2010; Degese *et al.*, 2012). On one hand, HO-1 accelerates pancreatic cancer growth by promoting tumour angiogenesis in mice, whilst HO-1 inhibition increases their responsiveness to anti-cancer therapy (Sunamura *et al.*, 2003; Berberat *et al.*, 2005). Consistent with this, HO-1 deficiency causes enhanced tumour regression in severe combined immune deficient (SCID) mice and reduces tumour growth in a mouse model of lung cancer (Fang *et al.*, 2003; Hirai *et al.*, 2007). On the other hand, protective, anti-tumour effects of HO-1 have been demonstrated in hepatoma and breast cancer. HO-1 inhibits the proliferation of breast carcinoma cells and induces apoptosis in these cells. Moreover, the chemopreventive agent sulforaphane contributes to tumour growth suppression through induction of HO-1 in hepatoma and breast cancer cells (Hill *et al.*, 2005; Keum *et al.*, 2006; Cornblatt *et al.*, 2007; Lin *et al.*, 2008).

The constitutive HO isoform, HO-2, may also play a role in inflammation and angiogenesis. Animals lacking HO-2 demonstrate impaired corneal wound healing, enhanced neovascularisation, and exaggerated inflammation (Seta *et al.*, 2006). Murine aortic EC from HO-2 null mice show an activated phenotype marked by oxidative stress, inflammation and angiogenesis (Bellner *et al.*, 2009). Interestingly, while HO-1 expression is downregulated in corneal tissue from HO-$2^{-/-}$ mice, MAEC from these animals show increased HO-1 levels. However, enzymatic activity of HO is significantly diminished in both and may account for the aggregated inflammation-dependent angiogenesis. These findings support a dual role for HO-1 in angiogenesis as postulated previously by our laboratory. Here, VEGF-mediated activation of HO-1 favours endothelial proliferation and prevents EC apoptosis, while anti-inflammatory actions of

HO-1 inhibit leukocyte migration, thus resulting in non-inflammatory angiogenesis. In contrast, inhibition of HO-1 activity increases leukocyte migration and subsequent local release of pro-angiogenic growth factors, so inducing inflammatory angiogenesis. Indeed, pharmacological inhibition of HO-1 by SnPP or ZnPP significantly increased vascularisation in an *in vivo* angiogenesis model, an effect associated with increased leukocyte infiltration. CoPP treatment however, significantly decreased LPS-induced angiogenesis and pro-inflammatory leukocytic infiltration into a Matrigel plug (Bussolati *et al.*, 2004; Bussolati and Mason, 2006).

A role in angiogenesis for the products of heme catabolism by HO enzymes, namely CO, biliverdin/bilirubin and ferrous iron has also been proposed but remains poorly understood (Fig. 1.12.). Exogenous CO induces proliferation of rat aortic EC and enhances their migratory capacity (Wegiel *et al.*, 2010). Low concentrations of CO are protective in EC and inhibit apoptosis through a p38 MAPK-dependent pathway. Thus, a reduced rate of apoptosis may also contribute to CO-mediated proliferation. Moreover, CO induces the production of angiogenic mediators. Indeed, CO supplementation increases HO-1 expression but also augments the synthesis of VEGF and SDF-1α and potentiates their synergistic effects on EC (Jozkowicz *et al.*, 2003; Lin *et al.*, 2009). Consistent with this, CO has been shown to significantly enhance VEGF synthesis in various organs in an animal model (Martin and Risau, 1998). In addition, CO exposure results in increased expression of the pro-angiogenic factor IL-8, but decreases the expression of anti-angiogenic factor sFlt1 and sEng. CO-mediated increase in pro-angiogenic mediators in turn results in enhanced endothelial proliferation and migration, and augmentation of vessel formation (Cudmore *et al.*, 2007; Dulak *et al.*, 2008; Kim *et al.*, 2011). Moreover, CO restores the impaired angiogenic responses of HO-1-deficient EC and EPC and enhances re-endothelisation after vascular injury by increasing circulating SDF-1α in a mouse model (Li Volti *et al.*, 2005; Deshane *et al.*, 2007).

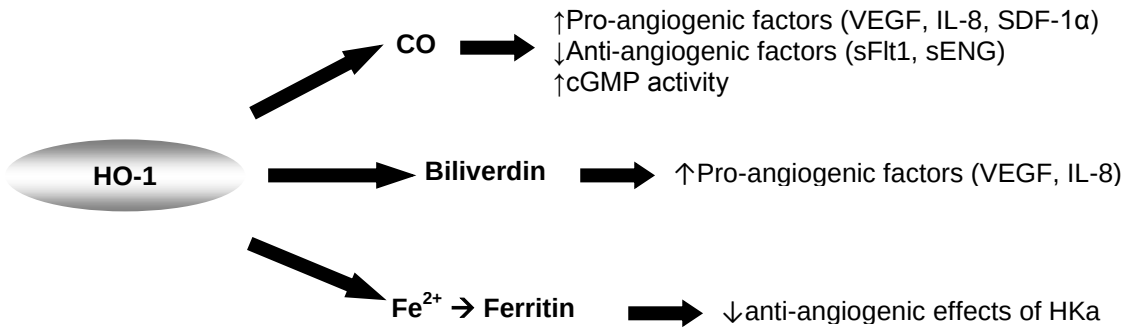

Figure 1. 14.: Pro-angiogenic effects of HO products. CO synthesised by the catalytic reaction of HO-1 induces the production of angiogenic mediators such as VEGF, IL-8 and SDF-1α, decreases the anti-angiogenic mediators soluble VEGF-R1 (sFlt1) and soluble endoglin (sEng) and increases soluble guanylate cyclase activity (cGMP). Biliverdin stimulates the induction of pro-angiogenic factors, such as VEGF and IL-8 in human keratinocytes. Ferritin binds cleaved high molecular weight kininogen (HKa) and antagonises its anti-angiogenic effects.

Iron can influence angiogenesis by acting as a co-factor for enzymes involved in the regulation of VEGF synthesis, or by enhancing oxidative stress through the Fenton reaction and formation of noxious hydroxyl radicals. On the other hand, ferrous iron induces the expression of ferritin, which acts as an anti-oxidant by catalysing the oxidation of toxic ferrous iron to its non-toxic form, ferric iron (Ponka, 1999; Watts, 2003). Potential pro-angiogenic effects of ferritin have been demonstrated by Coffman and colleagues. High molecular weight kininogen (HKa) acts as a potent inhibitor of angiogenesis by inducing the apoptosis of proliferating EC. Supplementation with serum ferritin significantly inhibited the anti-angiogenic effects of HKa, improving EC proliferation, migration and subsequent organisation into luminal vessel-like structures on Matrigel *in vitro* (Coffman *et al.*, 2009). Moreover, treatment of vascular SMC with the iron chelator deferoxamine mesylate (DFO) results in increased VEGF synthesis, and this may in turn indirectly promote angiogenesis (Dulak *et al.*, 2002).

The effects of biliverdin and bilirubin on angiogenesis are largely unknown and may be cell type-specific. Biliverdin has been shown to stimulate the production of pro-angiogenic factors such as VEGF and IL-1 in human keratinocytes in an ERK-dependent manner, but no biliverdin-mediated effect on VEGF expression was observed either in rat vascular SMC or in a human endothelial cell line (Dulak *et al.*, 2002; Jawza *et al.*, 2006; Lobada *et al.*, 2008).

1.4. HYPOTHESIS AND AIMS

Increasing evidence clearly demonstrates the functional importance of the cytoprotective enzyme HO-1 in the regulation of physiological and reparative but also pathological angiogenesis and data to date suggest that HO-1 may influence the angiogenic process at various levels. Based on these observations we hypothesised that the cytoprotective enzyme HO-1 and its products play an important role in VEGF-driven angiogenesis, whereby VEGF increases HO-1 expression and activity which in turn results in enhanced endothelial proliferation and migration and subsequent organisation into lumenised vessels. However, the precise transcriptional and signalling mechanisms through which HO-1 exerts its effects during angiogenesis and the role of the HO products CO, biliverdin/bilirubin, and iron remain elusive. A better understanding of the angiogenic effects of HO-1 may in turn reveal novel therapeutic targets for the manipulation of angiogenesis at sites of ischaemia and wound healing, or conversely to inhibit angiogenesis associated with atherosclerosis or tumourogenesis. Therefore, the aim of my work is to further elucidate the specific role of HO-1 and its products in the regulation of VEGF-induced angiogenesis, using a variety of *in vitro* and *in vivo* angiogenesis assays. In particular, this includes the following aims:

- To identify the transcriptional and signalling mechanisms regulating the induction of the cytoprotective enzyme HO-1 by the pro-angiogenic mediator VEGF
- To establish the functional importance of HO-1 during different stages of angiogenesis *in vitro*.
- To identify novel HO-1 downstream targets and to investigate their role in the regulation of VEGF-induced angiogenesis
- To elucidate the functional importance of HO-1 and its target proteins in *in vivo* angiogenesis.

CHAPTER 2 - MATERIALS AND METHODS

2.1. MATERIALS

2.1.1. Antibodies

The following primary and monoclonal antibodies (mAb) were used: Bcl-2 (C-2) mAb, cyclin A (B-8) mAb, and retinoblastoma protein (Rb; C-2) mAb were purchased from Santa Cruz Biotechnology, Inc. (Santa Cruz, California, USA). HO-1 mAb and anti-vimentin [RV202] mAb were from Stressgen (Exeter, UK) and Abcam plc (Cambridge, UK) respectively. Anti-VASP (9A2) was from Cell Signaling Technology, Inc. (Danvers, MA, USA). The anti-α-tubulin mAb was from Sigma-Aldrich Ltd. (Poole, Dorset, UK) and GAPDH mAb and anti-integrin $\alpha_v\beta_3$, clone LM609 were both purchased from Millipore (Billerica, MA, USA).

The polyclonal antibodies against HO-1 (H-105), Bcl-xl (H-62) and anti-PKCε were from Santa Cruz Biotechnology, Inc., and anti-phospho-PKCε (Ser^{729}) was from Millipore. HO-2 and anti-retinoblastoma (Rb) [pT^{821}] phosphospecific antibodies were purchased from Stressgen and Invitrogen (Paisley, UK), respectively. Anti-Phospho-VASP (Ser^{239}) was from Cell Signaling Technology, Inc.

The anti-VCAM-1 mAb 1.4C3 was generated in house. RMAC8 (anti-endoglin) was a kind gift from Dr A. d'Apice (St Vincent's Hospital, Victoria, Australia) and the anti-ICAM-2 mAB CBR-IC/2 was kindly provided by D. T. Springer (Harvard University, Cambridge, MA, USA). P2B1α (anti-CD31) was purchased from the Developmental Studies Hybridoma Bank (University of Iowa, Iowa, USA) and PCNA (PC-10) was from Santa Cruz Biotechnology, Inc.

The following secondary Abs were used: Fluorescein isothiocyanate (FITC)-labelled polyclonal rabbit anti-mouse immunoglobulin, swine anti-rabbit immunoglobulin/horseradish peroxidase (HRP), goat anti-mouse immunoglobulins/HRP were all purchased from DAKO (Glostrup, Denmark). Goat anti-mouse IgG1 Alexa Fluor 568, goat anti-mouse IgG1 Alexa Fluor 488 and goat anti-rabbit IgG1 Alexa Fluor 568 were from Invitrogen. A list of all antibody working dilutions used in this study is provided in the Appendix (Tab A.1. to Tab. A.6.).

2.1.2. Animals

Eight to ten-week old female C57BL/6 mice were purchased from Harlan Laboratories, Inc. (Bicester, Oxford, UK) and housed under controlled climatic conditions in microisolator cages with autoclaved bedding. Irradiated food and drinking water were readily available. All of the animals were housed and studied according to UK Home Office guidelines. Sentinel mice were housed alongside test animals and regularly screened for a standard panel of murine pathogens.

2.1.3. Compounds

Recombinant human $VEGF_{165}$ and recombinant human SDF-1α (CXCL12) were purchased from PeproTech EC Ltd., London, UK and reconstituted in 3% bovine serum albumin (BSA; Sigma-Aldrich Ltd.) in ultrapure water (H_2O; Millipore) to stock solutions of 1 mg/ml. Hemin and zinc (II) protoporphyrin IX chloride (ZnPP) were both obtained from Frontier Scientific (Logan, UT, USA) and dissolved in dimethyl sulfoxide (DMSO; Sigma-Aldrich Ltd.) to a stock concentration of 100 mM and 25 mM, respectively. Tricarbonyldichlorouthenium(II) dimer (CORM-2) and deferoxamine mesylate (DFO) were both from Sigma-Aldrich Ltd.. CORM-2 was dissolved in DMSO to a stock concentration of 50 mM and DFO was dissolved in ultrapure H_2O to a stock concentration of 10 mM. The enzyme-triggered CORMs (ET-CORMs) Stro074, SROM158, and Stro258 were all kind gifts from Prof H. G. Schmalz (Universität zu Köln, Köln, Germany) and dissolved in DMSO to stock concentrations of 100 mM. Actinomycin D was from Sigma-Aldrich Ltd. and dissolved in DMSO to stock concentration of 1 mg/ml.

2.1.4. Adenoviruses

The recombinant adenovirus expressing the HO-1 gene (AdHO-1) was a kind gift from Dr M. Soares (Instituto Gulbenkian de Ciencia, Oeiras, Portugal). Adenoviruses with an empty vector (Ad0) were provided by Dr E. Paleolog (Oxford University, Oxford, UK) and used as a control. Adenoviruses were amplified in human embryonic kidney (HEK) 293A cells in Dulbecco's Modified Eagle Medium (DMEM; Invitrogen) with 10% fetal calf serum (FCS; Biosera, Ringmer, UK) and grown at 37°C in 5% CO_2. When the cell monolayer reached 60-80% confluence, cells

were infected with the appropriate adenovirus. The infected cells were cultured at 37°C in 5% CO_2 for 3-5 days until HEK cells showed cytopathic effects, characterised by a round cell morphology and detachment from the culture flask. HEK293A cells were then harvested by pipetting, transferred into 50 ml tubes, and pelleted by centrifugation. The cell pellet was resuspended in 10 ml of the supernatant and the remaining supernatant was decanted into a sterile container and kept at 4°C. The cell suspension was freeze/thawed three times to disrupt the cells, and cell debris was pelleted by centrifugation at 3,500 x g for 15 min. The supernatant was removed and the previously reserved supernatant added. Adenoviruses were then purified using the AdEasyTM Virus Purification Kit (Stratagen, La Jolla, CA, USA) following the manufacturer's instructions. Purified adenoviruses were then titred using the Adeno-XTM Rapid Titer Kit (Clontech Laboratories Inc., Mountain View, CA, USA). The infectious units per ml (ifu/ml) for each virus was calculated as follows:

$$\text{Ifu/ml} = \frac{(\text{mean infected cell/field}) \times (\text{fields/well})}{\text{volume virus (ml)} \times (\text{dilution factor}).}$$

2.1.5. Cell Culture Reagents

Collagenase type II: Roche Diagnostics Ltd., West Sussex, UK. 2% gelatin and phosphate-buffered saline (PBS) with calcium (Ca^{2+}) and magnesium (Mg^{2+}): purchased from Gibco BRL Life Technologies, Paisley, UK. Heparin (1,000 U/ml): Leo Laboratories, Princes Risborough, UK. Fetal calf serum: Biosera, Ringmer, UK. EC culture medium 199 (M199), EC growth supplement (ECGS; 30 µg/ml), penicillin (100 IU/ml), streptomycin (0.1 mg/ml), and L-glutamine (2 mmol/L): all purchased from Sigma-Aldrich Ltd. EC culture medium MCDB-131 and Optimen: both Gibco BRL Life Technologies. Hank's balanced salt solution with Ca^{2+} and Mg^{2+} (HBSS) or without Ca^{2+} and Mg^{2+} (HBSS w/o), trypsin/ethylenediaminetetraacetic acid (EDTA): Sigma-Aldrich Ltd. Endothelial basal medium (EBM)-2 and endothelial growth medium (EGM)-2 supplemented with 2% fetal bovine serum (FBS), hydrocortisone, human fibroblast growth factor beta (h-FGF-β), VEGF, insulin-like growth factor analogue (R^3-IGF-1), ascorbic acid, human endothelial growth factor (hEGF), gentamicin, amphotericin-B (GA), and heparin: all purchased from Lonza, Basel, Switzerland. The 25 cm^2 and 75 cm^2 tissue culture flasks (T25 and T75) were from: Costar,

Cambridge, MA, USA. 6-well, 12-well, and 24-well tissue culture plates: Nunc, Thermo Fisher Scientific, Rochester, NY, USA. Flat bottom 96-well plates: Corning B. V. Life Sciences, Amsterdam, Netherlands.

2.1.6. Reagents and Apparatus for Western Blotting

Protein lysis: RIPA buffer was purchased from Thermo Fisher Scientific. Complete protease inhibitor cocktail and PhosSTOP phosphatase inhibitor cocktail: both Roche Diagnostics Ltd (Burgess Hill, West Sussex, UK).

Protein quantification: Bio-Rad Dc protein assay kit (Bio-Rad Laboratories, Hemel Hempstead, Herfordshire, UK) containing 250 ml alkaline copper tartrate solution (solution A), 2 ml dilute Folin reagent (solution B), 5 ml surfactant solution (solution S). Bovine gamma-globulin standard: Bio-Rad Laboratories.

Sodium dodecyl sulphate-polyacrylamide gel electrophoresis (SDS-Page): The XCell *SureLock*^{c} Mini-Cell was purchased from Invitrogen. NuPAGE® Novex System reagents and apparatus included: NuPAGE® Novex 10% or 4-12% Bis-Tris Gel 1.0 mm, 10 well or 10% Bis-Tris Gel, 1.5 mm, 15 well; NuPAGE® MOPS SDS Running Buffer (20X); NuPAGE® LDS Sample Buffer (4X); Protein size marker: SeaBlue Plus2 Pre-Stained Standard: all purchased from Invitrogen. DL-Dithiothreitol (DTT) was from Sigma-Aldrich Ltd. The Phos-tag™ SDS-Page System included: Phos-tag™ Acrylamide AAL-107: Wako Chemicals GmbH, Neuss, Germany. Acrylamide/Bis-acrylamide, 30% solution (29:1); manganese(II) chloride ($MnCl_2$), SDS, hydrochloric acid (HCl), Trizma^{c} base (Tris); N,N,N',N'-Tetramethylethylenediamine (TEMED); diammonium peroxydisulfate ($(NH_4)_2S_2O_8$): all Sigma-Aldrich Ltd. Novex® Sharp Unstained Protein Standard, Novex® Gel Cassettes, 1 mm, and Novex® combs, 1 mm, 10-well were all purchased from Invitrogen.

Transfer System: Trans-Blot SD Semi-Dry Transfer cell and 10X Tris/Glycine transfer buffer were from Bio-Rad. Immobilon™-P transfer membrane: Millipore.

Signal detection: Blocking buffer and Ab dilution buffer: 1X Tris buffered saline and Tween 20 (TBS-T) containing 5% BSA: all Sigma-Aldrich Ltd. Western Blotting Detection Reagents:

Amersham ECL™ (enhanced chemiluminescence) or Amersham ECL Plus™ Western Blotting Detection Reagents (GE Healthcare, Little Chalfont, Buckinghamshire, UK). Developing films: Kodak XOMat film (Sigma-Aldrich Ltd.). Developing machine: Compact X4 X-ray film processor (Xograph Healthcare Ltd., Tetbury, Gloucestershire, UK). Densitometry: ImageJ analysis software (National Institutes of Health, Bethesda, Maryland, USA).

2.1.7. HO-1 promoter constructs and luciferase reporter vectors

The HO-1 promoter construct pHOGL3/9.4 was kindly provided by Prof A. Agarwal (University of Alabama at Birmingham, Birmingham, Alabama, USA) and the plasmids pGL3-hHO4.9luc, pGL3-hHO2.2luc, and pGL3-hHO0.3luc were kind gifts from Prof N. Leitinger (Department of Vascular Biology and Thrombosis Research, University of Vienna, Vienna, Austria). pGL3-Basic luciferase reporter vector without the promoter insert (Promega, Madison, WI, USA) was used as a procedure control. pGL4.74[*hRluc*/TK] reporter vector (Promega) containing an herpes simplex virus thymidine kinase (HSV-TK) promoter and synthetic *Renilla* luciferase gene was used as the control vector for the dual luciferase reporter assay.

All plasmids were transformed in *Escherichia coli* (*E. coli*) DH5α competent cells (Invitrogen) and plasmid DNA was purified using the QIAGEN Plasmid Maxiprep Kit (Qiagen Ltd., Crawley, West Sussex, UK) in accordance with the manufacturer's instructions.

2.1.8. Reagents for Dual-Luciferase® Reporter Assay

The Dual-Luciferase® Reporter Assay System (DLR™ assay), containing Luciferase Assay Buffer II, Luciferase Assay Substrate, Stop&Glo® Buffer, Stop&Glo® Substrate, and 5X Passive Lysis Buffer (PLB) was purchased from Promega. The luminescence generated by the DLR™ assay was measured by a Biotek Synergy™ 4 Multi-Mode Microplate Reader (BioTek Instruments, Inc., Vermont, USA).

2.2. METHODS

2.2.1. Isolation and culture of endothelial cells

Human umbilical cords were donated by the Department of Obstetrics, Queen Charlotte's Hospital. The use of human umbilical vein endothelial cells (HUVEC) was approved by Hammersmith Hospital Research Ethics Committee (ref. no. 06/Q0406/21).

Fresh umbilical cords obtained at normal deliveries were stored in HBSS containing 0.1 mg/ml gentamicin and 1 mmol/l sodium pyruvate at 4°C. HUVEC were isolated from umbilical cords by digestion with collagenase type II based on a modified method from Jaffe *et al.* (1973). In brief, the umbilical vein was identified and washed with 50 ml HBSS w/o to remove blood in the lumen. The vein was then filled with 25 ml 0.5 mg/ml collagenase dissolved in HBSS w/o and incubated for 8 min at 37°C in 5% CO_2. After incubation, the cord was gently massaged to encourage cell detachment from extracellular matrix and the collagenase solution containing the EC was collected from the cord. The cord was then flushed with 25 ml HBSS w/o, which was added to the collagenase solution. To recover cells, the pooled solution was centrifuged at 335 x g for 10 min (Allegra X–15R Centrifuge, Beckman Coulter Ltd., High Wycombe, UK) and transferred to a 25 cm^2 1% gelatin-coated tissue culture flask containing complete M199 medium supplemented with 20% FCS, 100 IU/ml penicillin, 0.1 mg/ml streptomycin, 2 mmol/L L-glutamine, 10 U/ml heparin, and 30 µg/ml ECGS. The day after isolation, the cells were washed with HBSS twice and medium replaced. Upon confluency, EC were harvested by trypsin/EDTA and passaged into 75 cm^2 1% gelatin-coated tissue culture flasks. The morphological and molecular characteristics of isolated EC used in this study are detailed in Chapter 3.

2.2.2. Culture of human dermal microvascular endothelial cells

The human dermal microvascular endothelial cell line (HMEC-1) was a kind gift from Dr E. Ades (CDC Atlanta, USA). HMEC-1 were originally isolated from human dermal microvessels and immortalized by infection with an adenovirus carrying a SV40 promoter (Ades *et al.*, 1992). HMEC-1 were cultured on 1% gelatin-coated tissue culture flasks in MCDB-1 medium

supplemented with 10% FCS, 100 IU/ml penicillin, 0.1 mg/ml streptomycin. 2 mmol/L L-glutamine, and 10 ng/ml epidermal growth factor.

2.2.3. Culture of murine aortic endothelial cells

Murine aortic EC (MAEC) from HO-$1^{-/-}$ and HO-$1^{+/+}$ littermate controls (backcrossed 10 generations into the C57BL/6 background) were a kind gift from Dr M. Soares (Instituto Gulbenkian de Ciencia, Oeiras, Portugal). Cells were isolated as previously described and the MAEC phenotype was confirmed by characteristic cobblestone morphology and by uniform expression of endoglin (CD105) in more than 95% of cells, demonstrated by flow cytometry (Marelli-Berg *et al.*, 2000; Seldon *et al.*, 2007; Kinderlerer *et al.*, 2009). MAEC were cultured on 1% gelatin-coated tissue culture flasks in MCDB-131 medium supplemented with 20% FCS, 100 IU/ml penicillin, 0.1 mg/ml streptomycin, 2 mmol/l L-glutamine, and 30 µg/ml ECGS.

2.2.4. EC stimulation/treatment

All experiments with primary cells were conducted at passage 2 to 4. For each experiment, HUVEC were harvested by trypsin/EDTA and cultured in 1% gelatin-coated 6-, 12-, 24- or 96-well plates in EC plating M199 medium, supplemented with 10% FCS, 100 IU/ml penicillin, 0.1 mg/ml streptomycin, 2 mmol/L L-glutamine, 10 U/ml heparin, and 7.5 µg/ml ECGS. EC were allowed to settle overnight before stimulation/treatment.

EC were stimulated with 25 ng/ml VEGF or 100 ng/ml SDF-1α in growth factor free medium. ZnPP, CORM-2, ET-CORM and DFO were added directly to the culture medium. In all experiments, EC monolayers were treated with the appropriate vehicle controls (DMSO). The final concentration of DMSO was <0.1% in all samples. Stimulated cells were incubated for 2 to 72 h at 37°C in 5% CO_2 before further proceeding.

2.2.5. *In vitro* transfection of EC with siRNA by lipid-mediated transfection

Small interfering ribonucleic acid (siRNA) was introduced into EC by lipid-mediated transfection using the proprietary lipid complex geneFECTOR (VennNova, Pompano Beach, Florida, USA). A schematic of this process is shown in Fig. 2.1. Single sequence siRNAs against human HO-1 and PKCε were purchased from Qiagen Ltd. An siRNA pool of 4 sequences against human HO-1 was from Dharmacon, Inc. (Lafayette, Colorada, USA). Murine siRNA against HO-1 and cyclin A1 were both from Dharmacon, Inc. The non-targeting siRNA *Silencer*® Negative Control #1 was purchased from Ambion (Austin, Texas, USA). 3'-end Alexa Fluor 488-labelled siRNA against HO-1 and the AllStars Negative Control siRNA Alexa Fluor 488 were both from Qiagen Ltd (Tab. 2.1.).

HUVEC and MAEC were plated at 3 x 10^5 cells in 6-well plates in M199 or MCBD-131 plating medium, respectively to obtain 50% confluency. siRNA complexes were formed by mixing 100 µl geneFECTOR solution composed of 6 µl geneFECTOR in 100 µl Optimem and 100 µl siRNA solution containing 20 or 40 nM siRNA and 100 µl Optimem, followed by incubation at room temperature (RT) for 5 minutes (min). Culture medium was replaced with Optimem and siRNA complexes were added dropwise and incubated for 6 h. After incubation, culture medium was replaced with EBM-2 supplemented with 2% FCS, 100 IU/ml penicillin, 0.1 mg/ml streptomycin, 2 mmol/l L-glutamine, and 1.875 µg/ml ECGS. Transfected cells were incubated at 37°C in 5% CO_2 for up to 48 h before harvesting or further proceeding. Knockdown efficiency of siRNA sequences was assessed by quantitative real-time PCR (qRT-PCR) and western blotting (Chapter 5).

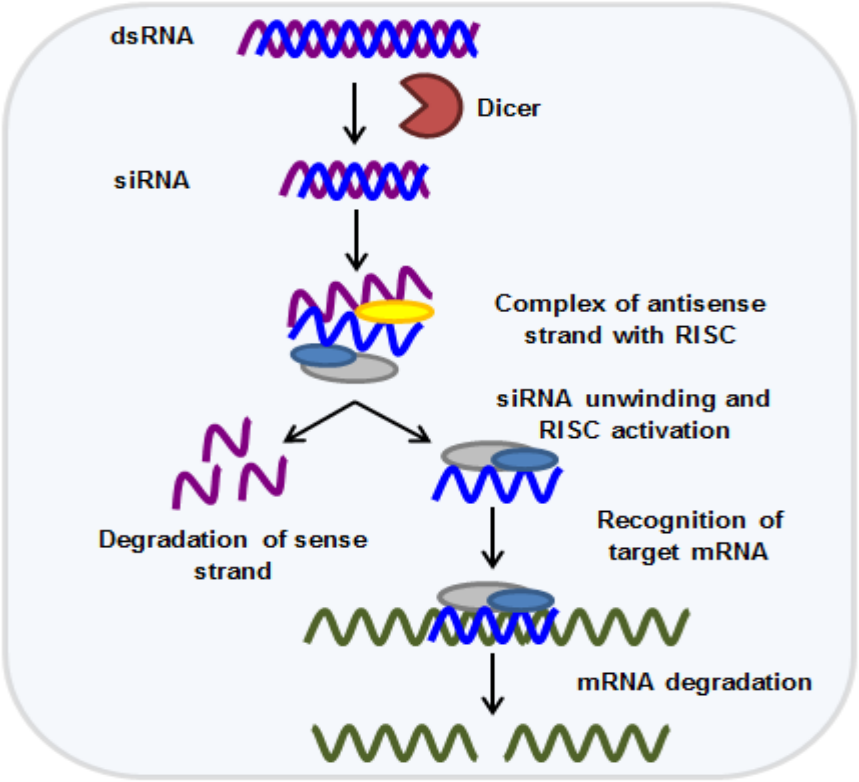

Figure 2. 1.: RNA interference by long double-stranded RNAs. Upon introduction, the long double-stranded RNAs (dsRNAs; typically >200 nt) enter a cellular pathway known as RNA interference (RNAi) pathway. During the initiation step, dsRNAs are cleaved into 20-25 nucleotide (nt) small interfering RNAs (siRNAs) by the RNase III-like enzyme Dicer. siRNAs then assemble into endoribonuclease-containing complexes known as RNA-induced silencing complexes (RISC), unwinding in the process and activating RISC (effector step). The siRNA strands subsequently guide the activated RISC to complementary RNA molecules, where they cleave and destroy the cognate RNA, thereby preventing protein translation (Meister and Tuschl, 2004). In this study, siRNA was introduced into cells by lipofection, which is not cleaved by dicer but directly recognised by RISC.

Table 2. 1.: Human and murine siRNA sequences.

Species	Target Gene	siRNA Name	mRNA target sequence 5'→3'
Human	HO-1	siHO-1 seq2	AAC AUU GCC AGU GCC ACC AAG
Human	HO-1	siHO-1 seq2 AF488	AAC AUU GCC AGU GCC ACC AAG
Human	HO-1	siHO-1 pool	GGC AGA GGG UGA UAG AAG A ACA CUC AGC UUU CUG GUG G AGA GAA UGC UGA GUU CAU G GAG GAG AUU GAG CGC AAC A
Human	HO-2	siHO-2 seq3	UGG GAG GUG AGU GGC CUG UAA
Human	HO-2	siHO-2 seq4	AAA GUG GGC UUU GCA AGC UAA
Human	HO-2	siHO-2 seq5	CAC GGC ACU UUA CUU CAC AUA
Human	HO-2	siHO-2 seq6	CAA GGA CUU CUU GAA AGG CAA
Human	PKCε	siPKCε seq5	CCC GAC CAU GGT AGU AGU GUU CAA
Mouse	HO-1	murine siHO-1 pool	GGA UUU GUC UGA GGC CUU G GGA GAU AGA GCG CAA CAA G CGA GAA UGC UGA GUU CAU G GGG AAU UUA UGC CAU GUA A
Mouse	cyclin A1	murine siCycA1 pool	UGA UUA ACG UAA CGG AGU A GGU CAA UGA ACC AGC CAA A AGU ACA AGG CUU CGA AGU A AUA CGU ACA CAA AGC GAC A
Human/Mouse/ Rat	N/A	siCTL	N/A
Human/Mouse/ Rat	N/A	siCTL AF488	N/A

2.2.6. Adenoviral infection of EC

EC were infected by incubation with the relevant adenovirus in serum-free M199 for 2 h at 37°C in 5% CO_2. Culture medium was then changed to M199 plating medium and cells were incubated overnight prior to harvesting and/or further proceeding. Infection of HUVEC with βgal or AdGFP control viruses previously demonstrated a transfection efficiency of 95% (Steinberg *et al.*, 2007). The multiplicity of infection (MOI) for adenoviruses used in this study was 100 virus particles per cell, which was determined by western blotting experiments (Chapter 5).

2.2.7. CellTiter 96® Aqueous One Solution cell proliferation assay

EC were plated at 5 x 10^3 cell/well in 1% gelatin-coated 96-well plates in growth factor-free medium supplemented with 5% FCS and incubated at 37°C in 5% CO_2 overnight. Cells were then treated with the compound of interest or the appropriate control for 24 to 72 h. Each treatment was performed in triplicate. After incubation, medium was replaced with 20% 3-(4,5-dimethylthiazol-2-yl)-5-(3-carboxymethoxyphenyl)-2-(4-sulfophenyl)-2H-tetrazolium (MTS) in growth factor-free medium and plates were incubated for another 3 h. The number of viable cells was determined with a Synergy HT plate reader (BioTek Instruments, Inc.) by measuring the absorbance at 490 nm.

2.2.8. *In vitro* cell proliferation assay

Cell proliferation was assessed using the Cell Proliferation ELISA, BrdU (colorimetric) from Roche Diagnostics Ltd. in accordance with the manufacturer's instructions. In brief, EC were plated at 5 x 10^3 cells/well in 1% gelatin-coated 96-well plates in growth factor-free medium supplemented with 5% FCS and incubated at 37°C in 5% CO_2 overnight. Cells were then treated with the compound of interest or the appropriate control for 24 to 72 h. Each treatment was performed in triplicate. After incubation, cells were labelled with 10 µM BrdU and re-incubated for 3 h. The labelling solution was removed and cells were fixed and denatured with FixDenat solution and incubation at RT for 30 min. The FixDenat solution was then replaced with anti-BrdU-POD working solution (mAb conjugated with peroxidase; POD) and the plate was incubated at RT for 90 min. Cell were

washed three times with 1x PBS and the immune complexes were detected by the addition of substrate solution (tetramethyl-benzidine) and incubated at RT up to 30 min until colour development was sufficient for photometric detection. The reaction product was quantified by measuring the absorbance at 370 nm on a Synergy HT plate reader. A reference wavelength was measured at 492 nm. The reaction product-specific absorbance at 370 nm was then normalised to the non-specific absorbance measured at 492 nm.

2.2.9. *In vitro* scratch assay

The *in vitro* scratch assay was used to study EC migration. EC were plated at 3 x 10^5 cell/well in 1% gelatin-coated 6-well plates in EBM-2 supplemented with 2% FCS and incubated at 37°C in 5% CO2 overnight. The confluent monolayers were scratched using a Gilson pipette tip (200 µl) and migration was assessed by live cell imaging. The migration path of individual cells in the leading edge of the scratch was tracked with the aid of time-lapse microscopy (LSM 510 Meta; Zeiss, Oberkochen, Germany) and image analysis software (ImageJ plugin Manual Tracking; National Institutes of Health; and Ibidi Chemotaxis and Migration tool; Ibidi GmbH, München, Germany). Cell motility was quantified in terms of the accumulated distance [µm], the Euclidean distance [µm], and velocity [µm/min].

2.2.10. Ibidi µ-slide chemotaxis assay

The Ibidi µ-slide chemotaxis assay was used to assess the directional migration of EC towards a growth factor gradient. EC suspended at a concentration of 3 x 10^6 cells/ml in complete EGM-2 supplemented with 10% FSC were prepared and 7 µl of the cell suspension was carefully pipetted into the observation area of collagen IV-coated chemotaxis µ-slides (Ibidi). Slides were placed into 15 mm Petri dishes and incubated at 37°C in 5% CO_2 for 3 h to allow EC to adhere. Floating cells were gently washed off and the medium within the observation area was replaced with growth factor-free EBM-2 supplemented with 2% FCS. One of the reservoirs was then filled with growth factor-free medium and the second reservoir with growth factor-supplemented medium. The directional migration of EC was assessed by live cell imaging. The migration path of

individual cells was tracked with the aid of time-lapse microscopy (LSM Meta 510) and image analysis software (ImageJ plugin Manual Tracking; and Ibidi Chemotaxis and Migration tool).

2.2.11. *In vitro* Matrigel tube formation assay

The Matrigel tube assay was used to investigate the effect of HO-1 inhibition on the ability of EC to form capillary-like structures *in vitro*. Pre-chilled 12-well plates were coated with growth factor-reduced Matrigel (BD Biosciences, San Jose, California, USA) and incubated at 37°C in 5% CO_2 for 30 min to allow gels to form. EC were plated onto the Matrigel at 1.2 x 10^5 cells/well in growth factor-free EBM-2 supplemented with 2% FCS. *In vitro* tube formation was assessed after 16 h. Five random pictures were captured for each well and tube length was quantified using the ImageJ plugin NeuronJ (National Institutes of Health).

2.2.12. *In vitro* adhesion assay

96-well plates were coated with 1% gelatin or 50 µg/ml collagen type I (BD Biosciences) for 1 h at 37°C, washed twice with PBS, and blocked with 1% BSA for 1 h. Control or HO-1 specific siRNA-treated HUVEC were labelled with 6.25 µM 5-chloromethylfluorescein diacetate in serum-free medium (Cell Tracker^{TM} Green CMFDA; Invitrogen) following the manufacturer's protocol. In brief, culture medium was removed and replaced with pre-warmed Cell Tracker^{TM} dye solution and incubated for 30 min at 37°C in 5% CO_2. After incubation, the dye working solution was replaced with fresh, pre-warmed medium and cells were incubated for another 30 min at 37°C. CMFDA-labelled cells were then reseeded at 20,000 cells per well onto the coated 96-well plates in EBM-2 supplemented with 2% FCS, 100 IU/ml penicillin, 0.1 mg/ml streptomycin, 2 mmol/l L-glutamine in the presence or absence of 25 ng/ml VEGF. After 40 min, the total cellular fluorescence was measured with a Synergy HT plate reader with absorption and emission settings at 492 and 517 nm respectively. Wells were then washed three times with PBS containing Ca^{2+} and Mg^{2+} at 37°C to remove non-adherent cells. The fluorescence of bound cells was then measured with the Synergy HT plate reader using the same settings. The percentage of bound cells relative to the total number seeded was then calculated.

2.2.13. *In vitro* immunofluorescent staining and confocal analysis

EC cultured on 1% gelatin-coated coverslips (VWR International Ltd., Lutterworth, UK) were fixed in methanol for 15 min at -20°C and permeabilized with 0.5% Triton X-100 (Sigma-Aldrich Ltd.) in PBS for 5 min. Non-specific Ab-binding was blocked by incubation with 10% normal goat serum (Sigma-Aldrich Ltd.) for 1 h at RT. EC were incubated with primary Ab (1:200) at 4°C overnight, washed with PBS and incubated with the appropriate AlexaFluor-conjugated secondary Ab (1:1,000; Invitrogen) for 1 h at RT. Cells were washed with PBS, stained with nuclear dye Draq5 (1:1,000: Cell Signaling Technology, Inc.) for 15 min and mounted onto microscope slides (VWR International Ltd.) with Fluoromount G (Cambridge Bioscience Ltd., Cambridge, UK). Immunofluorescent staining was analysed by z-stack confocal microscopy (LSM 510 Meta) using images at 63X magnification from 3 fields of view per experiment.

2.2.14. Apoptosis and cell cycle parameter analysis

Propidium iodide (PI) staining followed by flow cytometry was used to assess apoptosis and simultaneous analysis of cell cycle parameters of surviving cells. EC were harvested by exposure to trypsin/EDTA and fixed with 70% ethanol for 30 min at 4°C. After washing, cells were stained with propidium iodide staining solution composed of 50 µg/ml propidium iodide, 20 U/ml RNase (both Sigma-Aldrich Ltd.), 18 mg/ml EDTA, and 0.1% Triton X-100 for 45 min at 37°C prior to analysis by flow cytometry counting 20,000 cells per sample. Results are plotted as cell number versus DNA fluorescence and representative graphs are shown in Fig. 2.2. Apoptotic cells were identified by their hypodiploid nuclei resulting in a broad peak, clearly distinguishable from the sharp diploid DNA peak of normal cells.

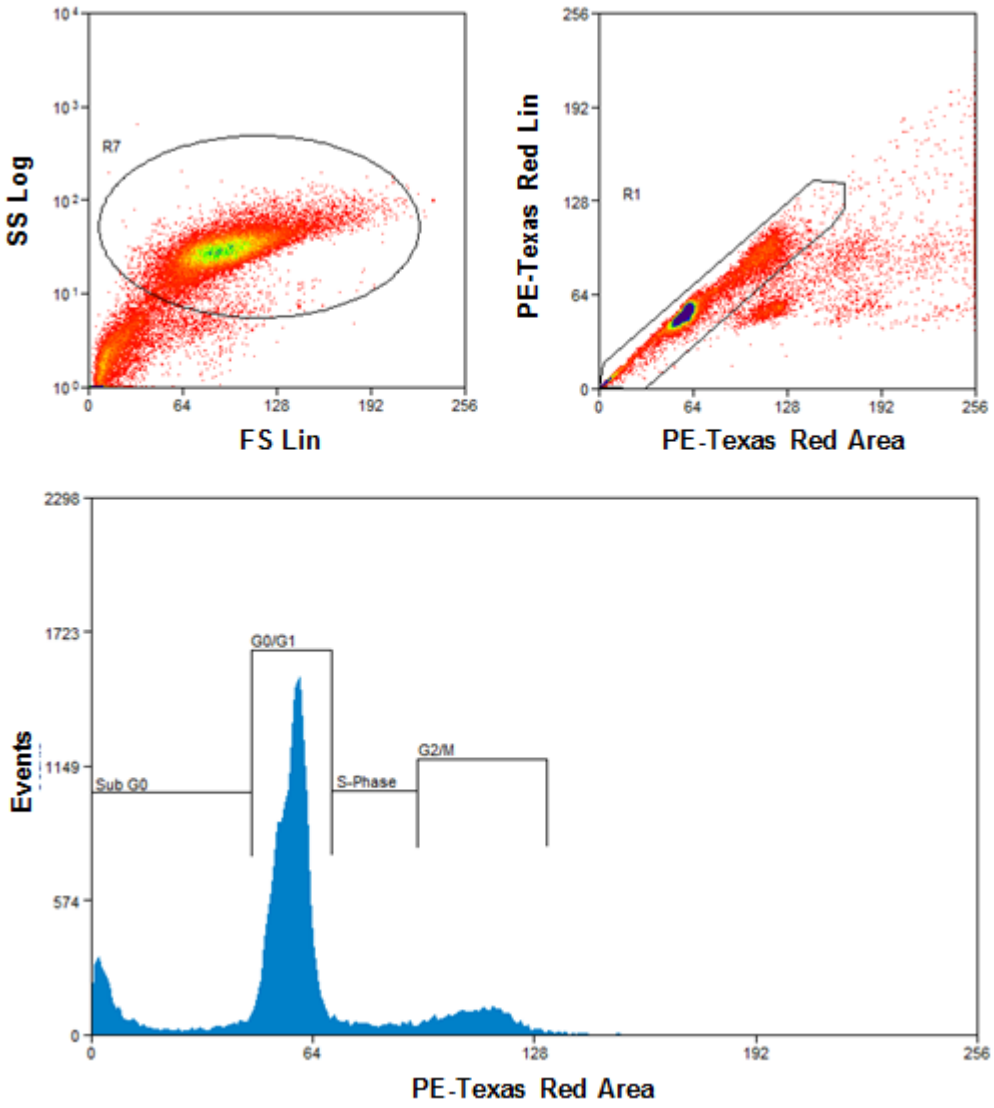

Figure 2. 2.: Apoptosis and cell cycle parameter analysis of human umbilical vein endothelial cells by propidium iodide staining and flow cytometry. A representative FACs blot of HUVEC stained with PI is shown. Cells were gated according to their DNA content into the different phases of the cell cycle. SS - side scatter, FS - forward scatter, PE-Texas Red – R-phycoerythrin Texas Red.

2.2.15. Senescence-associated beta-galactosidase (SA-β-gal) staining

EC cultured in 1% gelatin-coated 6-well plates were washed twice with PBS and fixed in 0.5% glutaraldehyde (Sigma-Aldrich Ltd.) in PBS for 15 min at RT. Cells were then washed twice with PBS supplemented with 1 mM magnesium chloride ($MgCl_2$; Sigma-Aldrich Ltd.) and incubated with X-gal staining solution composed of 20 mg/ml 5-bromo-4-chloro-3-indolyl β-D-galactosidase (X-gal) in N,N-dimethylformamide (both Sigma-Aldrich Ltd.), and 100 mM potassium hexacyano-

ferrate (III) ($K_3[Fe(CN)_6]$) and 100 mM potassium hexacyano-ferrate (II) trihydrate ($K_3[Fe(CN)_6]*3H_2O$; Sigma-Aldrich Ltd.) in PBS for 24 h at 37°C. After incubation, wells were washed with ultrapure H_2O and allowed to air dry. Blue-stained senescent cells were identified by phase-contrast microscopy (Leitz Labovert, Leica UK Ltd., Milton Keynes, UK) from 3 fields of view per experiment. Late passage cells (older/higher than P12) were used as a positive control for senescence.

2.2.16. Calpain activity assay

Calpain activity was measured using the calpain substrate 7-amino-4-chloromethlycoumarin (tBoc-LM-CMAC; Invitrogen). The substrate has an excitation/emission maxima of ~330/403. After cleavage by peptidases, the product produces blue-fluorescence with excitation/emission maxima ~351/430.

Control or HO-1 specific siRNA-treated HUVEC were loaded with 30 µM of the tBoc-LM-CMAC for 30 min at 37°C in 5% CO_2 in serum-free medium. EC were then treated with or without 25 ng/ml VEGF for the indicated time points. Fluorescence was measured by flow cytometry using the Violet-1 filter (FL6).

2.2.17. Exposure of EC to high shear unidirectional laminar flow *in vitro*

HUVEC were cultured on 10 µg/ml fibronectin-coated glass slides (Sigma-Aldrich Ltd.; glass slides: Thermo Fisher Scientific) in M199 plating medium and incubated at 37°C at 5% CO_2 overnight. Confluent monolayers were exposed to control static conditions or high shear unidirectional laminar flow (12 dynes/cm^2) for 24 h using the CytoDyne Streamer System (CytoDyne, La Jolla, CA, USA), consisting of the CytoShear Parallel Plate Flow Chamber and the CytoDyne Recirculating Flow Loop (Fig. 2.3.). The recirculating flow loop consists of two reservoirs, an upper and lower reservoir, with a parallel plate flow chamber positioned between them. Flow is governed by the hydrostatic pressure created by the vertical height distance between the upper and the lower reservoir. A constant pressure is maintained by continuous recirculation of culture medium from the lower to the upper reservoir at rates in excess of that

flowing through the chamber. The excess drains down the glass overflow manifold, which also serves to facilitate gas exchange with the medium. The flow chamber consists of machine-milled polycarbonate, a rectangular silastic gasket, and the glass slide with the attached endothelial monolayer, which are all held together by a vacuum maintained at the periphery of the slide, forming a channel of parallel-plate geometry (Frangos *et al.*, 1988). The system was assembled in a sterile class II laminar flow hood. Once the assembly was complete, the entire setup was moved into an enclosed chamber kept at 37°C and the system was gassed with a 95% air and 5% CO_2 mixture (BOC Industrial, London, UK). Morphologic and molecular characteristics of HUVEC exposed to high shear unidirectional laminar flow are described in Chapter 3.

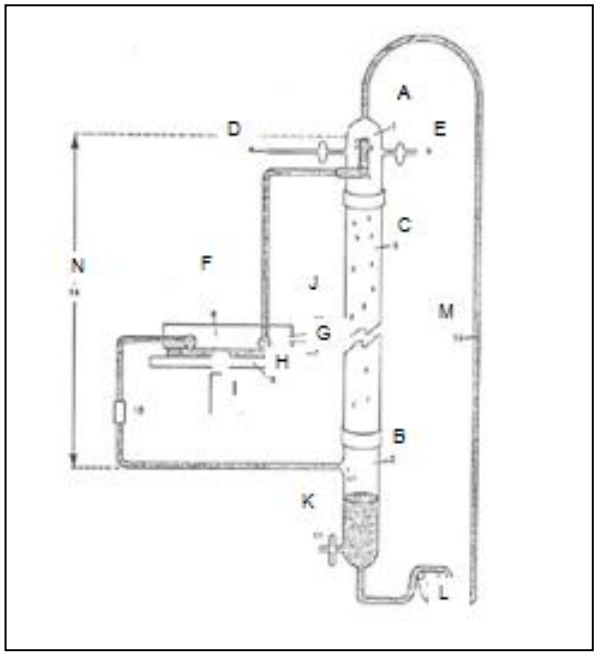

Figure 2. 3.: Schematic of the CytoDyne Streamer System. (a) upper reservoir, (b) lower reservoir, (c) overflow manifold, (d) filtered humidified 95% air + 5% CO2 input, (e) gas outlet, (f) flow chamber, (g) gasket, (h) slide with cell monolayer, (i) microscope (if required), (j) vacuum (k) sampling port, (l) roller pump, (m) PFA Teflon tubing, (n) height between upper and lower reservoir/constant pressure head (modified after Frangos *et al.*, 1988).

2.2.18. Flow cytometry

EC were harvested by exposure to trypsin/EDTA and cell suspensions were collected into FACs tubes (Marathon Laboratory Supplies, London, UK) and pelleted by centrifugation. EC were stained with the appropriate primary mAb or isotype-matched control for 30 min at 4°C. After washing, cells were pelleted and stained with FITC-labelled rabbit anti-mouse Ig for 30 min at 4°C followed by washing and fixation in 1% paraformaldehyde. Samples were analysed on a CyAn^{TM} ADP analyzer (Beckman Coulter Ltd., High Wycombe, UK) by counting 20,000 cells per sample. Representative histograms and plots are shown in Fig. 2.4. Results are expressed as a percentage of the relative fluorescent intensity (RFI) of non-stimulated cells. The RFI is calculated from the mean fluorescent intensity (MFI) of the test antibody divided by the MFI obtained with an isotype-matched irrelevant antibody.

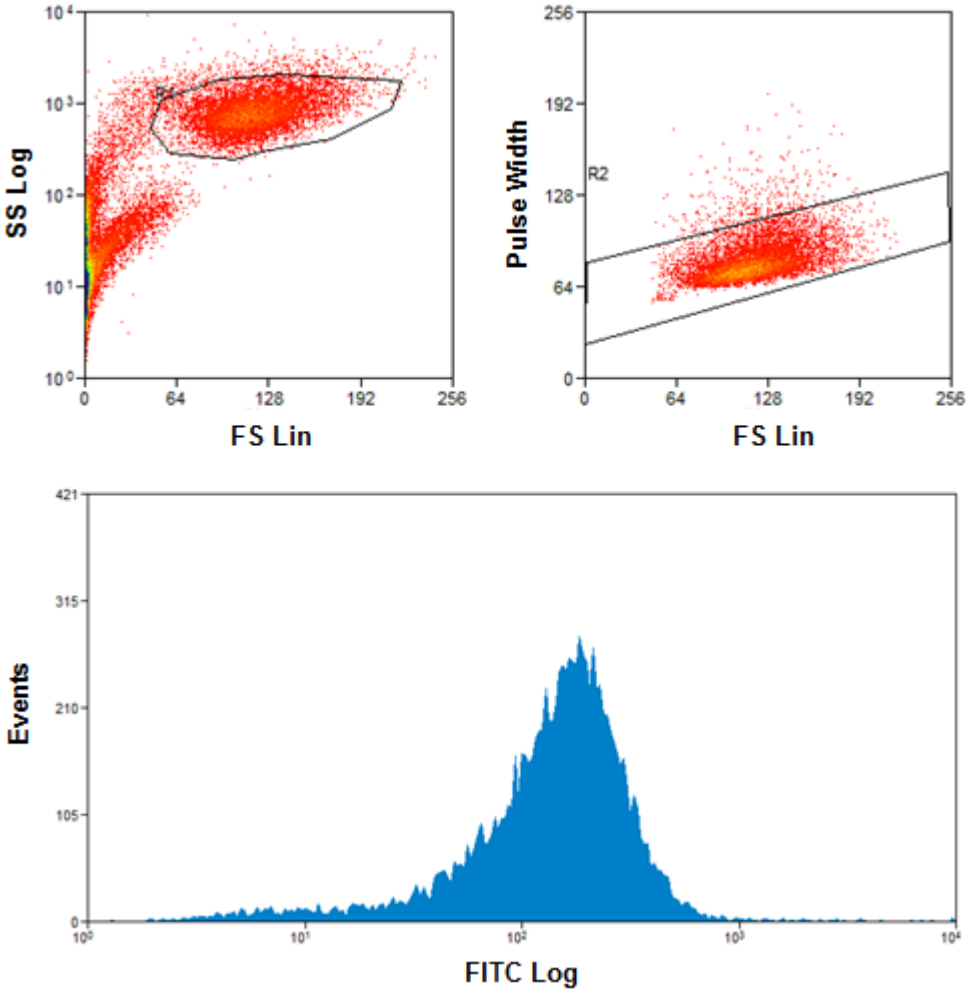

Figure 2. 4.: Flow cytometric analysis of human umbilical vein endothelial cells. A representative HUVEC FACs blot is shown. Gated cells were analysed for protein of interest. Molecular characterization of these cells is described in Chapter 3.2.2.. SS - side scatter, FS - forward scatter, FITC - fluorescein isothiocyanate.

2.2.19. Quantitative real-time polymerase chain reaction

Quantitative real-time PCR was performed using a CFX Connect real-time PCR detection system (Bio-Rad). β-actin was the housekeeping gene, with data calculated in relation to β-actin and verified using glyceraldehyde-3-phosphate dehydrogenase (GAPDH).

In brief, EC were washed with ice-cold PBS and lysed with Buffer RLT (Qiagen Ltd.) supplemented with 10 µl/ml β-mercaptoethanol (Sigma-Aldrich Ltd.) and total RNA was isolated using the RNeasy Mini Kit (Qiagen Ltd.) in accordance with the manufacturer's instructions.

Isolated RNA was quantified by spectrophotometry (Ultrospec 3000, Amersham Pharmacia Biotech Ltd.). DNase-1-digested total RNA (1 µg) was then reverse transcribed using 1 µM oligo(dT) (Invitrogen), 10 µM dNTP (Roche), and SuperScript II RNase Reverse Transcriptase (Invitrogen). cDNA was amplified in a 25 µl reaction containing 5 µl of cDNA template, 12.5 µl of iSYBR supermix, 0.5 pM sense and antisense gene-specific primers, and ultrapure water. Cycling parameters were 3 min at 95°C, and 40 cycles of 95°C for 10 sec and 60°C for 45 sec. Primers were previously designed, optimized and verified by other investigators within the laboratory (Kinderlerer *et al.*, 2006; Ali *et al.*, 2007; Partridge *et al.*, 2007; Hamdulay *et al.*, 2010). Human and mouse primer sequences are detailed in Tab. 2.2. and Tab. 2.3., respectively, and representative PCR curves are shown in Fig. 2.5. Gene expression was quantified using the comparative cycle threshold method (ΔΔCt). The Ct values of both the reference and the sample of interest were normalised to the housekeeping gene.

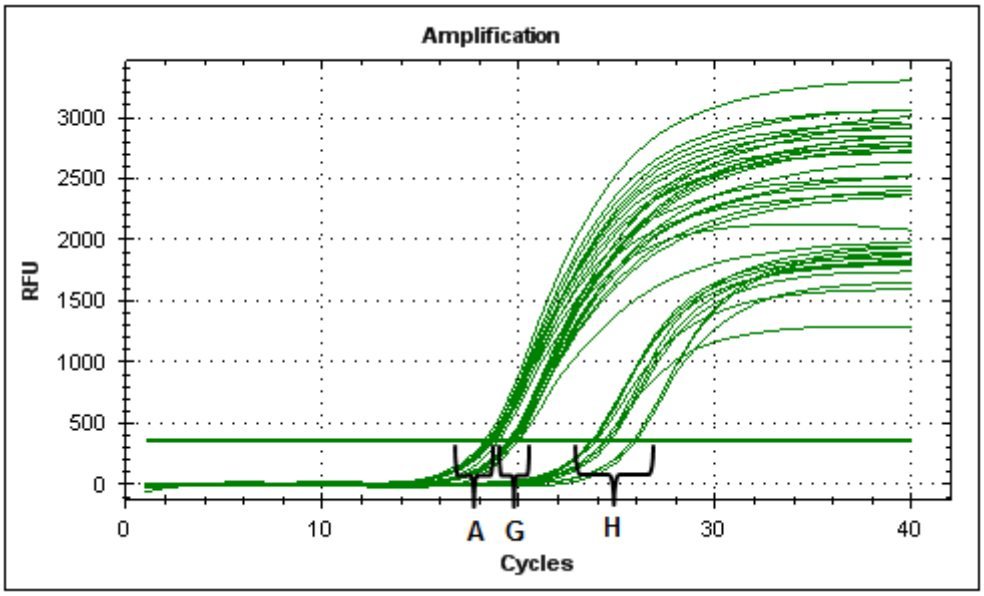

Figure 2. 5.: Representative quantitative PCR curves from cDNA prepared from EC. cDNA samples from HUVEC either transfected with 40 nM control siRNA (siCTL) or HO-1 specific siRNA (siHO-1 pool) and either left untreated or treated with 25 ng/ml VEGF for 24 h were analysed by qRT-PCR for mRNA expression of actin (A), GAPDH (G), and HO-1 (H). Three technical replicates for each condition are shown. RFU – relative fluorescence units.

Table 2. 2.: Human qRT-PCR primer sequences.

Gene Name	Target sequence 5' → 3'	
A1	forward	CAC AGG AGA ATG GAT AAG GCA AA
	reverse	AGT CAT CCA GCC AGA TTT AGG TCC
Actin	forward	GAG CTA CGA GCT GCC TGA CG
	reverse	GTA GTT TCG TGG ATG CCA CAG GAC T
Cdk1	forward	GAT TCT ATC CCT CCT GGT C
	reverse	AAT ATG GTG CCT ATA CTC C
Cdk2	forward	ATG GAG AAC TTC CAA AAG GTG GA
	reverse	CAG GCG GAT TTT CTT AAG CG
Cyclin A1	forward	TCA GGA CTG AGA ACC TGG CTA AGT ACG
	reverse	CCT AAT TGC TTG CTG AGG TCG ATG GG
Cyclin B1	forward	AAG AGC TTT AAA CTT TGG TCT GGG
	reverse	CTT TGT AAG TCC TTG ATT TAC CAT G
Cyclin D1	forward	CCG TCC ATG CGG AAG ATC
	reverse	GAA GAC CTC CTC CTC GCA CTT
Cyclin E1	forward	TCC AGG AAG AGG AAG GCA AAC
	reverse	CCT GTC GAT TTT GGC CAT TT
GAPDH	forward	CAA CAG CCT CAA GAT CAT C
	reverse	GAG TCC TTC CAC GAT ACC
HO-1	forward	CTT CTT CAC CTT CCC CAA CA
	reverse	TTC TAT CAC CCT CTG CCT GA
HO-2	forward	ATG TCA GCG GAA GTG GAA AC
	reverse	CGA GAG GTC AGC CAT TCT CA
p21	forward	GCA GAC CAG CAT GAC AGA TTT
	reverse	GGA TTA GGG CTT CCT CTT GGA
p27	forward	GCA ACC GAC GAT TCT TCT A
	reverse	GTC CAT TCC ATG AAG TCA GC

Table 2. 3.: Murine qRT-PCR primer sequences.

Gene Name	Target sequence 5' → 3'	
Actin	forward	GGC TGT ATT CCC CTC CAT CG
	reverse	CCA GTT GGT AAC AAT GCC ATG T
Cyclin A1	forward	TGC TCA AGT CAG ATC TCC ACT TCC
	reverse	TTA TAT TCT TCC CCA ACC TCC ACC
Cyclin A2	forward	GAG GGC GAT CCT TGT GGA T
	reverse	CAC AGC CAA ATG CAG GGT CT
HO-1	forward	AAG CCG AGA ATG CTG AGT TCA
	reverse	GCC GTG TAG ATA TGG TAC AAG GA
GAPDH	forward	AGG TCG GTG TGA ACG GAT TTG
	reverse	TGT AGA CCA TGT AGT TGA GGT CA

2.2.20. SABiosciences Human Cytoskeleton Regulators RT^2 Profiler^{TM} PCR Array

The SABiosciences Human Cytoskeleton Regulators RT^2 Profiler^{TM} PCR Array (Qiagen Ltd.) was used to compare the mRNA expression profile of HUVEC depleted of HO-1 by siRNA and control cells in response to VEGF. The array profiles the expression of 84 genes controlling the intracellular biogenesis, organisation, polymerisation, and depolymerisation of cytoskeleton components. In addition, the PCR array includes five housekeeping genes and controls for genomic DNA contamination, RNA quality, and general PCR performance.

In brief, HUVEC cultured on 1% gelatin-coated 6-well culture plates were washed with ice-cold PBS and lysed with Buffer RLT (Qiagen Ltd.) supplemented with 10 µl/ml β-mercaptoethanol (Sigma-Aldrich Ltd.). RNA lysates from three donor cords were pooled at time of collection and total RNA was isolated using the RNeasy Mini Kit (Qiagen Ltd.) in accordance with the manufacturer's instructions. Isolated RNA was quantified by Nanodrop analysis measuring the absorbance ratios A_{260nm}:A_{280nm} and A_{260nm}:A_{230nm} and ribosomal RNA band integrity was analysed on the Agilent® 2100 BioAnalyzer using an RNA 6000 Nano LabChip® (both Agilent Technologies, Inc., Santa Clara, CA, USA; Fig. 2.6.).

High-quality total RNA was then reversed transcribed using the RT^2 First Strand Kit (Qiagen Ltd.) in accordance with the manufacturer's instructions. In brief, the genomic DNA elimination mix was prepared by combining 1 µg of total RNA, 2 µl Buffer GE and RNase-free water to a final volume of 10 µl. The mix was incubated at 42°C for 5 min and then immediately placed on ice. The reverse-transcription mix was made up of 5X Buffer BC, Control P2, RE3 Reverse Transcriptase Mix, and RNase-free water to a final volume of 10 µl and combined with 10 µl genomic DNA elimination mix. The resulting mixture was incubated at 42°C for 15 min, followed by incubation at 95°C for 5 min. 91 µl RNase-free water was added to each cDNA synthesis reaction and kept on ice until further proceeding.

Real-time PCR was performed using the Bio-Rad iCycler (Bio-Rad). A 2.7 ml PCR components mix was prepared for each 96-well plate format composed of 2X RT^2 SYBR Green Mastermix, cDNA synthesis reaction, and RNase-free water, and 25 µl PCR components mix was dispensed into each well of the RT^2 Profiler^{TM} PCR array using an 8-channel pipettor. PCR plates were sealed with Optical Thin-wall 8-Cap Strips and centrifuged for 1 min at 1000 x g at RT and analysed by real-time PCR. Cycling parameters were 10 min at 95°C, and 40 cycles of 95°C for 15 sec and 60°C for 1 min. A melting curve program was run for 1 min at 95°C followed by 1 min at 60°C, and 70 cycles starting at 60°C for 10 sec with a temperature increase of 0.5°C after the second cycle. Gene expression was quantified using the RT^2 Profiler^{TM} PCR Array Data Analysis tool (Qiagen Ltd.). The Ct values of both the reference and the sample of interest were normalised to the housekeeping genes included on the PCR array.

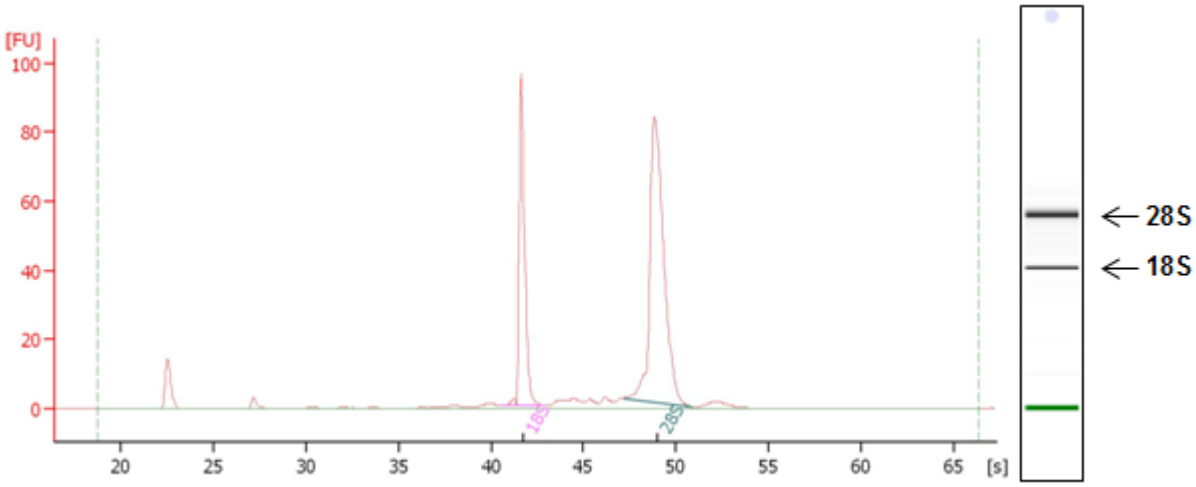

Figure 2. 6.: Ribosomal RNA band integrity. Agilent® 2100 BioAnalyzer electropherogram and gel-like image of high-quality total RNA showing sharp peaks and bands, respectively, for the 18S (left peak/lower band) and 28S (right peak/upper band) ribosomal RNA.

2.2.21. Western blotting

EC were washed with ice-cold PBS and lysed with RIPA buffer supplemented with complete protease inhibitor cocktail and PhosSTOP phosphatase inhibitor cocktail for 10 min at 4°C. The lysates were collected into Eppendorf tubes, sonicated for 1 min, and centrifuged at 17,968 x g for 20 min at 4°C (Sigma 1-15PK, Sigma-Aldrich Ltd.). The protein concentration of each sample was quantified using the Bio-Rad Dc protein assay kit according to the manufacturer's instructions using a gamma globulin standard. Proteins contained in cell lysates were separated by SDS PAGE. The samples were prepared by combining 15 µg of protein, 7.5 µl of 4xNuPAGE® LDS sample buffer and 2 µl DTT for 10% or 4-12%, 1 or 1.5 mm, 10 or 15 well Bis-Tris NuPAGE® gels. The final volume of each sample was diluted with ultrapure water to 30 µl and 20 µl for 10 and 15 well gels, respectively. Samples were denatured by boiling for 5 min, centrifuged for 1 min at 4°C and loaded onto the gels. Gels were run at 150 volts for 90 min. The separated proteins were transferred from gels to Immobilon™-P transfer membranes by semi-dry transfer for 1h with a current of 1 milliamp per membrane. The membrane was activated by methanol for 20 seconds and then washed with ultrapure water for 5 min followed by transfer buffer for 5 min. After transfer, the membranes were blocked in 5% BSA blocking buffer for 1 h at RT. Membranes were then probed with primary Ab, in 5% BSA dilution buffer at the working concentration, by

incubation on a rotator overnight at 4°C. On the second day, the membranes were rinsed and washed three times with TBS-T prior to incubation with the appropriate secondary HRP-conjugated Ab in 5% BSA dilution buffer at the working concentration. After incubation on a rotator at RT for 1 h, the membranes were washed three times with TBS-T and the signals were detected using an ECL detection kit. The blots were developed by exposing the membranes to Kodak XOMat films at varied time points to obtain the optimal results. Each film was developed by a Compact X4 X-ray processor. Membranes were stripped and/or reprobed for other proteins including a housekeeping gene as a loading control. Band intensity was quantified using ImageJ software.

2.2.22. Phos-tag™ SDS-PAGE

Protein lysates were collected and the protein concentration quantified as described in 2.2.21. Phosphorylated proteins were separated from non-phosphorylated proteins using Phos-tag™ SDS-PAGE (Fig. 2.7.). An 8% acrylamide resolving gel containing 50 µM Phos-tag™ acrylamide AAL-170 and 50 µM manganese chloride ($MnCL_2$) in 30% (w/v) acrylamide, 1.5 mol/L Tris/HCL buffered solution (pH=8.8), 0.5 % TEMED and 10% (w/v) diammonium peroxydisulfate solution was prepared and allowed to polymerize for 30 min at RT. 5.5% stacking gel composed of 30% (w/v) acrylamide and 0.5 mol/L Tris/HCL buffered solution (pH=6.8) was mixed with 0.5% TEMED and 10% (w/v) diammonium peroxydisulfate solution poured onto the polymerized resolving gel and allowed to settle for 60 min at RT. Protein samples were prepared by combining 20 µg protein with 3X bromphenol blue (BPB) sample buffer (Appendix), denatured by boiling for 5 min, centrifuged for 1 min at 4°C and loaded onto the gels. For lambda protein phosphatase treatment (λ PP; New England Biolabs, Inc., Ipswich, MA, USA), 20 µg protein was first mixed with 200 units λ PP, 1X NEBuffer, and 1 mM $MnCl_2$, and incubated for 30 min at 30°C prior to combining with BPB sample buffer. Gels were run at 150V for 120 min. After electrophoresis, gels were first soaked in general transfer buffer containing 1 mmol/L EDTA for 10 min, followed by soaking in general transfer buffer without EDTA for further 10 min, with gentle agitation to eliminate manganese ions from the gel and improve transfer of proteins onto PVDF membranes. Transfer

of proteins, probing of membranes with primary and appropriate secondary Abs, and signal detection was performed as described in 2.2.21.

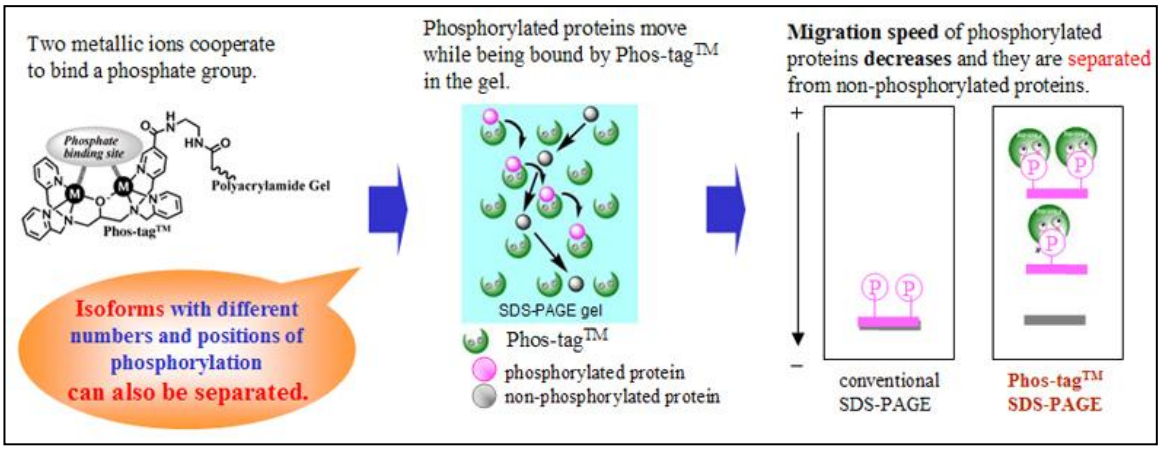

Figure 2. 7.: Phos-tag™ SDS-PAGE. Phos-tag™ acrylamide specifically binds to phosphorylated forms of Serine/Threonine/Tyrosine thereby separating phosphorylated proteins from non-phosphorylated proteins in the same sample. During electrophoresis, Phos-tag™ is directly added to the polyacrylamide gel and binds to phosphorylated proteins present in the cell lysate. Binding of Phos-tag™ alters the molecular weight (MW) of these proteins thereby decreasing migration speed and separating them from non-phosphorylated proteins. Membranes are then probed with total antibodies against the protein of interest and multiple bands become visible after chemiluminescent detection, with the lowest band representing non-phosphorylated proteins and upper bands representing phosphorylated forms of the protein of interest (Wako Chemicals GmbH; http://www.wako-chem.co.jp/english/labchem/product/life/phos-tag_aal_guidebook/index.htm).

2.2.23. Difference in-gel electrophoresis and Mass Spectroscopy

HUVEC cultured in 1% gelatin-coated T75 culture flasks were washed three times with DIGE washing buffer containing 5 mM magnesium acetate ($Mg(CH_3COO)_2$) and 10 mM Tris (pH=8). After the final wash, the buffer was replaced with 2 ml fresh DIGE washing buffer and cells were collected by scraping. Cells were then pelleted by centrifugation at 17,968 x g for 1 min at 4°C, lysed in DIGE lysis buffer containing 8 M urea, 4% CHAPS, and 30 mM Tris (pH=8.5) and sonicated for 2 min. DIGE washing and DIGE lysis buffer were both supplied by our collaborator Prof M. Mayr (King's College London, London, UK). Cell lysates were incubated on ice for 15 min with vigorous vortexing every 5 min. After centrifugation at 17,968 x g for 15 min at 4°C,

supernatant was harvested and protein concentration was quantified using the Bio-Rad Dc protein assay kit according to the manufacturer's instructions using a gamma globulin standard. Protein samples were then shipped to King's College London on dry ice and analysed by difference in-gel electrophoresis (DIGE) coupled to mass spectroscopy by our collaborators. Detailed protocols are available on: http://www.vascular-proteomics.com/. A list of differential expressed proteins was returned to our laboratory and then analysed by myself using DAVID Bioinformatics Resources 6.7 (National Institute of Allergy and Infectious Diseases (NIAID), National Institute of Health) and grouped according to gene ontology (GO).

2.2.24. *In vitro* transfection of EC with promoter constructs by lipofection

EC were co-transfected with the relevant promoter construct and pGL4.74[*hRluc*/TK] by lipofection using the proprietary lipid complex GeneJuice (Merck Chemicals Ltd., Nottingham, UK).

HUVEC were plated at 3 x 10^4 cells per well in 1% gelatin-coated 24-well plates in M199 plating medium and incubated at 37°C in 5% CO_2 overnight. GeneJuice solution was prepared by mixing 1.5 µl GeneJuice with 50 µl Optimen and incubated at RT for 5 min before addition of 250 ng of the relevant plasmid and 250 ng pGL4.74[*hRluc*]/TK]. The transfection mixture was incubated at RT for 15 min. Culture medium was replaced with Optimem and transfection mixture was added dropwise and incubated for 6 h. After incubation, culture medium was replaced with EBM-2 supplemented with 2% FCS, 100 IU/ml penicillin, 0.1 mg/ml streptomycin, 2 mmol/l L-glutamine, and 1.875 µg/ml ECGS. Transfected cells were incubated at 37°C in 5% CO_2 overnight and then treated with the appropriate compound for the indicated time points. Analysis of promoter activity was performed using the dual luciferase reporter assay.

2.2.25. Dual-Luciferase® Reporter Assay

The Dual-Luciferase® Reporter Assay System (DLR™ assay; Promega) was used as per instructions. The DLR™ assay enables the sequential measurement of the activities of both the firefly (*Photinus pyralis*) and *Renilla* (*Renilla reniformis*, also known as sea pansy) luciferases

from a single sample. The firefly luciferase reporter is measured first by adding Luciferase Assay Reagent II (LAR II) to generate a stabilized luminescent signal. After quantifying the firefly luminescence, this reaction is quenched, and the *Renilla* luciferase reaction is subsequently initiated by adding Stop&Glo® Reagent to the same tube. The Stop&Glo® Reagent also produces a stabilized signal from the *Renilla* luciferase, which decays slowly over the course of the measurement.

Cell lysis buffer was prepared by adding 1 volume of 5X Passive Lysis Buffer (PLB) to 4 volumes of ultrapure H_2O. LAR II was prepared by adding 10 ml Luciferase Assay Buffer II to Luciferase Assay Substrate. Stop&Glo® Reagent was prepared by adding 20 µl Stop&Glo® Substrate to 1 ml Stop&Glo® Buffer. Culture medium was aspirated and cell monolayers were washed with PBS twice. To each 24-well plate, 100 µl 1X PLB was added per well and plates were incubated at RT for 15 min on a rocking platform. Cell lysates were collected and transferred into Eppendorf tubes. For each reaction, 20 µl of cell lysate was transferred into one well of a white 96-well plate (Appleton Woods Ltd., Birmingham, UK). Each sample was prepared in triplicates. Plates were read on the Biotek SynergyTM 4 Multi-Mode Microplate Reader which dispensed LAR II and Stop&Glo® Reagent sequentially generating firefly and *Renilla* luminescence, respectively. Data was expressed as the ratio of firefly over *Renilla* luminescence.

2.2.26. *In vivo* Matrigel plug assay

The formation of new vessels *in vivo* was evaluated by the Matrigel plug assay as previously described (Bussolati *et al.*, 2004; Birdsey *et al.*, 2008). In brief, female C57BL/6 mice (10 weeks old) were anesthetized with an isoflurane gas (IsoFlo®, Abbott Laboratories Ltd., Queensborough, UK) and injected subcutaneously with Matrigel Basement Membrane Matrix mixture (BD Biosciences) near the abdominal midline, to induce the formation of a single solid gel plug. In gene silencing studies, Matrigel preparation included 350 µl Matrigel, 64 U/ml heparin, 40 ng/ml VEGF or vehicle, 2 µM siRNA (murine siHO-1 pool, murine siCycA1 pool, or siCTL), and PBS to a final volume of 500 µl. In gene over-expression studies, the recombinant adenovirus expressing the HO-1 gene (AdHO-1) and the control adenovirus containing an empty vector (Ad0) were used at 1×10^9 ifu/ml and combined with Matrigel preparations as described above. Plugs were

harvested after 7 days from CO_2-euthanised mice, fixed in 4% (w/v) paraformaldehyde for 2 h at RT, washed in PBS with Ca^{2+} and Mg^{2+} for 30 min, and stored in 70% ethanol/ultrapure H_2O at 4°C. Fixed plugs were then embedded in paraffin, and processed for hematoxylin and eosin staining by L. Lawrence (National Heart and Lung Institute, Imperial College London, London, UK). *In vivo* experiments were performed according to the Animals Scientific Procedures Act of 1986.

For quantification, vessels contained in the Matrigel plug were identified by the presence of nucleated cells surrounding a lumen containing red blood cells. Vessels were counted in 5 fields of view using a 20X objective lens (OLYMPUS BX50, OLYMPUS KEYMED, Southend on Sea, UK). Plugs from 3 mice were analysed for each treatment.

2.2.27. Statistical analysis

If not stated otherwise, data are expressed as the mean of individual experiments ± standard error of the mean (SEM). Data were grouped according to treatment and analysed using GraphPad PRISM Software (San Diego, CA, USA). Differences of the results between treatments were evaluated by analysis of variance (ANOVA) with Bonferroni correction, an unpaired Student's *t*-test, or column statistics using a one-sample *t*-test. Differences were considered significant at *p*-values <0.05.

CHAPTER 3 - MOLECULAR AND MORPHOLOGICAL CHARACTERISATION OF ENDOTHELIAL CELLS

3.1. INTRODUCTION

The vascular endothelium is a continuous cell monolayer lining the inner lumen of all blood vessels, thereby forming an interface between the circulating blood and the extravascular tissue. It is a highly dynamic tissue regulating the passage of materials from intravascular to extravascular sites. The endothelium uses its strategic location to maintain homeostasis through maintenance of a non-thrombotic environment facilitating laminar blood flow, by regulating vascular tone, haemostasis, vascular wall permeability, endothelial cell (EC) proliferation and angiogenesis, and innate and adaptive immunity. Due to its anatomical location and its extensive distribution throughout several organ systems, the endothelium is involved in many diseases; either having a primary role in pathogenesis or facilitating disease following EC bystander injury.

The endothelium is derived from the embryonic mesoderm via the differentiation of mesodermal cells into hemangioblasts leading to the formation of primitive blood islands. Hemangioblasts from the centre of the islands give rise to hematopoitic stem cells, and hemangioblasts at the periphery of the islands differentiate into angioblasts, the precursors of mature EC (Risau and Flamme, 1995; Cines *et al.*, 1998). EC are highly responsive to their micro-environment and exhibit marked plasticity with the ability to trans-differentiate into other cell lineages, whilst other cell types may also differentiate into EC (Aird, 2008). Although the endothelium was once viewed as an inert tissue consisting of a rather homogeneous population of cells, there is considerable evidence to suggest that although EC display many common features, they also exhibit remarkable heterogeneity (Garlanda and Dejana, 1997). Endothelial diversity is reflected by vessel size-specific, organ-specific and age-specific differences and is most evident at the morphological level, with a capillary phenotype classified as continuous, fenestrated or discontinuous. Other distinguishing criteria include cell size and shape, orientation with respect to the direction of blood flow, complexity of inter-endothelial adhesions, and composition of the recruited vessel wall (Thorin and Shreeve, 1998). Functional heterogeneity of EC is reflected by organ-specific roles in the control of vasoconstriction and dilation, blood coagulation and anti-coagulation, leukocyte homing and acute inflammation, wound healing and atherogenesis (Gerritsen, 1987). The

diversity of morphological and functional properties makes the endothelium uniquely adapted to communicate regionally with specific underlying tissue. For instance, liver cells lining the hepatic sinusoids are highly fenestrated and discontinuous, and mediate the exchange of metabolites and the processing of toxins between the portal blood, Kupffer cells and hepatocytes (Kmiec, 2001). Brain EC, in contrast, interact with astrocytes to produce the blood-brain barrier by forming a continuous endothelium with complex tight junctions and highly regulated polarised endocytosis and transcytosis (Abbott, 2002). Although all EC share common progenitors, there are very few defining structural and molecular markers which can be used to identify EC and distinguish one type of EC from another in a different vascular bed. Some structural, molecular and functional markers used to characterise EC are listed in Tab. 3.1 and Tab. 3.2.

As a result of their unique anatomical location EC are exposed to a variety of local haemodynamic mechanical forces. These include pressure, created by the hydrostatic forces of blood within the vessel; blood pressure-derived tensile stress, created as a result of defined intracellular connections between EC that exert longitudinal forces on the cell during vasomotion, and flow-generated shear stress, which is the frictional force exerted by the flowing blood on the endothelial surface, affecting cell morphology, cell metabolism and gene expression (Davies, 1995). For instance, within straight sections of the vasculature where high shear unidirectional laminar blood flow occurs, EC are transformed from their characteristic 'cobblestone'-shaped morphology into cells orientated parallel in the direction of flow. EC in these areas exhibit reduced endothelial turnover defined by both decreased proliferation and apoptosis, and enhanced anti-inflammatory and anti-thrombotic properties (Dewey *et al.*, 1981; Malek and Izumo, 1994; Kaiser *et al.*, 1997). Gene expression profiling demonstrated that cultured vascular EC respond to fluid mechanical forces by modulating the mRNA level of a large number of genes. Sustained laminar flow with high shear up-regulates expression of EC genes that are protective against atherosclerosis, including the transcription factors KLF-2 (Dekker *et al.*, 2002; Wang *et al.*, 2006), Nrf-2 (Chen *et al.*, 2003) and their downstream targets, such as the cytoprotective enzymes HO-1 (De Keulenaer *et al.*, 1998), MnSOD (Topper *et al.*, 1996) and Cu/ZnSOD (Inoue *et al.*, 1996). Laminar shear further facilitates secretion of the vasodilators PGI_2 and NO (Hanada *et al.*, 2000; Topper *et al.*, 1996; Malek *et al.*, 1999; Mashour and Boock, 1999), while suppressing the production of vasoconstrictors, such as ET-1 (Malek and Izumo, 1992), as well as inflammatory

mediators and adhesion molecules, including NFκB and VCAM-1, thereby contributing to a quiescent atheroprotective endothelial phenotype (Ando *et al.*, 1994). In contrast, disturbed flow, with associated reciprocating low shear stress, occurring at branch points and curvatures of the arterial tree, typically up-regulates genes that promote atherogenesis (Mohan *et al.*, 1999; De Keulenaer *et al.*, 1998).

The anatomical location of the endothelium makes it a difficult tissue to assess, thus impeding direct diagnostic and experimental studies. However, advances in microscopy, cell and molecular biology have improved our understanding of EC biology and function considerately. Of particular importance was the development of techniques to culture and characterise EC *in vitro*, which was initially attempted by Maruyama in the 1960's and later developed independently by Jaffe and Gimbrone in the 1970's (Maruyama, 1963; Jaffe *et al.*, 1973; Gimbrone *et al.*, 1974). The studies in this thesis employed EC isolated from human umbilical veins adopting the technique developed by Jaffe and colleagues which is detailed in Chapter 2. However, as already outlined in their original study, isolated EC populations may be contaminated with smooth muscle cells and fibroblasts, while EC may also differentiate into other cell types with different molecular and functional properties (Jaffe *et al*., 1973). Therefore this initial results chapter details the morphological and molecular characterisation of EC isolated from umbilical veins for use in my studies in the forthcoming chapters.

Table 3. 1.: Constitutive markers of endothelial cells. Modified after Garlanda and Dejana, 1997. EC – endothelial cell.

Constitutive Endothelial Markers		
Antigen	**Cell Type**	**Reference**
Angiotensin-converting enzyme	EC, epithelial cells, monocyte-macrophages, T lymphocytes	Belloni and Tressler, 1990
CD31/PECAM-1	EC, platelets, megakaryocytes, B and T lymphocyte subsets, monocytes, neutrophils	DeLisser *et al.*, 1994; Vecchi *et al.*, 1994
CD51/61 vitronectin receptor	EC, platelets, megakaryocytes, oesteoclasts, mast cells, B lymphocytes	Brooks *et al.*, 1996
CD102/ICAM-2	EC, lymphocytes, monocytes, platelets	Springer, 1990
CD105/endoglin	EC, monocyte-macrophages, erythroid cells, platelets, megakaryocytes	Gougos and Letarte, 1988
Griffonia simplicifolia aggulutinin binding	EC (rodent)	Sahagun *et al.*, 1989
Thrombomodulin	EC, smooth muscle cells	Esmon, 1995
Vascular endothelial cadherin	EC, trophoblasts, peripheral lymph node sinus macrophages	Lampugnani *et al.*, 1992
von Willebrand Factor	EC, platelets	Jaffe *et al.*, 1973, Wagner *et al.*, 1982
Weibel-Palade bodies	EC	Weibel and Palade, 1964

Table 3. 2.: Inducible markers of endothelial cells. Modified after Garlanda and Dejana, 1997. EC – endothelial cell.

Inducible Endothelial Markers			
Antigen	**Cell Type**	**Stimulus**	**Reference**
CD54/ICAM-1	EC, leukocytes, epithelium, fibroblasts	Upregulated in EC by inflammatory cytokines	Springer, 1990
CD62E/E-selectin	EC, post-capillary venules, restricted *in vivo*	inflammation, cytokines, neoangiogenesis	Kansas, 1996
CD62/P-selectin	EC, platelets	cytokines	Kansas, 1996
CD106/VCAM-1	EC, macrophages, synoviocytes, dendritic cells, mesothelium	Upregulated in EC by inflammatory cytokines	Springer, 1990
Tie 1	EC	neoangiogenesis	Mustonen and Alitalo, 1995
Tie 2/TEK	EC, monocytes	neoangiogenesis	Mustonen and Alitalo, 1995
VEGF receptor-1 (Flt-1)	EC	neoangiogenesis, Kaposi's sacroma	Peters *et al.*, 1993
VEGF receptor-2 (KDR/Flk-1)	EC	neoangiogenesis, Kaposi's sarcoma, vascular tumours	Quinn *et al.*, 1993

3.2. RESULTS

3.2.1. Morphological characterisation of endothelial cells

Cells were isolated from umbilical veins following collagenase treatment and grown to confluence on gelatin-coated culture flasks. Phase-contrast microscopy showed cellular monolayers with a characteristic ‘cobblestone’ morphology, composed of homogenous, closely opposed, polygonal shaped cells with distinct borders and centrally located nuclei (Fig. 3.1.A and B). These appearances were maintained beyond 5 passages and were also found with human microvascular endothelial cells (HMEC-1), representing EC of the human dermal microvasculature (Fig. 3.1.C and D). In contrast, human aortic smooth muscle cells exhibited a distinctly different appearance; they grew as long, slender overlapping cells in parallel arrays (Fig. 3.1.E and F).

3.2.2. Expression of constitutive and inducible surface markers of endothelial cells

Flow cytometric analysis was used to evaluate the purity of newly isolated primary cells from umbilical cords by assessing the constitutive expression of cell surface markers. Analysis of HUVEC showed a significant basal expression of EC markers CD31 (PECAM-1), endoglin (CD105), and ICAM-2 (Fig. 3.2.), but no basal expression of the leukocyte adhesion molecule VCAM-1 (Fig. 3.3.). Following TNF-α treatment for 16 h, there was a marked induction of VCAM-1 protein on the surface of EC. Both 1 ng/ml and 10 ng/ml TNF-α treatment, significantly enhanced VCAM-1 expression to a similar extent when compared to untreated control cells, with a relative fluorescent intensity (RFI) of 30 to 35 for TNF-α treated HUVEC compared to an RFI of 1.5 for untreated cells (Fig. 3.3.).

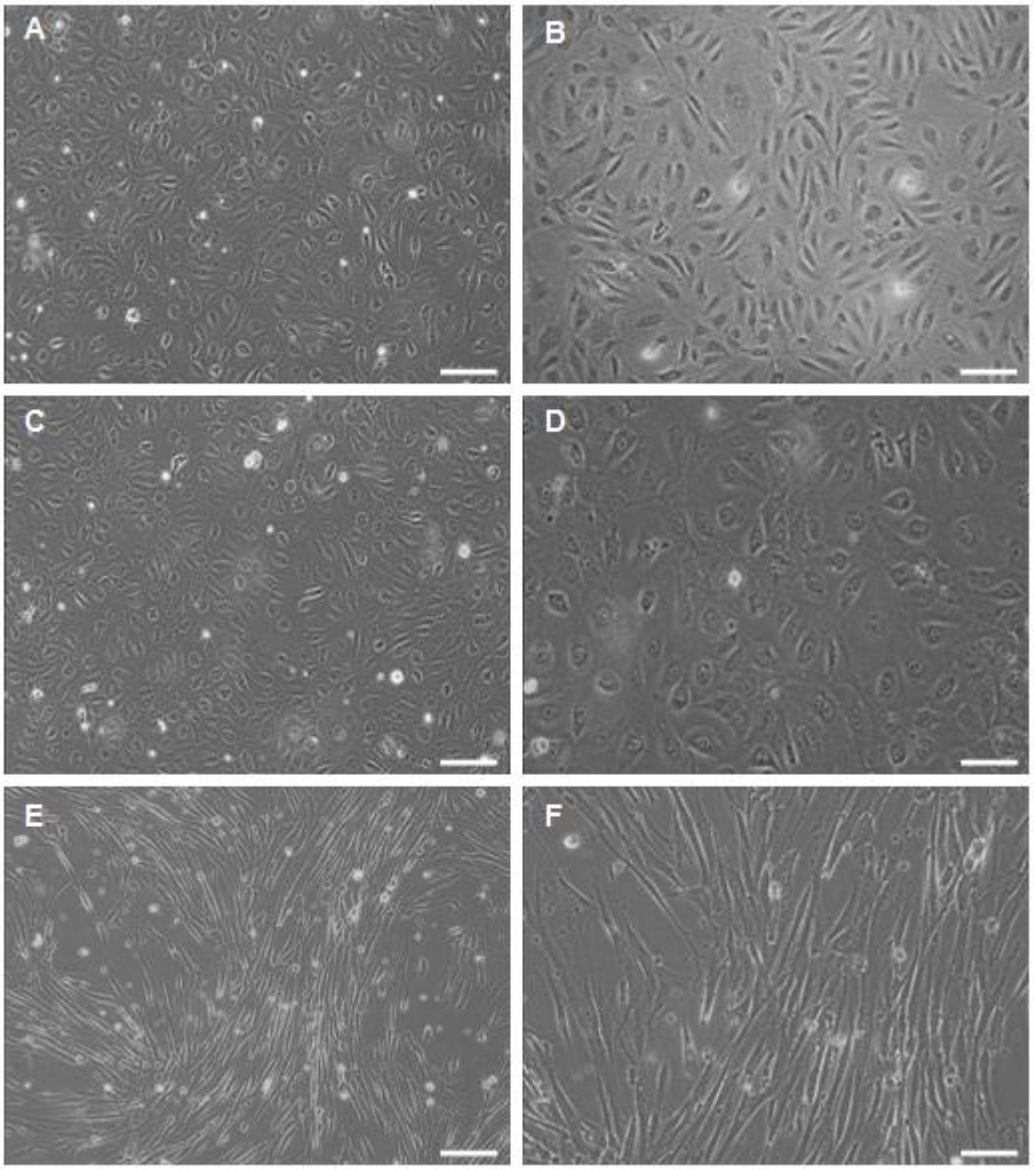

Figure 3. 1.: Morphological characterisation of human endothelial cells. Human endothelial cells were cultured on gelatin-coated culture flasks and visualised using phase-contrast microscopy. (A, B) Images of human umbilical vein endothelial cell (HUVEC) monolayers. (A) 10X and (B) 20X magnification. (C, D) Images of the human dermal microvascular endothelial cell (HMEC-1) monolayers (C) 10X and (D) 20X magnification. (E, F) Images of human aortic smooth muscle cell (HAoSMC) monolayers (E) 10X and (F) 20X magnification. Bars equal 50 µm.

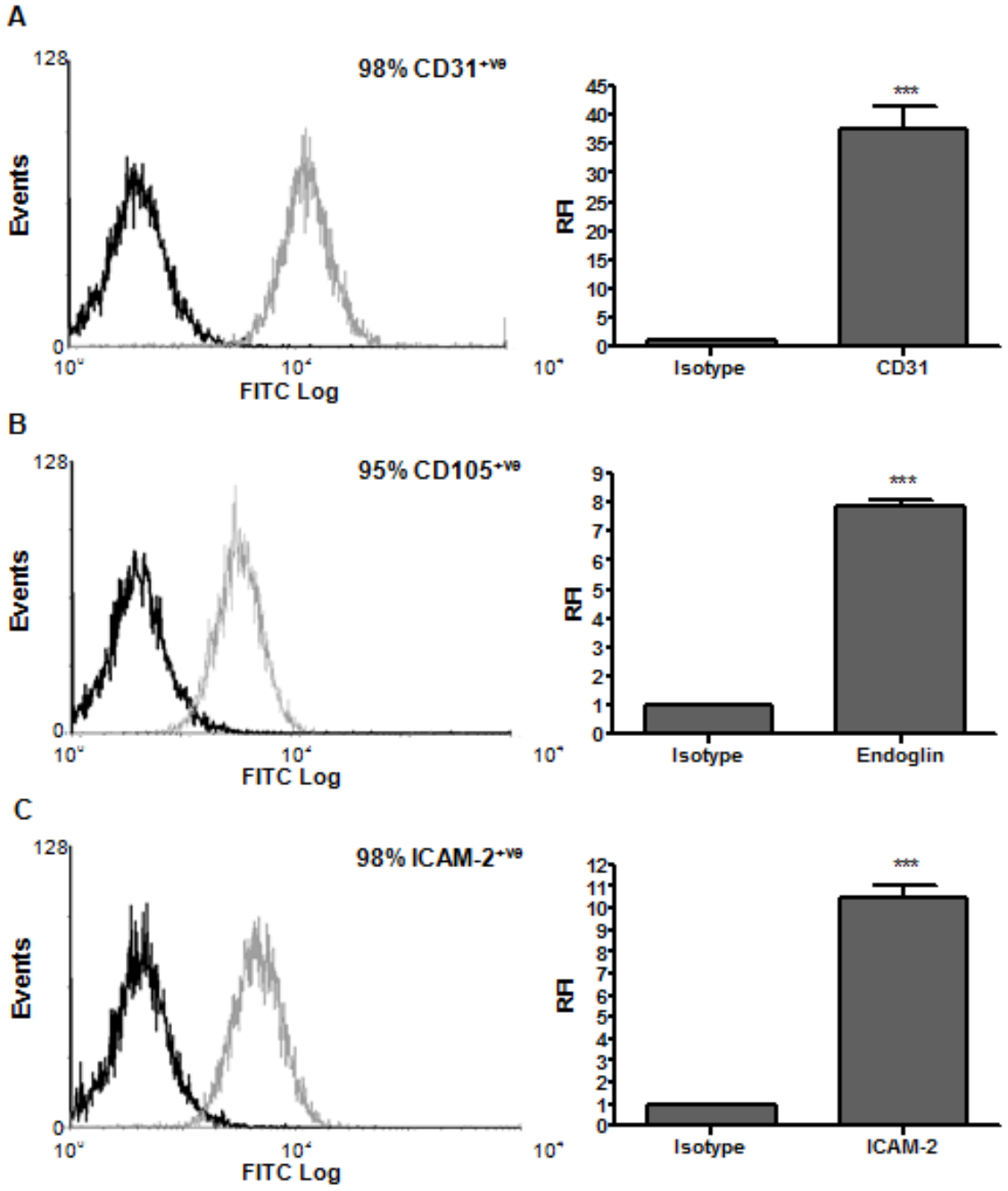

Figure 3. 2.: Expression of constitutive surface markers of endothelial cells. The expression of EC surface markers was assessed using flow cytometry. HUVEC monolayers were analysed for the expression of (A) CD31 (PECAM-1) using P2B1 mAb, (B) endoglin (CD105) using RMAC8 mAb, and (C) ICAM-2 using CBR-IC2/2 mAB. Black histograms represent the isotype control population, grey histograms present the antigen of interest with percent positivity in brackets. Bar charts display the relative fluorescence intensity (RFI). Data is presented as mean ± SEM (n=3 experiments), *** p<0.001. +ve – positive.

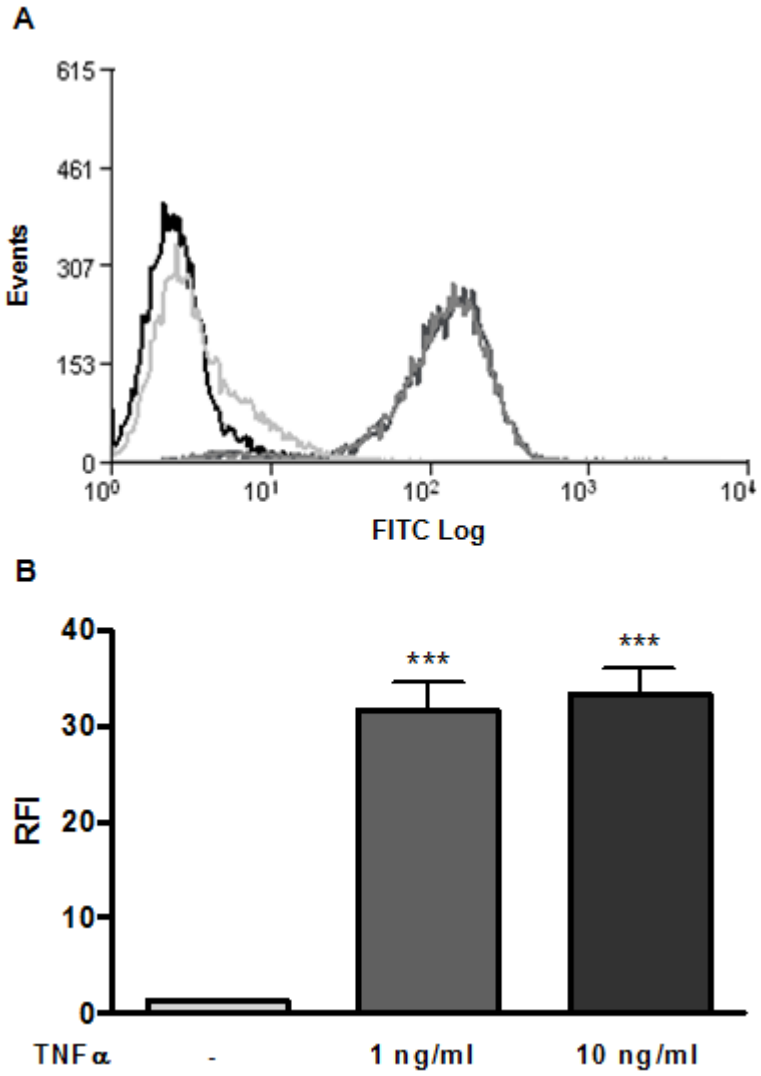

Figure 3. 3.: TNFα-induced surface expression of VCAM-1 on endothelial cells. HUVEC monolayers were left untreated (UT) or treated with 1 ng/ml TNFα or 10 ng/ml TNFα for 16 h prior to analysis of VCAM-1 surface expression by flow cytometry. (A) Black lines represent the isotype control population, grey shading represents VCAM-1 expression using 1.4C3 mAb with light grey untreated EC, medium grey 1 ng/ml TNFα, and dark grey 10 ng/ml TNFα treated HUVEC. (B) Bar charts display the relative fluorescence intensity (RFI) normalised to the isotype control. Data is presented as mean ± SEM (n=3 experiments), *** p<0.001 vs UT.

3.2.3. Morphological and molecular characterisation of EC exposed to high shear unidirectional laminar flow

Exposure to high shear unidirectional laminar flow *in vitro* alters morphological and molecular characteristics of EC. Phase-contrast microscopy showed that HUVEC maintained a confluent monolayer, and formation of intracellular gaps, denudation, and damage were not observed in

any of the experimental conditions. Cells cultured under static conditions maintained the characteristic 'cobblestone' morphology of EC with a polygonal cell shape and centrally located nuclei (Fig. 3.4.A). After exposure to high shear unidirectional flow (12 dynes/cm^2) for 24 h, EC exhibited an elongated cell shape and were orientated parallel in the direction of flow (Fig. 3.4.B). These morphological responses of EC to laminar flow are consistent with previous reports (Dewey *et al.*, 1981; Kataoka *et al.*, 1998).

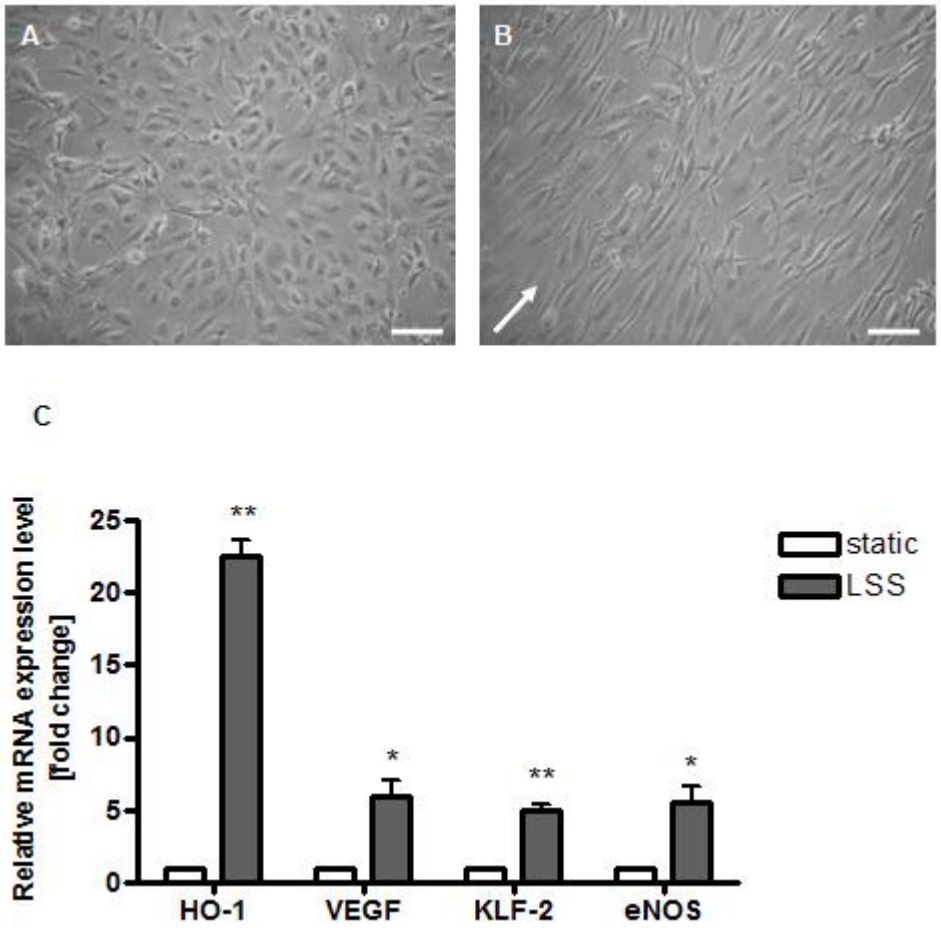

Figure 3. 4.: Morphological and molecular characterisation of endothelial cells exposed to high shear unidirectional laminar flow. HUVEC were cultured under (A) static conditions or (B) exposed to high shear unidirectional laminar flow (LSS; 12 dynes/cm^2) for 24 h prior to assessment of cell morphology by phase-contrast microscopy. Pictures are representative images from three experiments for (A) static and (B) LSS conditions, the arrow indicates the direction of flow. Bars equal 50 µm, 10X magnification; (C) mRNA quantification by qRT-PCR of known flow inducible genes. Data is presented as mean ± SEM and expressed relative to cells cultured under static conditions (n=3 experiments), * p<0.05, ** p<0.01.

Molecular analysis by quantitative RT-PCR revealed an increased induction of flow-responsive genes. HO-1 mRNA levels of cells exposed to high shear unidirectional flow for 24 h were significantly enhanced by >20-fold compared to cells cultured under static conditions (Fig. 3.4.C). Similarly, mRNA levels of the known flow inducible markers VEGF, KLF-2, and eNOS were increased by >5-fold by high shear stress compared to static cells, and again these results are in concordance with previous findings (De Keulenaer *et al.*, 1998; Chen *et al.*, 2003; Wang *et al.*, 2005; Malek *et al.*, 1999; Wang *et al.*, 2006).

3.3. DISCUSSION

Over the past decades, tremendous technological and methodological advances in cell and molecular biology have greatly improved our current understanding of the endothelium and its role in health and disease. The ability to isolate and characterise human EC *in vitro* created new possibilities to study the biology of EC, that are otherwise difficult to assess due to their anatomical location. The most common approach for EC harvesting is to enzymatically remove the cells by collagenase digestion from the internal lining of large blood vessels such as the human umbilical vein. Although a good yield of EC is generally achieved using this technique, it has been acknowledged by Jaffe and colleagues in 1973 that isolated EC populations may be contaminated with non-endothelial cells of the tissue surrounding the vessel, such as smooth muscle cells and fibroblasts. In addition, EC may differentiate into other cell types with different molecular and functional properties. The primary purpose of the studies described in this chapter were first to demonstrate the successful isolation and culture of EC from human umbilical veins, second to determine the purity of the isolated populations, and thirdly, to confirm the identity of these cells using well described morphological and molecular markers.

Cultured endothelial cells display certain characteristic features that can be used to confirm their identity after harvesting and plating the isolates, regardless of the method of isolation. They form confluent monolayers that restrict the movement of macromolecules and display a ‘cobblestone’ appearance, composed of homogenous, closely opposed, polygonal shaped cells with distinct borders and centrally located nuclei (Maruyama, 1963; Jaffe *et al.*, 1973,; Gimbrone *et al.*, 1974). Cells isolated from human umbilical veins in this study displayed the described morphological characteristics (Fig. 3.1.A and B) and similar appearances were seen with cultured cells of the dermal microvasculature (HMEC-1; Fig. 3.1.C and D). These appearances however differed markedly from those of smooth muscle cells (HAoSMC; obtained from Promocell), which were spindle shaped and grew in overlapping parallel arrays (Fig. 3.1.E and F).

Different cellular markers are localised in the cytoplasm or on the surface membrane of EC and are used for identification of EC in culture. Some of these markers are universal, such as CD31, others are specific for the vascular bed or the specific tissue, however the latter are relatively scarce. Some of the EC markers are constitutive and present in essentially all types of the

endothelium, while others are expressed after activation by inflammatory cytokines or growth factors (Tab. 3.1. and Tab. 3.2.). EC isolated from umbilical veins showed a marked expression of the surface molecules CD31, endoglin (CD105), and ICAM-2 (Fig. 3.2.). CD31 is a glycoprotein expressed at endothelial intercellular junctions, belongs to the immunoglobulin (Ig) superfamily and is important for the transendothelial migration of leukocytes, during angiogenesis and for integrin activation (Albelda *et al.*, 1991; DeLisser *et al.*, 1994; Newman and Newman, 2003). Endoglin is a homodimeric transmembrane protein which is a major glycoprotein of the vascular endothelium. The protein is part of the transforming growth factor-beta (TGF-β) receptor complex and is important in TGF signalling, cytoskeletal organisation and cell migration, and cardiovascular development and remodelling. Endoglin deficiency is embryonically lethal in mice due to cardiovascular defects (Gougos and Letarte, 1988; Barbara *et al.*, 1999; Sanz-Rodrigues *et al.*, 2004). ICAM-2 is a member of the intercellular adhesion molecule (ICAM) family and is expressed at high levels in EC. It is a type I transmembrane glycoprotein and binds the leukocyte integrin LFA-1, mediating leukocyte-endothelial cell interactions important for antigen-specific immune responses (Springer, 1990; Simmons, 1995; Hayflick *et al.*, 1998). VCAM-1 is a sialoglycoprotein and member of the Ig superfamily, mediating leukocyte-endothelial adhesion and signal transduction. VCAM-1 is not expressed in resting EC but strongly induced by pro-inflammatory cytokines including TNF-α, interferon-γ (IFN-γ), and interleukin-1 (IL-1) and expressed on the cell surface of EC (Springer, 1990; Cybulsky *et al.*, 1991; Preiss and Sattar, 2007). Isolated HUVEC demonstrated a similar VCAM-1 expression profile with no expression in the resting state, but following treatment with TNF-α there was a marked induction of VCAM-1 protein (Fig. 3.3.). In regard of future studies, it would be useful to further determine the purity of the isolated cell cultures by excluding a contamination with other cell types, such as fibroblasts and smooth muscle cells. Commonly used cellular markers for the characterisation of fibroblasts are ER-TR7 antigen and fibroblast-specific protein 1 (FSP1), and alpha smooth muscle actin (α-SMA) for smooth muscle cells.

A well-defined characteristic of EC is their morphological appearance when exposed to dynamic flow. Shear stress, which is the frictional force on the flowing blood on the endothelial surface, induces an elongation of the cell shape in the direction of the flow. This condition more closely resembles that of the blood vessel *in vivo* and is more physiologic than static culture for studying

dynamic-associated events (Dewey *et al.*, 1981; Kataoka *et al.*, 1998). The typical 'cobblestone' appearance of isolated primary cells used in this study was observed for cells cultured under static conditions, but was modified after exposure to high shear unidirectional laminar flow for 24 h. Cells became elongated in shape and aligned parallel in the direction of flow (Fig. 3.4.A and B). Gene expression analysis further revealed a marked increase in mRNA expression of the flow-responsive genes KLF-2, HO-1, eNOS and VEGF (Fig. 3.4.C) in response to high shear unidirectional laminar flow compared to static EC. Fluid shear stress maintains vascular homeostasis by influencing endothelial gene expression. One mechanism by which shear stress achieves this is through induction of transcription factors including KLF-2. The KLF-2 promoter contains a 62 bp shear stress-response element (SSRE) which is responsible for its shear stress-induced expression (Dekker *et al.*, 2002; Huddleson *et al.*, 2005). KLF-2 itself activates downstream targets through binding to the SSRE in the promoter of these flow-responsive genes, including HO-1 and eNOS (Topper *et al.*, 1996; SenBanerjee *et al.*, 2004; Huddleson *et al.*, 2005; Fledderus *et al.*, 2008). The expression of the pro-angiogenic factor VEGF is also induced by shear stress in a KLF-2-depedent manner (de la Paz *et al.*, 2012).

Another characteristic of EC is their ability to organise into tubules or capillary-like microtubes when plated onto two-dimensional Matrigel, fibrin or collagen matrixes in response to stimulants including growth factors and serum. The ability to form vessel-like structures on Matrigel of isolated HUVEC is described in detail in Chapter 5.

Morphological, structural and molecular characteristics that are restricted to the endothelium and can be used to define the identity of EC are limited. Many of these characteristics are shared with haemopoietic cells or mature blood cells, emphasising the idea of a common embryonic precursor (Risau, 1995). Instead the identity of EC is confirmed by the combination of a variety of morphological, structural, molecular and functional markers. Cell isolates from umbilical cords in this study demonstrated several morphological and functional characteristics of EC confirming the endothelial identity of these cells. The collection technique described in detail in Chapter 2 was therefore adopted for studies in the forthcoming chapters. Of note, there are limitations to an *in vitro* approach, as it is difficult to reproduce the *in vivo* endothelial micro-environment including aspects such as flow, interaction with other cells, connective tissues and signalling molecules.

This is evident from studies which demonstrated that culture disturbs EC from their quiescent *in vivo* phenotype (0.1% replications per day) to an activated state (1-10% replications per day), with associated loss of vessel type and organ-specific functions (Cines *et al.*, 1998). Nevertheless, provided all results are interpreted appropriately and with caution, the development of techniques to harvest and culture EC *in vitro* has immensely advanced our current understanding of the vascular endothelium and its role in physiology and disease.

CHAPTER 4 - THE PRO-ANGIOGENIC FACTORS VEGF AND SDF-1 ALPHA REGULATE THE EXPRESSION OF THE CYTOPROTECTIVE ENZYME HO-1 IN ENDOTHELIAL CELLS

4.1. INTRODUCTION

HO-1 is encoded by the gene *HMOX1*, located on chromosome 22, and its expression is mainly regulated at the transcriptional level (Gozzelino *et al.*, 2010). *HMOX1* transcription can be induced by a variety of signal transduction pathways in an inducer-, cell-type- and species-specific manner. A major role for mitogen-activated protein kinases (MAPK) has been implicated in the activation of HO-1 ultimately activating transcription factors that regulate *HMOX1* transcription by recognising specific response element-rich regions within the proximal (-0.3 kb) and distal (-4 kb and -10 kb) *HMOX1* promoter (Ryter *et al.*, 2006; H. Mylroie, unpublished data) (please see section 1.3.2.).

Biologic activities of the end-products of heme degradation, alone or in combination, and the HO-1 protein itself have been proven to possess important cytoprotective properties in the cardiovascular system, including anti-inflammatory, anti-apoptotic and anti-oxidant effects (Ali *et al.*, 2007; Kinderlerer *et al.*, 2008; Grochot-Przeczek *et al.*, 2012). Induction of HO-1 is an important cellular adaptive response, minimising tissue injury and facilitating repair, as revealed by the severe endothelial damage in human HO-1 deficiency (Yachie *et al.*, 1999). Of note, the recognised roles of HO-1 are far beyond cytoprotection. HO-1 has been implicated in the regulation of cell proliferation, differentiation and apoptosis. Moreover, the pro-angiogenic mediators vascular endothelial growth factor (VEGF), and more recently stromal cell-derived factor-1 alpha (SDF-1α), have been shown to activate HO-1 expression in EC implying a role for HO-1 in angiogenesis (Fernandez Bonkovsky, 2003; Bussolati *et al.*, 2004; Deshane *et al.*, 2007). Treatment of human umbilical vein endothelial cells (HUVEC) and human microvascular EC with VEGF increases HO-1 protein expression and enzymatic activity. Importantly, inhibition of HO-1 with pharmacologic antagonists, SnPP or ZnPP, significantly inhibits VEGF-induced proliferation in a dose-dependent manner *in vitro* and completely inhibits the development of capillary sprouting and neovessels in response to VEGF as shown using a murine muscle neovessel outgrowth model in Matrigel (Bussolati *et al.*, 2004). In concordance with these findings, VEGF increases HO-1 protein expression in the chick embryo chorioallantoic membrane, an effect

inhibited by staurosporine, indicating a potential role for protein kinase C (PKC; Fernandez and Bonkovsky, 2003). Furthermore, the chemokine SDF-1α, an important regulator of endothelial progenitor cell (EPC) migration and recruitment to sites of ischaemic injury, has been linked to HO-1-driven angiogenesis. Deshane *et al.* demonstrate increased HO-1 gene transcription and protein translation in human aortic EC in response to SDF-1α, and this is associated with increased enzymatic activity. Moreover, HO-1 depletion inhibits SDF-1α-induced endothelial tube formation and migration in HAEC, and aortic rings from HO-1-deficient mice, grown on Matrigel, fail to form capillary sprouts in response to SDF-1α (Deshane *et al.*, 2007).

Even though growing evidence suggests an important role for HO-1 in angiogenesis, the transcriptional and signalling mechanisms underlying growth factor-induced *HMOX1* activation remain elusive. The aim of this Chapter is therefore to determine the optimal time-point of HO-1 induction in response to the pro-angiogenic mediators VEGF and SDF-1α in proliferating human EC, and to use these findings to identify transcriptional and signalling mechanisms involved in growth factor-regulated HO-1 expression.

4.2. RESULTS

4.2.1. Heme oxygenase-1 is induced by the pro-angiogenic factors VEGF and SDF-1α

To assess changes in HO-1 expression in proliferating cells, primary HUVEC were cultured to sub-confluency (50-70%) on gelatin-coated culture dishes prior to treatment with the pro-angiogenic mediators VEGF-A or SDF-1α for up to 72 h. Expression levels of HO-1 in EC was assessed by qRT-PCR and western blotting. A significant increase in HO-1 mRNA levels following exposure to 25 ng/ml VEGF was seen after 8 h and peaked at 24 h (Fig. 4.1.A). HO-1 protein expression was significantly increased after 16 h VEGF treatment with maximal expression at 24 h in proliferating HUVEC (Fig. 4.1.B). Exposure to 100 ng/ml SDF-1α resulted in HO-1 induction at earlier time points compared to VEGF, with a significant increase in HO-1 mRNA after 2 h and maximal induction after 4 h (Fig. 4.2.A), resulting in enhanced protein expression after 4 h and 8 h treatment (Fig. 4.2.B). These findings are in concordance with previous studies reporting a significant induction of HO-1 protein after 24 h and 48 h in HUVEC and EC of the microvasculature (HMEC) in response to VEGF, and subsequent increase in HO-1 activity (Bussolati *et al.*, 2004). Likewise, SDF-1α has been reported to induce HO-1 mRNA and protein in human aortic EC (HAEC) with a maximum response after 4 h and 16 h exposure to SDF-1α, respectively (Deshane *et al.*, 2007). Of note, in this study utilising HUVEC, a significant variability in HO-1 induction was observed between cell isolates from different donors in response to both, VEGF and SDF-1α. Although I have not investigated this, this variability in responsiveness might result from the effect of HO-1 promoter polymorphisms (Taha *et al.*, 2010).

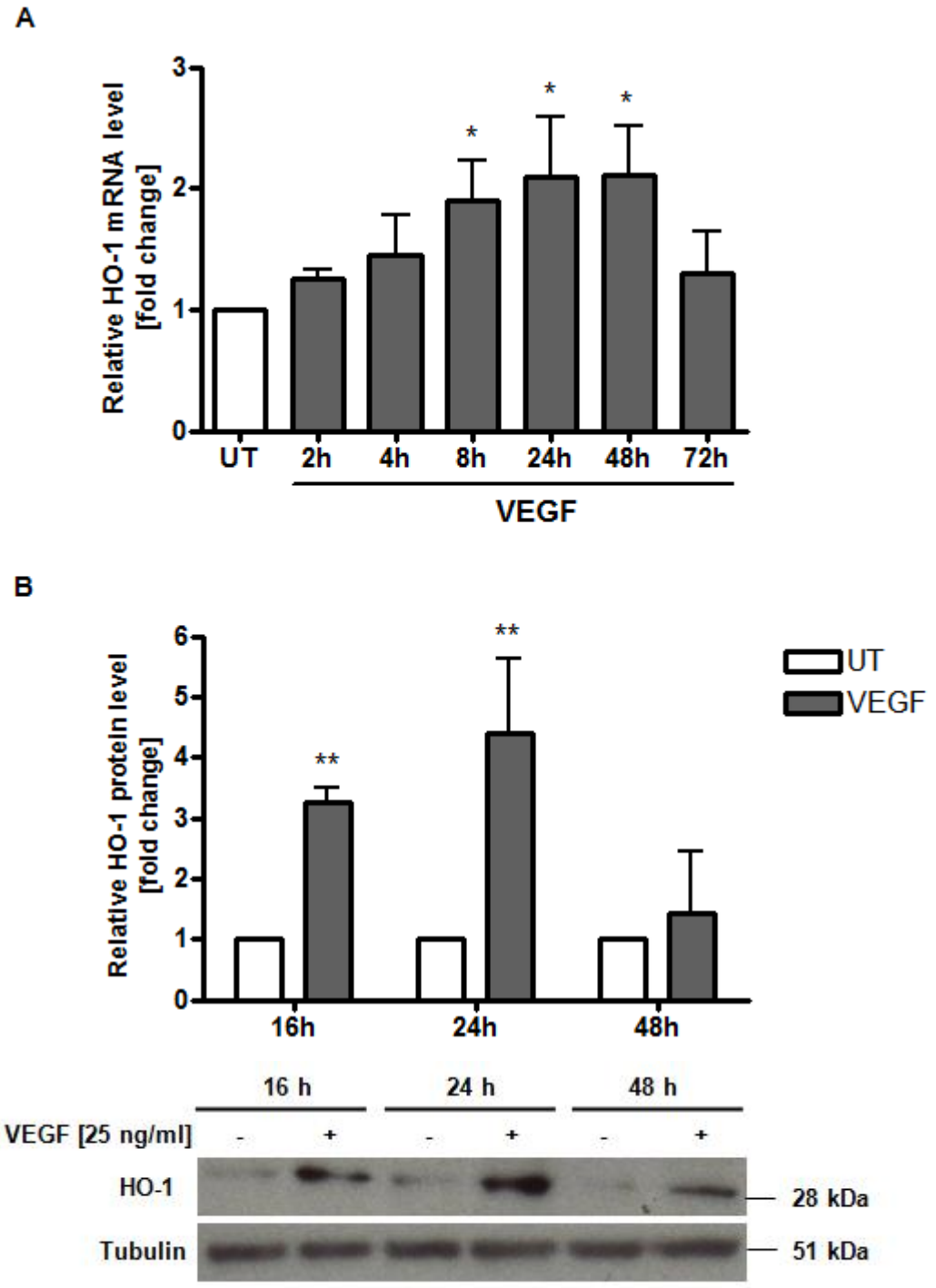

Figure 4. 1.: Heme oxygenase-1 is induced by the pro-angiogenic factor VEGF. HUVEC were cultured to sub-confluency (50-70%) prior to treatment with 25 ng/ml VEGF for the indicated time points. (A) mRNA levels were quantified by qRT-PCR and (B) protein expression was assessed by western blotting and quantified by densitometry. Tubulin was used as the loading control. In (A) untreated samples (UT) represent matched controls for each time point. (B) shows a representative blot and corresponding densitometry. Data is presented as mean ± SEM (n=8 experiments for mRNA levels; n=6 experiments for protein levels), * p<0.05 vs UT matched control.

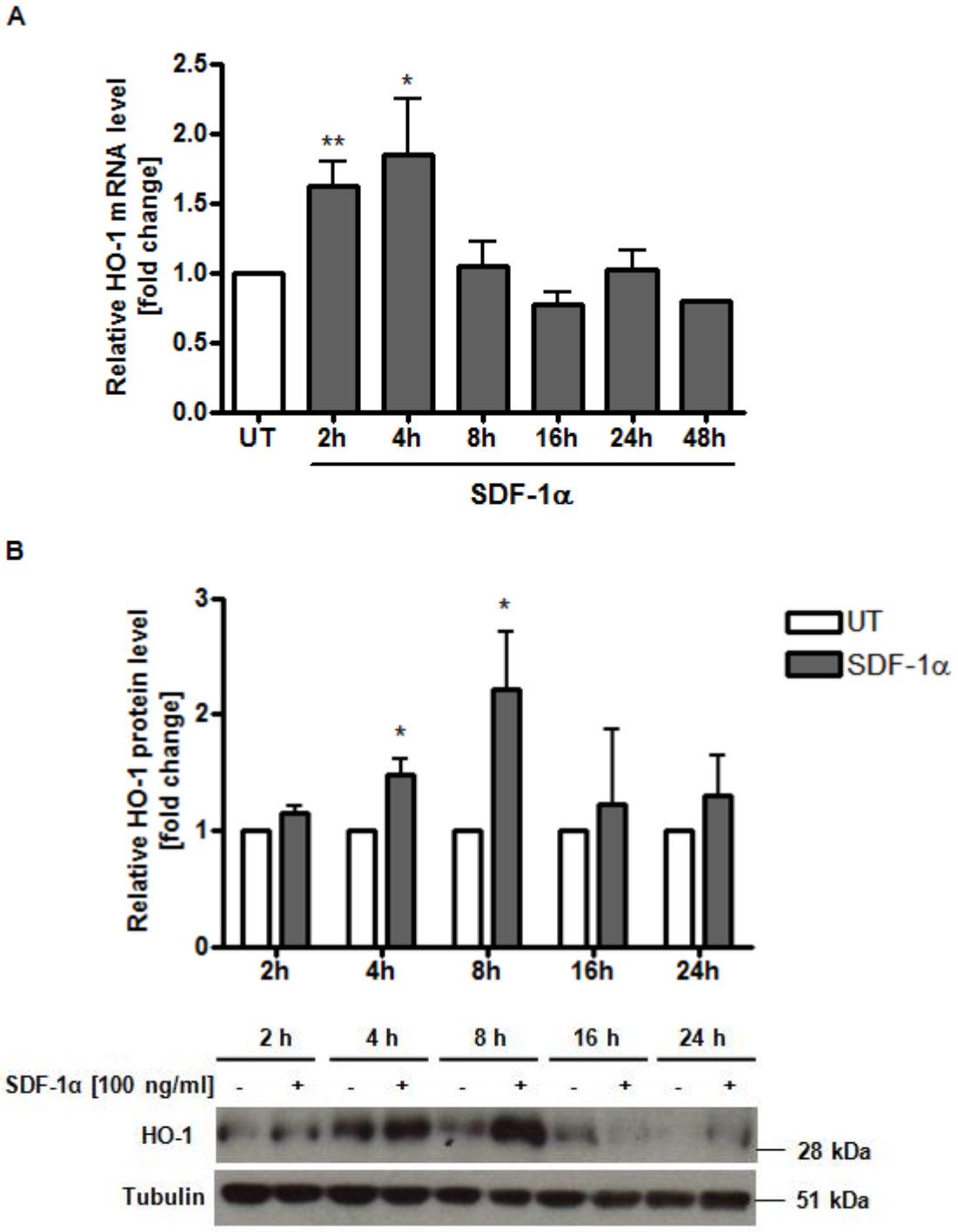

Figure 4. 2.: Heme oxygenase-1 is induced by the pro-angiogenic factor SDF-1α. HUVEC were cultured to sub-confluency (50-70%) prior to treatment with 100 ng/ml SDF-1α for the indicated time points. (A) mRNA levels were quantified by qRT-PCR and (B) protein expression was assessed by western blotting and quantified by densitometry. Tubulin was used as the loading control. In (A) untreated samples (UT) represent matched controls for each time point. (B) shows a representative blot and corresponding densitometry. Data is presented as mean ± SEM (n=5 experiments and n=1 for 48 h time point for mRNA levels; n=5 experiments for protein levels), * $p<0.05$, ** $p<0.01$ vs UT matched control.

4.2.2. Effect of VEGF and SDF-1α on *HMOX1* promoter activity

To identify transcription factors involved in HO-1 regulation by the pro-angiogenic factors VEGF and SDF-1α, the Dual-Luciferase® Reporter Assay System (DLR™ assay) was used. The DLR™ assay enables the sequential measurement of the activities of both the firefly and *Renilla* (*Renilla reniformis*) luciferases from a single sample.

HUVEC cultured on gelatin-coated 24-well culture plates were co-transfected with HO-1 promoter constructs ligated into the pGL3-Basic luciferase reporter vector (Fig. 4.3.) and the *Renilla* construct pGL4.74[*hRluc*/TK] prior to treatment with 25 ng/ml VEGF, 100 ng/ml SDF-1α, or the known HO-1 inducer hemin (0.2 µM) in a time course experiment for up to 48 h. The empty pGL3-Basic luciferase reporter vector was used as a procedure control in all experiments.

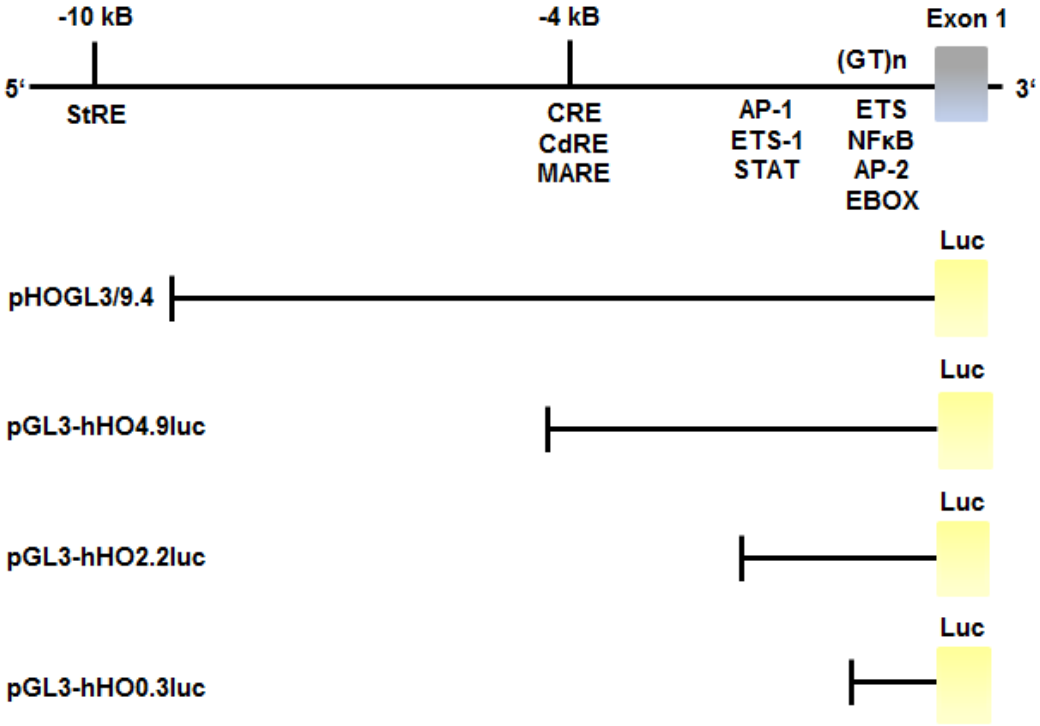

Figure 4. 3.: The human *HMOX1* promoter. The schematic depicts some of the known regulatory elements within the human *HMOX1* gene and *HMOX1* promoter constructs ligated into the pGL3-Basic luciferase reporter vector. AP – activator protein, CdRE – cadmium responsive element, CRE – cAMP responsive element, ETS – ETS binding site, Luc – luciferase, MARE – Maf response element, NFκB – nuclear factor kappa B, STAT – signal transducer and activator of transcription, StRE – stress response element (modified after Kronke *et al.*, 2003; Ryter *et al.*, 2006).

Hemin treatment resulted in a modest 3-fold increase in *HMOX1* promoter activity after 8 h compared to the untreated control and was used as a positive control for promoter activity (Fig. 4.4. and Fig. 4.5.). VEGF treatment had no effect on *HMOX1* activity after 4 h to 8 h. Of note, basal *HMOX1* promoter activity was significantly increased after 16 h to 48 h culture compared to earlier time points (4 h and 8 h), an effect attenuated by VEGF (Fig. 4.4.).

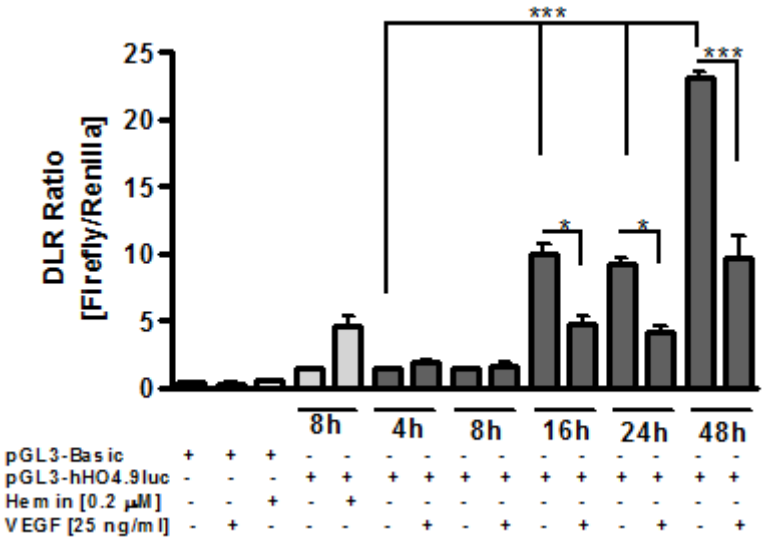

Figure 4. 4.: Effect of VEGF on *HMOX1* promoter activity. HUVEC were co-transfected with pGL3-hHO4.9luc or pGL3-basic control vector and pGL4.74[*hRluc*/TK] prior to treatment with hemin (0.2 µM) or VEGF (25 ng/ml) for the indicated time periods and *HMOX1* promoter activity was assessed using the DLRTM-assay. Data is presented as mean ± SEM (n=3 experiments), * $p<0.05$, *** $p<0.01$.

Likewise, exposure to the pro-angiogenic factor SDF-1α had no effect on *HMOX1* promoter activity after 2 h to 8 h compared to time-matched controls. But as seen in experiments utilising VEGF, basal *HMOX1* activity was notably enhanced at later time points (16 h to 24 h) and again SDF-1α treatment markedly decreased this response (Fig. 4.5.).

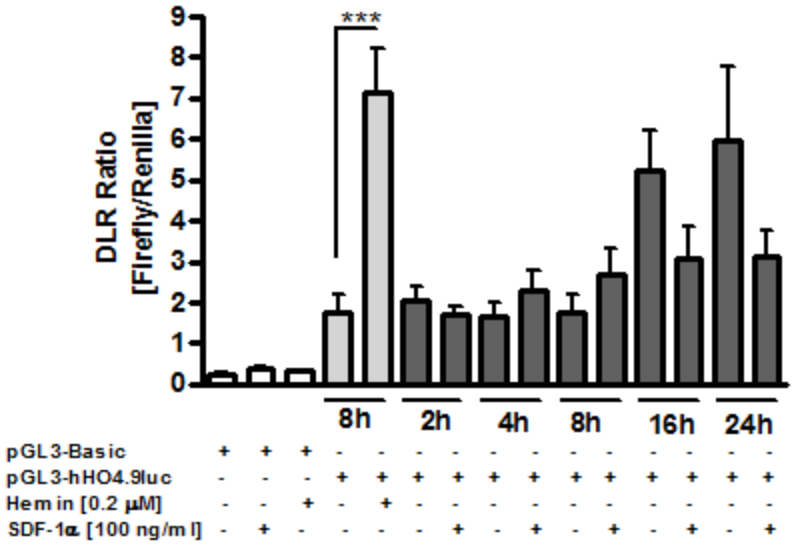

Figure 4. 5.: Effect of SDF-1α on *HMOX1* promoter activity. HUVEC were co-transfected with pGL3-hHO4.9luc or pGL3-basic control vector and pGL4.74[*hRluc*/TK] prior to treatment with hemin (0.2 µM) or SDF-1α (100 ng/ml) for the indicated time periods and *HMOX1* promoter activity was assessed using the DLRTM-assay. Data is presented as mean ± SEM (n=4 experiments), *** p<0.001 vs matched untreated control.

Recent studies demonstrated increased *HMOX1* promoter activity in response to the pro-angiogenic mediators VEGF and SDF-1α in human aortic EC (Deshane *et al.*, 2007). These experiments were conducted using a promoter construct containing an additional response element-rich region in the distal *HMOX1* promoter spanning the DNA sequence between -9.1 kb and -11.6 kb. To assess whether transcription factor binding sites within this region regulate *HMOX1* activity in HUVEC, time course experiments were repeated using the pHOGL3/9.4 promoter construct, containing 9.4 kb of the human HO-1 promoter. Here, exposure to the HO-1 inducer hemin (0.2 µM) for 8 h resulted in a minimal promoter response in pHOGL3/9.4 transfected cells, whereas cells transfected with pGL3-hHO4.9luc showed a 3-fold induction in *HMOX1* activity, a similar hemin-induced response as seen in previous experiments (Fig. 4.6.). Again, *HMOX1* activity was not altered by VEGF or SDF-1α after 2 h to 8 h compared to time-matched untreated controls and basal promoter activity was markedly enhanced after 16 h and 24 h culture. This effect was completely inhibited by VEGF and partially diminished by SDF-1α (Fig. 4.7.).

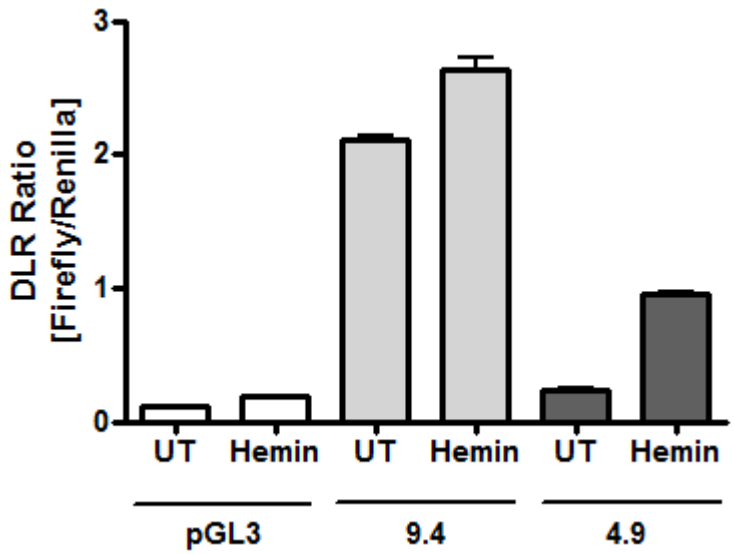

Figure 4. 6.: Investigating *HMOX1* promoter activity of HUVEC cultured in 6-well plates. HUVEC were co-transfected with pHOGL3/9.4 (9.4) or pGL3-hHO4.9luc (4.9) or pGL3-Basic control vector and pGL4.74[*hRluc*/TK] and left untreated (UT) or treated with hemin (0.2 µM) for 8 hrs. *HMOX1* promoter activity was assessed using the DLRTM-assay. Data is presented as mean ± SEM (n=1 experiment).

Numerous stress-responsive elements (StRE) have been identified within the distal *HMOX1* promoter that mediate transcriptional activation in response to a variety of inducers (Ryter *et al.*, 2006). The presence of these motifs might explain the differences in basal promoter activity between the pHOGL3/9.4 and pGL3-hHO4.9luc promoter plasmids. Further, the high basal *HMOX1* activity observed in cells transfected with the 9.4 kb promoter construct might counteract the effect of the HO-1 inducer hemin, which itself might regulate transcriptional motifs in the more proximal region of the *HMOX1* promoter.

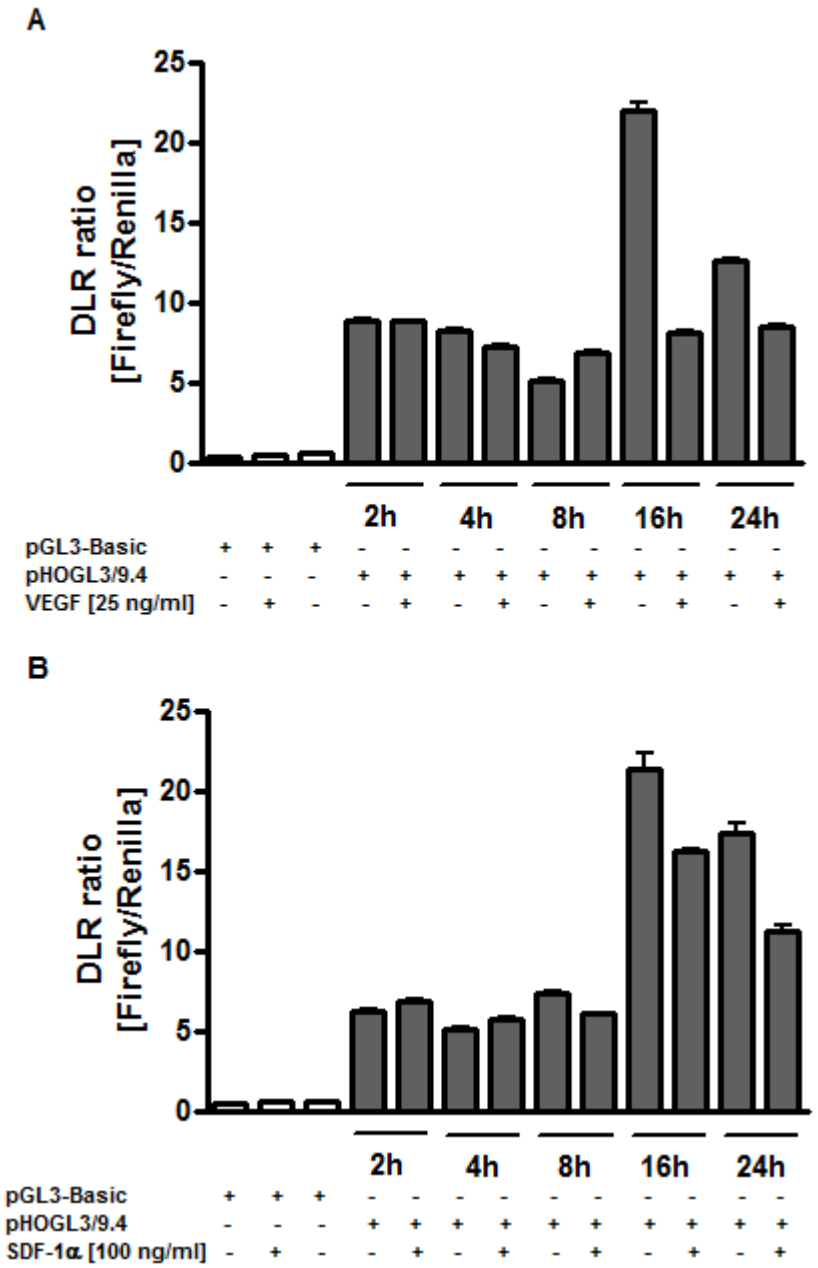

Figure 4. 7.: Effect of VEGF or SDF-1α on *HMOX1* promoter activity using the pHOGL3/9.4 promoter construct. HUVEC were co-transfected with pHOGL3/9.4 or pGL3-basic control vector and pGL4.74[*hRluc*/TK] prior to treatment with (A) VEGF (25 ng/ml), or (B) SDF-1α (100 ng/ml) for the indicated time periods and *HMOX1* promoter activity was assessed using the DLRTM-assay. Data is presented as mean ± SEM (n=1 experiment).

4.3. DISCUSSION

The heme oxygenase system has been proven to influence numerous molecular processes within the vasculature. The end-products of the degradation of the higly toxic heme moiety and the HO-1 enzyme itself regulate cell homeostasis and metabolism, and play a role in pathological processes. Moreover, HO-1 and its products, alone or in concert, perform important physiological functions in the vasculature that are linked to endothelial cytoprotection, including anti-inflammatory, anti-apoptotic, and anti-oxidant effects (please see section 1.3.3).

However, the recognised roles of HO-1 extend far beyond cytoprotection and growing evidence now suggests a role for HO-1 in angiogenesis. In recent years, research has implicated HO-1 in EC survival, proliferation, and tubule formation (Deramaudt *et al.*, 1998; Jozkowicz *et al.*, 2003; Bussolati *et al.*, 2004). This is supported by the findings that VEGF treatment results in HO-1 induction in the chick embryo chorioallantoic membrane, as well as increased expression in human EC, which is associated with increased enzymatic activity (Fernandez and Bonkovsky, 2003; Bussolati *et al.*, 2004). VEGF activates PI3K/Akt, p38, ERK1/2, and JNK MAPK signalling pathways, which also influence HO-1 expression in an inducer-, cell type-, and species-specific manner (Zachary, 2001; Ryter *et al.*, 2006). However, the identification of the acting pathway, alone or in combination, to regulate VEGF-mediated induction of HO-1 still remains elusive. The purpose of the studies in this chapter was to demonstrate induction of HO-1 in response to pro-angiogenic factors VEGF and SDF-1α in proliferating cultured human EC, and to identify transcriptional mechanisms that might regulate HO-1 driven angiogenesis in response to these factors.

Previous studies from our laboratory have reported an induction of HO-1 protein in response to VEGF after 24 h and 48 h in human EC isolated from umbilical veins (HUVEC) and EC of the microvasculature (HMEC-1) (Bussolati *et al.*, 2004). Likewise, time course experiments in this study resulted in a significant increase in HO-1 mRNA expression after 8 h VEGF treatment, with maximal expression after 24 h in proliferating HUVEC cultures (Fig. 4.1.A). Protein expression was significantly up-regulated after 16 h and peaked at 24 h in response to VEGF (Fig. 4.1.B). Deshane *et al.* (2007) recently proposed a relationship between the pro-angiogenic factor SDF-1α and HO-1. SDF-1α is the predominant chemokine for the mobilisation of hematopoietic stem cells

and endothelial progenitors to sites of injury and facilitates repair (Askari *et al.*, 2003; Kucia *et al.*, 2004; Walter *et al.*, 2005; Yamaguchi *et al.*, 2003). They found significantly increased HO-1 mRNA expression after 4 h, resulting in enhanced protein levels after 16 h exposure to SDF-1α in human aortic EC (HAEC). These findings are in concordance with the results from this study, showing SDF-1α-induced HO-1 mRNA after 2 h to 4 h and elevated HO-1 protein after 4 h and 8 h in proliferating HUVEC (Fig. 4.2.). Of note, high variability in basal HO-1 expression was observed between all experiments and induction of HO-1 by both VEGF and SDF-1α varied notably between cell isolates from different donors.

The proximal region of the human HO-1 promoter (~-243/-198 bp) contains a variable GT-rich region ($(GT)_n$), ranging from 11 to 42 repeats (Exner *et al.*, 2004). In recent years, research has shown that these $(GT)_n$ polymorphism affect transcription, modulate basal and induced HO-1 expression, and are of clinical relevance. For instance, type II diabetes patients with longer $(GT)_n$ repeats display reduced HO-1 expression and are at higher risk for the development of coronary artery disease (Chen *et al.*, 2002; Song *et al.*, 2009). In contrast, short $(GT)_n$ microsatellite polymorphisms are associated with reduced expression of pro-inflammatory markers (Li *et al.*, 2005). Moreover, transfection of aortic smooth muscle cells with reporter plasmids harbouring *HMOX1* promoter constructs with variable $(GT)_n$ repeats, demonstrated diminished HO-1 activity in cells transfected with constructs with longer $(GT)_n$ repeats (≥ 29) than those with short repeats (11, 16 or 20) (Chen *et al.*, 2002). Importantly, promoter polymorphism-dependent variability in HO-1 expression has also been reported in the human EC, affecting cytoprotective, anti-inflammatory, and pro-angiogenic properties of HO-1 (Taha *et al.*, 2010). Cell isolates from umbilical veins harbouring short $(GT)_n$ repeats in the HO-1 promoter show higher basal HO-1 expression and an increased HO-1 induction in response to a variety of inducers, are protected from oxidative stress, and show better responsiveness to VEGF resulting in enhanced EC proliferation (Taha *et al.*, 2010).

The presence of these DNA microsatellite polymorphisms within the *HMOX1* gene promoter might account for the high variability in basal and VEGF- and SDF-1α-induced HO-1 expression observed in this study. Genotyping the HO-1 promoter of human primary cell isolates and selection of cells possessing shorter HO-1 promoter alleles would be one approach to diminish

the high variability observed in HO-1 expression, and would assist studies to identify the signalling mechanisms involved in the regulation of HO-1 by pro-angiogenic factors with the aid of well-described synthetic MAPK inhibitors and/or dominant-negative adenovirus targeting MAPK. However, pre-selection of more active alleles does not represent the situation of the whole human population and therefore might result in contradictive outcomes. The use of cell lines or primary isolates from species that do not exhibit $(GT)_n$ polymorphisms could further assist in the identification of signalling mechanisms. It would be therefore of interest to screen promoter regions of endothelial cells from different species, including murine, porcine, and bovine EC, for the presence of microsatellite polymorphisms. Although clear species-specific differences exist in the regulation of HO-1, conserved regulatory regions within the promoter of the mouse and human gene have been identified, possibly allowing a more species-comprehensive conclusion from these studies (Alam *et al.*, 1994; Ryter *et al.*, 2006).

Numerous transcription factors regulating *HMOX1* gene activation have been identified in an inducer-, cell type-, and species-specific manner, including KLF-2, Nrf-2, and CREB among many others (Ryter *et al.*, 2006). The human HO-1 promoter possesses several regulatory element-rich domains; the distal -10 kb region has been implicated in the induction of HO-1 in response to the organic hydroperoxides (Hill-Kapturczak *et al.*, 2003a), and the -4 kb region mediates, in part, the induction response to heme and cadmium (Hill-Kapturczak *et al.*, 2003b; Takeda *et al.*, 1994), as well as shear stress, NO donor compounds, cigarette smoke, and oxidised phospholipids (Chen *et al.*, 2003; Hara *et al.*, 1999; Favatier and Polla, 2001; Kronke *et al.*, 2003). An additional response element-rich region, the -0.3 kb region, has been identified in the proximal promoter adjacent to the transcriptional start site, containing binding sites for ETS transcription factors, NFκB, and activator protein 2 (AP-2) (Deramaudt *et al.*, 1999; Lavrovsky *et al.*, 1993; Lavrovsky *et al.*, 1994). Currently, it remains unknown which of these regulatory element-rich regions and transcription factors mediate *HMOX1* gene activation in response the pro-angiogenic factors VEGF and SDF-1α, ultimately regulating the angiogenic properties of HO-1. Therefore, an additional purpose of this chapter was to elucidate transcriptional mechanisms of growth factor-mediated activation of *HMOX1* with the aid of HO-1 promoter constructs of various lengths (Fig. 4.3.). HUVEC transfected with the promoter construct pGL3-hHO4.9luc, spanning the -4 kb regulatory element-rich region and containing transcriptional binding sites for Nrf-2, CREB, and

ETS family members, exhibited a modest increase in promoter activity in response to the HO-1 inducer hemin after 8 h (Fig. 4.4. and Fig. 4.5.). However, in time course experiments utilising this promoter construct no change in *HMOX1* promoter activity was observed after 2 h to 8 h treatment with either VEGF or SDF-1α (Fig. 4.4. and Fig. 4.5.). Deshane *et al.* recently demonstrated significantly increased HO-1 promoter activity in response to SDF-1α and also VEGF in human aortic EC. Of note, these experiments were conducted using a promoter construct (pHOGL3/9.4) containing an additional response element-rich region in the distal *HMOX1* promoter spanning the DNA sequence between -9.1 kb and -11.6 kb (Deshane *et al.*, 2007). However as seen before, in our hands 2 h to 8 h VEGF and SDF-1α treatment did not alter *HMOX1* activity compared to time-matched controls in HUVEC transfected with the promoter construct pHOGL3/9.4 (Fig. 4.7.A and B).

Interestingly, in both experiments, either using the pGL3-hHO4.9luc or pHOGL3/9.4 plasmid, basal *HMOX1* promoter activity was significantly enhanced after 16 h to 24 h of culture compared to basal activity at earlier time points (2 h to 8 h), and this effect was completely inhibited by VEGF and in part diminished by SDF-1α (Fig. 4.4., Fig. 4.5., and Fig. 4.7.). This response might be explained by a stress-response of HUVEC during the course of the assay, resulting in transcriptional activation of HO-1, subsequently suppressed by the cytoprotective actions of VEGF. Indeed, along with the proliferating effects on EC, VEGF has been recognised as a cytoprotective modulator, by protecting EC from apoptosis through induction of the anti-apoptotic genes A1 and Bcl-2 (Gerber *et al.*, 1998), enhanced induction of DAF, thereby protecting EC against complement-mediated injury (Mason *et al.*, 2001), upregulation of eNOS (Bussolati *et al.*, 2001), and stimulating synthesis of NO and PGI_2 (Kroll and Waltenberger, 1999; Laitinen *et al.*, 1997; Murohara *et al.*, 1998; He *et al.*, 1999). Of note, pHOGL3/9.4-transfected HUVEC showed a more pronounced basal induction of HO-1 compared to cells transfected with pGL3-hHO4.9luc. Moreover, the *HMOX1* promoter response to hemin was minimal in cells transfected with the longer promoter construct compared to pGL3-hHO4.9luc-transfected HUVEC showing a 3-fold induction (Fig. 4.6.). Numerous stress-responsive elements (StRE) have been identified in the –10 kb regulatory region of the *HMOX1* gene promoter. StRE,10 bp long motifs of the consensus sequence of (T/C)GCTGAGTCA, are structurally conserved among the mouse, rat, and human HO-1 gene, and mediate transcriptional activation in response to a large variety of HO-1 inducers

(Ryter *et al.*, 2006). The presence of these motifs might explain the differences in basal promoter activity between the pHOGL3/9.4 and pGL3-hHO4.9luc promoter plasmids. Further, the high basal *HMOX1* activity observed in cells transfected with the 9.4 kb promoter construct might counteract the effect of the HO-1 inducer hemin, which itself might regulate transcriptional motifs in the more proximal region of the *HMOX1* promoter.

To date, it has not been proven possible to identify potential transcriptional pathways involved in the regulation of HO-1-driven angiogenesis utilising primary human EC isolated from umbilical cords. This results from high variability in basal and induced HO-1 expression, and high basal *HMOX1* gene promoter activity. Variability in basal and induced HO-1 expression possibly results from $(GT)_n$ polymorphisms within the gene promoter that have been shown to modulate HO-1 activity, and high basal promoter activity observed is maybe caused by a stress response of cells in culture. The use of cell lines or primary cells from species that do not possess DNA microsatellite repeats within their promoter might not only reduce the variability in HO-1 expression observed between cell isolates from different donors, but might also improve transfection efficiency and in turn assist in HO-1 promoter studies.

CHAPTER 5 - HO-1 INFLUENCES THE ANGIOGENIC PHENOTYPE OF ENDOTHELIAL CELLS

5.1. INTRODUCTION

The formation of new blood vessels is highly complex process and occurs in a series of steps (section 1.2.1). The angiogenic process is strictly regulated and depends on the concerted activities of various growth factors and their receptors expressed on the surface of endothelial and accessory cells. The most important molecule controlling blood vessel morphogenesis is vascular endothelial growth factor A (VEGF) (section 1.2.2.).

Recent research now demonstrates a link between the pro-angiogenic factor VEGF and the cytoprotective enzyme HO-1, indicating a potential role for HO-1 in the regulation of VEGF-mediated angiogenesis (please see section 1.3.4.). The first evidence came from Deramaudt and colleagues, demonstrating that gene transfer of human HO-1 into coronary EC enhances proliferation and formation of capillary-like structures (Deramaudt *et al.*, 1998). HO-1 overexpression promotes EC cycle progression, while inhibiting that of vascular SMC (Li Volti *et al.*, 2002). Supportive of these findings, studies from our laboratory show that overexpression of HO-1 utilising a recombinant adenovirus expressing the human HO-1 gene increases proliferation of EC isolated from human umbilical veins (HUVEC) (Bussolati and Mason, 2006). In contrast, inhibition of HO-1 decreases EC proliferation, capillary formation, and cell cycle progression. This effect is associated with an increased expression of the cell cycle inhibitors p21 and p27, and is significantly reversed by CO but not bilirubin (Li Volti *et al.*, 2002). Moreover, aortic EC isolated from HO-1 knockout (HO-$1^{-/-}$) mice, demonstrate reduced proliferation when compared with EC from matched HO-$1^{+/+}$ littermate controls (Chen *et al.*, 2004).

HO-1 may indirectly affect angiogenesis through its ability to increase VEGF synthesis (Dulak *et al.*, 2002; Jozkowicz *et al.*, 2002; Jozkowicz *et al.*, 2003). *In vivo* experiments using a rat model of hindlimb ischaemia, demonstrate that overexpression of HO-1 enhances VEGF synthesis and augments formation of vascular capillaries, improving the blood flow in ischaemic tissues, an effect abolished by the synthetic HO inhibitor ZnPP (Suzuki *et al.*, 2003). The role for HO-1 in angiogenesis is further supported by the finding that pro-angiogenic factors, including VEGF and more recently SDF-1α, activate HO-1 expression and activity (Bussolati *et al.*, 2004, Deshane *et*

al., 2007). Studies from our laboratory demonstrate that inhibition of HO-1 using the synthetic HO antagonists SnPP or ZnPP attenuates VEGF-induced EC proliferation *in vitro*, while induction of HO-1 with cobalt protoporphyrin (CoPP) alone results in EC proliferation comparable to that seen with VEGF (Bussolati *et al.*, 2004). HO-1 inhibition prevents development of VEGF-induced neovessels *in vitro* as well as *in vivo* and *ex vivo* (Bussolati *et al.*, 2004). Deshane *et al.* demonstrated that exposure of human aortic EC (HAEC) to SDF-1α results in marked upregulation of HO-1 mRNA and protein. Pharmacological and genetic inhibition of HO-1 impaired SDF-1α-mediated endothelial tube formation, an effect reversed by a CO donor, CO-releasing molecule (CORM-2), but not bilirubin. This study further confirms the functional significance of HO-1 in angiogenesis using HO-$1^{-/-}$ mouse models of Matrigel plug and wound healing. HO-1 inhibition is closely associated with impaired neovascularisation and wound healing in injured tissue (Deshane *et al.*, 2007).

The constitutive HO isoform, HO-2, may also play a role in inflammation and angiogenesis. Animals lacking HO-2 demonstrate impaired corneal wound closure, enhanced neovascularisation, and exaggerated inflammation (Seta *et al.*, 2006). Murine aortic EC (MAEC) isolated from HO-2 null mice show an activated phenotype marked by oxidative stress, inflammation and angiogenesis (Bellner *et al.*, 2009).

The role for HO-1 in angiogenesis is complex, intriguing, and remains to be fully understood. Data to date suggest that HO-1 may influence the angiogenic process at various levels. However, the precise mechanism through with HO-1 exerts its effects during angiogenesis and the role of the HO products CO, biliverdin/bilirubin, and iron remain elusive. The aim of this chapter is firstly to optimise various well-described *in vitro* angiogenesis assays for the use with primary EC. These assays will then be adopted for studies to elucidate the precise role of HO-1 during the different steps of angiogenesis with the aid of both, loss-of-function and gain-of-function approaches. A better understanding of the angiogenic effects of HO-1 may in turn not only reveal new insights into the role of its products but may also allow for the identification of novel downstream targets of HO-1 in the regulation of angiogenesis. This will be discussed in forthcoming chapters.

5.2. RESULTS

5.2.1. Validation of human siRNA sequences against the human HO-1 and HO-2 genes

Small interfering RNA (siRNA) was used for *in vitro* inhibition studies. Different siRNA sequences targeting the human HO genes were validated for their knockdown efficiency in human EC (HUVEC) by qRT-PCR, western blotting and/or immunofluorescence.

The basal expression level of the inducible HO isoform, HO-1, is low in the majority of mammalian cells, and therefore the HO-1 inducer hemin was utilised to determine the knockdown efficiency of siRNA sequences targeting HO-1. Hemin treatment (0.2 µM for 6 h) resulted in a marked upregulation in HO-1 mRNA and protein in untransfected control cells and to the same extent in cells transfected with a non-targeting control siRNA (siCTL; Fig. 5.1.). Knockdown of HO-1 using either a single sequence siRNA (siHO-1 seq2) or a pool of 4 siRNA sequences targeting HO-1 (siHO-1 pool), both used at 40 nM, significantly inhibited the hemin-induced response in HO-1 mRNA and protein. mRNA expression was inhibited by 70-80% and protein expression was decreased by 80-85% with either siRNA compared to siCTL-transfected cells (Fig. 5.1.). Moreover, the immunofluorescent signal detected by antibody-staining of HUVEC transfected with siHO-1 pool was notably reduced compared to cells treated with the siRNA delivery agent geneFECTOR (GF) or non-targeting control siRNA (Fig. 5.2.). Later in this chapter, 3'-AlexaFluor488-labelled siRNA was used in migration studies to assist quantification by single cell tracking. Western blotting analysis revealed a sufficient knockdown of HO-1 protein by 85% in HUVEC compared to GF-treated or siCTL-transfected cells. siHO-1 $seq2_{AF488}$ had no effect on HO-2 expression levels (Fig. 5.3.). In studies throughout this thesis, the validated siRNA sequences targeting HO-1 will be used in *in vitro* inhibition studies to specifically silence HO-1.

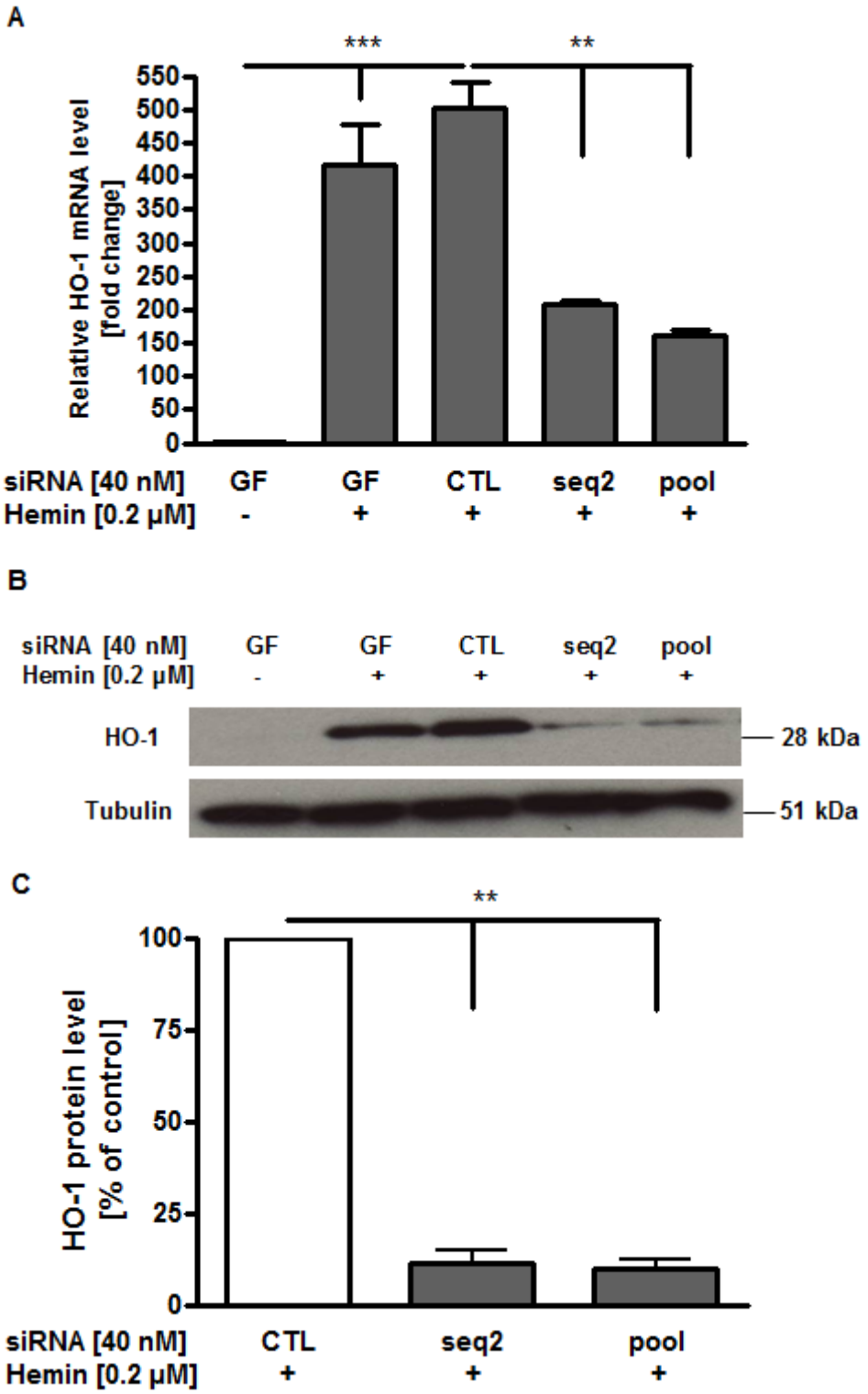

Figure 5. 1.: Knockdown efficiency of siRNA against HO-1 in HUVEC. HUVEC were either treated with geneFECTOR (GF) or transfected with 40 nM control siRNA (CTL) or HO-1 specific siRNA (seq2, pool) for 48 h in the presence of hemin (0.2 µM) for the last 6 h, prior to (A) mRNA quantification by qRT-PCR or (B, C) protein quantification by western blotting. (B) shows a representative blot, (C) shows the corresponding densitometry. Tubulin was used as a loading control. Data is presented as mean ± SEM (n=3 experiments), ** $p<0.01$, *** $p<0.001$.

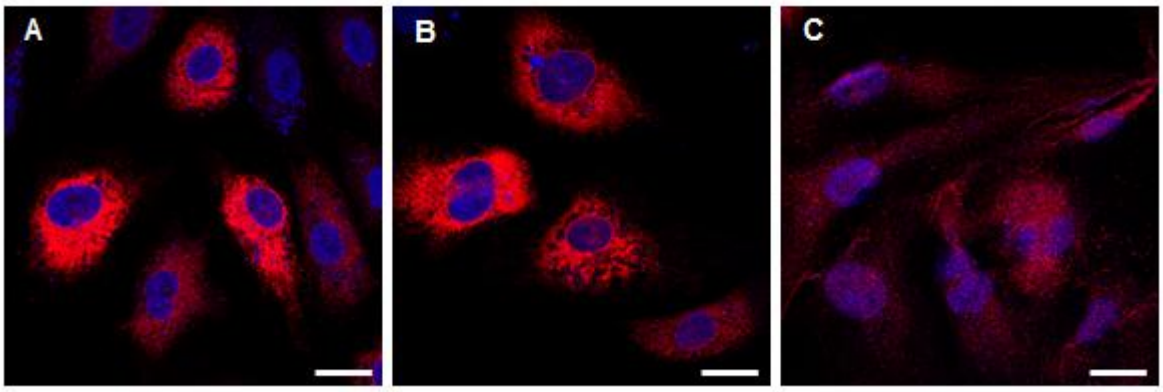

Figure 5. 2.: Validation of knockdown efficiency of siRNA against HO-1 in HUVEC by immunofluorescent staining. HUVEC were either treated with (A) geneFECTOR (GF) alone or transfected with 40 nM (B) control siRNA (CTL) or (C) HO-1 specific siRNA (pool) and seeded onto gelatin-coated coverslips for 48 h prior to methanol fixation and HO-1 staining using an anti-HO-1 mAb. Nuclei were stained with Draq5. Immunofluorescent staining was analysed by z-stack confocal microscopy. Pictures are representative images from n=3 experiments, 63X magnification. Bars equal 50 µm.

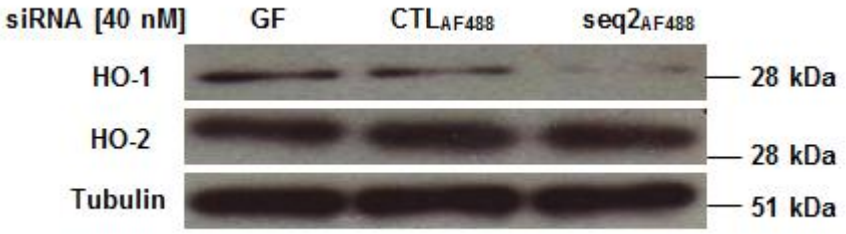

Figure 5. 3.: Knockdown efficiency of 3'-AlexaFluor488-labelled siRNA against HO-1 in HUVEC. HUVEC were either treated with geneFECTOR (GF) alone or transfected with 40 nM 3'-AlexaFluor488-labelled control siRNA (CTL_{AF488}) or HO-1 specific siRNA ($seq2_{AF488}$) for 48 h prior to protein level quantification by western blotting. Tubulin was used as a loading control. A representative blot from n=3 experiments is shown.

The constitutive isoform HO-2 is abundantly expressed in mammalian tissues. Different HO-2 targeting siRNA sequences (siHO-2 seq3, -4, -5, -6) were tested for their knockdown efficiency in HUVEC by western blotting. Transfection of HUVEC with siCTL had no effect on HO-2 protein compared to GF-treated cells. siHO-2 seq 3 and siHO-2 seq4 reduced protein levels to a minor extent, whereas siHO-2 seq5 and siHO-2 seq6 significantly decreased HO-2 protein by 75-80% (Fig. 5.4.). The latter two siRNA sequences targeting HO-2 will therefore be utilised for HO-2 gene silencing in forthcoming studies.

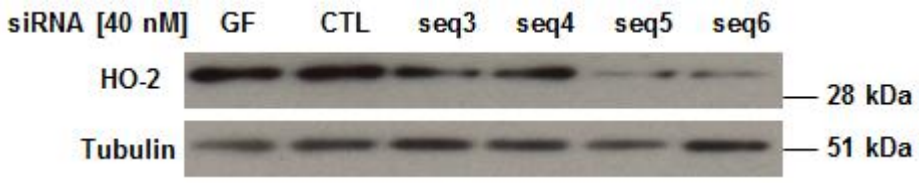

Figure 5. 4.: Knockdown efficiency of siRNA against HO-2 in HUVEC. HUVEC were either treated with geneFECTOR (GF) alone or transfected with 40 nM control siRNA (CTL) or different sequences of HO-2 specific siRNA (seq3, seq4, seq5, seq6) for 48 h prior to protein level quantification by western blotting. Tubulin was used as a loading control. A representative blot from n=3 experiments is shown.

5.2.2. Validation of the recombinant adenovirus expressing the human HO-1 gene

A recombinant adenovirus expressing the human HO-1 gene (AdHO-1) was used in gain-of-function studies in the course of this thesis. The optimal multiplicity of infection (MOI) in human EC was assessed by western blotting. As seen in Fig. 5.5., infection of HUVEC with the control adenovirus containing an empty vector (Ad0) had no effect on HO-1 protein levels when used at an MOI of 50 or 100 virus particles per cell when compared to non-infected control cells. AdHO-1 at an MOI of 50 markedly increased HO-1 protein and this effect was even more enhanced at an MOI of 100. Based on these findings, an adenoviral MOI of 100 virus particles per cell was used in this study.

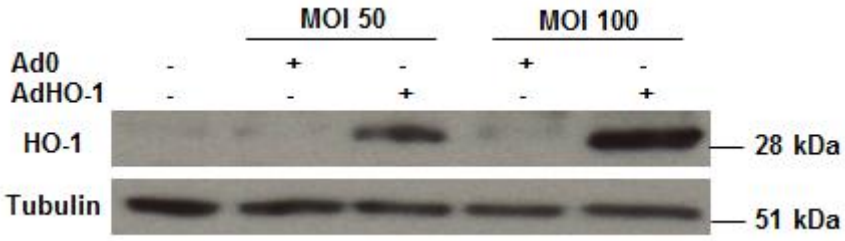

Figure 5. 5.: Validation of the recombinant adenovirus expressing the human HO-1 gene. HUVEC were either left uninfected of infected with a control adenovirus containing an empty vector (Ad0) or the recombinant adenovirus expressing the HO-1 gene (AdHO-1) at different multiplicities of infection (MOI) for 2 h in plain M199 medium prior to subsequent culture for 48 h. HO-1 protein expression was assessed by western blotting. Tubulin was used as a loading control. Representative blots from n=3 experiments are shown.

5.2.3. Inhibition of HO-1 impairs VEGF-mediated endothelial cell proliferation *in vitro*

The non-radioactive pyrimidine analogue 5-bromo-2'-deoxyuridine (BrdU) becomes incorporated into the genomic DNA of dividing cells in place of thymidine, allowing the detection and quantification of cell proliferation in culture.

To determine the optimal time point of vascular endothelial growth factor (VEGF)-induced proliferation of human EC *in vitro*, HUVEC were sparsely seeded onto gelatin-coated culture dishes in growth-factor-free medium in the absence or presence of 25 ng/ml VEGF for various time periods (Fig. 5.6.). Endothelial cell growth supplement (ECGS) was used as a positive control for proliferation and significantly increased EC proliferation after 72 h of culture. Likewise, treatment with the mitogen VEGF notably increased EC proliferation by 200% after 24 h compared to untreated control cells, and this effect was further enhanced after 48 h and 72 h of culture in the presence of VEGF, resulting in an increase in proliferation by 400% and up to 600%, respectively (Fig. 5.6.). The 48 h time point was chosen for forthcoming studies investigating the role of HO-1 in VEGF-mediated EC proliferation *in vitro*.

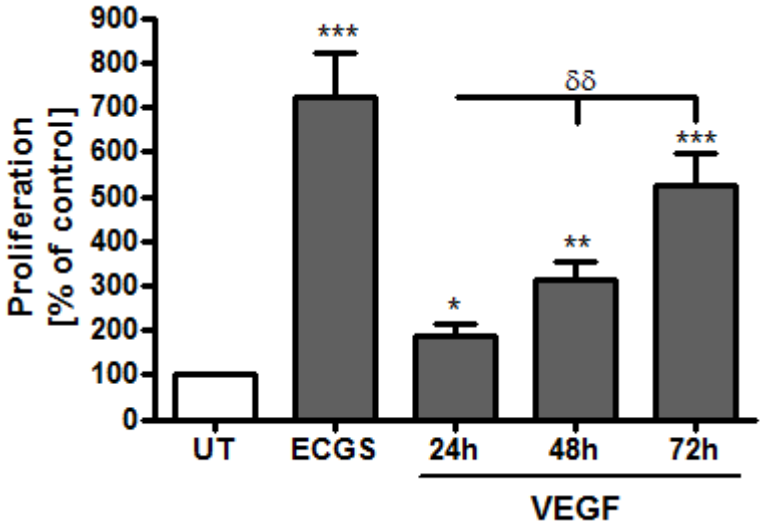

Figure 5. 6.: VEGF-induced human endothelial cell proliferation *in vitro*. HUVEC were left untreated (UT) or treated with 30 µg/ml ECGS for 72 h, or 25 ng/ml VEGF for the indicated time periods. EC proliferation was quantified by BrdU incorporation. Data is presented as mean ± SEM (n=5 experiment), * $p<0.05$, ** $p<0.01$, *** $p<0.001$ vs UT control, δδ $p<0.01$.

In initial studies, utilising the synthetic HO inhibitor zinc protoporphyrin (ZnPP), sparsely seeded HUVEC cultured in growth factor-free medium were treated with 25 ng/ml VEGF, ZnPP alone at 5 µM, 10 µM, or 20 µM, or VEGF and ZnPP in combination for 48 h (Fig. 5.7). ZnPP alone, at either concentration used, had no effect on EC proliferation. But as seen before, VEGF significantly enhanced proliferation after 48 h of culture. This effect was inhibited by ZnPP in a dose-dependent manner, resulting in complete inhibition of proliferation with ZnPP used at 20 µM.

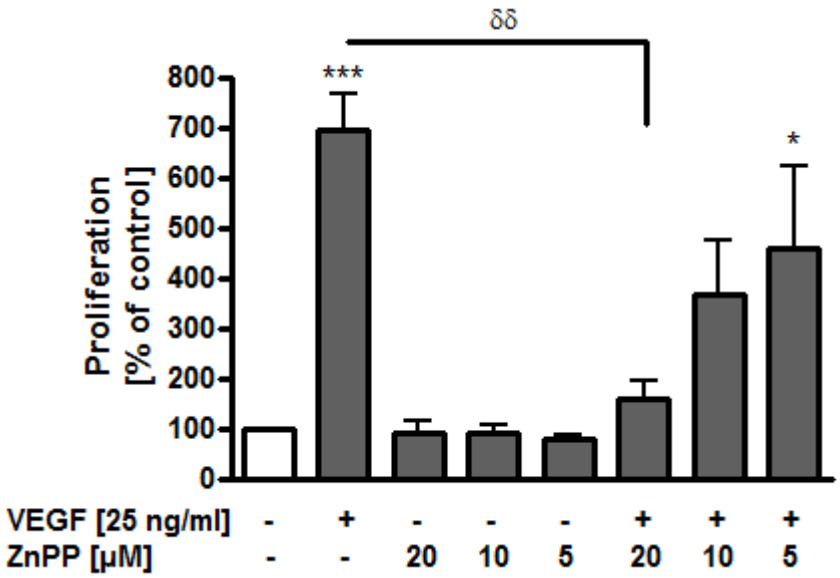

Figure 5. 7.: ZnPP inhibits VEGF-mediated proliferation in a dose-dependent manner. HUVEC were left untreated or treated with VEGF (25 ng/ml), ZnPP (5, 10, 20 µM), or VEGF and ZnPP in combination for 48 h. EC proliferation was quantified by BrdU incorporation. Data is presented as mean ± SEM (n=5 experiments), * $p<0.05$, *** $p<0.001$ vs UT control, δδ $p<0.01$.

Small interfering RNA (siRNA) is a more specific approach for silencing HO-1 in mammalian cells, as the synthetic inhibitor ZnPP not only inhibits the inducible isoform HO-1, but also HO-2 (Ryter *et al.*, 2006). HUVEC were treated with the siRNA delivery agent geneFECTOR (GF) or transfected with 40 nM control siRNA or HO-1 specific siRNA for 24 h, and re-seeded onto gelatin-coated 96-well plates in growth factor-free medium for the assessment of proliferation in response to VEGF by BrdU incorporation. However, HO-1-deficient cells appeared stressed after trypsin digestion and did not survive subsequent culture for 48 h either in the absence or presence of VEGF, emphasing the important protective role of HO-1.

Proliferating cell nuclear antigen (PCNA) is highly expressed in nuclei of cells in the G_1- and S-phase of the cell cycle, acting as a cofactor for DNA poymerase delta and increasing the processing of leading strand synthesis during DNA replication (Paunesku *et al.*, 2001). PCNA is a commonly used marker for cell proliferation. Of note, PCNA antibody staining coupled to FACs analysis does not require the transfer of cells to 96-well culture plates and therefore this assay was adopted to study the role of HO-1 in VEGF-induced proliferation. Exposure to VEGF for 48 h significantly increased the number of PCNA positive cells in GF-treated as well as in siCTL-transfected cultures. This effect was completely abrogated by siRNA-mediated HO-1 inhibition (Fig. 5.8.), confirming the findings obtained from inhibition studies utilising the HO inhibitor ZnPP.

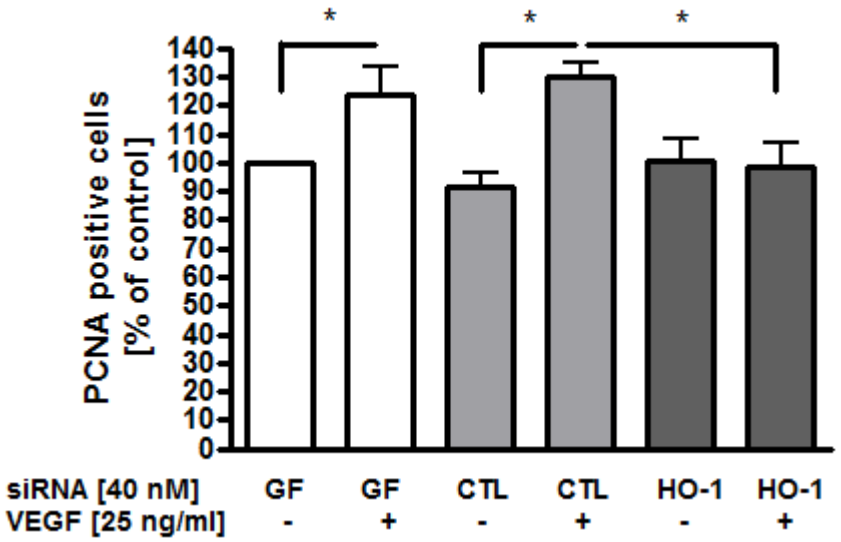

Figure 5. 8.: siRNA-mediated HO-1 depletion abrogates VEGF-induced HUVEC proliferation. HUVEC were treated with geneFECTOR (GF) or transfected with 40 nM control siRNA (CTL) or HO-1 specific siRNA (HO-1; represents pooled data from siHO-1 seq2 and siHO-1 pool) for 24 h. Cells were cultured in growth factor-free medium in the absence or presence of VEGF (25 ng/ml) for additional 48 h prior to PCNA staining and FACs analysis. Data is presented as mean ± SEM (n=5 experiments), * p<0.05.

In contrast, overexpression of the human HO-1 gene in HUVEC enhanced basal as well as VEGF-mediated proliferation *in vitro* (Fig. 5.9.). HUVEC responded to VEGF exposure with a significant increase in cell proliferation by 600%, measured as BrdU incorporation. Infection of cells with the control adenovirus containing an empty vector (Ad0) had no effect on either basal or VEGF-induced proliferation when compared to non-infected control cells, with a 6-fold increase in

proliferation in response to VEGF observed. Interestingly, basal EC proliferation was significantly enhanced in cells infected with the recombinant adenovirus expressing the HO-1 gene (AdHO-1) compared to Ad0-infected cells. Moreover, HO-1 overexpression had an effect on VEGF-mediated EC proliferation further amplifying the response by 1.5-fold compared to cells infected with the control adenovirus (Fig. 5.9).

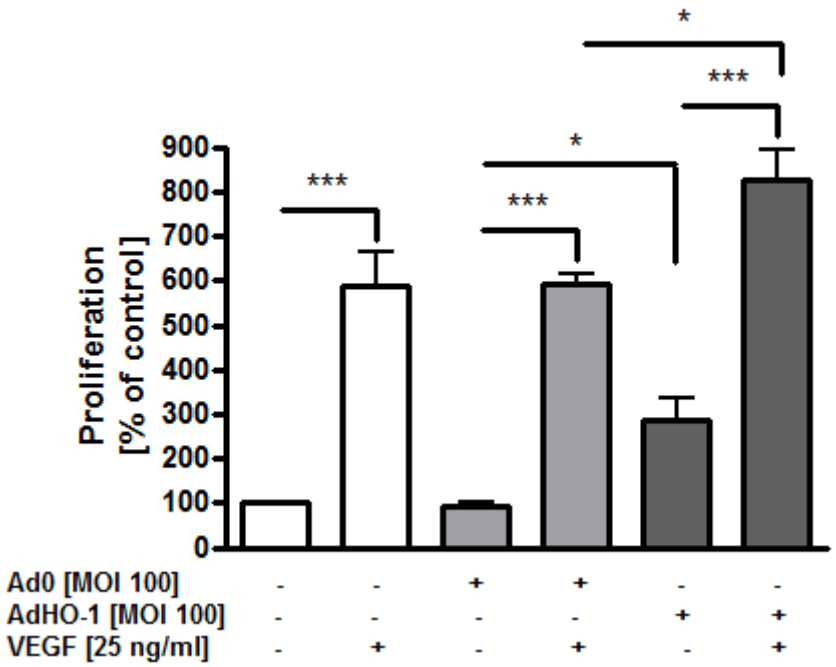

Figure 5. 9.: Recombinant adenovirus-induced expression of HO-1 enhances VEGF-mediated proliferation in HUVEC. HUVEC were left uninfected or infected with a control adenovirus containing an empty vector (Ad0) or the recombinant adenovirus expressing the human HO-1 gene (AdHO-1) for 2 h in plain M199 medium at a multiplicity of infection (MOI) of 100. Cells were cultured in the absence or the presence of VEGF (25 ng/ml) for additional 48 h. EC proliferation was quantified by BrdU incorporation. Data is presented as mean ± SEM (n=3 experiments), * p<0.05, *** p<0.001.

5.2.4. HO-1 inhibition has no effect on VEGF-mediated protection against cell death

Along with its proliferative effects, VEGF has been shown to act as a cytoprotective agent, protecting EC from apoptosis through increased induction of the anti-apoptotic genes A1 and Bcl-2 (Gerber *et al.*, 1998). HO-1 may also protect EC against apoptosis, indeed aortic EC isolated from HO-1 knockout mice are more susceptible to apoptotic stimuli and have increased caspase-3 activity compared with EC from HO-$1^{+/+}$ animals (Brouard *et al.*, 2000; Chen *et al.*, 2004). Thus,

the reduced proliferative properties of HO-1-deficient cells in response to VEGF may result from increased apoptosis of those cultures.

The CellTiter 96® Aqueous One Solution cell proliferation assay is a colorimetric method for determining the number of viable cells with the aid of a tetrazolium compound (MTS). MTS is bioreduced by cells into a formazan product that is soluble in tissue culture medium allowing measurement of absorbance (at 490 nm) directly from the culture-well plate (Cory *et al.*, 1991). The MTS assay was used to investigate a role for HO-1 in VEGF-mediated cell protection under serum-deprived conditions.

Initial optimising experiments were performed to determine the time point at which serum starvation results in a significant decrease in the number of viable cells in culture. HUVEC were cultured on gelatin-coated culture dishes in growth factor-free EC culture medium M199 supplemented with 10% FCS or serum-starved in M199 medium supplemented with 0.1% BSA in the absence or presence of VEGF (25 ng/ml) for 24 h to 48 h. Serum-deprivation for 24 h resulted in a modest but significant decrease in cell number (25-30%) compared to cells grown in the presence of 10% FCS. This effect was rescued by VEGF. The serum starvation-induced cell loss was more pronounced after 48 h of culture, resulting in a decrease in cell viability of 70-75% compared to the control. Again, this effect was significantly attenuated in the presence of VEGF (Fig. 5.10.). Based on these observations, the 48 h time point will be used in forthcoming HO-1 inhibition studies.

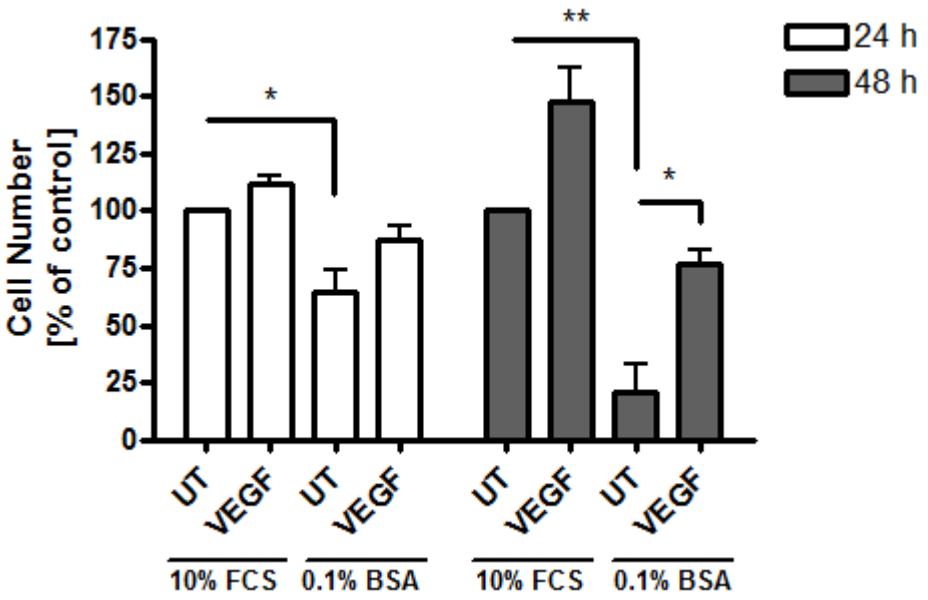

Figure 5. 10.: Serum starvation significantly decreases endothelial cell number after 48 h of culture, an effect attenuated by VEGF. HUVEC were cultured in M199 culture medium supplemented with 10% FCS or serum starved in M199 medium supplemented with 0.1% BSA in the absence (UT) or presence of VEGF (25 ng/ml) for 24 h (white bars) or 48 h (grey bars). The number of live cells was assessed using the MTS-assay. Data is presented as mean ± SEM (n=3 experiments), * $p<0.05$, ** $p<0.01$.

In HO-1 inhibition studies, enzyme activity was inhibited with the synthetic HO antagonist ZnPP or specific siRNA targeting the human HO-1 gene. ZnPP used at a concentration of 20 µM, which resulted in a significant inhibition of VEGF-mediated EC proliferation (Fig. 5.7.), had no significant effect on the cell viability of cells grown in 10% FCS after 48 h of culture. Moreover, the VEGF-induced increase in cell number was not affected by ZnPP at different concentrations (Fig. 5.11.A). Serum starvation resulted in 75% cell loss, an effect attenuated by VEGF. In the presence of ZnPP (20 µM), serum deprivation caused a decrease in cell viability to a similar extent (75%). Interestingly, HO-1 inhibition by ZnPP at either concentration had no significant effect on VEGF-mediated protection against serum starvation (Fig. 5.11.A). To confirm these observations, HO-1 was silenced using specific siRNA and the MTS-assay was repeated (Fig. 5.11.B). siCTL had no effect on cell number of cells grown in 10% compared to GF-treated cells, while VEGF significantly increased cell viability in these cultures. Inhibition of HO-1 using siHO-1 seq2 and siHO-1 pool decreased the number of viable cells by 50% and 40% respectively, but

this effect did not reach significance. Moreover, VEGF treatment was protective. Serum starvation decreased cell viability by 75% in siCTL-transfected cells and again this was rescued by VEGF. siRNA-mediated silencing of HO-1 resulted in a 90% and 75% reduction in EC viability for siHO-1 seq2 and siHO-1 pool, respectively, under serum-deprived conditions, an effect attenuated by VEGF (Fig. 5.11.B). These observations strengthen the findings observed with the ZnPP study, and suggest that HO-1 does not play an exclusive role in VEGF-mediated cell protection against serum starvation.

To further exclude apoptosis as an contributor to the impaired proliferative phenotype of HO-1-deficient EC, propidium iodide (PI) staining in combination with FACs analysis was utilised to identify apoptotic cells in culture. PI is a fluorogenic compound that binds stoichiometrically to nucleic acids so that fluorescence emission is proportional to the DNA content of a cell. When apoptotic cells are stained with PI and analysed by flow cytometry, they display a broad hypodiploid sub-G1-peak, which can be easily discriminated from the narrow peak of cells with diploid DNA content (Riccardi and Nicoletti, 2006).

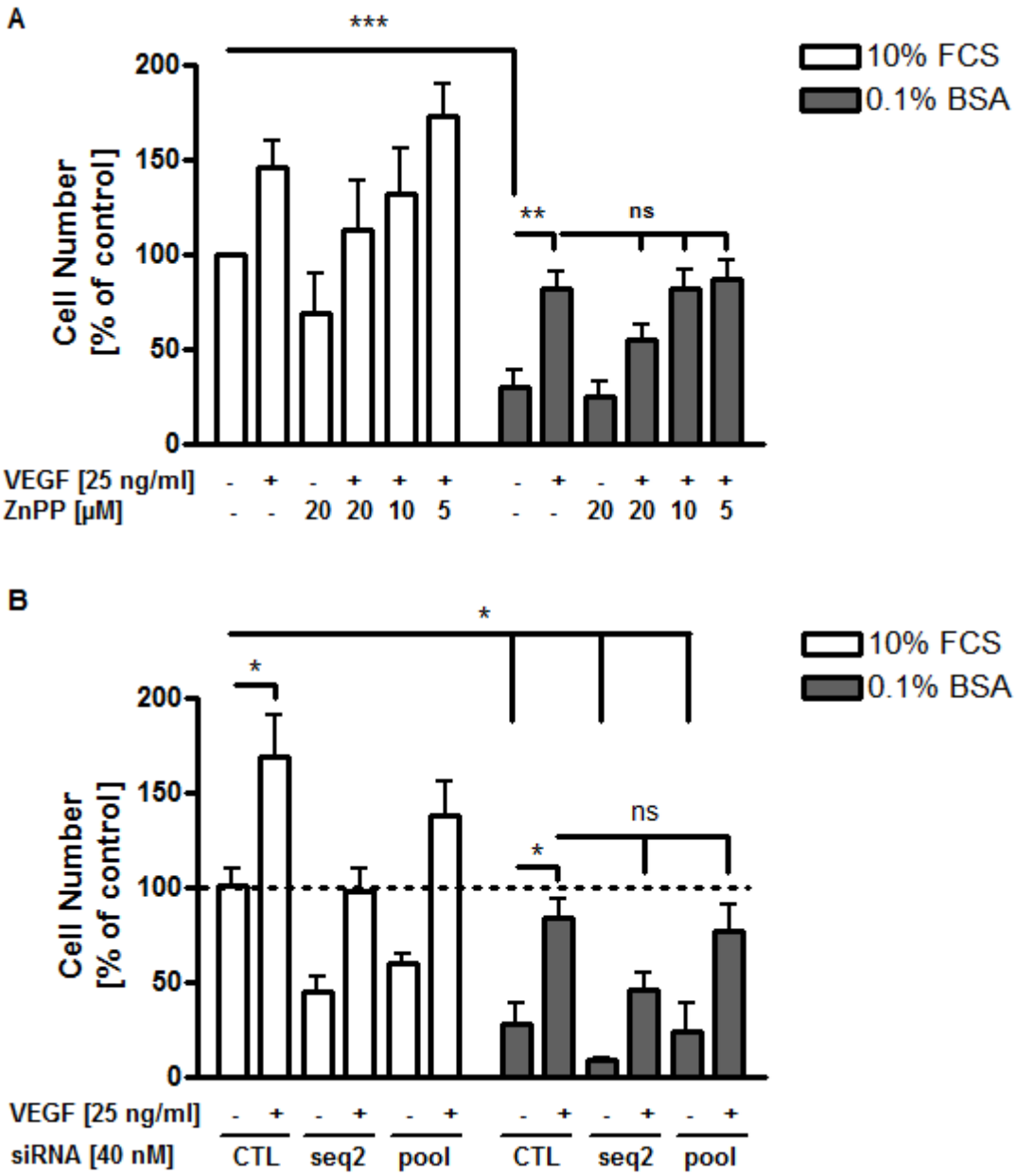

Figure 5. 11.: HO-1 inhibition has no effect on VEGF-mediated protection against serum starvation. (A) HUVEC were either grown in M199 culture medium supplemented with 10% FCS (white bars) or serum starved in M199 medium supplemented with 0.1% BSA (grey bars) in the absence or presence of VEGF (25 ng/ml), ZnPP (5, 10, 20 µM), or VEGF and ZnPP in combination for 48 h. (B) HUVEC were treated with geneFECTOR (dotted line) or transfected with 40 nM control siRNA (CTL) or HO-1 specific siRNA (seq2, pool) for 24 h. Cells were then either grown in M199 medium supplemented with 10% FCS (white bars) or serum starved in M199 medium supplemented with 0.1% BSA in the absence or presence of VEGF (25 ng/ml) for additional 48 h. The number of live cells was assessed using the MTS-assay. Data is presented as mean ± SEM (n=5 experiments for ZnPP study, n=3 experiments for siRNA study), ** p<0.01, *** p<0.001, ns – not significant.

As seen in Fig. 5.12., VEGF exposure for 48 h significantly decreased the number of apoptotic cells by 50% in cultures transfected with non-targeting control siRNA. Importantly, while HO-1 inhibition by siRNA increased apoptosis by 1.5-fold, VEGF-mediated protection was not affected in these cells, decreasing the number of apoptotic cells to a similar extent as seen in siCTL-transfected cultures (Fig. 5.12.). Moreover, as determined by qRT-PCR and western blotting, HO-1-deficient cells were still able to up-regulate the anti-apoptotic genes A1 and Bcl-2, respectively, in response to VEGF (Fig. 5.13.). Altogether these findings strongly suggest that HO-1 has no major effect on VEGF-mediated protection in endothelial cells *in vitro* and that the impaired angiogenic phenotype of HO-1-deficient cells is not caused by an increased rate of apoptosis.

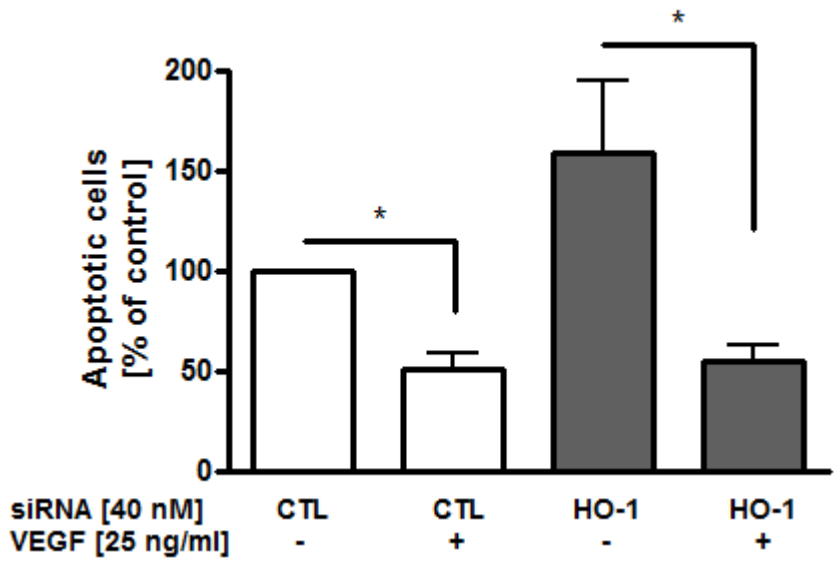

Figure 5. 12.: HO-1 inhibition has no effect on VEGF-mediated protection against cell death. HUVEC were transfected with 40 nM control siRNA (CTL) or HO-1 specific siRNA (HO-1; data represents pooled data from siHO-1 seq2 and siHO-1 pool) for 24 h prior to subsequent culture in the absence or presence of VEGF (25 ng/ml) for 48 h. Apoptotic cells were identified by propidium iodide staining prior to FACs analysis. Data is presented as mean ± SEM (n=4 experiments), * $p<0.05$.

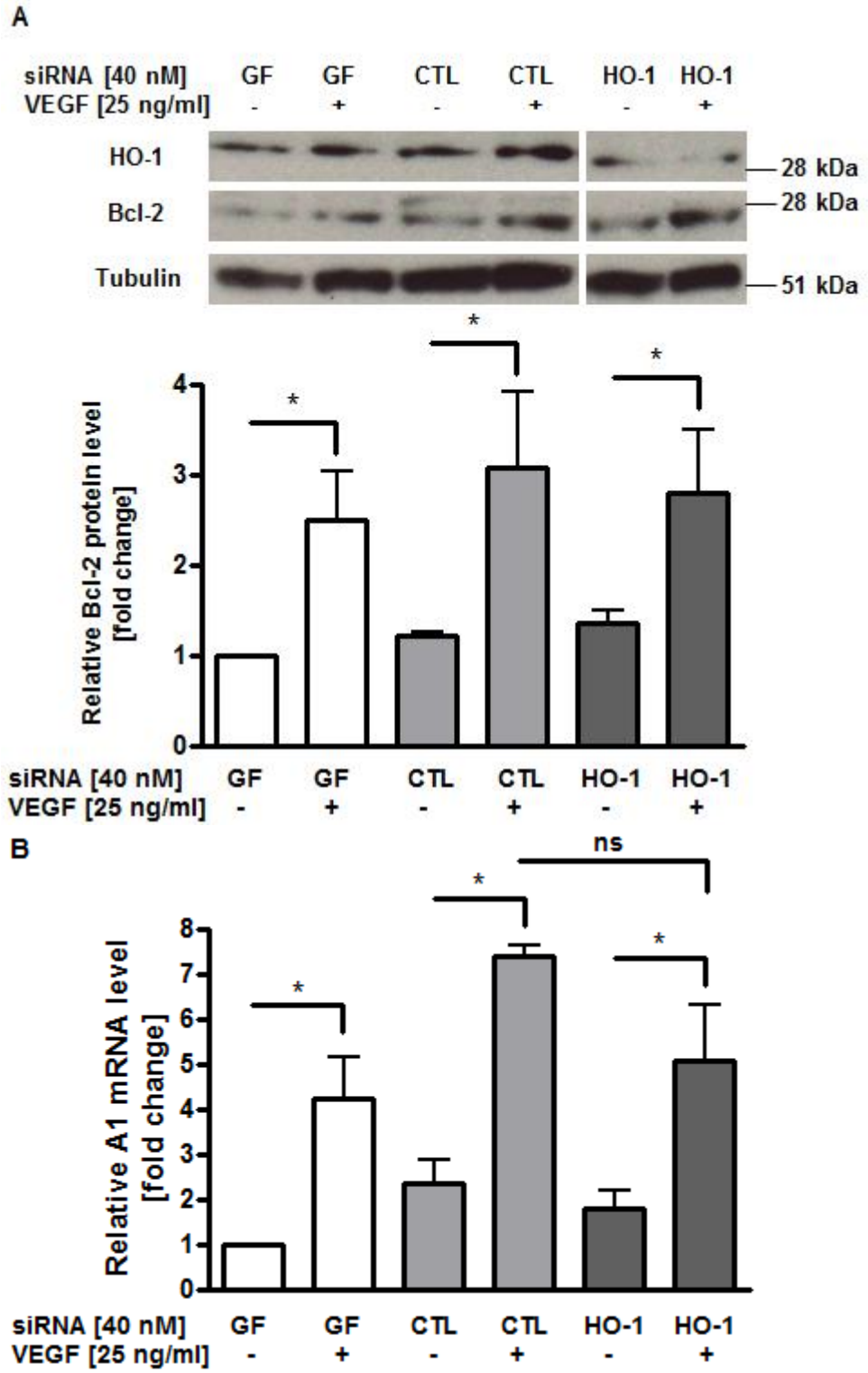

Figure 5. 13.: HO-1 inhibition has no effect on VEGF-induced expression of the anti-apoptotic genes A1 and Bcl-2. HUVEC were treated with geneFECTOR (GF) or transfected with 40 nM control siRNA (CTL) or HO-1 specific siRNA (HO-1; data represents pooled data from siHO-1 seq2 and siHO-1 pool) for 24 h prior to culture in the absence or presence of VEGF (25 ng/ml) for 48 h. (A) Bcl-2 protein levels were assessed by western blotting and quantified by densitometry. Tubulin was used as a loading control, (B) A1 mRNA expression was assessed by qRT-PCR. Data is presented as mean ± SEM (n=4 experiments), * $p<0.05$, ns – not significant.

5.2.5. HO-1 inhibition negatively affects the directional migration of endothelial cell *in vitro*

The *in vitro* scratch assay was used to study the role of HO-1 in EC migration *in vitro*. This assay is based on the observation that, upon creation of a new gap in a confluent monolayer, the so-called scratch, the cells on the edge of the newly created gap will migrate to close the scratch until new cell-cell contacts are established again. The basic steps involve creation of a scratch on monolayer cells, capture of images at the beginning and at regular intervals during cell migration to close the scratch, and comparison and quantification of the images to determine the rate of migration (Liang *et al.*, 2007). In this study, migratory properties of EC in the leading edge of the scratch were quantified by single cell tracking in terms of migration speed, and the accumulated and Euclidean distance travelled. Fluorescently-labelled siRNA was used in inhibition studies to specifically identify siRNA transfected cells for analysis. Non-transfected cells and dividing cells were excluded from the analysis.

Human EC (HUVEC) were seeded onto gelatin-coated culture dishes, transfected with either a 3'-AlexaFluor488-labelled non-targeting control siRNA (CTL_{AF488}) or an siRNA specifically targeting the HO-1 gene ($seq2_{AF488}$), and grown to confluency prior to creation of the monolayer scratch and subsequent culture for 16 h in the absence or presence of the pro-angiogenic mediator VEGF (25 ng/ml). Images of migrating cells were captured at regular 15 min intervals with the aid of time-lapse confocal microscopy and siRNA knockdown efficiency was validated by western blotting at the end of the assay. As seen in Fig. 5.14., siHO-1 $seq2_{AF488}$ sufficiently inhibited HO-1 expression in migrating EC in the absence and presence of VEGF, whereas both siRNAs, $siCTL_{AF488}$ and siHO-1 $seq2_{AF488}$, had no effect on the expression of the constitutive HO isoform HO-2. Single cell tracking revealed a modest increase in the accumulated distance and velocity of cells transfected with $siCTL_{AF488}$ in response to VEGF, however this effect was not significant. siRNA-mediated inhibition of HO-1 did not alter the accumulated distance migrated, neither in the absence nor the presence of VEGF, but had a minor effect on cell migration speed (Fig. 5.15.A and B). Interestingly, the Euclidean distance, which is the linear distance between the starting point and the end point of the migration path and thereby a measure of directionality, was significantly increased in the presence of VEGF in control siRNA transfected cells and this effect was completely inhibited by HO-1 (Fig. 5.15.C). Similar results were obtained from HO-1 inhibition studies in human EC of the microvasculature (HMEC-1). Exposure to VEGF significantly

increased the Euclidean distance travelled of cells transfected with the non-targeting control siRNA, an effect inhibited by HO-1 depletion (Fig. 5.15.D).

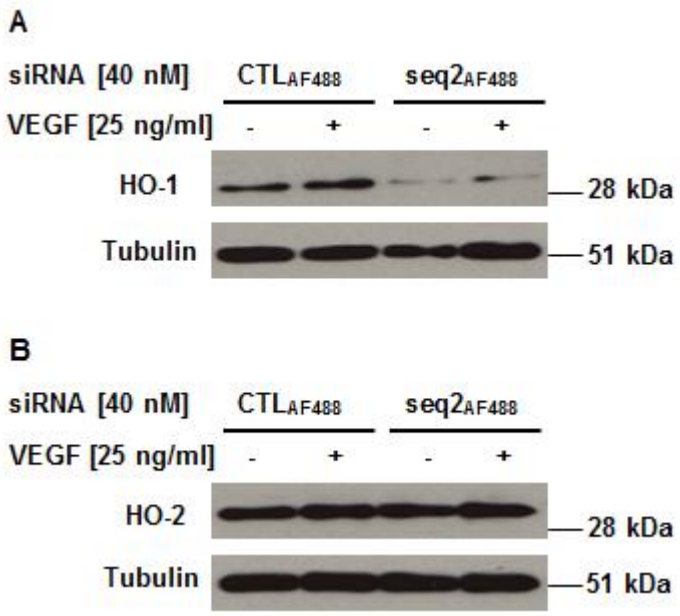

Figure 5. 14.: Validation of siRNA-mediated knockdown of HO-1 in migrating endothelial cells. HUVEC were transfected with 40 nM 3'-AlexaFluor488-labelled control siRNA (CTL_{AF488}) or HO-1 specific siRNA ($seq2_{AF488}$) for 24 h. Confluent cell monolayers were scratched and migration was assessed by live cell imaging in the absence or presence of VEGF (25 ng/ml) for 16 h. (A) HO-1 and (B) HO-2 protein levels were quantified by western blotting. Tubulin was used as a loading control. Representative blots of n=3 experiments are shown.

To further explore this observation the individual paths travelled by each cell were plotted in terms of their directionality, with the starting point of each path set to zero (Fig. 5.16). Exposure to VEGF resulted in a more linear directional movement of cells towards the scratch and the cells on the opposing side in the siCTL_{AF488}-transfected cultures, whereas HO-1-deficient cells migrated in a more random, circular pattern alongside the scratch edge.

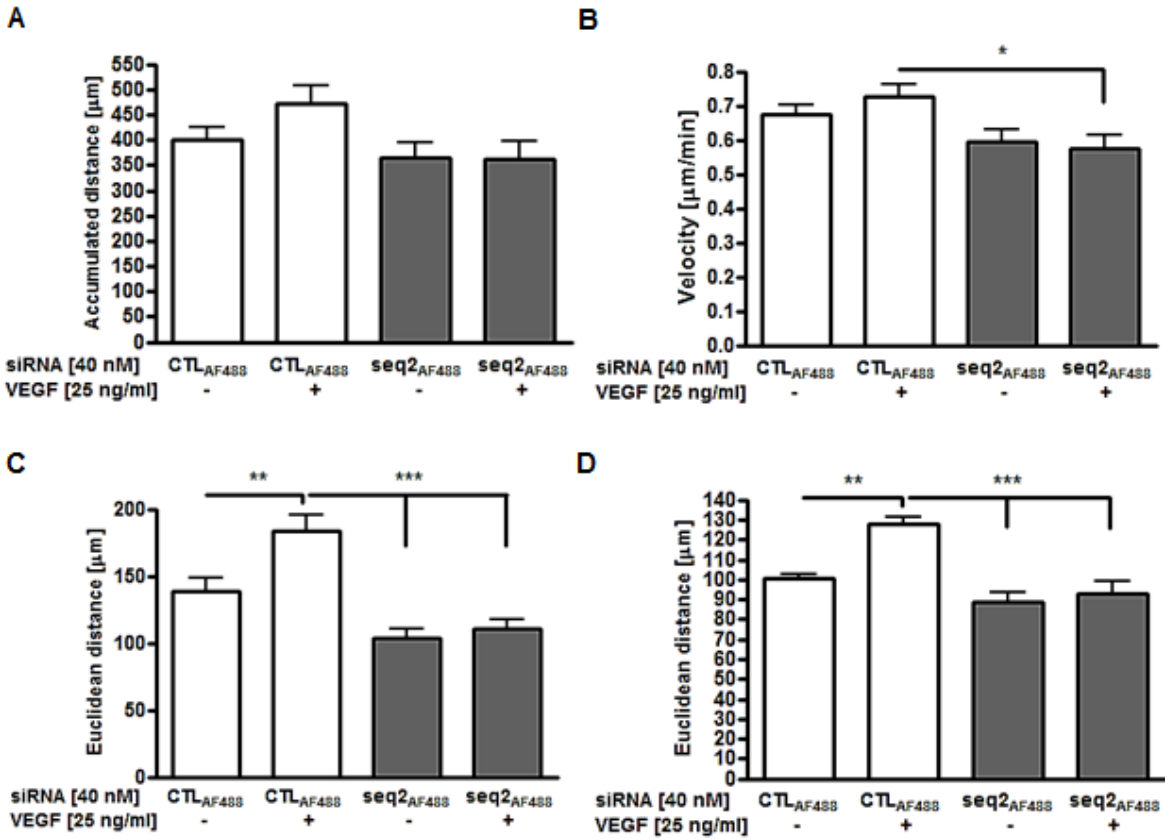

Figure 5. 15.: HO-1 inhibition impairs EC migration *in vitro*. (A, B, C) HUVEC or (D) HMEC were transfected with 40 nM 3'-AlexaFluor488-labelled control siRNA (CTL_{AF488}) or HO-1 specific siRNA ($seq2_{AF488}$) for 24 h. Confluent cell monolayers were scratched and migration was assessed by live cell imaging in the absence or presence of VEGF (25 ng/ml) for 16 h and quantified using ImageJ analysis software (Manual Tracking and Chemotaxis and Migration tool). (A) represents the accumulated distance, (B) the velocity, (C, D) the Euclidean distance. Data is presented as mean ± SD (n=3 experiments), * $p<0.05$, ** $p<0.01$, *** $p<0.001$.

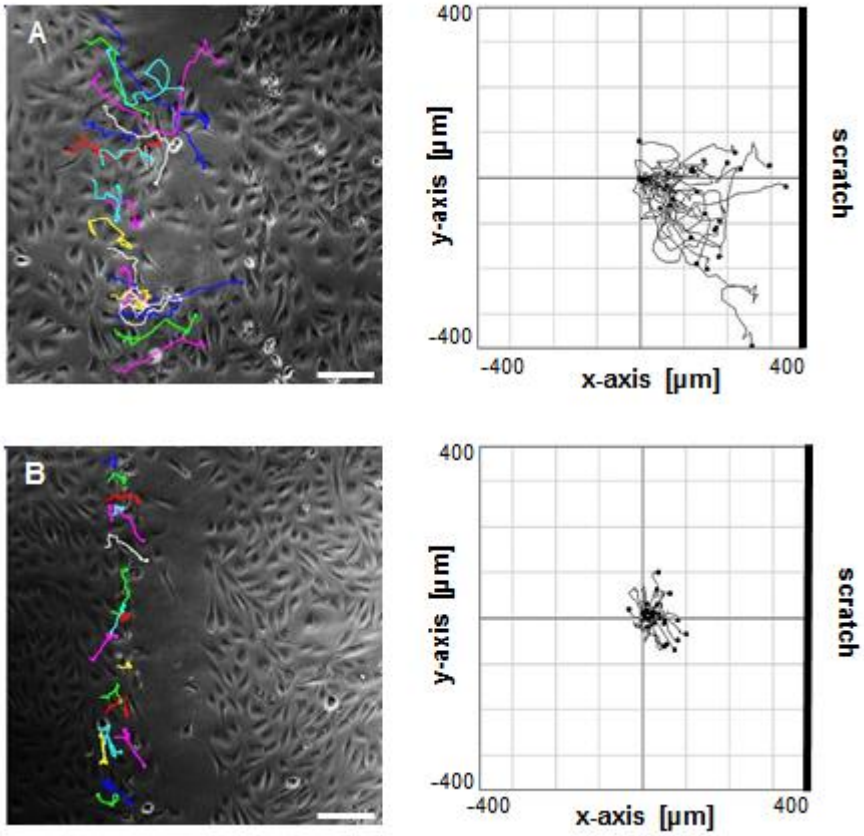

Figure 5. 16.: HO-1 inhibition alters the directional migration of EC in response to VEGF *in vitro*. The directional migration of HUVEC either transfected with 40 nM 3'-AlexaFluor488-labelled (A) control siRNA (CTL_{AF488}) or (B) HO-1 specific siRNA ($seq2_{AF488}$) in response to VEGF was quantified using ImageJ analysis software (Manual Tracking and Chemotaxis and Migration tool). Pictures are representative images from n=3 experiments and plots show the directional migration paths of individual cells. Bar equals 50 µm.

Moreover, overexpression of the human HO-1 gene in EC resulted in a modest but significant increase in Euclidean distance (Fig. 5.17.). Infection of migrating HUVEC with the recombinant adenovirus expressing the human HO-1 gene (AdHO-1) significantly increased HO-1 protein in the absence and also presence of VEGF (25 ng/ml) compared to cells infected with the control adenovirus (Ad0; Fig. 5.17.A). Quantification of the migration paths of individual cells demonstrated a significant increase in Euclidean distance in response to VEGF in control cells. Moreover, HO-1 overexpression alone or in combination with VEGF increased the Euclidean distance migrated by HUVEC, but with no synergistic effect (Fig. 5.17.B). Altogether, these findings are indicative of a role for HO-1 in the regulation of chemokinesis.

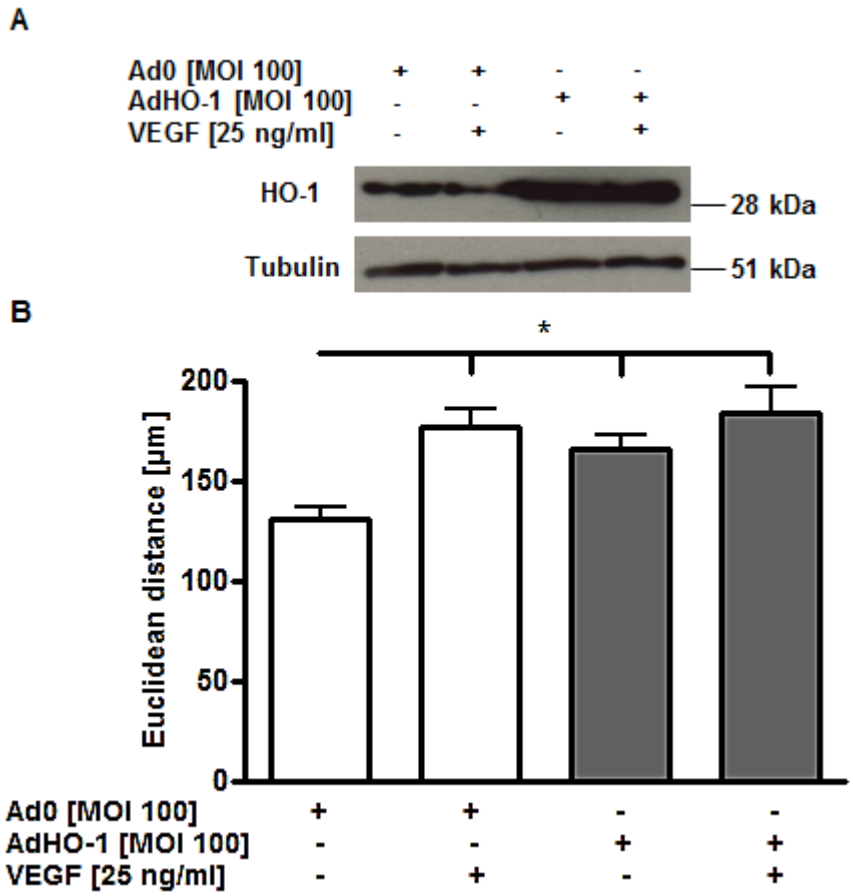

Figure 5. 17.: HO-1 overexpression favours EC migration *in vitro*. HUVEC were infected with control adenovirus containing an empty vector (Ad0) or the recombinant adenovirus expressing the HO-1 gene (AdHO-1) at an MOI of 100 for 2 h in plain M199 medium prior to subsequent culture for 16 h. Confluent cell monolayers were scratched and migration was assessed by live cell imaging in the absence or presence of VEGF (25 ng/ml) for 16 h. (A) HO-1 protein levels were quantified by western blotting. Tubulin was used as a loading control. A representative blot and data from n=3 experiments is shown. (B) The Euclidean distance was quantified by ImageJ analysis software (Manual Tracking and Chemotaxis and Migration tool). Data is presented as mean ± SD (n=3 experiments), * p<0.05.

The *in vitro* migration scratch assay is a simple and easy to perform assay that mimics to some extent the migration of EC *in vivo*. However, one of its limitations is the lack of the formation of a chemotactic gradient of growth factors over the course of the assay (Liang *et al.*, 2007). Therefore, to further investigate the potential role of HO-1 in mediating the directional migration of EC towards a pro-angiogenic stimulus, a more specific chemotaxis assay was utilised. The Ibidi µ-slide chemotaxis assay is optimised to analyse the chemotactic response of adherent cells in

linear and stable concentration profiles and was used to assess the directional migration of HO-1-deficient cells.

HUVEC transfected with either 3'-AlexaFluor488-labelled non-targeting control siRNA (CTL_{AF488}) or HO-1 specific siRNA ($seq2_{AF488}$) were re-seeded onto the collagen IV-coated observation area of the Ibidi µ-slide. The observation area is connected to two large reservoirs, one of which was filled with EC culture medium supplemented with 25 ng/ml VEGF and the second with growth factor-free medium, thereby generating a stable VEGF gradient. The migration of cells was captured by time-lapse microscopy in regular intervals (15 min) over a time period of 16 h and quantified by single cell tracking of fluorescently-labelled, non-dividing cells. Migration paths of individual cells were plotted with cells migrating towards the pro-angiogenic stimulus shown in black and cells migrating away from the stimulus shown in red (Fig. 5.18.). The majority of cells transfected with $siCTL_{AF488}$ migrated towards the VEGF gradient, whereas siRNA-mediated inhibition of HO-1 impaired the directional migration of EC, decreasing the number of cells migrating towards the VEGF gradient by >40%.

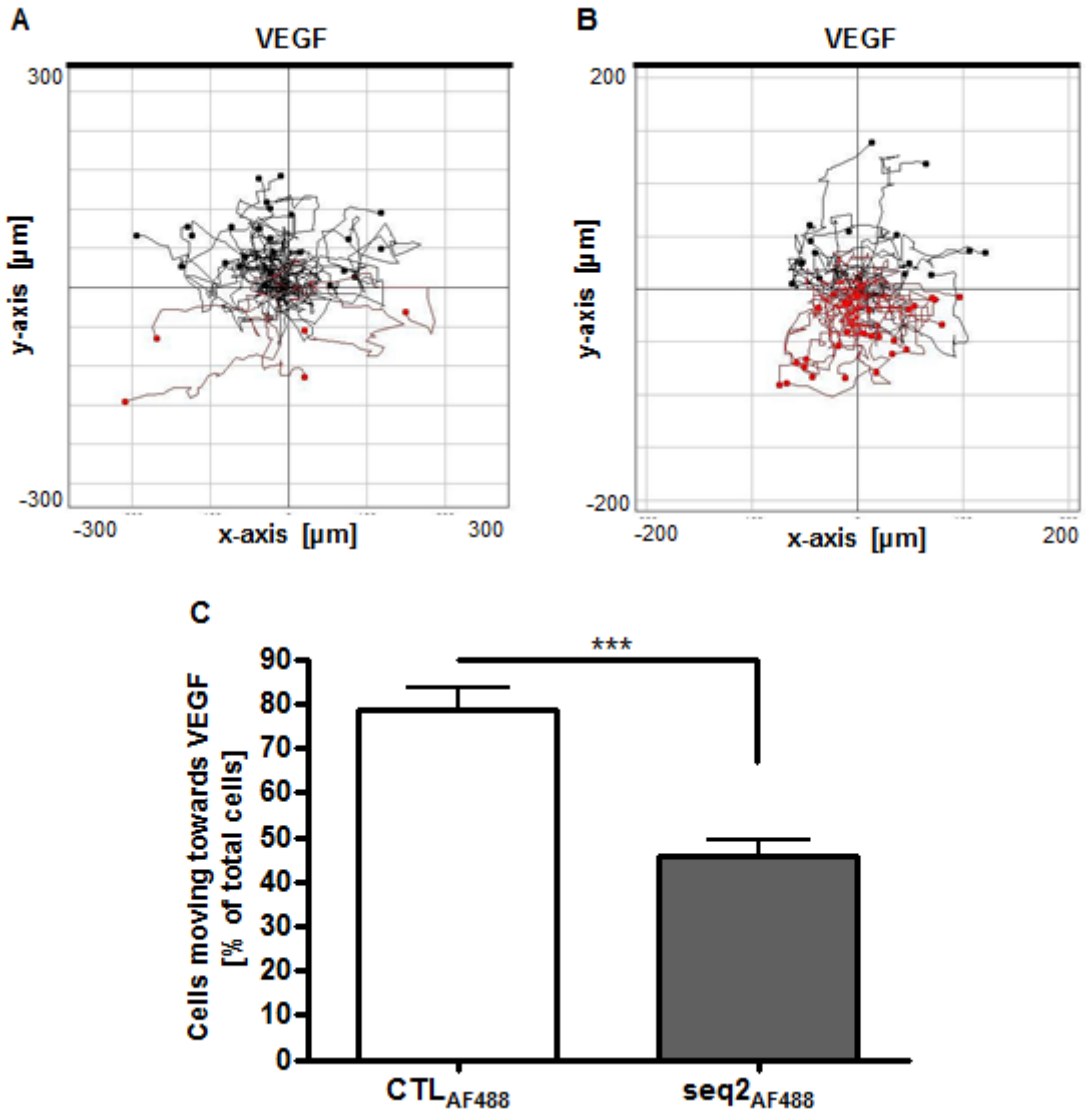

Figure 5. 18.: HO-1 inhibition impairs the directional migration of EC towards a VEGF-gradient. HUVEC were transfected with 40 nM 3'-AlexaFluor488-labelled (A) control siRNA (CTL_{AF488}) or (B) HO-1 specific siRNA ($seq2_{AF488}$) for 24 h and re-seeded onto collagen IV-coated Ibidi chemotaxis µ-slides. The upper reservoir was filled with EBM-2 culture medium supplemented with 25 ng/ml VEGF and the lower reservoir was filled with plain EBM-2 culture medium. The directional migration over a time period of 16 h was captured by time-lapse confocal microscopy and quantified using ImageJ analysis software (Manual Tracking and Chemotaxis and Migration tool). (A, B) Plots are representative images from n=3 experiments. Migration paths of cell moving towards the VEGF gradient are shown in black and migrations paths of cells migrating away from the VEGF gradient are shown in red, (C) represents the number of cells migrating towards the VEGF gradient. Data is presented as mean ± SEM (n=3 experiments), *** p<0.001.

Of note, depletion of the constitutive isoform HO-2 using specific siRNA also negatively affect the migratory properties of EC in culture. As with HO-1, knockdown efficiency was assessed by western blotting revealing a sufficient depletion of HO-2 protein in migrating HUVEC in the absence and also presence of VEGF (Fig. 5.19.). Interestingly, siRNA-mediated inhibition of HO-2 resulted in a marked upregulation of HO-1 protein, independently of VEGF.

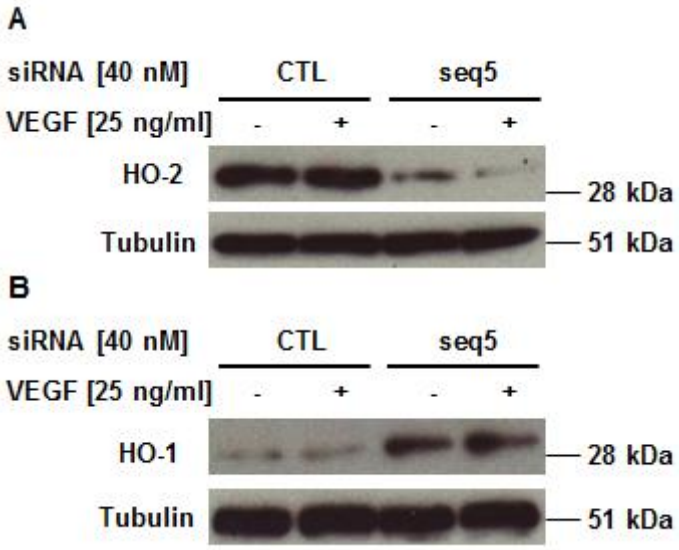

Figure 5. 19.: Validation of siRNA-mediated knockdown of HO-2 in cultures containing migrating endothelial cells. HUVEC were transfected with 40 nM control siRNA (CTL) or HO-2 specific siRNA (seq5) for 24 h. Confluent cell monolayers were scratched and migration was assessed by live cell imaging in the absence or presence of VEGF (25 ng/ml) for 16 h. (A) HO-2 and (B) HO-1 protein levels were quantified by western blotting. Tubulin was used as a loading control. Representative blots of n=3 experiments are shown.

Single cell tracking further demonstrated a significant reduction in migration speed, accumulated distance and the Euclidean distance migrated of HO-2-deficient cells compared to siCTL-transfected cells, both in the absence and the presence of VEGF (Fig. 5.20.), further supporting a role for the heme oxygenase system in the regulation of angiogenesis.

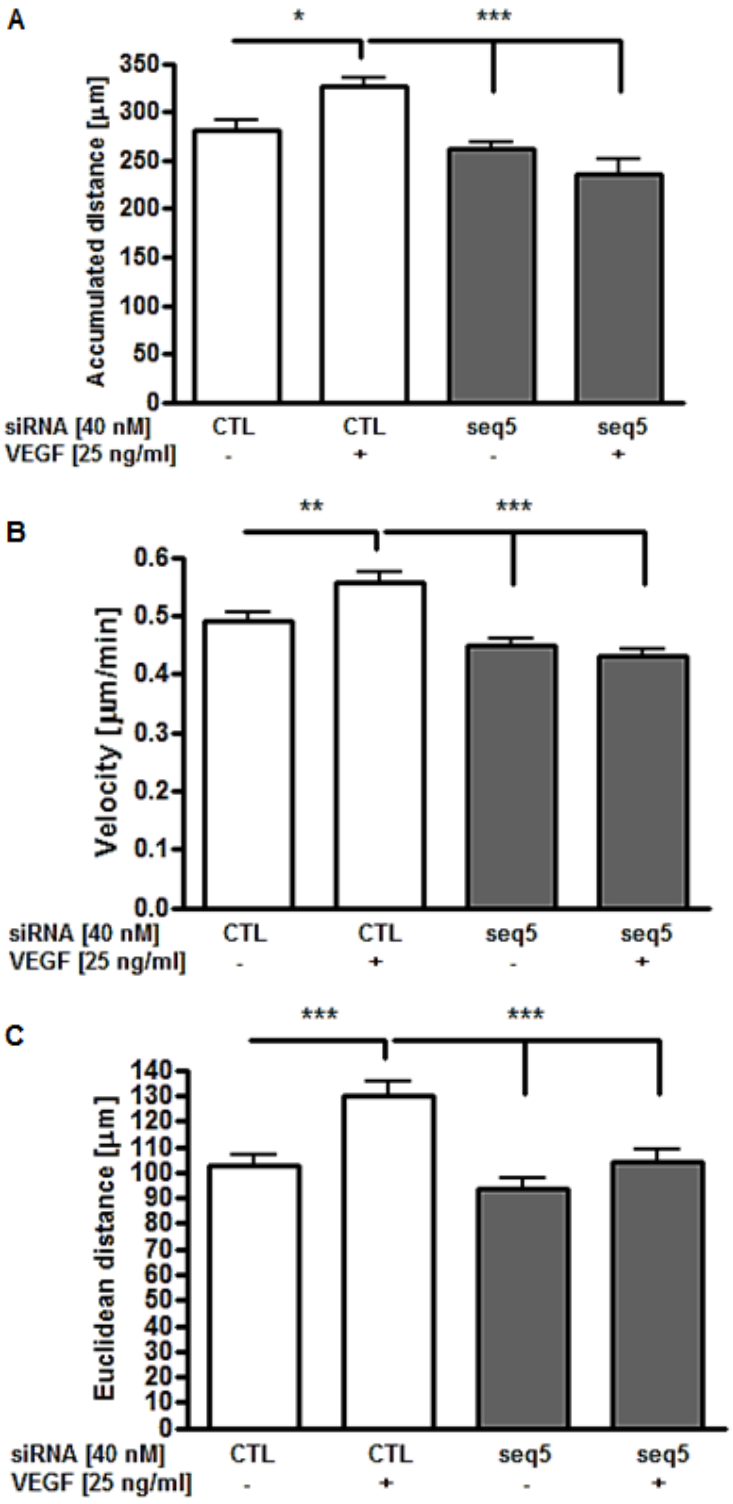

Figure 5. 20.: HO-2 inhibition impairs VEGF-mediated migration of EC *in vitro*. HUVEC were transfected with 40 nM control siRNA (CTL) or HO-2 specific siRNA (seq5) for 24 h. Confluent cell monolayers were scratched and migration was assessed by live cell imaging in the absence or presence of VEGF (25 ng/ml) for 16 h and quantified using ImageJ analysis software (Manual Tracking and Chemotaxis and Migration tool). (A) represents the accumulated distance, (B) the velocity, (C) the Euclidean distance. Data is presented as mean ± SD (n=3 experiments), * $p<0.05$, ** $p<0.01$, *** $p<0.001$.

5.2.6. HO-1 inhibition impairs endothelial cell tubule formation *in vitro*

Gene transfer of human HO-1 into coronary endothelial cells enhances formation of capillary-like structures in a 2D-Matrigel assay, whereas HO-1 antisense inhibits capillary formation (Deramaudt *et al.*, 1998; Li Volti *et al.*, 2002). Matrigel is a solubilised basement membrane preparation extracted from the Engelbreth-Holm-Swarm (EHS) mouse sarcoma, a tumour rich in extracellular matrix proteins. Its major component is laminin, followed by collagen IV, heparin sulphate proteoglycans, entactin/nidogen, and also contains TGF-β, epidermal growth factor, insulin-like growth factor, fibroblast growth factor, tissue plasminogen activator, and other growth factors which occur naturally in the EHS tumour. Endothelial cells seeded onto Matrigel rapidly attach, align, and form capillary-like tubules (6 h to 20 h for primary EC, 4 h to 8 h for cell lines), but do not proliferate. The vessels formed contain a lumen and tight cell-cell contacts (Arnaoutova *et al.*, 2009).

To further explore the role for HO-1 in tubule formation *in vitro*, HO-1 activity was inhibited using the synthetic HO inhibitor ZnPP or specific siRNA targeting the human HO-1 gene and tubule formation on 2D-Matrigel was assessed by phase-contrast microscopy. In inhibition studies utilising the synthetic compound ZnPP, HUVEC were seeded onto growth factor-reduced Matrigel in growth factor-free EC culture medium, and in the absence or presence of exogenous VEGF (25 ng/ml), ZnPP (20 µM), or VEGF and ZnPP in combination, and tube formation was assessed after 16 h (Fig. 5.21.). Exposure to VEGF significantly increased the average tube length compared to untreated control cells. Further, these cells appeared more advanced in their differentiation, having already formed a lumen, a response not seen in untreated cells (Fig. 5.21.A, B and E). Inhibition of HO by ZnPP impaired tube formation, resulting in a significant decrease in the average tube length, an effect not rescued by VEGF (Fig. 5.21.C, D and E).

These observations were subsequently confirmed using siRNA (Fig. 5.22.). HUVEC were transfected with either a non-targeting control siRNA (CTL) or HO-1 specific siRNA (seq2, pool) for 24 h and re-seeded on growth factor-reduced Matrigel in the absence or presence of VEGF for 16 h. Over the course of the assay control siRNA transfected cells formed an intact tubular network with lumenised vessels, and this was enhanced by VEGF, resulting in a significant increase in the average tube length (Fig. 5.21.A, B, and G). siRNA-mediated inhibition of HO-1

abrogated this response. Cells transfected either with siHO-1 seq2 or siHO-1 pool failed to form an intact tubular network over the time period of 16 h, resulting in short and fragile-looking structures, with an associated modest decrease in average tube length compared to untreated siCTL-transfected cells (Fig 5.22.C, E and G). Moreover, the VEGF-mediated increase in tube length as seen in siCTL-transfected cells was attenuated by HO-1 depletion (Fig. 5.22.D, F, and G). Similar observations were obtained from *in vitro* studies using HMEC-1. Here, VEGF exposure caused a significant increase in the average tube length of cells transfected with control siRNA and this response was completely attenuated by siRNA-mediated inhibition of HO-1 (Fig. 5.23.)

Murine aortic EC isolated from HO-1 knockout animals (HO-$1^{-/-}$) or wild type littermate controls (WT), have been recently shown to fail to form capillary-like structures on Matrigel *in vitro* in response to the chemokine SDF-1α (Deshane *et al.*, 2007). In this study, HO-$1^{-/-}$ MAEC and cells isolated from control animals were seeded onto growth factor-reduced Matrigel in growth factor-free EC culture medium in the absence (UT) or presence of VEGF for 16 h (Fig. 5.23.). Phase-contrast microscopy demonstrated an intact tubular network formed by WT MAEC in the absence and presence of VEGF, with the latter being more differentiated resulting in lumenised vessels with increased tube length (Fig. 5.23.A, B and E). Interestingly, EC from HO-$1^{-/-}$ animals also formed capillary-like structures on Matrigel *in vitro*, both in the absence and presence of VEGF. However, these vessels were shorter compared to vessels formed by WT cells and also appeared to be less differentiated. Cells were growing in clusters rather than aligned and forming luminal vessels (Fig. 5.23.C, D and E).

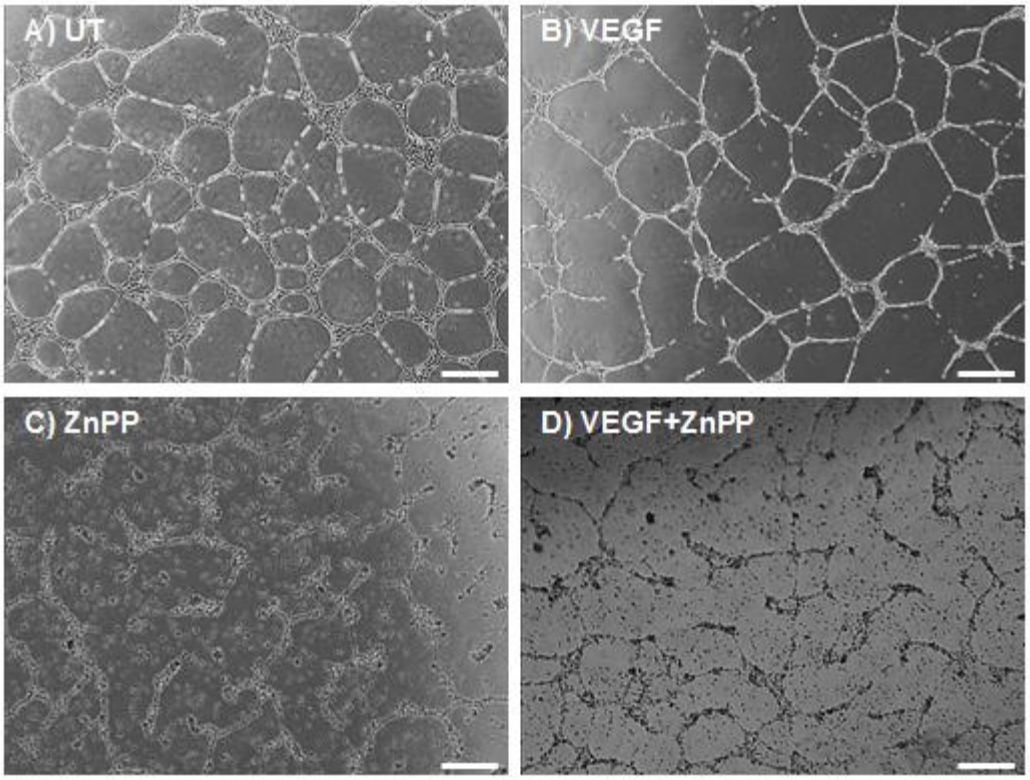

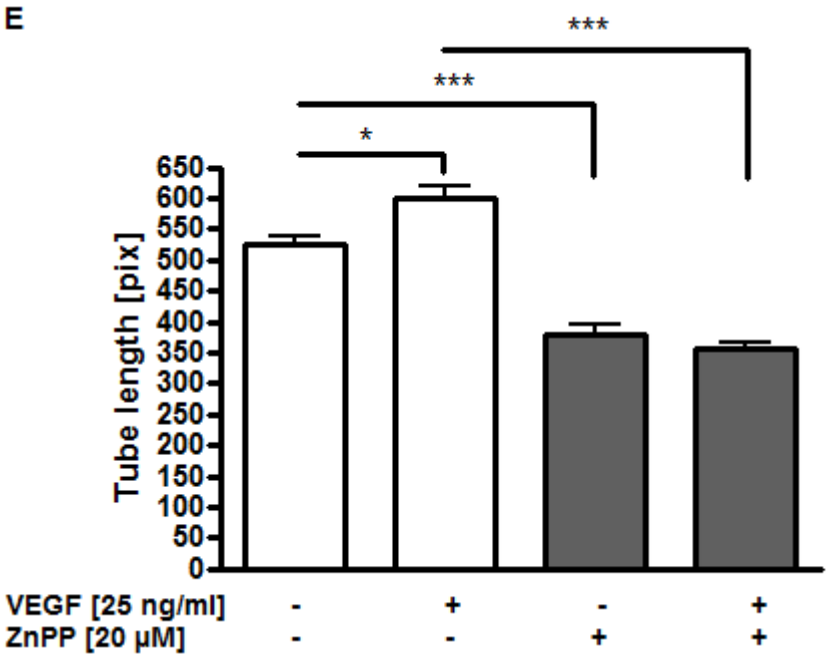

Figure 5. 21.: ZnPP inhibits human endothelial cell tubule formation *in vitro*. HUVEC were seeded onto growth factor-reduced Matrigel in plain EC culture medium and (A) left untreated or treated with (B) VEGF (25 ng/ml), (C) ZnPP (20 µM), or (D) VEGF and ZnPP in combination for 16 h and visualised using phase-contrast microscopy. Images from five fields per view were captured. Pictures are representative images from n=3 experiments, 4X magnification. Bar equals 50 µm. (E) Tube length was quantified using ImageJ analysis software (NeuronJ). Data is presented as mean ± SEM (n=3 experiments), * $p<0.05$, *** $p<0.001$.

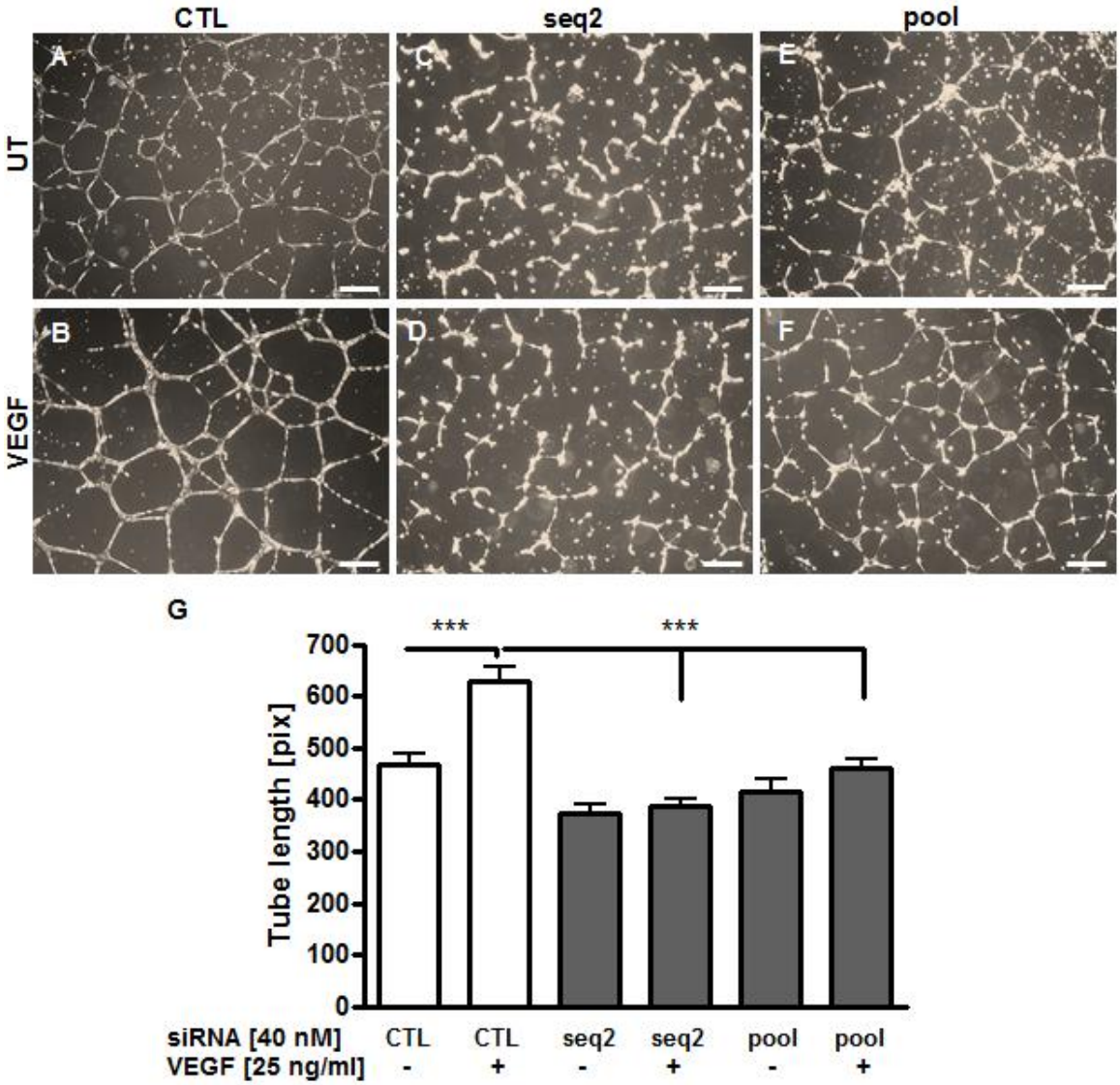

Figure 5. 22.: HO-1 inhibition inhibits human endothelial cell tubule formation *in vitro*. HUVEC were transfected with 40 nM (A, B) non-targeting control siRNA (CTL), (C, D) HO-1 specific siRNA (seq2) or (E, F) HO-1 specific siRNA (pool) for 24 h. Cells were seeded onto growth factor-reduced Matrigel in plain EC culture medium in the absence (A, C, E) or presence (B, D, F) of VEGF (25 ng/ml) for 16 h and visualized using phase-contrast microscopy. Images from five fields per view were captured. Pictures are representative images from n=3 experiments, 4X magnification. Bar equals 50 µm. (G) Tube length was quantified using ImageJ analysis software (NeuronJ). Data is presented as mean ± SEM (n=3 experiments), *** p<0.001.

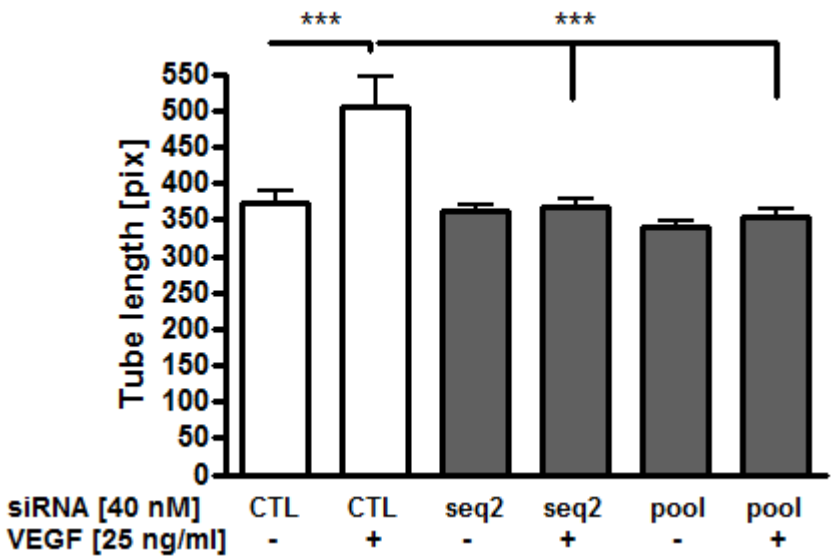

Figure 5. 23.: HO-1 inhibition impairs tubule formation of microvascular endothelial cells *in vitro*. Human microvascular EC (HMEC-1) were transfected with 40 nM non-targeting control siRNA (CTL), HO-1 specific siRNA (seq2, pool) for 24 h. Cells were seeded onto growth factor-reduced Matrigel in plain EC culture medium in the absence or presence of VEGF (25 ng/ml) for 6 h and visualised using phase-contrast microscopy. Images from five fields per view were captured and tube length was quantified using ImageJ analysis software (NeuronJ). Data is presented as mean ± SEM (n=3 experiments), *** $p<0.001$.

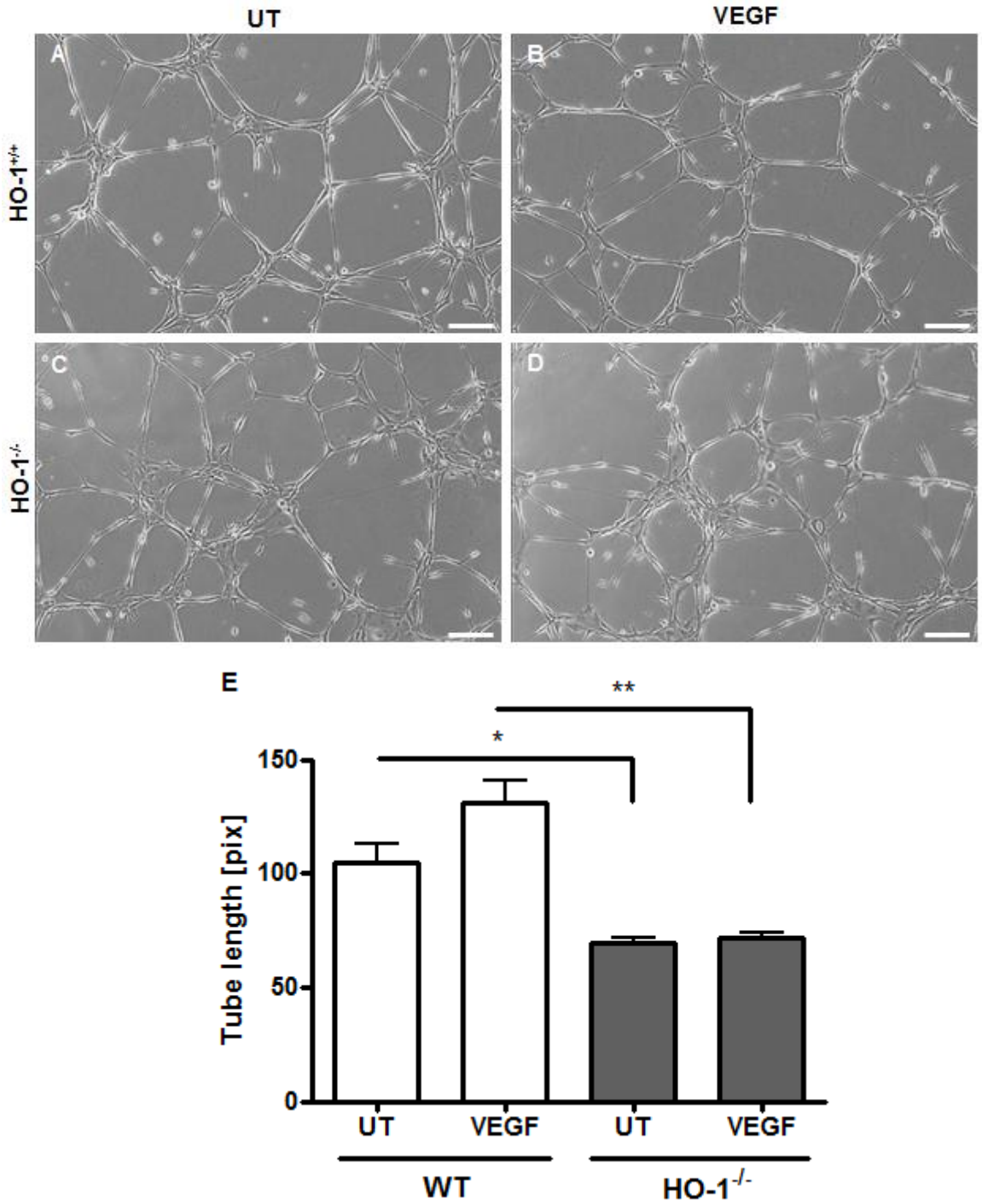

Figure 5. 24.: HO-1-deficient mouse aortic endothelial cells are delayed in their ability to form capillary-like tubules *in vitro*. Murine aortic EC (MAEC) isolated from (A, B) HO-$1^{+/+}$ littermate controls (WT), or (C, D) HO-$1^{-/-}$ mice, were seeded onto growth factor-reduced Matrigel in plain EC culture medium in the absence (C) (UT), or presence (D) of VEGF for 16 h and visualised using phase-contrast microscopy. Images from five fields per view were captured. Pictures are representative images from n=3 experiments, 10X magnification. Bar equals 50 µm. (E) Tube length was quantified using ImageJ analysis software (NeuronJ). Data is presented as mean ± SEM (n=3 experiments), * p<0.05, ** p<0.01.

5.3. DISCUSSION

Angiogenesis is a highly complex, multistep process and depends on the concerted activities of various growth factors and their receptors expressed on EC and accessory cells (Risau, 1997). The delicate balance between the release of pro- and anti-angiogenic mediators from these cells is essential for the regulation of angiogenesis. Besides the regulated process, angiogenesis is an inherent feature of numerous pathological conditions ranging from cancer to chronic inflammatory syndromes, resulting from either the overproduction of normal or aberrant forms of angiogenic mediators, or due to a relative deficiency in inhibitors (Sun and Schiller, 2007) (section 1.2.3.). Therefore, a better understanding of the mechanisms that regulate physiological but also pathological angiogenesis is crucial for the development of therapeutic strategies for manipulation of angiogenesis at sites of ischaemia or wound healing, or conversely to inhibit angiogenesis associated with atherosclerosis or tumourogenesis.

The major mediator of angiogenesis is vascular endothelial cell growth factor (VEGF), which regulates the proliferation, migration and survival of EC. During development, the level of VEGF is crucial for healthy growth, and the lack of even one functional allele of VEGF results in early embryonic lethality (Carmeliet *et al.*, 1996; Ferrara *et al.*, 1996). Moreover, in adult life, the synthesis of VEGF is potently induced by numerous stimuli, the major ones being hypoxia, cytokines, other growth factors, nitric oxide (NO), and reactive oxygen species (ROS) (Dulak and Jozkowicz, 2003; Dulak *et al.*, 2004).

Recent research now demonstrates a link between the pro-angiogenic factor VEGF and the cytoprotective enzyme HO-1 (Dulak *et al.*, 2004; Dulak *et al.*, 2008). Augmentation of HO-1 activity by inducers, such as heme, cobalt protoporphyrin (CoPP), prostaglandin J_2 (PGJ_2), hydrogen peroxide (H_2O_2), and hypoxia or genetic overexpression of HO-1 leads to the stimulation of VEGF synthesis in an HO-1-dependent manner in various cell types. (Dulak *et al.*, 2002; Jozkowicz *et al.*, 2002; Marinissen *et al.*, 2006; Dulak *et al.*, 2008). Moreover, HO-1 modulates the angiogenic effect of VEGF on EC. HO-1 overexpression enhances EC proliferation and *in vitro* tube formation or capillary sprouting in response to VEGF, while inhibition of HO-1 activity attenuates cell proliferation and VEGF-mediated migration of cultured EC (Deramaudt *et al.*, 1998; Jozkowicz *et al.*, 2003). Besides acting as an inducer of VEGF, HO-1 appears to be

involved downstream of the VEGF-mediated activation of EC. Studies from our laboratories have demonstrated increased HO-1 expression in response to the pro-angiogenic mediator VEGF in primary human EC and EC of the dermal microvasculature (Bussolati *et al.*, 2004). Accordingly, in studies performed in the chick chorioallantoic membrane model of angiogenesis, VEGF leads to enhanced HO-1 protein expression (Fernandez and Bonkovsky, 2003).

Despite considerable progress made in defining the role of HO-1 in the vasculature, further studies are required to identify the specific role of HO-1 during the different steps of the angiogenic process. In this study, siRNA was used to specifically silence HO-1 and to investigate how the angiogenic capabilities of cultured primary EC were affected. Sufficient knockdown efficiency of the different siRNA sequences targeting the human HO-1 gene used was confirmed by qRT-PCR, western blotting and immunofluorescent staining. As basal HO-1 expression is rather weak in cultured cells, the HO-1 inducer hemin was used to up-regulate HO-1 expression and this resulted in a potent induction of HO-1 mRNA and protein expression after 6 h exposure in non-transfected cells and cells transfected with a non-targeting control siRNA (siCTL) (Fig. 5.1.). However, this response was significantly attenuated in HUVEC either transfected with a single siRNA sequence (siHO-1 seq2) or a pool of four siRNA sequences targeting HO-1 (siHO-1 pool). HO-1 mRNA expression was inhibited by 70-80% and protein levels were decreased by 80-85% (Fig. 5.1.). Accordingly, fluorescein isothiocyanate (FITC)-labelled antibody staining of HO-1 in HUVEC revealed a significant decrease in the mean fluorescent intensity (MFI) of cells transfected with siHO-1 pool compared to non-transfected or siCTL-transfected EC (Fig. 5.2.). Based on these observations, the siRNAs targeting the human HO-1 gene, siHO-1 seq2 and siHO-1 pool, were used to silence HO-1 the forthcoming studies.

In response to angiogenic stimuli, EC proliferate, migrate, and coalesce to form primitive vascular networks that undergo maturation and remodelling, accompanied by recruitment of smooth muscle cells to give rise to mature blood vessels. Herein, we demonstrate a role for the cytoprotective enzyme HO-1 in all these highly regulated and complex steps of the angiogenic process using numerous well-described *in vitro* angiogenesis assays.

HO-1 and EC proliferation

In concordance with previous studies from our laboratory and others (Bussolati *et al.*, 2004; Jozkowicz *et al.*, 2003), synthetic inhibition of HO-1 using the metallophorphyrin ZnPP significantly diminished VEGF-induced EC proliferation in a dose-dependent manner, resulting in complete inhibition of proliferation at 20 µM (Fig. 5.7). *In vivo* ZnPP is formed in trace amounts during the metabolism of heme by HO enzymes, acting as a negative regulator of their enzymatic activity through competitive inhibition (Labbé *et al.*, 1999). Of note, naturally occurring as well as synthetic ZnPP not only inhibit the inducible isoform HO-1, but also the constitutive HO-2, and therefore lack specificity (Ryter *et al.*, 2006). A more specific approach to silence HO-1 without affecting the expression of constitutive HO-2 is afforded by the use of small interfering RNA targeting the human HO-1 gene, and this was used herein to determine the specific role of HO-1 in VEGF-mediated EC proliferation. In primary EC isolated from human umbilical veins siRNA-mediated inhibition of HO-1 abrogated VEGF-induced EC proliferation (Fig. 5.8.), confirming the findings obtained from HO inhibition studies utilising ZnPP and previously published data showing decreased EC proliferation and subsequent *in vitro* tube formation of EC expressing antisense HO-1 (Li Volti *et al.*, 2005). Accordingly, murine aortic EC isolated from HO-$1^{-/-}$ mice demonstrated reduced proliferation when compared to with EC from matched HO-$1^{+/+}$ littermate controls (Chen *et al.*, 2004). Moreover, these results suggest that depletion of the inducible isoform HO-1 is sufficient to impair the proliferative capacity of EC in culture, and that HO-2 does not compensate for the loss of HO-1.

Adenoviral overexpression of the human HO-1 gene, at an optimal multiplicity of infection (MOI 100), significantly increased HO-1 protein in HUVEC (Fig. 5.5.). HO-1 overexpressing EC demonstrated enhanced basal proliferation and increased HO-1 protein levels had a synergistic effect on VEGF-mediated EC proliferation *in vitro* (Fig. 5.9.). These observations are in line with earlier studies, showing an increase in the proliferative capacity of EC in response to the HO inducer CoPP and reproduce previous studies from our laboratory demonstrating a significant increase in proliferation of HO-1 overexpressing HUVEC (Bussolati *et al.*, 2004; Bussolati and Mason, 2006). Likewise, Deramaudt and colleagues reported enhanced endothelial proliferation of coronary microvascular EC transfected with a plasmid vector harbouring the human HO-1 gene (Deramaudt *et al.*, 1998).

Altogether, these findings are indicative for a role of HO-1 in EC proliferation in response to the angiogenic mediator VEGF and are in concordance with previous studies demonstrating the proliferative effect of HO-1 in the vasculature. However, the proliferative effects of HO-1 vary depending on the cell type and disease status of the tissue. Indeed HO-1 overexpression inhibited proliferation of vascular SMC and induced apoptosis in these cells (Li Volti *et al.*, 2002; Li Volti *et al.*, 2005). Moreover, gain-of-function studies reported anti-proliferative effects of HO-1 in rat and human breast cancer cells lines (Hill *et al.*, 2005), and HO-1 inhibition augmented mesangial cell proliferation, a hallmark of many progressive renal diseases (Kumar *et al.*, 2010).

HO-1 and EC survival

HO-1 is an important regulator of cell survival. Murine aortic EC isolated from HO-1 knockout mice are more susceptible to apoptotic stimuli and have increased caspase-3 activity compared with EC from HO-$1^{+/+}$ littermate controls (Brouard *et al.*, 2000; Chen *et al.*, 2004). The paradigm that HO-1 is an important molecule in defence against oxidative stress is supported by the only human case of HO-1 deficiency who died prematurely at age six, revealing intravascular hemolysis, increased sensitivity to oxidant injury and EC dysfunction post-mortem (Yachie *et al.*, 1999). In addition, a recent report demonstrated an important role for HO-1 in the regulation of DNA repair by diminishing radiation-induced DNA damage and improving cell survival (Otterbein *et al.*, 2011). Moreover, alongside its proliferative actions, the pro-angiogenic mediator VEGF is cytoprotective and anti-apoptotic, protecting EC from apoptosis through increased induction of the anti-apoptotic genes A1 and Bcl-2 (Gerber *et al.*, 1998).

Herein, we investigated whether the anti-apoptotic effects of HO-1 contribute to VEGF-mediated EC protection using loss-of-function studies. Exposure to VEGF protected against serum starvation-induced cell death in control cells and this effect was not significantly attenuated by HO-1 inhibition, either afforded by the synthetic antagonist ZnPP or HO-1 specific siRNA (Fig. 5.11.). Interpretation of these results has to be carried out with caution. The MTS assay is a measure of viable cells in culture rather than a specific apoptosis assay, i.e. changes in cell number can either result from increased cell death or on the other hand from decreased proliferation of cells. Cell counting in combination with trypan blue staining of cells, is a useful

measure of cell number and allows distinguishing between the number of viable and dead cells in culture. Moreover, more specific apoptosis assays are required to determine the effect of HO-1 inhibition on cell viability. Herein, PI staining was utilised to specifically distinguish between aopotic and viable cells. The increase in apoptotic cells resulting from HO-1 deficiency was significantly decreased in the presence of VEGF and this was accompanied by increased VEGF-induced expression of the anti-apoptotic mediators A1 and Bcl-2 (Fig. 5.12. and Fig. 5.13.). These findings are indicative of an HO-1-independent cytoprotective action of VEGF and further suggest that the reduced proliferative properties observed in HO-1-deficient EC in response to VEGF (Fig. 5.7. and Fig. 5.8.) do not reflect increased apoptosis.

HO-1 and EC migration

Endothelial motility is essential to angiogenesis. EC migration is directionally regulated by chemotactic, haptotactic, and mechanotactic stimuli and also requires the degradation of the ECM to enable the forward progression of migrating cells. This involves the activation of numerous signalling pathways that initiate the rearrangement of the cytoskeleton, followed by a series of events in which the EC extend, contract, and pull their rear to the front of the cell to enable forward movement (Lamalice *et al.*, 2007).

A role for HO-1 in endothelial migration is emerging but is so far poorly understood. Deshane and colleagues recently demonstrated a link between HO-1 and EC and EPC migration in response to the chemokine SDF-1α. HO-1 depletion abrogated SDF-1α-induced migration of human aortic EC (HAEC), an effect also seen in aortic EC and EPC isolated from HO-1 knockout mice (Deshane *et al.*, 2007). Furthermore, the synthetic HO-1 antagonist SnPP inhibited the VEGF-induced migration of HUVEC as assessed using a modified Boyden chamber (Jozkowicz *et al.*, 2003). Moreover, the migratory properties of HO-1 overexpressing coronary microvascular EC were enhanced as demonstrated by increased propensity to form vascular tubes in Matrigel (Deramaudt *et al.*, 1998). Herein, we show that HO-1 plays an important role in the directional migration of EC towards a gradient of the pro-angiogenic mediator VEGF.

The *in vitro* scratch assay is a reliable tool for analysis of the migration patterns of cells in culture. Confocal time lapse microscopy coupled to single cell tracking allows the quantification of

migration paths of individual cells in terms of their accumulated distance and velocity, as well as their directionality expressed as the Euclidean distance. In this study, fluorescently-labelled siRNA was used to silence HO-1 in primary human EC and to specifically identify cells successfully transfected with siRNA and with depleted HO-1 (Fig. 5.3. and Fig. 5.14). Non-fluorescent cells were excluded from analysis. HO-1 depletion by siRNA had no significant effect on the accumulated distance travelled or the velocity when compared to HUVEC transfected with a control siRNA ($siCTL_{AF488}$), either in the absence or the presence of VEGF (Fig. 5.15.A and B). The Euclidean distance was significantly increased in response to VEGF in $siCTL_{AF488}$-transfected HUVEC and this effect was completely abolished in HO-1-deficient cells (Fig. 5.15.C). Further analysis of the directional movement of individual cells revealed that HO-1-depleted cells migrated in a rather random, circular pattern alongside the scratch edge, whereas control cells showed a more linear, directional movement towards the scratch and the cells on the opposite site (Fig. 5.16.). Moreover, a similar migratory pattern was observed for HO-1-deficient human EC derived from the dermal microvasculature (HMEC) with a diminished Euclidean distance travelled in response to VEGF when compared to $siCTL_{AF488}$-transfected cells (Fig. 5.15.D). In contrast, we show that adenoviral overexpression of the human HO-1 gene significantly improves the Euclidean distance of HUVEC (Fig. 5.17.).

Taken together, these results strongly suggest a role for HO-1 in the directional migration of EC mediated by VEGF. One of the disadvantages and limitations of the migration scratch assay is the lack of the formation of a chemotactic gradient of growth factors over the course of the assay, and this assay does not replace other well-established methods for chemotaxis, including the Boyden chamber (Liang *et al.*, 2007). The Boyden chamber consists of two fluid-containing compartments separated by a microporous membrane, with the upper compartment containing the cells of interest. For the induction of chemotactic response of cells, attractants are added to the lower compartment and cells begin to migrate through the pores of the membrane (Chen, 2005). Disadvantages of this assay include that the chemotactic gradient is unknown and variable (Chen 2005; Hulkower and Herber, 2011) Moreover, transmigration through a membrane does not depict the migratory behaviour of EC *in vivo*. Thus, herein, the Ibidi µ-slide chemotaxis assay was used to further investigate a potential role for HO-1 in mediating the directional migration of EC towards a pro-angiogenic stimulus. The µ-slide assay is optimised to analyse the chemotactic

response of adherent cells in linear and stable concentration profiles over a period of 48 h. In principle, the µ-slide consists of two large reservoirs: one filled with attractant-free and one with VEGF-supplemented culture medium. The two reservoirs are connected by a narrow observation area and cells that are seeded within the observation area become superimposed by a linear and time-stable VEGF gradient. Time-lapse migration coupled to single cell tracking of cells allows quantification of the chemotactic responses. Quantification of the directional migration paths of individual, fluorescently-labelled, non-dividing cells revealed that significantly less HO-1-depleted cells (40%) migrated towards the VEGF gradient when compared to HUVEC transfected with a non-targeting control siRNA (80%) (Fig. 5.18.).

These findings, to our knowledge for the first time, demonstrate a link between the cytoprotective enzyme HO-1 and the directed movement of EC in response to a VEGF gradient. The cellular and molecular machinery underlying EC migration is highly regulated and complex. Further studies are required to establish the specific role of HO-1 and its products in this process. In response to angiogenic stimuli, EC undergo morphological changes allowing their directed forward movement. Lamellipodia and filopodia are highly dynamic structures, generated within minutes at the moving front of the EC (Huber *et al.*, 2003). Both structures are capable of probing the environment, thereby sensing the presence of attractive guidance cues and initiating migration towards these (Defilippi *et al.*, 1999). It would be of great interest to assess whether changes in the morphological appearance of HO-1-deficient cells, i.e. changes in lamellipodia and filopodia extensions, are accountable for their impaired migratory capacity in response to VEGF. Interference Reflection microscopy (IRM) could be one approach to address this. Furthermore, the identification of HO-1 downstream targets and signalling pathways regulating HO-1-driven migration are of great importance and will be discussed in in forthcoming chapters.

HO-1 and EC tubule formation

In the final step of the angiogenic process, migrating EC rearrange into lumenised capillary structures that undergo maturation and remodelling to give rise to mature blood vessels. Using the *in vitro* 2D-Matrigel assay, we demonstrate a role for HO-1 in this process.

Synthetic inhibition afforded by the HO inhibitor ZnPP or specific silencing of HO-1 by siRNA abolished HUVEC tubule formation on growth factor-reduced Matrigel in response to VEGF (Fig. 5.21. and Fig. 5.22.). Moreover, a similar response was observed with HO-1-depleted human dermal microvascular EC and murine aortic EC (MAEC) isolated from HO-$1^{-/-}$ mice when compared to HO-$1^{+/+}$ littermate controls (Fig 5.23. and Fig. 5. 24.). Of note, the results have to be interpreted with caution. While the 2D Matrigel assay is a commonly used *in vitro* angiogenesis assay and has been found to be the most potent matrix for tube formation, there is some debate as to whether these tubules represent capillaries. While some groups have confirmed lumen formation of these newly formed tubes by electron microscopy, others could not demonstrate the presence of a lumen (Grant *et al.*, 1991; Connolly *et al.*, 2002; Bikfalvi *et al.*, 1991). In addition, it should be noted that other non-endothelial cell types including primary human fibroblasts, human prostate carcinoma cell lines and glioblastoma cells have been shown to rearrange in tubular structures on Matrigel (Donovan *et al.*, 2001). Therefore, to investigate the effect on HO-1 inhibition on tube formation, the findings should be confirmed by the use of other *in vitro* angiogenesis assays, such as a three dimensional (3D) Matrigel assay or a co-culture assay of EC with human fibroblasts that more closely mimic the *in vivo* situation in terms of tubulogenesis. Fibroblasts secret matrix components that act as a scaffold and enables EC to form tubules that contain a lumen, with a heterogenous tubes length pattern, more closely resembling the capillary bed in *in vivo* (Bishop et al., 1999; Donovan *et al.*, 2001).

Nontheless, the findings observed in this study demonstrate a role for HO-1 in the assembly of EC into blood vessels and are in concordance with previously published reports. Gene transfer of human HO-1 into coronary endothelial cells enhanced formation of capillary-like structures in a 2D-Matrigel assay, whereas inhibition of HO-1 decreased capillary formation (Deramaudt *et al.*, 1998; Li Volti *et al.*, 2002). Moreover, HO-1 inhibition with both SnPP and ZnPP completely inhibited capillary sprouting and neovessel outgrowth in response to VEGF in a murine abdominal muscle model (Bussolati *et al.*, 2004). Further, Deshane *et al.* demonstrated that MAEC isolated from HO-1 knockout mice fail to form tubules on 2D-Matrigel *in vitro* in response to the chemokine SDF-1α and aortic rings isolated from these animals were unable to form SDF-1α-induced capillary sprouts *ex vivo* (Deshane *et al.*, 2007). Moreover, HO-1 inhibition delayed cutaneous

wound healing in mice which was accompanied by impaired neovascularisation of tissues (Deshane *et al.*, 2007; Grochot-Przeczek *et al.*, 2009).

Our findings and previously published data clearly demonstrate an important role for HO-1 in VEGF- and SDF-1α-mediated angiogenesis for vascular remodelling and repair. But despite the progress made in identifying the role for HO-1 in angiogenesis *in vitro*, further *in vivo* studies using murine specific siRNA targeting the mouse HO-1 gene in the Matrigel plug assay are now necessary to define the role of HO-1 in VEGF-mediated angiogenesis (see Chapter 7).

HO-2 and angiogenesis

The role of HO-2, the constitutive HO isoform, in endothelial homeostasis is poorly understood and may include a regulatory role in heme homeostasis, by sequestering heme to maintain the intracellular heme level. HO-2 may also function as an oxygen sensor and HO-2 deletion causes EC activation marked by oxidative stress, inflammation, and angiogenesis, underscoring important functions of this enzyme in endothelial homeostasis (Kemp, 2005; Bellner *et al.*, 2009). Moreover, it has been postulated that HO-2 is critical for HO-1 expression and function, which may explain the reason why HO-$2^{-/-}$ mice could not compensate for the loss of HO-2 by increasing HO-1 expression (Sodhi *et al.*, 2009).

In this study, we show an impaired migratory phenotype of HO-2-deficient primary human EC in culture. Wound closure of an artificial scratch on a confluent monolayer of HUVEC, was significantly impaired by HO-2 inhibition afforded by specific siRNA in terms of the accumulated distance, velocity and Euclidean distance both in the absence and presence of VEGF (Fig. 5.20.). These observations reflect those from previous studies postulating a role for HO-2 in angiogenesis. Animals lacking HO-2 are characterised by impaired corneal wound closure, enhanced neovascularisation, and exaggerated inflammation as demonstrated by NFκB activation and increased expression of inflammatory cytokines including MCP-1, IL-1 and IL-6 (Seta *et al.*, 2006; Bellner *et at.*, 2009). Moreover, MAEC isolated from HO-$2^{-/-}$ mice showed an activated phenotype marked by oxidative stress, inflammation and angiogenesis (Bellner *et al.*, 2009). Interestingly, while HO-1 expression was downregulated in corneal tissue, MAEC from HO-$2^{-/-}$ mice showed increased HO-1 expression. However, in both cases HO activity was significantly

reduced, suggesting that decreased enzymatic activity of HO-$2^{-/-}$ mice is responsible for the aggravated inflammation-dependent angiogenesis supporting the dual role of HO-1 in angiogenesis, postulated by our laboratory. This hypothesis suggests that activation of HO-1 by VEGF favours EC proliferation and prevents EC apoptosis, while inhibiting leukocyte migration, thus resulting in non-inflammatory reparative angiogenesis, whereas inhibition of HO activity increases leukocyte migration and subsequent local release of growth factors inducing pro-inflammatory angiogenesis (Bussolati *et al.*, 2004; Bussolati and Mason, 2006).

Of note, migrating HUVEC deficient in HO-2 also showed a significant upregulation in HO-1 protein, independent of VEGF exposure (Fig. 5.19.), which could be a response to injury resulting from the generation of the scratch. The HO-2-deficient cells exhibited impaired migration despite an increase in HO-1, suggesting that HO-1 function requires HO-2. Thus, it would be of interest to assess whether HO activity is also altered in these cultures, as a decrease in enzymatic activity may explain the impaired migratory capacity of the HO-2 depleted HUVEC.

Summary

Herein, we show that HO-1 deficiency affects the angiogenic capacity of EC in culture at various levels. VEGF-induced endothelial proliferation was significantly inhibited and HO-1-depleted cells failed to form an intact tubular network in a 2D-Matrigel assay in response to VEGF. Moreover, the directional migration of EC towards a VEGF gradient was negatively affected by HO-1 inhibition, with significantly less cells migrating towards the angiogenic stimulus in HO-1-depleted cultures compared to control cells.

Despite the considerable progress made in defining the angiogenic properties of HO-1, further studies are required to identify the signalling pathways involved and those activated by HO-1 products. Likewise, further studies are required to define the role of HO-1 in angiogenesis *in vivo*. HO-1-deficient mice and tissue-specific or inducible knockout models, as well as murine specific siRNA used in combination with the Matrigel plug assay will help to establish the angiogenic functions of HO-1.

CHAPTER 6 - HO-1 PRODUCTS AND DOWNSTREAM TARGETS IN ANGIOGENESIS

6.1. INTRODUCTION

The precise mechanisms through which HO-1 exerts its effects during angiogenesis and the role of its products CO, biliverdin/bilirubin, and iron remain poorly understood (please see section 1.3.4.). A better understanding of the signalling pathways and downstream targets of HO-1 and its products in the process of angiogenesis may lead to identification of novel therapeutic targets.

To date, only one potential downstream target of HO-1-mediated angiogenesis has been identified. Vasodilator-stimulated phosphoprotein (VASP) is a cytoskeletal-associated protein located at regions of dynamic actin remodelling, such as cell-cell contacts and filopodia protrusions (Krause *et al.*, 2003; Bear and Gertler *et al.*, 2009; Trichet *et al.*, 2008). In cells, differential VASP phosphorylation controls remodelling of the actin cytoskeleton affecting anti-capping, bundling, and anti-branching activities of F-actin (Barzik *et al.*, 2005; Pasic *et al.*, 2008; Applewhite *et al.*, 2007; Bachmann *et al.*, 2009; Schirenbeck *et al.*, 2006; Bear *et al.*, 2002; Skoble *et al.*, 2001). Human VASP harbours three phosphorylation sites serine 157 (Ser157), Ser239, and threonine 278 (Thr278) which are substrates of serine/threonine kinases (Butt *et al.*, 1994; Blume *et al.*, 2007). Ser157 and Ser239 are phosphorylated by cAMP-dependent protein kinase (PKA) and cGMP-dependent protein kinase (PKG) respectively (Butt *et al.*, 1994; Zhuang *et al.*, 2004). Thr278 phosphorylation is initiated by AMP-activated protein kinase (AMPK) (Blume *et al.*, 2007). Recently, it was shown that phosphorylation of VASP at Ser239 in response to SDF-1α is lost in HO-1-deficient mice, but can be restored by the CO-releasing molecule (CORM)-2 (Deshane *et al.*, 2007), suggesting a role for HO-1 in the regulation of VASP activity. In addition exposure to VEGF results in VASP phosphorylation (Ser239) in HUVEC and bovine aortic EC (BAEC), and this is associated with increased capillary-like formation in an *in vitro* Matrigel assay (Fiedler *et al.*, 2009; Chen *et al.*, 2008). Moreover, Price and Brindle demonstrate a role for VASP in stress-fibre and membrane ruffle formation in endothelial cells, which can influence endothelial migration and organisation during capillary formation, and modulate vascular permeability via effects on EC contractility (Price and Brindle, 2000).

Despite the considerable progress made in establishing a role for HO-1 in angiogenesis, the functions of HO products CO, biliverdin/bilirubin and iron and other downstream targets in HO-1

driven angiogenesis still remain elusive. This chapter aims to investigate whether the HO products CO and iron mediate the pro-migratory effects of HO-1 and whether supplementation with a CO donor or DFO would restore the impaired angiogenic capacity of HO-1-deficient HUVEC. Moreover, we aim to determine whether VEGF-mediated phosphorylation of the potential HO-1 downstream target VASP is affected in HO-1-deficient HUVEC, thereby contributing to their impaired migratory phenotype. Finally, to further elucidate downstream effectors of HO-1 in angiogenesis, a targeted PCR array and a proteomic screen will be performed between HO-1-deficient EC and control cells in response to the mitogen VEGF, with the ultimate aim of identifying novel therapeutic targets for the manipulation of angiogenesis.

6.2. RESULTS

6.2.1. DFO does not reverse the impaired migratory phenotype of HO-1-deficient EC *in vitro*

The generation and release of intracellular Fe^{2+} during heme metabolism, leads to the subsequent up-regulation of the iron-binding protein ferritin heavy chain (FHC). FHC associates with ferritin light chain to form a multimeric complex (Harrison and Arosio, 1996) and catalyses the oxidation of iron from the ferrous (Fe^{2+}) to the ferric form (Fe^{3+}) thereby removing excess iron from the system (Balla *et al.*, 1992; Berberat *et al.*, 2003). In this study, the synthetic compound deferoxamine mesylate (DFO) was used to mimic the action of FHC. DFO acts as an iron chelator by binding free iron (Fe^{2+}). Once bound to an iron chelator, Fe^{2+} is inert and lacks the ability to perform in chemical reactions as it is removed from the system.

To investigate whether HO-1 products regulate the pro-migratory effects of HO-1, primary human EC (HUVEC) were cultured onto gelatin-coated culture dishes (6-well) and transfected with 40 nM 3'-AlexaFluor488-labelled non-targeting control siRNA ($siCTL_{AF488}$) or HO-1 specific siRNA (siHO-1 $seq2_{AF488}$) for 24 h. Cells were then left untreated or pre-treated with 100 µM DFO prior to exposure to VEGF and generation of a scratch on the confluent monolayer. Scratch closure was observed by live cell confocal imaging over a period of 16 h and the directional migration of individual cells was assessed by single cell tracking. Exposure to the iron chelator DFO had no effect on the Euclidean distance travelled by HUVEC transfected with the control siRNA in response to VEGF (Fig. 6.1.). Moreover, HO-1 depletion significantly reduced the Euclidean distance travelled in response to VEGF in the absence of DFO, and this response reproduced previous observations made during this study (compare Fig. 5.15.C). Interestingly, the presence of DFO in HO-1-deficient cultures did not alter the response to VEGF and the directional migration paths of cells were still significantly diminished compared to $siCTL_{AF488}$-transfected cells exposed to DFO (Fig. 6.1.). Taken together these observations suggest that DFO, at least on its own, is not sufficient to restore the impaired directional migration of HO-1-deficient cells.

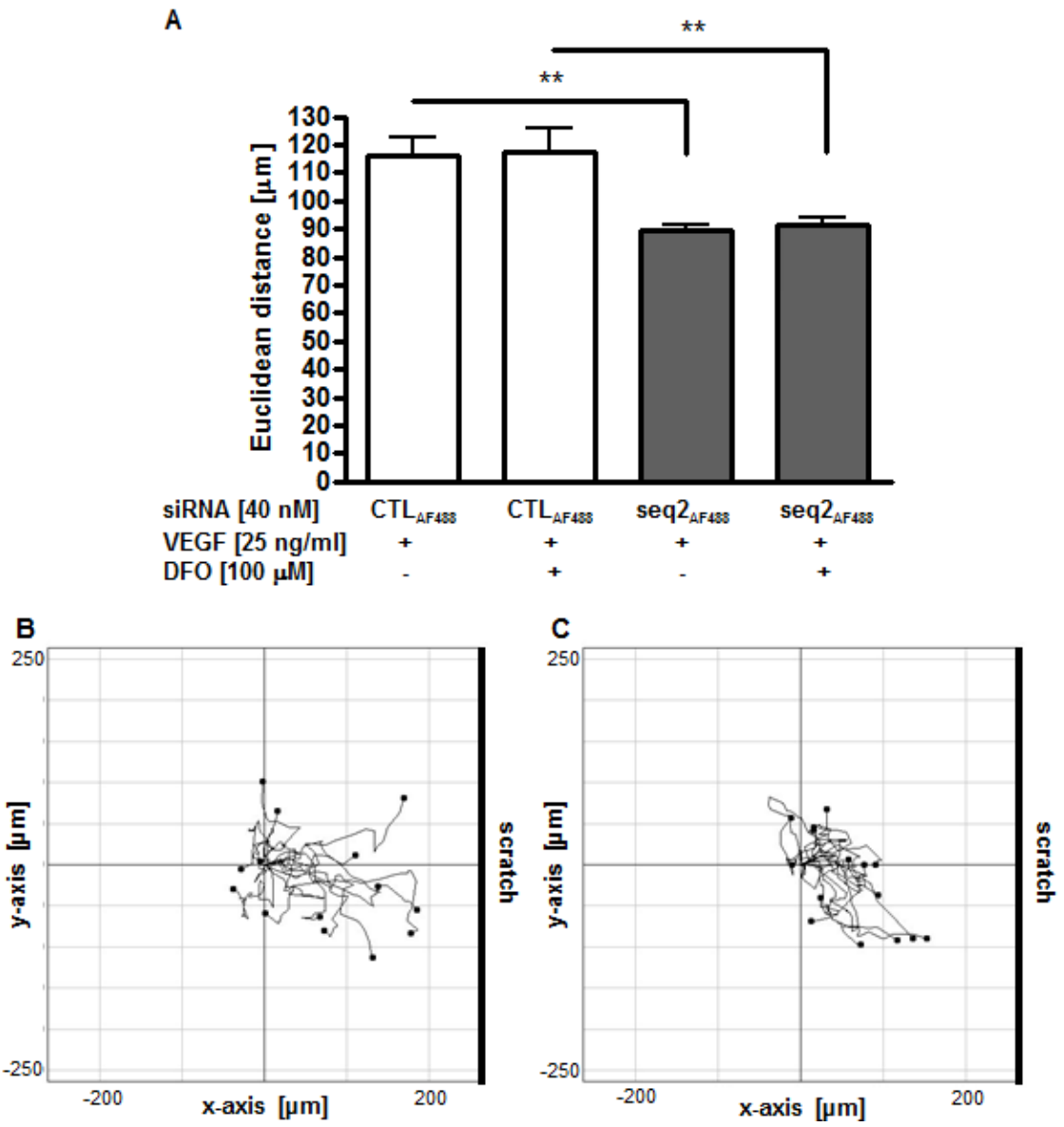

Figure 6. 1.: DFO alone is not sufficient to reverse the impaired migratory phenotype of HO-1-deficient endothelial cells in response to VEGF. HUVEC were transfected with 40 nM 3'-AlexaFluor488-labelled control siRNA (CTL_{AF488}) or HO-1 specific siRNA ($seq2_{AF488}$) for 24 h. Cells were left untreated or pre-treated with DFO (100 µM) for 2 h. Confluent monolayers were then scratched and treated with 25 ng/ml VEGF for 16 h. Migration was assessed by live cell imaging and quantified using ImageJ analysis software (Manual Tracking and Chemotaxis Migration tool). (A) represents the Euclidean distance. Plots show the directional migration of HUVEC (B) transfected with CTL_{AF488} or (C) $seq2_{AF488}$ and pre-treated with DFO. Data is presented as mean ± SD (n=3 experiments), ** p<0.01.

6.2.2. CO-releasing molecules are not sufficient to reverse the impaired migratory phenotype of HO-1-deficient EC *in vitro*

Like NO, HO-1 derived CO has been recognised as an important signalling molecule in the vascular system inducing numerous beneficial effects including cytoprotection, vasodilation and inhibition of inflammation and is likely to be attributable for the angiogenic effects of HO-1 (Choi and Otterbein, 2002; Ryter *et al.*, 2006). One approach to deliver CO directly into living cells in culture, in an accurate, safe and measurable manner, is the use of CO-releasing molecules (CORMs). The dinuclear ruthenium complex 1, known as CORM-2 ($[Ru(CO)_3Cl_2]_2$), is a water soluble transition metal-carbonyl complex that liberates CO upon ligand exchange with DMSO, and is frequently used as a CO-releasing molecule in biological studies (Motterlini *et al.*, 2002).

To investigate whether pro-migratory effects of HO-1 are mediated by its product CO and whether delivery of CO reverses the impaired directional migration of HO-1-deficient cells, $siCTL_{AF488}$ or siHO-1 $seq2_{AF488}$-transfected HUVEC were pre-treated with vehicle (DMSO) or the CO donor CORM-2 (50 µM) for 2 h prior to the generation of a scratch on the confluent cell monolayer and subsequent exposure to VEGF for 16 h. Time lapse microscopy coupled to single cell tracking revealed no change in Euclidean distance of control cells in response to CORM-2. Moreover, the diminished migration of HO-1-deficient HUVEC was not improved by CORM-2 treatment (Fig. 6.2.). Noteworthy, CO release from CORM-2 is very fast ($t_{1/2}$ ≈ 1min) and unspecific thereby hampering the delivery of controlled amounts of CO to the target cells (Motterlini *et al.*, 2005). To improve CO delivery in our system, a novel class of enzyme-triggered CORMs (ET-CORMs) were utilised. ET-CORMS exist as stable precursor complexes and, once take up by a cell, are cleaved by intracellular esterases releasing CO (Romanski *et al.*, 2011).

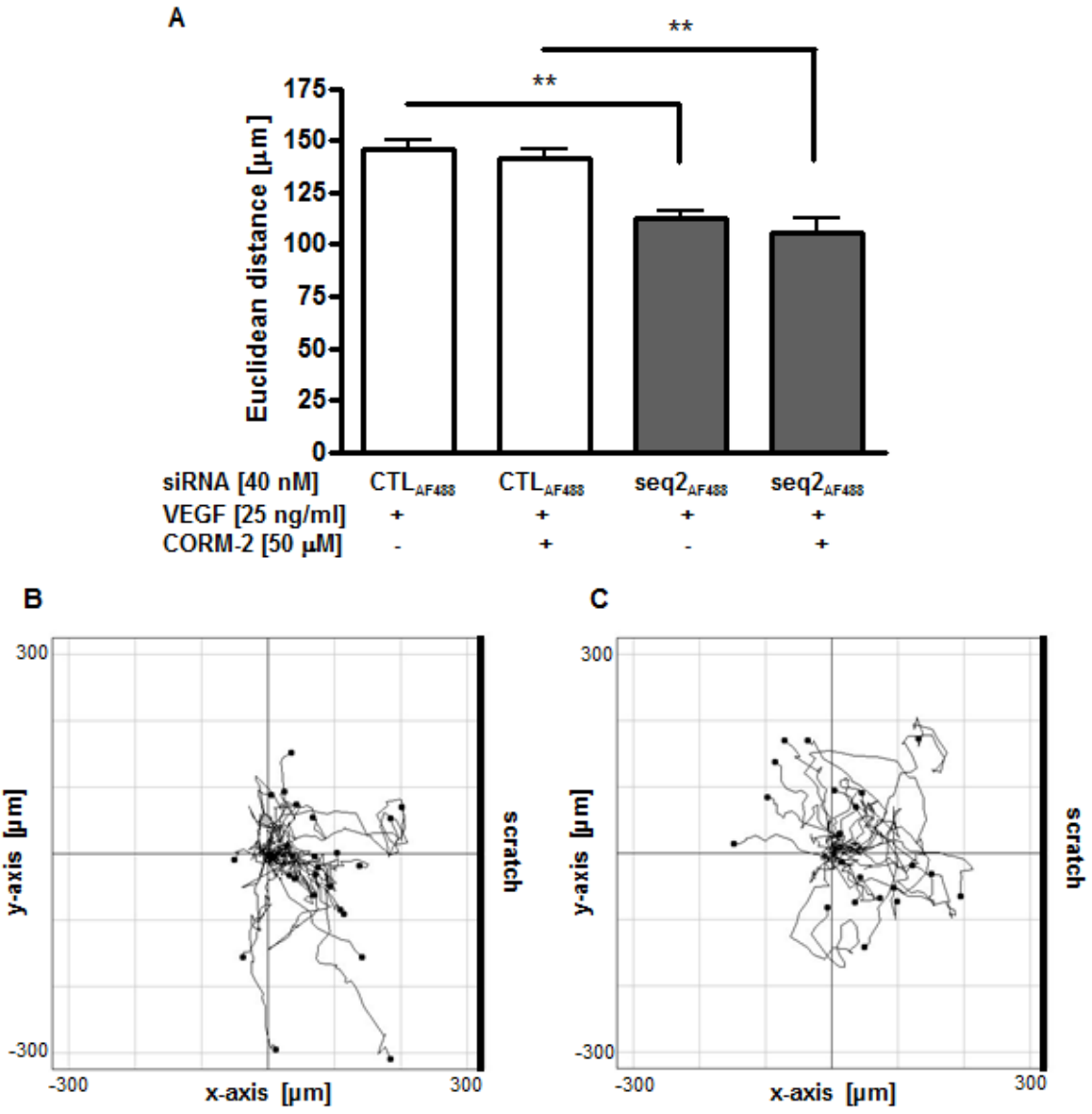

Figure 6. 2.: CORM-2 alone is not sufficient to reverse the impaired migratory phenotype of HO-1-deficient endothelial cells in response to VEGF. HUVEC were transfected with 40 nM 3'-AlexaFluor488-labelled control siRNA (CTL_{AF488}) or HO-1 specific siRNA ($seq2_{AF488}$) for 24 h. Cells were left untreated or pre-treated wit CORM-2 (50 µM) for 2 h. Confluent monolayers were then scratched and treated with 25 ng/ml VEGF for 16 h. Migration was assessed by live cell imaging and quantified using ImageJ analysis software (Manual Tracking and Chemotaxis Migration tool). (A) represents the Euclidean distance. Plots show the directional migration of HUVEC (B) transfected with siCTL_{AF488} or (C) $seq2_{AF488}$ and pre-treated with DFO. Data is presented as mean ± SD (n=3 experiments), ** p<0.01.

ET-CORMs, namely Stro074, Stro258 and SROM158, used in this study were kindly provided by Prof H. G. Schmalz (Universität zu Köln, Köln, Germany) and initial experiments were conducted to validate their toxicity and activity in primary human EC. Cell viability in response to ET-CORMs in the absence or presence of VEGF was assessed using the MTS-assay (Fig. 6.3.) Here, dose-titration experiments demonstrated that all three ET-CORMs used significantly decreased the number of viable cells at 100 µM (Fig. 6.3.A) and 50 µM (Fig. 6.3.B) independent of exposure to VEGF. Of note, exposure to 50 µM SROM158 had the least toxic effect on HUVEC with or without VEGF, resulting in a 20-30% decrease in cell viability compared to ~50% and ~40% for Stro074 and Stro258, respectively (Fig. 6.3.B). Based on these observations, the dose-dependent effect of SROM158 on EC viability was further assessed using concentrations ranging from 12.5 µM to 50 µM (Fig. 6.4.). Again, pre-treatment and exposure to 50 µM SROM158 for 16 h significantly decreased the number of viable cells by 20-25% both in the absence and the presence of VEGF compared to DMSO-treated control cells. However, when used at 12.5 µM or 25 µM, SROM158 had no effect on HUVEC viability (Fig. 6.4.).

HO-1-derived CO modulates inflammatory responses and CORMs have been shown to inhibit TNF-α-induced expression of inflammatory adhesion molecules, including VCAM-1 and E-selectin (Sun *et al.*, 2007; Song *et al.*, 2009; Bergstraesser *et al.*, 2012). These anti-inflammatory effects of CORMs were used to test for the activity of SROM158 in HUVEC by assessing its effect on TNF-α-induced VCAM-1 expression (Fig. 6.5.). As assessed by flow cytometry, VCAM-1 upregulation in response to 1 ng/ml or 10 ng/ml TNF-α was significantly reduced by the CO donor SROM158. Treatment of HUVEC with 12.5 µM SROM158 resulted in a minor but significant reduction in TNF-α-induced VCAM-1 in the absence and presence of VEGF for 16h, and this effect was more pronounced (~25%) when used at a concentration of 25 µM (Fig. 6.5.). Moreover, western blot analysis demonstrated treatment with SROM158 up-regulated HO-1 protein in a dose-dependent manner in HUVEC in the absence and presence of VEGF, but with no synergistic effect on HO-1 induction between VEGF and SROM158 (Fig. 6.6.)

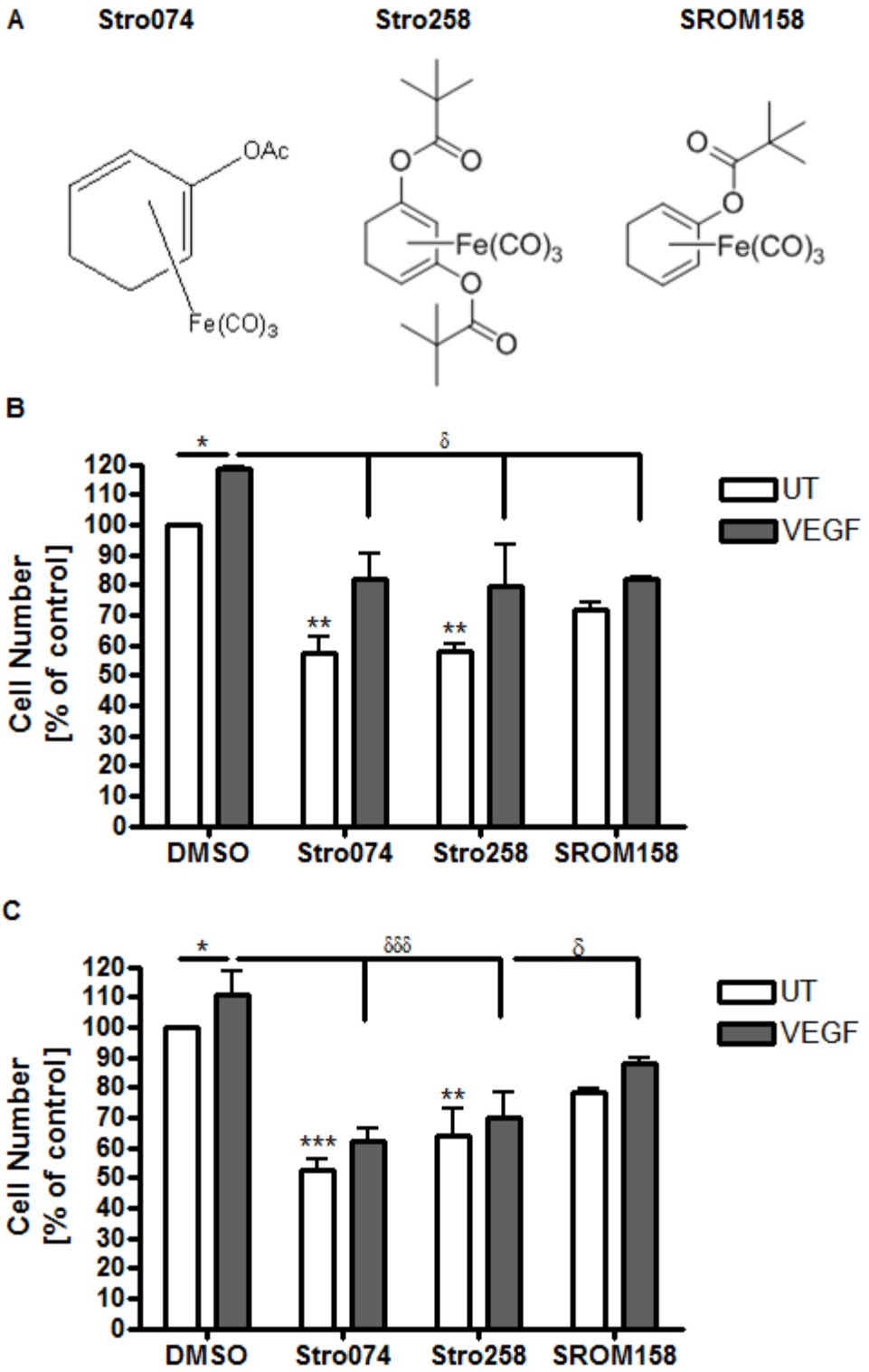

Figure 6. 3.: Dose-dependent effect of ET-CORMs on EC number. (A) shows the chemical formulas of the ET-CORMs Stro074, Stro258 and SROM158. (B, C) HUVEC were sparsely seeded onto gelatin-coated culture plates in growth factor-free EBM-2 culture medium supplemented with 2% FCS and pre-treated for 30 min with vehicle (DMSO) or ET-CORMs (Stro074, Stro258, SROM158) at (B) 100 µM, or (C) 50 µM. Cells were then left untreated (UT) or treated with 25 ng/ml VEGF for 16 h. The number of live cells was assessed using the MTS-assay. Data is presented as mean ± SEM (n=3 experiments), * p<0.05, ** p<0.01 vs untreated DMSO control, δ p<0.05, δδδ p<0.001 vs VEGF treated DMSO control.

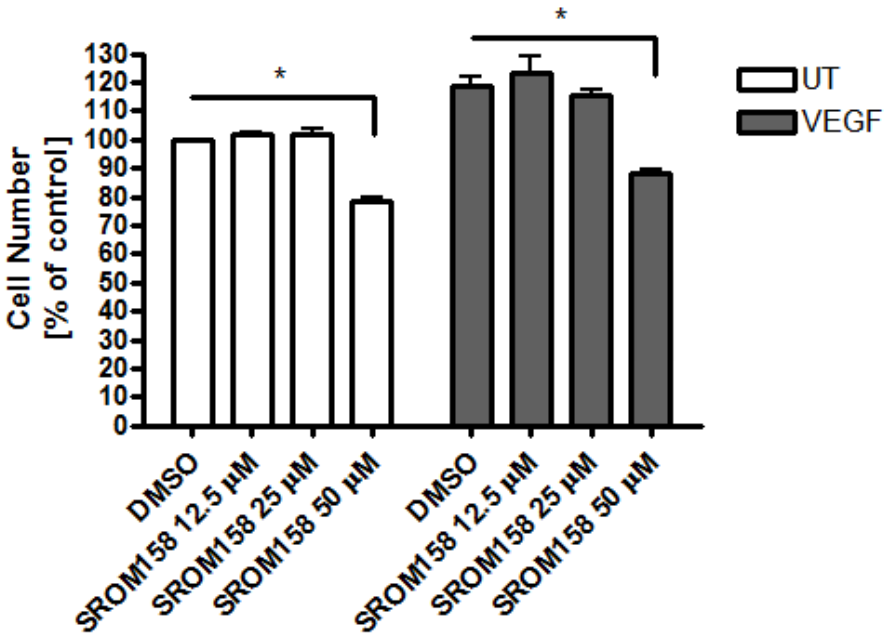

Figure 6. 4.: SROM158 has no effect on EC number at low concentrations. HUVEC were sparsely seeded onto gelatin-coated culture plates in growth factor-free EBM-2 culture medium supplemented with 2% FCS and pre-treated for 30 min with SROM158 at the indicated concentrations. Cells were then left untreated (UT) or treated with 25 ng/ml VEGF for 16 h. The number of live cells was assessed using the MTS-assay. Data is presented as mean ± SEM (n=3 experiments), * p<0.05.

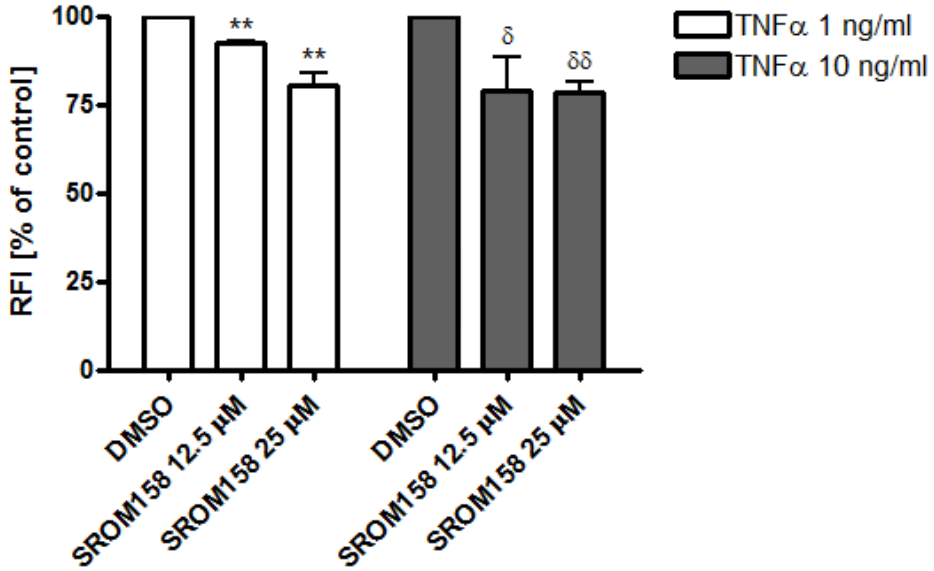

Figure 6. 5.: SROM158 suppresses TNF-α-induced VCAM-1 surface expression on EC. HUVEC were pre-treated with vehicle (DMSO) or SROM158 at the indicated concentrations. Cells were then left untreated or treated with 1 ng/ml TNF-α or 10 ng/ml TNF-α for 16 h prior to analysis of VCAM-1 surface expression by flow cytometry using mAb 1.4C3. Data is presented as mean ± SEM (n=3 experiments), ** p<0.01 untreated DMSO control vs 1 ng/ml TNF-α, δ p<0.05, δδ p<0.01 untreated DMSO control vs 10 ng/ml TNF-α. RFI – relative fluorescence intensity.

Taken together, SROM158 used at a concentration of 25 µM has no toxic effect on EC viability and partially suppresses expression of VCAM-1 in response to pro-inflammatory stimuli, demonstrating its activity. Furthermore, SROM158 markedly induced HO-1 protein. Based on these observations, SROM158 at a concentration of 25 µM was used for forthcoming experiments investigating the role of CO in HO-1 driven angiogenesis.

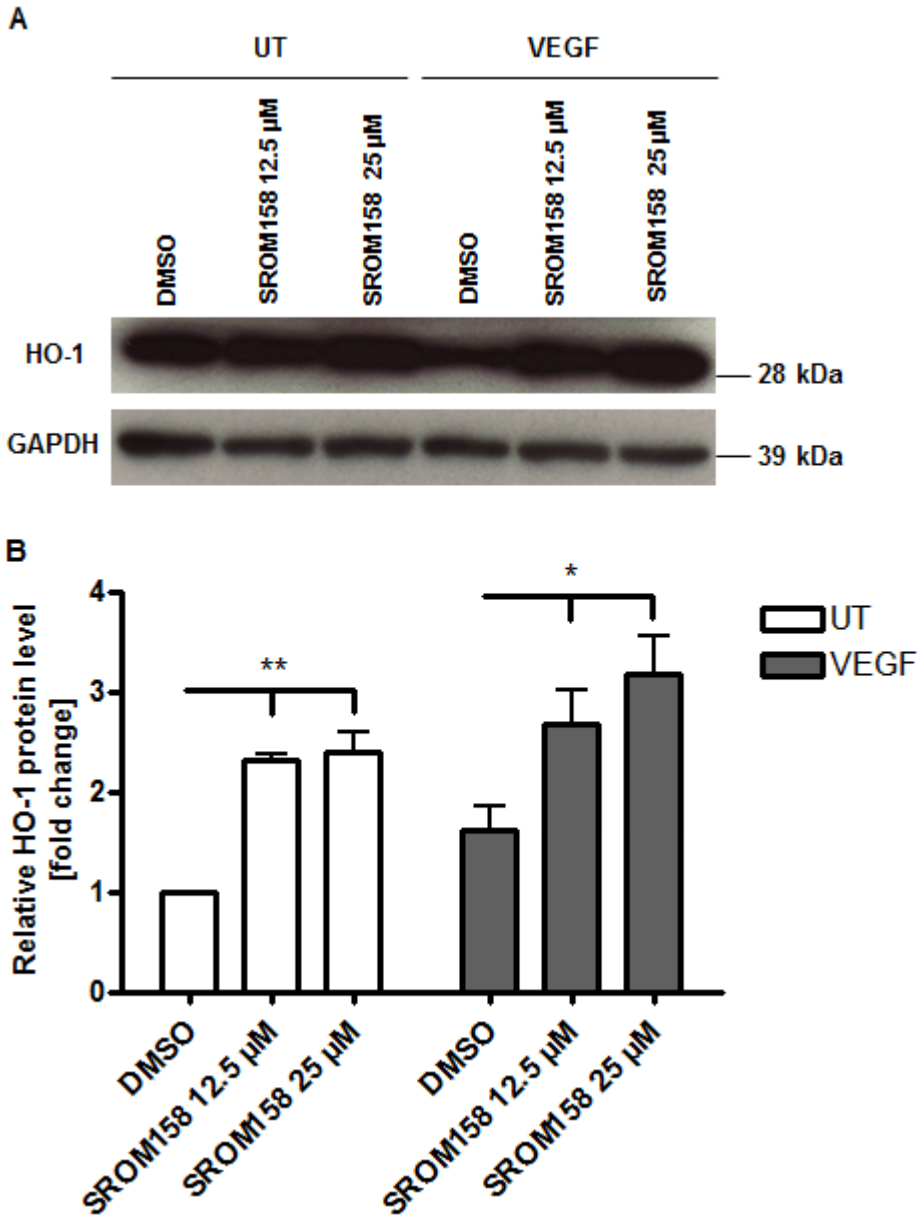

Figure 6. 6.: SROM158 induces HO-1 protein expression in human EC. HUVEC were pre-treated with vehicle (DMSO) or SROM158 at the indicated concentrations. Cells were then left untreated (UT) or treated with 25 ng/ml VEGF for 16 h prior to assessment of HO-1 protein expression by western blotting. GAPDH was used as a loading control. (A) shows a representative blot, and (B) shows the corresponding densitometry. Data is presented as mean ± SEM (n=3 experiments), * p<0.05, ** p<0.01.

To investigate the effect of SROM158 on VEGF-mediated cell proliferation, cells transfected with a non-targeting control siRNA (siCTL) or siRNA targeting HO-1 (siHO-1 seq2, siHO-1 pool) were stained with the proliferation marker PCNA and PCNA positive cell were identified by flow cytometry (Fig. 6.7.). In siCTL-transfected cells exposure to the mitogen VEGF for 24 h resulted in a significant increase in EC proliferation compared to vehicle (DMSO)-treated cells. VEGF treatment in combination with 25 µM SROM158 enhanced proliferation to a similar extent as seen with VEGF alone. In concordance with our previous findings, siRNA-mediated inhibition of HO-1 attenuated the VEGF-induced proliferation (compare Fig. 6.7. and Fig. 5.8.). Moreover, 30 min pre-treatment with SROM158 and subsequent culture for 24 h had no effect on VEGF-induced proliferation in siHO-1-transfected cells (Fig. 6.7.).

Furthermore, as assessed by the migration scratch *in vitro* assay, SROM158 did not rescue the impaired directional migration of HO-1-depleted EC in response to VEGF (Fig. 6.8.). Here, scratch closure and the directional migration of HUVEC, quantified by single cell tracking of fluorescently-labelled cells and expressed as the Euclidean distance, was not affected by SROM158 treatment in control siRNA-transfected cultures. As seen before, siRNA-mediated silencing of HO-1 significantly reduced the Euclidean distance compared to vehicle-treated control siRNA-transfected cells (compare Fig. 5.15.C and Fig. 6.8.A), and this response was not improved in the presence of SROM158 (Fig. 6.8.A). Accordingly, the migration pathway of individual siCTL-transfected cells treated with SROM158 in combination with VEGF was directed towards the scratch and the cells on the opposite site, whereas the migration path of HO-1-depleted cells migrated in a non-linear, more circular pattern alongside the edge of the scratch (Fig 6.8.B and C).

Altogether, these findings suggest that CO, at least own its own, does not mediate the angiogenic properties of HO-1, but might act in concert with other HO products or so far unknown downstream targets of HO-1.

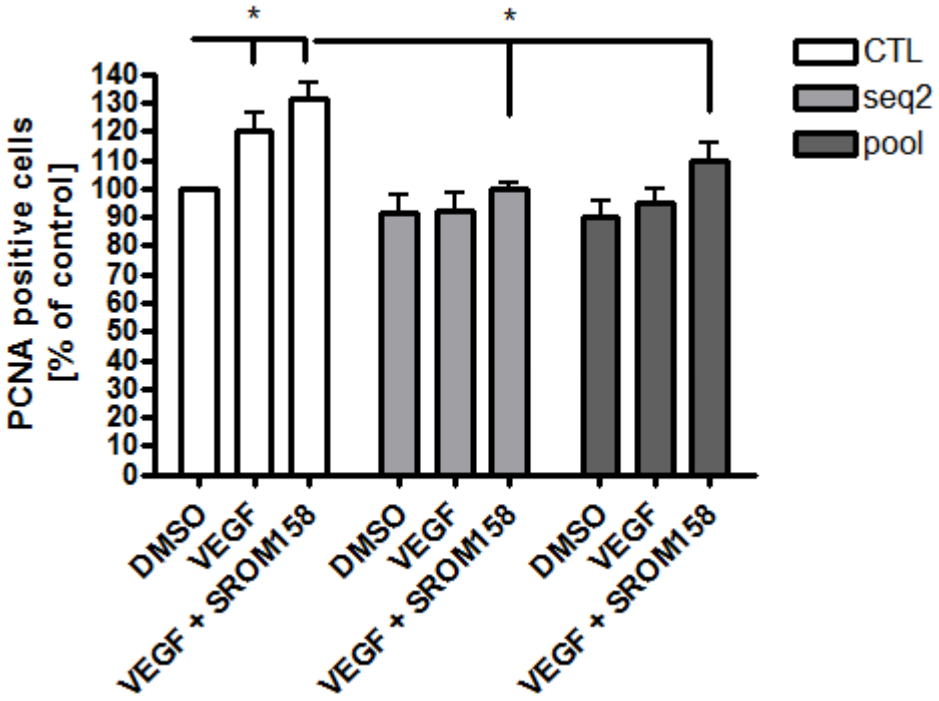

Figure 6. 7.: SROM158 alone is not sufficient to reverse the impaired proliferative phenotype of HO-1-deficient endothelial cells in response to VEGF. HUVEC were transfected with 40 nM control siRNA (CTL) or HO-1 specific siRNA (seq2, pool) for 24 h. Cells were pre-treated with vehicle or 25 µM SROM158 for 30 min prior to subsequent culture in growth factor-free medium in the absence (UT) or presence of 25 ng/ml VEGF for 24 h. Cell proliferation was assessed by PCNA staining and FACs analysis. Data is presented as mean ± SEM (n=6 experiments), * $p<0.05$.

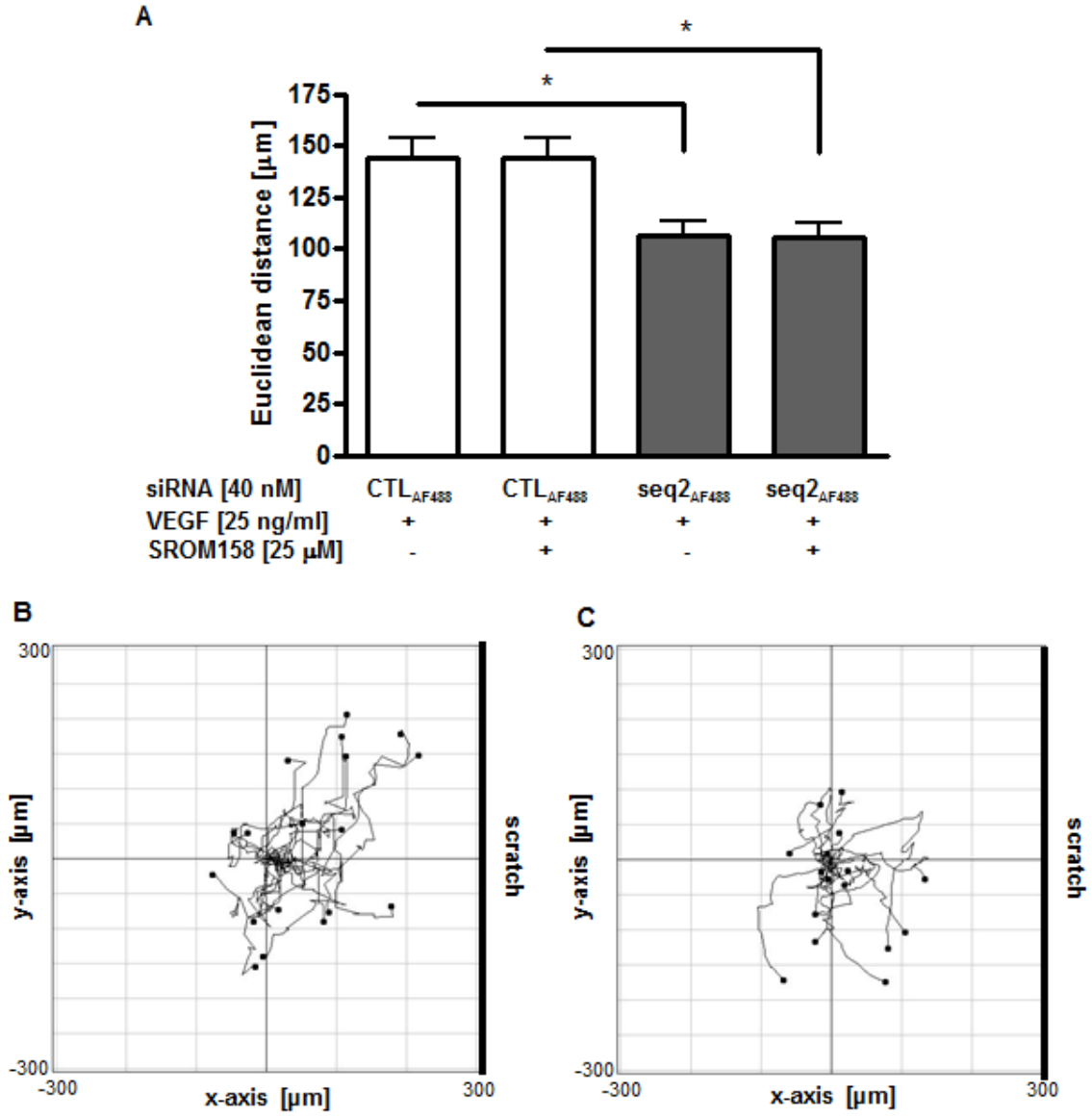

Figure 6. 8.: SROM158 alone is not sufficient to reverse the impaired migratory phenotype of HO-1-deficient endothelial cells in response to VEGF. HUVEC were transfected with 40 nM 3'-AlexaFluor488 control siRNA (CTL_{AF488}) or HO-1 specific siRNA ($seq2_{AF488}$) for 24 h. Cells were pre-treated with vehicle (DMSO) or 25 µM SROM158 for 30 min. Confluent monolayers were then scratched and treated with 25 ng/ml VEGF for 16 h. Migration was assessed by live cell imaging and quantified using ImageJ analysis software (Manual Tracking and Chemotaxis and Migration tool). (A) represents the Euclidean distance. Plots show the directional migration of HUVEC (B) transfected with $siCTL_{AF488}$, or (C) siHO-1 $seq2_{AF488}$ and pre-treated with SROM158. Data is presented as mean ± SD (n=3 experiments), * p<0.05.

6.2.3. HO-1 and vasodilator-stimulated phosphoprotein

Recent work by Deshane and co-workers has demonstrated a link between HO-1 and vasodilator-stimulated phosphoprotein (VASP), a cytoskeletal-associated protein localised at cell-cell contacts and microfilaments (Deshane *et al.*, 2007; Krause *et al.*, 2003). Treatment of MAEC isolated from HO-$1^{+/+}$ littermate control mice with SDF-1α resulted in VASP phosphorylation at serine 239 (Ser239) but not in cells from HO-1 knockout mice. Importantly, treatment with the CO donor CORM-2 resulted in phosphorylation of VASP in both HO-$1^{+/+}$ and HO-$1^{-/-}$, suggesting that SDF-1-α-mediated phosphorylation of VASP is HO-1 dependent. These findings led us to examine the effects of VEGF on VASP and to investigate if VASP acts as a downstream effector of HO-1 in VEGF-induced angiogenesis.

Time course experiments were conducted to determine the optimal time point of VEGF-mediated phosphorylation of VASP. Here, treatment of HUVEC with 25 ng/ml VEGF had no effect on total VASP protein at any time point, but resulted in VASP phosphorylation at Ser239 after 15 min exposure, and peaked after 30 min. No increase in phosphorylation compared to untreated control cells was observed after 240 min VEGF treatment (Fig. 6.9.). Therefore, 30 min exposure to VEGF was adapted for HO-1 inhibition studies.

To determine if VASP phosphorylation by VEGF is HO-1 dependent, HO-1 expression and activity was silenced by siRNA. In HUVEC transfected with siCTL, 30 min VEGF treatment resulted in a significant increase in phospho-VASP (Ser239). Even though variable results were obtained, inhibition either by siHO-1 seq2 or siHO-1 pool had no significant effect on the phosphorylation status of VASP both in the absence and presence of VEGF (Fig. 6.10.). Accordingly, no difference in VASP phosphorylation at Ser239 was observed between MAEC isolated from HO-$1^{-/-}$ animals and HO-$1^{+/+}$ littermate controls after 30 min VEGF exposure (Fig. 6.11.). In addition, the CO donor SROM158 alone or in combination with VEGF had no effect on VEGF-mediated VASP phosphorylation either in HO-$1^{+/+}$ or HO-$1^{-/-}$ MAEC (Fig. 6.11.). Altogether, these results suggest that VEGF-mediated VASP phosphorylation is HO-1 independent.

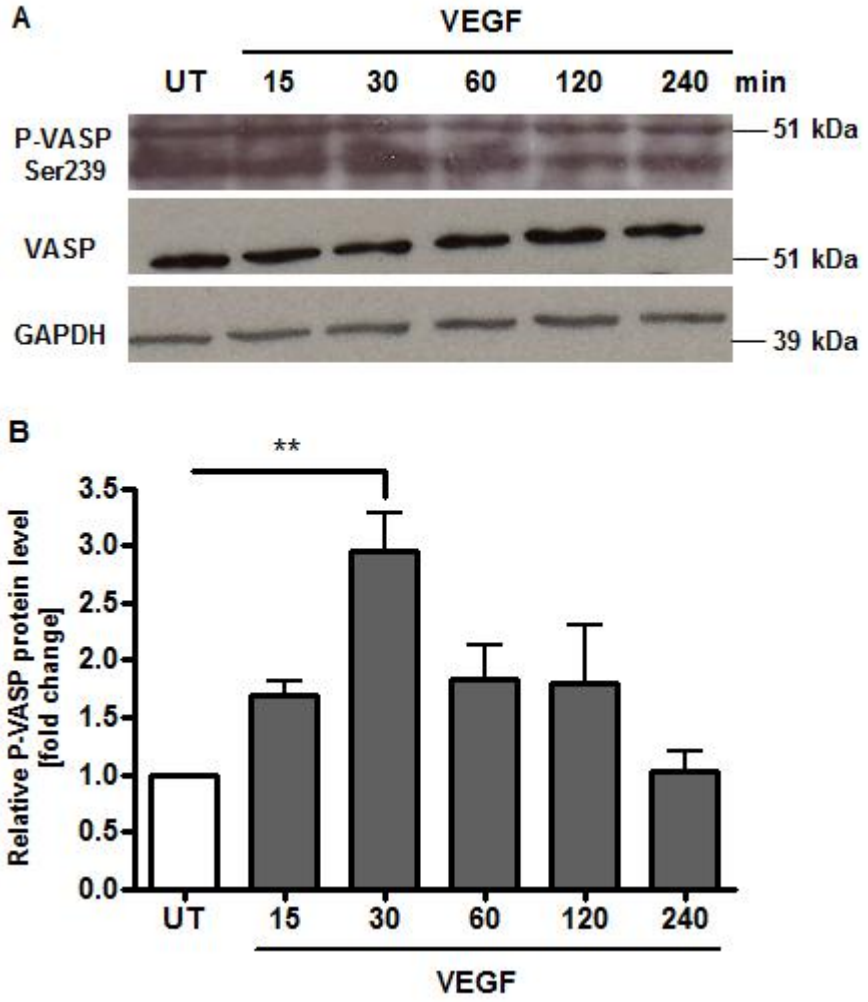

Figure 6. 9.: VEGF-mediated phosphorylation of vasodilator-stimulated protein is optimal after 30 min exposure. HUVEC were cultured in growth factor-free culture medium and left untreated (UT) or treated with 25 ng/ml VEGF for the indicated time periods (in min). Phosphorylation of VASP at serine 239 (Ser239) was assessed by western blotting and quantified by densitometry and is expressed as phospho-VASP (P-VASP) relative to total VASP protein. Phospo-VASP (Ser239) antibody only detects endogenous VASP when phosphorylated at serine 239 as indicated by a double band. GAPDH was used as a loading control. (A) shows a representative blot and (B) shows the corresponding densitometry. Data is presented as mean ± SEM (n=3 experiments), ** $p<0.01$.

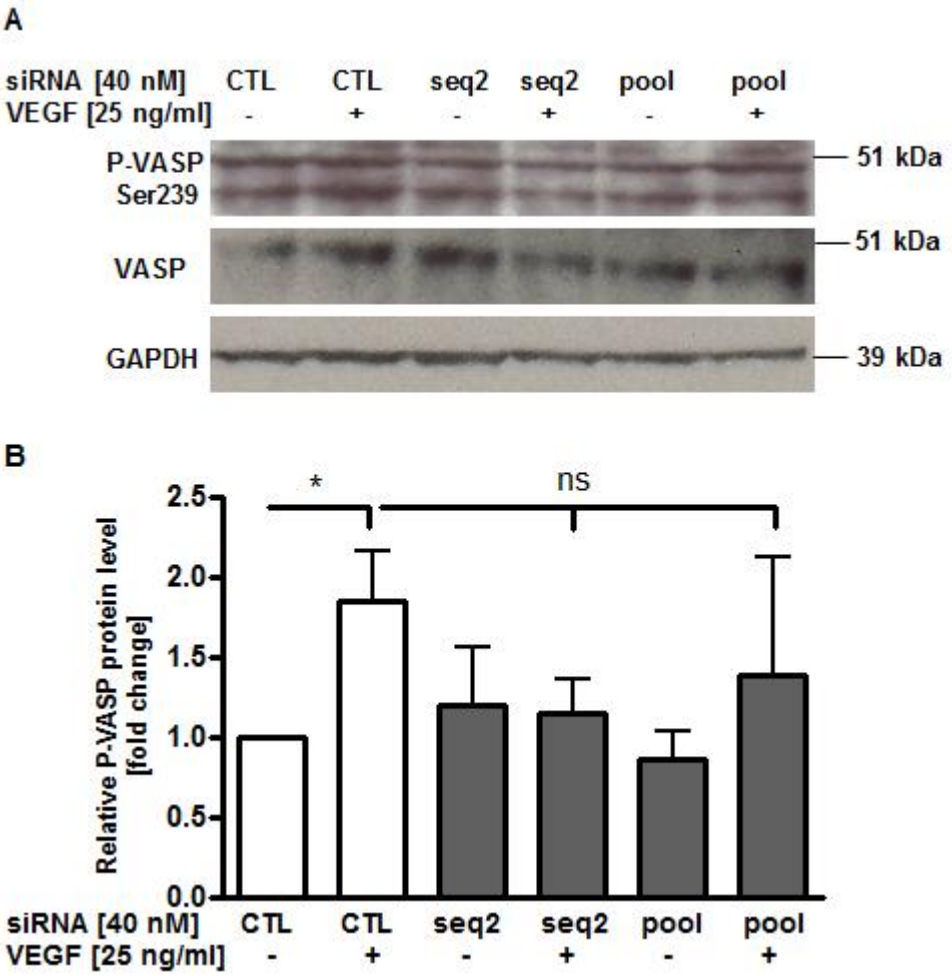

Figure 6. 10.: VEGF-mediated VASP phosphorylation in primary human endothelial cells is not HO-1 dependent. HUVEC transfected with 40 nM control siRNA (CTL) or HO-1 specific siRNA (seq2, pool) were cultured in growth factor-free medium and left untreated or treated with 25 ng/ml VEGF for 30 min. Phosphorylation of VASP at serine 239 (Ser239) was assessed by western blotting and quantified by densitometry and is expressed as phospho-VASP (P-VASP) relative to total VASP protein. GAPDH was used as a loading control. (A) shows a representative blot and (B) shows the corresponding densitometry. Data is presented as mean ± SEM (n=3 experiments), * p<0.05, ns – not significant.

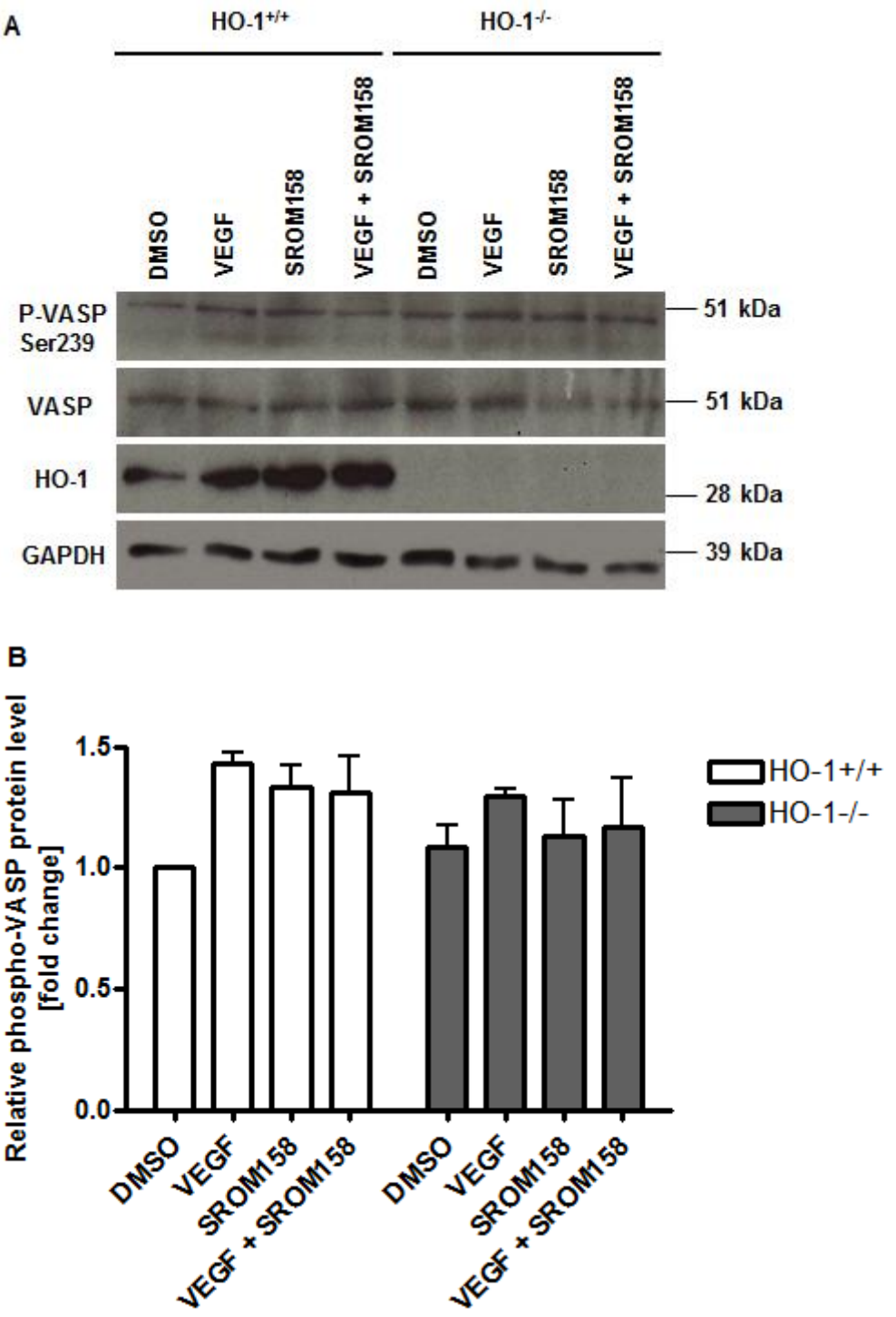

Figure 6. 11.: VEGF-mediated phosphorylation of VASP is not altered in murine aortic EC isolated from HO-1 knockout mice. MAEC isolated from HO-$1^{+/+}$ littermate controls or HO-$1^{-/-}$ animals were treated with vehicle control (DMSO), 25 ng/ml VEGF, 25 µM SROM158, or VEGF and SROM158 in combination for 30 min. Protein expression and phosphorylation of VASP at serine 239 (Ser239) was assessed by western blotting and quantified by densitometry. VASP phosphorylation is expressed as phospho-VASP (P-VASP) relative to total VASP protein. GAPDH was used as a loading control. (A) shows a representative blot and (B) shows the corresponding densitometry. Data is presented as mean ± SEM (n=3 experiments).

6.2.4. Identification of novel HO-1 downstream targets – PCR array

To begin to elucidate downstream effectors of HO-1 in VEGF-driven angiogenesis, the mRNA expression profile of HUVEC depleted of HO-1 by siRNA and control cells in response to VEGF was compared with the aid of the SABiosciences Human Cytoskeleton Regulators RT^2 Profiler™ PCR Array (Qiagen Ltd.). The array profiles the expression of 84 genes controlling the biogenesis, organisation and rearrangement, as well as the polymerisation and depolymerisation of the cytoskeleton, an important precondition for the process of angiogenesis.

Umbilical vein EC isolated from three human donors were pooled and either transfected with a non-targeting control siRNA (siCTL) or HO-1 specific siRNA (siHO-1 pool) for 24 h prior to treatment with 25 ng/ml VEGF and subsequent culture for 16 h. For best results from the PCR array, isolated total RNA was quality controlled for concentration and purity by Nanodrop analysis and ribosomal RNA band integrity on an Agilent BioAnalyzer using an RNA 6000 Nano LabChip®. The ratio of absorbance at 260 nm and 280 nm (A_{260nm}:A_{280nm}) is used to assess the purity of RNA and a ratio of ~2.0 is generally accepted to describe high-quality 'pure' RNA. The A_{260nm}:A_{230nm} ratio is used as a secondary measure of nucleic purity and should be greater than 1.7 (Schroeder *et al.*, 2006). Here, total RNA isolation from siCTL-transfected cells yielded a concentration of 614.5 ng/µl RNA, with an absorbance ratio A_{260nm}:A_{280nm}=2.16 and A_{260nm}:A_{230nm}=1.8 (Tab. 6.1.). Similar results were obtained for HO-1-depleted cultures with a total RNA concentration of 626.0 ng/µl, absorbance ratio A_{260nm}:A_{280nm}=2.12 and A_{260nm}:A_{230nm}=2.07 (Tab. 6.1.). Moreover, analysis of ribosomal band integrity demonstrated sharp peaks and bands for the 18S and 28S ribosomal RNA (rRNA) on electropherograms and gel-like images, respectively, resulting in an RNA integrity number (RIN) of 8.1 for control cells and a RIN of 10.0 for HO-1-depleted cells (Fig. 6.12.). RIN values range from 1 (totally degraded) to 10 (intact) (Schroeder *et al.*, 2006). Taken together, these results indicate high-quality total RNA isolated from both control and HO-1 siRNA-transfected cultures, which meets the standards of integrity and purity from protein, organic, or genomic DNA contamination required for reliable results from the RT^2 Profiler PCR array. In addition, the siRNA-mediated knockdown of the human HO-1 gene in these samples was assessed by qRT-PCR and revealed a sufficient reduction in HO-1 mRNA of 70% in siHO-1 pool-transfected cells compared to siCTL-transfected cells (Fig. 6.13.).

Table 6. 1.: Nanodrop analysis of isolated total RNA. Total RNA from HUVEC pooled from three donors either transfected with 40 nM control siRNA (siCTL) or HO-1 specific siRNA (siRNA pool) and treated with 25 ng/ml VEGF for 16 h was isolated using the RNeasy Mini Kit and quantified by Nanodrop analysis.

Sample	Concentration [ng/µl]	Absorbance ratio A_{260nm}:A_{280nm}	Absorbance ratio A_{260nm}:A_{230nm}
siCTL + VEGF	614.5	2.16	1.8
siHO-1 pool + VEGF	626.0	2.12	2.07

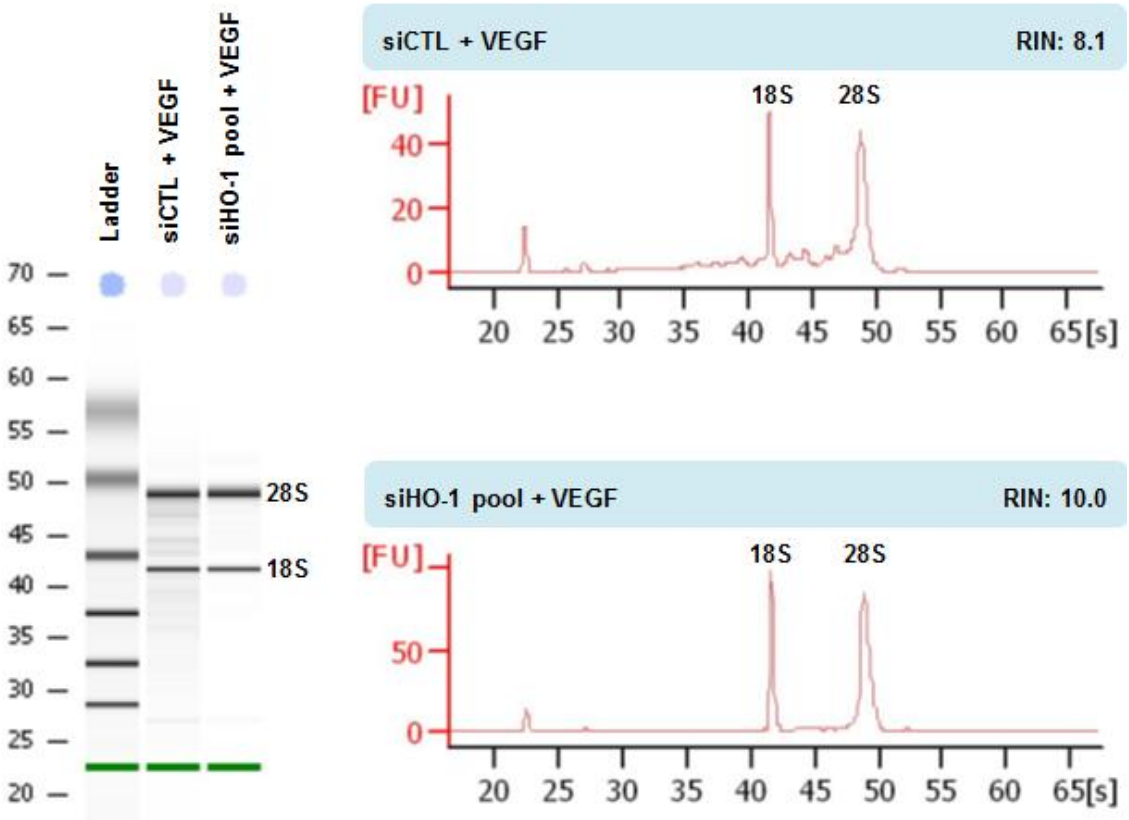

Figure 6. 12.: Ribosomal band integrity analysed on the Agilent® 2100 BioAnalyzer. Total RNA isolated from HUVEC pooled from three donors either transfected with 40 nM control siRNA (siCTL) or HO-1 specific siRNA (siHO-1 pool) and treated with 25 ng/ml VEGF for 16 h was analysed using an RNA 6000 Nano LabChip®. The gel-like image and corresponding electropherogram show high-quality total RNA as sharp bands and peaks, respectively. RIN – RNA integrity number, 28S – 28S ribosomal RNA, 18S – 18S ribosomal RNA.

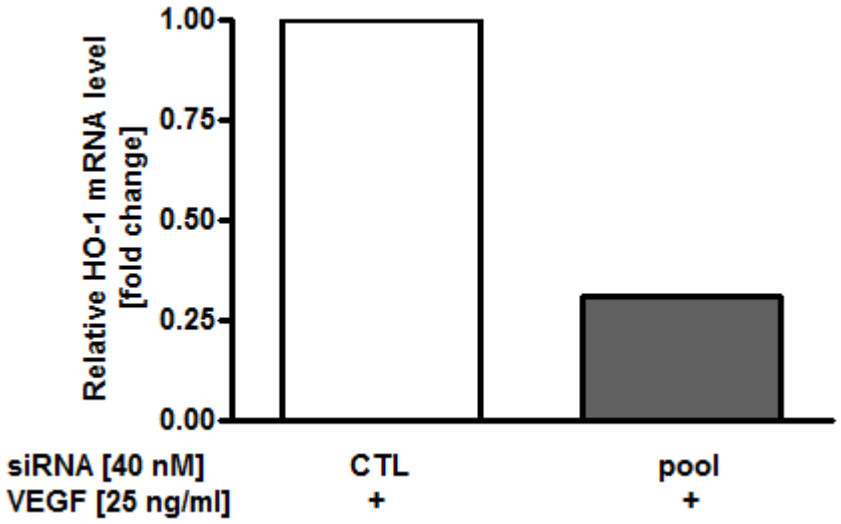

Figure 6. 13.: Validation of siRNA-mediated silencing of HO-1 in human EC. HUVEC either transfected with 40 nM control siRNA (CTL) or HO-1 specific siRNA (pool) were treated with 25 ng/ml VEGF for 16 h. Cells from isolated from three donor were pooled and HO-1 mRNA expression was quantified by qRT-PCR.

Gene expression profiling using the Cytoskeleton Regulator PCR array identified numerous genes that were differentially expressed between siCTL and siHO-1 pool-transfected cells in response to VEGF exposure for 16 h (Tab. 6.2.). In this study, fold changes in mRNA expression were considered significantly upregulated when ≥ 2.00 and significantly downregulated when ≤0.50. Genes that were significantly upregulated in HO-1-depleted cells compared to control cells include ARPC2 (fold change = 2.17), CIT (fold change = 2.03), FSCN2 (fold change = 2.17), and PPP1R12B (fold change = 2.03). Among the identified hits, only one gene was significantly downregulated by HO-1 inhibition, the positive cell cycle regulator cyclin A1 (CCNA1; fold change = 0.44) (Tab. 6.2.).

Table 6. 2.: Cytoskeleton Regulator PCR array results. Changes in mRNA expression of siCTL- or siHO-1 pool-transfected HUVEC in response to VEGF were assessed using the SABiosciences Human Cytoskeleton Regulators RT^2 Profiler^{TM} PCR Array and quantified using the SABiosciences RT^2 Profiler^{TM} PCR Array Data Analysis version 3.5 online service. Fold up- and downregulation ≥ 2.00 and ≤ 0.50 were considered as significant changes in gene expression and are highlighted in bold.

Gene Symbol	Gene Name	Fold Up- or Down-Regulation
ACTR2	ARP2 actin-related protein 2 homolog (yeast)	1.01
ACTR3	ARP3 actin-related protein 3 homolog (yeast)	0.77
ARFIP2	ADP-ribosylation factor interacting protein 2	1.34
ARHGAP6	Rho GTPase activating protein 6	1.16
ARHGDIB	Rho GDP dissociation inhibitor (GDI) beta	0.82
ARHGEF11	Rho guanine nucleotide exchange factor (GEF) 11	1.43
ARPC1B	Actin related protein 2/3 complex, subunit 1B, 41kDa	1.34
ARPC2	**Actin related protein 2/3 complex, subunit 2, 34kDa**	**2.17**
ARPC3	Actin related protein 2/3 complex, subunit 3, 21kDa	0.82
ARPC4	Actin related protein 2/3 complex, subunit 4, 20kDa	1.54
ARPC5	Actin related protein 2/3 complex, subunit 5, 16kDa	0.58
AURKA	Aurora kinase A	1.43
AURKB	Aurora kinase B	1.34
AURKC	Aurora kinase C	1.65
BAIAP2	BAI1-associated protein 2	1.09
CALD1	Caldesmon 1	0.88
CALM1	Calmodulin 1 (phosphorylase kinase, delta)	0.95
CASK	Calcium/calmodulin-dependent serine protein kinase (MAGUK family)	1.09
CCNA1	**Cyclin A1**	**0.44**
CCNB2	Cyclin B2	1.43
CDC42	Cell division cycle 42 (GTP binding protein, 25kDa)	0.95
CDC42BPA	CDC42 binding protein kinase alpha (DMPK-like)	1.25
CDC42EP2	CDC42 effector protein (Rho GTPase binding) 2	1.01
CDC42EP3	CDC42 effector protein (Rho GTPase binding) 3	1.16
CDK5	Cyclin-dependent kinase 5	1.43
CDK5R1	Cyclin-dependent kinase 5, regulatory subunit 1 (p35)	1.43

Table 6.2 continued

ARAP1	ArfGAP with RhoGAP domain, ankyrin repeat and PH domain 1	1.25
CFL1	Cofilin 1 (non-muscle)	1.01
CIT	**Citron (rho-interacting, serine/threonine kinase 21)**	**2.03**
CLASP1	Cytoplasmic linker associated protein 1	0.88
CLASP2	Cytoplasmic linker associated protein 2	0.88
CLIP1	CAP-GLY domain containing linker protein 1	1.09
CLIP2	CAP-GLY domain containing linker protein 2	1.25
CRK	V-crk sarcoma virus CT10 oncogene homolog (avian)	0.82
CTTN	Cortactin	1.01
CYFIP1	Cytoplasmic FMR1 interacting protein 1	0.95
CYFIP2	Cytoplasmic FMR1 interacting protein 2	1.77
DIAPH1	Diaphanous homolog 1 (Drosophila)	0.95
DSTN	Destrin (actin depolymerizing factor)	1.01
EZR	Ezrin	1.65
FNBP1L	Formin binding protein 1-like	1.16
FSCN2	**Fascin homolog 2, actin-bundling protein, retinal (Strongylocentrotus purpuratus)**	**2.17**
GSN	Gelsolin (amyloidosis, Finnish type)	1.09
IQGAP1	IQ motif containing GTPase activating protein 1	0.88
IQGAP2	IQ motif containing GTPase activating protein 2	1.09
LIMK1	LIM domain kinase 1	1.09
LIMK2	LIM domain kinase 2	0.82
LLGL1	Lethal giant larvae homolog 1 (Drosophila)	1.25
MACF1	Tubule-actin crosslinking factor 1	0.82
MAP3K11	Mitogen-activated protein kinase kinase kinase 11	1.54
MAP4	Tubule-associated protein 4	0.72
MAPK13	Mitogen-activated protein kinase 13	1.16
MAPRE1	Tubule-associated protein, RP/EB family, member 1	0.82
MAPRE2	Tubule-associated protein, RP/EB family, member 2	0.58
MAPT	Tubule-associated protein tau	0.72
MARK2	MAP/tubule affinity-regulating kinase 2	1.09
MID1	Midline 1 (Opitz/BBB syndrome)	0.88
MSN	Moesin	0.62

Table 6.2. continued

MYLK	Myosin light chain kinase	1.16
MYLK2	Myosin light chain kinase 2	1.34
NCK1	NCK adaptor protein 1	1.01
NCK2	NCK adaptor protein 2	1.01
PAK1	P21 protein (Cdc42/Rac)-activated kinase 1	1.43
PAK4	P21 protein (Cdc42/Rac)-activated kinase 4	1.09
PFN2	Profilin 2	1.09
PHLDB2	Pleckstrin homology-like domain, family B, member 2	0.95
PIKFYVE	Phosphoinositide kinase, FYVE finger containing	1.16
PPP1R12A	Protein phosphatase 1, regulatory (inhibitor) subunit 12A	1.43
PPP1R12B	**Protein phosphatase 1, regulatory (inhibitor) subunit 12B**	**2.03**
PPP3CA	Protein phosphatase 3 (formerly 2B), catalytic subunit, alpha isoform	0.82
PPP3CB	Protein phosphatase 3 (formerly 2B), catalytic subunit, beta isoform	0.51
RAC1	Ras-related C3 botulinum toxin substrate 1 (rho family, small GTP binding protein Rac1)	0.88
RACGAP1	Rac GTPase activating protein 1	1.25
RDX	Radixin	0.82
RHOA	Ras homolog gene family, member A	0.82
ROCK1	Rho-associated, coiled-coil containing protein kinase 1	0.95
SSH1	Slingshot homolog 1 (Drosophila)	1.16
SSH2	Slingshot homolog 2 (Drosophila)	0.77
STMN1	Stathmin 1	1.09
TIAM1	T-cell lymphoma invasion and metastasis 1	1.65
VASP	Vasodilator-stimulated phosphoprotein	1.01
WAS	Wiskott-Aldrich syndrome (eczema-thrombocytopenia)	0.51
WASF1	WAS protein family, member 1	1.01
WASL	Wiskott-Aldrich syndrome-like	1.16

To validate the PCR array result, HUVEC were either treated with the siRNA delivery agent geneFECTOR (GF) or transfected with siCTL or siHO-1 (seq2, pool) for 24 h prior to treatment with VEGF and subsequent culture for 16 h. VEGF treatment of GF-treated and siCTL-transfected cells resulted in a significant increase in cyclin A1 mRNA. Moreover, siRNA-mediated silencing of HO-1 not only diminished basal cyclin A1 expression but also inhibited the VEGF response (Fig. 6.14), thereby confirming the PCR array result.

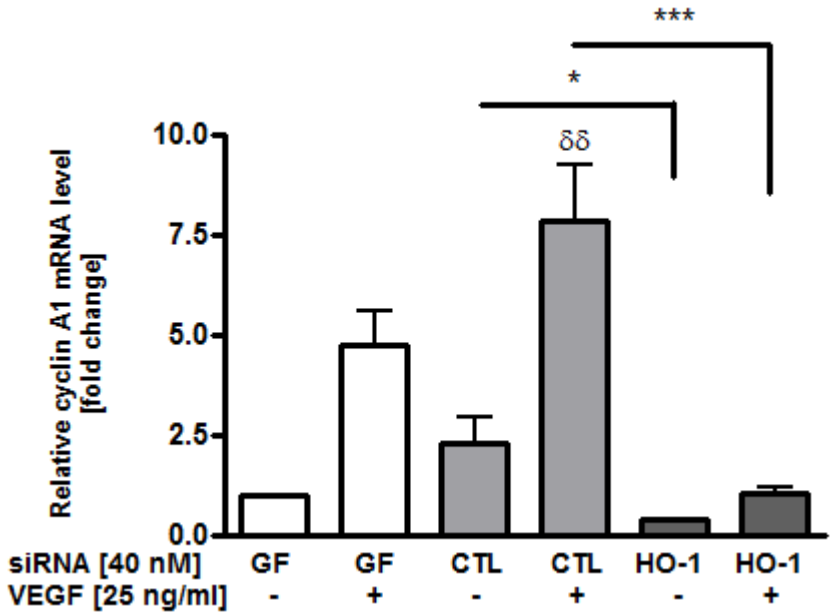

Figure 6. 14.: Validation of the PCR array hit cyclin A1 by quantitative real-time PCR. HUVEC were either treated with geneFECTOR (GF) or transfected with 40 nM control siRNA (CTL) or HO-1 specific siRNA (HO-1; represents pooled data from siHO-1 seq2 and siHO-1 pool) for 16 h. Cells were then left untreated or treated with 25 ng/ml VEGF for 24 h prior to mRNA quantification by qRT-PCR. Data is presented as mean ± SEM (n=3 experiments), * $p<0.05$, ** $p<0.01$. δδ $p<0.01$ vs untreated siCTL-transfected cells.

6.2.5. Identification of novel HO-1 downstream targets - Proteomics

In collaboration with Prof M. Mayr (King's College London, UK) a proteomic screen of primary human EC was performed as a second approach to identify novel HO-1 downstream targets that are involved in HO-1-dependent VEGF-mediated angiogenesis.

Cellular lysates of primary human EC (HUVEC), pooled from three donors either transfected with 40 nM control siRNA (siCTL) or HO-1 specific siRNA (siHO-1 pool) and treated with VEGF for 16 h, or alternatively, lysates of HUVEC either infected with a control adenovirus containing an empty vector (Ad0) or the recombinant adenovirus expressing the human HO-1 gene (AdHO-1) were collected by myself and HO-1 protein expression was assessed by western blotting (Fig. 6.15.). Silencing of HO-1 by siRNA in HUVEC resulted in a sufficient decrease in HO-1 expression compared to siCTL-transfected cells (Fig. 6.15.A). Likewise, infection of cells with AdHO-1 markedly upregulated HO-1 protein, an effect not seen with Ad0 (Fig. 6.15.B).

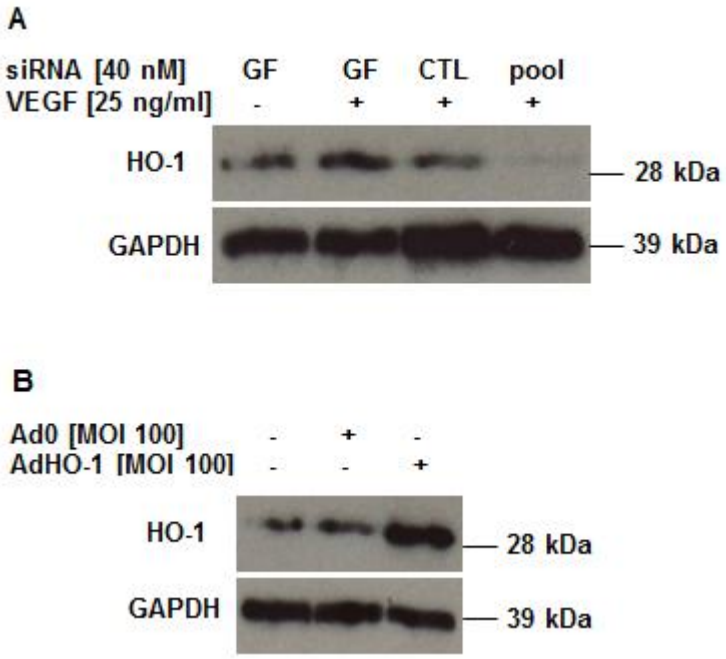

Figure 6. 15.: Validation of HO-1 protein expression in human primary EC. HUVEC pooled from three donors were cultured in gelatin-coated T75 culture flasks and either (A) treated with geneFECTOR (GF) or transfected with 40 nM control siRNA (CTL) or HO-1 specific siRNA (pool) for 24 h and then left untreated or treated with 25 ng/ml VEGF for 16 h, or (B) left uninfected or infected with a control adenovirus containing an empty vector (Ad0) or the recombinant adenovirus expressing the HO-1 gene at a MOI of 100 for 2 h in plain M199 medium prior to subsequent culture for 16 h. HO-1 protein expression was assessed by western blotting. GAPDH was used as a loading control.

The validated protein lysates were analysed by difference in-gel electrophoresis (DIGE) coupled to mass spectroscopy by our collaborators and a list of differentially expressed proteins was returned to our laboratory (Fig. 6.16. and Tab. 6.3.).

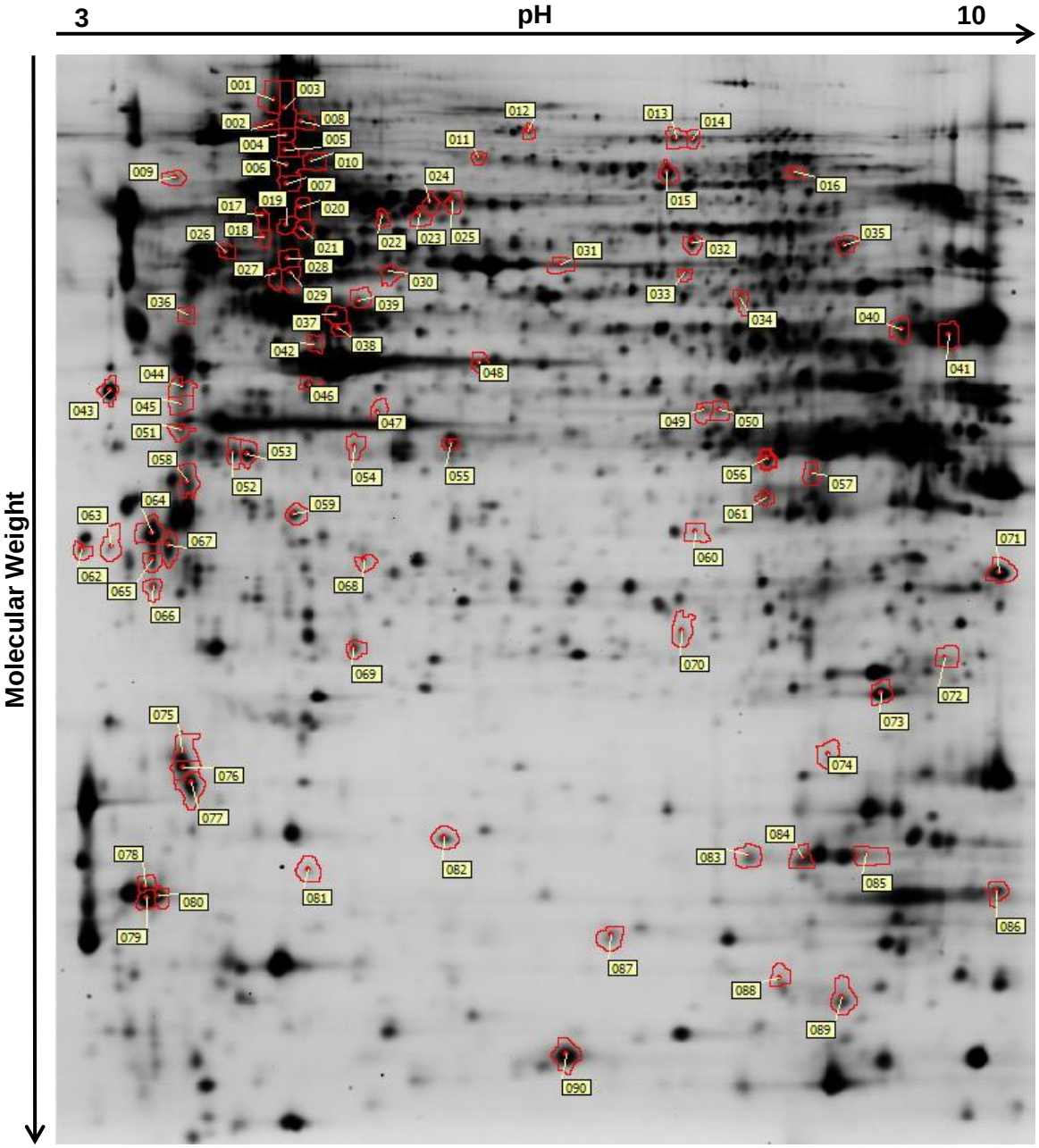

Figure 6. 16.: Difference in-gel electrophoresis results. Different samples (GF, GF + VEGF, siCRL + VEGF, siHO-1 pool + VEGF, UT, Ad0, AdHO-1; all in triplicates) were labelled with Cy3 and Cy5 fluorescent dyes and separated by difference in-gel electrophoresis (DIGE). Fluorescent images were captured and visualised by silver staining and scanned in transmission scan mode. Spots showing a significant difference in intensity, here indicated by red circles and numbers, were excised for in-gel tryptic digestion and analysed by mass spectroscopy.

Table 6. 3.: Full list of differential expressed proteins. Each sample was labelled with a fluorescent dye (Cy3 or Cy5) and mixed with the internal standard (a mixture of all samples tested and labelled wirh Cy2). The table represents the combined hits resulting from each sample normalised to the internal standard.

No.	Protein name	Accession No.	Mw (Da)	Protein identification probability	No. of unique peptides	No. of unique spectra	No. of total spectra	Coverage
1	Vimentin	VIME_HUMAN	53634,6	100,00%	16	18	30	0,363
2	Vimentin	VIME_HUMAN	53634,6	100,00%	21	25	43	0,483
3	Vimentin	VIME_HUMAN	53634,6	100,00%	35	48	90	0,687
4	Vimentin	VIME_HUMAN	53634,6	100,00%	38	44	81	0,792
5	Vimentin	VIME_HUMAN	53634,6	100,00%	34	40	69	0,71
6	Vimentin	VIME_HUMAN	53634,6	100,00%	34	40	76	0,725
7	Vimentin	VIME_HUMAN	53634,6	100,00%	28	32	52	0,629
8	Heat shock 70 kDa protein 4	HSP74_HUMAN	94313,9	100,00%	14	17	31	0,202
9	Periodic tryptophan protein 1 homolog	PWP1_HUMAN	55810,6	100,00%	3	3	5	0,0639
10	Lamin-B1	LMNB1_HUMAN	66391,6	100,00%	4	4	5	0,0785
10	Ran GTPase-activating protein 1	RAGP1_HUMAN	63525,3	100,00%	4	4	6	0,0784
11	Zyxin	ZYX_HUMAN	61258	99,80%	2	2	4	0,0455
11	Gelsolin	GELS_HUMAN	85679,8	100,00%	3	3	4	0,0409
12	Neutral alpha-glucosidase AB	GANAB_HUMAN	106857,9	100,00%	4	5	8	0,0424
13	Procollagen-lysine,2-oxoglutarate 5-dioxygenase 2	PLOD2_HUMAN	84669,4	100,00%	8	9	17	0,13
14	Nucleolin	NUCL_HUMAN	76597,9	100,00%	3	3	6	0,0437
14	Procollagen-lysine,2-oxoglutarate 5-dioxygenase 2	PLOD2_HUMAN	84669,4	100,00%	9	9	14	0,137
15	Caldesmon	CALD1_HUMAN	93232,8	100,00%	10	15	28	0,173
16	Lamina-associated polypeptide 2, isoform alpha	LAP2A_HUMAN	75475,8	100,00%	7	9	13	0,117
16	Lamin-A/C	LMNA_HUMAN	74122,6	100,00%	6	6	11	0,101
17	Vimentin	VIME_HUMAN	53634,6	100,00%	19	22	39	0,438
18	Vimentin	VIME_HUMAN	53634,6	100,00%	10	10	16	0,24
19	Vimentin	VIME_HUMAN	53634,6	100,00%	23	25	47	0,496
20	Vimentin	VIME_HUMAN	53634,6	100,00%	18	20	43	0,397

Table 6.3 continued

21	Heterogeneous nuclear ribonucleoprotein K	HNRPK_HUMAN	50960,5	100,00%	7	11	19	0,179
22	Lamin-B2	LMNB2_HUMAN	67671,7	100,00%	6	6	10	0,123
22	Vimentin	VIME_HUMAN	53634,6	100,00%	8	8	16	0,152
23	Ras GTPase-activating protein-binding protein 1	G3BP1_HUMAN	52144,8	99,90%	3	3	5	0,0622
24	Annexin A6	ANXA6_HUMAN	75859,5	100,00%	9	10	15	0,146
25	Heat shock cognate 71 kDa protein	HSP7C_HUMAN	70881,8	100,00%	5	5	7	0,0975
26	Vimentin	VIME_HUMAN	53634,6	100,00%	12	13	23	0,311
26	Protein disulfide-isomerase	PDIA1_HUMAN	57100,1	100,00%	6	9	16	0,14
27	Tubulin beta chain	TBB5_HUMAN	49652,6	100,00%	5	5	8	0,133
27	Vimentin	VIME_HUMAN	53634,6	100,00%	9	10	17	0,215
28	Tubulin alpha-1A chain	TBA1A_HUMAN	50117,7	100,00%	12	16	30	0,335
28	Vimentin	VIME_HUMAN	53634,6	100,00%	20	26	48	0,472
29	Polymerase I and transcript release factor	PTRF_HUMAN	43458,5	100,00%	9	14	26	0,254
29	Vimentin	VIME_HUMAN	53634,6	100,00%	12	15	25	0,322
30	Heterogeneous nuclear ribonucleoprotein K	HNRPK_HUMAN	50960,5	100,00%	4	4	7	0,0929
30	Vimentin	VIME_HUMAN	53634,6	100,00%	7	7	11	0,157
31	Protein disulfide-isomerase A3	PDIA3_HUMAN	56766,6	100,00%	11	14	23	0,234
32	T-complex protein 1 subunit zeta	TCPZ_HUMAN	58007,3	100,00%	19	21	36	0,282
33	Succinyl-CoA:3-ketoacid-coenzyme A transferase 1, mitochondrial	SCOT1_HUMAN	56140,8	100,00%	5	6	9	0,104
34	Seryl-tRNA synthetase, mitochondrial	SYSM_HUMAN	58265,5	95,00%	1	1	2	0,0193
35	Pyruvate kinase isozymes M1/M2	KPYM_HUMAN	57919,5	100,00%	10	10	19	0,175
36	Vimentin	VIME_HUMAN	53634,6	100,00%	9	9	15	0,155
37	Thioredoxin domain-containing protein 5	TXND5_HUMAN	47611,1	100,00%	16	18	31	0,352
38	Heterogeneous nuclear ribonucleoprotein F	HNRPF_HUMAN	45653,8	100,00%	8	11	20	0,234
39	Endophilin-A2	SH3G1_HUMAN	41473,2	100,00%	11	11	20	0,293

Table 6.3. continued

40	Serpin H1	SERPH_HUMAN	46424	100,00%	8	9	16	0,167
41	Serpin H1	SERPH_HUMAN	46424	100,00%	17	22	44	0,409
42	Eukaryotic translation initiation factor 3 subunit F	EIF3F_HUMAN	37545,5	100,00%	6	7	13	0,216
42	Perilipin-3	PLIN3_HUMAN	47027,6	100,00%	5	5	9	0,184
43	Protein SET	SET_HUMAN	33471,4	100,00%	7	11	18	0,224
44	Tropomyosin alpha-1 chain	TPM1_HUMAN	32692	100,00%	10	12	19	0,306
45	Tropomyosin alpha-1 chain	TPM1_HUMAN	32692	100,00%	5	5	7	0,155
45	Vimentin	VIME_HUMAN	53634,6	100,00%	4	4	7	0,0751
46	Unidentified	-	-	-	-	-	-	-
47	Unidentified	-	-	-	-	-	-	-
48	Actin, cytoplasmic 1	ACTB_HUMAN	41719,8	100,00%	8	8	15	0,205
49	Ubiquitin fusion degradation protein 1 homolog	UFD1_HUMAN	34483,2	99,80%	3	4	7	0,0782
50	Heterogeneous nuclear ribonucleoproteins C1/C2	HNRPC_HUMAN	33652,5	100,00%	5	5	7	0,134
51	Tropomyosin alpha-1 chain	TPM1_HUMAN	32692	100,00%	7	7	13	0,201
52	Elongation factor 1-delta	EF1D_HUMAN	31103,9	96,60%	2	2	3	0,0391
53	Elongation factor 1-delta	EF1D_HUMAN	31103,9	100,00%	13	15	25	0,47
54	Guanine nucleotide-binding protein subunit beta-4	GBB4_HUMAN	37549,8	100,00%	4	4	7	0,115
55	60S acidic ribosomal protein P0	RLA0_HUMAN	34256,3	100,00%	10	12	20	0,385
56	Calponin-2	CNN2_HUMAN	33679,6	100,00%	4	5	9	0,149
57	Voltage-dependent anion-selective channel protein 2	VDAC2_HUMAN	31549,3	100,00%	6	6	10	0,255
58	Tropomyosin alpha-1 chain	TPM1_HUMAN	32692	100,00%	6	6	12	0,155
59	Tubule-associated protein RP/EB family member 1	MARE1_HUMAN	29981,5	100,00%	6	7	13	0,254
60	Purine nucleoside phosphorylase	PNPH_HUMAN	32100	100,00%	5	5	13	0,218
61	Voltage-dependent anion-selective channel protein 2	VDAC2_HUMAN	31549,3	99,80%	2	2	3	0,068

Table 6.3. continued

62	Unidentified	-	-	-	-	-	-	-
63	Unidentified	-	-	-	-	-	-	-
64	Elongation factor 1-delta	EF1D_HUMAN	31103,9	99,20%	3	3	4	0,0712
64	Elongation factor 1-beta	EF1B_HUMAN	24746,2	100,00%	4	5	7	0,231
65	Elongation factor 1-delta	EF1D_HUMAN	31103,9	99,90%	3	3	5	0,0712
65	Elongation factor 1-beta	EF1B_HUMAN	24746,2	100,00%	5	5	7	0,307
66	Eukaryotic translation initiation factor 6	IF6_HUMAN	26580,2	100,00%	6	7	13	0,294
67	14-3-3 protein epsilon	1433E_HUMAN	29157	100,00%	12	16	30	0,353
68	Prohibitin	PHB_HUMAN	29786,6	100,00%	7	7	13	0,228
69	Unidentified	-	-	-	-	-	-	-
70	LDLR chaperone MESD	MESD_HUMAN	26059,9	100,00%	7	8	16	0,325
71	39S ribosomal protein L24, mitochondrial	RM24_HUMAN	24897	100,00%	4	4	7	0,208
71	FK506-binding protein 3	FKBP3_HUMAN	25159,4	100,00%	6	6	10	0,263
72	Cysteine and glycine-rich protein 1	CSRP1_HUMAN	20549,1	100,00%	9	10	17	0,508
73	Transgelin-2	TAGL2_HUMAN	22373,9	100,00%	9	13	23	0,442
74	Unidentified	-	-	-	-	-	-	-
75	Myosin regulatory light chain 12A	ML12A_HUMAN	19777,2	100,00%	3	3	6	0,175
76	Myosin regulatory light chain 12A	ML12A_HUMAN	19777,2	100,00%	6	7	16	0,404
77	Myosin regulatory light chain 12A	ML12A_HUMAN	19777,2	100,00%	7	9	19	0,509
78	Myosin light polypeptide 6	MYL6_HUMAN	16911,8	100,00%	4	5	9	0,364
79	Myosin light polypeptide 6	MYL6_HUMAN	16911,8	100,00%	9	12	24	0,636
80	Myosin light polypeptide 6	MYL6_HUMAN	16911,8	100,00%	4	4	6	0,364
81	Unidentified	-	-	-	-	-	-	-
82	Actin-related protein 2/3 complex subunit 5	ARPC5_HUMAN	16302,6	100,00%	5	6	12	0,311
83	Peptidyl-prolyl cis-trans isomerase A	PPIA_HUMAN	17994,9	100,00%	6	8	16	0,394
84	Peptidyl-prolyl cis-trans isomerase A	PPIA_HUMAN	17994,9	100,00%	6	8	20	0,358

Table 6.3. continued

85	Peptidyl-prolyl cis-trans isomerase A	PPIA_HUMAN	17994,9	100,00%	7	8	16	0,358
86	Histone H2B type 1-B	H2B1B_HUMAN	13932,8	100,00%	3	3	5	0,167
86	60S ribosomal protein L22	RL22_HUMAN	14769,3	100,00%	4	4	7	0,242
86	40S ribosomal protein S19	RS19_HUMAN	16042,5	99,90%	3	3	5	0,172
87	Unidentified	-	-	-	-	-	-	-
88	Unidentified	-	-	-	-	-	-	-
89	Hemoglobin subunit alpha	HBA_HUMAN	15239,6	100,00%	4	5	9	0,282
90	Protein S100-A11	S10AB_HUMAN	11723,1	100,00%	3	5	9	0,219

Of the identified hits, 29 proteins were differentially expressed between the proteome of HUVEC transfected with a non-targeting control siRNA and HO-1-depleted HUVEC exposed to VEGF for 16 h. These hits were then analysed using the DAVID Bioinformatics Resources 6.7 online software (National Institute of Allergy and Infectious Diseases (NIAID), National Institute of Health) and grouped according to gene ontology (GO), in terms of cellular component, molecular function, and biological process (Tab. 6.4.). The main purpose of the proteomic screen was to identify potential downstream targets of HO-1 mediating VEGF-driven angiogenesis. Here, gene ontology identified several proteins that are involved in the regulation of angiogenesis and related GO-groups including cytoskeletal proteins and intermediate filaments, and proteins that regulate cell structure/morphology and motility (Tab. 6.4. highlighted in bolt). Of note, a common hit to all these groups was the intermediate filament vimentin, and its role in HO-1-driven angiogenesis will be discussed in more detail in Chapter 8.

Table 6. 4.: Differentially expressed proteins between HO-1-deficient and control human EC in response to VEGF. 29 identified proteins were analysed and grouped according to gene ontology (GO) using DAVID Bioinformatics Resources 6.7. Groups of particular importance to this study are highlighted in bold.

Cellular Component GO Term	**Count**	**Gene Name**
intracellular organelle lumen	12	SCOT1 SET IF6 HNRPF HNPRK LMNB1 NUCL PHB PDIA3 SERPH TXNDC5 VDAC2
organelle lumen	12	SCOT1 SET IF6 HNRPF HNPRK LMNB1 NUCL PHB PDIA3 SERPH TXNDC5 VDAC2
membrane-enclosed lumen	12	SCOT1 SET IF6 HNRPF HNPRK LMNB1 NUCL PHB PDIA3 SERPH TXNDC5 VDAC2
nuclear lumen	7	SET IF6 HNRPF HNPRK LMNB1 NUCL PHB
spliceosome	3	HNRPC HNRPF HNPRK
ribonucleoprotein complex	4	HNRPC HNRPF HNPRK NUCL
nucleoplasm	5	SET HNRPF HNPRK NUCL PHB
nucleolus	4	IF6 HNRPF HNPRK NUCL

Table 6.4. continued		
organelle envelope	6	RAGP1 IF6 LMNB1 PHB TAGL2 VDAC2
envelope	6	RAGP1 IF6 LMNB1 PHB TAGL2 VDAC2
nuclear envelope	4	RAGP1 IF6 LMNB1 TAGL2
nuclear membrane	3	IF6 LMNB1 TAGL2
organelle inner membrane	3	IF6 LMNB1 PHB
organelle membrane	5	IF6 LMNB1 PHB TAGL2 VDAC2
endomembrane system	4	RAGP1 IF6 LMNB1 TAGL2
endoplasmic reticulum lumen	3	PDIA3 SERPH TXNDC5
endoplasmic reticulum	6	SET MESD PLOD2 PDIA3 SERPH TXNDC5
endoplasmic reticulum part	3	SET MESD PDIA3 SERPH TXNDC5
integral to membrane	3	RAGP1 PHB VDAC2
intrinsic to membrane	3	RAGP1 PHB VDAC2
intermediate filament	**3**	**Eukaryotic translation initiation factor (IF6)** **Lamin B1(LMNB1)** **Vimentin (VIME)**
intermediate filament cytoskeleton	**3**	**Eukaryotic translation initiation factor (IF6)** **Lamin B1(LMNB1)** **Vimentin (VIME)**
non-membrane-bound organelle	9	RAGP1 HNRPK HNRPF IF6 LMNB1 NUCL TPM1 VDAC2 VIME

Table 6.4. continued		
intracellular non-membrane bound organelle	9	RAGP1 HNRPK HNRPF IF6 LMNB1 NUCL TPM1 VDAC2 VIME
cytoskeletal part	**4**	**Eukaryotic translation initiation factor (IF6)** **Lamin B1 (LMNB1)** **Tropomyosin alpha-1 chain (TPM1)** **Vimentin (VIME)**
cytoskeleton	**4**	**Eukaryotic translation initiation factor (IF6)** **Lamin B1 (LMNB1)** **Tropomyosin alpha-1 chain (TPM1)** **Vimentin (VIME)**
mitochondrial part	3	SCOT1 PHB VDAC2
mitochondrion	4	SCOT1 PHB 1433E VDAC2
cytosol	9	G3BP1 SET EF1B EF1D EIF3F 1433E KPYM UFD1 VIME
plasma membrane	7	G3BP1 RAGP1 PLIN3 PHB TAGL2 TPM1 VIME
plasma membrane part	4	RAGP1 PLIN3 PHB TPM1
Molecular Function **GO Term**	**Count**	**Gene Name**
translation factor activity, nucleic acid binding		
RNA binding	5	G3BP1 HNRPC HNRPK HNRPF NUCL
nucleotide binding	5	G3BP1 HNRPC HNRPF NUCL VDAC2
DNA binding	3	G3BP1 HNRPK NUCL
structural molecule activity	**3**	**Lamin B1 (LMNB1)** **Tropomyosin alpha-1 chain (TPM1)** **Vimentin (VIME)**
metal ion binding	3	CSRP1 PLOD2 KPYM
cation binding	3	CSRP1 PLOD2 KPYM
ion binding	3	CSRP1 PLOD2 KPYM

Table 6.4. continued

Biological Process GO Term	Count	Gene Name
translation	4	EF1B EF1D EIF3F IF6
RNA splicing, via transesterification reactions	3	HNRPC HNRPF HNPRK
nuclear mRNA splicing, via spliceosome	3	HNRPC HNRPF HNPRK
RNA splicing	3	HNRPC HNRPF HNPRK
mRNA processing	3	HNRPC HNRPF HNPRK
mRNA metabolic process	3	HNRPC HNRPF HNPRK
RNA processing	3	HNRPC HNRPF HNPRK
intracellular transport	5	SET PDIA3 1433E TXDN5 TPM1
regulation of apoptosis	4	PHB PDIA3 1433E TXDN5
regulation of programmed cell death	4	PHB PDIA3 1433E TXDN5
regulation of cell death	4	PHB PDIA3 1433E TXDN5
cell motion	**3**	**14-3-3 protein epsilon (1433E)** **Tropomyosin alpha-1 chain (TPM1)** **Vimentin (VIME)**
negative regulation of macromolecule metabolic process	3	SET PHB 1433E

6.3. DISCUSSION

This study and data from previous studies clearly demonstrate a link between the cytoprotective enzyme HO-1 and the angiogenic capacity of EC with HO-1 affecting endothelial proliferation, migration and vessel assembly (Bussolati and Mason, 2006; Dulak *et al.*, 2008; Kim *et al.*, 2011). However, the signalling pathways involved in the regulation of HO-1-driven angiogenesis and those used by the HO products CO, biliverdin/bilirubin, and iron remain to be determined.

Herein, we show that siRNA-mediated inhibition negatively affects chemotactic migration of EC in response to the pro-angiogenic mediator VEGF resulting in a significant decrease in the number of cell migrating towards the chemotactic stimuli (Fig. 5.15, Fig. 5.16. and Fig. 5.18), whereas adenoviral overexpression of HO-1 reverses this response (Fig. 5.17.). To determine whether HO-1-derived iron and subsequent induction of ferritin subunit ferritin heavy chain (FHC) regulate HO-1-mediated migration, HUVEC depleted of HO-1 were exposed to the iron chelator deferoxamine mesylate (DFO) prior to the assessment of their migratory capacities. DFO chelates intracelluar iron, mimicking the activities of ferritin. Ferritin is a ubiquitously existing intracellular multimeric protein complex consisting of a heavy chain and a light chain subunit (Harrison and Arosio, 1996). Ferritin is able to effectively sequester intracellular iron and, hence, limits the pro-oxidant capacity of ferrous iron (Fe^{2+}) by catalysing the oxidation to the ferric form (Fe^{3+}) (Balla *et al.*, 1992; Berberat *et al.*, 2003). It is likely that increased ferritin expression in conjunction with HO-1 expression may contribute to additional protection afforded by HO-1 (Balla *et al.*, 1992; Ryter *et al.*, 2006). In addition, a potential pro-angiogenic function of ferritin has been demonstrated by Coffman and colleagues. High molecular weight kininogen (HKa) is a potent inhibitor of angiogenesis by inducing the apoptosis of proliferating EC. Supplementation with serum ferritin significantly inhibited the anti-angiogenic effects of HKa improving EC proliferation, migration and subsequent formation of capillary-like structures (Coffman *et al.*, 2009). Moreover, exposure of vascular SMC to DFO increased VEGF synthesis and may influence angiogenesis indirectly (Dulak *et al.*, 2002). However, treatment with DFO of HO-1-deficient HUVEC was not able to restore their impaired migratory phenotype in response to VEGF (Fig. 6.1.). These data suggest that the HO product iron and resulting increased ferritin at least not solely mediate the pro-migratory properties of HO-1, suggesting a possible role for HO-1-derived CO and/or biliverdin/bilirubin in this process.

HO-1-derived CO has been recognised as an important intracellular signalling molecule in the vascular system inducing numerous beneficial effects including cytoprotection, vasodilation and inhibition of inflammation and is likely to be attributable for the angiogenic properties of HO-1. Indeed, CO supplementation increased HO-1 expression but also augmented the synthesis of VEGF and SDF-1α and potentiated their synergistic effects on EC (Jozkowicz *et al.*, 2003; Lin *et al.*, 2009). In an animal model, CO exposure significantly enhanced VEGF synthesis in various organs (Marti and Risau, 1998). Moreover, genetic overexpression of HO-1 enhances VEGF synthesis in EC, and VEGF was also able to stimulate HO-1 expression. Such a positive feedback can be beneficial for angiogenesis (Dulak *et al.*, 2002; Bussolati *et al.*, 2004). HO-1 and CO are closely linked to the pro-angiogenic effects of SDF-1α. Treatment with CO enhanced re-endothelialisation after vascular injury by increasing circulating SDF-1α in a mouse model (Deshane *et al.*, 2007). Further, SDF-1α augmented capillary sprouting in EPC and aortic EC isolated from HO-$1^{+/+}$ mice. This effect was markedly inhibited in cells from HO-1 knockout mice, but restored by CO exposure (Deshane *et al.*, 2007).

Effective delivery of CO to cells is challenging. The use of gaseous CO is risky and strongly limited by the high affinity of CO towards haemoglobin and the resulting systemic effects on oxygen transport and low bioavailability. Moreover, gaseous CO is difficult to delivery directly to living cells in an accurate, safe and measurable fashion (Johnson *et al.*, 2003; Motterlini *et al.*, 2005). A promising strategy to circumvent these problems and to deliver controlled amounts of CO directly to a tissue is the use of the transition metal carbonyls CO-releasing molecules (CORMs). To date, numerous CORMs have been developed and are generally composed of a transition metal such as manganese, cobalt, ruthenium or iron, surrounded by a certain number of carbonyl (CO) groups as coordinated ligands, thereby storing CO in a stable chemical form. Dissociation of CO from the metal centre can be induced by UV activation, ligand substitution, pH, or metal oxidation, and is dependent on the relevant CORM (Motterlini *et al.*, 2005). The tricarbonlydichlororuthenium II dimer ($[Ru(CO)_3Cl_2]_2$), generally known as CORM-2, is a water soluble transition metal-carbonyl complex that liberates CO upon ligand exchange with DMSO, and has been shown to play a critical role in the resolution of inflammatory responses and alleviation of cardiovascular diseases (Motterlini *et al.*, 2002; Motterlini *et al.*, 2003). CORM-2 caused vasodilation of pre-contracted rat aortic rings and attenuated coronary vasoconstriction in

hearts *ex vivo*, significantly reduced acute hypertension and diminished ischaemia/reperfusion induced injury *in vivo*. Moreover, blood platelet aggregation was partially inhibited by CORM-2 and macrophages pre-treated with CORM-2 displayed a significant reduction in NO production in response to LPS compared to control cells (Motterlini *et al.*, 2002; Johnson *et al.*, 2003). Moreover, CORMs have been shown to have anti-inflammatory and anti-apoptotic effects on vascular EC. They inhibit EC death via suppression of IL-18-mediated NFκB activation, TNF-α-induced expression of VCAM-1 and E-selectin in HUVEC and high glucose-induced ICAM-1 expression on EC (Tranter and Jones, 2008; Sun *et al.*, 2007; Song *et al.*, 2009; Bergstraesser *et al.*, 2012; Nizamutdinova *et al.*, 2009). Based on these observations, CORM-2 was used as a CO donor to study the role of CO in HO-1-driven angiogenesis. However, pre-treatment and subsequent culture of HO-1-deficient HUVEC with CORM-2 did not restore their impaired migratory phenotype in response to VEGF when compared to control cells (Fig. 6.2.). This may indicate that HO-1-driven migration of EC is not CO-dependent, or that there was insufficient CO delivery to the cells in culture over the course of the assay (16 h). CO release from CORM-2 is very fast ($t_{1/2}$ ≈ 1min) and non-specific (Motterlini *et al.*, 2005), which may hamper the delivery of controlled amounts of CO to the target cells. Therefore, to further elucidate the role of CO in HO-1-driven angiogenesis and to improve CO delivery in our system, a novel class of powerful CORMs, so called enzyme-triggered CORMs (ET-CORMs), were adopted.

ET-CORMs are acylocyclohexadiene-iron tricarbonyl complexes which are stable under physiological conditions but are readily converted to the active form by means of enzymatic hydrolysis. Once taken up by the cell, ET-CORMs are activated by enzymatic cleavage of the ester functionality mediated by intracellular esterases resulting in the dissociative loss of CO. The esterase-triggered release of CO was confirmed by means of the carbonmonoxy myoglobin (MbCO) content (Romanski *et al.*, 2011; Romanski *et al.*, 2012). Herein, the cytotoxic effect of three different ET-CORMs, namely Sto074, Stro258 and SROM158, on primary human EC was determined. High doses (50-100 µM) significantly reduced cell viability with all three tested ET-CORMs. Of note, the cytotoxic effect of SROM158 at high concentration was less pronounced than Stro074 and Stro258, and had no effect on cell viability when used at concentrations ranging from 12.5 µM to 25 µM (Fig. 6.3. and Fig. 6.4.). Moreover, SROM158 significantly suppressed TNF-α-induced surface expression of VCAM-1 on HUVEC (Fig. 6.5.), confirming its activity and

reproducing previously published reports demonstrating the inhibitory effect of CORMs on expression of inflammatory adhesion molecules in response to TNF-α (Sun *et al.*, 2007; Song *et al.*, 2009; Bergstraesser *et al.*, 2012). Further, we can show that exposure to SROM158 significantly enhanced HO-1 protein in HUVEC both in the absence and presence of VEGF, but no synergistic effect was observed (Fig. 6.6.). CO exposure, either administered as a gas or in the form of a CORM, induced proliferation of rat aortic EC and enhanced their migratory capacity (Wegiel *et al.*, 2010). Moreover, CO has been shown to restore the impaired angiogenic responses of EC transduced with antisense HO-1 (Li Volti *et al.*, 2005). However in our study, supplementation with the CO donor SROM158 was not sufficient to restore the impaired angiogenesis observed in HO-1-deficient cultures, in terms of VEGF-mediated endothelial proliferation and migration. In control cells, VEGF alone and in combination with SROM158 significantly increased EC proliferation, however this effect was diminished by siRNA-mediated silencing of HO-1 and not rescued by SROM158 (Fig. 6.7.). Likewise, HO-1-deficient cells demonstrated reduced migration in response to VEGF, depicted as the Euclidean distance, and this defect in directional migration was not restored by SROM158 (Fig. 6.8.). These findings reproduce the observations obtained from CORM-2 studies, showing that even the more powerful CORM is not sufficient to reverse the impaired angiogenic phenotype of HO-1-deficient EC.

Collectively, these data suggest that HO-1 induced angiogenesis and EC migration are dependent on HO-1 but are not mediated, at least solely, by the HO products CO or iron. The effect of biliverdin/bilirubin on HO-1-driven angiogenesis was not investigated during the course of this study, due to technical and time limitations. Of note, a role for the HO products in HO-1 driven angiogenesis cannot be completely excluded based on the data from this study, as the products may act in concert and may be dependent on each other. Indeed, a cooperative effect of CO and biliverdin has been demonstrated in a mouse model of inflammatory liver damage. While single administration of a CO donor or biliverdin had some beneficial effects on protection against liver damage in response to LPS, only co-administration of both HO products significantly prolonged survival of the animals and reduced expression of pro-inflammatory cytokines, including TNF-α and IFN-γ (Sass *et al.*, 2004).

So far, only one potential downstream effector in HO-1 driven angiogenesis has been described. Deshane and colleagues demonstrated that SDF-1α-mediated phosphorylation of vasodilator-stimulated phosphoprotein (VASP) is HO-1-dependent. Treatment of MAEC with the chemokine SDF-1α resulted in VASP phosphorylation at Ser239 in HO-$1^{+/+}$ cells but not in EC from HO-$1^{-/-}$ mice. Importantly, treatment with CORM-2 was able to phosphorylate VASP in both HO-$1^{+/+}$ and HO-$1^{-/-}$ cells (Deshane et al., 2007). VASP, a member of the highly conserved Ena/VASP family of actin regulatory proteins, is a cytoskeletal-associated protein localised at cell-cell contacts and microfilaments (Krause *et al.*, 2003). VASP has been implicated in actin-based processes such as fibroblast and neuronal migration and axon guidance (Bear *et al*., 2000; Goh *et al.*, 2002; Lanier *et al.*, 1999; Krause *et al.*, 2003). In the endothelium, phospho-VASP is localised to cell junctions and can be co-immunoprecipated with the tight-junction marker zonula-occludens (ZO)-1 in EC (Comerford *et al.*, 2002). Further, VASP has been shown to regulate stress-fibre and membrane ruffle formation in EC, thereby influencing endothelial migration and organisation during capillary formation (Price and Brindle, 2000). Moreover, the link between VASP and HO-1-driven angiogenesis is further strengthened by the finding that CORM-2 supplementation resulted in a considerable redistribution of VASP to the filopodia of equine EPCs (Deshane *et al.*, 2007). Filopodia are highly dynamic structures generated within minutes after stimulation at the moving front of EC (Huber *et al.*, 2003). They probe the environment for the presence of attractive guidance cues and initiate migration towards these (Defilippi *et al.*, 1999). Redistribution of VASP to filopodia in response to CO suggests a role for VASP in HO-1-driven migration and led us to investigate the effect of VEGF on VASP phosphorylation in primary human EC and HO-1-deficient cells. In concordance with previous studies, we show VASP phosphorylation at Ser239 in response to the mitogen VEGF (Fig. 6.9.) (Fiedler *et al.*, 2009; Chen *et al.*, 2008). However, siRNA-mediated inhibition of HO-1 had no effect on VEGF-induced VASP phosphorylation in HUVEC (Fig. 6.10.). Further, VASP phosphorylation in response to VEGF was not altered in MAEC from HO-$1^{-/-}$ mice when compared to HO-$1^{+/+}$ littermate control cells (Fig. 6.11), suggesting that VEGF-mediated VASP phosphorylation is not dependent on HO-1.

As no link between VEGF-mediated VASP phosphorylation and HO-1-driven angiogenesis could be observed, further studies to identify novel downstream effectors of HO-1 regulating this pathway are required. We performed a target PCR array and compared the gene expression

profiles of HO-1-depleted HUVEC with control cells in response to VEGF. To obtain optimal results from the PCR array, isolated total RNA was quality controlled for concentration and purity and ribosomal RNA band integrity. The samples showed RNA integrity numbers (RIN) above 7, with a RIN of 8.1 for control cells and a RIN of 10.0 for HO-1-depleted cells (Fig. 6.12.). RIN values are an algorithm for assessing integrity values to RNA measurements. RIN values range from 1 to 10, with 1 describing totally degraded RNA and 10 intact RNA (Schroeder *et al.*, 2006). Quantitative RT-PCR revealed a sufficient reduction (~70%) in HO-1 mRNA expression in siHO-1 pool transfected cells compared to control cells (Fig. 6.13.). Thus, collectively, the prepared samples met the standards required to achieve the best results with the PCR array.

We chose an array which profiles genes involved in the regulation of the cytoskeleton such as those controlling the biogenesis, organisation and rearrangement, as well as polymerisation and depolymerisation of the cytoskeleton. Cytoskeletal rearrangement is required for endothelial migration, an early step in angiogenesis. Genes that were significantly upregulated (fold change ≥ 2.0) included actin-related protein 2/3 complex, subunit 2 (ARPC2), citron (CIT), fascin homolog 2 (FSCN2), and protein phosphatase 1, regulatory (inhibitor) subunit 12A (PPP1R12A) (Tab. 6.2.). FSCN2 and ARPC2 have been shown to be involved in actin filament assembly, with the latter also affecting migratory capacity of epithelial cells (Tubb *et al.*, 2000; Welch *et al.*, 1997; Machesky *et al.*, 1997). PPP1R12A has been demonstrated to regulate the formation of cell protrusions, including lamellipodia, at the moving front of cells, and CIT regulates cell cycle progression during cell mitosis (Kimura *et al.*, 1996; Bavaria *et al.*, 2011; Liu *et al.*, 2003). Among the identified hits, the positive cell cycle regulator cyclin A1 (CCNA1) was the only gene to be significantly downregulated by HO-1 inhibition (fold change ≤ 0.5) (Tab. 6.2.). Moreover the PCR array result was confirmed by qRT-PCR, demonstrating a significant reduction in basal as well as VEGF-induced CCNA1 mRNA expression in HO-1-depleted cells compared to the control (Fig. 6.14.). Cyclin A1 belongs to the highly conserved cyclin family, whose members are characterised by a dramatic periodicity in protein abundance through the cell cycle. Cyclin A1 functions as a cell cycle regulator though binding to and activation of cyclin-dependent kinases (Cdks) and was shown to interact with numerous important cell cycle regulators, including Cdk2, retinoblastoma protein (Rb) family members, the transcription factor E2F-1, and the negative cell cycle regulators p21 and p27 (Obaya and Sedivy, 2002; Satyanarayana and Kaldis; 2009). HO-1 has been linked

to cell cycle progression. Indeed, HO-1 and CO induced cell cycle progression in EC, but not in vascular SMC (Li Volti *et al.*, 2002; Liu *et al.*, 2002). Further, HO-1 inhibition resulted in cell cycle arrest in EC, an effect associated with increased expression of the cell cycle inhibitors p21 and p27 (Li Volti *et al.*, 2005). Moreover, Abraham and colleagues performed a microarray study of the genome of human dermal microvascular EC (HMEC-1) transduced with the human HO-1 gene. Major findings were upregulation of growth factors VEGF, endothelial growth factor (EGF), and hepatic-derived growth factor (HDGF). Importantly, several genes associated with cell cycle progression, including cyclin A1 (4-fold increase), cyclin E and D, were significantly upregulated in HO-1 overexpressing cells, whereas the expression of the Cdk inhibitors p21 and p27 was markedly reduced (Abraham *et al.*, 2003). In addition, the observation that cell cycle regulators such as Cdk2, cyclin E and cyclin A are highly expressed in proliferating cells as well as the notion that cyclin A1 protein is upregulated after scraping injury to bovine aortic EC monolayers, which induces transient EC proliferation and migration (Chen *et al.*, 2000), make cyclin A1 a promising candidate as a potential downstream target of HO-1, and may regulate HO-1-dependent angiogenesis. A more detailed investigation of a role for cyclin A1 in HO-1-mediated proliferation and migration will be discussed in Chapter 7.

As a second approach to identify HO-1 downstream effectors in the regulation of angiogenesis, a proteomic screen was performed in collaboration with Prof M. Mayr (King's College London). We compared the proteome of HO-1-deficient HUVEC with control cells in the presence of VEGF. In addition, a comparison of differentially expressed proteins between HO-1 overexpressing cells and control cells was performed. Difference in-gel electrophoresis (DIGE) coupled to mass spectroscopy revealed 90 differential expressed proteins (Tab. 6.3.), of which 29 were differentially expressed between HUVEC transfected with a non-targeting control siRNA (siCTL) and HO-1-deficient HUVEC treated with VEGF for 16 h (Tab. 6.4.). Gene ontology analysis further revealed the intermediate filament vimentin as an interesting hit with regard to the impaired angiogenic capacities of HO-1-deficient EC observed in this study. Vimentin belongs to the protein family of intermediate filaments (IFs) and detailed studies of vimentin knockout mice revealed a role for vimentin in wound healing, cell migration, vasodilation and homing of leukocytes to lymph nodes (Eckes *et al.*, 2000; Eckes *et al.*, 1998; Henrion *et al.*, 1997; Nieminen *et al.*, 2006). Further, vimentin$^{-/-}$ animals are characterised by a lack of integrity in vascular endothelium

(Nieminen *et al.*, 2006). Interestingly, HO-1-deficient mice also demonstrate impaired neovascularisation during wound healing and HO-1-deficient EPC show defective homing and re-endothelisation of the retinal vasculature compared with wild-type cells following ischaemia (Deshane *et al.*, 2007; Grochot-Prezecezek *et al.*, 2009). Vimentin has been also shown to participate in a number of important cellular functions such as cell adhesion and migration, as well as cell signalling, and more recently angiogenic sprouting (Ivaska *et al.*, 2007; Kwak *et al.*, 2012). In Chapter 5, I have demonstrated an impaired angiogenic phenotype of EC depleted of HO-1 in terms of their proliferative and migratory capacities as well as *in vitro* assembly into capillary-like structures on 2D Matrigel. The emerging role of vimentin in angiogenesis combined with the defective angiogenic responses of HO-1-deficient EC make vimentin a promising candidate as a downstream effector of HO-1. This hypothesis is further strengthend by the similiarites between vimentin$^{-/-}$ and HO-1$^{-/-}$ animals. Alltoghter, due to its role in cell migration and angiogenesis, as well as the similar characteristics between vimentin and HO-1 deficiency, vimentin is of particular interest to our study and Chapter 8 will focus on the role of vimentin in HO-1-driven angiogenesis.

CHAPTER 7 - ROLE FOR HO-1 AND CYCLIN A1 IN CELL CYCLE REGULATION AND VEGF-MEDIATED ANGIOGENESIS

7.1. INTRODUCTION

The mammalian cell cycle is a precisely regulated process driven by the coordinated regulation of activities of the cyclin-dependent kinases (Cdks), a family of serine/threonine kinases, and expression of their binding partners, the cyclins (Morgan, 1997; Satyanarayana and Kaldis, 2009) (please see section 1.2.1). The observation that cyclin A1, a positive cell cycle regulator, was significantly reduced in proliferating HO-1-deficient EC led us to investigate the potential function of HO-1 in cell cycle progression.

Recent reports postulated a role for the cytoprotective enzyme HO-1 in cell cycle regulation. Indeed, EC transfected with the human HO-1 gene demonstrate a significant increase in the percentage of cells in G_1-phase when compared to control cells (Kushida *et al.*, 2002a). Moreover, retroviral overexpression of HO-1 protects human microvessel cells from pyrrolidine dithiocarbamate (PDTC)-induced abnormalities in DNA distribution and cell cycle progression, whereas inhibition of HO-1 activity results in increased PDTC-mediated abnormalities in cell cycle progression (Kushida *et al.*, 2002b). Colombrita and colleagues further demonstrated that HO-1 expression is cell cycle dependent. Human endothelial cells in G_0/G_1-phase show a several fold higher increase in HO-1 mRNA in response to angiotensin (Ang) II when compared to cycling, exponentially grown cells, which might be a protective mechanism against oxidative stress to assure normal cell proliferation and decreased DNA damage (Colombrita *et al.*, 2003). Moreover, decreased HO-1 activity is associated with endothelial cell cycle arrest, an effect restored by CO but not bilirubin (Li Volti *et al.*, 2005). The abnormalities in cell cycle progression in HO-1-deficient cells are accompanied by increased expression of the cell cycle inhibitors p21 and p27 (Li Volti *et al.*, 2005). Of note, the effect of HO-1 on cell cycle progression appears to be cell type specific. While HO-1 deficiency arrests EC in cell cycle progression, the opposite effect is observed in SMC (Li Volti *et al.*, 2002). Furthermore, CO negatively regulates the expression of the cell cycle-specific transcription factor E2F-1 in vascular SMC, thereby suppressing the expression of genes required for cell cycle progression (Morita *et al.*, 1997). In an elegant microarray study by Abraham and colleagues several cell cycle regulating genes were shown to be differentially

expressed between HO-1 overexpressing and control EC. The positive cell cycle regulators cyclin D, cyclin E and cyclin A were found to be significantly upregulated in human EC overexpressing HO-1, whereas expression of p21 and p27 was downregulated (Abraham *et al.*, 2003). In addition, cell cycle regulation is also closely related to cell migration. Indeed, Chen and colleagues demonstrated increased Cdk2 activity in proliferating and migrating bovine aortic EC (BAEC), an effect accompanied by increased cyclin A but decreased p27 expression (Chen *et al.*, 2000).

The aim of this chapter was to further elucidate the role of HO-1 in the regulation of endothelial cell cycle progression and to investigate the role for cyclin A1 as a potential downstream target of HO-1 in the regulation of angiogenesis.

7.2. RESULTS

7.2.1. HO-1 inhibition arrests EC in cell cycle progression

The propidium iodide (PI) staining flow cytometric assay, which has been widely used to analyse cell cycle parameters of mammalian cells, was here adopted to assess changes in cell cycle progression of HO-1-deficient cells in response to VEGF.

HUVEC, either transfected with a non-targeting control siRNA (siCTL) or siRNA targeting the human HO-1 gene (siHO-1 seq2 and siHO-1 pool) were left untreated or treated with VEGF for 48 h prior to PI staining and subsequent flow cytometric analysis. In response to VEGF, siCTL-transfected cells progressed from G_0/G_1-phase to the S-phase of the cell cycle as indicated by an increase in DNA content (12.75 ± 0.54% for untreated siCTL vs 15.75 ± 0.81% VEGF-treated siCTL). This response was significantly diminished by siRNA-mediated HO-1 inhibition, both in the absence and presence of VEGF, resulting in 7.95 ± 0.43% and 11.27 ± 0.62% DNA distribution (Fig. 7.1.).

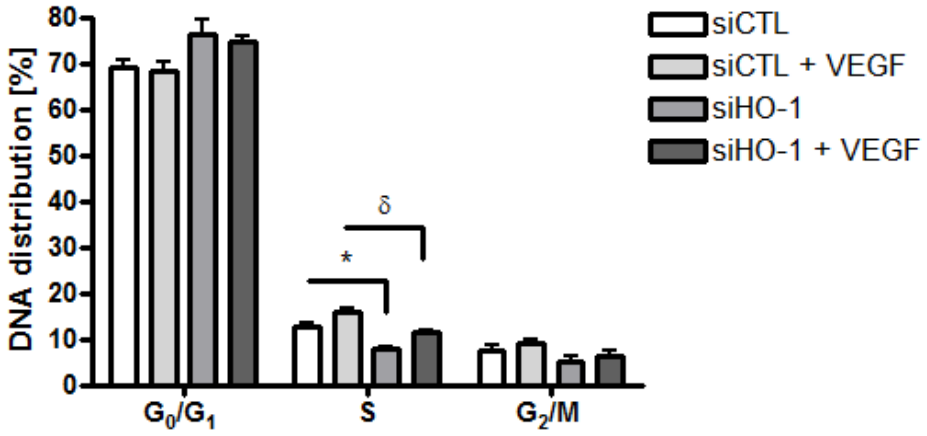

	DNA Distribution [%]		
Treatment	**G_0/G_1**	**S**	**G_2/M**
siCTL	68.98 ± 1.69	12.75 ± 0.54	7.40 ± 1.16
siCTL + VEGF	65.40 ± 1.96	15.75 ± 0.81	9.2 ± 0.71
siHO-1	76.24 ± 3.18	7.95 ± 0.43*	5.09 ± 1.11
siHO-1 + VEGF	74.76 ± 1.30	11.27 ± 0.62$^{\delta}$	6.42 ± 0.96

Figure 7. 1.: HO-1-deficient EC are arrested in cell cycle progression from G1- to S-phase. siCTL-transfected or siHO-1-transfected HUVEC were left untreated or treated with 25 ng/ml VEGF for 48 h prior to propidium iodide staining and FACs analysis. Data represents pooled data from siHO-1 seq2 and siHO-1 pool and is presented as mean ± SEM (n=3 experiments), * $p<0.05$ vs siCTL, δ $p<0.05$ vs siCTL + VEGF.

Due to cellular stress and other stimuli, cells can permanently lose their ability to proliferate, a process termed cellular senescence (Debacq-Chainiaux *et al.*, 2009). To investigate whether the arrest in cell cycle progression of HO-1-depleted cells resulted from premature senescence, siCTL-transfected and siHO-1-transfected HUVEC in the absence and presence of VEGF were stained for senescence-associated beta-galactosidase (SA-β-gal) activity, which permits the identification of senescent cells in culture (Debacq-Chainiaux *et al.*, 2009).

Prolonged culture of HUVEC, for 12 passages, resulted in a marked increase in the number of SA-β-gal positive cells in the absence and presence of VEGF when compared to control cells (cultured for 4 passages) and was used as a positive control for senescence (Fig. 7.2.). VEGF exposure resulted in a minor but non-significant increase in SA-β-gal activity in both siCTL-transfected cells and HO-1-deficient EC. Moreover, siRNA-mediated silencing of HO-1 had no effect on senescence, either in the absence or presence of VEGF when compared to matched control cells (Fig. 7.2.), suggesting that the observed cell cycle arrest of HO-1-depleted cells does not result from premature senescence of those cultures.

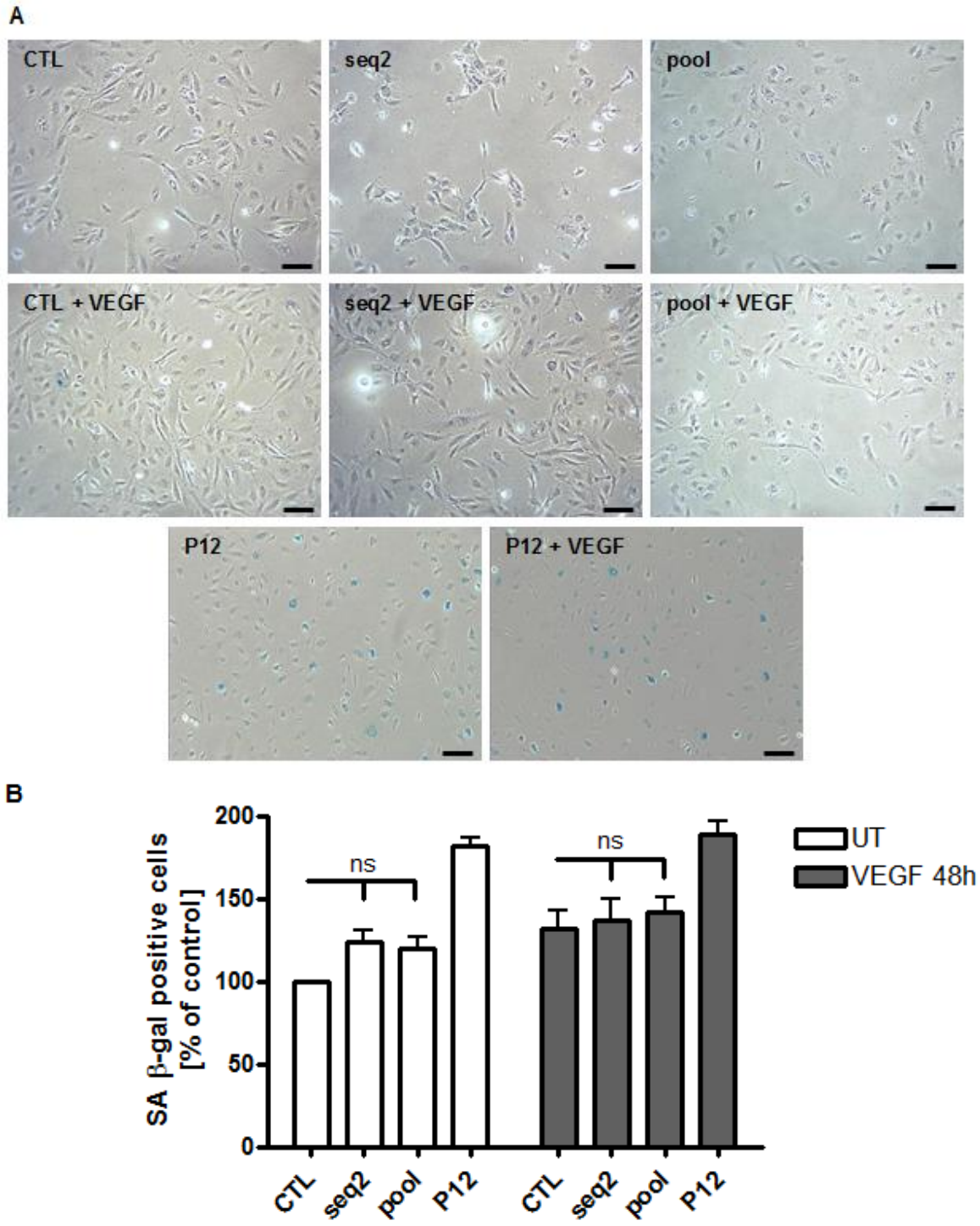

Figure 7. 2.: HO-1 inhibition does not result in premature senescence in HUVEC. HUVEC either transfected with 40 nM control siRNA (siCTL) or HO-1 specific siRNA (siHO-1 seq2 or siHO-1 pool) were left untreated or treated with 25 ng/ml VEGF for 48 h. Senescent cells were identified by SA-β-gal staining and phase-contrast microscopy. HUVEC cultured for 12 passages were used as a positive control for senescence. (A) Pictures are representative images from n=3 experiments, 10X magnification. Bars equal 50 µM. (B) Quantification of SA-β-gal positive cells. Data is presented as mean ± SEM (n=3 experiments), ns – not significant.

7.2.2. HO-1 inhibition alters the expression profile of cell cycle regulators in proliferating EC

As basal and VEGF-induced cyclin A1 mRNA expression was significantly decreased in HO-1-deficient cells, as determined by the target PCR and subsequent validation of the results (Tab. 6.2. and Fig. 6.14.), and HO-1 depletion arrested EC in cell cycle progression (Fig. 7.1.), we investigated the effect of HO-1 inhibition on the expression levels of other cell cycle regulators in proliferating EC.

Initially, knockdown efficiency of HO-1 specific siRNA in proliferating HUVEC was validated and revealed a sufficient reduction in HO-1 mRNA of 75%, both in the absence and presence of VEGF when compared to control siRNA-transfected cells (Fig. 7.3.).

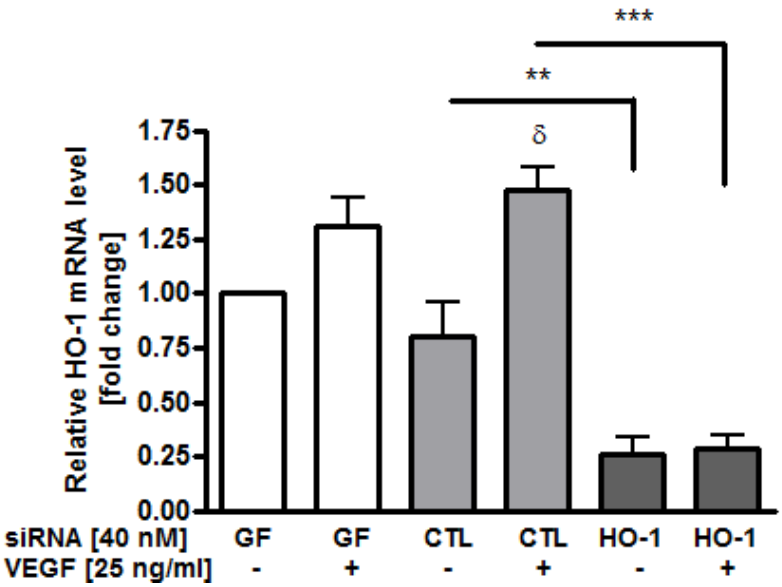

Figure 7. 3.: Knockdown efficiency of HO-1 specific siRNA in proliferating EC. HUVEC were either treated with geneFECTOR (GF) alone or transfected with 40 nM control siRNA (CTL) or HO-1 specific siRNA (HO-1; data represents pooled data from seq2 and pool) for 16 h. Cells were then left untreated or treated with 25 ng/ml VEGF for 24 h prior to mRNA quantification by qRT-PCR. Data is presented as mean ± SEM (n=3 experiments), ** p<0.01, *** p<0.001. δ p<0.05 vs untreated siCTL-transfected cells.

VEGF exposure significantly increased cyclin mRNA expression of all four tested cyclins, i.e. cyclin D1, cyclin E1, cyclin A1, and cyclin B1, in siCTL-transfected cells (Fig. 7.4.). Moreover, VEGF treatment markedly upregulated the expression of cyclin B1 and cyclin D1 in HO-1-deficient cells (Fig. 7.4.A and D). However, basal as well as VEGF-induced mRNA expression of cyclin E1 and A1 was significantly reduced by HO-1 inhibition in proliferating HUVEC compared to siCTL-transfected cells (Fig. 7.4.B and C).

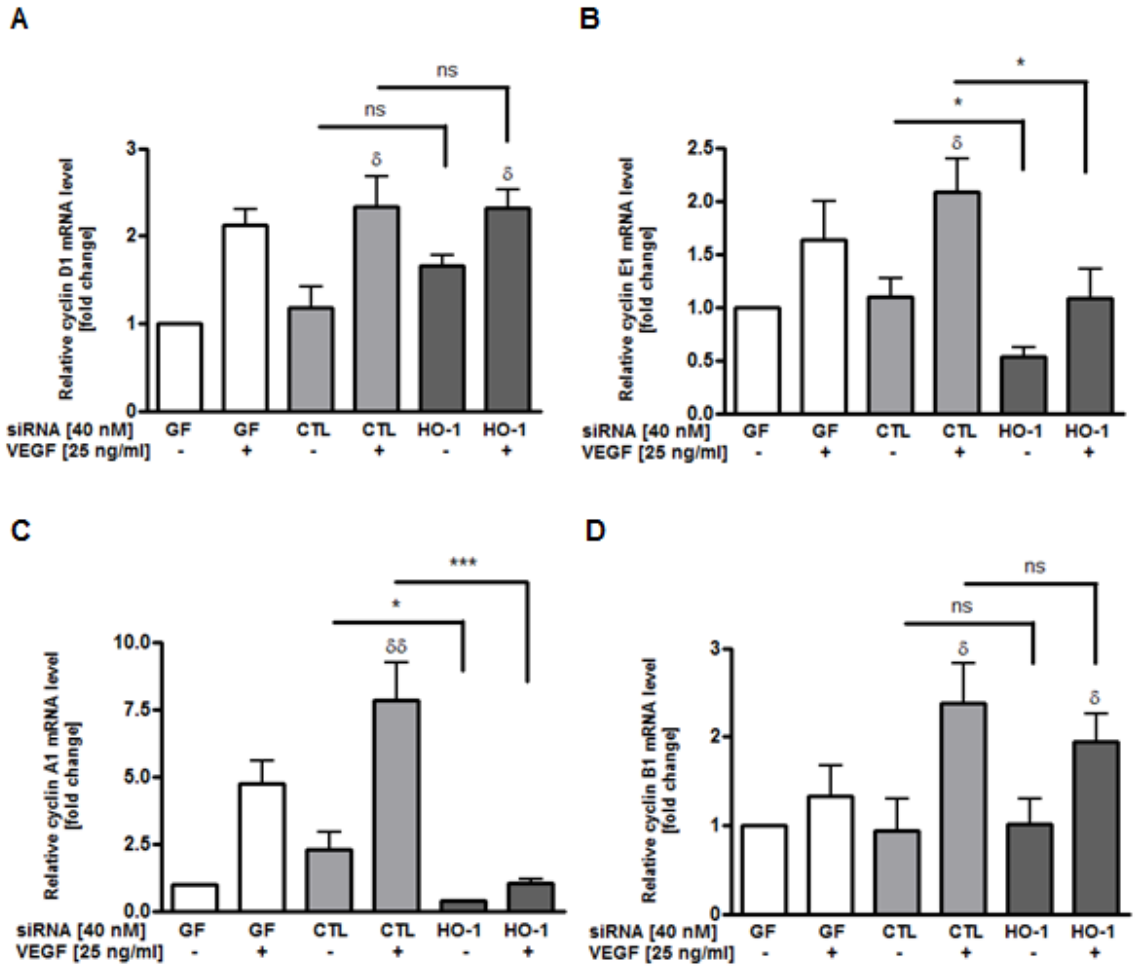

Figure 7. 4.: Effect of HO-1 inhibition on cyclin mRNA expression in proliferating EC. HUVEC were either treated with geneFECTOR (GF) alone or transfected with 40 nM control siRNA (CTL) or HO-1 specific siRNA (HO-1; data represents pooled data from seq2 and pool) for 16 h. Cells were then left untreated or treated with 25 ng/ml VEGF for 24 h prior to mRNA quantification by qRT-PCR. (A) cyclin D1, (B) cyclin E1, (C) cyclin A1, (D) cyclin B1. Data is presented as mean ± SEM (n=3-5 experiments), * $p<0.05$, *** $p<0.001$. δ $p<0.05$, δδ $p<0.01$ vs untreated siCTL-transfected cells. ns – not significant.

Cyclin E1 regulates the transition of cells from G_0/G_1-phase into the S-phase of the cell cycle, while cyclin A1 promotes progression through the S-phase and into G_2-phase. Both cyclins form complexes with and regulate the activity of Cdk2, while cyclin D1 and B1 regulate Cdk4/6 and Cdk1 activity respectively (Obaya and Sedivy, 2002; Satyanarayana and Kaldis, 2009). Quantitative RT-PCR demonstrated a 2-fold increase in Cdk2 mRNA in response to VEGF in control cells, while the results for Cdk1 were more variable between cords, and no significant

difference could be observed (Fig. 7.5.). In addition, basal as well as VEGF-induced Cdk1 mRNA was not altered by HO-1 siRNA (Fig. 7.5.A). However, HO-1 inhibition abrogated the VEGF-induced increase in Cdk2 mRNA, but had no effect on basal Cdk2 (Fig. 7.5.B).

The CKIs p21 and p27 of the CIP/KIP family inhibit activity of Cdk2 when in complex with either cyclin E1 or cyclin A1, but also regulate the activity of other Cdks (Sherr and Roberts, 1995; Obaya and Sedivy, 2002). VEGF exposure had no effect on p21 and p27 mRNA expression in control cells, and HO-1 inhibition did not affect p21 expression either in untreated or VEGF-treated HUVEC (Fig. 7.6.A). In contrast, expression of p27 was slightly but significantly upregulated by HO-1 inhibition in the absence and the presence of VEGF (Fig. 7.6.B).

In summary, HO-1 depletion alters the mRNA expression profile of cell cycle regulators resulting in a reduced expression of the positive regulators cyclin E1 and cyclin A1, and their binding partner Cdk2, but increasing mRNA levels of p27, an inhibitor of cyclin E1/Cdk2 and cyclin A1/Cdk2 complexes.

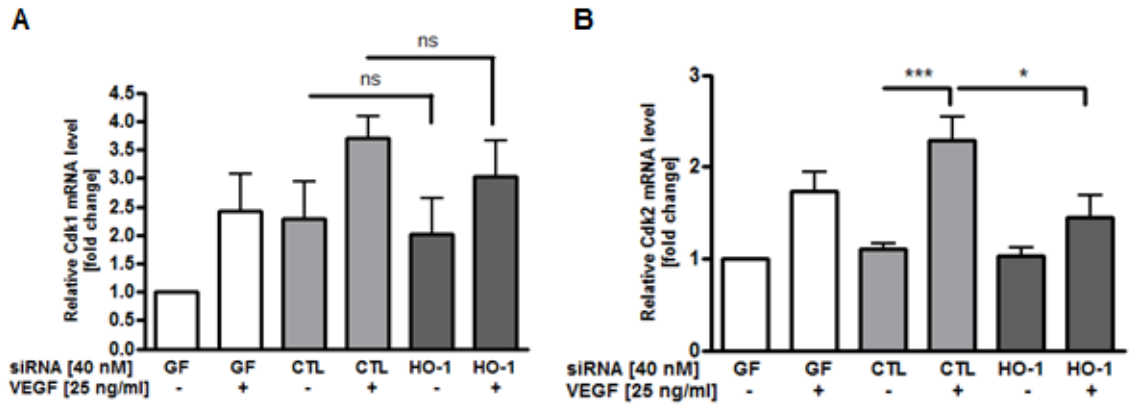

Figure 7. 5.: Effect of HO-1 inhibition on Cdk mRNA expression in proliferating EC. HUVEC were either treated with geneFECTOR (GF) alone or transfected with 40 nM control siRNA (CTL) or HO-1 specific siRNA (HO-1; data represents pooled data from seq2 and pool) for 16 h. Cells were then left untreated or treated with 25 ng/ml VEGF for 24 h prior to mRNA quantification by qRT-PCR. (A) Cdk1, (B) Cdk2. Data is presented as mean ± SEM (n=3-5 experiments), * p<0.05, *** p<0.001. ns – not significant.

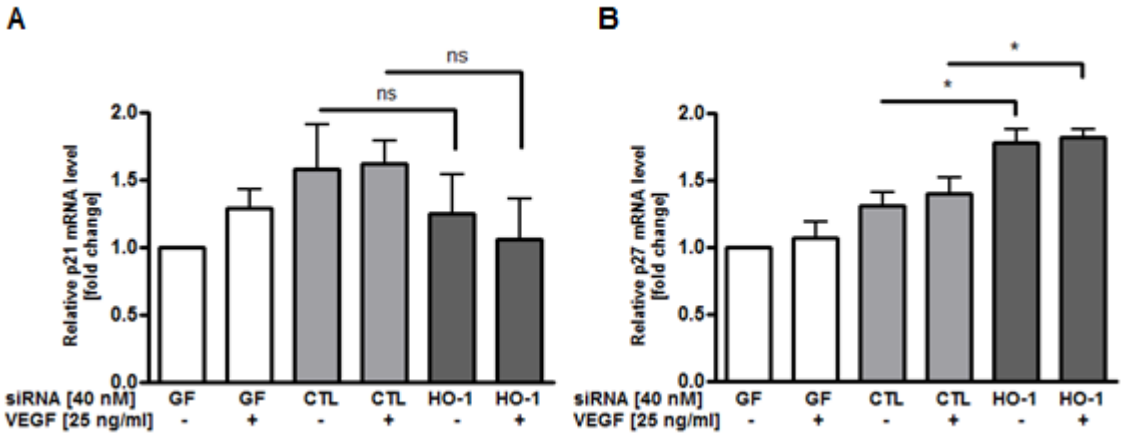

Figure 7. 6.: Effect of HO-1 inhibition on p21 and p27 mRNA expression in proliferating EC. HUVEC were either treated with geneFECTOR (GF) alone or transfected with 40 nM control siRNA (CTL) or HO-1 specific siRNA (HO-1; data represents pooled data from seq2 and pool) for 16 h. Cells were then left untreated or treated with 25 ng/ml VEGF for 24 h prior to mRNA quantification by qRT-PCR. (A) p21, (B) p27. Data is presented as mean ± SEM (n=5 experiments), * p<0.05. ns - not significant.

7.2.3. Migrating HO-1$^{-/-}$ EC show decreased cyclin A1 and reduced Cdk2 activity

Chen and colleagues demonstrated increased Cdk2 activity in proliferating and migrating bovine aortic EC in response to scratch-induced injury. Moreover, this effect coincided with a maximal increase in cyclin A and a maximal decrease in p27 protein, after 4 to 8 h after scratching (Chen *et al.*, 2000). Based on these findings, and my observation that proliferating HO-1-deficient EC show an altered cell cycle regulator expression profile, we investigated the effect of HO-1 inhibition on Cdk2 activity and cyclin A expression in migrating EC.

HO-1 inhibition significantly inhibited the VEGF-induced increase in Euclidean distance of migrating EC when compared to control cells (Fig. 7.7.A and Fig. 5.15.). Western blotting revealed a sufficient knockdown of HO-1 protein by siRNA both in the absence and presence of VEGF. Interestingly, cyclin A expression was also significantly reduced in HO-1-depleted migrating HUVEC (Fig. 7.7.B).

Cdk2 activity was assessed by phosphorylation of retinoblastoma protein (pRb) at threonine 821 (Thr821). pRb is a negative regulator of the cell cycle and its active non-phosphorylated form binds the transcription factor E2F-1 thereby rendering it inactive and inhibiting the transcription of genes necessary for cell cycle progression. Phosphorylation of pRb by active cyclin/Cdk complexes results in its inactivation, the release of E2F-1, transcription of cell cycle regulatory genes, such as cyclin E and cyclin A, and in turn cell cycle progression (Weinberg, 1995; Dyson, 1998). Phosphorylation of pRb at Thr821 is mediated by active cyclin E/Cdk2 and cyclin A/Cdk2 complexes and is thereby a measure of Cdk2 activity (Zarkowska and Mittnacht, 1997). Protein analysis of lysates from migrating HUVEC showed an increase in phospho-pRb in response to 16 h VEGF treatment in siCTL-transfected cells, indicating active Cdk2. However, this effect was significantly attenuated by siRNA-mediated silencing of HO-1, demonstrating reduced Cdk2 activity in migrating HO-1-deficient EC (Fig. 7.8.). Collectively, these findings demonstrate a link between cell cycle regulation and HO-1-driven endothelial migration.

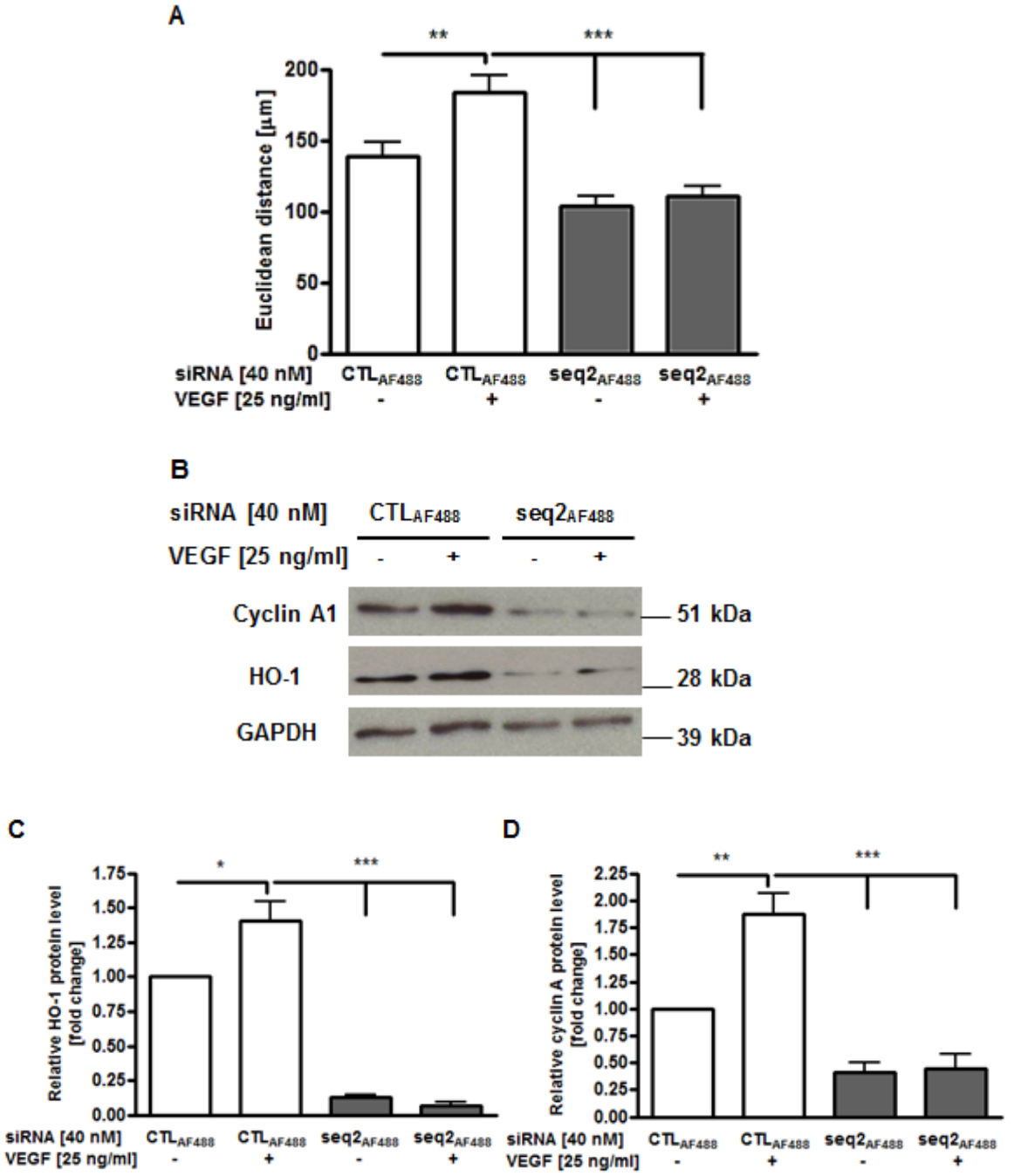

Figure 7. 7.: Migrating HO-1-deficient EC show reduced cyclin A1 protein. HUVEC were either transfected with 40 nM 3'-AlexaFluor488-labelled control siRNA (CTL_{AF488}) or HO-1 specific siRNA ($seq2_{AF488}$) for 24 h. Confluent cell monolayers were scratched and migration was assessed by live cell imaging in the absence or presence of VEGF (25 ng/ml) for 16 h and quantified using ImageJ analysis software (Manual Tracking and Chemotaxis and Migration tool). (A) Represents the Euclidean distance. Data is presented as mean ± SD (n=3 experiments), ** p<0.01, p<0.001. (B, C, D) HO-1 and cyclin A1 protein levels were quantified by western blotting and quantified by densitometry. GAPDH was used as a loading control. (B) Representative blots from n=3 experiments are shown, (C, D) shows the corresponding densitometry for (C) HO-1 and (D) cyclin A1. Data is presented as mean ± SEM (n=3 experiments), * p<0.05, ** p<0.01; *** p<0.001.

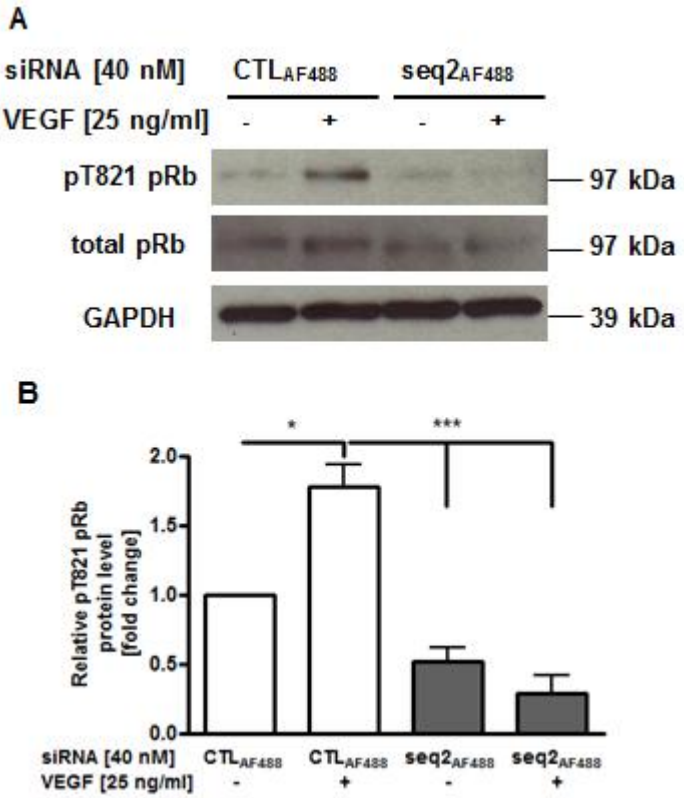

Figure 7. 8.: Cdk2 activity is significantly reduced in migrating HO-1-deficient HUVEC. HUVEC were either transfected with 40 nM 3'-AlexaFluor488-labelled control siRNA (CTL_{AF488}) or HO-1 specific siRNA ($seq2_{AF488}$) for 24 h. Confluent cell monolayers were scratched and migration was assessed by live cell imaging in the absence or presence of VEGF (25 ng/ml) for 16 h. Cdk2 was assessed by phosphorylation of retinoblastoma protein (pRb) and is expressed as phospho-pRb (pT821) relative to total pRb. GAPDH was used as a loading control. (A) Representative blots from n=3 experiments are shown, (B) shows the corresponding densitometry. Data is presented as mean ± SEM (n=3 experiments), * p<0.05, *** p<0.001.

7.2.4. HO-1 and cyclin A1 regulate VEGF-driven angiogenesis *in vivo*

The *in vivo* Matrigel plug assay was used to further elucidate the role of HO-1 in angiogenesis and to investigate the function of the positive cell cycle regulator cyclin A1, a potential downstream target of HO-1, in HO-1-driven angiogenesis.

In gene-silencing studies, non-targeting control siRNA (siCTL) or murine specific siRNA targeting the mouse HO-1 (murine siHO-1 pool) or mouse cyclin A1 (murine siCycA1 pool) gene were co-injected with Matrigel supplemented with VEGF and heparin near the abdominal midline of female C57BL/6 mice. Knockdown efficiency of murine specific siRNA was validated in murine aortic EC isolated from HO-$1^{+/+}$ animals by western blotting and/or qRT-PCR prior to the use of siRNA in Matrigel plugs *in vivo*. HO-1 protein and mRNA expression was markedly reduced by siHO-1 pool when compared to siCTL-transfected cells, whereas siCycA1 pool had no effect on HO-1 expression. Moreover, neither of the siRNAs altered the expression of HO-2 (Fig. 7.9.A and B). siCycA1 pool decreased cyclin A1 mRNA by 75% in MAEC, but had no effect on the expression of cyclin A2 isoform. Interestingly, siHO-1 pool also notably reduced cyclin A1 but not cyclin A2 mRNA when compared to control cells (Fig. 7.9.C and D), suggesting a potential function for HO-1 in the regulation of cyclin A1 mRNA expression.

After 7 days, Matrigel plugs were carefully harvested from CO_2-euthanised mice, fixed in 4% paraformaldehyde, paraffin embedded, and processed for staining. H&E staining showed that VEGF-supplementation of Matrigel plugs containing siCTL resulted in a significant increase in their vascularisation in the Matrigel plugs when compared to plugs without VEGF (Fig. 7.10.A and B). This was also demonstrated by a significant increase in the percentage area occupied by neovessels per field of view (Fig. 7.11.). Although reduced, there was still a significant effect on VEGF-induced neovessel formation in plugs containing siHO-1 pool (Fig. 7.11.). Of note, this response was quite variable between plugs from different animals with some plugs being highly vascularised and others showing a marked inhibition in VEGF-mediated vessel formation (Fig. 7.10.C and D). Interestingly, siRNA-mediated inhibition of cyclin A1 significantly attenuated vessel formation in response to VEGF (Fig. 7.10.E and F), indicative for a role of cyclin A1 in angiogenesis *in vivo*.

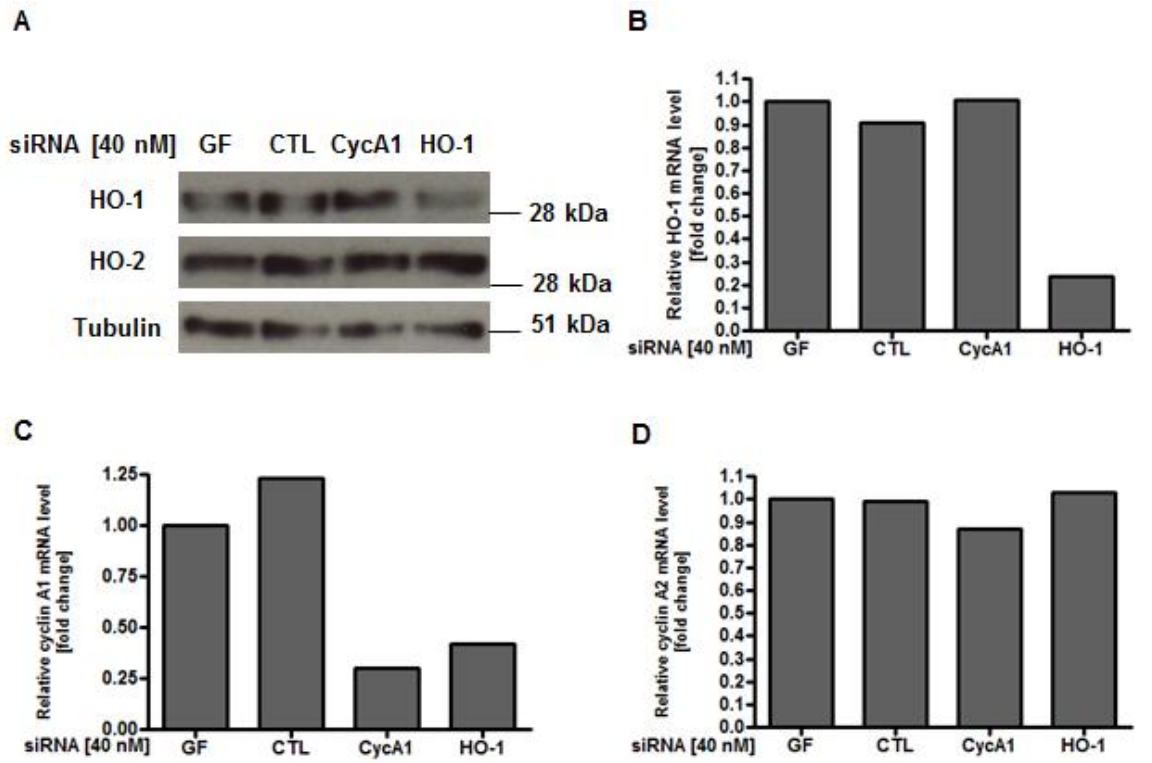

Figure 7. 9.: Validation of murine siRNA in mouse aortic EC. Mouse aortic EC isolated from HO-$1^{+/+}$ littermate control mice were either treated with geneFECTOR (GF) alone or transfected with 40 nM control siRNA (CTL), murine cyclin A1 specific siRNA (CycA1), or murine HO-1 specific siRNA (HO-1) and cultured for 48 h. (A) Protein expression was assessed by western blotting, (B, C, D) mRNA expression was assessed by qRT-PCR. (B) HO-1, (C) cyclin A1, (D) cyclin A2 (n=1 experiment).

To further elucidate the role of cyclin A1 in angiogenesis and to investigate whether inhibition of VEGF-induced vascularisation of Matrigel plugs containing siRNA targeting the cyclin A1 gene is reversed by HO-1, we adopted an adenoviral overexpression approach in combination with the Matrigel plug assay. H&E staining showed that overexpression of HO-1 significantly increased (> 2-fold) vascularisation of Matrigel plugs when compared to plugs supplemented with an empty control adenovirus (Ad0), an effect also seen in siCTL-containing plugs (Fig. 7.12.A, B, C and E). Importantly, a similar response was observed in HO-1 overexpressing plugs in which cyclin A1 expression was inhibited by siRNA, resulting in a 2-fold increase in vascularisation (Fig. 7.12. D and E). Taken together, these results suggest that HO-1 and cyclin A1 regulate VEGF-induced angiogenesis *in vivo*, where cyclin A1 deficiency results in reduced VEGF-mediated vessel formation, an effect restored by HO-1.

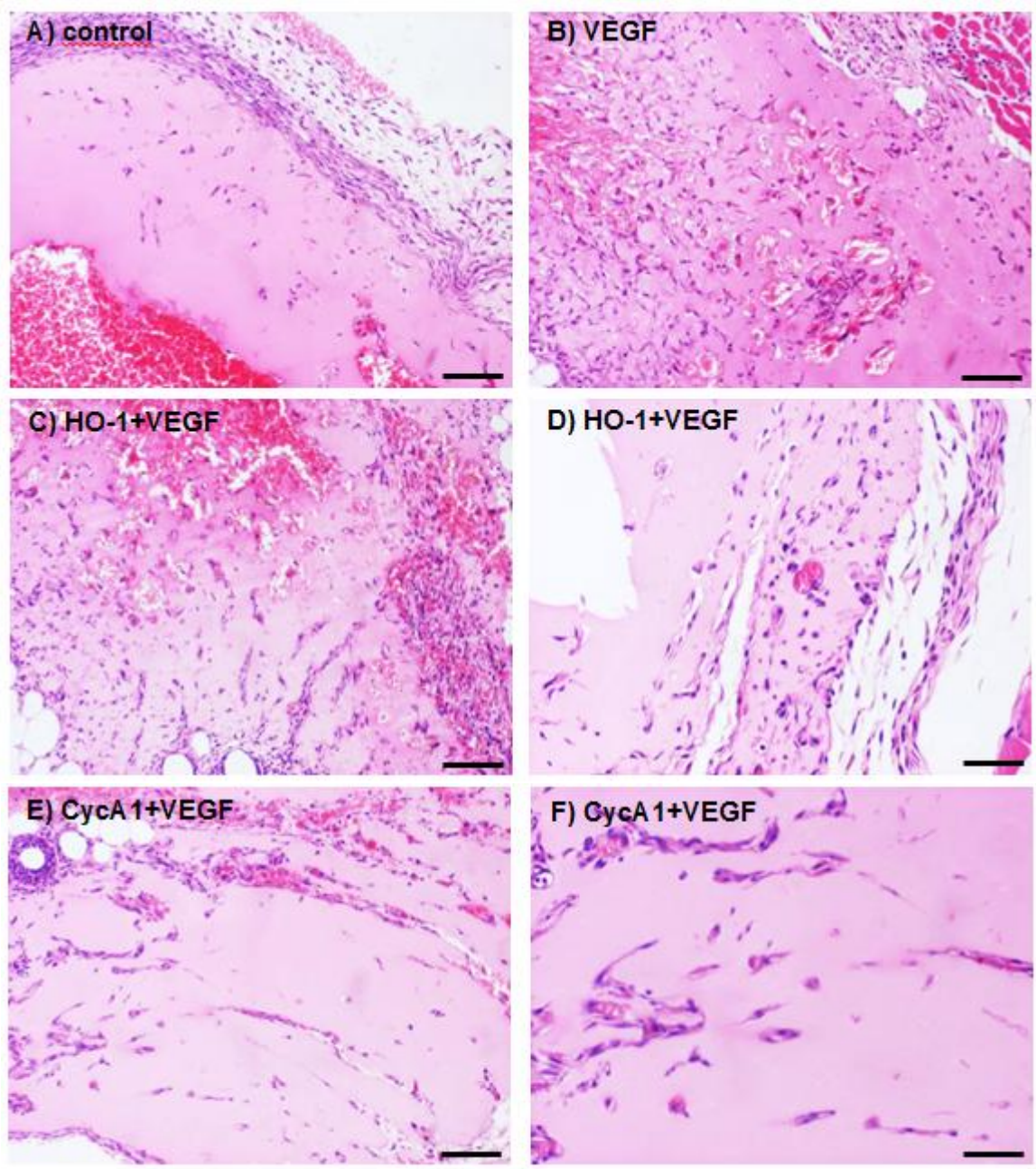

Figure 7. 10.: Silencing of HO-1 and cyclin A1 impairs angiogenesis *in vivo*. Female C57BL/6 mice (10 weeks old) were injected with Matrigel preparations containing (A) a vehicle control, (B) 40 ng/ml VEGF in combination with 2 µM control siRNA (CTL), (C, D) VEGF in combination with murine siRNA against the HO-1 gene (HO-1), (E, F) VEGF in combination with murine siRNA against the CycA1 gene (CycA1). (A, B, C, E) 10X magnification, (D, F) 20X magnification, bars equal 50 µm. Representative images are shown (n=3 mice per treatment).

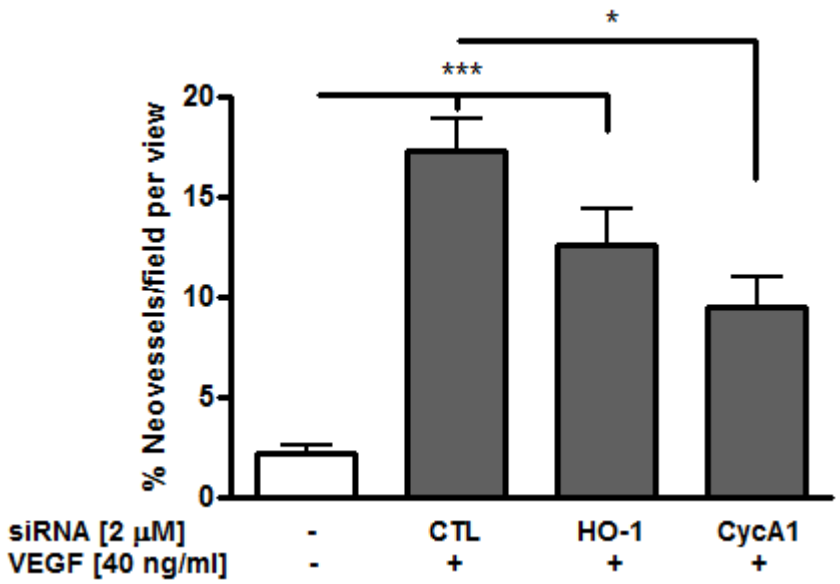

Figure 7. 11.: Quantification of vascularised areas relative to the total area. Female C57BL/6 mice (10 weeks old) were injected with Matrigel preparations containing a vehicle control, 40 ng/ml VEGF in combination with 2 µM control siRNA (CTL), VEGF in combination with murine siRNA against the HO-1 gene (HO-1), or VEGF in combination with murine siRNA against the CycA1 gene (CycA1). Vessels were counted in 5 fields of views. Data is presented as mean ± SEM (n=3 mice per treatment), * $p<0.05$, *** $p<0.001$.

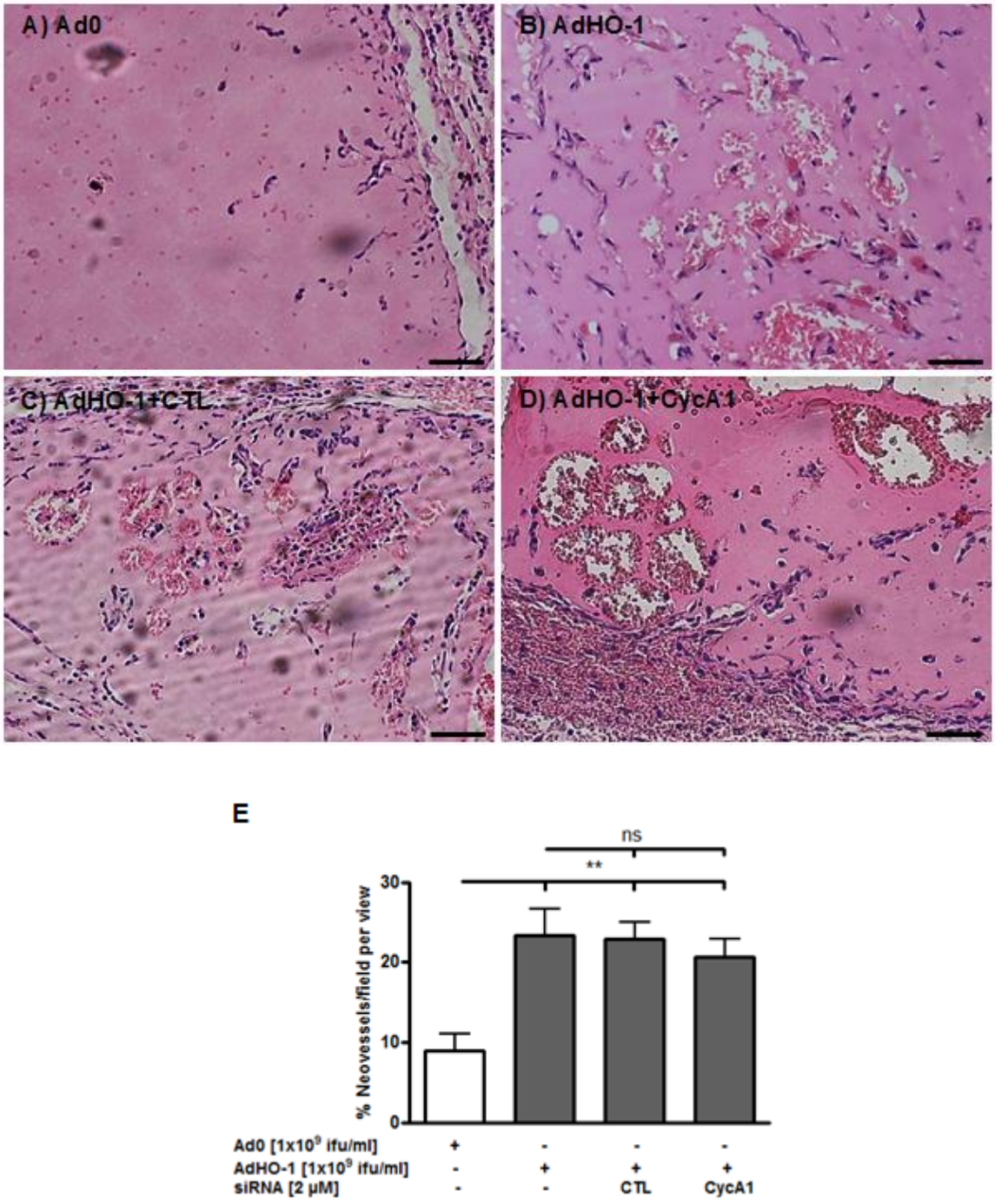

Figure 7. 12.: Overexpression of heme oxygenase-1 rescues cyclin A1-impaired angiogenesis *in vivo*. Female C57BL/6 mice (10 weeks old) were injected with Matrigel preparations containing (A) an empty control adenovirus (Ad0), (B) the recombinant adenovirus expressing the HO-1 gene (AdHO-1), (C) AdHO-1 in combination with 2 µM control siRNA (CTL), (D) AdHO-1 in combination with murine siRNA against the CycA1 gene (CycA1). (E) Quantification of vascularised areas relative to the total area. Vessels were counted in 5 fields of views. Representative images are shown, 20X magnification, bars equal 50 µm. Data is presented as mean ± SEM (n=3 mice per treatment), ** p<0.01. ns – not significant.

7.2.5. HO-1 and cyclin A1 mRNA stability

Based on the observation that siRNA-mediated inhibition of HO-1 results in decreased expression of cyclin A1 mRNA in proliferating and migrating human primary EC (Tab. 6.2., Fig. 6.14., Fig. 7.4.C. and Fig. 7.7.B) and also in mouse aortic EC (Fig. 7.9.C), we investigated a potential role for HO-1 in the transcriptional regulation of cyclin A1.

We performed an actinomycin D time course experiment to determine whether HO-1 inhibition affects cyclin A1 mRNA stability in migrating EC. HUVEC monolayers treated with either the siRNA-delivery agent geneFECTOR (GF) alone or transfected with a non-targeting control siRNA (siCTL) or siRNA targeting the human HO-1 gene (siHO-1 pool), were scratched and then left untreated or treated with VEGF for 16 h prior to subsequent treatment with actinomycin D. Quantitative RT-PCR showed no difference in mRNA stability between GF-treated and siCTL-transfected EC in response to VEGF when compared to untreated control cells (Fig. 7.13.). However, a significant decrease in total mRNA of cyclin A1 in HO-1-depleted cells treated with VEGF was observed after 2 h and 4 h exposure to actinomycin D when compared to siCTL-transfected cells (Fig. 7.13.A). This effect was reflected in a 30% decrease in mRNA half-life as determined by curve fitting depicting the one-phase exponential decay (Fig. 7.13.B). These preliminary results suggest that the observed downregulation of cyclin A1 mRNA in HO-1-deficient cells may result from a decrease in mRNA stability and might be indicative for a potential function of HO-1 in the transcriptional regulation of gene expression.

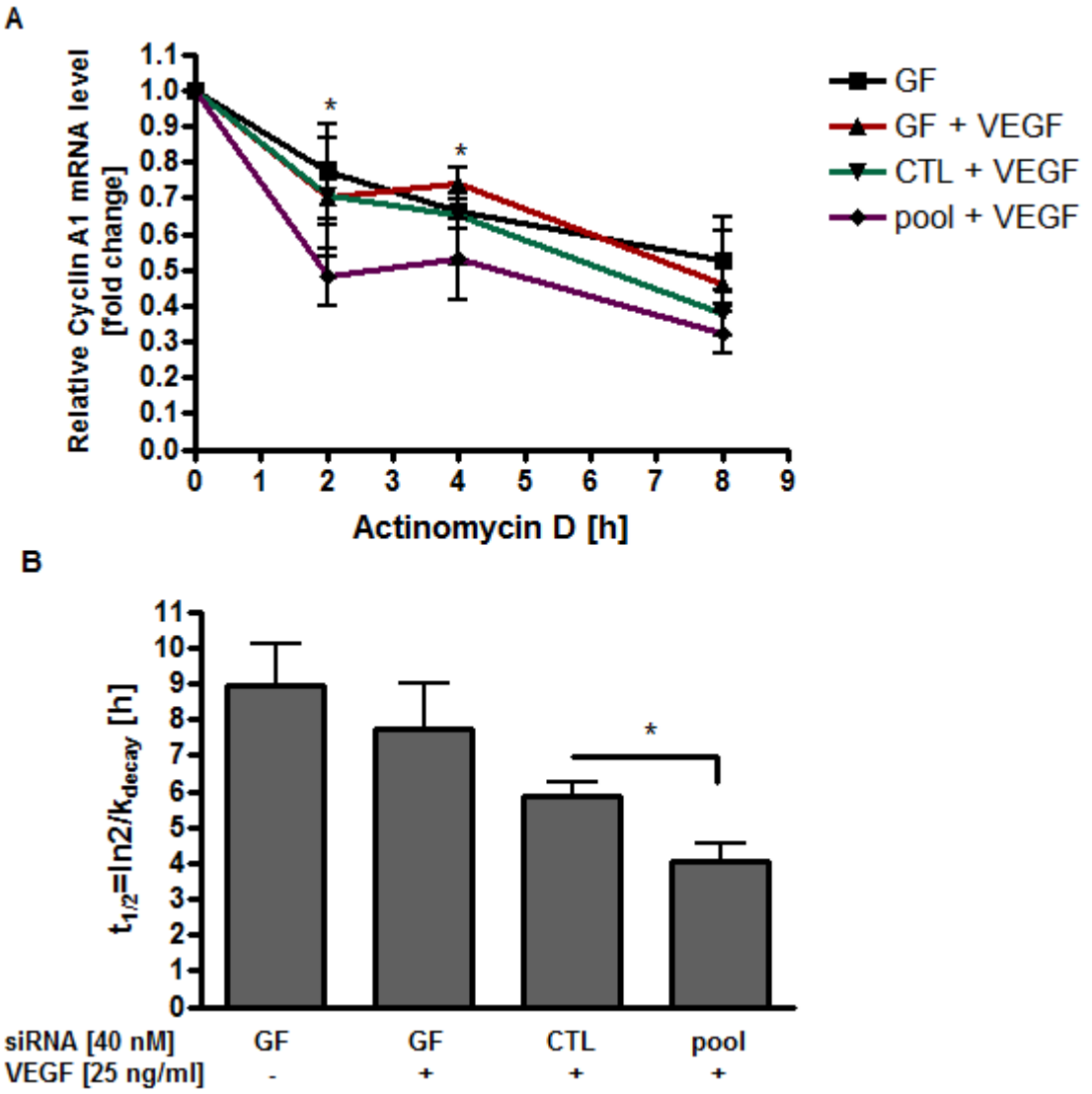

Figure 7. 13.: HO-1 inhibition decreases cyclin A1 mRNA stability. Confluent HUVEC monolayers either treated with geneFECTOR (GF) alone or transfected with 40 nM control siRNA (CTL) or HO-1 specific siRNA (pool) were scratched and left untreated or treated with VEGF for 16 h. (A) mRNA stability was assessed by 5 µg/ml actinomycin D treatment for the indicated time points and cyclin A1 mRNA levels were quantified by qRT-PCR. (B) Corresponding one-phase exponential decay curves showing cyclin mRNA half-lives were fitted using the TableCurve 2D analysis software (Systat Software GmbH, Erkrath, Germany). Data is presented as mean ± SEM (n=4 experiments), * $p<0.05$.

7.3. DISCUSSION

The mammalian cell cycle is a complex, highly regulated process driven by distinct, cell cycle phase-specific cyclin-dependent kinases (Cdks) and the sequential expression of their regulatory units, the cyclins (Morgan, 1997; Satyanarayana and Kaldis, 2009). Activity of Cdks is further controlled by phosphorylation and binding to inhibitory proteins, cyclin-dependent kinase inhibitor (CKIs) (Sherr and Robert, 1999). Herein, we show a relationship between the cytoprotective enzyme HO-1 and the cell cycle regulator cyclin A1.

We performed a targeted PCR array comparing the differential expression of genes regulating cytoskeletal functions between human primary EC and HO-1-deficient EC in response to the mitogen VEGF and demonstrated a significant downregulation in cyclin A1 mRNA following HO-1 depletion (Tab. 6.2.). We further showed that HO-1 deficiency results in decreased basal as well as VEGF-induced expression of cyclin A1 in proliferating HUVEC (Fig. 6.14.). Based on these findings we hypothesized a regulatory role for HO-1 in the mammalian cell cycle. Indeed, cell cycle analysis by propidium iodide staining revealed that HO-1 deficiency inhibits in EC cell cycle progression. The EC demonstrated significant abnormalities in their DNA distribution. HO-1 depletion resulted in an increased number of cells in the G_0/G_1-phase, with a subsequent significant decrease of cells in S-phase, an effect observed for both untreated and VEGF-treated HO-1-depleted EC (Fig. 7.1.). These results suggest that HO-1 deficiency inhibits endothelial cell cycle progression from G_1- to S-phase and moreover are in agreement with earlier studies by Li Volti and colleagues demonstrating impaired cell cycle progression of human microvascular cells in response to the HO inhibitor SnPP or transduced with anti-sense HO-1 (Li Volti *et al.*, 2002; Li Volti *et al.*, 2005).

To elucidate the mechanisms underlying the impaired cell cycle progression resulting from HO-1-deficiency, cells were stained for senescence-associated beta-galactosidase (SA-β-gal) activity, permitting the identification of senescent cells in culture (Debacq-Chainiaux *et al.*, 2009). Prolonged culture of cells eventually results in their inability to proliferate, a process known as cellular senescence (Debacq-Chainiaux *et al.*, 2009). Senescence is a stress and damage response phenomenon that locks up mitotically competent diploid cells in a permanent growth arrest. Senescence is associated with progressive shortening of telomeres, the physical ends of

chromosomes, comprising their functional integrity eventually leading to the induction of a DNA damage checkpoint response that halts the cell cycle permanently (Greider, 1998; Shay and Wright, 2000; d'Adda di Fagagna *et al.*, 2003). Senescent cells differ in their morphology from normal diploid EC, their volume increases and they lose their original shape, acquiring a flattened and enlarged appearance (Ben-Porath and Weinberg, 2004). At the molecular level, senescent cells undergo distinct changes in gene expression that may cause impairment of cellular function, resulting in a pro-inflammatory and pro-thrombotic phenotype in EC (Erusalimsky, 2008). The main signalling pathways involved are the p53/p21 and p16/retinoblastoma protein tumour suppressor pathway (Campisi and d'Adda di Fagagna, 2007). Herein, we show that HO-1 deficiency does not result in an increase in SA-β-gal positive cells as seen with EC cultured over a prolonged period (Fig. 7.2.), suggesting that the observed cell cycle arrest and proliferative defects of HO-1-deficient EC do not result from premature senescence. A small but non-significant increase in SA-β-gal activity was observed in all tested cultures in response to VEGF (Fig. 7.2.). Of note, presence of VEGF resulted in more confluent cell monolayers and this may induce senescence in cells in culture (Debacq-Chainiaux *et al.*, 2009).

To further investigate the underlying mechanisms regulating cell cycle arrest in response to HO-1 inhibition in EC, we compared the expression profile of numerous cell cycle regulators of HO-1-depleted cells with control cells. VEGF supplementation increased mRNA levels of all tested cyclins, i.e. cyclin D1, cyclin E1, cyclin A1 and cyclin B1, in proliferating control cells (Fig. 7.4.). Interestingly, while expression of cyclin D1 and cyclinB1 was not affected by siRNA-mediated silencing of HO-1, basal as well as VEGF-induced mRNA levels of cyclin E1 and cyclin A1 were significantly downregulated (Fig. 7.4.). Moreover, VEGF-induced Cdk2 was significantly diminished in HO-1-depleted EC, whereas expression of the cell cycle inhibitor p27 was upregulated both in untreated and VEGF-treated HO-1-deficient EC when compared to control cells (Fig. 7.5.B and Fig. 7.6.B). Expression of Cdk1 and p21 was not affected by HO-1 inhibition (Fig. 7.5.A and Fig. 7.6.A). This finding further strengthened the results obtained from the SA-β-gal studies demonstrating that HO-1 inhibition does not induce premature senescence in EC. Expression of the cell cycle inhibitor p21 is also linked to senescence. p21 is induced directly by p53 in response to DNA damage, and is also upregulated during replicative senescence (El-Deiry

et al., 1994; Dulic *et al.*, 1994; Noda *et al.*, 1994; Stein *et al.*, 1999; Campisi and d'Agga di Fagagna, 2007).

Transcription of both cyclin E1 and cyclin A1 is controlled by the cell cycle transcription factor E2F-1, which is released from retinoblastoma protein (pRb) upon phosphorylation by active cyclin D/Cdk4/6 complexes (Sherr and Roberts, 1999). The E-type cyclins, cyclin E1 and cyclin E2, are expressed in mid to late G_1-phase and bind to and activate Cdk2. CyclinE/Cdk2 activity is required for S-phase entry and the initiation of DNA replication and further phosphorylates pRb (Dulic *et al.*, 1992; Koff *et al.*, 1992; Zarkowska and Mittnacht, 1997; Lundberg and Weinberg, 1998). This hyperphosphorylation of pRb is required for its complete inactivation and in turn leads to further E2F-1-mediated transcription (Lundberg and Weinberg, 1998; Stayanarayana and Kaldis, 2009). Cyclin A1 together with cyclin A2 belongs to the A-type cyclins and they are expressed from late G_1- until M-phase of the cell cycle (Lundberg and Weinberg, 1998; Sherr and Roberts, 1999). Cyclin A binds to and activates Cdk2 and, to a lesser extent Cdk1. The activity of cyclin A/Cdk2 is required for S-phase transition and control of DNA replication (Elledge *et al.*, 1992; Cardoso *et al.*, 1993), and cyclin A/Cdk1 activity is required for the initiation of prophase during mitosis (Furuno *et al.*, 1999).

Cyclin E/Cdk2 and cyclin A/Cdk2 activities are inhibited by p27. p27 belongs to CIP/KIP family of cyclin-dependent kinase inhibitors (CKIs) and negatively regulates progression through the cell cycle. p27 levels are generally low in cells transitioning through G_1, due to reduced gene transcription as well as increased protein turnover (Mateyak *et al.*, 1999; Hengst and Reed, 1996). However, forced expression of p27 results in a G_1 cell cycle arrest of cells through its association with cyclin D/Cdk4/6, cyclin E/Cdk2 or cyclin A/Cdk2 complexes (Polyak *et al.*, 1994; Toyoshima and Hunter, 1994), suggesting the halt in cell cycle progression observed in HO-1-deficient cells results from a decrease in Cdk2 activity due to reduced expression of the positive regulators cyclin E1 and cyclin A1 and increased levels of p27. The increase in p27 may also reflect a decrease in Cdk2 activity, as p27 expression is regulated by Cdk2. In late G_1 and early S-phase, active cyclin E/Cdk2 and cyclin A/Cdk2 complexes phosphorylate p27 at threonine 187 (Thr187), which targets p27 for degradation via ubiquitination (Nakayama and Nakayama, 2006).

CIP/KIP members were almost solely viewed as nuclear proteins with a principal function as cell cycle inhibitors. However, emerging evidence indicates a role for cytoplasmic p27 in the regulation of actin dynamics and cell migration. Delivery of p27 into hepatocellular carcinoma cell, induced cell migration, whereas p27-deficient fibroblasts were impaired in cell motility, an effect rescued by reconstitution of p27. Moreover, p27-mediated cell migration was dependent on phosphorylation of cytoplasmic p27 at Ser10 (Nagahara *et al.*, 1998; McAllister *et al.*, 2003). In a subsequent study, Besson and colleagues demonstrated that p27-deficient fibroblasts displayed an increased amount of stress fibres and focal adhesions, which failed to rearrange into membrane ruffles and lamellipodia in response to exposure to PDGF thereby impairing cell motility (Besson *et al.*, 2004). Importantly, these properties of cytoplasmic p27 were independent on cyclin/Cdk inhibition (Denicourt and Dowdy, 2004). In contrast, another study demonstrated a role for p27 in endothelial cell proliferation and migration dependent on cyclin/Cdk activity (Chen *et al.*, 2000). They showed that proliferating cells express higher levels of cyclin E and cyclin A but reduced p27 associated with increased Cdk2 activity when compared to quiescent control cells. Moreover, migrating EC revealed increased Cdk2 activity which was accompanied by a maximal increase in cyclin A and a maximal decrease in p27 protein 4 h to 8 h after generation of a scratch on a confluent cell monolayer (Chen *et al.*, 2000). Herein, we show that migrating HUVEC deficient in HO-1 also show reduced cyclin A1 protein and decreased Cdk2 activity when compared to control cells (Fig. 7.7. and Fig. 7.8.), suggesting that the impaired migratory phenotype of HO-1-depleted cells results, at least partially, from reduced Cdk2 activity. The low level of cyclin A1 is likely to contribute to the reduced Cdk2 activity. In addition high levels of p27 may be responsible for the low Cdk2 activity in HO-1-deficient cells, and it would be of interest to look further at expression levels of p27 and other cell cycle regulators in migrating HO-1-deficient EC.

Altogether, the results obtained during this study link the cytoprotective enzyme HO-1 to cell cycle regulation and angiogenesis. We therefore hypothesise that HO-1 plays an important role in the regulation of VEGF-mediated angiogenesis and that loss of HO-1 arrests EC early in the cell cycle, due to less availability of positive cell cycle regulators cyclin A1 and cyclin E1 and/or increased levels of the negative regulator p27, resulting in decreased Cdk2 activity. This not only

negatively regulates cell proliferation but also migration of EC towards angiogenic stimuli, resulting in impaired vessel formation.

The role of HO-1 and cyclin A1 in vessel formation was further investigated in an *in vivo* Matrigel plug angiogenesis assay. Here, supplementation of Matrigel plugs with VEGF injected into female C57BL/6 mice significantly induced vessel formation when compared to untreated plus (Fig. 7.10. and Fig 7.11.). siRNA-mediated inhibition of HO-1 partially inhibited VEGF-induced neovascularisation (Fig. 7.10. and Fig. 7.11.). Of note, vessel formation in plugs containing murine specific HO-1 siRNA varied between animals, with some animals showing a marked response in vessel formation while others showed almost no vessel growth (Fig. 7.10.B and C). Previous studies from our laboratory postulated a dual role for HO-1 in VEGF-driven angiogenesis, based on earlier findings that pharmacological inhibition of HO-1 by SnPP increased VEGF-driven angiogenesis *in vivo*, with dense leukocytic inflammatory infiltrates seen around vessels (Bussolati and Mason, 2006). Here, under physiological conditions, HO-1 activation by VEGF favours EC proliferation and prevents EC apoptosis, while inhibiting leukocyte migration, thus resulting in predominantly non-inflammatory angiogenesis. In contrast, when HO-1 activation by VEGF is inhibited, increased leukocyte migration occurs with subsequent local release of growth factors and induction of inflammatory angiogenesis. This hypothesis is confirmed by the observation that supplementation of Matrigel plugs with the HO-1 inducer CoPP inhibits LPS-driven leukocyte-dependent angiogenesis *in vivo* (Bussolati and Mason, 2006). This dual effect of HO-1 on angiogenesis might account for the differences in vessel formation in HO-1$^{-/-}$ plugs observed in this study. Interestingly, siRNA-mediated silencing of cyclin A1 in Matrigel plugs supplemented with VEGF resulted in a significant decrease in the vascularised area (Fig. 7.10.E and F and Fig. 7.11.), indicating a role for the cell cycle regulator cyclin A1 in VEGF-mediated angiogenesis *in vivo*.

To investigate the relationship between HO-1 and cyclin A1 during angiogenesis we adopted an adenoviral approach to overexpress HO-1 in cyclin A1 siRNA-treated Matrigel plugs. Addition of an adenovirus overexpressing HO-1 (AdHO-1) to Matrigel significantly enhanced vessel formation when compared to plugs containing an empty control adenovirus (Ad0) (Fig. 7.12.) A similar response was observed in plugs supplemented with AdHO-1 in combination with a non-targeting

control siRNA (Fig. 7.12.C and E). Importantly, AdHO-1 also significantly increased vessel growth in cyclin A1 depleted plugs (Fig. 7.12.D and E), so restoring the impaired angiogenic response seen with cyclin A1 deficiency. Based on this observation we propose that HO-1 regulates expression of cyclin A1 which in turn is an essential contributor to the pro-angiogenic capacities of HO-1 during VEGF-driven angiogenesis. Of note, knockdown efficiency of siRNA sequences targeting murine HO-1 or cyclin A1 was only sufficiently demonstrated *in vitro* using MAEC isolated from HO-$1^{+/+}$ littermate control mice and not tested *in vivo* due to time constrains. However, in future experiments, murine-specific fluorescently-labelled siRNA can be used to assess knockdown efficiency directly. Alternatively, immunofluorescent staining of the target gene co-stained with an endothelial marker, such as CD31, could be used to monitor transfection efficiency. In addition, as shown previously, mRNA expression levels can be assessed by qRT-PCR from total RNA isolated from harvested plugs, using murine specific primers as against the gene of interest (Birdsey *et al.*, 2008). This does not only allow the determination of knockdown efficiency of murine specific siRNAs but simulatenously allows measuring the levels of expression in the plug of various angiogenic and/or inflammatory genes. Taken together, this in turn could assist interpretation of the results and changes in transfection and knockdown efficiency may explain the variability observed in neovessel formation in HO-1 siRNA-treated Matrigel plugs.

Interestingly, while siRNA-mediated silencing of cyclin A1 had no effect on HO-1 expression in murine aortic EC, depletion of HO-1 significantly decreased cyclin A1 mRNA (Fig. 7.9.), an effect also observed in primary human EC (Tab. 6.2., Fig. 6.14., Fig. 7.4.C. and Fig. 7.7.B). These findings are supportive for a role of HO-1 upstream of cyclin A1 and may suggest a function for HO-1 as a transcriptional regulator. Thus, it would be of a great interest to look at expression levels of cyclin A1, and other cell cycle regulators, in neovessels in Matrigel plugs supplemented with (i) HO-1 siRNA and (ii) AdHO-1.

To start to elucidate the function of HO-1 as a potential regulator of gene transcription, we performed an actinomycin D chase experiment and compared cyclin A1 mRNA half-lives in HO-1-deficient EC and control cells in response to VEGF. Inhibition of HO-1 significantly decreased total cyclin A1 mRNA, resulting in a 30% decrease in cyclin A1 half-life when compared to siCTL-transfected HUVEC (Fig. 7.13.). These preliminary results suggest that the observed

downregulation of cyclin A1 mRNA in HO-1-deficient cells may result from decreased mRNA stability and might be indicative for a potential function of HO-1 in the transcriptional regulation of gene expression. Cyclin A expression is controlled by protein degradation through the ubiquitination/proteasome pathway involving the anaphase-promoting (APC/C) complex and/or acetylation (Mateo et al., 2009). However, it has been long recognised that the expression of cell cycle regulators, including cyclin A, is also critically regulated by altering the stability of their mRNA (Howe *et al.*, 1995; Maity *et al.*, 1997; Wang *et al.*, 2000). Wang and colleagues demonstrated that cyclin A and also cyclin B1 mRNA stability is regulated by the RNA-binding protein HuR during cell proliferation (Wang *et al.*, 2000). HuR proteins have been found to bind to ARE-containing mRNAs and either stabilise them and/or enhance their translation in turn protecting them from degradation (Fan and Steitz, 1998). HO-1 mRNA stability has also been shown to be regulated by HuR in human fibroblasts (Kuwano *et al.*, 2009). However, whether HO-1 itself can function as a transcriptional regulator via a HuR-dependent pathway remains to be determined and it would be of interest to investigate the effect of HO-1 on HuR expression and its subsequent mRNA-stabilising function.

In summary, this chapter highlights a role for the cytoprotective enzyme HO-1 in cell cycle regulation and strengthens previously published data (Abraham *et al.*, 2003: Li Volit *et al.*, 2002, Li Volti *et al.*, 2005). We propose that HO-1 affects the transition of cells through the cell cycle by influencing the expression of cell cycle regulators, and in turn by affecting Cdk2 activity. Moreover, we have started to elucidate a potential role for cyclin A1 in HO-1-driven angiogenesis. However a direct link between HO-1 and cyclin A1 remains to be determined as changes in the proliferative capacity of cells and cell cycle progression are ultimately linked to changes in cell cycle regulator expression, and reduced cyclin A1 levels might not be specific to HO-1 deficiency. Follow-up experiments are required to further explore a potential interaction between HO-1 and cyclin A1, i.e. cylin A1 promoter and immunoprecipitation studies. Nontheless, these findings might be of importantance in the identification of new therapeutic targets for the manipulation of angiogenesis.

CHAPTER 8 - THE INTERMEDIATE FILAMENT VIMENTIN – A NOVEL HO-1 TARGET

8.1. INTRODUCTION

A proteomic screen identified vimentin as a potential downstream target of HO-1 in the regulation of VEGF-mediated angiogenesis (Tab. 6.3. and Tab. 6.4.). Vimentin belongs to the large protein family of intermediate filaments (IFs), which along with actin-containing microfilaments and tubules are the three main cyctoskeletal systems of vertebrates and many invertebrate cells. Dynamic interactions among the three cytoskeletal systems regulate the structural organisation of the cytoplasm of the cell (Chang and Goldman, 2004).

IF proteins have been classified into five distinct types on the basis of their structure, assembly properties and their tissue distribution (Tab. 8.1.).

Table 8. 1.: Classification of IF proteins. (Modified after Chang and Goldman, 2004).

Type	IF protein	Localisation
Type I	acidic keratins	epithelia
Type II	basic keratins	epithelia
Type III	vimentin	mesenchymal cells, endothelial cells
	desmin	muscle cells
	glial fibrillary acidic protein	glial cells, astrocytes, stellate liver cells
	peripherin	diverse neuronal cells
	synemin	muscle cells
Type IV	neurofilament-L	neurons
	neurofilament-M	neurons
	neurofilament-H	neurons
	nestin	neuroepithelial stem cells, muscle cells
	α-internexin	neurons
	syncolin	muscle cells
Type V	lamins	nuclear
unclassified	phakinin	lens
	filensin	lens

Vimentin belongs to the type-III IF proteins and is expressed in mesenchymal cells and some ectodermal cells during early development. Like all cytoplasmic IF proteins, vimentin consists of a central α-helical domain, the rod domain, that is flanked by two non-α-helical domains, the head and tail domains (Fig. 8.1.). The rod domain is the most conserved region among different IF proteins, whereas the amino-terminal head and the carboxy-terminal tail domain share little homology among different IFs (Parry and Steinert, 1999). The head domain has been demonstrated to regulate filament assembly and the tail domain plays a proposed role in lateral interactions and organisation of IF networks (Herrmann *et al.*, 2003). Both non-α-helical domains of vimentin have numerous phosphorylation sites that are involved in the regulation of filament assembly/disassembly and subcellular organisation (Fig. 8.1.) (Helfand *et al.*, 2003). Type-III IF proteins exist in several morphological states, including non-filamentous particles, short filaments known as squiggles, and long mature filaments (Prahlad *et al.*, 1998; Yoon *et al.*, 1998). *In vitro* studies show that filament assembly takes place in a three-step process. First vimentin tetramers assemble laterally to form unit-length filaments of approximately 16 nm in diameter and 60 nm in length. These unit-length filaments associate end-to-end forming loosely packed filaments several hundred nm long, reducing their diameter while extending in length. Eventually, loosely packed filaments reorganise into compact mature filaments (Strelkov *et al.*, 2003). Filament assembly is controlled by rapid phosphorylation and dephosphorylation of vimentin (Eriksson *et al.*, 2004). Moreover, many of the novel functions of vimentin are regulated by these post-translational modifications, such as cell adhesion and integrin trafficking, cell migration and cell signalling.

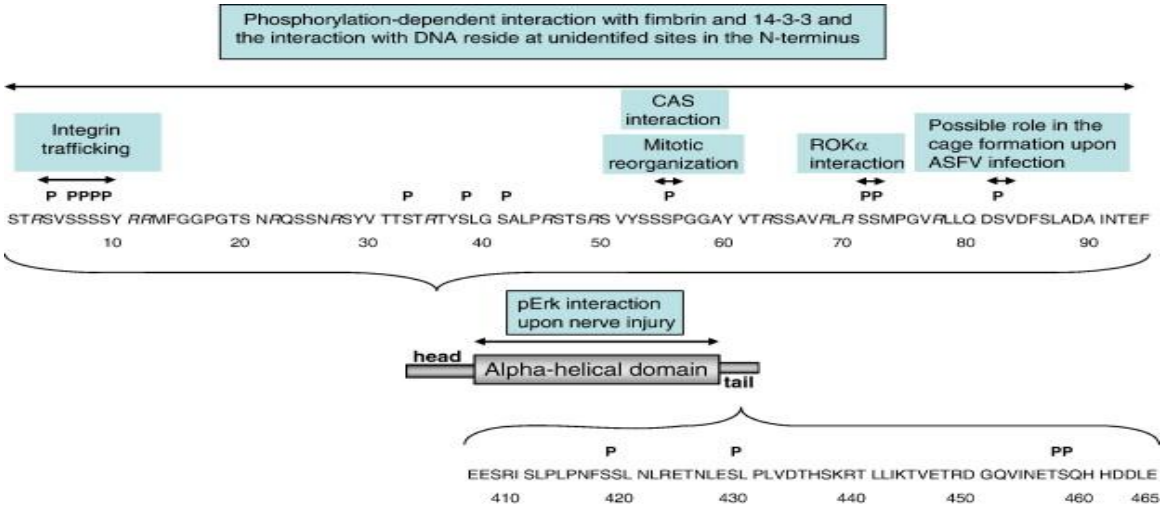

Figure 8. 1.: Vimentin structure and phosphorylation sites. Vimentin consists of a central α-helical rod domain, flanked by the amino-terminal head and the carboxy-terminal tail domain. Vimentin has a highly complex phosphorylation pattern, with sites specific for different cellular states. Many of its functions are regulated by phosphorylation. (Adapted from Ivaska *et al.*, 2007).

Vimentin is a major component of the cytoskeleton and was initially thought to solely function in the stabilisation of cells, but subsequent analyses now reveal a more complex role for vimentin. Detailed studies of vimentin knockout mice demonstrate that these animals are characterised by impaired wound healing due to defects in the capacity of fibroblasts to migrate, decreased flow-induced dilation of resistance arteries, reflecting a role in the mechanotransduction of shear stress, disturbed homing of leukocytes to lymph nodes, and lack of vascular endothelial integrity (Eckes *et al.*, 2000; Eckes *et al.*, 1998; Henrion *et al.*, 1997; Nieminen *et al.*, 2006). Moreover, vimentin$^{-/-}$ mice show reduced corneal neovascularisation and hypoxia-induced retinal neovascularisation (Eckes *et al.*, 2000; Lundkvist *et al.*, 2004). Interestingly, HO-1-deficient mice also demonstrate impaired neovascularisation during wound healing and HO-1-deficient EPC show defective homing and re-endothelisation of the retinal vasculature compared with wild-type cells following ischaemia (Deshane *et al.*, 2007; Grochot-Przeczek *et al.*, 2009).

Vimentin has been shown to play an essential role in adhesion and cell-cell contacts by regulating integrin functions, especially in endothelial cells (Vincent *et al.*, 2004; Green *et al.*, 2005). An important adhesion receptor linking EC to the extracellular matrix is $\alpha_v\beta_3$ integrin. Once bound to matrix in EC, $\alpha_v\beta_3$ can be found linked to vimentin in structures termed vimentin associated matrix

adhesions (VAMs). VAMs are sites where vimentin associates with integrins either via actin, or indirectly via actin regulatory proteins such as vinculin and plectin (Gonzales *et al.*, 2001). Interestingly, VAMs have been shown to be assembled at the moving front of migrating cells and in response to shear stress (Geiger *et al.*, 2001; Tsuruta *et al.*, 2003). siRNA-mediated knockdown of vimentin results in decreased cell adhesion, strengthening the importance of vimentin in the regulation of cell-ECM adhesions (Tsuruta *et al.*, 2003). More recently, vimentin was found to associate with $\alpha_2\beta_1$ integrin in EC, mediating cell adhesion to collagen matrices (Kreis *et al.*, 2005).

Moreover, growing evidence points to vimentin as a pro-migratory molecule. In fibroblasts, site-directed mutagenesis studies revealed that PKCε-dependent phosphorylation of vimentin is essential for the haptotactic motility of cells (Ivaska *et al.*, 2002; Ivaska *et al.*, 2005). Furthermore, phosphorylation regulated changes in vimentin filament assembly have been implicated in smooth muscle cell migration and contraction (Tang *et al.*, 2005). In the endothelium, vimentin has been linked to sprouting angiogenesis. In an elegant study, Kwak and colleagues demonstrated that growth factor-induced activation of calpains results in vimentin cleavage and increased vimentin solubility. Moreover, calpain-dependent cleavage and depolymerisation of vimentin was required for the initiation of endothelial sprouting in three-dimensional collagen matrices (Kwak *et al.*, 2012).

In a proteomic screen of primary human EC, we found that the intermediate filament vimentin was differentially expressed between control and HO-1-deficient cells in the presence of the pro-angiogenic mediator VEGF. The similarities between vimentin$^{-/-}$ and HO-1$^{-/-}$ mice in regard to their neovasularisation responses, as well as vimentin's role as a regulator of cell adhesion and integrin traffic, and its newly reported role in the regulation of cell migration and sprouting angiogenesis, make vimentin a promising candidate as a downstream effector of HO-1 in the regulation of VEGF-mediated angiogenesis. This chapter aims to validate the result of the proteomic study and to further investigate the effect of HO-1 inhibition on vimentin in terms of morphology, cellular localisation and phosphorylation state.

8.2. RESULTS

8.2.1. HO-1 inhibition impairs $a_v\beta_3$-dependent adhesion of EC to gelatin matrices

In proliferation studies using the BrdU ELISA, we observed reduced cell survival in HO-1-deficient EC following re-seeding after trypsin digestion when compared to control cells, and hypothesised that this defect resulted from impaired cell adhesion of HO-1-deficient EC (Chapter 5).

To investigate a potential role for HO-1 in cell adhesion, HUVEC were pre-loaded with a fluorescent dye 5-chloromethylfluorescein diacetate (Cell Tracker™ dye solution) and re-seeded onto either gelatin-coated or collagen type I-coated culture dishes in the presence or absence of VEGF for 40 min and cell adhesion was quantified as the cellular fluorescence of bound cells relative to the total cellular fluorescence. Cell adhesion onto collagen type I to matrices is mainly regulated via the integrin β_1, whereas the main integrin regulating cell adhesion to gelatin matrices is integrin $\alpha_v\beta_3$ (Davis, 1992; Kuhn and Eble, 1994).

VEGF treatment had no significant effect on β_1-dependent adhesion of HUVEC to collagen type I. Moreover, no difference in the number of adherent cells was observed between control and HO-1-deficient EC, suggesting that HO-1 depletion has no effect on β_1-dependent cell adhesion (Fig. 8.2.). Similarly, VEGF did not result in a significant change in the adhesion of HUVEC to gelatin matrices. However, both in the absence and presence of VEGF, siRNA-mediated inhibition of HO-1 significantly reduced the number of adherent cells by ~40% for siHO-1 seq2-transfected cells and ~15-20% for siHO-1 pool-transfected cells when compared to cells transfected with siCTL (Fig. 8.3.), suggesting a function of HO-1 in $\alpha_v\beta_3$-dependent EC-ECM adhesion.

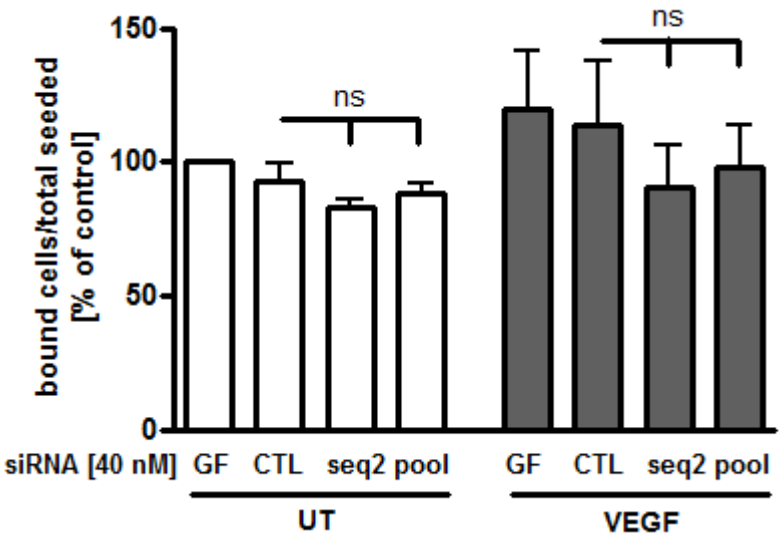

Figure 8. 2.: HO-1 depletion by siRNA has no effect on β_1-dependent adhesion of HUVEC to collagen type I-matrices. HUVEC either treated with GeneFector (GF) or transfected with control siRNA (CTL) or HO-1 specific siRNA (seq2, pool) were labelled with 5-chloromethylfluorescein diacetate (Cell TrackerTM Green CMFDA) (6.25 µM) and seeded onto collagen type I-coated 96-well plates in the absence (UT) or the presence of 25 ng/ml VEGF and allowed to adhere for 40 min. Total cellular fluorescence was measured prior to washing and subsequent fluorescence measurement of bound cells. Adhesion is expressed as the percentage of bound cells relative to the total number seeded. Data is presented as mean ± SEM (n=4 experiments), ns – not significant.

Flow cyctometric analysis was used to investigate the effect of HO-1 inhibition on $\alpha_v\beta_3$ surface expression. HUVEC expressed $\alpha_v\beta_3$ constitutively. In geneFECTOR (GF)-treated cells, VEGF exposure had no effect on $\alpha_v\beta_3$ surface levels when compared to untreated HUVEC. In addition, $\alpha_v\beta_3$ protein was not affected by siCTL. Moreover, siRNA-mediated silencing of HO-1, either with siHO1 seq2 or siHO-1 pool, had no significant effect on $\alpha_v\beta_3$ surface expression on EC when compared to that on GF-treated cells (Fig. 8.4.), suggesting that the observed impairment in cell adhesion of HO-1-deficient EC does not result from changes in $\alpha_v\beta_3$ expression.

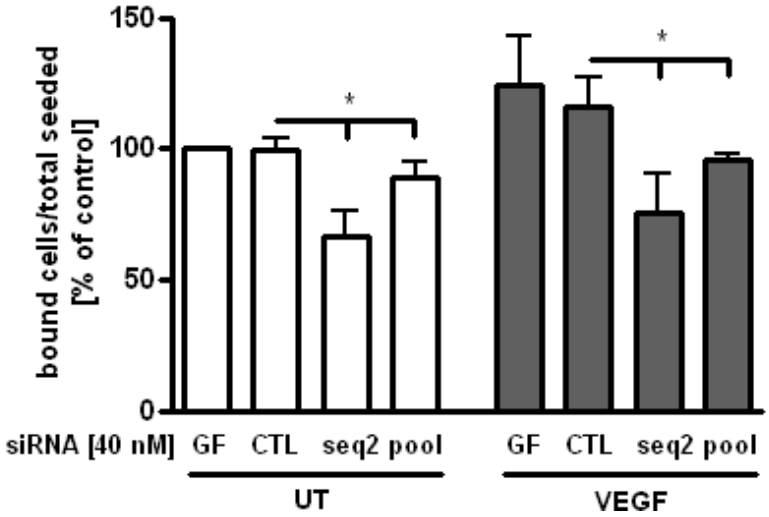

Figure 8. 3.: HO-1 depletion reduces $\alpha_v\beta_3$-dependent adhesion of HUVEC to gelatin-matrices. HUVEC either treated with geneFECTOR (GF) alone or transfected with 40 nM control siRNA (CTL) or HO-1 specific siRNA (seq2, pool) were labelled with 5-chloromethylfluorescein diacetate (Cell TrackerTM Green CMFDA) (6.25 µM) and seeded onto gelatin-coated 96-well plates in the absence (UT) or the presence of 25 ng/ml VEGF and allowed to adhere for 40 min. Total cellular fluorescence was measured prior to washing and subsequent fluorescence measurement of bound cells. Adhesion is expressed as the percentage of bound cells relative to the total number seeded. Data is presented as mean ± SEM (n=3 experiments), * p<0.05.

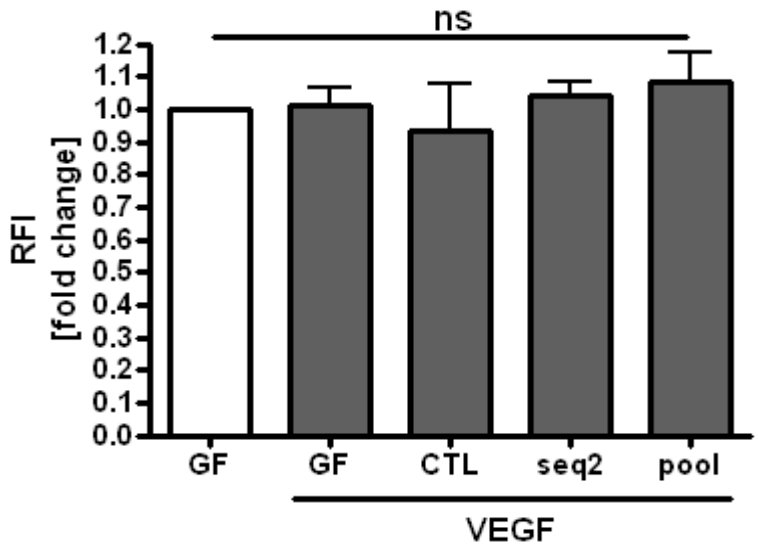

Figure 8. 4.: HO-1 depletion by siRNA has no effect on $\alpha_v\beta_3$-integrin surface expression on HUVEC. HUVEC either treated with geneFECTOR (GF) alone or transfected with 40 nM control siRNA (CTL) or HO-1 specific siRNA (seq2, pool) were left untreated or treated with 25 ng/ml VEGF for 40 min prior to assessing αvβ3-integrin surface expression by flow cytometry. The bar chart displays the relative fluorescence intensity (RFI). Data is presented relative to expression in cells treated with GF alone and expressed as mean ± SEM (n=4 experiments), ns - not significant vs untreated GF.

8.2.2. HO-1 inhibition has no effect on vimentin protein expression in EC

As both HO-1-deficient as well as vimentin-depleted cells show alterations in integrin-mediated adhesion to ECM, we further investigated the role of vimentin as a potential downstream effector of HO-1.

The proteomic screen identified vimentin to be differentially expressed between siCTL-transfected and HO-1-depleted HUVEC treated with VEGF for 16 h (Tab. 6.3. and Tab.6.4.). To investigate this finding, vimentin and HO-1 protein levels were assessed by conventional one-dimensional western blotting. HO-1 expression was not significantly altered by VEGF in GF-treated or siCTL-transfected EC when compared to untreated control cells, while siHO-1 pool decreased HO-1 protein by 85-90% in HUVEC (Fig. 8.5.A and C). Vimentin was highly expressed constitutively and no change in expression in response to VEGF was detected. Furthermore, the vimentin protein level was not affected by siRNA-mediated depletion of HO-1 when compared to siCTL-transfected cells (Fig. 8.5.B and C). These results suggest that the change in intensity on the 2D gel may reflect changes in size or phosphorylation.

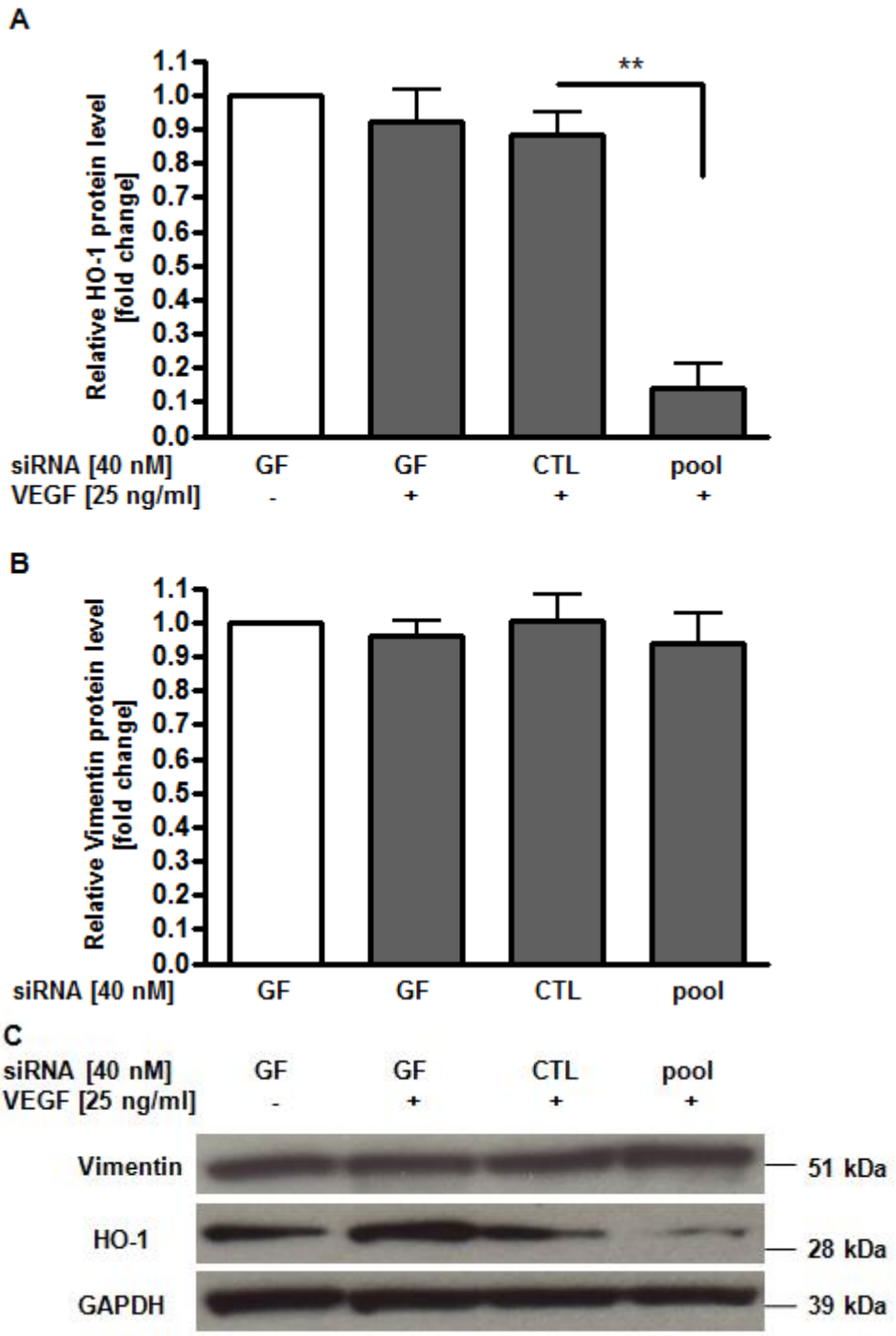

Figure 8. 5.: HO-1 depletion by siRNA has no effect on HUVEC vimentin protein expression. HUVEC were either treated with geneFECTOR (GF) alone or transfected with 40 nM control siRNA (CTL) or HO-1-specific siRNA (pool) for 24 h prior to treatment with 25 ng/ml VEGF or vehicle for additional 16 h. Protein expression was assessed by western blotting and quantified by densitometry for (A) HO-1 and (B) vimentin. (C) shows a representative blot. GAPDH was used a loading control. Data is presented as mean ± SEM (n=3 experiments), ** p<0.01.

8.2.3. Vimentin filament assembly is impaired in HO-1-depleted EC

To investigate if morphological changes in vimentin account for the differences observed during the proteomic study between control and HO-1-deficient EC in response to VEGF, vimentin filaments were visualised by immunofluorescent staining. Confocal z-stack analysis revealed that siCTL-transfected cells cultured on gelatin-coated coverslips for 16 h demonstrate a punctuate vimentin staining pattern, suggesting the presence of vimentin particles and short filaments (Fig. 8.6.A). Exposure of siCTL-transfected cell to VEGF resulted in the development of widespread dense vimentin filament networks (Fig. 8.6.B), and a significant increase in cell area (Fig. 8.6.E). HO-1 depletion per se did not markedly change the vimentin staining pattern or cell area when compared to untreated siCTL-transfected cells, suggesting the presence of predominately short vimentin filaments and particles (Fig. 8.6.C and E). However, the VEGF-induced increase in cell area and filament assembly into a mature, well-defined vimentin network was significantly attenuated in siHO-1 seq2$_{AF488}$-transfected cells, as indicated by a disturbed, punctuated vimentin staining (Fig. 8.6.D and E).

Vimentin filament assembly is controlled by rapid phosphorylation and dephosphorylation of the protein (Chou *et al.*, 2007), and we therefore hypothesised that impaired or delayed filament assembly in HO-1-deficient cells might result from differential phosphorylation.

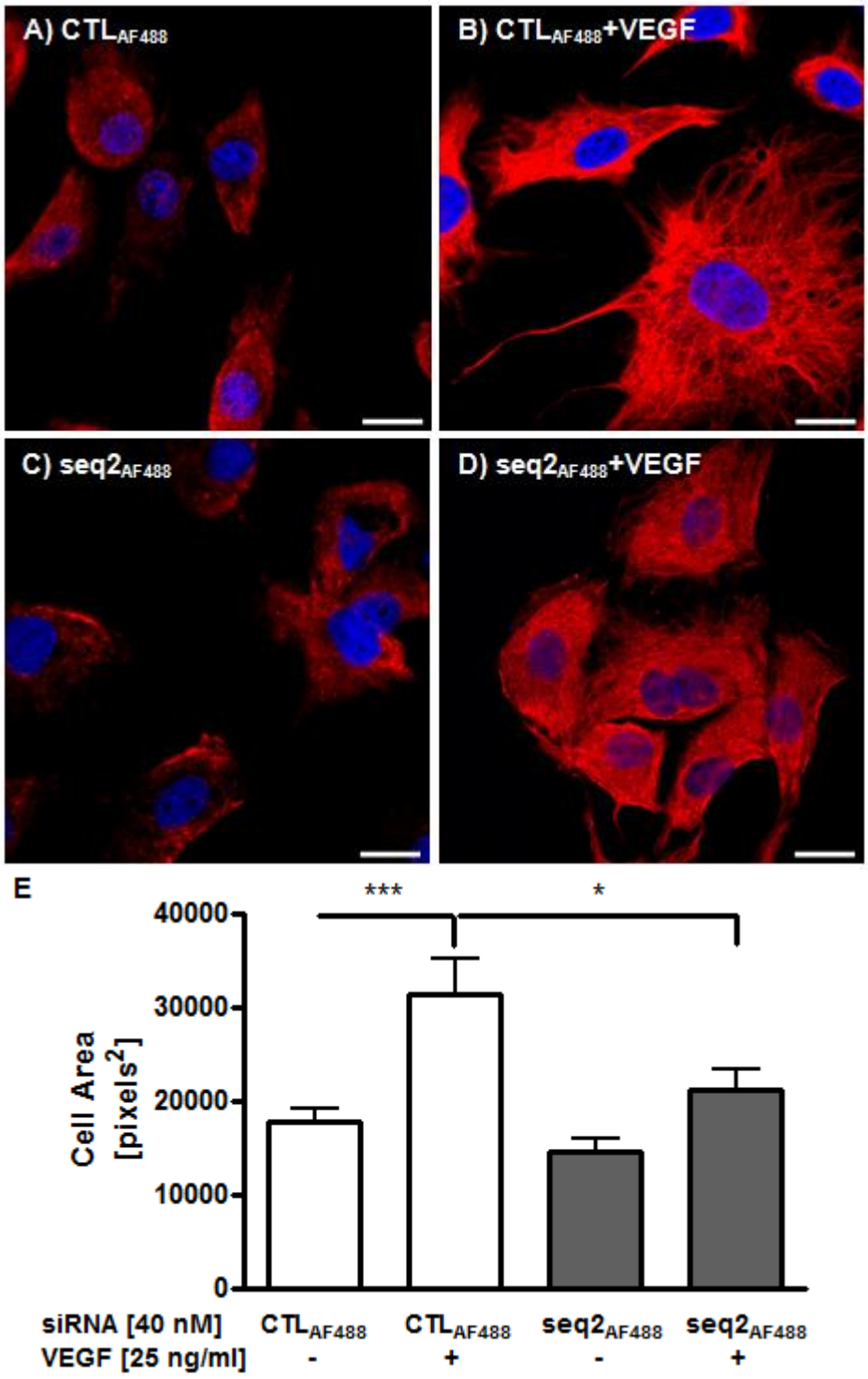

Figure 8. 6.: Vimentin filament assembly is impaired in HO-1-depleted HUVEC. HUVEC transfected with 40 nM 3'-AlexaFluor488-labelled control (CTL_{AF488}) (A, B), or HO-1 specific siRNA ($seq2_{AF488}$) (C, D) were seeded onto gelatin-coated coverslips in the absence (UT) or the presence of 25 ng/ml VEGF for 16 h prior to methanol fixation and vimentin staining with mAb RV202. Nuclei were stained with Draq5. Immunofluorescent staining was analysed by z-stack confocal microscopy and representative images are shown, 63X magnification. Bar equals 50 µm. (E) The cell area in 15 cells was quantified using ImageJ and is expressed in pixels. Data is presented as mean ± SEM (n=5 experiments), * p<0.05, *** p<0.001.

8.2.4. Phos-tag™ SDS-PAGE reveals multiple bands for vimentin

Vimentin is an abundant protein and present in multiple isoforms and post-translational modifications (Chang and Goldman, 2004; Chou *et al.*, 2007). To identify if the changes in vimentin observed during the proteomic study are due to changes in vimentin phosphorylation rather than expression, we used a novel technique called Phos-tag™ SDS-PAGE gel electrophoresis. Phos-tag™ is a functional molecule that binds specifically to phosphorylated forms of serine, threonine and tyrosine residues thereby separating phosphorylated from non-phosphorylated proteins in the same sample. Binding of Phos-tag™ to phosphorylated proteins alters their MW thereby decreasing their migration speed and resulting in multiple bands on SDS-PAGE gels after visualisation by antibody staining.

Phos-tag™ SDS-PAGE resulted in one band for vimentin in HUVEC treated with the siRNA delivery agent (GF) alone. However, exposure to VEGF for 16 h resulted in multiple bands in GF-treated and also siCTL-transfected cells, suggesting that VEGF alters the phosphorylation status of vimentin (Fig. 8.7). Interestingly, the appearance of multiple bands for vimentin was markedly reduced in siHO-1 pool-transfected cells (Fig. 8.7.), which might indicate differential phosphorylation of vimentin resulting from the different treatments and in turn suggesting a function for HO-1 in VEGF-mediated phosphorylation of vimentin.

To confirm that the multiple bands appearing in response to VEGF represent phosphorylated forms of vimentin, protein lysates were treated with lambda phosphatase (λ PP) prior to analysis on Phos-tag™ SDS-PAGE. However, λ PP treatment had no marked effect on the appearance on band number and intensity appearing in response to VEGF when compared to untreated GF-treated cells (Fig. 8.8.). Moreover, band number and intensity was not affected by λ PP in HO-1-deficient cells (compare Fig. 8.7. and Fig. 8.8.), suggesting that the multiple bands observed by Phos-tag™ SDS-PAGE do not represent *de novo* phosphorylation.

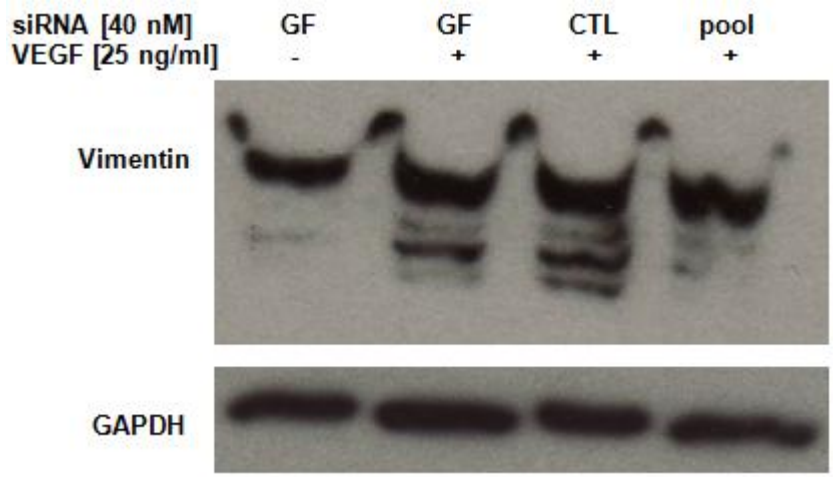

Figure 8. 7.: Phos-tag™ SDS-PAGE electrophoresis reveals multiple bands for vimentin. HUVEC were either treated with geneFECTOR alone (GF) or transfected with 40 nM control siRNA (siCTL) or HO-1-specific siRNA (pool) for 24 h prior to treatment with 25 ng/ml VEGF or vehicle for additional 16 h. Vimentin protein expression was assessed by Phos-tag™ SDS-PAGE and a representative blot is shown. GAPDH was used as a loading control (n=3 experiments).

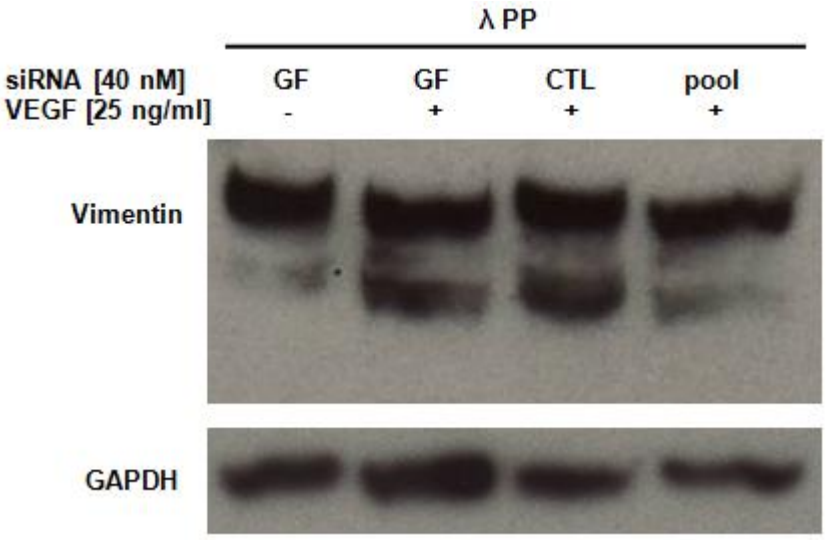

Figure 8. 8.: Lambda phosphatase treatment has no effect on vimentin protein band intensity observed on Phos-tag™ SDS-PAGE blots. HUVEC were either treated with geneFECTOR (GF) or transfected with 40 nM control siRNA (siCTL) or HO-1-specific siRNA (pool) for 24 h prior to treatment with 25 ng/ml VEGF or vehicle for additional 16 h. Protein lysates were treated with 200 units lambda phosphatase (λ PP) and vimentin protein expression was assessed by Phos-tag™ SDS-PAGE and a representative blot is shown. GAPDH was used as a loading control (n=2 experiments).

8.2.5. HO-1 inhibition results in reduced vimentin cleavage in EC

Growth factors, including VEGF and bFGF, have been shown to result in vimentin cleavage via the activation of calpains (Kwak *et al.*, 2012). Cleaved vimentin appears on 1D SDS-PAGE as multiple bands due to differences in their molecular weight compared to full-length vimentin. As the number and intensity of vimentin bands observed on Phos-tag^{TM} SDS-PAGE gels in response to VEGF was not affected by λ PP, we hypothesised that the multiple bands represent cleaved fragments rather than new phosphorylated forms of vimentin.

Conventional 1D western blotting revealed a sufficient knockdown of HO-1 protein in siHO-1 pool transfected HUVEC, whereas siCTL had no effect on HO-1 expression (Fig. 8.9.A). Over-exposure of membranes probed with a total vimentin antibody, showed one major band at approximately 51 kDa for all tested conditions, with no obvious difference in band intensity (Fig. 8.9.A). This band appeared at the same molecular weight as previously (Fig. 8.5.). VEGF exposure for 16 h resulted in multiple new bands appearing in GF-treated and siCTL-transfected cells (Fig. 8.9.A), suggesting the presence of cleaved vimentin fragments of different sizes as indicated by the reduced molecular weights (~40-50 kDa). Interestingly, this effect was notably diminished by HO-1 inhibition, with a reduction in band number and intensity (Fig. 8.9.A). To quantify these observations, for each condition band intensity was determined by densitometry for full-length vimentin and all cleaved fragments. The accumulated band intensity was then normalised to GAPDH and is expressed as the total vimentin fragment intensity. Here, VEGF significantly increased the fragment intensity by ~50% in GF-treated and siCTL-transfected HUVEC, an effect attenuated by HO-1 depletion (Fig. 8.9.B).

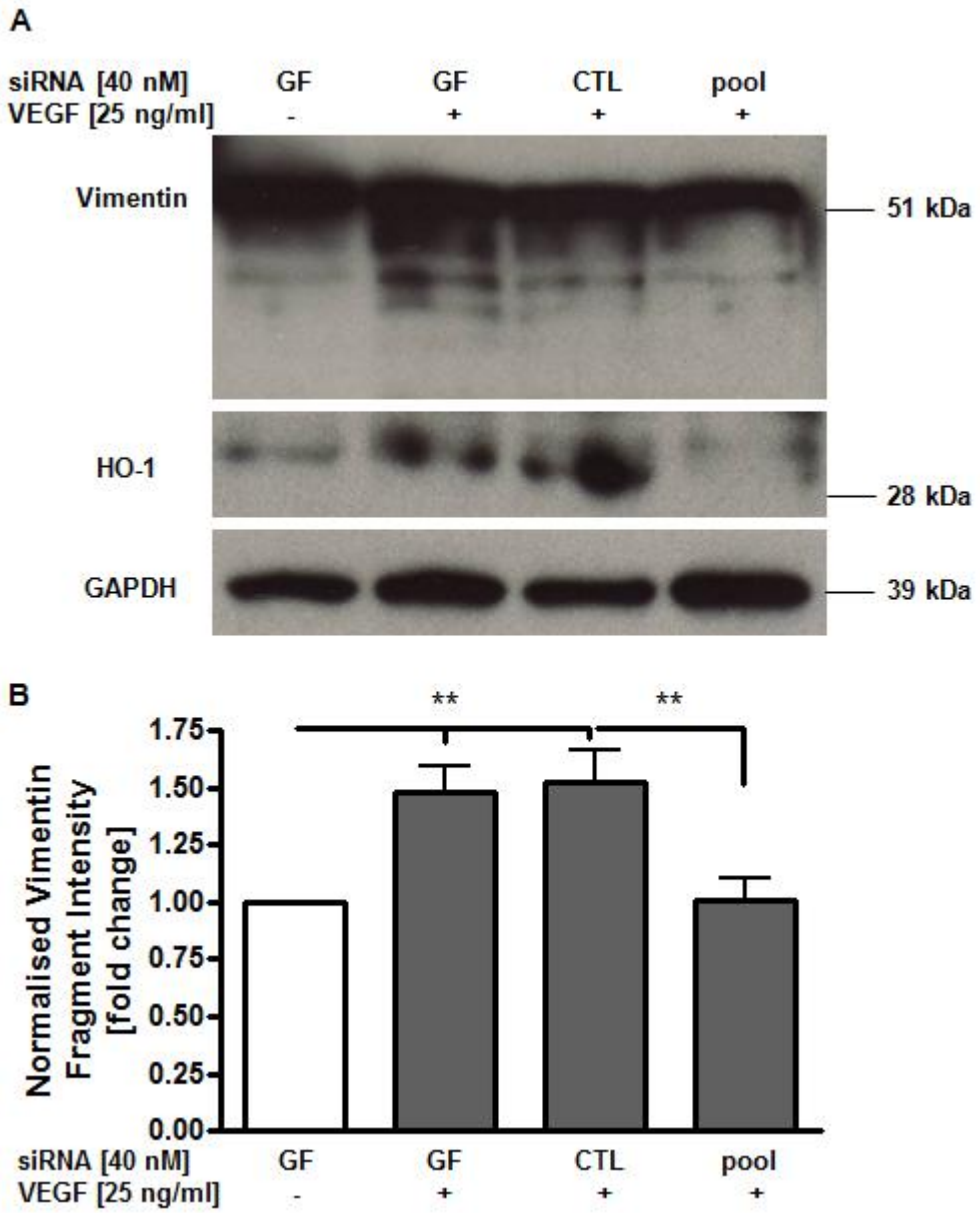

Figure 8. 9.: HO-1 depletion by siRNA results in reduced vimentin cleavage in human umbilical vein endothelial cells. HUVEC were either treated with geneFECTOR (GF) alone or transfected with 40 nM control siRNA (CTL) or HO-1-specific siRNA (pool) for 24 h prior to treatment with 25 ng/ml VEGF or vehicle for additional 16 h. Vimentin and HO-1 protein expression was assessed by western blotting and GAPDH was used as a loading control. A representative blot is shown. (B) Intensity of vimentin cleavage products was quantified by densitometry and normalised to GAPDH. Data is presented as mean ± SEM (n=5 experiments), ** $p<0.01$.

VEGF-dependent cleavage of vimentin requires calpain activity (Kwak *et al.*, 2012). To investigate whether HO-1 depletion has an effect on calpain activation, HUVEC were loaded with the calpain substrate tBoc-LM-CMAC prior to VEGF exposure and subsequent validation of calpain activity by flow cytometry. Calpain activity was significantly increased after 60 min and 90 min VEGF treatment in GF-treated and siCTL-transfected HUVEC compared to the control (Fig. 8.10.). Interestingly, the VEGF-induced increase in calpain activity was partially but significantly reduced by HO-1 inhibition (Fig. 8.10.), suggesting that the impaired vimentin cleavage observed in HO-1-deficient cells might result from decreased calpain activity.

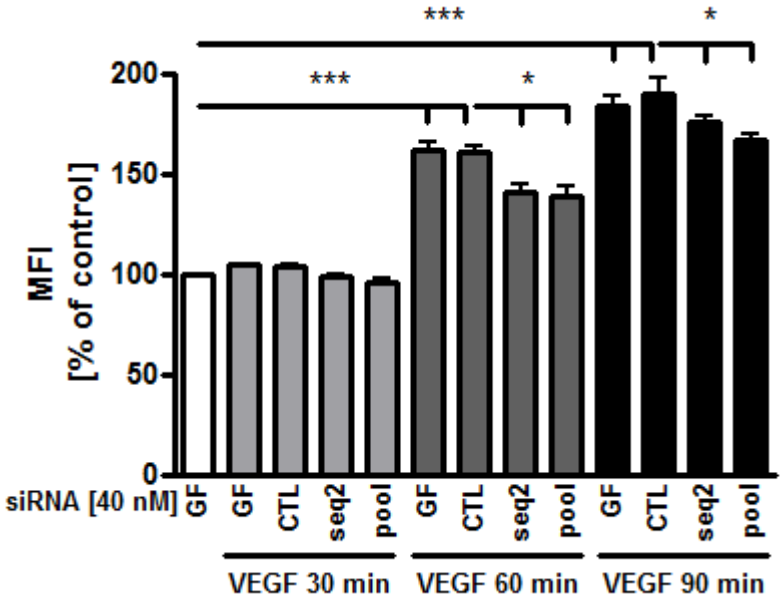

Figure 8. 10.: Calpain activation by VEGF is inhibited in HO-1-depleted HUVEC. HUVEC were either treated with geneFECTOR (GF) alone or transfected with 40 nM control siRNA (CTL) or HO-1-specific siRNA (seq2, pool) for 24 h. Cells were pre-loaded with the calpain substrate tBoc-LM-CMAC prior to treatment with 25 ng/ml VEGF or vehicle for the indicated time points. Calpain activity was assessed by flow cytometry and is expressed as the mean fluorescence intensity (MFI). Data is presented as mean ± SEM (n=2 experiments for 30 min, n=4 experiments for 60 min, and n=3 experiments for 90 min VEGF treatment), * $p<0.05$, *** $p<0.001$.

8.3. DISCUSSION

The comparison of the proteome of HO-1-depleted primary EC exposed to the pro-angiogenic factor VEGF and HO-$1^{+/+}$ control cells, identified the intermediate filament vimentin as a potential downstream target of HO-1 in VEGF-mediated angiogenesis. Vimentin is the major IF protein of mesenchymal cells and is highly conserved throughout all vertebrates, indicating an important role for the protein in cell physiology (Chang and Goldman, 2004; Ivaska *et al*., 2007). Vimentin was long thought to function solely in the stabilisation of cells through dynamic interactions with the other two major components of the cytoskeleton, actin-containing microfilaments and tubules. However, detailed studies of vimentin knockout mice recently revealed a more complex function for vimentin in the regulation of cell adhesion, integrin trafficking, and cell migration, as well as a regulator of signal transduction (Ivaska *et al.*, 2007).

Vimentin regulates cell adhesion and cell-cell contacts through association with hemidesmosomes, and has also been shown to regulate integrin function. Integrins are heterodimeric transmembrane receptors comprised of a non-covalently associated α- and a β-subunit. They mediate cell-cell and cell-matrix adhesions by binding extracellular ligands with their long N-terminal extracellular domain. The transmembrane segments and the short intracellular domain connect the extracellular ligand to the cytoskeleton and signal transduction machinery translating matrix-derived signals into cellular responses, including changes in cell morphology, cell migration, and proliferation (Brakebusch and Fassler, 2003; Calderwood, 2004; Liu *et al.*, 2000). Vimentin has been found to associate with integrin receptors either via actin, or via actin regulatory proteins in complexes known as vimentin associated matrix adhesion (VAMs) (Gonzales *et al.*, 2001). In endothelial cells, the integrin $\alpha_v\beta_3$ is an important regulator of cell-matrix adhesions and was found in VAMs (Geiger *et al.*, 2001). Moreover, VAMs are actively assembled at the forefront of migrating cells and vimentin appears to be an important regulator of VAM size and stability, as flow-induced VAM assembly is inhibited by siRNA-mediated depletion of vimentin, resulting in decreased cell adhesion (Tsuruta *et al.*, 2003). Furthermore, vimentin has been shown to regulate cell adhesion to collagen matrices via association with the $\alpha_2\beta_1$ integrin receptor (Kreis *et al.*, 2005).

Herein, we show that HO-1 inhibition results in reduced $\alpha_v\beta_3$-dependent adhesion of cells to gelatin-matrices, whereas β_1-dependent adhesion is not affected (Fig. 8.2. and Fig. 8.3.). Vimentin has been shown to regulate endo- and exocytic traffic of integrins through PKCε-dependent phosphorylation of the protein, in turn facilitating directional cell motility (Parsons *et al.*, 2002; Woods *et al.*, 2004; Ivaska *et al.*, 2002; Ivaska *et al.*, 2005). Based on this observation, we hypothesised that the reduced adherence of HO-1-deficient EC might result from impaired vimentin regulation and/or expression and subsequent decreased integrin surface expression. However, flow cytometric analysis showed no differences in $\alpha_v\beta_3$ surface levels in HO-1-deficient EC when compared to control cells (Fig. 8.4.). These data suggest that the impaired attachment of HO-1-deficient EC is not resulting from decreased availability of binding receptors but rather due to a functional defect possibly affecting the capacity of integrins to recognise and bind to ECM ligands, and/or to signal to the cytoskeleton.

The finding that siRNA-mediated knockdown of either vimentin or HO-1 decreased endothelial adhesive properties suggested vimentin was a promising candidate as a potential HO-1 target. The idea of an interplay between the cytoprotective enzyme HO-1 and the IF protein might be supported by the phenotypic similarities between vimentin$^{-/-}$ and HO-1$^{-/-}$ mice. Vimentin knockout animals demonstrate vascular endothelial dysfunction characterised by defects in barrier function (Nieminen *et al.*, 2006), as well as dysregulated formation of granulation tissue, a process that involves extensive angiogenic sprouting (Eckes *et al.*, 2000). A pro-angiogenic function for vimentin is strengthened by the finding that growth-factor induced activation of calpains is required for vimentin cleavage and subsequent endothelial sprouting (Kwak *et al.*, 2012), and by their proposed role in cell migration (Ivaska *et al.*, 2007). Furthermore, vimentin deficient mice show reduced flow-induced dilation of resistance arteries, and disturbed homing of leukocytes to lymph nodes (Eckes *et al.*, 2000; Eckes *et al.*, 1998; Henrion *et al.*, 1997). HO-1 knockout mice also demonstrate reduced neovascularisation during wound healing and defective EPC homing and re-endothelisation of the retinal vasculature in response to ischaemia-induced injury (Deshane *et al.*, 2007; Grochot-Przeczek *et al.*, 2009). Of note, vimentin$^{-/-}$ mice also show reduced corneal neovascularisation and hypoxia-induced retinal neovascularisation (Eckes *et al.*, 2000; Lundkvist *et al.*, 2004).

In order to further investigate a potential function for vimentin in HO-1-driven angiogenesis, the initial step was to validate the results obtained from the proteomic study. Conventional one-dimensional western blotting suggested that HO-1 inhibition had no effect on vimentin protein expression (Fig. 8.5.). 1D electrophoresis separates proteins only according to their molecular weight not taking into account any post-translational modifications. In contrast, two-dimensional SDS-PAGE, as used in the proteomic study, separates proteins according to their molecular weight in the first dimension and according to their isoelectric point (pI) in the second dimension. The pI is the pH at which a protein carries no net electrical charge and a shift in pI is indicative of post-translational modifications of a protein, such as a change in the phosphorylation state (Halligan, 2009). The technical limitations in terms of sensitivity of 1D western blotting might explain why no differences in total vimentin were observed, whereas the proteomic screen identified vimentin as a protein to be differentially expressed between HO-1-deficient and HO-$1^{+/+}$ control cells.

As vimentin is abundantly expressed and exists in many different morphological states, isoforms, and with various post-translational modifications (Chang and Goldman, 2004), we hypothesised that differences in vimentin morphology, localisation and/or phosphorylation account for the differential expression of vimentin as observed by 2D SDS-PAGE.

Depending on the functional state of a cell, vimentin exists as non-filamentous particles, short filaments, or long mature filaments (Prahlad *et al.*, 1998; Chou *et al.*, 2007). Immunofluorescent staining of vimentin with confocal z-stack analysis revealed a punctuate staining pattern for vimentin in HUVEC transfected with a non-targeting control siRNA, suggesting vimentin exists in the form of non-filamentous particles or short filaments (Fig. 8.6.A). VEGF exposure of siCTL-transfected cells resulted in a significant increase in cell area and development of a dense vimentin network consisting of long mature filaments covering the complete cell area (Fig. 8.6.B and E). Similar responses in vimentin reorganisation have been reported in the spreading fibroblast, where during early spreading vimentin was found in the form of non-filamentous particles or short filaments predominately near the edges of the cell. In contrast, in fully spread cells an extensive and complex vimentin network was formed from the assembly of these short filaments and particles into long mature filaments covering the complete area of the cell (Prahlad

et al., 1998; Chou *et al.*, 2007). This suggests that VEGF initiates cell spreading, and reorganisation of vimentin in EC, resulting in increased cell area and a complex vimentin filament network, which in turn might regulate, at least to some extent, the angiogenic properties of EC in response to VEGF. Interestingly, while HO-1 depletion alone had no significant effect on vimentin morphology and cell size when compared to siCTL-transfected EC, the VEGF-induced increase in cell area was significantly inhibited (Fig. 8.6.A, C and E). Moreover, cells showed a disturbed, punctuate staining pattern and failed to form an intact filamentous vimentin network in response to VEGF (Fig. 8.6.D). These data suggest a role for HO-1 in vimentin filament assembly, where HO-1 inhibition impairs and/or delays filament assembly in response to VEGF which might in turn result in defective angiogenic capacities of EC.

Vimentin filament assembly is a three step process involving the primary association of vimentin tetramers, which then bind each other end-to-end forming unit-length filaments. These unit-length filaments further expand into loosely packed filaments which simultaneously compact in diameter and reorganise into long mature vimentin filaments (Strelkov *et al.*, 2003). Vimentin filament assembly is controlled by rapid phosphorylation and dephosphorylation of the protein (Eriksson *et al.*, 2004; Chou *et al.*, 2007) and we therefore hypothesised that the impaired or maybe delayed filament assembly in HO-1-deficient cells might result from differential phosphorylation.

In this study, we adopted a novel western blotting technique which allows the identification of phosphorylated and non-phosphorylated forms of a protein in the same sample. Phos-tag^{TM} SDS-PAGE utilises just a total antibody targeting the protein of interest rather than numerous phospho-specific antibodies. Phos-tag^{TM} is a functional molecule that is directly added to the electrophoresis gel and binds specifically to phosphorylated serine, threonine and tyrosine residues, thereby affecting the molecular weight and migration speed of proteins, and resulting in multiple separate bands after antibody staining and chemiluminescent visualisation.

Phos-tag^{TM} SDS-PAGE revealed one band, with a similar expression intensity at the same molecular weight for all four tested conditions (Fig. 8.7.). VEGF exposure resulted in the appearance of multiple lower molecular weight bands underneath in cells treated with the siRNA delivery agent alone of cell transfected with a control siRNA (Fig 8.7.), suggesting that VEGF phosphorylates vimentin at multiple phosphorylation sites. Of note, the appearance of multiple

bands in response to VEGF was diminished in HO-1-depleted EC (Fig. 8.7.). These data suggest that VEGF-induced phosphorylation of vimentin is at least in part dependent on HO-1 and that HO-1 deficiency impairs VEGF-induced vimentin phosphorylation which might affect vimentin filament assembly and in turn the angiogenic properties of EC.

To confirm the hypothesis that HO-1 is required for VEGF-mediated phosphorylation, the same protein lysates as used for Phos-tag™ SDS-PAGE were treated with a lambda phosphatase (λ PP) prior to electrophoresis. λ PP is a protein phosphatase with activity towards phosphorylated serine, threonine and tyrosine residues, mediating the release of phosphate groups (Cohen and Cohen, 1989). Thus, λ PP treatment should reduce the appearance and/or intensity of multiple bands on Phos-tag™ gels. However, band number and intensity was not affected by λ PP treatment in either control cells or in HO-1-deficient EC (Fig. 8.8.), indicating that the observed bands do not represent new phosphorylated forms of vimentin and hence that HO-1 inhibition has no effect on vimentin phosphorylation. More likely, these lower molecular weight bands are vimentin cleavage products. To strengthen this hypothesis and further exclude *de novo* phosphorylation as an explanation for the presence of multiple bands, a positive control for λ PP activity should be used in future experiments. A variety of protein kinases, including PKA, PKC, and Cdc2 kinase have been shown to phosphorylate vimentin (Tzivion *et al.*, 2000). In addition, Kinoshita and colleagues recently reported rapid hyperphosphorylation of vimentin in the presence of the protein phosphatase inhibitor calyculin A as shown by Phos-tag™ western blotting (Kinoshita *et al.*, 2012). Thus in future experiments, vimentin phosphorylation in human EC could be induced by either protein kinases or calyculin A and serve as a positive control for phosphorylation. Moreover, λ PP treatment should markedly inhibit vimentin phosphorylation in these samples in turn serving as a positive control for λ PP activity.

Recently, Kwak and colleagues demonstrated that growth factor-induced activation of calpains results in vimentin cleavage which in turn is required for angiogenic sprouting of EC (Kwak *et al.*, 2012). Calpains are intracellular calcium-activated cysteine proteases and have been shown to regulate cell migration through cleavage of numerous actin regulatory proteins, including talin, vinculin and paxillin. Calpains are required for the formation of membrane protrusions and cell membrane release during cell spreading (Franco *et al.*, 2004; Wells *et al.*, 2005). Moreover,

calpains can cleave the amino-terminus of vimentin (Fischer *et al.*, 1986; Tompa *et al.*, 2004). The amino-terminal head domain of vimentin has been shown to regulate filament assembly, thus calpain-induced cleavage renders vimentin incapable of forming insoluble, polymerised filaments (Herrmann *et al.*, 2003).

In the study by Kwak and colleagues vimentin cleavage was demonstrated by western blotting analysis of total cell lysates (Kwak *et al.*, 2012). Here full-length vimentin resulted in a band at approximately 60 kDa, which is in agreement with the molecular weight of vimentin, which is 57 kDa (Dahl *et al.*, 1981). Cleaved vimentin fragments were identified as multiple bands below the full-length vimentin with reduced molecular weights (Kwak *et al.*, 2012). We hypothesised that full-length vimentin is the most abundant form of vimentin expressed in human EC and therefore easy to identify by conventional 1D SDS-PAGE, whereas cleaved vimentin fragments are less abundantly expressed and might be more difficult to identify on electrophoresis. This might also explain the fact, that no differences in vimentin expression could be observed in our initial validation studies (Fig. 8.5.). To further investigate this hypothesis, 1D western blot analyses comparing the expression of vimentin in HO-1-deficient EC with control cells were repeated, but the blots were exposed for longer durations. Indeed, in all tested conditions one highly expressed band was apparent at approximately 51 kDa with no significant differences in expression between treatments (Fig. 8.9.A). We identified this band as full-length vimentin. Interestingly, VEGF treatment resulted in multiple bands with a lower molecular weight appearing underneath the band for full-length vimentin in geneFECTOR-treated and siCTL-transfected cells, but not in HO-1-deficient HUVEC (Fig. 8.9.A). We identified those bands as truncated forms of vimentin, with molecular weights ranging from approximately 40-50 kDa. Accordingly, quantification revealed a significant decrease in vimentin fragment intensity in HO-1-depleted cells in response to VEGF when compared to HO-$1^{+/+}$ control cells (Fig. 8.9.B). Moreover, we can show that VEGF-mediated calpain activation is significantly inhibited by siRNA-mediated silencing of HO-1 (Fig. 8.10.), which might account for the defect in vimentin fragmentation in response to VEGF observed in HO-1-deficient EC. In their study, Kwak and colleagues demonstrated the re-localisation of vimentin to cell edges in response to growth factor treatment, an effect attenuated in the presence of calpain inhibitors (Kwak *et al.*, 2012). Thus, impaired vimentin filament assembly, as observed in HO-1-

deficient cells (Fig. 8.6.), might also result from decreased calpain activation and subsequent inhibition of vimentin re-localisation to cell edges.

Altogether, these results are indicative of a role of vimentin as a downstream target of HO-1 in VEGF-mediated angiogenesis, where VEGF induces HO-1 expression and/or activity which is required for activation of the calcium-dependent protease calpain. Calpain activation in turn leads to cleaved, soluble, depolymerised vimentin localising to cell edges thereby driving the angiogenic responses of EC.

CHAPTER 9 - CONCLUDING REMARKS

9.2. DISCUSSION

Over the past decades, tremendous technological and methodological advances in cell and molecular biology have greatly improved our understanding of the vascular endothelium and its role in health and disease. The endothelium constitutes the cellular lining of all vessels in the cardiovascular system, and forms a physiological and structural barrier between the intravascular space and extravascular tissue. The endothelium is no longer viewed as an inert structure, but rather has been recognised to be a highly complex, dynamic and heterogeneous organ important in several house-keeping functions. It actively regulates the passage of solutes, macromolecules and blood cells across the wall, generates and integrates biological signals and plays an essential role in haemostasis, leukocyte traffic and vascular tone, maintaining an anti-thrombotic, fibrinolytic and anti-inflammatory surface (Cines *et al.*, 1998). Endothelial cells are also involved in the control of growth, development and differentiation of the vessel wall in the processes of vasculogenesis and angiogenesis (Risau, 1997). Impairment of these endothelial cell-mediated processes leads to a dysfunctional endothelium and has been implicated in the pathogenesis of atherosclerosis and other pathological conditions affecting the cardiovascular system, including hypertension, coronary and peripheral artery disease, chronic heart failure, as well as autoimmune diseases such as diabetes mellitus and systemic lupus erythematosus (Ross, 1999; Schachinger *et al.*, 2000; Heitzer *et al.*, 2001; Bijl, 2003; Endemann and Schiffrin, 2004, Higashi *et al.*, 2009). To counteract harmful stimuli and limit local and systemic pathogenic responses following vascular injury, the vascular endothelium has developed intrinsic cytoprotective signalling pathways and expresses several anti-inflammatory and cytoprotective proteins, including soluble anti-inflammatory molecules, cell surface proteins and receptors, as well as intercellular adhesion molecules. The principal aim of our research group is to identify these intrinsic mediators and the signalling pathways regulating them. By establishing a more detailed understanding of the underlying cytoprotective mechanisms of the endothelium, we hope that they might represent future therapeutic targets for the restoration of endothelial homeostasis, the prevention of endothelial dysfunction and subsequent atherogenesis in patients with systemic inflammatory diseases.

Of particular interest to our group is the role of the enzyme heme oxygenase-1 and its products in vascular cytoprotection and angiogenesis. HO-1 catalyses the degradation of free heme into equal molar amounts of carbon monoxide, ferrous iron with subsequent induction of ferritin, and biliverdin, which is rapidly converted into bilirubin. Biologic activities of the end-products alone or in combination with HO-1 protein itself exhibit multiple cytoprotective effects in the cardiovascular system (Ali *et al.*, 2007; Kinderlerer *et al.*, 2008; Grochot-Przeczek *et al.*, 2012). Moreover, induction of HO-1 is an important cellular adaptive response, minimising tissue injury and facilitating repair, as revealed in multiple models of disease and the severe endothelial damage in human HO-1 deficiency (Yachie *et al.*, 1999). But the recognised roles for HO-1 are far beyond cytoprotection, and HO-1 and its products have been implicated in cell proliferation, differentiation and apoptosis (Dulak *et al.*, 2008). Recently, it has been shown that the pro-angiogenic factors VEGF and SDF-1α induce HO-1 expression and enhance its enzymatic activity, in turn modulating the angiogenic capacities of endothelial cells (Bussolati *et al.*, 2004; Deshane *et al.*, 2007). Accordingly, VEGF treatment results in HO-1 induction in the chick embryo chorioallantoic membrane (Fernandez and Bonkovsky, 2003). However, the precise transcriptional and signalling pathways underlying growth factor-induced HO-1 activation remain elusive. Therefore, in Chapter 4, I determined the optimal time point of HO-1 induction in response to VEGF and SDF-1α in primary human umbilical vein EC in the hope of identifying transcriptional regulators and signalling pathways mediating this effect.

In accordance with previously published studies, exposure to VEGF or SDF-1α significantly up-regulated HO-1 message and protein levels in EC. Of note, high variability in basal HO-1 expression was observed between all experiments, and induction of HO-1 by both VEGF and SDF-1α varied notably between cell isolates from different donors. Moreover, high basal *HMOX1* promoter activity was observed in HO-1 promoter studies, while no difference in promoter activity was observed in cells exposed to VEGF or SDF-1α. We hypothesise that the variability in basal and induced HO-1 may results from microsatellite polymorphisms within the gene promoter. These variable GT-rich regions have been shown to affect transcription, modulate basal and induced HO-1 expression and are of clinical relevance (Chen *et al.*, 2002; Song *et al.*, 2009). Moreover, longer $(GT)_n$ repeats have been shown to diminish the responsiveness of EC to the pro-angiogenic factor VEGF, as indicated by reduced VEGF-mediated proliferation (Taha *et al.*,

2010). The basal promoter activity observed may be caused by a stress-response of cells in culture. Indeed, HO-1 is a stress-inducible enzyme and numerous stress responsive elements have been identified within the *HMOX1* promoter sequence. These in turn meditate transcriptional activation in response to a large variety of HO-1 inducers (Ryter *et al.*, 2006). The high basal *HMOX1* promoter activity may mask any effects afforded by VEGF and SDF-1α. Therefore, to date it has not been proven possible to identify potential transcriptional pathways involved in the regulation of HO-1-driven angiogenesis utilising primary human EC. Genotyping of the HO-1 promoter of human cell isolates for $(GT)_n$ repeats, as well as the use of cell lines or primary cell isolates from species not possessing these polymorphisms, may assist in follow-up studies to identify transcriptional and signalling mechanisms involved in the regulation of HO-1 by pro-angiogenic mediators.

VEGF is the most important molecule in the regulation of blood vessel morphogenesis, controlling cell permeability, endothelial proliferation, migration and survival (Ferrara *et al.*, 2003). The notion that VEGF induces expression of the cytoprotective enzyme HO-1, which itself has been shown to induce the synthesis of VEGF, implicates a potential role for HO-1 in VEGF-mediated angiogenesis (Dulak *et al.*, 2008). Indeed, HO-1 overexpression enhanced proliferation and *in vitro* tube formation or capillary sprouting in response to VEGF, while inhibition of HO-1 activity attenuated cell proliferation and migration of cultured EC (Deramaudt *et al.*, 1998; Jozkowicz *et al.*, 2003; Bussolati and Mason, 2006). Despite the considerable progress made in defining the role for HO-1 in the vasculature, further studies are required to identify the specific role of HO-1 during the individual steps of the angiogenic process. Moreover, the functions of the end-products of HO-1-mediated degradation of heme, carbon monoxide, biliverdin/bilirubin, and ferritin, in the regulation of angiogenesis remain poorly understood. We tried to further shed light onto this field of research by specific silencing of HO-1 using targeted siRNAs, or conversely by the use of an adenoviral vector expressing the human HO-1 gene. Herein, we show that specific inhibition of human HO-1 significantly decreased the proliferative capacity of primary EC in response to the potent pro-angiogenic mitogen VEGF, whereas adenoviral-induced overexpression of HO-1 significantly enhanced EC proliferation and exhibited a synergistic effect on VEGF-driven proliferation. These observations confirm previous findings from our laboratory utilising the less specific pharmacological agonist CoPP or the synthetic HO-1 antagonists SnPP and ZnPP

(Bussolati *et al.*, 2004; Bussolati and Mason, 2006). Of note, the metalloprotoporphyrins SnPP and ZnPP not only inhibit the activity of HO-1 but also interfere with the constitutive HO-2, and therefore lack specificity (Ryter *et al.*, 2006). The use of specific siRNA targeting the human HO-1 gene in this study now demonstrated that loss of only the inducible isoform HO-1 is sufficient to impair the proliferative capacity of EC in culture, and that HO-2 does not compensate for the loss of HO-1 in our system.

Both VEGF and HO-1 have been shown to play important anti-apoptotic functions in the vasculature. VEGF protected EC from serum starvation through the induction of the anti-apoptotic genes A1 and Bcl-2, while murine aortic EC from HO-1 null mice are more susceptible to apoptotic stimuli and have increased caspase-3 activity compared with EC from HO-$1^{+/+}$ littermate controls (Gerber *et al.*, 1998; Berberat *et al.*, 2000; Chen *et al.*, 2004). Thus, an increased rate of apoptosis may contribute to the apparent proliferative defects of HO-1-depleted EC. In line with this, we show increased apoptosis in EC cultures depleted of HO-1, however this effect is rescued by VEGF and associated with an upregulation in A1 message and Bcl-2 protein. Moreover, VEGF protected HO-1-deficient HUVEC from serum starvation-induced cell death. These findings suggest that the reduced proliferation properties observed in HO-1-deficient EC in response to VEGF do not reflect increased apoptosis. Moreover, cytoprotective mechanisms of VEGF mediated through increased induction of A1 and Bcl-2 are HO-1-independent.

Endothelial motility is essential to the angiogenic growth. Deshane and colleagues recently demonstrated a link between HO-1 and both EC and EPC migration in response to the chemokine SDF-1α. Furthermore, pharmacological inhibition of HO-1 was shown to reduce the migratory capacity of EC, whilst HO-1 overexpression enhanced endothelial migration as demonstrated by increased propensity to form capillary-like structures in Matrigel (Jozkowicz *et al.*, 2003; Deramaudt *et al.*, 1998). Herein, we demonstrate that HO-1 is an important regulator of endothelial migration in response to VEGF. Closure of artificial wounds generated on HUVEC monolayers was impaired by HO-1 inhibition, and HO-1-deficient cells demonstrated a significant reduction in their linear migration, expressed as the Euclidean distance, in response to VEGF when compared to control cells. These findings are confirmed by analysis of the directional movement of individual cells, revealing that HO-1-deficient cells migrated in a rather random,

circular pattern alongside the scratch edge, whereas control cells showed a more linear, directional movement across the scratch and towards cells on the opposite site. Conversely, the migratory capacity of EC was notably enhanced in cells overexpressing the human HO-1 gene. Moreover, we report, to our knowledge for the first time, impaired chemotactic migration of HO-1-deficient EC towards a pro-angiogenic stimuli. HO-1 deficiency significantly reduced the number of EC migrating towards a VEGF gradient as assessed by the Ibidi µ-slide chemotaxis assay. However, further studies are required to establish the specific role of HO-1 and its products in the process. The directed forward movement of EC requires the rearrangement of the cytoskeleton and subsequent morphological changes resulting in the expansion of cell protrusion at the moving front. Lamellipodia and filopodia are both capable of probing the environment for attractive guidance cues and initiate migration towards these (Defilippi *et al.*, 1999). Their formation is regulated by activation of the small GTPases Rac1 and Cdc42, respectively (Lamalice *et al.*, 2007). It would be of great interest to investigate whether (i) changes in the morphological appearance, i.e. changes in lamellipodia and filopodia protrusions, or (ii) changes in small GTPase-mediated signalling contribute to the impaired migratory capacity of HO-1-deficient cells in response to VEGF. In the final step of the angiogenic process, migrating EC rearrange into lumenised capillary structures that undergo maturation and remodelling. Herein, we show that formation of capillary-like structures on Matrigel in response to VEGF is significantly impaired by HO-1 depletion. Altogether our data demonstrate a role for HO-1 in the regulation of VEGF-induced angiogenesis, and demonstrate that the cytoprotective enzyme HO-1 affects the angiogenic capacity of EC in culture at various levels.

The products of HO-1-dependent heme degradation carbon monoxide, biliverdin/bilirubin and ferritin are well recognised for their cytoprotective effects in the vascular system and have also been linked to angiogenesis. Moreover, HO-1 products are likely to be responsible for its biological activity and anti-inflammatory, anti-oxidant and anti-apoptotic actions. In this study we investigated whether the end-products of heme metabolism also contribute to the pro-angiogenic effects of HO-1. Deferoxamine mesylate chelates intracellular iron and mimics the activity of ferritin, which has been shown to inhibit the anti-apoptotic effects of high molecular weight kininogen, improving the proliferation, migration and subsequent formation of capillary-like structures of EC (Coffman *et al.*, 2009). Moreover, exposure of vascular SMC to DFO increased

VEGF synthesis and may influence angiogenesis indirectly (Dulak *et al.*, 2002). However, in my experiments, treatment of HO-1-deficient HUVEC with DFO did not restore their impaired migratory phenotype in response to VEGF.

HO-1-derived CO is likely to be predominantly responsible for the angiogenic properties of HO-1. CO supplementation increased HO-1 expression and augmented the synthesis of VEGF in EC in culture (Jozkowicz *et al.*, 2003; Lin *et al.*, 2009). This effect has also been described in an animal model, resulting in increased VEGF biosynthesis in various tissues and organs following CO exposure (Marti and Risau, 1998). Herein, we used CO-releasing molecules to delivery CO in a safe, accurate and measurable fashion to cells in culture. CORM-2 is a water soluble transition metal-carbonyl complex that liberates CO upon ligand exchange with DMSO, and has been shown to play a critical role in the resolution of inflammatory responses and alleviation of cardiovascular diseases (Motterlini *et al.*, 2002; Motterlini *et al.*, 2003). However, pre-treatment and subsequent culture of HO-1-deficient HUVEC with CORM-2 did not restore their impaired migratory phenotype in response to VEGF. CO release from CORM-2 is very fast ($t_{1/2}$ ≈ 1min) and non-specific, which may hamper the delivery of controlled amounts of CO to the target cells (Motterlini *et al.*, 2005). Thus inadequate CO_2 may have been responsible for the lack of effect.

Enzyme-triggered CORMs represent a novel class of powerful CORMs, which are stable under physiological conditions, but are rapidly converted to the active form by means of enzymatic hydrolysis when taken up by cells. Enzymatic cleavage of the ester functionality by intracellular esterases results in the dissociative loss of CO (Romanski *et al.*, 2011; Romanski *et al.*, 2012). The biological activity of the ET-CORM SROM158 was confirmed by its inhibitory effect on TNF-α-induced surface expression of VCAM-1, and SROM158 either on its own or in combination with VEGF significantly induced HO-1 in HUVEC. However, as seen with CORM-2, the more powerful SROM158 was not sufficient to reverse the dysfunctional angiogenic capacities of HUVEC deficient in HO-1, in terms of VEGF-mediated proliferation and migration. Collectively, these data suggest that HO-1-induced angiogenesis and EC migration are dependent on HO-1 but are not mediated, at least solely, by the HO products CO or iron. The role of the bile pigments biliverdin and bilirubin in angiogenesis is poorly understood, but biliverdin may have an indirect effect on angiogenesis by stimulating the production of pro-angiogenic factors, such as VEGF and IL-8 in

human keratinocytes (Jawza *et al.*, 2006; Lobada *et al.*, 2008). Thus, HO-1-derived biliverdin/bilirubin might contribute to the pro-angiogenic effects of HO-1 and human EC. Moreover, a role for CO and iron in HO-1-driven angiogenesis cannot be completely excluded solely based on the data from this study, as the products may act in concert and may be dependent on each other. Indeed, co-administration of CO and biliverdin greatly enhanced their anti-inflammatory and anti-apoptotic effects in a mouse model of liver damage when compared to single administration of either CO or biliverdin (Sass *et al.*, 2004).

Angiogenesis is involved in the progression of numerous diseases. Excessive angiogenesis, due to the overproduction of normal or aberrant forms of angiogenic mediators, or a relative deficiency in angiogenic inhibitors, is associated with chronic inflammatory diseases, such as atherosclerosis, diabetes mellitus and rheumatoid arthritis, as well as tumour growth and metastasis. In other diseases, such as ischaemic heart disease or preeclampsia, the angiogenic switch is insufficient, causing EC dysfunction, vessel malformation or regression, or preventing revascularisation, healing and regeneration (Carmeliet, 2005). Study of anti-angiogenic agents for the treatment of various malignant diseases is of special interest, and a variety of angiogenic inhibitors, targeting VEGF or VEGF-R2, such as bevacizumab, are available for clinical use, with others in clinical trials (Buysschaert *et al.*, 2007; Carmeliet *et al.*, 2009). Conversely, the use of angiogenic stimulators, although initially promising in animal models and small uncontrolled pilot studies in patients with ischaemic heart disease or peripheral arterial occlusive disease, so far do not show any convincing therapeutic benefit, demonstrating the need for further studies to identify novel therapeutic targets for the manipulation of angiogenesis. HO-1 and its associated pathways may represent a new target. However, a better understanding of the signalling pathways and downstream effectors of HO-1 in the regulation of angiogenesis is required and one of the main aspects of my project.

Vasodilator-stimulated phosphoprotein has been proposed as a potential downstream target of HO-1 in SDF-1α-mediated angiogenesis. SDF-1α-induced VASP phosphorylation was attenuated in HO-1-deficient murine aortic EC, an effect restored by a CO donor (Deshane *et al.*, 2007). However herein we show that VEGF-mediated VASP phosphorylation is not altered by HO-1 depletion, suggesting that VASP is not a downstream effector of HO-1 in VEGF-induced

angiogenesis. Therefore, to identify potential novel targets of HO-1 in angiogenesis, we performed (i) a targeted PCR array and (ii) a proteomic screen comparing the differential expression of genes and proteins, respectively, in HO-1-deficient human primary EC and control cells in response to the mitogen VEGF.

Cyclin A1 mRNA levels were significantly reduced by HO-1 depletion as identified by the PCR array. In addition, further analyses revealed a significant reduction in basal and VEGF-induced expression of the positive cell cycle regulators cyclin E1 and the cyclin-dependent kinase Cdk2, but increased expression of the Cdk2 inhibitor p27 in proliferating HUVEC. These findings are in line with previously a published microarray study, demonstrating increased cyclin E and cyclin A expression in EC transduced with the human HO-1 gene (Abraham *et al.*, 2003). Moreover, we show that migrating EC deficient in HO-1 exhibit reduced cyclin A1 protein and this is accompanied by a decrease in Cdk2 activity. The altered expression profile of cell cycle regulators might in turn be responsible for the halt in transition from G_1- to S-phase observed in HO-1-deficient HUVEC in the absence and also the presence of VEGF. Both E-type cyclins as well as A-type cyclins bind to and activate Cdk2. The active cyclin E/Cdk2 complex is required for S-phase entry, while active cyclin A/Cdk triggers the progression through S-phase (Dulic *et al.*, 1992; Koff *et al.*, 1992; Elledge *et al.*, 1992; Cardoso *et al.*, 1993). In addition, the activity of both complexes is inhibited by p27 (Mateyak et al., 1999; Hengst and Reed, 1996). Thus, reduced Cdk2 activity, resulting from reduced availability of the positive cell cycle regulators cyclin A1 and cyclin E1 and/or increased levels of the negative regulator p27, may contribute to the impaired angiogenic capacities of HO-1-deficient EC, not only inhibiting their proliferation but also chemotactic migration, and subsequently resulting in vascular malformations.

In this study, human EC isolated from the umbilical vein were used as an *in vitro* model for studies on angiogenesis. The use of primary cells has the advantage that the characteristics of early passage cells in culture are closer to their parent EC when compared to cell lines, in terms of their gene expression profile and reponses to stimuli. They often more closely resemble the tissue they are taken from and they are more representative of the human population, due to the high degree of heterogeneity between preparations form different individuals. However, when studying angiogenesis, it this fundamental to consider the *in vivo* angiogenic characteristics of the cells

used, as some EC, including cells lining the human umblical vein, do not undergo extensive angiogenic sprouting *in vivo*. Moreover, it has to be considered that EC from different tissues are locally specialised in their functional characteristics. Cells express specific subsets of genes according to tissue origin as well as source, i.e. arterial versus venous EC and/or EC of the microvasculature versus cell of the macrovasculature. Thus, the use of HUVEC alone is not sufficient to model endothelial function in multiple vascular beds, and caution is needed when interpretating the results of *in vitro* studies, stressing the need for more sophisticated *in vivo* angiogenesis models.

We further started to elucidate a potential role for HO-1 and cyclin A1 in *in vivo* angiogenesis. siRNA-mediated inhibition of HO-1 partially inhibited VEGF-induced neovascularisation, and cyclin A1 silencing in Matrigel plugs resulted in a significant decrease in the vascularised area in response to VEGF. Conversely, adenoviral overexpression of HO-1 in Matrigel plugs significantly enhanced vessel formation when compared to plugs containing an empty control adenovirus. Interestingly, AdHO-1 also significantly increased vessel growth in cyclin A1 depleted plugs, so restoring the impaired angiogenic response seen with cyclin A1 deficiency. We therefore propose that HO-1 regulates expression of cyclin A1, which in turn is an essential contributor to the pro-angiogenic capacities of HO-1 during VEGF-driven angiogenesis. The role for HO-1 as an upstream effector of cyclin A1 is further supported by the finding that depletion of HO-1 significantly decreased cyclin A1 mRNA levels in murine aortic EC and human primary EC. Moreover, actinomycin D chase experiments demonstrated a significant reduction in cyclin A1 mRNA stability and subsequent a decrease in cyclin A1 half-lives in HO-1-deficient HUVEC, suggesting a potential function for HO-1 as a transcriptional regulator of gene expression.

The proteomic screen identified the intermediate filament vimentin as a potential downstream target of HO-1 in the regulation of angiogenesis. Vimentin is the major IF protein expressed in mesenchymal cells and is involved in integrin trafficking, cell adhesion and migration, and has been proposed to be an important mediator of signal transduction (Ivaska *et al.*, 2007). Interestingly, HO-1 and vimentin deficiency share similar characteristics. siRNA-mediated silencing of vimentin has been shown to reduce integrin-mediated endothelial cell adhesion (Tsuruta *et al.*, 2003). We show that HO-1 depletion significantly reduces $\alpha_v\beta_3$-dependent

adhesion of HUVEC when compared to control cells, an effect not resulting from altered $\alpha_v\beta_3$ surface expression levels. Thus, the impaired adherence of HO-1-deficient EC is not due to decreased availability of binding receptors but rather due to a functional defect, possibly affecting the capacity of integrins to recognise and bind to ECM ligands, and/or to signal to the cytoskeleton. Moreover, vimentin null mice are characterised by impaired wound healing due to defects in the capacity of fibroblast to migrate, and they show reduced corneal neovascularisation and hypoxia-induced retinal neovascularisation (Eckes *et al.*,1998; Eckes *et al.*, 2000; Lundkvist *et al.*, 2004). HO-1-deficient mice also demonstrate impaired neovascularisation during wound healing and HO-1-deficient EPC show defective homing and re-endothelisation of the retinal vasculature compared with wild-type cells following ischaemia (Deshane *et al.*, 2007; Grochot-Przeczek *et al.*, 2009).

These similarities between vimentin$^{-/-}$ and HO-1$^{-/-}$ animals make vimentin a promising candidate as a downstream effector of HO-1. To further investigate a potential function for vimentin in HO-1-driven angiogenesis, we initially validated the results obtained from the proteomic screen, but were not able to show an effect of HO-1 depletion on vimentin protein expression by conventional one-dimensional electrophoresis. This may be explained by technical limitations and reduced sensitivity of 1D electrophoresis when compared to 2D SDS-PAGE. 2D electrophoresis not only separates proteins according to their molecular weight, but also according to their isoelectric point in the second dimension, allowing the identification of post-translational modifications (Halligan, 2009). Vimentin is abundantly expressed and exists in many morphological states, isoforms and has numerous phosphorylation sites (Chang and Goldman 2004). Thus, changes in vimentin observed by 2D SDS-PAGE may represent differences in vimentin morphology, localisation, and/or phosphorylation. Indeed, using immunofluorescent staining we demonstrate differences in vimentin organisation and filament assembly between control cells and HO-1-depleted HUVEC. In control cells vimentin predominantly exists as non-filamentous particles or short vimentin filaments that reorganise into long mature vimentin filaments and form a dense, widespread filamentous network in response to VEGF, while HO-1 depletion inhibits or and/or delays VEGF-induced filament assembly.

Vimentin filament assembly is controlled by rapid phosphorylation and dephosphorylation of the protein (Eriksson et al., 2004; Chou et al., 2007), and thus defective filament assembly of HO-1-deficient cells might result from differential phosphorylation. In fact, Phos-tag™ SDS-PAGE revealed multiple lower molecular weight bands in response to VEGF in control cells, suggesting that VEGF phosphorylates vimentin at multiple sites. Interestingly, the appearance of multiple bands in response to VEGF was diminished by HO-1 depletion, suggesting that VEGF-induced vimentin phosphorylation is at least in part dependent on HO-1. However, the appearance and intensity of low molecular weight bands either in control or HO-1-deficient cells was not affected by treatment with a lambda phosphatase. This indicates that the observed bands do not represent new phosphorylated forms of vimentin and hence that HO-1 inhibition has no effect on vimentin phosphorylation. More likely, these lower molecular weight bands represent cleaved vimentin fragments. Kwak and colleagues recently demonstrated that growth factor-induced activation of calpains results in vimentin cleavage which in turn is required for angiogenic sprouting of EC (Kwak *et al.*, 2012). In line with these observations, we demonstrate calpain activation and vimentin cleavage in response to VEGF in control cells, as indicated by the presence of low molecular weight vimentin, ranging from 40-50 kDa, in addition to full-length vimentin (51 kDa). Interestingly, VEGF-induced calpain activation was significantly reduced by HO-1 depletion and vimentin fragmentation was inhibited in HO-1-deficient EC. Re-localisation of vimentin to cell edges in response to growth factors has also been shown to be dependent on calpain activity (Kwak *et al.*, 2012). Thus, impaired vimentin filament assembly, as observed in HO-1-deficient HUVEC, might also result from decreased calpain activation and subsequent inhibition of vimentin re-localisation to cell edges. This in turn may impair the angiogenic properties of endothelial cells in response to growth factor stimulation.

9.3. CONCLUSION

Herein we show an important role for the cytoprotective enzyme HO-1 in the regulation of *in vitro* and *in vivo* angiogenesis. HO-1 deficiency alters the angiogenic phenotype of endothelial cells at various levels; HO-1 inhibition attenuates endothelial proliferation in response to the mitogen VEGF and significantly impairs EC directional migration towards a pro-angiogenic stimulus. Furthermore, HO-1-deficient EC fail to form an intact tubular network in a 2D Matrigel assay and VEGF-driven neovascularisation of Matrigel plugs is partially reduced by siRNA-mediated HO-1 knockdown.

HO-1 deficiency prevents cell cycle progression. Moreover, HO-1-deficient proliferating and migrating EC exhibit altered cell cycle regulator expression, with reduced positive cell cycle regulators cyclin A1 and cyclin E1, but increased levels of the cell cycle inhibitor p27, resulting in reduced Cdk2 activity. We propose that the aberrant expression of cell cycle regulators and subsequent impaired Cdk2 activation of HO-1-deficient EC not only affects their proliferative capacity but also their migration, which in turn accounts for the impaired organisation into blood vessels.

We further propose a role for the intermediate filament vimentin as a downstream effector of HO-1 in the regulation of VEGF-mediated angiogenesis, where VEGF induced HO-1 is required expression for activation of the calcium-dependent protease calpain. Calpain activation in turn leads to cleaved, soluble, depolymerised vimentin localising to cell edges, thereby driving the angiogenic responses of EC.

The identification of cyclin A1, and other cell cycle regulators, as well as vimentin as HO-1 downstream effectors in the regulation of VEGF-mediated angiogenesis may assist studies in the development of new therapeutic agents for the manipulation of angiogenesis.

9.4. FUTURE WORK

The role of HO-1 during angiogenesis is complex and remains to be fully understood. The data obtained during the course of this thesis provide a better understanding of the functional importance of HO-1 in the regulation of VEGF-mediated angiogenesis but in turn raises several new questions:

1. How does HO-1 deficiency impair the chemotactic migration of endothelial cells? Has HO-1 inhibition an effect on small GTPase activation and signalling? Do changes in protrusion formation account for the impaired migratory phenotype of HO-1-deficient EC?
2. Does the halt in cell cycle progression account for the impaired migratory capacities of HO-1-deficient EC. Are expression levels of cell cycle regulators other than cyclin A1 affected by HO-1 depletion in migrating EC? What is the role for p27 in HO-1-driven migration?
3. Do the end-products of HO-1-mediated heme metabolism have an effect on cell cycle regulator expression and cell cycle progression?
4. How does cell cycle progression affect angiogenesis *in vivo*? Are cell cycle regulator expression levels altered in (i) HO-1 siRNA treated, or (ii) AdHO-1 treated Matrigel plugs?
5. Does HO-1 act as a transcriptional regulator of gene expression? If so, what are the mechanisms?
6. Is there a role for the intermediate filament vimentin in HO-1-driven angiogenesis *in vivo*? Is vimentin expression altered in HO-1 siRNA treated Matrigel plugs?
7. Do CO, biliverdin/bilirubin, and or ferritin have an effect on vimentin expression, morphology and localisation, and/or phosphorylation?
8. Is there a link between vimentin, cyclin A1 and HO-1?

CHAPTER 10 - REFERENCES

ABBOTT, N. J. 2002. Astrocyte-endothelial interactions and blood-brain barrier permeability. J Anat, 200, 629-38.

ABBOTT, N. J., PATABENDIGE, A. A., DOLMAN, D. E., YUSOF, S. R. & BEGLEY, D. J. 2010. Structure and function of the blood-brain barrier. Neurobiol Dis, 37, 13-25.

ABEDI, H. & ZACHARY, I. 1997. Vascular endothelial growth factor stimulates tyrosine phosphorylation and recruitment to new focal adhesions of focal adhesion kinase and paxillin in endothelial cells. J Biol Chem, 272, 15442-51.

ABRAHAM, D. & DASHWOOD, M. 2008. Endothelin--role in vascular disease. Rheumatology (Oxford), 47 Suppl 5, v23-4.

ABRAHAM, N. G., KUSHIDA, T., MCCLUNG, J., WEISS, M., QUAN, S., LAFARO, R., DARZYNKIEWICZ, Z. & WOLIN, M. 2003. Heme oxygenase-1 attenuates glucose-mediated cell growth arrest and apoptosis in human microvessel endothelial cells. Circulation Research, 93, 507-14.

ABRAHAM, N. G., SCAPAGNINI, G. & KAPPAS, A. 2003. Human heme oxygenase: cell cycle-dependent expression and DNA microarray identification of multiple gene responses after transduction of endothelial cells. J Cell Biochem, 90, 1098-111.

ABRAHAM, S., YEO, M., MONTERO-BALAGUER, M., PATERSON, H., DEJANA, E., MARSHALL, C. J. & MAVRIA, G. 2009. VE-Cadherin-mediated cell-cell interaction suppresses sprouting via signaling to MLC2 phosphorylation. Curr Biol, 19, 668-74.

ABU-GHAZALEH, R., KABIR, J., JIA, H., LOBO, M. & ZACHARY, I. 2001. Src mediates stimulation by vascular endothelial growth factor of the phosphorylation of focal adhesion kinase at tyrosine 861, and migration and anti-apoptosis in endothelial cells. Biochem J, 360, 255-64.

ACHEN, M. G., JELTSCH, M., KUKK, E., MAKINEN, T., VITALI, A., WILKS, A. F., ALITALO, K. & STACKER, S. A. 1998. Vascular endothelial growth factor D (VEGF-D) is a ligand for the tyrosine kinases VEGF receptor 2 (Flk1) and VEGF receptor 3 (Flt4). Proc Natl Acad Sci U S A, 95, 548-53.

ADAMS, R. H. & ALITALO, K. 2007. Molecular regulation of angiogenesis and lymphangiogenesis. Nat Rev Mol Cell Biol, 8, 464-78.

ADES, E. W., CANDAL, F. J., SWERLICK, R. A., GEORGE, V. G., SUMMERS, S., BOSSE, D. C. & LAWLEY, T. J. 1992. HMEC-1: establishment of an immortalized human microvascular endothelial cell line. J Invest Dermatol, 99, 683-90.

AGARWAL, S., ELLIOTT, J. R. & MANZI, S. 2009. Atherosclerosis risk factors in systemic lupus erythematosus. Curr Rheumatol Rep, 11, 241-7.

AIRD, W. C. 2007. Phenotypic heterogeneity of the endothelium: I. Structure, function, and mechanisms. Circulation Research, 100, 158-73.

AIRD, W. C. 2008. Endothelium in health and disease. Pharmacol Rep, 60, 139-43.

AIT-OUFELLA, H., MAURY, E., LEHOUX, S., GUIDET, B. & OFFENSTADT, G. 2010. The endothelium: physiological functions and role in microcirculatory failure during severe sepsis. Intensive Care Medicine, 36, 1286-1298.

AKHTAR, N., DICKERSON, E. B. & AUERBACH, R. 2002. The sponge/Matrigel angiogenesis assay. Angiogenesis, 5, 75-80.

ALAM, J., CAI, J. & SMITH, A. 1994. Isolation and characterization of the mouse heme oxygenase-1 gene. Distal 5' sequences are required for induction by heme or heavy metals. J Biol Chem, 269, 1001-9.

ALBELDA, S. M., MULLER, W. A., BUCK, C. A. & NEWMAN, P. J. 1991. Molecular and cellular properties of PECAM-1 (endoCAM/CD31): a novel vascular cell-cell adhesion molecule. J Cell Biol, 114, 1059-68.

ALI, F., HAMDULAY, S. S., KINDERLERER, A. R., BOYLE, J. J., LIDINGTON, E. A., YAMAGUCHI, T., SOARES, M. P., HASKARD, D. O., RANDI, A. M. & MASON, J. C. 2007. Statin-mediated cytoprotection of human vascular endothelial cells: a role for Kruppel-like factor 2-dependent induction of heme oxygenase-1. J Thromb Haemost, 5, 2537-46.

ALI, F., ZAKKAR, M., KARU, K., LIDINGTON, E. A., HAMDULAY, S. S., BOYLE, J. J., ZLOH, M., BAUER, A., HASKARD, D. O., EVANS, P. C. & MASON, J. C. 2009. Induction of the Cytoprotective Enzyme Heme Oxygenase-1 by Statins Is Enhanced in Vascular Endothelium Exposed to Laminar Shear Stress and Impaired by Disturbed Flow. Journal of Biological Chemistry, 284, 18882-18892.

ALMAGRO, S., DURMORT, C., CHERVIN-PETINOT, A., HEYRAUD, S., DUBOIS, M., LAMBERT, O., MAILLEFAUD, C., HEWAT, E., SCHAAL, J. P., HUBER, P. & GULINO-DEBRAC, D. 2010. The motor protein myosin-X transports VE-cadherin along filopodia to allow the formation of early endothelial cell-cell contacts. Mol Cell Biol, 30, 1703-17.

AMERSI, F., SHEN, X. D., ANSELMO, D., MELINEK, J., IYER, S., SOUTHARD, D. J., KATORI, M., VOLK, H. D., BUSUTTIL, R. W., BUELOW, R. & KUPIEC-WEGLINSKI, J. W. 2002. Ex vivo exposure to carbon monoxide prevents hepatic ischaemia/reperfusion injury through p38 MAP kinase pathway. Hepatology, 35, 815-23.

AMIT, Y. & BONEH, A. 1993. Bilirubin inhibits protein kinase C activity and protein kinase C-mediated phosphorylation of endogenous substrates in human skin fibroblasts. Clin Chim Acta, 223, 103-11.

ANDERSON, A. O. & ANDERSON, N. D. 1976. Lymphocyte emigration from high endothelial venules in rat lymph nodes. Immunology, 31, 731-48.

ANDERSON, N. D., ANDERSON, A. O. & WYLLIE, R. G. 1976. Specialized structure and metabolic activities of high endothelial venules in rat lymphatic tissues. Immunology, 31, 455-73.

ANDERSON, T. J., ELSTEIN, E., HABER, H. & CHARBONNEAU, F. 2000. Comparative study of ACE-inhibition, angiotensin II antagonism, and calcium channel blockade on flow-mediated vasodilation in patients with coronary disease (BANFF study). J Am Coll Cardiol, 35, 60-6.

ANDO, J., TSUBOI, H., KORENAGA, R., TAKADA, Y., TOYAMA-SORIMACHI, N., MIYASAKA, M. & KAMIYA, A. 1994. Shear stress inhibits adhesion of cultured mouse endothelial cells to lymphocytes by downregulating VCAM-1 expression. Am J Physiol, 267, C679-87.

ANDO, J. & YAMAMOTO, K. 2011. Effects of shear stress and stretch on endothelial function. Antioxid Redox Signal, 15, 1389-403.

APPLEWHITE, D. A., BARZIK, M., KOJIMA, S., SVITKINA, T. M., GERTLER, F. B. & BORISY, G. G. 2007. Ena/VASP proteins have an anti-capping independent function in filopodia formation. Mol Biol Cell, 18, 2579-91.

ARNAOUTOVA, I., GEORGE, J., KLEINMAN, H. K. & BENTON, G. 2009. The endothelial cell tube formation assay on basement membrane turns 20: state of the science and the art. Angiogenesis, 12, 267-74.

ARNOUT, J., HOYLAERTS, M. F. & LIJNEN, H. R. 2006. Haemostasis. Handb Exp Pharmacol, 1-41.

ASKARI, A. T., UNZEK, S., POPOVIC, Z. B., GOLDMAN, C. K., FORUDI, F., KIEDROWSKI, M., ROVNER, A., ELLIS, S. G., THOMAS, J. D., DICORLETO, P. E., TOPOL, E. J. & PENN, M. S. 2003. Effect of stromal-cell-derived factor 1 on stem-cell homing and tissue regeneration in ischaemic cardiomyopathy. Lancet, 362, 697-703.

AUGUSTIN, H. G., KOZIAN, D. H. & JOHNSON, R. C. 1994. Differentiation of Endothelial-Cells - Analysis of the Constitutive and Activated Endothelial-Cell Phenotypes. Bioessays, 16, 901-906.

BACH, F. H., HANCOCK, W. W. & FERRAN, C. 1997. Protective genes expressed in endothelial cells: a regulatory response to injury. Immunol Today, 18, 483-6.

BACHMANN, C., FISCHER, L., WALTER, U. & REINHARD, M. 1999. The EVH2 domain of the vasodilator-stimulated phosphoprotein mediates tetramerization, F-actin binding, and actin bundle formation. J Biol Chem, 274, 23549-57.

BAINBRIDGE, S. A. & SMITH, G. N. 2005. HO in pregnancy. Free Radic Biol Med, 38, 979-88.

BALLA, G., JACOB, H. S., BALLA, J., ROSENBERG, M., NATH, K., APPLE, F., EATON, J. W. & VERCELLOTTI, G. M. 1992. Ferritin - a Cytoprotective Antioxidant Strategem of Endothelium. Journal of Biological Chemistry, 267, 18148-18153.

BALLA, J., VERCELLOTTI, G. M., JENEY, V., YACHIE, A., VARGA, Z., JACOB, H. S., EATON, J. W. & BALLA, G. 2007. Heme, heme oxygenase, and ferritin: how the vascular endothelium survives (and dies) in an iron-rich environment. Antioxid Redox Signal, 9, 2119-37.

BARANANO, D. E., RAO, M., FERRIS, C. D. & SNYDER, S. H. 2002. Biliverdin reductase: a major physiologic cytoprotectant. Proc Natl Acad Sci U S A, 99, 16093-8.

BARBARA, N. P., WRANA, J. L. & LETARTE, M. 1999. Endoglin is an accessory protein that interacts with the signaling receptor complex of multiple members of the transforming growth factor-beta superfamily. J Biol Chem, 274, 584-94.

BARLOVIC, D. P., SORO-PAAVONEN, A. & JANDELEIT-DAHM, K. A. 2011. RAGE biology, atherosclerosis and diabetes. Clin Sci (Lond), 121, 43-55.

BARRETT, T. B. & BENDITT, E. P. 1988. Platelet-derived growth factor gene expression in human atherosclerotic plaques and normal artery wall. Proc Natl Acad Sci U S A, 85, 2810-4.

BARZIK, M., KOTOVA, T. I., HIGGS, H. N., HAZELWOOD, L., HANEIN, D., GERTLER, F. B. & SCHAFER, D. A. 2005. Ena/VASP proteins enhance actin polymerization in the presence of barbed end capping proteins. J Biol Chem, 280, 28653-62.

BAVARIA, M. N., RAY, R. M. & JOHNSON, L. R. 2011. The phosphorylation state of MRLC is polyamine dependent in intestinal epithelial cells. Am J Physiol Cell Physiol, 300, C164-75.

BAYLESS, K. J. & DAVIS, G. E. 2002. The Cdc42 and Rac1 GTPases are required for capillary lumen formation in three-dimensional extracellular matrices. J Cell Sci, 115, 1123-36.

BEAR, J. E. & GERTLER, F. B. 2009. Ena/VASP: towards resolving a pointed controversy at the barbed end. J Cell Sci, 122, 1947-53.

BEAR, J. E., LOUREIRO, J. J., LIBOVA, I., FASSLER, R., WEHLAND, J. & GERTLER, F. B. 2000. Negative regulation of fibroblast motility by Ena/VASP proteins. Cell, 101, 717-28.

BEAR, J. E., SVITKINA, T. M., KRAUSE, M., SCHAFER, D. A., LOUREIRO, J. J., STRASSER, G. A., MALY, I. V., CHAGA, O. Y., COOPER, J. A., BORISY, G. G. & GERTLER, F. B. 2002. Antagonism between Ena/VASP proteins and actin filament capping regulates fibroblast motility. Cell, 109, 509-21.

BECK, L., JR. & D'AMORE, P. A. 1997. Vascular development: cellular and molecular regulation. FASEB J, 11, 365-73.

BELLNER, L., MARTINELLI, L., HALILOVIC, A., PATIL, K., PURI, N., DUNN, M. W., REGAN, R. F. & SCHWARTZMAN, M. L. 2009. Heme oxygenase-2 deletion causes endothelial cell activation marked by oxidative stress, inflammation, and angiogenesis. J Pharmacol Exp Ther, 331, 925-32.

BELLONI, P. N. & TRESSLER, R. J. 1990. Microvascular endothelial cell heterogeneity: interactions with leukocytes and tumor cells. Cancer Metastasis Rev, 8, 353-89.

BENEDITO, R., ROCA, C., SORENSEN, I., ADAMS, S., GOSSLER, A., FRUTTIGER, M. & ADAMS, R. H. 2009. The notch ligands Dll4 and Jagged1 have opposing effects on angiogenesis. Cell, 137, 1124-35.

BEN-PORATH, I. & WEINBERG, R. A. 2004. When cells get stressed: an integrative view of cellular senescence. Journal of Clinical Investigation, 113, 8-13.

BERBERAT, P. O., DAMBRAUSKAS, Z., GULBINAS, A., GIESE, T., GIESE, N., KUNZLI, B., AUTSCHBACH, F., MEUER, S., BUCHLER, M. W. & FRIESS, H. 2005. Inhibition of heme oxygenase-1 increases responsiveness of pancreatic cancer cells to anticancer treatment. Clin Cancer Res, 11, 3790-8.

BERBERAT, P. O., KATORI, M., KACZMAREK, E., ANSELMO, D., LASSMAN, C., KE, B., SHEN, X., BUSUTTIL, R. W., YAMASHITA, K., CSIZMADIA, E., TYAGI, S., OTTERBEIN, L. E., BROUARD, S., TOBIASCH, E., BACH, F. H., KUPIEC-WEGLINSKI, J. W. & SOARES, M. P. 2003. Heavy chain ferritin acts as an anti-apoptotic gene that protects livers from ischaemia-reperfusion injury. Faseb Journal, 17, 1724-+.

BERGSTRAESSER, C., HOEGER, S., SONG, H., ERMANTRAUT, L., HOTTENROT, M., CZYMAI, T., SCHMIDT, M., GOEBELER, M., PONELIES, N., STICH, C., LOESEL, R., MOLEMA, G., SEELEN, M., VAN SON, W., YARD, B. A. & RAFAT, N. 2012. Inhibition of VCAM-1 expression in endothelial cells by CORM-3: the role of the ubiquitin-proteasome system, p38, and mitochondrial respiration. Free Radic Biol Med, 52, 794-802.

BESSON, A., GURIAN-WEST, M., SCHMIDT, A., HALL, A. & ROBERTS, J. M. 2004. p27Kip1 modulates cell migration through the regulation of RhoA activation. Genes Dev, 18, 862-76.

BIJL, M. 2003. Endothelial activation, endothelial dysfunction and premature atherosclerosis in systemic autoimmune diseases. Neth J Med, 61, 273-7.

BIKFALVI, A., CRAMER, E. M., TENZA, D. & TOBELEM, G. 1991. Phenotypic modulations of human umilical vein endothelial cells and human dermal fibroblasts using two angiogenic assays. Biol Cell, 72, 275-8.

BIRDSEY, G. M., DRYDEN, N. H., AMSELLEM, V., GEBHARDT, F., SAHNAN, K., HASKARD, D. O., DEJANA, E., MASON, J. C. & RANDI, A. M. 2008. Transcription factor Erg regulates angiogenesis and endothelial apoptosis through VE-cadherin. Blood, 111, 3498-506.

BISHOP, E. T., BELL, G. T., BLOOR, I. J., HENDRY, N. F. & WHEATLEY, D. N. 1999. An in vitro model of angiogenesis: basic features. Angiogenesis, 3, 335-44.

BLUME, C., BENZ, P. M., WALTER, U., HA, J., KEMP, B. E. & RENNE, T. 2007. AMP-activated protein kinase impairs endothelial actin cytoskeleton assembly by phosphorylating vasodilator-stimulated phosphoprotein. J Biol Chem, 282, 4601-12.

BOEHNING, D., MOON, C., SHARMA, S., HURT, K. J., HESTER, L. D., RONNETT, G. V., SHUGAR, D. & SNYDER, S. H. 2003. Carbon monoxide neurotransmission activated by CK2 phosphorylation of heme oxygenase-2. Neuron, 40, 129-37.

BOONYASRISAWAT, W., EBERLE, D., BACCI, S., ZHANG, Y. Y., NOLAN, D., GERVINO, E. V., JOHNSTONE, M. T., TRISCHITTA, V., SHOELSON, S. E. & DORIA, A. 2007. Tag polymorphisms at the A20 (TNFAIP3) locus are associated with lower gene expression and increased risk of coronary artery disease in type 2 diabetes. Diabetes, 56, 499-505.

BOUIS, D., KUSUMANTO, Y., MEIJER, C., MULDER, N. H. & HOSPERS, G. A. 2006. A review on pro- and anti-angiogenic factors as targets of clinical intervention. Pharmacol Res, 53, 89-103.

BRAKEBUSCH, C. & FASSLER, R. 2003. The integrin-actin connection, an eternal love affair. EMBO J, 22, 2324-33.

BRATT, J. & PALMBLAD, J. 1997. Cytokine-induced neutrophil-mediated injury of human endothelial cells. J Immunol, 159, 912-8.

BREIER, G., ALBRECHT, U., STERRER, S. & RISAU, W. 1992. Expression of vascular endothelial growth factor during embryonic angiogenesis and endothelial cell differentiation. Development, 114, 521-32.

BRETSCHER, M. S. 1996. Moving membrane up to the front of migrating cells. Cell, 85, 465-7.

BRINDLE, N. P., SAHARINEN, P. & ALITALO, K. 2006. Signaling and functions of angiopoietin-1 in vascular protection. Circulation Research, 98, 1014-23.

BROOKS, P. C., STROMBLAD, S., SANDERS, L. C., VON SCHALSCHA, T. L., AIMES, R. T., STETLER-STEVENSON, W. G., QUIGLEY, J. P. & CHERESH, D. A. 1996. Localization of matrix metalloproteinase MMP-2 to the surface of invasive cells by interaction with integrin alpha v beta 3. Cell, 85, 683-93.

BROOS, K., FEYS, H. B., DE MEYER, S. F., VANHOORELBEKE, K. & DECKMYN, H. 2011. Platelets at work in primary hemostasis. Blood Rev, 25, 155-67.

BROUARD, S., OTTERBEIN, L. E., ANRATHER, J., TOBIASCH, E., BACH, F. H., CHOI, A. M. K. & SOARES, M. P. 2000. Carbon monoxide generated by heme oxygenase 1 suppresses endothelial cell apoptosis. Journal of Experimental Medicine, 192, 1015-1025.

BRUNE, B. & ULLRICH, V. 1987. Inhibition of platelet aggregation by carbon monoxide is mediated by activation of guanylate cyclase. Molecular Pharmacology, 32, 497-504.

BUSSOLATI, B., AHMED, A., PEMBERTON, H., LANDIS, R. C., DI CARLO, F., HASKARD, D. O. & MASON, J. C. 2004. Bifunctional role for VEGF-induced heme oxygenase-1 in vivo: induction of angiogenesis and inhibition of leukocytic infiltration. Blood, 103, 761-6.

BUSSOLATI, B., DUNK, C., GROHMAN, M., KONTOS, C. D., MASON, J. & AHMED, A. 2001. Vascular endothelial growth factor receptor-1 modulates vascular endothelial growth factor-mediated angiogenesis via nitric oxide. Am J Pathol, 159, 993-1008.

BUSSOLATI, B. & MASON, J. C. 2006. Dual role of VEGF-induced heme-oxygenase-1 in angiogenesis. Antioxid Redox Signal, 8, 1153-63.

BUTCHER, E. C. 1991. Leukocyte-endothelial cell recognition: three (or more) steps to specificity and diversity. Cell, 67, 1033-6.

BUTT, E., ABEL, K., KRIEGER, M., PALM, D., HOPPE, V., HOPPE, J. & WALTER, U. 1994. cAMP- and cGMP-dependent protein kinase phosphorylation sites of the focal adhesion vasodilator-stimulated phosphoprotein (VASP) in vitro and in intact human platelets. J Biol Chem, 269, 14509-17.

BUYSSCHAERT, I., CARMELIET, P. & DEWERCHIN, M. 2007. Clinical and fundamental aspects of angiogenesis and anti-angiogenesis. Acta Clin Belg, 62, 162-9.

CALDERWOOD, D. A. 2004. Integrin activation. J Cell Sci, 117, 657-66.

CAMPISI, J. & D'ADDA DI FAGAGNA, F. 2007. Cellular senescence: when bad things happen to good cells. Nat Rev Mol Cell Biol, 8, 729-40.

CARDOSO, M. C., LEONHARDT, H. & NADAL-GINARD, B. 1993. Reversal of terminal differentiation and control of DNA replication: cyclin A and Cdk2 specifically localize at subnuclear sites of DNA replication. Cell, 74, 979-92.

CARMELIET, P. 2000. Mechanisms of angiogenesis and arteriogenesis. Nat Med, 6, 389-95.

CARMELIET, P. 2005. Angiogenesis in life, disease and medicine. Nature, 438, 932-6.

CARMELIET, P. & COLLEN, D. 1995. Role of the plasminogen/plasmin system in thrombosis, hemostasis, restenosis and atherosclerosis evaluation in transgenic animals. Trends Cardiovasc Med, 5, 117-22.

CARMELIET, P., DE SMET, F., LOGES, S. & MAZZONE, M. 2009. Branching morphogenesis and antiangiogenesis candidates: tip cells lead the way. Nat Rev Clin Oncol, 6, 315-26.

CARMELIET, P., FERREIRA, V., BREIER, G., POLLEFEYT, S., KIECKENS, L., GERTSENSTEIN, M., FAHRIG, M., VANDENHOECK, A., HARPAL, K., EBERHARDT, C., DECLERCQ, C., PAWLING, J., MOONS, L., COLLEN, D., RISAU, W. & NAGY, A. 1996. Abnormal blood vessel development and lethality in embryos lacking a single VEGF allele. Nature, 380, 435-9.

CARMELIET, P., LAMPUGNANI, M. G., MOONS, L., BREVIARIO, F., COMPERNOLLE, V., BONO, F., BALCONI, G., SPAGNUOLO, R., OOSTHUYSE, B., DEWERCHIN, M., ZANETTI, A., ANGELLILO, A., MATTOT, V., NUYENS, D., LUTGENS, E., CLOTMAN, F., DE RUITER, M. C., GITTENBERGER-DE GROOT, A., POELMANN, R., LUPU, F., HERBERT, J. M., COLLEN, D. & DEJANA, E. 1999. Targeted deficiency or cytosolic truncation of the VE-cadherin gene in mice impairs VEGF-mediated endothelial survival and angiogenesis. Cell, 98, 147-57.

CARO, C. G., FITZ-GERALD, J. M. & SCHROTER, R. C. 1969. Arterial wall shear and distribution of early atheroma in man. Nature, 223, 1159-60.

CAVALLARO, U. & CHRISTOFORI, G. 2000. Molecular mechanisms of tumor angiogenesis and tumor progression. J Neurooncol, 50, 63-70.

CELLETTI, F. L., WAUGH, J. M., AMABILE, P. G., BRENDOLAN, A., HILFIKER, P. R. & DAKE, M. D. 2001. Vascular endothelial growth factor enhances atherosclerotic plaque progression. Nat Med, 7, 425-9.

CEPONIS, A., KONTTINEN, Y. T., IMAI, S., TAMULAITIENE, M., LI, T. F., XU, J. W., HIETANEN, J., SANTAVIRTA, S. & FASSBENDER, H. G. 1998. Synovial lining, endothelial and inflammatory mononuclear cell proliferation in synovial membranes in psoriatic and reactive arthritis: a comparative quantitative morphometric study. Br J Rheumatol, 37, 170-8.

CHANG, L. & GOLDMAN, R. D. 2004. Intermediate filaments mediate cytoskeletal crosstalk. Nat Rev Mol Cell Biol, 5, 601-13.

CHAPPELL, D. C., VARNER, S. E., NEREM, R. M., MEDFORD, R. M. & ALEXANDER, R. W. 1998. Oscillatory shear stress stimulates adhesion molecule expression in cultured human endothelium. Circulation Research, 82, 532-539.

CHATZIZISIS, Y. S., COSKUN, A. U., JONAS, M., EDELMAN, E. R., FELDMAN, C. L. & STONE, P. H. 2007. Role of endothelial shear stress in the natural history of coronary atherosclerosis and vascular remodeling: molecular, cellular, and vascular behavior. J Am Coll Cardiol, 49, 2379-93.

CHEN, D., WALSH, K. & WANG, J. 2000. Regulation of cdk2 activity in endothelial cells that are inhibited from growth by cell contact. Arterioscler Thromb Vasc Biol, 20, 629-35.

CHEN, H. C. 2005. Boyden chamber assay. Methods Mol Biol, 294, 15-22.

CHEN, H. J., LEVINE, Y. C., GOLAN, D. E., MICHEL, T. & LIN, A. J. 2008. Atrial natriuretic peptide-initiated cGMP pathways regulate vasodilator-stimulated phosphoprotein phosphorylation and angiogenesis in vascular endothelium. Journal of Biological Chemistry, 283, 4439-4447.

CHEN, K. & MAINES, M. D. 2000. Nitric oxide induces heme oxygenase-1 via mitogen-activated protein kinases ERK and p38. Cell Mol Biol (Noisy-le-grand), 46, 609-17.

CHEN, S., SEGA, M. & AGARWAL, A. 2004. "Lumen digestion" technique for isolation of aortic endothelial cells from heme oxygenase-1 knockout mice. Biotechniques, 37, 84-6, 88-9.

CHEN, X. L., VARNER, S. E., RAO, A. S., GREY, J. Y., THOMAS, S., COOK, C. K., WASSERMAN, M. A., MEDFORD, R. M., JAISWAL, A. K. & KUNSCH, C. 2003. Laminar flow induction of antioxidant response element-mediated genes in endothelial cells. A novel anti-inflammatory mechanism. J Biol Chem, 278, 703-11.

CHEN, Y. H., LIN, S. J., LIN, M. W., TSAI, H. L., KUO, S. S., CHEN, J. W., CHARNG, M. J., WU, T. C., CHEN, L. C., DING, Y. A., PAN, W. H., JOU, Y. S. & CHAU, L. Y. 2002. Microsatellite polymorphism in promoter of heme oxygenase-1 gene is associated with susceptibility to coronary artery disease in type 2 diabetic patients. Hum Genet, 111, 1-8.

CHENG, C., TEMPEL, D., VAN HAPEREN, R., VAN DER BAAN, A., GROSVELD, F., DAEMEN, M. J., KRAMS, R. & DE CROM, R. 2006. Atherosclerotic lesion size and vulnerability are determined by patterns of fluid shear stress. Circulation, 113, 2744-53.

CHENG, C., VAN HAPEREN, R., DE WAARD, M., VAN DAMME, L. C., TEMPEL, D., HANEMAAIJER, L., VAN CAPPELLEN, G. W., BOS, J., SLAGER, C. J., DUNCKER, D. J., VAN DER STEEN, A. F., DE CROM, R. & KRAMS, R. 2005. Shear stress affects the intracellular distribution of eNOS: direct demonstration by a novel in vivo technique. Blood, 106, 3691-8.

CHENG, Y. F., CLYMAN, R. I., ENENSTEIN, J., WALEH, N., PYTELA, R. & KRAMER, R. H. 1991. The integrin complex alpha v beta 3 participates in the adhesion of microvascular endothelial cells to fibronectin. Exp Cell Res, 194, 69-77.

CHHABRA, E. S. & HIGGS, H. N. 2007. The many faces of actin: matching assembly factors with cellular structures. Nat Cell Biol, 9, 1110-21.

CHIN, B. Y., JIANG, G., WEGIEL, B., WANG, H. J., MACDONALD, T., ZHANG, X. C., GALLO, D., CSZIMADIA, E., BACH, F. H., LEE, P. J. & OTTERBEIN, L. E. 2007. Hypoxia-inducible factor 1alpha stabilization by carbon monoxide results in cytoprotective preconditioning. Proc Natl Acad Sci U S A, 104, 5109-14.

CHOI, A. M. & OTTERBEIN, L. E. 2002. Emerging role of carbon monoxide in physiologic and pathophysiologic states. Antioxid Redox Signal, 4, 227-8.

CHOU, Y. H., FLITNEY, F. W., CHANG, L., MENDEZ, M., GRIN, B. & GOLDMAN, R. D. 2007. The motility and dynamic properties of intermediate filaments and their constituent proteins. Exp Cell Res, 313, 2236-43.

CHUA, C. C., HAMDY, R. C. & CHUA, B. H. 1998. Upregulation of vascular endothelial growth factor by H2O2 in rat heart endothelial cells. Free Radic Biol Med, 25, 891-7.

CINES, D. B., POLLAK, E. S., BUCK, C. A., LOSCALZO, J., ZIMMERMAN, G. A., MCEVER, R. P., POBER, J. S., WICK, T. M., KONKLE, B. A., SCHWARTZ, B. S., BARNATHAN, E. S., MCCRAE, K. R., HUG, B. A., SCHMIDT, A. M. & STERN, D. M. 1998. Endothelial cells in physiology and in the pathophysiology of vascular disorders. Blood, 91, 3527-61.

CISOWSKI, J., LOBODA, A., JOZKOWICZ, A., CHEN, S., AGARWAL, A. & DULAK, J. 2005. Role of heme oxygenase-1 in hydrogen peroxide-induced VEGF synthesis: effect of HO-1 knockout. Biochem Biophys Res Commun, 326, 670-6.

CLEAVER, O. & MELTON, D. A. 2003. Endothelial signaling during development. Nat Med, 9, 661-8.

COFFMAN, L. G., PARSONAGE, D., D'AGOSTINO, R., JR., TORTI, F. M. & TORTI, S. V. 2009. Regulatory effects of ferritin on angiogenesis. Proc Natl Acad Sci U S A, 106, 570-5.

COHEN, P. T. & COHEN, P. 1989. Discovery of a protein phosphatase activity encoded in the genome of bacteriophage lambda. Probable identity with open reading frame 221. Biochem J, 260, 931-4.

CONNOLLY, J. O., Simpson, N. HEWLETT, L. & HALL, A. 2002. Rac regulates endothelial morphogenesis and capillary formation. Mol Biol Cell, 13, 2474-85.

COLAS, C. & ORTIZ DE MONTELLANO, P. R. 2003. Autocatalytic radical reactions in physiological prosthetic heme modification. Chem Rev, 103, 2305-32.

COLOMBRITA, C., LOMBARDO, G., SCAPAGNINI, G. & ABRAHAM, N. G. 2003. Heme oxygenase-1 expression levels are cell cycle dependent. Biochem Biophys Res Commun, 308, 1001-8.

COMERFORD, K. M., LAWRENCE, D. W., SYNNESTVEDT, K., LEVI, B. P. & COLGAN, S. P. 2002. Role of vasodilator-stimulated phosphoprotein in PKA-induced changes in endothelial junctional permeability. FASEB J, 16, 583-5.

COOPER, J. T., STROKA, D. M., BROSTJAN, C., PALMETSHOFER, A., BACH, F. H. & FERRAN, C. 1996. A20 blocks endothelial cell activation through a NF-kappaB-dependent mechanism. J Biol Chem, 271, 18068-73.

CORNBLATT, B. S., YE, L., DINKOVA-KOSTOVA, A. T., ERB, M., FAHEY, J. W., SINGH, N. K., CHEN, M. S., STIERER, T., GARRETT-MAYER, E., ARGANI, P., DAVIDSON, N. E., TALALAY, P., KENSLER, T. W. & VISVANATHAN, K. 2007. Preclinical and clinical evaluation of sulforaphane for chemoprevention in the breast. Carcinogenesis, 28, 1485-90.

CORY, A. H., OWEN, T. C., BARLTROP, J. A. & CORY, J. G. 1991. Use of an aqueous soluble tetrazolium/formazan assay for cell growth assays in culture. Cancer Commun, 3, 207-12.

COUGHLIN, S. R. 1999. How the protease thrombin talks to cells. Proc Natl Acad Sci U S A, 96, 11023-7.

COWAN, K. J. & STOREY, K. B. 2003. Mitogen-activated protein kinases: new signaling pathways functioning in cellular responses to environmental stress. J Exp Biol, 206, 1107-15.

CUDMORE, M., AHMAD, S., AL-ANI, B., FUJISAWA, T., COXALL, H., CHUDASAMA, K., DEVEY, L. R., WIGMORE, S. J., ABBAS, A., HEWETT, P. W. & AHMED, A. 2007. Negative regulation of soluble Flt-1 and soluble endoglin release by heme oxygenase-1. Circulation, 115, 1789-97.

CYBULSKY, M. I., FRIES, J. W., WILLIAMS, A. J., SULTAN, P., EDDY, R., BYERS, M., SHOWS, T., GIMBRONE, M. A., JR. & COLLINS, T. 1991. Gene structure, chromosomal location, and basis for alternative mRNA splicing of the human VCAM1 gene. Proc Natl Acad Sci U S A, 88, 7859-63.

DABEK, J., KULACH, A., MONASTYRSKA-CUP, B. & GASIOR, Z. 2006. Transforming growth factor beta and cardiovascular diseases: the other facet of the 'protective cytokine'. Pharmacological Reports, 58, 799-805.

D'ADDA DI FAGAGNA, F., REAPER, P. M., CLAY-FARRACE, L., FIEGLER, H., CARR, P., VON ZGLINICKI, T., SARETZKI, G., CARTER, N. P. & JACKSON, S. P. 2003. A DNA damage checkpoint response in telomere-initiated senescence. Nature, 426, 194-8.

DAHL, D., RUEGER, D. C., BIGNAMI, A., WEBER, K. & OSBORN, M. 1981. Vimentin, the 57 000 molecular weight protein of fibroblast filaments, is the major cytoskeletal component in immature glia. Eur J Cell Biol, 24, 191-6.

DATLA, S. R., DUSTING, G. J., MORI, T. A., TAYLOR, C. J., CROFT, K. D. & JIANG, F. 2007. Induction of heme oxygenase-1 in vivo suppresses NADPH oxidase-derived oxidative stress. Hypertension, 50, 636-642.

DAVIES, P. F. 1995. Flow-mediated endothelial mechanotransduction. Physiol Rev, 75, 519-60.

DAVIES, P. F. 2000. Spatial haemodynamics, the endothelium, and focal atherogenesis: a cell cycle link? Circulation Research, 86, 114-6.

DAVIES, P. F., REMUZZI, A., GORDON, E. J., DEWEY, C. F., JR. & GIMBRONE, M. A., JR. 1986. Turbulent fluid shear stress induces vascular endothelial cell turnover in vitro. Proc Natl Acad Sci U S A, 83, 2114-7.

DAVIS, G. E. 1992. Affinity of integrins for damaged extracellular matrix: alpha v beta 3 binds to denatured collagen type I through RGD sites. Biochem Biophys Res Commun, 182, 1025-31.

DAVIS, G. E. & BAYLESS, K. J. 2003. An integrin and Rho GTPase-dependent pinocytic vacuole mechanism controls capillary lumen formation in collagen and fibrin matrices. Microcirculation, 10, 27-44.

DAVIS, G. E. & SENGER, D. R. 2005. Endothelial extracellular matrix: biosynthesis, remodeling, and functions during vascular morphogenesis and neovessel stabilization. Circulation Research, 97, 1093-107.

DAVIS, S., ALDRICH, T. H., JONES, P. F., ACHESON, A., COMPTON, D. L., JAIN, V., RYAN, T. E., BRUNO, J., RADZIEJEWSKI, C., MAISONPIERRE, P. C. & YANCOPOULOS, G. D. 1996. Isolation of angiopoietin-1, a ligand for the TIE2 receptor, by secretion-trap expression cloning. Cell, 87, 1161-9.

DE CATERINA, R., LIBBY, P., PENG, H. B., THANNICKAL, V. J., RAJAVASHISTH, T. B., GIMBRONE, M. A., JR., SHIN, W. S. & LIAO, J. K. 1995. Nitric oxide decreases cytokine-induced endothelial activation. Nitric oxide selectively reduces endothelial expression of adhesion molecules and proinflammatory cytokines. Journal of Clinical Investigation, 96, 60-8.

DE DOMENICO, I., WARD, D. M. & KAPLAN, J. 2009. Serum ferritin regulates blood vessel formation: a role beyond iron storage. Proc Natl Acad Sci U S A, 106, 1683-4.

DE KEULENAER, G. W., CHAPPELL, D. C., ISHIZAKA, N., NEREM, R. M., ALEXANDER, R. W. & GRIENDLING, K. K. 1998. Oscillatory and steady laminar shear stress differentially affect human endothelial redox state: role of a superoxide-producing NADH oxidase. Circulation Research, 82, 1094-101.

DE NUCCI, G., GRYGLEWSKI, R. J., WARNER, T. D. & VANE, J. R. 1988. Receptor-mediated release of endothelium-derived relaxing factor and prostacyclin from bovine aortic endothelial cells is coupled. Proc Natl Acad Sci U S A, 85, 2334-8.

DE SMET, F., SEGURA, I., DE BOCK, K., HOHENSINNER, P. J. & CARMELIET, P. 2009. Mechanisms of vessel branching: filopodia on endothelial tip cells lead the way. Arterioscler Thromb Vasc Biol, 29, 639-49.

DE VRIES, C., ESCOBEDO, J. A., UENO, H., HOUCK, K., FERRARA, N. & WILLIAMS, L. T. 1992. The fms-like tyrosine kinase, a receptor for vascular endothelial growth factor. Science, 255, 989-91.

DEBACQ-CHAINIAUX, F., ERUSALIMSKY, J. D., CAMPISI, J. & TOUSSAINT, O. 2009. Protocols to detect senescence-associated beta-galactosidase (SA-betagal) activity, a biomarker of senescent cells in culture and in vivo. Nat Protoc, 4, 1798-806.

DEFILIPPI, P., OLIVO, C., VENTURINO, M., DOLCE, L., SILENGO, L. & TARONE, G. 1999. Actin cytoskeleton organization in response to integrin-mediated adhesion. Microscopy Research and Technique, 47, 67-78.

DEGESE, M. S., MENDIZABAL, J. E., GANDINI, N. A., GUTKIND, J. S., MOLINOLO, A., HEWITT, S. M., CURINO, A. C., COSO, O. A. & FACCHINETTI, M. M. 2012. Expression of heme oxygenase-1 in non-small cell lung cancer (NSCLC) and its correlation with clinical data. Lung Cancer, 77, 168-75.

DEJANA, E., CORADA, M. & LAMPUGNANI, M. G. 1995. Endothelial cell-to-cell junctions. FASEB J, 9, 910-8.

DEJANA, E. & LAURI, D. 1990. Biochemical and functional characteristics of integrins: a new family of adhesive receptors present in hematopoietic cells. Haematologica, 75, 1-6.

DEJANA, E., TOURNIER-LASSERVE, E. & WEINSTEIN, B. M. 2009. The control of vascular integrity by endothelial cell junctions: molecular basis and pathological implications. Dev Cell, 16, 209-21.

DEKKER, R. J., VAN SOEST, S., FONTIJN, R. D., SALAMANCA, S., DE GROOT, P. G., VANBAVEL, E., PANNEKOEK, H. & HORREVOETS, A. J. 2002. Prolonged fluid shear stress induces a distinct set of endothelial cell genes, most specifically lung Kruppel-like factor (KLF2). Blood, 100, 1689-98.

DEL ZOPPO, G. J. & MILNER, R. 2006. Integrin-matrix interactions in the cerebral microvasculature. Arterioscler Thromb Vasc Biol, 26, 1966-75.

DELA PAZ, N. G., WALSHE, T. E., LEACH, L. L., SAINT-GENIEZ, M. & D'AMORE, P. A. 2012. Role of shear-stress-induced VEGF expression in endothelial cell survival. J Cell Sci, 125, 831-43.

DELISSER, H. M., NEWMAN, P. J. & ALBELDA, S. M. 1994. Molecular and functional aspects of PECAM-1/CD31. Immunol Today, 15, 490-5.

DENG, Y. M., WU, B. J., WITTING, P. K. & STOCKER, R. 2004. Probucol protects against smooth muscle cell proliferation by upregulating heme oxygenase-1. Circulation, 110, 1855-60.

DENICOURT, C. & DOWDY, S. F. 2004. Cip/Kip proteins: more than just CDKs inhibitors. Genes Dev, 18, 851-5.

DENNERY, P. A.2005. Novel Functions of Heme Oxygenase Protein. In Heme Oxygenase The Elegant Orchestration of its Products in Medicine, p. 127-140.

DENNERY, P. A., MCDONAGH, A. F., SPITZ, D. R., RODGERS, P. A. & STEVENSON, D. K. 1995. Hyperbilirubinemia results in reduced oxidative injury in neonatal Gunn rats exposed to hyperoxia. Free Radic Biol Med, 19, 395-404.

DERAMAUDT, B. M., BRAUNSTEIN, S., REMY, P. & ABRAHAM, N. G. 1998. Gene transfer of human heme oxygenase into coronary endothelial cells potentially promotes angiogenesis. J Cell Biochem, 68, 121-7.

DERAMAUDT, B. M., REMY, P. & ABRAHAM, N. G. 1999. Upregulation of human heme oxygenase gene expression by Ets-family proteins. J Cell Biochem, 72, 311-21.

DERYNCK, R. & ZHANG, Y. E. 2003. Smad-dependent and Smad-independent pathways in TGF-beta family signalling. Nature, 425, 577-584.

DESHANE, J., CHEN, S., CABALLERO, S., GROCHOT-PRZECZEK, A., WAS, H., LI CALZI, S., LACH, R., HOCK, T. D., CHEN, B., HILL-KAPTURCZAK, N., SIEGAL, G. P., DULAK, J., JOZKOWICZ, A., GRANT, M. B. & AGARWAL, A. 2007. Stromal cell-derived factor 1 promotes angiogenesis via a heme oxygenase 1-dependent mechanism. J Exp Med, 204, 605-18.

DEWEY, C. F., JR., BUSSOLARI, S. R., GIMBRONE, M. A., JR. & DAVIES, P. F. 1981. The dynamic response of vascular endothelial cells to fluid shear stress. J Biomech Eng, 103, 177-85.

DICHIARA, M. R., KIELY, J. M., GIMBRONE, M. A., LEE, M. E., PERRELLA, M. A. & TOPPER, J. N. 2000. Inhibition of E-selectin gene expression by transforming growth factor beta in endothelial cells involves coactivator integration of Smad and nuclear factor kappa B-mediated signals. Journal of Experimental Medicine, 192, 695-704.

DIMMELER, S., DERNBACH, E. & ZEIHER, A. M. 2000. Phosphorylation of the endothelial nitric oxide synthase at ser-1177 is required for VEGF-induced endothelial cell migration. FEBS Lett, 477, 258-62.

DIMMELER, S., FLEMING, I., FISSLTHALER, B., HERMANN, C., BUSSE, R. & ZEIHER, A. M. 1999. Activation of nitric oxide synthase in endothelial cells by Akt-dependent phosphorylation. Nature, 399, 601-5.

DONOVAN, D., BROWN, N. J., BISHOP, E. T. & LEWIS, C. E. 2001. Comparison of three in vitro human angiogenesis assays with capillaries formed in vivo. Angiogenesis, 4, 113-25.

DORE, S., TAKAHASHI, M., FERRIS, C. D., ZAKHERY, R., HESTER, L.D. & GUASTELLA, D. 1999. Bilirubin, formed by activation of heme oxygenase-2, protects neurons against oxidative stress injury. Proc Natl Acad Sci U S A, 96, 2445-50.

DUCKERS, H. J., BOEHM, M., TRUE, A. L., YET, S. F., SAN, H., PARK, J. L., CLINTON WEBB, R., LEE, M. E., NABEL, G. J. & NABEL, E. G. 2001. Heme oxygenase-1 protects against vascular constriction and proliferation. Nat Med, 7, 693-8.

DULAK, J., DESHANE, J., JOZKOWICZ, A. & AGARWAL, A. 2008. Heme oxygenase-1 and carbon monoxide in vascular pathobiology: focus on angiogenesis. Circulation, 117, 231-41.

DULAK, J. & JOZKOWICZ, A. 2003. Regulation of vascular endothelial growth factor synthesis by nitric oxide: facts and controversies. Antioxid Redox Signal, 5, 123-32.

DULAK, J., JOZKOWICZ, A., FORESTI, R., KASZA, A., FRICK, M., HUK, I., GREEN, C. J., PACHINGER, O., WEIDINGER, F. & MOTTERLINI, R. 2002. Heme oxygenase activity modulates vascular endothelial growth factor synthesis in vascular smooth muscle cells. Antioxid Redox Signal, 4, 229-40.

DULAK, J., LOBODA, A. & JOZKOWICZ, A. 2008. Effect of heme oxygenase-1 on vascular function and disease. Curr Opin Lipidol, 19, 505-12.

DULAK, J., LOBODA, A., ZAGORSKA, A. & JOZKOWICZ, A. 2004. Complex role of heme oxygenase-1 in angiogenesis. Antioxid Redox Signal, 6, 858-66.

DULIC, V., KAUFMANN, W. K., WILSON, S. J., TLSTY, T. D., LEES, E., HARPER, J. W., ELLEDGE, S. J. & REED, S. I. 1994. p53-dependent inhibition of cyclin-dependent kinase activities in human fibroblasts during radiation-induced G1 arrest. Cell, 76, 1013-23.

DULIC, V., LEES, E. & REED, S. I. 1992. Association of human cyclin E with a periodic G1-S phase protein kinase. Science, 257, 1958-61.

DUMONT, D. J., FONG, G. H., PURI, M. C., GRADWOHL, G., ALITALO, K. & BREITMAN, M. L. 1995. Vascularization of the mouse embryo: a study of flk-1, tek, tie, and vascular endothelial growth factor expression during development. Dev Dyn, 203, 80-92.

DYSON, N. 1998. The regulation of E2F by pRB-family proteins. Genes Dev, 12, 2245-62.

ECKES, B., COLUCCI-GUYON, E., SMOLA, H., NODDER, S., BABINET, C., KRIEG, T. & MARTIN, P. 2000. Impaired wound healing in embryonic and adult mice lacking vimentin. J Cell Sci, 113 (Pt 13), 2455-62.

ECKES, B., DOGIC, D., COLUCCI-GUYON, E., WANG, N., MANIOTIS, A., INGBER, D., MERCKLING, A., LANGA, F., AUMAILLEY, M., DELOUVEE, A., KOTELIANSKY, V., BABINET, C. & KRIEG, T. 1998. Impaired mechanical stability, migration and contractile capacity in vimentin-deficient fibroblasts. J Cell Sci, 111 (Pt 13), 1897-907.

EILKEN, H. M. & ADAMS, R. H. 2010. Dynamics of endothelial cell behavior in sprouting angiogenesis. Curr Opin Cell Biol, 22, 617-25.

ELBIRT, K. K. & BONKOVSKY, H. L. 1999. Heme oxygenase: recent advances in understanding its regulation and role. Proc Assoc Am Physicians, 111, 438-47.

EL-DEIRY, W. S., HARPER, J. W., O'CONNOR, P. M., VELCULESCU, V. E., CANMAN, C. E., JACKMAN, J., PIETENPOL, J. A., BURRELL, M., HILL, D. E., WANG, Y. & ET AL. 1994. WAF1/CIP1 is induced in p53-mediated G1 arrest and apoptosis. Cancer Res, 54, 1169-74.

ELLEDGE, S. J., RICHMAN, R., HALL, F. L., WILLIAMS, R. T., LODGSON, N. & HARPER, J. W. 1992. CDK2 encodes a 33-kDa cyclin A-associated protein kinase and is expressed before CDC2 in the cell cycle. Proc Natl Acad Sci U S A, 89, 2907-11.

ENDEMANN, D. H. & SCHIFFRIN, E. L. 2004. Endothelial dysfunction. J Am Soc Nephrol, 15, 1983-92.

ERIKSSON, J. E., BRAUTIGAN, D. L., VALLEE, R., OLMSTED, J., FUJIKI, H. & GOLDMAN, R. D. 1992. Cytoskeletal integrity in interphase cells requires protein phosphatase activity. Proc Natl Acad Sci U S A, 89, 11093-7.

ERIKSSON, J. E., HE, T., TREJO-SKALLI, A. V., HARMALA-BRASKEN, A. S., HELLMAN, J., CHOU, Y. H. & GOLDMAN, R. D. 2004. Specific in vivo phosphorylation sites determine the assembly dynamics of vimentin intermediate filaments. J Cell Sci, 117, 919-32.

ERUSALIMSKY, J. D. 2009. Vascular endothelial senescence: from mechanisms to pathophysiology. J Appl Physiol, 106, 326-32.

ESMON, C. T. 1992. The protein C anticoagulant pathway. Arterioscler Thromb, 12, 135-45.

ESMON, C. T. 1995. Thrombomodulin as a model of molecular mechanisms that modulate protease specificity and function at the vessel surface. FASEB J, 9, 946-55.

ESSER, S., LAMPUGNANI, M. G., CORADA, M., DEJANA, E. & RISAU, W. 1998. Vascular endothelial growth factor induces VE-cadherin tyrosine phosphorylation in endothelial cells. J Cell Sci, 111 (Pt 13), 1853-65.

EXNER, M., MINAR, E., WAGNER, O. & SCHILLINGER, M. 2004. The role of heme oxygenase-1 promoter polymorphisms in human disease. Free Radic Biol Med, 37, 1097-104.

FABBRI, M., BIANCHI, E., FUMAGALLI, L. & PARDI, R. 1999. Regulation of lymphocyte traffic by adhesion molecules. Inflamm Res, 48, 239-46.

FAN, X. C. & STEITZ, J. A. 1998. Overexpression of HuR, a nuclear-cytoplasmic shuttling protein, increases the in vivo stability of ARE-containing mRNAs. EMBO J, 17, 3448-60.

FANG, J., SAWA, T., AKAIKE, T., AKUTA, T., SAHOO, S. K., KHALED, G., HAMADA, A. & MAEDA, H. 2003. In vivo antitumor activity of pegylated zinc protoporphyrin: targeted inhibition of heme oxygenase in solid tumor. Cancer Res, 63, 3567-74.

FANTIN, A., VIEIRA, J. M., GESTRI, G., DENTI, L., SCHWARZ, Q., PRYKHOZHIJ, S., PERI, F., WILSON, S. W. & RUHRBERG, C. 2010. Tissue macrophages act as cellular chaperones for vascular anastomosis downstream of VEGF-mediated endothelial tip cell induction. Blood, 116, 829-40.

FAVA, R. A., OLSEN, N. J., SPENCER-GREEN, G., YEO, K. T., YEO, T. K., BERSE, B., JACKMAN, R. W., SENGER, D. R., DVORAK, H. F. & BROWN, L. F. 1994. Vascular permeability factor/endothelial growth factor (VPF/VEGF): accumulation and expression in human synovial fluids and rheumatoid synovial tissue. J Exp Med, 180, 341-6.

FAVATIER, F. & POLLA, B. S. 2001. Tobacco-smoke-inducible human haem oxygenase-1 gene expression: role of distinct transcription factors and reactive oxygen intermediates. Biochem J, 353, 475-82.

FELDMAN, L. J., AGUIRRE, L., ZIOL, M., BRIDOU, J. P., NEVO, N., MICHEL, J. B. & STEG, P. G. 2000. Interleukin-10 inhibits intimal hyperplasia after angioplasty or stent implantation in hypercholesterolemic rabbits. Circulation, 101, 908-16.

FELETOU, M. & VANHOUTTE, P. M. 2009. EDHF: an update. Clin Sci (Lond), 117, 139-55.

FENG, D., NAGY, J. A., DVORAK, H. F. & DVORAK, A. M. 2002. Ultrastructural studies define soluble macromolecular, particulate, and cellular transendothelial cell pathways in venules, lymphatic vessels, and tumor-associated microvessels in man and animals. Microsc Res Tech, 57, 289-326.

FERNANDEZ, M. & BONKOVSKY, H. L. 2003. Vascular endothelial growth factor increases heme oxygenase-1 protein expression in the chick embryo chorioallantoic membrane. Br J Pharmacol, 139, 634-40.

FERRAN, C., STROKA, D. M., BADRICHANI, A. Z., COOPER, J. T., WRIGHTON, C. J., SOARES, M., GREY, S. T. & BACH, F. H. 1998. A20 inhibits NF-kappaB activation in endothelial cells without sensitizing to tumor necrosis factor-mediated apoptosis. Blood, 91, 2249-58.

FERRARA, N. 2000. VEGF: an update on biological and therapeutic aspects. Curr Opin Biotechnol, 11, 617-24.

FERRARA, N., CARVER-MOORE, K., CHEN, H., DOWD, M., LU, L., O'SHEA, K. S., POWELL-BRAXTON, L., HILLAN, K. J. & MOORE, M. W. 1996. Heterozygous embryonic lethality induced by targeted inactivation of the VEGF gene. Nature, 380, 439-42.

FERRARA, N., GERBER, H. P. & LECOUTER, J. 2003. The biology of VEGF and its receptors. Nat Med, 9, 669-76.

FIEDLER, L. R., BACHETTI, T., LEIPER, J., ZACHARY, I., CHEN, L. H., RENNE, T. & WOJCIAK-STOTHARD, B. 2009. The ADMA/DDAH Pathway Regulates VEGF-Mediated Angiogenesis. Arteriosclerosis Thrombosis and Vascular Biology, 29, 2117-U309.

FISCHER, S., VANDEKERCKHOVE, J., AMPE, C., TRAUB, P. & WEBER, K. 1986. Protein-chemical identification of the major cleavage sites of the Ca2+ proteinase on murine vimentin, the mesenchymal intermediate filament protein. Biol Chem Hoppe Seyler, 367, 1147-52.

FLEDDERUS, J. O., BOON, R. A., VOLGER, O. L., HURTTILA, H., YLA-HERTTUALA, S., PANNEKOEK, H., LEVONEN, A. L. & HORREVOETS, A. J. 2008. KLF2 primes the antioxidant transcription factor Nrf2 for activation in endothelial cells. Arterioscler Thromb Vasc Biol, 28, 1339-46.

FLEINER, M., KUMMER, M., MIRLACHER, M., SAUTER, G., CATHOMAS, G., KRAPF, R. & BIEDERMANN, B. C. 2004. Arterial neovascularization and inflammation in vulnerable patients: early and late signs of symptomatic atherosclerosis. Circulation, 110, 2843-50.

FRANCO, S., PERRIN, B. & HUTTENLOCHER, A. 2004. Isoform specific function of calpain 2 in regulating membrane protrusion. Exp Cell Res, 299, 179-87.

FRANGOS, J. A., MCINTIRE, L. V. & ESKIN, S. G. 1988. Shear stress induced stimulation of mammalian cell metabolism. Biotechnol Bioeng, 32, 1053-60.

FRANK, P. G., PAVLIDES, S. & LISANTI, M. P. 2009. Caveolae and transcytosis in endothelial cells: role in atherosclerosis. Cell Tissue Res, 335, 41-7.

FUJITA, T., TODA, K., KARIMOVA, A., YAN, S. F., NAKA, Y., YET, S. F. & PINSKY, D. J. 2001. Paradoxical rescue from ischaemic lung injury by inhaled carbon monoxide driven by derepression of fibrinolysis. Nat Med, 7, 598-604.

FULTON, D., GRATTON, J. P., MCCABE, T. J., FONTANA, J., FUJIO, Y., WALSH, K., FRANKE, T. F., PAPAPETROPOULOS, A. & SESSA, W. C. 1999. Regulation of endothelium-derived nitric oxide production by the protein kinase Akt. Nature, 399, 597-601.

FURUNO, N., DEN ELZEN, N. & PINES, J. 1999. Human cyclin A is required for mitosis until mid prophase. J Cell Biol, 147, 295-306.

GALBRAITH, C. G., YAMADA, K. M. & GALBRAITH, J. A. 2007. Polymerizing actin fibers position integrins primed to probe for adhesion sites. Science, 315, 992-5.

GALE, N. W. & YANCOPOULOS, G. D. 1999. Growth factors acting via endothelial cell-specific receptor tyrosine kinases: VEGFs, angiopoietins, and ephrins in vascular development. Genes Dev, 13, 1055-66.

GALLEY, H. F. & WEBSTER, N. R. 2004. Physiology of the endothelium. Br J Anaesth, 93, 105-13.

GAMBLE, J. R., BRADLEY, S., NOACK, L. & VADAS, M. A. 1995. Tgf-Beta and Endothelial-Cells Inhibit Vcam-1 Expression on Human Vascular Smooth-Muscle Cells. Arteriosclerosis Thrombosis and Vascular Biology, 15, 949-955.

GAMBLE, J. R., DREW, J., TREZISE, L., UNDERWOOD, A., PARSONS, M., KASMINKAS, L., RUDGE, J., YANCOPOULOS, G. & VADAS, M. A. 2000. Angiopoietin-1 is an antipermeability and anti-inflammatory agent in vitro and targets cell junctions. Circulation Research, 87, 603-7.

GARLANDA, C. & DEJANA, E. 1997. Heterogeneity of endothelial cells. Specific markers. Arterioscler Thromb Vasc Biol, 17, 1193-202.

GAVARD, J. & GUTKIND, J. S. 2008. VE-cadherin and claudin-5: it takes two to tango. Nat Cell Biol, 10, 883-5.

GEIGER, B., BERSHADSKY, A., PANKOV, R. & YAMADA, K. M. 2001. Transmembrane crosstalk between the extracellular matrix--cytoskeleton crosstalk. Nat Rev Mol Cell Biol, 2, 793-805.

GERALDES, P., HIRAOKA-YAMAMOTO, J., MATSUMOTO, M., CLERMONT, A., LEITGES, M., MARETTE, A., AIELLO, L. P., KERN, T. S. & KING, G. L. 2009. Activation of PKC-delta and SHP-1 by hyperglycemia causes vascular cell apoptosis and diabetic retinopathy. Nat Med, 15, 1298-306.

GERBER, H. P., DIXIT, V. & FERRARA, N. 1998. Vascular endothelial growth factor induces expression of the antiapoptotic proteins Bcl-2 and A1 in vascular endothelial cells. J Biol Chem, 273, 13313-6.

GERHARDT, H., GOLDING, M., FRUTTIGER, M., RUHRBERG, C., LUNDKVIST, A., ABRAMSSON, A., JELTSCH, M., MITCHELL, C., ALITALO, K., SHIMA, D. & BETSHOLTZ, C. 2003. VEGF guides angiogenic sprouting utilizing endothelial tip cell filopodia. J Cell Biol, 161, 1163-77.

GERRITSEN, M. E. 1987. Functional heterogeneity of vascular endothelial cells. Biochem Pharmacol, 36, 2701-11.

GHOSH, D. K. & SALERNO, J. C. 2003. Nitric oxide synthases: domain structure and alignment in enzyme function and control. Front Biosci, 8, d193-209.

GIBBS, P. E. & MAINES, M. D. 2007. Biliverdin inhibits activation of NF-kappaB: reversal of inhibition by human biliverdin reductase. Int J Cancer, 121, 2567-74.

GIMBRONE, M. A., JR., COTRAN, R. S. & FOLKMAN, J. 1974. Human vascular endothelial cells in culture. Growth and DNA synthesis. J Cell Biol, 60, 673-84.

GINGRAS, D., LAMY, S. & BELIVEAU, R. 2000. Tyrosine phosphorylation of the vascular endothelial-growth-factor receptor-2 (VEGFR-2) is modulated by Rho proteins. Biochem J, 348 Pt 2, 273-80.

GLIKI, G., ABU-GHAZALEH, R., JEZEQUEL, S., WHEELER-JONES, C. & ZACHARY, I. 2001. Vascular endothelial growth factor-induced prostacyclin production is mediated by a protein kinase C (PKC)-dependent activation of extracellular signal-regulated protein kinases 1 and 2 involving PKC-delta and by mobilization of intracellular Ca2+. Biochem J, 353, 503-12.

GLIKI, G., WHEELER-JONES, C. & ZACHARY, I. 2002. Vascular endothelial growth factor induces protein kinase C (PKC)-dependent Akt/PKB activation and phosphatidylinositol 3'-kinase-mediates PKC delta phosphorylation: role of PKC in angiogenesis. Cell Biol Int, 26, 751-9.

GOH, K. L., CAI, L., CEPKO, C. L. & GERTLER, F. B. 2002. Ena/VASP proteins regulate cortical neuronal positioning. Curr Biol, 12, 565-9.

GONZALES, M., WEKSLER, B., TSURUTA, D., GOLDMAN, R. D., YOON, K. J., HOPKINSON, S. B., FLITNEY, F. W. & JONES, J. C. 2001. Structure and function of a vimentin-associated matrix adhesion in endothelial cells. Mol Biol Cell, 12, 85-100.

GONZALEZ, W., FONTAINE, V., PUEYO, M. E., LAQUAY, N., MESSIKA-ZEITOUN, D., PHILIPPE, M., ARNAL, J. F., JACOB, M. P. & MICHEL, J. B. 2000. Molecular plasticity of vascular wall during N(G)-nitro-L-arginine methyl ester-induced hypertension: modulation of proinflammatory signals. Hypertension, 36, 103-9.

GOODMAN, A. I., CHOUDHURY, M., DA SILVA, J. L., SCHWARTZMAN, M. L. & ABRAHAM, N. G. 1997. Overexpression of the heme oxygenase gene in renal cell carcinoma. Proc Soc Exp Biol Med, 214, 54-61.

GOUGOS, A. & LETARTE, M. 1988. Identification of a human endothelial cell antigen with monoclonal antibody 44G4 produced against a pre-B leukemic cell line. J Immunol, 141, 1925-33.

GOZZELINO, R., JENEY, V. & SOARES, M. P. 2010. Mechanisms of Cell Protection by Heme Oxygenase-1. Annual Review of Pharmacology and Toxicology, 50, 323-354.

GOZZELINO, R., JENEY, V. & SOARES, M. P. 2010. Mechanisms of cell protection by heme oxygenase-1. Annu Rev Pharmacol Toxicol, 50, 323-54.

GRAINGER, D. J., KEMP, P. R., LIU, A. C., LAWN, R. M. & METCALFE, J. C. 1994. Activation of Transforming Growth-Factor-Beta Is Inhibited in Transgenic Apolipoprotein(a) Mice. Nature, 370, 460-462.

GRAINGER, D. J., MOSEDALE, D. E., METCALFE, J. C. & BOTTINGER, E. P. 2000. Dietary fat and reduced levels of TGF beta 1 act synergistically to promote activation of the vascular endothelium and formation of lipid lesions. Journal of Cell Science, 113, 2355-2361.

GRANT, D. S., LELKES, P. I., FUKUDA, K. & KLEINMAN, H. K. 1991. Intracellular mechanisms involved in basement membrane induced blood vessel differentiation in vitro. In Vitro Cell Dev Biol, 27, 327-36.

GREEN, K. J., BOHRINGER, M., GOCKEN, T. & JONES, J. C. 2005. Intermediate filament associated proteins. Adv Protein Chem, 70, 143-202.

GREENAWAY, J., CONNOR, K., PEDERSEN, H. G., COOMBER, B. L., LAMARRE, J. & PETRIK, J. 2004. Vascular endothelial growth factor and its receptor, Flk-1/KDR, are cytoprotective in the extravascular compartment of the ovarian follicle. Endocrinology, 145, 2896-905.

GREIDER, C. W. 1998. Telomeres and senescence: the history, the experiment, the future. Curr Biol, 8, R178-81.

GROCHOT-PRZECZEK, A., DULAK, J. & JOZKOWICZ, A. 2012. Haem oxygenase-1: non-canonical roles in physiology and pathology. Clin Sci (Lond), 122, 93-103.

GROCHOT-PRZECZEK, A., LACH, R., MIS, J., SKRZYPEK, K., GOZDECKA, M., SROCZYNSKA, P., DUBIEL, M., RUTKOWSKI, A., KOZAKOWSKA, M., ZAGORSKA, A., WALCZYNSKI, J., WAS, H., KOTLINOWSKI, J., DRUKALA, J., KUROWSKI, K., KIEDA, C., HERAULT, Y., DULAK, J. & JOZKOWICZ, A. 2009. Heme oxygenase-1 accelerates cutaneous wound healing in mice. PLoS One, 4, e5803.

GUNNETT, C. A., HEISTAD, D. D., BERG, D. J. & FARACI, F. M. 2000. IL-10 deficiency increases superoxide and endothelial dysfunction during inflammation. Am J Physiol Heart Circ Physiol, 279, H1555-62.

GUO, W. & GIANCOTTI, F. G. 2004. Integrin signalling during tumour progression. Nat Rev Mol Cell Biol, 5, 816-26.

HAJRA, L., EVANS, A. I., CHEN, M., HYDUK, S. J., COLLINS, T. & CYBULSKY, M. I. 2000. The NF-kappa B signal transduction pathway in aortic endothelial cells is primed for activation in regions predisposed to atherosclerotic lesion formation. Proceedings of the National Academy of Sciences of the United States of America, 97, 9052-9057.

HALLIGAN, B. D. 2009. ProMoST: a tool for calculating the pI and molecular mass of phosphorylated and modified proteins on two-dimensional gels. Methods Mol Biol, 527, 283-98, ix.

HAMDULAY, S. S., WANG, B., BIRDSEY, G. M., ALI, F., DUMONT, O., EVANS, P. C., HASKARD, D. O., WHEELER-JONES, C. P. & MASON, J. C. 2010. Celecoxib activates PI-3K/Akt and mitochondrial redox signaling to enhance heme oxygenase-1-mediated anti-inflammatory activity in vascular endothelium. Free Radic Biol Med, 48, 1013-23.

HANADA, T., HASHIMOTO, M., NOSAKA, S., SASAKI, T., NAKAYAMA, K., MASUMURA, S., YAMAUCHI, M. & TAMURA, K. 2000. Shear stress enhances prostacyclin release from endocardial endothelial cells. Life Sci, 66, 215-20.

HANSEN, T. W., MATHIESEN, S. B. & WALAAS, S. I. 1996. Bilirubin has widespread inhibitory effects on protein phosphorylation. Pediatr Res, 39, 1072-7.

HANSSON, G. K. 2005. Inflammation, atherosclerosis, and coronary artery disease. N Engl J Med, 352, 1685-95.

HARA, E., TAKAHASHI, K., TAKEDA, K., NAKAYAMA, M., YOSHIZAWA, M., FUJITA, H., SHIRATO, K. & SHIBAHARA, S. 1999. Induction of heme oxygenase-1 as a response in sensing the signals evoked by distinct nitric oxide donors. Biochem Pharmacol, 58, 227-36.

HARRISON, P. M. & AROSIO, P. 1996. Ferritins: Molecular properties, iron storage function and cellular regulation. Biochimica Et Biophysica Acta-Bioenergetics, 1275, 161-203.

HAWKINS, B. T. & DAVIS, T. P. 2005. The blood-brain barrier/neurovascular unit in health and disease. Pharmacol Rev, 57, 173-85.

HAYASHI, S., TAKAMIYA, R., YAMAGUCHI, T., MATSUMOTO, K., TOJO, S. J., TAMATANI, T., KITAJIMA, M., MAKINO, N., ISHIMURA, Y. & SUEMATSU, M. 1999. Induction of heme oxygenase-1 suppresses venular leukocyte adhesion elicited by oxidative stress: role of bilirubin generated by the enzyme. Circulation Research, 85, 663-71.

HAYFLICK, J. S., KILGANNON, P. & GALLATIN, W. M. 1998. The intercellular adhesion molecule (ICAM) family of proteins. New members and novel functions. Immunol Res, 17, 313-27.

HAYWARD, R., NOSSULI, T. O., SCALIA, R. & LEFER, A. M. 1997. Cardioprotective effect of interleukin-10 in murine myocardial ischaemia-reperfusion. Eur J Pharmacol, 334, 157-63.

HE, H., VENEMA, V. J., GU, X., VENEMA, R. C., MARRERO, M. B. & CALDWELL, R. B. 1999. Vascular endothelial growth factor signals endothelial cell production of nitric oxide and prostacyclin through flk-1/KDR activation of c-Src. J Biol Chem, 274, 25130-5.

HEISTAD, D. D. & MARCUS, M. L. 1979. Role of vasa vasorum in nourishment of the aorta. Blood Vessels, 16, 225-38.

HEITZER, T., SCHLINZIG, T., KROHN, K., MEINERTZ, T. & MUNZEL, T. 2001. Endothelial dysfunction, oxidative stress, and risk of cardiovascular events in patients with coronary artery disease. Circulation, 104, 2673-8.

HELFAND, B. T., CHANG, L. & GOLDMAN, R. D. 2003. The dynamic and motile properties of intermediate filaments. Annu Rev Cell Dev Biol, 19, 445-67.

HELLSTROM, M., PHNG, L. K., HOFMANN, J. J., WALLGARD, E., COULTAS, L., LINDBLOM, P., ALVA, J., NILSSON, A. K., KARLSSON, L., GAIANO, N., YOON, K., ROSSANT, J., IRUELA-ARISPE, M. L., KALEN, M., GERHARDT, H. & BETSHOLTZ, C. 2007. Dll4 signalling through Notch1 regulates formation of tip cells during angiogenesis. Nature, 445, 776-80.

HENGST, L. & REED, S. I. 1996. Translational control of p27Kip1 accumulation during the cell cycle. Science, 271, 1861-4.

HENRION, D., TERZI, F., MATROUGUI, K., DURIEZ, M., BOULANGER, C. M., COLUCCI-GUYON, E., BABINET, C., BRIAND, P., FRIEDLANDER, G., POITEVIN, P. & LEVY, B. I. 1997. Impaired flow-induced dilation in mesenteric resistance arteries from mice lacking vimentin. Journal of Clinical Investigation, 100, 2909-14.

HERRMANN, H., HESSE, M., REICHENZELLER, M., AEBI, U. & MAGIN, T. M. 2003. Functional complexity of intermediate filament cytoskeletons: from structure to assembly to gene ablation. Int Rev Cytol, 223, 83-175.

HERRMANN, J., LERMAN, L. O., MUKHOPADHYAY, D., NAPOLI, C. & LERMAN, A. 2006. Angiogenesis in atherogenesis. Arterioscler Thromb Vasc Biol, 26, 1948-57.

HIGAKI, T., SAWADA, S., KONO, Y., IMAMURA, H., TADA, Y., YAMASAKI, S., TORATANI, A., SATO, T., KOMATSU, S., AKAMATSU, N., TAMAGAKI, T., TSUDA, Y., TSUJI, H. & NAKAGAWA, M. 1999. A role of protein kinase C in the regulation of cytosolic phospholipase A(2) in bradykinin-induced PGI(2) synthesis by human vascular endothelial cells. Microvasc Res, 58, 144-55.

HIGASHI, Y., NOMA, K., YOSHIZUMI, M. & KIHARA, Y. 2009. Endothelial function and oxidative stress in cardiovascular diseases. Circ J, 73, 411-8.

HILL, M., PEREIRA, V., CHAUVEAU, C., ZAGANI, R., REMY, S., TESSON, L., MAZAL, D., UBILLOS, L., BRION, R., ASGHAR, K., MASHREGHI, M. F., KOTSCH, K., MOFFETT, J., DOEBIS, C., SEIFERT, M., BOCZKOWSKI, J., OSINAGA, E. & ANEGON, I. 2005. Heme oxygenase-1 inhibits rat and human breast cancer cell proliferation: mutual cross inhibition with indoleamine 2,3-dioxygenase. FASEB J, 19, 1957-68.

HILL-KAPTURCZAK, N., SIKORSKI, E., VOAKES, C., GARCIA, J., NICK, H. S. & AGARWAL, A. 2003. An internal enhancer regulates heme- and cadmium-mediated induction of human heme oxygenase-1. Am J Physiol Renal Physiol, 285, F515-23.

HILL-KAPTURCZAK, N., VOAKES, C., GARCIA, J., VISNER, G., NICK, H. S. & AGARWAL, A. 2003. A cis-acting region regulates oxidized lipid-mediated induction of the human heme oxygenase-1 gene in endothelial cells. Arterioscler Thromb Vasc Biol, 23, 1416-22.

HIRAI, K., SASAHIRA, T., OHMORI, H., FUJII, K. & KUNIYASU, H. 2007. Inhibition of heme oxygenase-1 by zinc protoporphyrin IX reduces tumor growth of LL/2 lung cancer in C57BL mice. Int J Cancer, 120, 500-5.

HODIVALA-DILKE, K. M., REYNOLDS, A. R. & REYNOLDS, L. E. 2003. Integrins in angiogenesis: multitalented molecules in a balancing act. Cell Tissue Res, 314, 131-44.

HOFMANN, J. J. & IRUELA-ARISPE, M. L. 2007. Notch signaling in blood vessels: who is talking to whom about what? Circulation Research, 100, 1556-68.

HONDA, H. M., LEITINGER, N., FRANKEL, M., GOLDHABER, J. I., NATARAJAN, R., NADLER, J. L., WEISS, J. N. & BERLINER, J. A. 1999. Induction of monocyte binding to endothelial cells by MM-LDL - Role of lipoxygenase metabolites. Arteriosclerosis Thrombosis and Vascular Biology, 19, 680-686.

HORNIG, C. & WEICH, H. A. 1999. Soluble VEGF receptors. Angiogenesis, 3, 33-9.

HOTULAINEN, P. & LAPPALAINEN, P. 2006. Stress fibers are generated by two distinct actin assembly mechanisms in motile cells. J Cell Biol, 173, 383-94.

HOUCK, K. A., FERRARA, N., WINER, J., CACHIANES, G., LI, B. & LEUNG, D. W. 1991. The vascular endothelial growth factor family: identification of a fourth molecular species and characterization of alternative splicing of RNA. Mol Endocrinol, 5, 1806-14.

HOUCK, K. A., LEUNG, D. W., ROWLAND, A. M., WINER, J. & FERRARA, N. 1992. Dual regulation of vascular endothelial growth factor bioavailability by genetic and proteolytic mechanisms. J Biol Chem, 267, 26031-7.

HOWE, J. A., HOWELL, M., HUNT, T. & NEWPORT, J. W. 1995. Identification of a developmental timer regulating the stability of embryonic cyclin A and a new somatic A-type cyclin at gastrulation. Genes Dev, 9, 1164-76.

HSU, S., THAKAR, R., LIEPMANN, D. & LI, S. 2005. Effects of shear stress on endothelial cell haptotaxis on micropatterned surfaces. Biochem Biophys Res Commun, 337, 401-9.

HUBER, A. B., KOLODKIN, A. L., GINTY, D. D. & CLOUTIER, J. F. 2003. Signaling at the growth cone: Ligand-receptor complexes and the control of axon growth and guidance. Annual Review of Neuroscience, 26, 509-563.

HUDDLESON, J. P., AHMAD, N., SRINIVASAN, S. & LINGREL, J. B. 2005. Induction of KLF2 by fluid shear stress requires a novel promoter element activated by a phosphatidylinositol 3-kinase-dependent chromatin-remodeling pathway. J Biol Chem, 280, 23371-9.

HUGHES, S. E., CROSSMAN, D. & HALL, P. A. 1993. Expression of basic and acidic fibroblast growth factors and their receptor in normal and atherosclerotic human arteries. Cardiovasc Res, 27, 1214-9.

HUSSAIN, A. S., MARKS, G. S., BRIEN, J. F. & NAKATSU, K. 1997. The soluble guanylyl cyclase inhibitor 1H-[1,2,4]oxadiazolo[4,3-alpha]quinoxalin-1-one (ODQ) inhibits relaxation of rabbit aortic rings induced by carbon monoxide, nitric oxide, and glyceryl trinitrate. Can J Physiol Pharmacol, 75, 1034-7.

HYNES, R. O. 2007. Cell-matrix adhesion in vascular development. J Thromb Haemost, 5 Suppl 1, 32-40.

HYNES, R. O., BADER, B. L. & HODIVALA-DILKE, K. 1999. Integrins in vascular development. Braz J Med Biol Res, 32, 501-10.

IGNATESCU, M. C., GHAREHBAGHI-SCHNELL, E., HASSAN, A., REZAIE-MAJD, S., KORSCHINECK, I., SCHLEEF, R. R., GLOGAR, H. D. & LANG, I. M. 1999. Expression of the angiogenic protein, platelet-derived endothelial cell growth factor, in coronary atherosclerotic plaques: In vivo correlation of lesional microvessel density and constrictive vascular remodeling. Arterioscler Thromb Vasc Biol, 19, 2340-7.

ILAN, N., MAHOOTI, S. & MADRI, J. A. 1998. Distinct signal transduction pathways are utilized during the tube formation and survival phases of in vitro angiogenesis. J Cell Sci, 111 (Pt 24), 3621-31.

IMAIZUMI, T. A., STAFFORINI, D. M., YAMADA, Y., MCINTYRE, T. M., PRESCOTT, S. M. & ZIMMERMAN, G. A. 1995. Platelet-activating factor: a mediator for clinicians. J Intern Med, 238, 5-20.

IMHOF, B. A. & AURRAND-LIONS, M. 2004. Adhesion mechanisms regulating the migration of monocytes. Nat Rev Immunol, 4, 432-44.

IMMENSCHUH, S. & RAMADORI, G. 2000. Gene regulation of heme oxygenase-1 as a therapeutic target. Biochem Pharmacol, 60, 1121-8.

INABA, T., MATSUSHIME, H., VALENTINE, M., ROUSSEL, M. F., SHERR, C. J. & LOOK, A. T. 1992. Genomic organization, chromosomal localization, and independent expression of human cyclin D genes. Genomics, 13, 565-74.

INOUE, A., YANAGISAWA, M., KIMURA, S., KASUYA, Y., MIYAUCHI, T., GOTO, K. & MASAKI, T. 1989. The human endothelin family: three structurally and pharmacologically distinct isopeptides predicted by three separate genes. Proc Natl Acad Sci U S A, 86, 2863-7.

INOUE, N., RAMASAMY, S., FUKAI, T., NEREM, R. M. & HARRISON, D. G. 1996. Shear stress modulates expression of Cu/Zn superoxide dismutase in human aortic endothelial cells. Circulation Research, 79, 32-7.

ISHIKAWA, K., NAVAB, M., LEITINGER, N., FOGELMAN, A. M. & LUSIS, A. J. 1997. Induction of heme oxygenase-1 inhibits the monocyte transmigration induced by mildly oxidized LDL. Journal of Clinical Investigation, 100, 1209-16.

ISHIKAWA, K., SATO, M. & YOSHIDA, T. 1991. Expression of rat heme oxygenase in Escherichia coli as a catalytically active, full-length form that binds to bacterial membranes. Eur J Biochem, 202, 161-5.

ISHIKAWA, K., SUGAWARA, D., WANG, X., SUZUKI, K., ITABE, H., MARUYAMA, Y. & LUSIS, A. J. 2001. Heme oxygenase-1 inhibits atherosclerotic lesion formation in ldl-receptor knockout mice. Circulation Research, 88, 506-12.

ISHIZAKA, N., DE LEON, H., LAURSEN, J. B., FUKUI, T., WILCOX, J. N., DE KEULENAER, G., GRIENDLING, K. K. & ALEXANDER, R. W. 1997. Angiotensin II-induced hypertension increases heme oxygenase-1 expression in rat aorta. Circulation, 96, 1923-9.

IVASKA, J., PALLARI, H. M., NEVO, J. & ERIKSSON, J. E. 2007. Novel functions of vimentin in cell adhesion, migration, and signaling. Exp Cell Res, 313, 2050-62.

IVASKA, J., VUORILUOTO, K., HUOVINEN, T., IZAWA, I., INAGAKI, M. & PARKER, P. J. 2005. PKCepsilon-mediated phosphorylation of vimentin controls integrin recycling and motility. EMBO J, 24, 3834-45.

IVASKA, J., WHELAN, R. D., WATSON, R. & PARKER, P. J. 2002. PKC epsilon controls the traffic of beta1 integrins in motile cells. EMBO J, 21, 3608-19.

JAFFE, E. A., NACHMAN, R. L., BECKER, C. G. & MINICK, C. R. 1973. Culture of human endothelial cells derived from umbilical veins. Identification by morphologic and immunologic criteria. Journal of Clinical Investigation, 52, 2745-56.

JAIN, R. K. 2003. Molecular regulation of vessel maturation. Nat Med, 9, 685-93.

JAZWA, A., LOBODA, A., GOLDA, S., CISOWSKI, J., SZELAG, M., ZAGORSKA, A., SROCZYNSKA, P., DRUKALA, J., JOZKOWICZ, A. & DULAK, J. 2006. Effect of heme and heme oxygenase-1 on vascular endothelial growth factor synthesis and angiogenic potency of human keratinocytes. Free Radic Biol Med, 40, 1250-63.

JENEY, V., BALLA, J., YACHIE, A., VARGA, Z., VERCELLOTTI, G. M., EATON, J. W. & BALLA, G. 2002. Pro-oxidant and cytotoxic effects of circulating heme. Blood, 100, 879-87.

JEZIORSKA, M. & WOOLLEY, D. E. 1999. Local neovascularization and cellular composition within vulnerable regions of atherosclerotic plaques of human carotid arteries. J Pathol, 188, 189-96.

JOHNSON, T. R., MANN, B. E., CLARK, J. E., FORESTI, R., GREEN, C. J. & MOTTERLINI, R. 2003. Metal carbonyls: a new class of pharmaceuticals? Angew Chem Int Ed Engl, 42, 3722-9.

JOHNSON-LEGER, C., AURRAND-LIONS, M. & IMHOF, B. A. 2000. The parting of the endothelium: miracle, or simply a junctional affair? J Cell Sci, 113 (Pt 6), 921-33.

JOUKOV, V., PAJUSOLA, K., KAIPAINEN, A., CHILOV, D., LAHTINEN, I., KUKK, E., SAKSELA, O., KALKKINEN, N. & ALITALO, K. 1996. A novel vascular endothelial growth factor, VEGF-C, is a ligand for the Flt4 (VEGFR-3) and KDR (VEGFR-2) receptor tyrosine kinases. EMBO J, 15, 1751.

JOZKOWICZ, A., HUK, I., NIGISCH, A., WEIGEL, G., DIETRICH, W., MOTTERLINI, R. & DULAK, J. 2003. Heme oxygenase and angiogenic activity of endothelial cells: stimulation by carbon monoxide and inhibition by tin protoporphyrin-IX. Antioxid Redox Signal, 5, 155-62.

JOZKOWICZ, A., HUK, I., NIGISCH, A., WEIGEL, G., WEIDINGER, F. & DULAK, J. 2002. Effect of prostaglandin-J(2) on VEGF synthesis depends on the induction of heme oxygenase-1. Antioxid Redox Signal, 4, 577-85.

JOZKOWICZ, A., HUK, I., NIGISCH, A., WEIGEL, G., WEIDINGER, F. & DULAK, J. 2002. Effect of prostaglandin-J(2) on VEGF synthesis depends on the induction of heme oxygenase-1. Antioxid Redox Signal, 4, 577-85.

JUAN, S. H., LEE, T. S., TSENG, K. W., LIOU, J. Y., SHYUE, S. K., WU, K. K. & CHAU, L. Y. 2001. Adenovirus-mediated heme oxygenase-1 gene transfer inhibits the development of atherosclerosis in apolipoprotein E-deficient mice. Circulation, 104, 1519-25.

JUCKETT, M. B., BALLA, J., BALLA, G., JESSURUN, J., JACOB, H. S. & VERCELLOTTI, G. M. 1995. Ferritin protects endothelial cells from oxidized low density lipoprotein in vitro. Am J Pathol, 147, 782-9.

KACIMI, R., CHENTOUFI, J., HONBO, N., LONG, C. S. & KARLINER, J. S. 2000. Hypoxia differentially regulates stress proteins in cultured cardiomyocytes: role of the p38 stress-activated kinase signaling cascade, and relation to cytoprotection. Cardiovasc Res, 46, 139-50.

KAIPAINEN, A., KORHONEN, J., MUSTONEN, T., VAN HINSBERGH, V. W., FANG, G. H., DUMONT, D., BREITMAN, M. & ALITALO, K. 1995. Expression of the fms-like tyrosine kinase 4 gene becomes restricted to lymphatic endothelium during development. Proc Natl Acad Sci U S A, 92, 3566-70.

KAIPAINEN, A., KORHONEN, J., PAJUSOLA, K., APRELIKOVA, O., PERSICO, M. G., TERMAN, B. I. & ALITALO, K. 1993. The related FLT4, FLT1, and KDR receptor tyrosine kinases show distinct expression patterns in human fetal endothelial cells. J Exp Med, 178, 2077-88.

KAISER, D., FREYBERG, M. A. & FRIEDL, P. 1997. Lack of haemodynamic forces triggers apoptosis in vascular endothelial cells. Biochem Biophys Res Commun, 231, 586-90.

KAISER, D., FREYBERG, M. A. & FRIEDL, P. 1997. Lack of haemodynamic forces triggers apoptosis in vascular endothelial cells. Biochem Biophys Res Commun, 231, 586-90.

KANETO, H., KATAKAMI, N., MATSUHISA, M. & MATSUOKA, T. A. 2010. Role of reactive oxygen species in the progression of type 2 diabetes and atherosclerosis. Mediators Inflamm, 2010, 453892.

KANSAS, G. S. 1996. Selectins and their ligands: current concepts and controversies. Blood, 88, 3259-87.

KATAOKA, N., UJITA, S. & SATO, M. 1998. Effect of flow direction on the morphological responses of cultured bovine aortic endothelial cells. Medical & Biological Engineering & Computing, 36, 122-128.

KATER, S. B. & REHDER, V. 1995. The sensory-motor role of growth cone filopodia. Curr Opin Neurobiol, 5, 68-74.

KAWAMURA, K., ISHIKAWA, K., WADA, Y., KIMURA, S., MATSUMOTO, H., KOHRO, T., ITABE, H., KODAMA, T. & MARUYAMA, Y. 2005. Bilirubin from heme oxygenase-1 attenuates vascular endothelial activation and dysfunction. Arterioscler Thromb Vasc Biol, 25, 155-60.

KAWASHIMA, A., ODA, Y., YACHIE, A., KOIZUMI, S. & NAKANISHI, I. 2002. Heme oxygenase-1 deficiency: the first autopsy case. Hum Pathol, 33, 125-30.

KEMP, P. J. 2005. Hemeoxygenase-2 as an O2 sensor in K+ channel-dependent chemotransduction. Biochem Biophys Res Commun, 338, 648-52.

KESHAVAN, P., DEEM, T. L., SCHWEMBERGER, S. J., BABCOCK, G. F., COOK-MILLS, J. M. & ZUCKER, S. D. 2005. Unconjugated bilirubin inhibits VCAM-1-mediated transendothelial leukocyte migration. J Immunol, 174, 3709-18.

KEUM, Y. S., YU, S., CHANG, P. P., YUAN, X., KIM, J. H., XU, C., HAN, J., AGARWAL, A. & KONG, A. N. 2006. Mechanism of action of sulforaphane: inhibition of p38 mitogen-activated protein kinase isoforms contributing to the induction of antioxidant response element-mediated heme oxygenase-1 in human hepatoma HepG2 cells. Cancer Res, 66, 8804-13.

KEYSE, S. M. & TYRRELL, R. M. 1989. Heme oxygenase is the major 32-kDa stress protein induced in human skin fibroblasts by UVA radiation, hydrogen peroxide, and sodium arsenite. Proc Natl Acad Sci U S A, 86, 99-103.

KHURANA, R., SIMONS, M., MARTIN, J. F. & ZACHARY, I. C. 2005. Role of angiogenesis in cardiovascular disease: a critical appraisal. Circulation, 112, 1813-24.

KIM, H. P., WANG, X., GALBIATI, F., RYTER, S. W. & CHOI, A. M. 2004. Caveolae compartmentalization of heme oxygenase-1 in endothelial cells. FASEB J, 18, 1080-9.

KIM, H. P., WANG, X., NAKAO, A., KIM, S. I., MURASE, N., CHOI, M. E., RYTER, S. W. & CHOI, A. M. 2005. Caveolin-1 expression by means of p38beta mitogen-activated protein kinase mediates the antiproliferative effect of carbon monoxide. Proc Natl Acad Sci U S A, 102, 11319-24.

KIM, I., KIM, H. G., SO, J. N., KIM, J. H., KWAK, H. J. & KOH, G. Y. 2000. Angiopoietin-1 regulates endothelial cell survival through the phosphatidylinositol 3'-kinase/Akt signal transduction pathway. Circulation Research, 86, 24-29.

KIM, I., MOON, S. O., HAN, C. Y., PAK, Y. K., MOON, S. K., KIM, J. J. & KOH, G. Y. 2001. The angiopoietin-tie2 system in coronary artery endothelium prevents oxidized low-density lipoprotein-induced apoptosis. Cardiovasc Res, 49, 872-81.

KIM, I., MOON, S. O., PARK, S. K., CHAE, S. W. & KOH, G. Y. 2001. Angiopoietin-1 reduces VEGF-stimulated leukocyte adhesion to endothelial cells by reducing ICAM-1, VCAM-1, and E-selectin expression. Circulation Research, 89, 477-9.

KIM, I., OH, J. L., RYU, Y. S., SO, J. N., SESSA, W. C., WALSH, K. & KOH, G. Y. 2002. Angiopoietin-1 negatively regulates expression and activity of tissue factor in endothelial cells. FASEB J, 16, 126-8.

KIM, Y. M., PAE, H. O., PARK, J. E., LEE, Y. C., WOO, J. M., KIM, N. H., CHOI, Y. K., LEE, B. S., KIM, S. R. & CHUNG, H. T. 2011. Heme oxygenase in the regulation of vascular biology: from molecular mechanisms to therapeutic opportunities. Antioxid Redox Signal, 14, 137-67.

KIMURA, K., ITO, M., AMANO, M., CHIHARA, K., FUKATA, Y., NAKAFUKU, M., YAMAMORI, B., FENG, J., NAKANO, T., OKAWA, K., IWAMATSU, A. & KAIBUCHI, K. 1996. Regulation of myosin phosphatase by Rho and Rho-associated kinase (Rho-kinase). Science, 273, 245-8.

KINDERLERER, A. R., ALI, F., JOHNS, M., LIDINGTON, E. A., LEUNG, V., BOYLE, J. J., HAMDULAY, S. S., EVANS, P. C., HASKARD, D. O. & MASON, J. C. 2008. KLF2-dependent, shear stress-induced expression of CD59: a novel cytoprotective mechanism against complement-mediated injury in the vasculature. J Biol Chem, 283, 14636-44.

KINDERLERER, A. R., GREGOIRE, I. P., HAMDULAY, S. S., ALI, F., STEINBERG, R., SILVA, G., ALI, N., WANG, B. F., HASKARD, D. O., SOARES, M. P. & MASON, J. C. 2009. Heme oxygenase-1 expression enhances vascular endothelial resistance to complement-mediated injury through induction of decay-accelerating factor: a role for increased bilirubin and ferritin. Blood, 113, 1598-1607.

KINDERLERER, A. R., STEINBERG, R., JOHNS, M., HARTEN, S. K., LIDINGTON, E. A., HASKARD, D. O., MAXWELL, P. H. & MASON, J. C. 2006. Statin-induced expression of CD59 on vascular endothelium in hypoxia: a potential mechanism for the anti-inflammatory actions of statins in rheumatoid arthritis. Arthritis Res Ther, 8, R130.

KIRKBY, K. A. & ADIN, C. A. 2006. Products of heme oxygenase and their potential therapeutic applications. Am J Physiol Renal Physiol, 290, F563-71.

KITAMOTO, S., EGASHIRA, K., KATAOKA, C., KOYANAGI, M., KATOH, M., SHIMOKAWA, H., MORISHITA, R., KANEDA, Y., SUEISHI, K. & TAKESHITA, A. 2000. Increased activity of nuclear factor-kappa B participates in cardiovascular remodeling induced by chronic inhibition of nitric oxide synthesis in rats. Circulation, 102, 806-812.

KINOSHITA, E., KINOSHITA-KIKUTA, E. & KOIKE, T. 2012. Phos-tag SDS-PAGE systems for phosphorylation profiling of proteins with a wide range of molecular masses under neutral pH conditions. Proteomics, 12, 192-202.

KITAMURA, Y., ISHIDA, Y., TAKATA, K., MIZUTANI, H., KAKIMURA, J., INDEN, M., NAKATA, J., TANIGUCHI, T., TSUKAHARA, T., AKAIKE, A. & SHIMOHAMA, S. 2003. Hyperbilirubinemia protects against focal ischaemia in rats. J Neurosci Res, 71, 544-50.

KLEMKE, R. L., CAI, S., GIANNINI, A. L., GALLAGHER, P. J., DE LANEROLLE, P. & CHERESH, D. A. 1997. Regulation of cell motility by mitogen-activated protein kinase. J Cell Biol, 137, 481-92.

KMIEC, Z. 2001. Cooperation of liver cells in health and disease. Adv Anat Embryol Cell Biol, 161, III-XIII, 1-151.

KNOWLES, J. W., REDDICK, R. L., JENNETTE, J. C., SHESELY, E. G., SMITHIES, O. & MAEDA, N. 2000. Enhanced atherosclerosis and kidney dysfunction in eNOS(-/-)Apoe(-/-) mice are ameliorated by enalapril treatment. Journal of Clinical Investigation, 105, 451-8.

KNOWLES, R. G. & MONCADA, S. 1994. Nitric oxide synthases in mammals. Biochem J, 298 (Pt 2), 249-58.

KOCH, A. E. 2000. The role of angiogenesis in rheumatoid arthritis: recent developments. Ann Rheum Dis, 59 Suppl 1, i65-71.

KOCH, A. E., HARLOW, L. A., HAINES, G. K., AMENTO, E. P., UNEMORI, E. N., WONG, W. L., POPE, R. M. & FERRARA, N. 1994. Vascular endothelial growth factor. A cytokine modulating endothelial function in rheumatoid arthritis. J Immunol, 152, 4149-56.

KOCHIN, V., IMANISHI, S. Y. & ERIKSSON, J. E. 2006. Fast track to a phosphoprotein sketch - MALDI-TOF characterization of TLC-based tryptic phosphopeptide maps at femtomolar detection sensitivity. Proteomics, 6, 5676-82.

KOFF, A., GIORDANO, A., DESAI, D., YAMASHITA, K., HARPER, J. W., ELLEDGE, S., NISHIMOTO, T., MORGAN, D. O., FRANZA, B. R. & ROBERTS, J. M. 1992. Formation and activation of a cyclin E-cdk2 complex during the G1 phase of the human cell cycle. Science, 257, 1689-94.

KOLLURU, G. K., BIR, S. C. & KEVIL, C. G. 2012. Endothelial dysfunction and diabetes: effects on angiogenesis, vascular remodeling, and wound healing. Int J Vasc Med, 2012, 918267.

KOLODGIE, F. D., GOLD, H. K., BURKE, A. P., FOWLER, D. R., KRUTH, H. S., WEBER, D. K., FARB, A., GUERRERO, L. J., HAYASE, M., KUTYS, R., NARULA, J., FINN, A. V. & VIRMANI, R. 2003. Intraplaque hemorrhage and progression of coronary atheroma. N Engl J Med, 349, 2316-25.

KOMAROVA, Y. & MALIK, A. B. 2010. Regulation of endothelial permeability via paracellular and transcellular transport pathways. Annu Rev Physiol, 72, 463-93.

KOYANAGI, M., EGASHIRA, K., KITAMOTO, S., NI, W., SHIMOKAWA, H., TAKEYA, M., YOSHIMURA, T. & TAKESHITA, A. 2000. Role of monocyte chemoattractant protein-1 in cardiovascular remodeling induced by chronic blockade of nitric oxide synthesis. Circulation, 102, 2243-8.

KRAUSE, M., DENT, E. W., BEAR, J. E., LOUREIRO, J. J. & GERTLER, F. B. 2003. Ena/VASP proteins: regulators of the actin cytoskeleton and cell migration. Annu Rev Cell Dev Biol, 19, 541-64.

KREIS, S., SCHONFELD, H. J., MELCHIOR, C., STEINER, B. & KIEFFER, N. 2005. The intermediate filament protein vimentin binds specifically to a recombinant integrin alpha2/beta1 cytoplasmic tail complex and co-localizes with native alpha2/beta1 in endothelial cell focal adhesions. Exp Cell Res, 305, 110-21.

KREISER, D., NGUYEN, X., WONG, R., SEIDMAN, D., STEVENSON, D., QUAN, S., ABRAHAM, N. & DENNERY, P. A. 2002. Heme oxygenase-1 modulates fetal growth in the rat. Lab Invest, 82, 687-92.

KROLL, J. & WALTENBERGER, J. 1999. A novel function of VEGF receptor-2 (KDR): rapid release of nitric oxide in response to VEGF-A stimulation in endothelial cells. Biochem Biophys Res Commun, 265, 636-9.

KRONKE, G., BOCHKOV, V. N., HUBER, J., GRUBER, F., BLUML, S., FURNKRANZ, A., KADL, A., BINDER, B. R. & LEITINGER, N. 2003. Oxidized phospholipids induce expression of human heme oxygenase-1 involving activation of cAMP-responsive element-binding protein. J Biol Chem, 278, 51006-14.

KUBES, P., SUZUKI, M. & GRANGER, D. N. 1991. Nitric oxide: an endogenous modulator of leukocyte adhesion. Proc Natl Acad Sci U S A, 88, 4651-5.

KUCIA, M., JANKOWSKI, K., RECA, R., WYSOCZYNSKI, M., BANDURA, L., ALLENDORF, D. J., ZHANG, J., RATAJCZAK, J. & RATAJCZAK, M. Z. 2004. CXCR4-SDF-1 signalling, locomotion, chemotaxis and adhesion. J Mol Histol, 35, 233-45.

KUHLENCORDT, P. J., GYURKO, R., HAN, F., SCHERRER-CROSBIE, M., ARETZ, T. H., HAJJAR, R., PICARD, M. H. & HUANG, P. L. 2001. Accelerated atherosclerosis, aortic aneurysm formation, and ischaemic heart disease in apolipoprotein E/endothelial nitric oxide synthase double-knockout mice. Circulation, 104, 448-54.

KUHN, K. & EBLE, J. 1994. The structural bases of integrin-ligand interactions. Trends Cell Biol, 4, 256-61.

KUKK, E., LYMBOUSSAKI, A., TAIRA, S., KAIPAINEN, A., JELTSCH, M., JOUKOV, V. & ALITALO, K. 1996. VEGF-C receptor binding and pattern of expression with VEGFR-3 suggests a role in lymphatic vascular development. Development, 122, 3829-37.

KUMAR, D., BHASKARAN, M., ALAGAPPAN, L., TORI, D., YADAV, I., KONKIMALLA, S., MAGOON, S. & SINGHAL, P. C. 2010. Heme oxygenase-1 modulates mesangial cell proliferation by p21 Waf1 upregulation. Ren Fail, 32, 254-8.

KUSHIDA, T., LIVOLTI, G., GOODMAN, A. I. & ABRAHAM, N. G. 2002. TNF-alpha-mediated cell death is attenuated by retrovirus delivery of human heme oxygenase-1 gene into human microvessel endothelial cells. Transplant Proc, 34, 2973-8.

KUSHIDA, T., QUAN, S., YANG, L., IKEHARA, S., KAPPAS, A. & ABRAHAM, N. G. 2002. A significant role for the heme oxygenase-1 gene in endothelial cell cycle progression. Biochem Biophys Res Commun, 291, 68-75.

KUWANO, Y., RABINOVIC, A., SRIKANTAN, S., GOROSPE, M. & DEMPLE, B. 2009. Analysis of nitric oxide-stabilized mRNAs in human fibroblasts reveals HuR-dependent heme oxygenase 1 upregulation. Mol Cell Biol, 29, 2622-35.

KWAK, H. I., KANG, H., DAVE, J. M., MENDOZA, E. A., SU, S. C., MAXWELL, S. A. & BAYLESS, K. J. 2012. Calpain-mediated vimentin cleavage occurs upstream of MT1-MMP membrane translocation to facilitate endothelial sprout initiation. Angiogenesis, 15, 287-303.

KWAK, H. J., SO, J. N., LEE, S. J., KIM, I. & KOH, G. Y. 1999. Angiopoietin-1 is an apoptosis survival factor for endothelial cells. FEBS Lett, 448, 249-53.

KYRIAKIS, J. M. & AVRUCH, J. 2001. Mammalian mitogen-activated protein kinase signal transduction pathways activated by stress and inflammation. Physiol Rev, 81, 807-69.

LABBE, R. F., VREMAN, H. J. & STEVENSON, D. K. 1999. Zinc protoporphyrin: A metabolite with a mission. Clin Chem, 45, 2060-72.

LAITINEN, M., ZACHARY, I., BREIER, G., PAKKANEN, T., HAKKINEN, T., LUOMA, J., ABEDI, H., RISAU, W., SOMA, M., LAAKSO, M., MARTIN, J. F. & YLA-HERTTUALA, S. 1997. VEGF gene transfer reduces intimal thickening via increased production of nitric oxide in carotid arteries. Hum Gene Ther, 8, 1737-44.

LAMALICE, L., LE BOEUF, F. & HUOT, J. 2007. Endothelial cell migration during angiogenesis. Circulation Research, 100, 782-94.

LAMPUGNANI, M. G., ORSENIGO, F., GAGLIANI, M. C., TACCHETTI, C. & DEJANA, E. 2006. Vascular endothelial cadherin controls VEGFR-2 internalization and signaling from intracellular compartments. J Cell Biol, 174, 593-604.

LAMPUGNANI, M. G., RESNATI, M., RAITERI, M., PIGOTT, R., PISACANE, A., HOUEN, G., RUCO, L. P. & DEJANA, E. 1992. A novel endothelial-specific membrane protein is a marker of cell-cell contacts. J Cell Biol, 118, 1511-22.

LANIER, L. M., GATES, M. A., WITKE, W., MENZIES, A. S., WEHMAN, A. M., MACKLIS, J. D., KWIATKOWSKI, D., SORIANO, P. & GERTLER, F. B. 1999. Mena is required for neurulation and commissure formation. Neuron, 22, 313-25.

LAPPALAINEN, H., LAINE, P., PENTIKAINEN, M. O., SAJANTILA, A. & KOVANEN, P. T. 2004. Mast cells in neovascularized human coronary plaques store and secrete basic fibroblast growth factor, a potent angiogenic mediator. Arterioscler Thromb Vasc Biol, 24, 1880-5.

LASKY, L. A. 1992. Selectins: interpreters of cell-specific carbohydrate information during inflammation. Science, 258, 964-9.

LAU, A. K., LEICHTWEIS, S. B., HUME, P., MASHIMA, R., HOU, J. Y., CHAUFOUR, X., WILKINSON, B., HUNT, N. H., CELERMAJER, D. S. & STOCKER, R. 2003. Probucol promotes functional reendothelialization in balloon-injured rabbit aortas. Circulation, 107, 2031-6.

LAUFFENBURGER, D. A. & HORWITZ, A. F. 1996. Cell migration: a physically integrated molecular process. Cell, 84, 359-69.

LAVROVSKY, Y., SCHWARTZMAN, M. L. & ABRAHAM, N. G. 1993. Novel regulatory sites of the human heme oxygenase-1 promoter region. Biochem Biophys Res Commun, 196, 336-41.

LAVROVSKY, Y., SCHWARTZMAN, M. L., LEVERE, R. D., KAPPAS, A. & ABRAHAM, N. G. 1994. Identification of binding sites for transcription factors NF-kappa B and AP-2 in the promoter region of the human heme oxygenase 1 gene. Proc Natl Acad Sci U S A, 91, 5987-91.

LEE, E. G., BOONE, D. L., CHAI, S., LIBBY, S. L., CHIEN, M., LODOLCE, J. P. & MA, A. 2000. Failure to regulate TNF-induced NF-kappaB and cell death responses in A20-deficient mice. Science, 289, 2350-4.

LEE, S. S., JOO, Y. S., KIM, W. U., MIN, D. J., MIN, J. K., PARK, S. H., CHO, C. S. & KIM, H. Y. 2001. Vascular endothelial growth factor levels in the serum and synovial fluid of patients with rheumatoid arthritis. Clin Exp Rheumatol, 19, 321-4.

LEFER, A. M. 1991. Mechanisms of the Protective Effects of Transforming Growth-Factor-Beta in Reperfusion Injury. Biochemical Pharmacology, 42, 1323-1327.

LEFER, A. M., TSAO, P., AOKI, N. & PALLADINO, M. A. 1990. Mediation of Cardioprotection by Transforming Growth-Factor-Beta. Science, 249, 61-64.

LEHOUX, S., CASTIER, Y. & TEDGUI, A. 2006. Molecular mechanisms of the vascular responses to haemodynamic forces. J Intern Med, 259, 381-92.

LERNER-MARMAROSH, N., SHEN, J., TORNO, M. D., KRAVETS, A., HU, Z. & MAINES, M. D. 2005. Human biliverdin reductase: a member of the insulin receptor substrate family with serine/threonine/tyrosine kinase activity. Proc Natl Acad Sci U S A, 102, 7109-14.

LEVIN, E. R. 1995. Endothelins. N Engl J Med, 333, 356-63.

LEY, K., LAUDANNA, C., CYBULSKY, M. I. & NOURSHARGH, S. 2007. Getting to the site of inflammation: the leukocyte adhesion cascade updated. Nat Rev Immunol, 7, 678-89.

LI, P., ELRAYESS, M. A., GOMMA, A. H., PALMEN, J., HAWE, E., FOX, K. M. & HUMPHRIES, S. E. 2005. The microsatellite polymorphism of heme oxygenase-1 is associated with baseline plasma IL-6 level but not with restenosis after coronary in-stenting. Chin Med J (Engl), 118, 1525-32.

LI, S., HUANG, N. F. & HSU, S. 2005. Mechanotransduction in endothelial cell migration. J Cell Biochem, 96, 1110-26.

LI VOLTI, G., SACERDOTI, D., SANGRAS, B., VANELLA, A., MEZENTSEV, A., SCAPAGNINI, G., FALCK, J. R. & ABRAHAM, N. G. 2005. Carbon monoxide signaling in promoting angiogenesis in human microvessel endothelial cells. Antioxid Redox Signal, 7, 704-10.

LI VOLTI, G., WANG, J., TRAGANOS, F., KAPPAS, A. & ABRAHAM, N. G. 2002. Differential effect of heme oxygenase-1 in endothelial and smooth muscle cell cycle progression. Biochem Biophys Res Commun, 296, 1077-82.

LI, Y. S., HAGA, J. H. & CHIEN, S. 2005. Molecular basis of the effects of shear stress on vascular endothelial cells. J Biomech, 38, 1949-71.

LIANG, C. C., PARK, A. Y. & GUAN, J. L. 2007. In vitro scratch assay: a convenient and inexpensive method for analysis of cell migration in vitro. Nat Protoc, 2, 329-33.

LIN, C. W., SHEN, S. C., HOU, W. C., YANG, L. Y. & CHEN, Y. C. 2008. Heme oxygenase-1 inhibits breast cancer invasion via suppressing the expression of matrix metalloproteinase-9. Mol Cancer Ther, 7, 1195-206.

LINNENBAUM, M., BUSKER, M., KRAEHLING, J.R. & BEHRENDS, S. 2012. Heme Oxygenase Isoforms Differ in Their Subcellular Trafficking during Hypoxia and Are Differentially Modulated by Cytochrome P450 Reductase. PLoS ONE, 7, e35483.

LIP, P. L., BELGORE, F., BLANN, A. D., HOPE-ROSS, M. W., GIBSON, J. M. & LIP, G. Y. 2000. Plasma VEGF and soluble VEGF receptor FLT-1 in proliferative retinopathy: relationship to endothelial dysfunction and laser treatment. Invest Ophthalmol Vis Sci, 41, 2115-9.

LIU, H., DI CUNTO, F., IMARISIO, S. & REID, L. M. 2003. Citron kinase is a cell cycle-dependent, nuclear protein required for G2/M transition of hepatocytes. J Biol Chem, 278, 2541-8.

LIU, S., CALDERWOOD, D. A. & GINSBERG, M. H. 2000. Integrin cytoplasmic domain-binding proteins. J Cell Sci, 113 (Pt 20), 3563-71.

LIU, X. M., CHAPMAN, G. B., WANG, H. & DURANTE, W. 2002. Adenovirus-mediated heme oxygenase-1 gene expression stimulates apoptosis in vascular smooth muscle cells. Circulation, 105, 79-84.

LIU, Y., WEI, S. H., HO, A. S., DE WAAL MALEFYT, R. & MOORE, K. W. 1994. Expression cloning and characterization of a human IL-10 receptor. J Immunol, 152, 1821-9.

LOBODA, A., JAZWA, A., GROCHOT-PRZECZEK, A., RUTKOWSKI, A. J., CISOWSKI, J., AGARWAL, A., JOZKOWICZ, A. & DULAK, J. 2008. Heme oxygenase-1 and the vascular bed: from molecular mechanisms to therapeutic opportunities. Antioxid Redox Signal, 10, 1767-812.

LOOTS, M. A., LAMME, E. N., MEKKES, J. R., BOS, J. D. & MIDDELKOOP, E. 1999. Cultured fibroblasts from chronic diabetic wounds on the lower extremity (non-insulin-dependent diabetes mellitus) show disturbed proliferation. Arch Dermatol Res, 291, 93-9.

LOPEZ-PEDRERA, C., PEREZ-SANCHEZ, C., RAMOS-CASALS, M., SANTOS-GONZALEZ, M., RODRIGUEZ-ARIZA, A. & CUADRADO, M. J. 2012. Cardiovascular risk in systemic autoimmune diseases: epigenetic mechanisms of immune regulatory functions. Clin Dev Immunol, 2012, 974648.

LORANT, D. E., ZIMMERMAN, G. A., MCINTYRE, T. M. & PRESCOTT, S. M. 1995. Platelet-activating factor mediates procoagulant activity on the surface of endothelial cells by promoting leukocyte adhesion. Semin Cell Biol, 6, 295-303.

LUKAS, J., LUKAS, C. & BARTEK, J. 2004. Mammalian cell cycle checkpoints: signalling pathways and their organization in space and time. DNA Repair (Amst), 3, 997-1007.

LUNDBERG, A. S. & WEINBERG, R. A. 1998. Functional inactivation of the retinoblastoma protein requires sequential modification by at least two distinct cyclin-cdk complexes. Mol Cell Biol, 18, 753-61.

LUNDKVIST, A., REICHENBACH, A., BETSHOLTZ, C., CARMELIET, P., WOLBURG, H. & PEKNY, M. 2004. Under stress, the absence of intermediate filaments from Muller cells in the retina has structural and functional consequences. J Cell Sci, 117, 3481-8.

LUPIA, E., PUCCI, A., PEASSO, P., MERLO, M., BARON, P., ZANINI, C., DEL SORBO, L., RIZEA-SAVU, S., SILVESTRO, L., FORNI, M., EMANUELLI, G., CAMUSSI, G. & MONTRUCCHIO, G. 2003. Intra-plaque production of platelet-activating factor correlates with neoangiogenesis in human carotid atherosclerotic lesions. Int J Mol Med, 12, 327-34.

LUVARA, G., PUEYO, M. E., PHILIPPE, M., MANDET, C., SAVOIE, F., HENRION, D. & MICHEL, J. B. 1998. Chronic blockade of NO synthase activity induces a proinflammatory phenotype in the arterial wall - Prevention by angiotensin II antagonism. Arteriosclerosis Thrombosis and Vascular Biology, 18, 1408-1416.

LYALL, F. & MYATT, L. 2002. The role of the placenta in pre-eclampsia--a workshop report. Placenta, 23 Suppl A, S142-5.

MA, H., CALDERON, T. M., FALLON, J. T. & BERMAN, J. W. 2002. Hepatocyte growth factor is a survival factor for endothelial cells and is expressed in human atherosclerotic plaques. Atherosclerosis, 164, 79-87.

MACHESKY, L. M., REEVES, E., WIENTJES, F., MATTHEYSE, F. J., GROGAN, A., TOTTY, N. F., BURLINGAME, A. L., HSUAN, J. J. & SEGAL, A. W. 1997. Mammalian actin-related protein 2/3 complex localizes to regions of lamellipodial protrusion and is composed of evolutionarily conserved proteins. Biochem J, 328 (Pt 1), 105-12.

MAINES, M. D. 1997. The heme oxygenase system: a regulator of second messenger gases. Annu Rev Pharmacol Toxicol, 37, 517-54.

MAINES, M. D. & ABRAHAMSSON, P. A. 1996. Expression of heme oxygenase-1 (HSP32) in human prostate: normal, hyperplastic, and tumor tissue distribution. Urology, 47, 727-33.

MAINES, M. D., MAYER, R. D., EWING, J. F. & MCCOUBREY, W. K., JR. 1993. Induction of kidney heme oxygenase-1 (HSP32) mRNA and protein by ischaemia/reperfusion: possible role of heme as both promotor of tissue damage and regulator of HSP32. J Pharmacol Exp Ther, 264, 457-62.

MAINES, M. D., TRAKSHEL, G. M. & KUTTY, R. K. 1986. Characterization of two constitutive forms of rat liver microsomal heme oxygenase. Only one molecular species of the enzyme is inducible. J Biol Chem, 261, 411-9.

MAISONPIERRE, P. C., SURI, C., JONES, P. F., BARTUNKOVA, S., WIEGAND, S. J., RADZIEJEWSKI, C., COMPTON, D., MCCLAIN, J., ALDRICH, T. H., PAPADOPOULOS, N., DALY, T. J., DAVIS, S., SATO, T. N. & YANCOPOULOS, G. D. 1997. Angiopoietin-2, a natural antagonist for Tie2 that disrupts in vivo angiogenesis. Science, 277, 55-60.

MAITY, A., MCKENNA, W. G. & MUSCHEL, R. J. 1997. Cyclin A message stability varies with the cell cycle. Cell Growth Differ, 8, 311-8.

MALEK, A. & IZUMO, S. 1992. Physiological fluid shear stress causes downregulation of endothelin-1 mRNA in bovine aortic endothelium. Am J Physiol, 263, C389-96.

MALEK, A. M., ALPER, S. L. & IZUMO, S. 1999. Haemodynamic shear stress and its role in atherosclerosis. JAMA, 282, 2035-42.

MALEK, A. M. & IZUMO, S. 1994. Molecular aspects of signal transduction of shear stress in the endothelial cell. J Hypertens, 12, 989-99.

MALEK, A. M., IZUMO, S. & ALPER, S. L. 1999. Modulation by pathophysiological stimuli of the shear stress-induced up-regulation of endothelial nitric oxide synthase expression in endothelial cells. Neurosurgery, 45, 334-44; discussion 344-5.

MALLAT, Z., BESNARD, S., DURIEZ, M., DELEUZE, V., EMMANUEL, F., BUREAU, M. F., SOUBRIER, F., ESPOSITO, B., DUEZ, H., FIEVET, C., STAELS, B., DUVERGER, N., SCHERMAN, D. & TEDGUI, A. 1999. Protective role of interleukin-10 in atherosclerosis. Circulation Research, 85, e17-24.

MALLER, J. L. 1991. Mitotic control. Curr Opin Cell Biol, 3, 269-75.

MANCUSO, C., PANI, G. & CALABRESE, V. 2006. Bilirubin: an endogenous scavenger of nitric oxide and reactive nitrogen species. Redox Rep, 11, 207-13.

MANN, G. E., YUDILEVICH, D. L. & SOBREVIA, L. 2003. Regulation of amino acid and glucose transporters in endothelial and smooth muscle cells. Physiol Rev, 83, 183-252.

MARADIT-KREMERS, H., NICOLA, P. J., CROWSON, C. S., BALLMAN, K. V. & GABRIEL, S. E. 2005. Cardiovascular death in rheumatoid arthritis: a population-based study. Arthritis Rheum, 52, 722-32.

MARELLI-BERG, F. M., PEEK, E., LIDINGTON, E. A., STAUSS, H. J. & LECHLER, R. I. 2000. Isolation of endothelial cells from murine tissue. J Immunol Methods, 244, 205-15.

MARINISSEN, M. J., TANOS, T., BOLOS, M., DE SAGARRA, M. R., COSO, O. A. & CUADRADO, A. 2006. Inhibition of heme oxygenase-1 interferes with the transforming activity of the Kaposi sarcoma herpesvirus-encoded G protein-coupled receptor. J Biol Chem, 281, 11332-46.

MARTI, H. H. & RISAU, W. 1998. Systemic hypoxia changes the organ-specific distribution of vascular endothelial growth factor and its receptors. Proc Natl Acad Sci U S A, 95, 15809-14.

MARTIN, A., KOMADA, M. R. & SANE, D. C. 2003. Abnormal angiogenesis in diabetes mellitus. Med Res Rev, 23, 117-45.

MARUYAMA, Y. 1963. The human endothelial cell in tissue culture. Z Zellforsch Mikrosk Anat, 60, 69-79.

MASHOUR, G. A. & BOOCK, R. J. 1999. Effects of shear stress on nitric oxide levels of human cerebral endothelial cells cultured in an artificial capillary system. Brain Res, 842, 233-8.

MASON, J. C., LIDINGTON, E. A., YARWOOD, H., LUBLIN, D. M. & HASKARD, D. O. 2001. Induction of endothelial cell decay-accelerating factor by vascular endothelial growth factor: a mechanism for cytoprotection against complement-mediated injury during inflammatory angiogenesis. Arthritis Rheum, 44, 138-50.

MATEO, F., VIDAL-LALIENA, M., CANELA, N., BUSINO, L., MARTINEZ-BALBAS, M. A., PAGANO, M., AGELL, N. & BACHS, O. 2009. Degradation of cyclin A is regulated by acetylation. Oncogene, 28, 2654-66.

MATEYAK, M. K., OBAYA, A. J. & SEDIVY, J. M. 1999. c-Myc regulates cyclin D-Cdk4 and -Cdk6 activity but affects cell cycle progression at multiple independent points. Mol Cell Biol, 19, 4672-83.

MATTILA, P. K. & LAPPALAINEN, P. 2008. Filopodia: molecular architecture and cellular functions. Nat Rev Mol Cell Biol, 9, 446-54.

MCALLISTER, S. S., BECKER-HAPAK, M., PINTUCCI, G., PAGANO, M. & DOWDY, S. F. 2003. Novel p27(kip1) C-terminal scatter domain mediates Rac-dependent cell migration independent of cell cycle arrest functions. Mol Cell Biol, 23, 216-28.

MCCOUBREY, W.K. & MAINES, M.D. 1993. Domains of rat heme oxygenase-2: the amino terminus and histidine 151 are required as tge axial heme iron ligand of heme oxygenase-2. J Biol Chem, 272, 1268-74.

MCCOUBREY, W.K. & MAINES, M.D. 1994. The structure, organization and differential expression of the gene encoding rat heme oxygenase-2. Gene 139, 155-161.

MEGIAS, J., BUSSEROLLES, J. & ALCARAZ, M. J. 2007. The carbon monoxide-releasing molecule CORM-2 inhibits the inflammatory response induced by cytokines in Caco-2 cells. Br J Pharmacol, 150, 977-86.

MEHTA, D. & MALIK, A. B. 2006. Signaling mechanisms regulating endothelial permeability. Physiol Rev, 86, 279-367.

MEISTER, G. & TUSCHL, T. 2004. Mechanisms of gene silencing by double-stranded RNA. Nature, 431, 343-9.

MENSE, S. M. & ZHANG, L. 2006. Heme: a versatile signaling molecule controlling the activities of diverse regulators ranging from transcription factors to MAP kinases. Cell Res, 16, 681-92.

MILEI, J., PARODI, J. C., ALONSO, G. F., BARONE, A., GRANA, D. & MATTURRI, L. 1998. Carotid rupture and intraplaque hemorrhage: immunophenotype and role of cells involved. Am Heart J, 136, 1096-105.

MINSHALL, R. D., SESSA, W. C., STAN, R. V., ANDERSON, R. G. & MALIK, A. B. 2003. Caveolin regulation of endothelial function. Am J Physiol Lung Cell Mol Physiol, 285, L1179-83.

MITCHELL, J. A. & WARNER, T. D. 1999. Cyclo-oxygenase-2: pharmacology, physiology, biochemistry and relevance to NSAID therapy. Br J Pharmacol, 128, 1121-32.

MOHAN, S., MOHAN, N., VALENTE, A. J. & SPRAGUE, E. A. 1999. Regulation of low shear flow-induced HAEC VCAM-1 expression and monocyte adhesion. American Journal of Physiology-Cell Physiology, 276, C1100-C1107.

MONCADA, S., GRYGLEWSKI, R., BUNTING, S. & VANE, J. R. 1976. An enzyme isolated from arteries transforms prostaglandin endoperoxides to an unstable substance that inhibits platelet aggregation. Nature, 263, 663-5.

MONCADA, S. & HIGGS, E. A. 2006. Nitric oxide and the vascular endothelium. Handb Exp Pharmacol, 213-54.

MONCADA, S., PALMER, R. M. & HIGGS, E. A. 1991. Nitric oxide: physiology, pathophysiology, and pharmacology. Pharmacol Rev, 43, 109-42.

MORENO, P. R., PURUSHOTHAMAN, K. R., FUSTER, V., ECHEVERRI, D., TRUSZCZYNSKA, H., SHARMA, S. K., BADIMON, J. J. & O'CONNOR, W. N. 2004. Plaque neovascularization is increased in ruptured atherosclerotic lesions of human aorta: implications for plaque vulnerability. Circulation, 110, 2032-8.

MORGAN, D. O. 1997. Cyclin-dependent kinases: engines, clocks, and microprocessors. Annu Rev Cell Dev Biol, 13, 261-91.

MORISE, Z., EPPIHIMER, M., GRANGER, D. N., ANDERSON, D. C. & GRISHAM, M. B. 1999. Effects of lipopolysaccharide on endothelial cell adhesion molecule expression in interleukin-10 deficient mice. Inflammation, 23, 99-110.

MORITA, T. & KOUREMBANAS, S. 1995. Endothelial cell expression of vasoconstrictors and growth factors is regulated by smooth muscle cell-derived carbon monoxide. Journal of Clinical Investigation, 96, 2676-82.

MORITA, T., MITSIALIS, S. A., KOIKE, H., LIU, Y. & KOUREMBANAS, S. 1997. Carbon monoxide controls the proliferation of hypoxic vascular smooth muscle cells. J Biol Chem, 272, 32804-9.

MORITA, T., PERRELLA, M. A., LEE, M. E. & KOUREMBANAS, S. 1995. Smooth muscle cell-derived carbon monoxide is a regulator of vascular cGMP. Proc Natl Acad Sci U S A, 92, 1475-9.

MORSE, D., PISCHKE, S. E., ZHOU, Z., DAVIS, R. J., FLAVELL, R. A., LOOP, T., OTTERBEIN, S. L., OTTERBEIN, L. E. & CHOI, A. M. 2003. Suppression of inflammatory cytokine production by carbon monoxide involves the JNK pathway and AP-1. J Biol Chem, 278, 36993-8.

MORSE, D. & SETHI, J. 2002. Carbon monoxide and human disease. Antioxid Redox Signal, 4, 331-8.

MORSI, W. G., SHAKER, O. G., ISMAIL, E. F., AHMED, H. H., EL-SERAFI, T. I., MAKLADY, F. A., ABDEL-AZIZ, M. T., EL-ASMAR, M. F. & ATTA, H. M. 2006. HO-1 and VGEF gene expression in human arteries with advanced atherosclerosis. Clin Biochem, 39, 1057-62.

MOTTERLINI, R., CLARK, J. E., FORESTI, R., SARATHCHANDRA, P., MANN, B. E. & GREEN, C. J. 2002. Carbon monoxide-releasing molecules: characterization of biochemical and vascular activities. Circulation Research, 90, E17-24.

MOTTERLINI, R., MANN, B. E. & FORESTI, R. 2005. Therapeutic applications of carbon monoxide-releasing molecules. Expert Opin Investig Drugs, 14, 1305-18.

MOTTERLINI, R., MANN, B. E., JOHNSON, T. R., CLARK, J. E., FORESTI, R. & GREEN, C. J. 2003. Bioactivity and pharmacological actions of carbon monoxide-releasing molecules. Curr Pharm Des, 9, 2525-39.

MOULTON, K. S., HELLER, E., KONERDING, M. A., FLYNN, E., PALINSKI, W. & FOLKMAN, J. 1999. Angiogenesis inhibitors endostatin or TNP-470 reduce intimal neovascularization and plaque growth in apolipoprotein E-deficient mice. Circulation, 99, 1726-32.

MOULTON, K. S., VAKILI, K., ZURAKOWSKI, D., SOLIMAN, M., BUTTERFIELD, C., SYLVIN, E., LO, K. M., GILLIES, S., JAVAHERIAN, K. & FOLKMAN, J. 2003. Inhibition of plaque neovascularization reduces macrophage accumulation and progression of advanced atherosclerosis. Proc Natl Acad Sci U S A, 100, 4736-41.

MULLER, W. A. 2003. Leukocyte-endothelial-cell interactions in leukocyte transmigration and the inflammatory response. Trends Immunol, 24, 327-34.

MUROHARA, T. & ASAHARA, T. 2002. Nitric oxide and angiogenesis in cardiovascular disease. Antioxid Redox Signal, 4, 825-31.

MUROHARA, T., HOROWITZ, J. R., SILVER, M., TSURUMI, Y., CHEN, D., SULLIVAN, A. & ISNER, J. M. 1998. Vascular endothelial growth factor/vascular permeability factor enhances vascular permeability via nitric oxide and prostacyclin. Circulation, 97, 99-107.

MUSTONEN, T. & ALITALO, K. 1995. Endothelial receptor tyrosine kinases involved in angiogenesis. J Cell Biol, 129, 895-8.

NAGAHARA, H., VOCERO-AKBANI, A. M., SNYDER, E. L., HO, A., LATHAM, D. G., LISSY, N. A., BECKER-HAPAK, M., EZHEVSKY, S. A. & DOWDY, S. F. 1998. Transduction of full-length TAT fusion proteins into mammalian cells: TAT-p27Kip1 induces cell migration. Nat Med, 4, 1449-52.

NAKAYAMA, K. I. & NAKAYAMA, K. 2006. Ubiquitin ligases: cell-cycle control and cancer. Nat Rev Cancer, 6, 369-81.

NESSA, A., LATIF, S. A., SIDDIQUI, N. I., HUSSAIN, M. A., BHUIYAN, M. R., HOSSAIN, M. A., AKTHER, A. & RAHMAN, M. 2009. Angiogenesis-a novel therapeutic approach for ischaemic heart disease. Mymensingh Med J, 18, 264-72.

NEUFELD, G., COHEN, T., GENGRINOVITCH, S. & POLTORAK, Z. 1999. Vascular endothelial growth factor (VEGF) and its receptors. FASEB J, 13, 9-22.

NEUZIL, J. & STOCKER, R. 1994. Free and albumin-bound bilirubin are efficient co-antioxidants for alpha-tocopherol, inhibiting plasma and low density lipoprotein lipid peroxidation. J Biol Chem, 269, 16712-9.

NEWMAN, P. J. & NEWMAN, D. K. 2003. Signal transduction pathways mediated by PECAM-1: new roles for an old molecule in platelet and vascular cell biology. Arterioscler Thromb Vasc Biol, 23, 953-64.

NIEMINEN, M., HENTTINEN, T., MERINEN, M., MARTTILA-ICHIHARA, F., ERIKSSON, J. E. & JALKANEN, S. 2006. Vimentin function in lymphocyte adhesion and transcellular migration. Nat Cell Biol, 8, 156-62.

NIZAMUTDINOVA, I. T., KIM, Y. M., KIM, H. J., SEO, H. G., LEE, J. H. & CHANG, K. C. 2009. Carbon monoxide (from CORM-2) inhibits high glucose-induced ICAM-1 expression via AMP-activated protein kinase and PPAR-gamma activations in endothelial cells. Atherosclerosis, 207, 405-11.

NODA, A., NING, Y., VENABLE, S. F., PEREIRA-SMITH, O. M. & SMITH, J. R. 1994. Cloning of senescent cell-derived inhibitors of DNA synthesis using an expression screen. Exp Cell Res, 211, 90-8.

NOVOTNY, L. & VITEK, L. 2003. Inverse relationship between serum bilirubin and atherosclerosis in men: a meta-analysis of published studies. Exp Biol Med (Maywood), 228, 568-71.

NURSE, P. 1990. Universal control mechanism regulating onset of M-phase. Nature, 344, 503-8.

OBAYA, A. J. & SEDIVY, J. M. 2002. Regulation of cyclin-Cdk activity in mammalian cells. Cell Mol Life Sci, 59, 126-42.

OLLINGER, R., BILBAN, M., ERAT, A., FROIO, A., MCDAID, J., TYAGI, S., CSIZMADIA, E., GRACA-SOUZA, A. V., LILOIA, A., SOARES, M. P., OTTERBEIN, L. E., USHEVA, A., YAMASHITA, K. & BACH, F. H. 2005. Bilirubin: a natural inhibitor of vascular smooth muscle cell proliferation. Circulation, 112, 1030-9.

OLLINGER, R., YAMASHITA, K., BILBAN, M., ERAT, A., KOGLER, P., THOMAS, M., CSIZMADIA, E., USHEVA, A., MARGREITER, R. & BACH, F. H. 2007. Bilirubin and biliverdin treatment of atherosclerotic diseases. Cell Cycle, 6, 39-43.

ONAT, D., BRILLON, D., COLOMBO, P. C. & SCHMIDT, A. M. 2011. Human vascular endothelial cells: a model system for studying vascular inflammation in diabetes and atherosclerosis. Curr Diab Rep, 11, 193-202.

OTTERBEIN, L., CHIN, B. Y., OTTERBEIN, S. L., LOWE, V. C., FESSLER, H. E. & CHOI, A. M. 1997. Mechanism of hemoglobin-induced protection against endotoxemia in rats: a ferritin-independent pathway. Am J Physiol, 272, L268-75.

OTTERBEIN, L. E., BACH, F. H., ALAM, J., SOARES, M., TAO LU, H., WYSK, M., DAVIS, R. J., FLAVELL, R. A. & CHOI, A. M. 2000. Carbon monoxide has anti-inflammatory effects involving the mitogen-activated protein kinase pathway. Nat Med, 6, 422-8.

OTTERBEIN, L. E., HEDBLOM, A., HARRIS, C., CSIZMADIA, E., GALLO, D. & WEGIEL, B. 2011. Heme oxygenase-1 and carbon monoxide modulate DNA repair through ataxia-telangiectasia mutated (ATM) protein. Proc Natl Acad Sci U S A, 108, 14491-6.

OTTERBEIN, L. E., SOARES, M. P., YAMASHITA, K. & BACH, F. H. 2003. Heme oxygenase-1: unleashing the protective properties of heme. Trends Immunol, 24, 449-55.

PAE, H. O., LEE, Y. C. & CHUNG, H. T. 2008. Heme oxygenase-1 and carbon monoxide: emerging therapeutic targets in inflammation and allergy. Recent Pat Inflamm Allergy Drug Discov, 2, 159-65.

PALEOLOG, E. M. 2002. Angiogenesis in rheumatoid arthritis. Arthritis Res, 4 Suppl 3, S81-90.

PALEOLOG, E. M., YOUNG, S., STARK, A. C., MCCLOSKEY, R. V., FELDMANN, M. & MAINI, R. N. 1998. Modulation of angiogenic vascular endothelial growth factor by tumor necrosis factor alpha and interleukin-1 in rheumatoid arthritis. Arthritis Rheum, 41, 1258-65.

PALMER, R. M., ASHTON, D. S. & MONCADA, S. 1988. Vascular endothelial cells synthesize nitric oxide from L-arginine. Nature, 333, 664-6.

PALMER, R. M., FERRIGE, A. G. & MONCADA, S. 1987. Nitric oxide release accounts for the biological activity of endothelium-derived relaxing factor. Nature, 327, 524-6.

PAN, S. 2009. Molecular mechanisms responsible for the atheroprotective effects of laminar shear stress. Antioxid Redox Signal, 11, 1669-82.

PAPAPETROPOULOS, A., FULTON, D., MAHBOUBI, K., KALB, R. G., O'CONNOR, D. S., LI, F., ALTIERI, D. C. & SESSA, W. C. 2000. Angiopoietin-1 inhibits endothelial cell apoptosis via the Akt/survivin pathway. J Biol Chem, 275, 9102-5.

PAPAPETROPOULOS, A., GARCIA-CARDENA, G., DENGLER, T. J., MAISONPIERRE, P. C., YANCOPOULOS, G. D. & SESSA, W. C. 1999. Direct actions of angiopoietin-1 on human endothelium: evidence for network stabilization, cell survival, and interaction with other angiogenic growth factors. Lab Invest, 79, 213-23.

PARDANAUD, L., YASSINE, F. & DIETERLEN-LIEVRE, F. 1989. Relationship between vasculogenesis, angiogenesis and haemopoiesis during avian ontogeny. Development, 105, 473-85.

PARK, J. E., KELLER, G. A. & FERRARA, N. 1993. The vascular endothelial growth factor (VEGF) isoforms: differential deposition into the subepithelial extracellular matrix and bioactivity of extracellular matrix-bound VEGF. Mol Biol Cell, 4, 1317-26.

PARK, S. K., YANG, W. S., LEE, S. K., AHN, H., PARK, J. S., HWANG, O. & LEE, J. D. 2000. TGF-beta(1) down-regulates inflammatory cytokine-induced VCAM-1 expression in cultured human glomerular endothelial cells. Nephrology Dialysis Transplantation, 15, 596-604.

PARSONS, M., KEPPLER, M. D., KLINE, A., MESSENT, A., HUMPHRIES, M. J., GILCHRIST, R., HART, I. R., QUITTAU-PREVOSTEL, C., HUGHES, W. E., PARKER, P. J. & NG, T. 2002. Site-directed perturbation of protein kinase C- integrin interaction blocks carcinoma cell chemotaxis. Mol Cell Biol, 22, 5897-911.

PARTANEN, J., ARMSTRONG, E., MAKELA, T. P., KORHONEN, J., SANDBERG, M., RENKONEN, R., KNUUTILA, S., HUEBNER, K. & ALITALO, K. 1992. A novel endothelial cell surface receptor tyrosine kinase with extracellular epidermal growth factor homology domains. Mol Cell Biol, 12, 1698-707.

PARTRIDGE, J., CARLSEN, H., ENESA, K., CHAUDHURY, H., ZAKKAR, M., LUONG, L., KINDERLERER, A., JOHNS, M., BLOMHOFF, R., MASON, J. C., HASKARD, D. O. & EVANS, P. C. 2007. Laminar shear stress acts as a switch to regulate divergent functions of NF-kappaB in endothelial cells. FASEB J, 21, 3553-61.

PASIC, L., KOTOVA, T. & SCHAFER, D. A. 2008. Ena/VASP proteins capture actin filament barbed ends. J Biol Chem, 283, 9814-9.

PASSANITI, A., TAYLOR, R. M., PILI, R., GUO, Y., LONG, P. V., HANEY, J. A., PAULY, R. R., GRANT, D. S. & MARTIN, G. R. 1992. A simple, quantitative method for assessing angiogenesis and antiangiogenic agents using reconstituted basement membrane, heparin, and fibroblast growth factor. Lab Invest, 67, 519-28.

PATAN, S. 2000. Vasculogenesis and angiogenesis as mechanisms of vascular network formation, growth and remodeling. J Neurooncol, 50, 1-15.

PAUNESKU, T., MITTAL, S., PROTIC, M., ORYHON, J., KOROLEV, S. V., JOACHIMIAK, A. & WOLOSCHAK, G. E. 2001. Proliferating cell nuclear antigen (PCNA): ringmaster of the genome. Int J Radiat Biol, 77, 1007-21.

PEDRAM, A., RAZANDI, M. & LEVIN, E. R. 1998. Extracellular signal-regulated protein kinase/Jun kinase cross-talk underlies vascular endothelial cell growth factor-induced endothelial cell proliferation. J Biol Chem, 273, 26722-8.

PELLEGRIN, S. & MELLOR, H. 2007. Actin stress fibres. J Cell Sci, 120, 3491-9.

PETERS, K. G., DE VRIES, C. & WILLIAMS, L. T. 1993. Vascular endothelial growth factor receptor expression during embryogenesis and tissue repair suggests a role in endothelial differentiation and blood vessel growth. Proc Natl Acad Sci U S A, 90, 8915-9.

PETIT, V. & THIERY, J. P. 2000. Focal adhesions: structure and dynamics. Biol Cell, 92, 477-94.

PETRACHE, I., OTTERBEIN, L. E., ALAM, J., WIEGAND, G. W. & CHOI, A. M. 2000. Heme oxygenase-1 inhibits TNF-alpha-induced apoptosis in cultured fibroblasts. Am J Physiol Lung Cell Mol Physiol, 278, L312-9.

PETROVA, T. V., MAKINEN, T. & ALITALO, K. 1999. Signaling via vascular endothelial growth factor receptors. Exp Cell Res, 253, 117-30.

PHAM, C. G., BUBICI, C., ZAZZERONI, F., PAPA, S., JONES, J., ALVAREZ, K., JAYAWARDENA, S., DE SMAELE, E., CONG, R., BEAUMONT, C., TORTI, F. M., TORTI, S. V. & FRANZOSO, G. 2004. Ferritin heavy chain upregulation by NF-kappaB inhibits TNFalpha-induced apoptosis by suppressing reactive oxygen species. Cell, 119, 529-42.

PIAO, M. & TOKUNAGA, O. 2006. Significant expression of endoglin (CD105), TGFbeta-1 and TGFbeta R-2 in the atherosclerotic aorta: an immunohistological study. J Atheroscler Thromb, 13, 82-9.

PINDERSKI OSLUND, L. J., HEDRICK, C. C., OLVERA, T., HAGENBAUGH, A., TERRITO, M., BERLINER, J. A. & FYFE, A. I. 1999. Interleukin-10 blocks atherosclerotic events in vitro and in vivo. Arterioscler Thromb Vasc Biol, 19, 2847-53.

PINES, J. & HUNTER, T. 1989. Isolation of a human cyclin cDNA: evidence for cyclin mRNA and protein regulation in the cell cycle and for interaction with p34cdc2. Cell, 58, 833-46.

POLLARD, T. D. & BORISY, G. G. 2003. Cellular motility driven by assembly and disassembly of actin filaments. Cell, 112, 453-65.

POLLOCK, J. S., FORSTERMANN, U., MITCHELL, J. A., WARNER, T. D., SCHMIDT, H. H., NAKANE, M. & MURAD, F. 1991. Purification and characterization of particulate endothelium-derived relaxing factor synthase from cultured and native bovine aortic endothelial cells. Proc Natl Acad Sci U S A, 88, 10480-4.

POLYAK, K., KATO, J. Y., SOLOMON, M. J., SHERR, C. J., MASSAGUE, J., ROBERTS, J. M. & KOFF, A. 1994. p27Kip1, a cyclin-Cdk inhibitor, links transforming growth factor-beta and contact inhibition to cell cycle arrest. Genes Dev, 8, 9-22.

PONKA, P. 1999. Cellular iron metabolism. Kidney Int Suppl, 69, S2-11.

POSS, K. D. & TONEGAWA, S. 1997. Heme oxygenase 1 is required for mammalian iron reutilization. Proc Natl Acad Sci U S A, 94, 10919-24.

POTTEAUX, S., DELEUZE, V., MERVAL, R., BUREAU, M. F., ESPOSITO, B., SCHERMAN, D., TEDGUI, A. & MALLAT, Z. 2006. In vivo electrotransfer of interleukin-10 cDNA prevents endothelial upregulation of activated NF-kappaB and adhesion molecules following an atherogenic diet. Eur Cytokine Netw, 17, 13-8.

PRAHLAD, V., YOON, M., MOIR, R. D., VALE, R. D. & GOLDMAN, R. D. 1998. Rapid movements of vimentin on tubule tracks: kinesin-dependent assembly of intermediate filament networks. J Cell Biol, 143, 159-70.

PREDESCU, S. A., PREDESCU, D. N. & MALIK, A. B. 2007. Molecular determinants of endothelial transcytosis and their role in endothelial permeability. Am J Physiol Lung Cell Mol Physiol, 293, L823-42.

PREISS, D. J. & SATTAR, N. 2007. Vascular cell adhesion molecule-1: a viable therapeutic target for atherosclerosis? Int J Clin Pract, 61, 697-701.

PRICE, C. J. & BRINDLE, N. P. 2000. Vasodilator-stimulated phosphoprotein is involved in stress-fiber and membrane ruffle formation in endothelial cells. Arterioscler Thromb Vasc Biol, 20, 2051-6.

PUFE, T., PETERSEN, W., TILLMANN, B. & MENTLEIN, R. 2001. Splice variants VEGF121 and VEGF165 of the angiogenic peptide vascular endothelial cell growth factor are expressed in the synovial tissue of patients with rheumatoid arthritis. J Rheumatol, 28, 1482-5.

QI, J. H. & CLAESSON-WELSH, L. 2001. VEGF-induced activation of phosphoinositide 3-kinase is dependent on focal adhesion kinase. Exp Cell Res, 263, 173-82.

QUINN, T. P., PETERS, K. G., DE VRIES, C., FERRARA, N. & WILLIAMS, L. T. 1993. Fetal liver kinase 1 is a receptor for vascular endothelial growth factor and is selectively expressed in vascular endothelium. Proc Natl Acad Sci U S A, 90, 7533-7.

RAJU, V. S., MCCOUBREY, W. K., JR. & MAINES, M. D. 1997. Regulation of heme oxygenase-2 by glucocorticoids in neonatal rat brain: characterization of a functional glucocorticoid response element. Biochim Biophys Acta, 1351, 89-104.

RICCARDI, C. & NICOLETTI, I. 2006. Analysis of apoptosis by propidium iodide staining and flow cytometry. Nat Protoc, 1, 1458-61.

RIDDELL, D. R. & OWEN, J. S. 1999. Nitric oxide and platelet aggregation. Vitam Horm, 57, 25-48.

RIDLEY, A. J. 2001. Rho GTPases and cell migration. J Cell Sci, 114, 2713-22.

RIDLEY, A. J., SCHWARTZ, M. A., BURRIDGE, K., FIRTEL, R. A., GINSBERG, M. H., BORISY, G., PARSONS, J. T. & HORWITZ, A. R. 2003. Cell migration: integrating signals from front to back. Science, 302, 1704-9.

RILEY, J. K., TAKEDA, K., AKIRA, S. & SCHREIBER, R. D. 1999. Interleukin-10 receptor signaling through the JAK-STAT pathway. Requirement for two distinct receptor-derived signals for anti-inflammatory action. J Biol Chem, 274, 16513-21.

RISAU, W. 1995. Differentiation of endothelium. FASEB J, 9, 926-33.

RISAU, W. 1997. Mechanisms of angiogenesis. Nature, 386, 671-4.

RISAU, W. & FLAMME, I. 1995. Vasculogenesis. Annu Rev Cell Dev Biol, 11, 73-91.

ROBB, L. & ELEFANTY, A. G. 1998. The hemangioblast--an elusive cell captured in culture. Bioessays, 20, 611-4.

ROCA, C. & ADAMS, R. H. 2007. Regulation of vascular morphogenesis by Notch signaling. Genes Dev, 21, 2511-24.

ROCHA, V. Z. & LIBBY, P. 2009. Obesity, inflammation, and atherosclerosis. Nat Rev Cardiol, 6, 399-409.

ROMANSKI, S., KRAUS, B., GUTTENTAG, M., SCHLUNDT, W., RUCKER, H., ADLER, A., NEUDORFL, J. M., ALBERTO, R., AMSLINGER, S. & SCHMALZ, H. G. 2012. Acyloxybutadiene tricarbonyl iron complexes as enzyme-triggered CO-releasing molecules (ET-CORMs): a structure-activity relationship study. Dalton Trans, 41, 13862-75.

ROMANSKI, S., KRAUS, B., SCHATZSCHNEIDER, U., NEUDORFL, J. M., AMSLINGER, S. & SCHMALZ, H. G. 2011. Acyloxybutadiene iron tricarbonyl complexes as enzyme-triggered CO-releasing molecules (ET-CORMs). Angew Chem Int Ed Engl, 50, 2392-6.

ROONEY, M., CONDELL, D., QUINLAN, W., DALY, L., WHELAN, A., FEIGHERY, C. & BRESNIHAN, B. 1988. Analysis of the histologic variation of synovitis in rheumatoid arthritis. Arthritis Rheum, 31, 956-63.

ROSS, R. 1999. Atherosclerosis--an inflammatory disease. N Engl J Med, 340, 115-26.

ROSSANT, J. & HOWARD, L. 2002. Signaling pathways in vascular development. Annu Rev Cell Dev Biol, 18, 541-73.

ROTH, G. J. 1992. Platelets and blood vessels: the adhesion event. Immunol Today, 13, 100-5.

ROUSSEAU, S., HOULE, F. & HUOT, J. 2000. Integrating the VEGF signals leading to actin-based motility in vascular endothelial cells. Trends Cardiovasc Med, 10, 321-7.

ROUSSEL, M. F. 1999. The INK4 family of cell cycle inhibitors in cancer. Oncogene, 18, 5311-7.

RUDINI, N. & DEJANA, E. 2008. Adherens junctions. Curr Biol, 18, R1080-2.

RUGGERI, Z. M. 1999. Structure and function of von Willebrand factor. Thromb Haemost, 82, 576-84.

RYTER, S. W., ALAM, J. & CHOI, A. M. 2006. Heme oxygenase-1/carbon monoxide: from basic science to therapeutic applications. Physiol Rev, 86, 583-650.

RYTER, S. W. & CHOI, A. M. 2002. Heme oxygenase-1: molecular mechanisms of gene expression in oxygen-related stress. Antioxid Redox Signal, 4, 625-32.

SAHAGUN, G., MOORE, S. A., FABRY, Z., SCHELPER, R. L. & HART, M. N. 1989. Purification of murine endothelial cell cultures by flow cytometry using fluorescein-labeled griffonia simplicifolia agglutinin. Am J Pathol, 134, 1227-32.

SALIM, M., BROWN-KIPPHUT, B. A. & MAINES, M. D. 2001. Human biliverdin reductase is autophosphorylated, and phosphorylation is required for bilirubin formation. J Biol Chem, 276, 10929-34.

SAMPATH, R., KUKIELKA, G. L., SMITH, C. W., ESKIN, S. G. & MCINTIRE, L. V. 1995. Shear Stress-Mediated Changes in the Expression of Leukocyte Adhesion Receptors on Human Umbilical Vein Endothelial-Cells in-Vitro. Annals of Biomedical Engineering, 23, 247-256.

SANDER, E. E., TEN KLOOSTER, J. P., VAN DELFT, S., VAN DER KAMMEN, R. A. & COLLARD, J. G. 1999. Rac downregulates Rho activity: reciprocal balance between both GTPases determines cellular morphology and migratory behavior. J Cell Biol, 147, 1009-22.

SANZ-RODRIGUEZ, F., GUERRERO-ESTEO, M., BOTELLA, L. M., BANVILLE, D., VARY, C. P. & BERNABEU, C. 2004. Endoglin regulates cytoskeletal organization through binding to ZRP-1, a member of the Lim family of proteins. J Biol Chem, 279, 32858-68.

SASS, G., SEYFRIED, S., PARREIRA SOARES, M., YAMASHITA, K., KACZMAREK, E., NEUHUBER, W. L. & TIEGS, G. 2004. Cooperative effect of biliverdin and carbon monoxide on survival of mice in immune-mediated liver injury. Hepatology, 40, 1128-35.

SATYANARAYANA, A. & KALDIS, P. 2009. Mammalian cell-cycle regulation: several Cdks, numerous cyclins and diverse compensatory mechanisms. Oncogene, 28, 2925-39.

SAVAGE, B., SALDIVAR, E. & RUGGERI, Z. M. 1996. Initiation of platelet adhesion by arrest onto fibrinogen or translocation on von Willebrand factor. Cell, 84, 289-97.

SCHACHINGER, V., BRITTEN, M. B. & ZEIHER, A. M. 2000. Prognostic impact of coronary vasodilator dysfunction on adverse long-term outcome of coronary heart disease. Circulation, 101, 1899-906.

SCHIFFRIN, E. L. 2001. A critical review of the role of endothelial factors in the pathogenesis of hypertension. J Cardiovasc Pharmacol, 38 Suppl 2, S3-6.

SCHILLINGER, M., EXNER, M., MLEKUSCH, W., AHMADI, R., RUMPOLD, H., MANNHALTER, C., WAGNER, O. & MINAR, E. 2002. Heme oxygenase-1 genotype is a vascular anti-inflammatory factor following balloon angioplasty. J Endovasc Ther, 9, 385-94.

SCHIRENBECK, A., ARASADA, R., BRETSCHNEIDER, T., STRADAL, T. E., SCHLEICHER, M. & FAIX, J. 2006. The bundling activity of vasodilator-stimulated phosphoprotein is required for filopodium formation. Proc Natl Acad Sci U S A, 103, 7694-9.

SCHROEDER, A., MUELLER, O., STOCKER, S., SALOWSKY, R., LEIBER, M., GASSMANN, M., LIGHTFOOT, S., MENZEL, W., GRANZOW, M. & RAGG, T. 2006. The RIN: an RNA integrity number for assigning integrity values to RNA measurements. BMC Mol Biol, 7, 3.

SCHWERTNER, H. A. 1998. Association of smoking and low serum bilirubin antioxidant concentrations. Atherosclerosis, 136, 383-7.

SCHWERTNER, H. A., JACKSON, W. G. & TOLAN, G. 1994. Association of low serum concentration of bilirubin with increased risk of coronary artery disease. Clin Chem, 40, 18-23.

SCHWERTNER, H. A. & VITEK, L. 2008. Gilbert syndrome, UGT1A1*28 allele, and cardiovascular disease risk: possible protective effects and therapeutic applications of bilirubin. Atherosclerosis, 198, 1-11.

SCOTT-BURDEN, T. 1995. Regulation of nitric oxide production by tetrahydrobiopterin. Circulation, 91, 248-50.

SELDON, M. P., SILVA, G., PEJANOVIC, N., LARSEN, R., GREGOIRE, I. P., FILIPE, J., ANRATHER, J. & SOARES, M. P. 2007. Heme oxygenase-1 inhibits the expression of adhesion molecules associated with endothelial cell activation via inhibition of NF-kappaB RelA phosphorylation at serine 276. J Immunol, 179, 7840-51.

SELZMAN, C. H., MELDRUM, D. R., CAIN, B. S., MENG, X., SHAMES, B. D., AO, L. & HARKEN, A. H. 1998. Interleukin-10 inhibits postinjury tumor necrosis factor-mediated human vascular smooth muscle proliferation. J Surg Res, 80, 352-6.

SENBANERJEE, S., LIN, Z., ATKINS, G. B., GREIF, D. M., RAO, R. M., KUMAR, A., FEINBERG, M. W., CHEN, Z., SIMON, D. I., LUSCINSKAS, F. W., MICHEL, T. M., GIMBRONE, M. A., JR., GARCIA-CARDENA, G. & JAIN, M. K. 2004. KLF2 Is a novel transcriptional regulator of endothelial proinflammatory activation. J Exp Med, 199, 1305-15.

SERINI, G., VALDEMBRI, D. & BUSSOLINO, F. 2006. Integrins and angiogenesis: a sticky business. Exp Cell Res, 312, 651-8.

SETA, F., BELLNER, L., REZZANI, R., REGAN, R. F., DUNN, M. W., ABRAHAM, N. G., GRONERT, K. & LANIADO-SCHWARTZMAN, M. 2006. Heme oxygenase-2 is a critical determinant for execution of an acute inflammatory and reparative response. Am J Pathol, 169, 1612-23.

SHALABY, F., ROSSANT, J., YAMAGUCHI, T. P., GERTSENSTEIN, M., WU, X. F., BREITMAN, M. L. & SCHUH, A. C. 1995. Failure of blood-island formation and vasculogenesis in Flk-1-deficient mice. Nature, 376, 62-6.

SHAY, J. W. & WRIGHT, W. E. 2000. Hayflick, his limit, and cellular ageing. Nat Rev Mol Cell Biol, 1, 72-6.

SHERER, Y., ZINGER, H. & SHOENFELD, Y. 2010. Atherosclerosis in systemic lupus erythematosus. Autoimmunity, 43, 98-102.

SHERR, C. J. & ROBERTS, J. M. 1999. CDK inhibitors: positive and negative regulators of G1-phase progression. Genes Dev, 13, 1501-12.

SHI, Y. & MASSAGUE, J. 2003. Mechanisms of TGF-beta signaling from cell membrane to the nucleus. Cell, 113, 685-700.

SHIBAHARA, S., MULLER, R., TAGUCHI, H. & YOSHIDA, T. 1985. Cloning and expression of cDNA for rat heme oxygenase. Proc Natl Acad Sci U S A, 82, 7865-9.

SHIBAHARA, S., SATO, M., MULLER, R. M. & YOSHIDA, T. 1989. Structural organization of the human heme oxygenase gene and the function of its promoter. Eur J Biochem, 179, 557-63.

SHIBUYA, M. 2006. Differential roles of vascular endothelial growth factor receptor-1 and receptor-2 in angiogenesis. J Biochem Mol Biol, 39, 469-78.

SHIBUYA, M., YAMAGUCHI, S., YAMANE, A., IKEDA, T., TOJO, A., MATSUSHIME, H. & SATO, M. 1990. Nucleotide sequence and expression of a novel human receptor-type tyrosine kinase gene (flt) closely related to the fms family. Oncogene, 5, 519-24.

SHULL, M. M., ORMSBY, I., KIER, A. B., PAWLOWSKI, S., DIEBOLD, R. J., YIN, M. Y., ALLEN, R., SIDMAN, C., PROETZEL, G., CALVIN, D., ANNUNZIATA, N. & DOETSCHMAN, T. 1992. Targeted Disruption of the Mouse Transforming Growth Factor-Beta-1 Gene Results in Multifocal Inflammatory Disease. Nature, 359, 693-699.

SICA, A., LARGHI, P., MANCINO, A., RUBINO, L., PORTA, C., TOTARO, M. G., RIMOLDI, M., BISWAS, S. K., ALLAVENA, P. & MANTOVANI, A. 2008. Macrophage polarization in tumour progression. Semin Cancer Biol, 18, 349-55.

SIEDLECKI, C. A., LESTINI, B. J., KOTTKE-MARCHANT, K. K., EPPELL, S. J., WILSON, D. L. & MARCHANT, R. E. 1996. Shear-dependent changes in the three-dimensional structure of human von Willebrand factor. Blood, 88, 2939-50.

SIEMEISTER, G., SCHIRNER, M., REUSCH, P., BARLEON, B., MARME, D. & MARTINY-BARON, G. 1998. An antagonistic vascular endothelial growth factor (VEGF) variant inhibits VEGF-stimulated receptor autophosphorylation and proliferation of human endothelial cells. Proc Natl Acad Sci U S A, 95, 4625-9.

SIMMONS, D. L. 1995. The role of ICAM expression in immunity and disease. Cancer Surv, 24, 141-55.

SIMMONS, D. L., BOTTING, R. M. & HLA, T. 2004. Cyclooxygenase isozymes: the biology of prostaglandin synthesis and inhibition. Pharmacol Rev, 56, 387-437.

SINER, J. M., JIANG, G., COHEN, Z. I., SHAN, P., ZHANG, X., LEE, C. G., ELIAS, J. A. & LEE, P. J. 2007. VEGF-induced heme oxygenase-1 confers cytoprotection from lethal hyperoxia in vivo. FASEB J, 21, 1422-32.

SKOBLE, J., AUERBUCH, V., GOLEY, E. D., WELCH, M. D. & PORTNOY, D. A. 2001. Pivotal role of VASP in Arp2/3 complex-mediated actin nucleation, actin branch-formation, and Listeria monocytogenes motility. J Cell Biol, 155, 89-100.

SMITH, W. B., NOACK, L., KHEWGOODALL, Y., ISENMANN, S., VADAS, M. A. & GAMBLE, J. R. 1996. Transforming growth factor-beta 1 inhibits the production of IL-8 and the transmigration of neutrophils through activated endothelium. Journal of Immunology, 157, 360-368.

SOARES, M. P., SELDON, M. P., GREGOIRE, I. P., VASSILEVSKAIA, T., BERBERAT, P. O., YU, J., TSUI, T. Y. & BACH, F. H. 2004. Heme oxygenase-1 modulates the expression of adhesion molecules associated with endothelial cell activation. J Immunol, 172, 3553-63.

SODHI, K., INOUE, K., GOTLINGER, K. H., CANESTRARO, M., VANELLA, L., KIM, D. H., MANTHATI, V. L., KODURU, S. R., FALCK, J. R., SCHWARTZMAN, M. L. & ABRAHAM, N. G. 2009. Epoxyeicosatrienoic acid agonist rescues the metabolic syndrome phenotype of HO-2-null mice. J Pharmacol Exp Ther, 331, 906-16.

SOKER, S., TAKASHIMA, S., MIAO, H. Q., NEUFELD, G. & KLAGSBRUN, M. 1998. Neuropilin-1 is expressed by endothelial and tumor cells as an isoform-specific receptor for vascular endothelial growth factor. Cell, 92, 735-45.

SOLOMON, M. J., GLOTZER, M., LEE, T. H., PHILIPPE, M. & KIRSCHNER, M. W. 1990. Cyclin activation of p34cdc2. Cell, 63, 1013-24.

SONG, F., LI, X., ZHANG, M., YAO, P., YANG, N., SUN, X., HU, F. B. & LIU, L. 2009. Association between heme oxygenase-1 gene promoter polymorphisms and type 2 diabetes in a Chinese population. Am J Epidemiol, 170, 747-56.

SPENCER, S. D., DI MARCO, F., HOOLEY, J., PITTS-MEEK, S., BAUER, M., RYAN, A. M., SORDAT, B., GIBBS, V. C. & AGUET, M. 1998. The orphan receptor CRF2-4 is an essential subunit of the interleukin 10 receptor. J Exp Med, 187, 571-8.

SPIECKER, M., PENG, H. B. & LIAO, J. K. 1997. Inhibition of endothelial vascular cell adhesion molecule-1 expression by nitric oxide involves the induction and nuclear translocation of IkappaBalpha. J Biol Chem, 272, 30969-74.

SPRINGER, T. A. 1990. Adhesion receptors of the immune system. Nature, 346, 425-34.

SPRINGER, T. A. 1995. Traffic signals on endothelium for lymphocyte recirculation and leukocyte emigration. Annu Rev Physiol, 57, 827-72.

STAMLER, J. S., SINGEL, D. J. & LOSCALZO, J. 1992. Biochemistry of nitric oxide and its redox-activated forms. Science, 258, 1898-902.

STASSEN, J. M., ARNOUT, J. & DECKMYN, H. 2004. The hemostatic system. Curr Med Chem, 11, 2245-60.

STEIN, G. H., DRULLINGER, L. F., SOULARD, A. & DULIC, V. 1999. Differential roles for cyclin-dependent kinase inhibitors p21 and p16 in the mechanisms of senescence and differentiation in human fibroblasts. Mol Cell Biol, 19, 2109-17.

STEINBERG, R., HARARI, O. A., LIDINGTON, E. A., BOYLE, J. J., NOHADANI, M., SAMAREL, A. M., OHBA, M., HASKARD, D. O. & MASON, J. C. 2007. A protein kinase Cepsilon-anti-apoptotic kinase signaling complex protects human vascular endothelial cells against apoptosis through induction of Bcl-2. J Biol Chem, 282, 32288-97.

STOCKER, R., YAMAMOTO, Y., MCDONAGH, A. F., GLAZER, A. N. & AMES, B. N. 1987. Bilirubin is an antioxidant of possible physiological importance. Science, 235, 1043-6.

STRELKOV, S. V., HERRMANN, H. & AEBI, U. 2003. Molecular architecture of intermediate filaments. Bioessays, 25, 243-51.

STROKA, D. M., BADRICHANI, A. Z., BACH, F. H. & FERRAN, C. 1999. Overexpression of A1, an NF-kappaB-inducible anti-apoptotic bcl gene, inhibits endothelial cell activation. Blood, 93, 3803-10.

SUBURO, A. M. & D'AMORE, P. A. 2006. Development of the endothelium. Handb Exp Pharmacol, 71-105.

SUCHTING, S. & EICHMANN, A. 2009. Jagged gives endothelial tip cells an edge. Cell, 137, 988-90.

SUN, B. W., CHEN, Z. Y., CHEN, X. & LIU, C. 2007. Attenuation of leukocytes sequestration by carbon monoxide-releasing molecules: liberated carbon monoxide in the liver of thermally injured mice. J Burn Care Res, 28, 173-81.

SUN, J., HOSHINO, H., TAKAKU, K., NAKAJIMA, O., MUTO, A., SUZUKI, H., TASHIRO, S., TAKAHASHI, S., SHIBAHARA, S., ALAM, J., TAKETO, M. M., YAMAMOTO, M. & IGARASHI, K. 2002. Hemoprotein Bach1 regulates enhancer availability of heme oxygenase-1 gene. EMBO J, 21, 5216-24.

SUN, S. & SCHILLER, J. H. 2007. Angiogenesis inhibitors in the treatment of lung cancer. Crit Rev Oncol Hematol, 62, 93-104.

SUNAMURA, M., DUDA, D. G., GHATTAS, M. H., LOZONSCHI, L., MOTOI, F., YAMAUCHI, J., MATSUNO, S., SHIBAHARA, S. & ABRAHAM, N. G. 2003. Heme oxygenase-1 accelerates tumor angiogenesis of human pancreatic cancer. Angiogenesis, 6, 15-24.

SUO, J., OSHINSKI, J. N. & GIDDENS, D. P. 2008. Blood flow patterns in the proximal human coronary arteries: relationship to atherosclerotic plaque occurrence. Mol Cell Biomech, 5, 9-18.

SUTTLES, J., MILHORN, D. M., MILLER, R. W., POE, J. C., WAHL, L. M. & STOUT, R. D. 1999. CD40 signaling of monocyte inflammatory cytokine synthesis through an ERK1/2-dependent pathway. A target of interleukin (il)-4 and il-10 anti-inflammatory action. J Biol Chem, 274, 5835-42.

SUZUKI, M., ISO-O, N., TAKESHITA, S., TSUKAMOTO, K., MORI, I., SATO, T., OHNO, M., NAGAI, R. & ISHIZAKA, N. 2003. Facilitated angiogenesis induced by heme oxygenase-1 gene transfer in a rat model of hindlimb ischaemia. Biochem Biophys Res Commun, 302, 138-43.

SZEKANECZ, Z., KEREKES, G., DER, H., SANDOR, Z., SZABO, Z., VEGVARI, A., SIMKOVICS, E., SOOS, L., SZENTPETERY, A., BESENYEI, T., SZUCS, G., SZANTO, S., TAMASI, L., SZEGEDI, G., SHOENFELD, Y. & SOLTESZ, P. 2007. Accelerated atherosclerosis in rheumatoid arthritis. Ann N Y Acad Sci, 1108, 349-58.

TAHA, H., SKRZYPEK, K., GUEVARA, I., NIGISCH, A., MUSTAFA, S., GROCHOT-PRZECZEK, A., FERDEK, P., WAS, H., KOTLINOWSKI, J., KOZAKOWSKA, M., BALCERCZYK, A., MUCHOVA, L., VITEK, L., WEIGEL, G., DULAK, J. & JOZKOWICZ, A. 2010. Role of heme oxygenase-1 in human endothelial cells: lesson from the promoter allelic variants. Arterioscler Thromb Vasc Biol, 30, 1634-41.

TAILLE, C., EL-BENNA, J., LANONE, S., DANG, M. C., OGIER-DENIS, E., AUBIER, M. & BOCZKOWSKI, J. 2004. Induction of heme oxygenase-1 inhibits NAD(P)H oxidase activity by down-regulating cytochrome b558 expression via the reduction of heme availability. J Biol Chem, 279, 28681-8.

TAKAHASHI, S., TAKAHASHI, Y., ITO, K., NAGANO, T., SHIBAHARA, S. & MIURA, T. 1999. Positive and negative regulation of the human heme oxygenase-1 gene expression in cultured cells. Biochim Biophys Acta, 1447, 231-5.

TAKAHASHI, T., UENO, H. & SHIBUYA, M. 1999. VEGF activates protein kinase C-dependent, but Ras-independent Raf-MEK-MAP kinase pathway for DNA synthesis in primary endothelial cells. Oncogene, 18, 2221-30.

TAKEDA, K., ISHIZAWA, S., SATO, M., YOSHIDA, T. & SHIBAHARA, S. 1994. Identification of a cis-acting element that is responsible for cadmium-mediated induction of the human heme oxygenase gene. J Biol Chem, 269, 22858-67.

TAKEDA, K., ISHIZAWA, S., SATO, M., YOSHIDA, T. & SHIBAHARA, S. 1994. Identification of a cis-acting element that is responsible for cadmium-mediated induction of the human heme oxygenase gene. J Biol Chem, 269, 22858-67.

TALLQUIST, M. D., SORIANO, P. & KLINGHOFFER, R. A. 1999. Growth factor signaling pathways in vascular development. Oncogene, 18, 7917-32.

TAMMELA, T., ZARKADA, G., WALLGARD, E., MURTOMAKI, A., SUCHTING, S., WIRZENIUS, M., WALTARI, M., HELLSTROM, M., SCHOMBER, T., PELTONEN, R., FREITAS, C., DUARTE, A., ISONIEMI, H., LAAKKONEN, P., CHRISTOFORI, G., YLA-HERTTUALA, S., SHIBUYA, M., PYTOWSKI, B., EICHMANN, A., BETSHOLTZ, C. & ALITALO, K. 2008. Blocking VEGFR-3 suppresses angiogenic sprouting and vascular network formation. Nature, 454, 656-60.

TANG, D. D., BAI, Y. & GUNST, S. J. 2005. Silencing of p21-activated kinase attenuates vimentin phosphorylation on Ser-56 and reorientation of the vimentin network during stimulation of smooth muscle cells by 5-hydroxytryptamine. Biochem J, 388, 773-83.

TEDGUI, A. & MALLAT, Z. 2001. Anti-inflammatory mechanisms in the vascular wall. Circulation Research, 88, 877-87.

TEDGUI, A. & MALLAT, Z. 2006. Cytokines in atherosclerosis: pathogenic and regulatory pathways. Physiol Rev, 86, 515-81.

TENHUNEN, R., MARVER, H. S. & SCHMID, R. 1969. Microsomal heme oxygenase. Characterization of the enzyme. J Biol Chem, 244, 6388-94.

TERMAN, B. I., CARRION, M. E., KOVACS, E., RASMUSSEN, B. A., EDDY, R. L. & SHOWS, T. B. 1991. Identification of a new endothelial cell growth factor receptor tyrosine kinase. Oncogene, 6, 1677-83.

TESFAMARIAM, B. & DEFELICE, A. F. 2007. Endothelial injury in the initiation and progression of vascular disorders. Vascul Pharmacol, 46, 229-37.

THORIN, E. & SHREEVE, S. M. 1998. Heterogeneity of vascular endothelial cells in normal and disease states. Pharmacol Ther, 78, 155-66.

TISCHER, E., MITCHELL, R., HARTMAN, T., SILVA, M., GOSPODAROWICZ, D., FIDDES, J. C. & ABRAHAM, J. A. 1991. The human gene for vascular endothelial growth factor. Multiple protein forms are encoded through alternative exon splicing. J Biol Chem, 266, 11947-54.

TOMPA, P., BUZDER-LANTOS, P., TANTOS, A., FARKAS, A., SZILAGYI, A., BANOCZI, Z., HUDECZ, F. & FRIEDRICH, P. 2004. On the sequential determinants of calpain cleavage. J Biol Chem, 279, 20775-85.

TOPPER, J. N., CAI, J., FALB, D. & GIMBRONE, M. A., JR. 1996. Identification of vascular endothelial genes differentially responsive to fluid mechanical stimuli: cyclooxygenase-2, manganese superoxide dismutase, and endothelial cell nitric oxide synthase are selectively up-regulated by steady laminar shear stress. Proc Natl Acad Sci U S A, 93, 10417-22.

TOYOSHIMA, H. & HUNTER, T. 1994. p27, a novel inhibitor of G1 cyclin-Cdk protein kinase activity, is related to p21. Cell, 78, 67-74.

TRACHE, A., TRZECIAKOWSKI, J. P., GARDINER, L., SUN, Z., MUTHUCHAMY, M., GUO, M., YUAN, S. Y. & MEININGER, G. A. 2005. Histamine effects on endothelial cell fibronectin interaction studied by atomic force microscopy. Biophys J, 89, 2888-98.

TRACZ, M. J., JUNCOS, J. P., GRANDE, J. P., CROATT, A. J., ACKERMAN, A. W., RAJAGOPALAN, G., KNUTSON, K. L., BADLEY, A. D., GRIFFIN, M. D., ALAM, J. & NATH, K. A. 2007. Renal haemodynamic, inflammatory, and apoptotic responses to lipopolysaccharide in HO-1-/- mice. Am J Pathol, 170, 1820-30.

TRAKSHEL, G. M., KUTTY, R. K. & MAINES, M. D. 1986. Purification and characterization of the major constitutive form of testicular heme oxygenase. The noninducible isoform. J Biol Chem, 261, 11131-7.

TRAKSHEL, G. M. & MAINES, M. D. 1989. Multiplicity of heme oxygenase isozymes. Ho-1 and HO-2 are different molecular species in rat and rabbit. J Biol Chem, 264, 1323-8.

TRAN, J., RAK, J., SHEEHAN, C., SAIBIL, S. D., LACASSE, E., KORNELUK, R. G. & KERBEL, R. S. 1999. Marked induction of the IAP family antiapoptotic proteins survivin and XIAP by VEGF in vascular endothelial cells. Biochem Biophys Res Commun, 264, 781-8.

TRANTER, M. & JONES, W. K. 2008. Anti-inflammatory effects of HO-1 activity in vascular endothelial cells, commentary on "Carbon monoxide donors or heme oxygenase (HO-1) overexpression blocks interleukin-18-mediated NF-kappaB-PTEN-dependent human cardiac endothelial cell death". Free Radic Biol Med, 44, 261-3.

TRAUB, O. & BERK, B. C. 1998. Laminar shear stress: mechanisms by which endothelial cells transduce an atheroprotective force. Arterioscler Thromb Vasc Biol, 18, 677-85.

TRICHET, L., SYKES, C. & PLASTINO, J. 2008. Relaxing the actin cytoskeleton for adhesion and movement with Ena/VASP. J Cell Biol, 181, 19-25.

TROY, G. C. 1988. An overview of hemostasis. Vet Clin North Am Small Anim Pract, 18, 5-20.

TSURUTA, D. & JONES, J. C. 2003. The vimentin cytoskeleton regulates focal contact size and adhesion of endothelial cells subjected to shear stress. J Cell Sci, 116, 4977-84.

TUBB, B. E., BARDIEN-KRUGER, S., KASHORK, C. D., SHAFFER, L. G., RAMAGLI, L. S., XU, J., SICILIANO, M. J. & BRYAN, J. 2000. Characterization of human retinal fascin gene (FSCN2) at 17q25: close physical linkage of fascin and cytoplasmic actin genes. Genomics, 65, 146-56.

TULIS, D. A., DURANTE, W., LIU, X., EVANS, A. J., PEYTON, K. J. & SCHAFER, A. I. 2001. Adenovirus-mediated heme oxygenase-1 gene delivery inhibits injury-induced vascular neointima formation. Circulation, 104, 2710-5.

TULIS, D. A., DURANTE, W., PEYTON, K. J., EVANS, A. J. & SCHAFER, A. I. 2001. Heme oxygenase-1 attenuates vascular remodeling following balloon injury in rat carotid arteries. Atherosclerosis, 155, 113-22.

TZIVION, G., LUO, Z. J. & AVRUCH, J. 2000. Calyculin A-induced vimentin phosphorylation sequesters 14-3-3 and displaces other 14-3-3 partners in vivo. J Biol Chem, 275, 29772-29778.

USHIO-FUKAI, M. 2006. Redox signaling in angiogenesis: role of NADPH oxidase. Cardiovasc Res, 71, 226-35.

USUI, M., EGASHIRA, K., TOMITA, H., KOYANAGI, M., KATOH, M., SHIMOKAWA, H., TAKEYA, M., YOSHIMURA, T., MATSUSHIMA, K. & TAKESHITA, A. 2000. Important role of local angiotensin II activity mediated via type 1 receptor in the pathogenesis of cardiovascular inflammatory changes induced by chronic blockade of nitric oxide synthesis in rats. Circulation, 101, 305-310.

VALENZUELA, D. M., GRIFFITHS, J. A., ROJAS, J., ALDRICH, T. H., JONES, P. F., ZHOU, H., MCCLAIN, J., COPELAND, N. G., GILBERT, D. J., JENKINS, N. A., HUANG, T., PAPADOPOULOS, N., MAISONPIERRE, P. C., DAVIS, S. & YANCOPOULOS, G. D. 1999. Angiopoietins 3 and 4: diverging gene counterparts in mice and humans. Proc Natl Acad Sci U S A, 96, 1904-9.

VAN DER MEEREN, A., SQUIBAN, C., GOURMELON, P., LAFONT, H. & GAUGLER, M. H. 1999. Differential regulation by IL-4 and IL-10 of radiation-induced IL-6 and IL-8 production and ICAM-1 expression by human endothelial cells. Cytokine, 11, 831-8.

VAN NIEUW AMERONGEN, G. P., KOOLWIJK, P., VERSTEILEN, A. & VAN HINSBERGH, V. W. 2003. Involvement of RhoA/Rho kinase signaling in VEGF-induced endothelial cell migration and angiogenesis in vitro. Arterioscler Thromb Vasc Biol, 23, 211-7.

VANDERLAAN, P. A., REARDON, C. A. & GETZ, G. S. 2004. Site specificity of atherosclerosis: site-selective responses to atherosclerotic modulators. Arterioscler Thromb Vasc Biol, 24, 12-22.

VANHOUTTE, P. M. 1997. Endothelial dysfunction and atherosclerosis. Eur Heart J, 18 Suppl E, E19-29.

VANHOUTTE, P. M., SHIMOKAWA, H., TANG, E. H. & FELETOU, M. 2009. Endothelial dysfunction and vascular disease. Acta Physiol (Oxf), 196, 193-222.

VECCHI, A., GARLANDA, C., LAMPUGNANI, M. G., RESNATI, M., MATTEUCCI, C., STOPPACCIARO, A., SCHNURCH, H., RISAU, W., RUCO, L., MANTOVANI, A. & ET AL. 1994. Monoclonal antibodies specific for endothelial cells of mouse blood vessels. Their application in the identification of adult and embryonic endothelium. Eur J Cell Biol, 63, 247-54.

VESTWEBER, D. 2003. Lymphocyte trafficking through blood and lymphatic vessels: more than just selectins, chemokines and integrins. Eur J Immunol, 33, 1361-4.

VESTWEBER, D. 2008. VE-cadherin: the major endothelial adhesion molecule controlling cellular junctions and blood vessel formation. Arterioscler Thromb Vasc Biol, 28, 223-32.

VINCENT, P. A., XIAO, K., BUCKLEY, K. M. & KOWALCZYK, A. P. 2004. VE-cadherin: adhesion at arm's length. Am J Physiol Cell Physiol, 286, C987-97.

WAGNER, C. T., DURANTE, W., CHRISTODOULIDES, N., HELLUMS, J. D. & SCHAFER, A. I. 1997. Haemodynamic forces induce the expression of heme oxygenase in cultured vascular smooth muscle cells. Journal of Clinical Investigation, 100, 589-596.

WAGNER, D. D., OLMSTED, J. B. & MARDER, V. J. 1982. Immunolocalization of von Willebrand protein in Weibel-Palade bodies of human endothelial cells. J Cell Biol, 95, 355-60.

WALSH, D. A., WADE, M., MAPP, P. I. & BLAKE, D. R. 1998. Focally regulated endothelial proliferation and cell death in human synovium. Am J Pathol, 152, 691-702.

WALTER, D. H., HAENDELER, J., REINHOLD, J., ROCHWALSKY, U., SEEGER, F., HONOLD, J., HOFFMANN, J., URBICH, C., LEHMANN, R., ARENZANA-SEISDESDOS, F., AICHER, A., HEESCHEN, C., FICHTLSCHERER, S., ZEIHER, A. M. & DIMMELER, S. 2005. Impaired CXCR4 signaling contributes to the reduced neovascularization capacity of endothelial progenitor cells from patients with coronary artery disease. Circulation Research, 97, 1142-51.

WANG, D., ANDERSON, J. C. & GLADSON, C. L. 2005. The role of the extracellular matrix in angiogenesis in malignant glioma tumors. Brain Pathol, 15, 318-26.

WANG, H., RIHA, G. M., YAN, S., LI, M., CHAI, H., YANG, H., YAO, Q. & CHEN, C. 2005. Shear stress induces endothelial differentiation from a murine embryonic mesenchymal progenitor cell line. Arterioscler Thromb Vasc Biol, 25, 1817-23.

WANG, L. J., LEE, T. S., LEE, F. Y., PAI, R. C. & CHAU, L. Y. 1998. Expression of heme oxygenase-1 in atherosclerotic lesions. Am J Pathol, 152, 711-20.

WANG, N., MIAO, H., LI, Y. S., ZHANG, P., HAGA, J. H., HU, Y., YOUNG, A., YUAN, S., NGUYEN, P., WU, C. C. & CHIEN, S. 2006. Shear stress regulation of Kruppel-like factor 2 expression is flow pattern-specific. Biochem Biophys Res Commun, 341, 1244-51.

WANG, R., WU, L. & WANG, Z. 1997. The direct effect of carbon monoxide on KCa channels in vascular smooth muscle cells. Pflugers Arch, 434, 285-91.

WANG, W., CALDWELL, M. C., LIN, S., FURNEAUX, H. & GOROSPE, M. 2000. HuR regulates cyclin A and cyclin B1 mRNA stability during cell proliferation. EMBO J, 19, 2340-50.

WARE, J. A. & SIMONS, M. 1997. Angiogenesis in ischaemic heart disease. Nat Med, 3, 158-64.

WAS, H., CICHON, T., SMOLARCZYK, R., RUDNICKA, D., STOPA, M., CHEVALIER, C., LEGER, J. J., LACKOWSKA, B., GROCHOT, A., BOJKOWSKA, K., RATAJSKA, A., KIEDA, C., SZALA, S., DULAK, J. & JOZKOWICZ, A. 2006. Overexpression of heme oxygenase-1 in murine melanoma: increased proliferation and viability of tumor cells, decreased survival of mice. Am J Pathol, 169, 2181-98.

WAS, H., DULAK, J. & JOZKOWICZ, A. 2010. Heme oxygenase-1 in tumor biology and therapy. Curr Drug Targets, 11, 1551-70.

WATTS, R. N., PONKA, P. & RICHARDSON, D. R. 2003. Effects of nitrogen monoxide and carbon monoxide on molecular and cellular iron metabolism: mirror-image effector molecules that target iron. Biochem J, 369, 429-40.

WEGIEL, B., BATY, C. J., GALLO, D., CSIZMADIA, E., SCOTT, J. R., AKHAVAN, A., CHIN, B. Y., KACZMAREK, E., ALAM, J., BACH, F. H., ZUCKERBRAUN, B. S. & OTTERBEIN, L. E. 2009. Cell surface biliverdin reductase mediates biliverdin-induced anti-inflammatory effects via phosphatidylinositol 3-kinase and Akt. J Biol Chem, 284, 21369-78.

WEGIEL, B., GALLO, D. J., RAMAN, K. G., KARLSSON, J. M., OZANICH, B., CHIN, B. Y., TZENG, E., AHMAD, S., AHMED, A., BATY, C. J. & OTTERBEIN, L. E. 2010. Nitric oxide-dependent bone marrow progenitor mobilization by carbon monoxide enhances endothelial repair after vascular injury. Circulation, 121, 537-48.

WEIBEL, E. R. & PALADE, G. E. 1964. New Cytoplasmic Components in Arterial Endothelia. J Cell Biol, 23, 101-12.

WEINBERG, R. A. 1995. The retinoblastoma protein and cell cycle control. Cell, 81, 323-30.

WELCH, M. D., DEPACE, A. H., VERMA, S., IWAMATSU, A. & MITCHISON, T. J. 1997. The human Arp2/3 complex is composed of evolutionarily conserved subunits and is localized to cellular regions of dynamic actin filament assembly. J Cell Biol, 138, 375-84.

WELLNER, M., MAASCH, C., KUPPRION, C., LINDSCHAU, C., LUFT, F. C. & HALLER, H. 1999. The proliferative effect of vascular endothelial growth factor requires protein kinase C-alpha and protein kinase C-zeta. Arterioscler Thromb Vasc Biol, 19, 178-85.

WELLS, A., HUTTENLOCHER, A. & LAUFFENBURGER, D. A. 2005. Calpain proteases in cell adhesion and motility. Int Rev Cytol, 245, 1-16.

WIDLANSKY, M. E., GOKCE, N., KEANEY, J. F., JR. & VITA, J. A. 2003. The clinical implications of endothelial dysfunction. J Am Coll Cardiol, 42, 1149-60.

WIJAYANTI, N., HUBER, S., SAMOYLENKO, A., KIETZMANN, T. & IMMENSCHUH, S. 2004. Role of NF-kappaB and p38 MAP kinase signaling pathways in the lipopolysaccharide-dependent activation of heme oxygenase-1 gene expression. Antioxid Redox Signal, 6, 802-10.

WITTING, P. K., RAYNER, B. S., WU, B. J., ELLIS, N. A. & STOCKER, R. 2007. Hydrogen peroxide promotes endothelial dysfunction by stimulating multiple sources of superoxide anion radical production and decreasing nitric oxide bioavailability. Cell Physiol Biochem, 20, 255-68.

WOLFRUM, S., TEUPSER, D., TAN, M., CHEN, K. Y. & BRESLOW, J. L. 2007. The protective effect of A20 on atherosclerosis in apolipoprotein E-deficient mice is associated with reduced expression of NF-kappaB target genes. Proc Natl Acad Sci U S A, 104, 18601-6.

WOLINSKY, H., KATZ, D., MARKLE, R., MILLS, J., BREM, S. & WASSERTHEILSMOLLER, S. 1980. Hydrolase Activities in the Rat Aorta .4. Relation between Clearance Rates of Circulating I-125-Labeled Low-Density Lipoproteins and Levels of Tissue Hydrolase Activity. Circulation Research, 47, 433-442.

WOODS, A. J., WHITE, D. P., CASWELL, P. T. & NORMAN, J. C. 2004. PKD1/PKCmu promotes alphavbeta3 integrin recycling and delivery to nascent focal adhesions. EMBO J, 23, 2531-43.

WOOLKALIS, M. J., DEMELFI, T. M., JR., BLANCHARD, N., HOXIE, J. A. & BRASS, L. F. 1995. Regulation of thrombin receptors on human umbilical vein endothelial cells. J Biol Chem, 270, 9868-75.

WU, M. H. 2005. Endothelial focal adhesions and barrier function. J Physiol, 569, 359-66.

XIA, P., AIELLO, L. P., ISHII, H., JIANG, Z. Y., PARK, D. J., ROBINSON, G. S., TAKAGI, H., NEWSOME, W. P., JIROUSEK, M. R. & KING, G. L. 1996. Characterization of vascular endothelial growth factor's effect on the activation of protein kinase C, its isoforms, and endothelial cell growth. Journal of Clinical Investigation, 98, 2018-26.

YACHIE, A., NIIDA, Y., WADA, T., IGARASHI, N., KANEDA, H., TOMA, T., OHTA, K., KASAHARA, Y. & KOIZUMI, S. 1999. Oxidative stress causes enhanced endothelial cell injury in human heme oxygenase-1 deficiency. Journal of Clinical Investigation, 103, 129-35.

YAMAGUCHI, J., KUSANO, K. F., MASUO, O., KAWAMOTO, A., SILVER, M., MURASAWA, S., BOSCH-MARCE, M., MASUDA, H., LOSORDO, D. W., ISNER, J. M. & ASAHARA, T. 2003. Stromal cell-derived factor-1 effects on ex vivo expanded endothelial progenitor cell recruitment for ischaemic neovascularization. Circulation, 107, 1322-8.

YAMAGUCHI, T. P., DUMONT, D. J., CONLON, R. A., BREITMAN, M. L. & ROSSANT, J. 1993. flk-1, an flt-related receptor tyrosine kinase is an early marker for endothelial cell precursors. Development, 118, 489-98.

YAMASHITA, K., MCDAID, J., OLLINGER, R., TSUI, T. Y., BERBERAT, P. O., USHEVA, A., CSIZMADIA, E., SMITH, R. N., SOARES, M. P. & BACH, F. H. 2004. Biliverdin, a natural product of heme catabolism, induces tolerance to cardiac allografts. FASEB J, 18, 765-7.

YANAGISAWA, M., KURIHARA, H., KIMURA, S., TOMOBE, Y., KOBAYASHI, M., MITSUI, Y., YAZAKI, Y., GOTO, K. & MASAKI, T. 1988. A novel potent vasoconstrictor peptide produced by vascular endothelial cells. Nature, 332, 411-5.

YET, S. F., LAYNE, M. D., LIU, X., CHEN, Y. H., ITH, B., SIBINGA, N. E. & PERRELLA, M. A. 2003. Absence of heme oxygenase-1 exacerbates atherosclerotic lesion formation and vascular remodeling. FASEB J, 17, 1759-61.

YOON, M., MOIR, R. D., PRAHLAD, V. & GOLDMAN, R. D. 1998. Motile properties of vimentin intermediate filament networks in living cells. J Cell Biol, 143, 147-57.

ZACHARY, I. 2001. Signaling mechanisms mediating vascular protective actions of vascular endothelial growth factor. Am J Physiol Cell Physiol, 280, C1375-86.

ZAKHARY, R., GAINE, S. P., DINERMAN, J. L., RUAT, M., FLAVAHAN, N. A. & SNYDER, S. H. 1996. Heme oxygenase 2: endothelial and neuronal localization and role in endothelium-dependent relaxation. Proc Natl Acad Sci U S A, 93, 795-8.

ZEIHER, A. M., FISSLTHALER, B., SCHRAY-UTZ, B. & BUSSE, R. 1995. Nitric oxide modulates the expression of monocyte chemoattractant protein 1 in cultured human endothelial cells. Circulation Research, 76, 980-6.

ZENCLUSSEN, A. C., SCHUMACHER, A., ZENCLUSSEN, M. L., WAFULA, P. & VOLK, H. D. 2007. Immunology of pregnancy: cellular mechanisms allowing fetal survival within the maternal uterus. Expert Rev Mol Med, 9, 1-14.

ZENG, H., ZHAO, D. & MUKHOPADHYAY, D. 2002. KDR stimulates endothelial cell migration through heterotrimeric G protein Gq/11-mediated activation of a small GTPase RhoA. J Biol Chem, 277, 46791-8.

ZHANG, X., BEDARD, E. L., POTTER, R., ZHONG, R., ALAM, J., CHOI, A. M. & LEE, P. J. 2002. Mitogen-activated protein kinases regulate HO-1 gene transcription after ischaemia-reperfusion lung injury. Am J Physiol Lung Cell Mol Physiol, 283, L815-29.

ZHANG, X., SHAN, P., JIANG, G., ZHANG, S. S., OTTERBEIN, L. E., FU, X. Y. & LEE, P. J. 2006. Endothelial STAT3 is essential for the protective effects of HO-1 in oxidant-induced lung injury. FASEB J, 20, 2156-8.

ZHUANG, S., NGUYEN, G. T., CHEN, Y., GUDI, T., EIGENTHALER, M., JARCHAU, T., WALTER, U., BOSS, G. R. & PILZ, R. B. 2004. Vasodilator-stimulated phosphoprotein activation of serum-response element-dependent transcription occurs downstream of RhoA and is inhibited by cGMP-dependent protein kinase phosphorylation. J Biol Chem, 279, 10397-407.

ZIEGLER, S. F., BIRD, T. A., SCHNERINGER, J. A., SCHOOLEY, K. A. & BAUM, P. R. 1993. Molecular cloning and characterization of a novel receptor protein tyrosine kinase from human placenta. Oncogene, 8, 663-70.

APPENDIX

Table A. 1.: Monoclonal and polyclonal primary antibodies for western blotting. Target antigens are listed in an alphabetical order and working dilutions were prepared in 1X TBS-T.

Target Antigen	Source Species	Supplier	Dilution
α-tubulin	mouse, ascites fluid	Sigma-Aldrich Ltd.	1:30,000
Bcl-2 (C-2)	mouse monoclonal	Santa Cruz Biotechnology, Inc.	1:1,000
Bcl-xl (H-62)	rabbit polyclonal	Santa Cruz Biotechnology, Inc.	1:1,000
cyclin A (B-8)	mouse monoclonal	Santa Cruz Biotechnology, Inc.	1:1,000
GAPDH	mouse monoclonal	Millipore	1:30,000
HO-1	mouse monoclonal	Stressgen	1:1,000
HO-2	rabbit polyclonal	Stressgen	1:1,000
PKCε	rabbit polyclonal	Santa Cruz Biotechnology, Inc.	1:1,000
Phospho-PKCε (Ser729)	rabbit polyclonal	Millipore	1:1,000
Rb (C-2)	mouse monoclonal	Santa Cruz Biotechnology, Inc.	1:1,000
Phospho-Rb (pT821)	rabbit polyclonal	Invitrogen	1:1,000
VASP (9A2)	rabbit monoclonal	Cell Signaling	1:1,000
Phospho-VASP (Ser239)	rabbit polyclonal	Cell Signaling	1:1,000
Vimentin	mouse monoclonal	Abcam	1:10,000

Table A. 2.: Secondary antibodies for western blotting. Working dilutions were prepared in 1X TBS-T.

Target Antigen	Source Species	Supplier	Dilution
HRP-conjugated anti-mouse	goat	Dako	1:1,500 – 1:30,000
HRP-conjugated anti-rabbit	swine	Dako	1:3,000

Table A. 3.: Primary antibodies for immunofluorescence staining. Target antigens are listed in an alphabetical order and working dilutions were prepared in 3% BSA in PBS with Ca^{2+} and Mg^{2+}.

Target Antigen	Source Species	Supplier	Dilution
HO-1	rabbit polyclonal	Santa Cruz Biotechnology, Inc.	1:200
Vimentin	mouse monoclonal	Abcam	1:200
Negative control mouse IgG1	mouse	Dako	1:20

Table A. 4.: Secondary antibodies for immunofluorescence staining. Working dilutions were prepared in 3% BSA in PBS with Ca^{2+} and Mg^{2+}.

Target Antigen	Source Species	Supplier	Dilution
anti-mouse IgG1 Alexa Fluor 488	goat	Invitrogen	1:1,000
anti-mouse IgG1 Alexa Fluor 568	goat	Invitrogen	1:1,000
anti-rabbit IgG1 Alexa Fluor 568	goat	Invitrogen	1:1,000

Table A. 5.: Primary antibodies for flow cytometry. Target antigens are listed in an alphabetical order and working dilutions were prepared in HBSS with Ca^{2+} and Mg^{2+} supplemented with 1% FCS.

Target Antigen	Source Species	Supplier	Dilution
CD31	mouse monoclonal	Developmental Studies Hybridoma Bank	neat supernatant
Endoglin	mouse monoclonal	Dr A. d'Apice	1:50
ICAM-2	mouse monoclonal	D. T. Springer	1:50
Integrin $\alpha_v\beta_3$	mouse monoclonal	Millipore	1:50
PCNA	mouse monoclonal	Santa Cruz Biotechnology, Inc.	1:50
VCAM-1	mouse monoclonal	generated in house	neat supernatant

Table A. 6.: Secondary antibodies for flow cytometry. Working dilutions were prepared in HBSS with Ca^{2+} and Mg^{2+} supplemented with 1% FCS.

Target Antigen	Source Species	Supplier	Dilution
FITC-labelled anti-mouse	rabbit polyclonal	Dako	1: 50